Herpes Simplex Virus type 1 lytic viral gene expression during the establishment and maintenance of latency

Tiffany Ann Russell

A thesis submitted for the degree of Doctor of Philosophy of the Australian National University

August 2015

Research School of Biology

The Australian National University

Declaration

This is to certify that:

- The work presented in this thesis was conducted at the Australian National University in the laboratory of Associate Professor David C. Tscharke. This thesis comprises my original work towards the degree of Doctor of Philosophy, except where indicated.
- To the best of my knowledge, this thesis does not contain material previously published by another person, except where due acknowledgement is made in the text.
- This thesis is less than 100 000 words in length, exclusive of figures, tables, references and appendices.

Tiffany Russell

Acknowledgements

I can't believe that I am finally here and it's time to thank all of the truly remarkable people who have helped me during this long, often torturous, but rewarding journey that has been my PhD. In many ways this is an exciting and joyous time, and I feel incredibly privileged to have had this opportunity. I hope I am eloquent enough to convey my heartfelt appreciation for all those who have supported me through this time.

Firstly, I would like to thank my supervisor, Associate Professor David Tscharke, for providing invaluable guidance, while still managing to maintain his sanity and sense of optimism in the face of my despair. It has been challenging, which is part of the fun. I have come so far, both as a scientist and a scholar, but also personally, and I cannot express how grateful I am for the opportunities you have provided me. Thank you.

I need to thank our fantastic collaborators, Dr. Frank Carbone, Dr. Claerwen Jones and Dr. Joel Ma, for their assistance. I would like to thank all the members of my supervisory panel for their guidance and support during this process – Dr. Ian Searle, Dr. Barbara van Leeuwen, Dr. Inge Flesch and Dr. Alex Maier. I would also like to thank Shannon and Matt for their assistance in the animal house, as well as Sharon and James in the autoclave room for always being so ready to help and cheerful.

I also want to thank all members of the Tscharke lab, both past and present: Stewart Smith, Inge Flesch, Michael Wong, Leon Lin, Bianca Dobson, Thilaga Velusamy, Natasha Hollett, Tijana Stefanovic, Kathryn Dickson, Erica Wynne-Jones, Mel Soda, Jana Pickering, Erica Keller, Emily Spierings, and Barbara Quinan. I could not have survived without your help and unwavering support. In particular, I would like to thank Stewart, for answering my inane questions, and always being ready with a sympathetic ear when I am having a Sisyphus moment. I also want to thank mW – I didn't really need another younger brother, but I'm glad you tried to fill the void. Your advice was not always reassuring, but your proofreading skills and knowledge of all things immunology was awe-inspiring. I also need to thank my cell mate, Bianca. I'm sure I drove you mad in our little cubicle, but I could not have done this without your calm and perseverance. Finally, to my herpes gang – Thilaga, Tijana and Erica – I wouldn't be where I am today without you, and I can't wait to see the amazing things you all go on to achieve.

I need to thank my family. Mum, Dad, Tom and Carla – I couldn't have survived without you. Words can't express how I feel. Looking at where we all are twenty years later, I'm so proud of how far we have come together. I love you all!

Finally, I want to thank all the people who remind me every day how magical it is to be a scientist. When I despair at a failing experiment, you make me realise that even the smallest achievements in science are special, and I find it easier to hold on for those amazing moments that take my breath away. Thanks Dad and Tom, for being amazed by my cultures of Vero cells in our fancy lab. I can't believe I actually get paid to do this either! Thanks Queenie, and my 3rd year students – I have loved seeing you learn and grow, and it is privilege to be able to teach you. Thanks also to Brayden and Gracie for your wonderful, supportive emails – this is for you:

A virus enters a bar.
The bartender says, "We don't serve your kind in here".
The virus replies, "Well, you're not a very good host".

Publications arising from this project

Russell, T.A., Stefanovic, T., and Tscharke, D.C. (2015). Engineering herpes simplex viruses by infection–transfection methods including recombination site targeting by CRISPR/Cas9 nucleases. Journal of Virological Methods *213*, 18-25.

Macleod, B.L., Bedoui, S., Hor, J.L., Mueller, S.N., **Russell, T.A.**, Hollett, N.A., Heath, W.R., Tscharke, D.C., Brooks, A.G., and Gebhardt, T. (2014). Distinct APC subtypes drive spatially segregated $CD4^+$ and $CD8^+$ T-cell effector activity during skin infection with HSV-1. PLoS Pathogens *10*, e1004303.

Ma, J.Z., **Russell, T.A.**, Spelman, T., Carbone, F.R., and Tscharke, D.C. (2014). Lytic gene expression is frequent in HSV-1 latent infection and correlates with the engagement of a cell-intrinsic transcriptional response. PLoS Pathogens *10*, e1004237.

Abstract

Herpes Simplex Virus (HSV) type I causes cold sores but is also associated with severe outcomes such as encephalitis and blindness. The primary lytic HSV-1 infection in the skin and peripheral nervous system (PNS) is limited to around a week, but latent virus persists in neurons, from which it can reactivate periodically. A black and white view of lytic versus latent infection persists in the HSV literature. Somewhat paradoxically, there remains concern that 'true' latent infection cannot be assumed to occur in animal models within a month of primary infection. In this thesis, the ROSA26R/Cre mouse model was used that allows historic assessment of virus activity. In this model, β-galactosidase (β-gal) expression is switched on permanently in any cells that had experienced HSV-1-driven Cre recombinase expression. Further, placing the *Cre* gene under the control of various HSV-1 promoters allowed the number of cells that have experienced different types of viral activity to be determined, from entry of a virus genome to expression of lytic genes.

This historical analysis found substantial lytic gene expression and spread of virus occurs in the PNS for at least five days beyond the peak of infectious virus load. This suggests that the period immediately after the bulk of the lytic infection is quelled remains highly dynamic. Further, there was continued accumulation in β-gal marked cells in mice infected with viruses that express Cre from the gB and infected cell protein (ICP) 6 promoters. Therefore, transient, likely low level, promoter activity does occur during latency, which can lead to protein production. This was not observed for the ICP0 promoter, indicating that expression from various lytic gene promoters differs during this time.

More striking, when expression of *Cre* was directed by the promoter for ICP47, a viral gene that functions to inhibit adaptive immune responses, the number of β-gal-expressing neurons continued to rise sharply until day 20 after infection. Further, β-gal marked cells continued to accumulate throughout latency, suggesting that ICP47 may function during latency to facilitate evasion of the immune response, and potentially reactivation. However, attempts to overcome the effect of ICP47 expression by increasing antigen presentation on infected neurons did not have a substantial impact on the establishment or maintenance of latency.

In summary, this thesis has provided insights into the dynamic interaction between viral lytic gene expression and the immune response during latency, challenging the traditional paradigm of an almost-quiescent form of HSV-1 latency. The results presented in this thesis further our understanding HSV-1 and α-herpesvirus latency, and with further research will hopefully lead to better therapeutic outcomes.

Table of contents

List of figures

List of tables

Abbreviations

6-FAM	6-carboxylfluorescein
acH3K9	acetylation of lysine 9 of histone 3
acH3K14	acetylation of lysine 14 of histone 3
α	Immediate Early
ANOVA	A one-way analysis of variance
ANU	the Australian National University
APC	Antigen Presenting Cell
APC-Cy7	Allophycocyanin-cyanine 7
APS	Ammonium Persulphate
BAC	Bacterial Artificial Chromosome
β	Early
β-gal	β-galactosidase
BGH	Bovine Growth Hormone
BV421	Brilliant Violet 421
CAT	Chloramphenicol Acetyltransferase
CENP	Centromere Protein
ChIP	Chromatin Immunoprecipitation
CMC	Carboxymethylcellulose
CMV	Cytomegalovirus
CMV IE	Cytomegalovirus Immediate-Early
CNS	Central Nervous System
CoREST	Corepressor element-1 silencing transcription factor
CPE	Cytopathic Effect
CreER	Cre that has been fused to mutated hormone-binding domains of the Estrogen Receptor
CRISPR	Clustered Regularly Spaced Palindromic Repeats
C_T	Threshold Cycle
CTCF	CCCTC-binding factor
CTF	CCAAT Binding Factor
CXA	Contextual analysis
DAS	Downstream Activator Sequence
DDAO-galactosidase	9H-(1,3-dichloro-9,9-dimethylacridin-2-one-7-yl β-D-galactopyranoside
DMEM	Dulbecco's Modified Eagle Medium
DMF	*N, N* Dimethylformamide

DMSO	Dimethyl sulfoxide
dNTP	deoxynucleotide triphosphate
DRG	Dorsal Root Ganglia
DTT	Dithioreitol
eGC	eGFP/Cre fusion protein
ECMV	Encephalomyocarditis Virus
eGFP	enhanced Green Fluorescent Protein
ER	Endoplasmic Reticulum
FBS	Foetal Bovine Serum
FITC	Fluorescein Isothiocyanate
γ_1	Leaky late
γ_2	True late
gB	glycoprotein B
gC	glycoprotein C
gE	glycoprotein E
GFP	Green Fluorescent Protein
gzmB	granzyme B
gRNA	guide RNA
HCF-1	Host Cell Factor 1
HDAC	Histone Deacetylase
HIV	Human Immunodeficiency Virus
HP1	Heterochromatin binding Protein 1
HSV	Herpes Simplex Virus
I	Internal
ICP	Infected Cell Protein
IFN	Interferon
IL	Interleukin
INR	Initiator
IRES	Internal Ribosome Entry Site
IRF1	Interferon Regulatory Factor 1
ISH	*In Situ* Hybridisation
JCSMR	John Curtin School of Medical Research
LAT	Latency Associated Transcript
LB	Luria-Bertani
LCM	Laser Cutting Microdissection
LSD1	Lysine Specific Demethylase 1

MCS	Multiple Cloning Site
MEM	Minimum Essential Medium
metH3K4	methylation of lysine 4 of histone 3
metH3K9	methylation of lysine 9 of histone 3
metH3K27	methylation of lysine 27 of histone 3
MGBNFQ	3' Minor Groove Binder Non Fluorescent Quencher
MHC	Major Histocompatibility Complex
miRNA	microRNA
MOI	Multiplicity Of Infection
NGF	Neuron Growth Factor
NK	Natural Killer
OCT-1	Octamer binding protein 1
OHT	4-hydroxytamoxifen
ONPG	Ortho-Nitrophenyl-β-galactoside
opm	oscillations per minute
OriS	Origin of Replication in the Short region of the HSV-1 genome
p.i.	post infection
PAM	Protospacer Adjacent Motif
PBS	Phosphate Buffered Saline
PE	Phycoerythrin
PE-Cy7	Phycoerythrin-cyanine 7
PFA	Paraformaldehyde
PNS	Peripheral Nervous System
qPCR	quantitative PCR
qRT-PCR	quantitative Reverse Transcriptase-Polymerase Chain Reaction
RAG	Recombination Activating Genes
REST	RE1-Silencing Transcription factor
RISC	RNA Induced Silencing Complex
R_L	Long Repeat
rNTP	ribonucleotide triphosphate
ROSA26R	B6.129S4-Gt(ROSA)26Sor^{tm1So}/J
R_S	Short Repeat
RT	Reverse Transcriptase
SDS	Sodium Dodecyl Sulphate
SOC	Super Optimal broth with Catabolite repressor
SP1	GC bp-rich motifs for Stimulator Protein

SV40	Simian Virus 40
T	Terminal
TAE	Tris-Acetate-EDTA
TAP	Transporter associated with Antigen Presentation
TBE	Tris-Borate-EDTA
TCR	T Cell Receptor
TEMED	N-N-N'-N'-tetramethylethylenediamine
TG	Trigeminal Ganglia
TK	thymidine kinase
TLR	Toll-Like Receptor
T_m	Melting Temperature
TNF-α	Tumour Necrosis Factor α
TRIID/TBP	Transcription factor II D/TATA Binding Protein
T_{RM} cells	Tissue Resident Memory cells
U_L	Unique Long region of the HSV-1 genome
U_S	Unique Short region of the HSV-1 genome
VP	Virion Protein
VRE	VP16 Responsiveness Element
VZV	Varicella Zoster Virus
X-gal	5-bromo-4-chloro-3-indolyl-beta-D-galacto-pyranoside
YFP	Yellow Fluorescent Protein

1 | Introduction

1.1 Overview with an introduction to Herpes Simplex Virus

HSV is a large double-stranded DNA virus of the family *Herpesviridae*. All herpesviruses share three distinct characteristics. Firstly, they all have the same typical particle morphology (Section 1.1.1). Secondly, all possess a large double-stranded DNA genome, ranging from approximately 125 to 235 kb in size (Section 1.1.2; Davison et al., 2009; Roizmann et al., 1992). Finally, all have the ability to produce disease following productive infection, as well as enter a latent phase in some cells of the infected natural host characterised by an absence of detectable infectious virus. The virus can then periodically reactivate from this reservoir to re-enter the lytic program of infection (Section 1.1.3; Stevens and Cook, 1971). It is this characteristic that is the defining quality of HSV-1, but despite decades of research, the role of virus and host factors that dictate the progression of infection remains poorly defined. This thesis will attempt to investigate the establishment of the latent HSV-1 infection and the extent to which this is dictated by the productive infection and its associated gene expression. It will also investigate the limited viral gene expression that may take place during latency and consider a more dynamic model of HSV-1 latency.

1.1.1 The mammalian herpesviruses

Mammalian herpesviruses can be classified into α, β and γ subgroups (Davison et al., 2009). This is based primarily on biological characteristics, such as host range, spread in culture, the speed of their reproductive cycle and, most importantly, the primary site in which latency is established (Roizman et al., 1981; Roizmann et al., 1992). In simplistic terms, the α herpesviruses primarily establish latency in sensory neurons, while the β herpesviruses establish latency in cells of the monocyte lineage and the γ herpesviruses establish latency in T or B cells (Davison, 2007). At least seven distinct human *herpesviruses* have currently been identified and sequenced (Baer et al., 1984; Cha et al., 1996; Davison and Scott, 1986; Dolan et al., 1998; Gompels et al., 1995; McGeoch et al., 1986; Nicholas, 1996). Three of these are classified as α herpesviruses: varicella-zoster virus (VZV), HSV-1 and HSV-2 (Subak-Sharpe and Dargan, 1998). HSV-1 and HSV-2 are closely related, with approximately 80% genetic homology within coding regions (Dolan et al., 1998).

1.1.2 Epidemiology and disease resulting from HSV-1 infection

HSV-1 is a ubiquitous human pathogen, with seropositivity of 76% in Australia (Cunningham et al., 2006). Most recent estimates suggest that the global prevalence of HSV-1 is approximately 90%, and is much greater than that of HSV-2 (as reviewed by

Smith and Robinson, 2002). HSV-1 seropositivity varies with age, sex, geographical location (rural versus metropolitan) and Indigenous status (Cunningham et al., 2006; Smith and Robinson, 2002).

Both HSV-1 and HSV-2 infect primarily through mucosal surfaces or damaged skin. In the majority of cases, HSV-1 is acquired via the oro-labial route, although the incidence of genital herpes as a result of HSV-1 infection is rising in many developed countries, including Australia (Tran et al., 2004). Both the primary HSV-1 infection and any subsequence episodes of reactivation can be either symptomatic or asymptomatic, with this being at least partially dependent on the immunological status of the host (Knaup et al., 2000; as reviewed by Knipe and Cliffe, 2008). Generally, it has been estimated that around one third of those who are seropositive will experience at least one symptomatic HSV-1 episode (Whitley et al., 1998).

The majority of HSV-1 infections are mild or asymptomatic but for others they can be highly debilitating (Knaup et al., 2000). HSV-1 is responsible for a variety of pathological conditions, including herpes labialis (commonly known as cold sores), eczema herpeticum, genital lesions, herpes simplex encephalitis and herpes keratitis (Bader et al., 1978; McGrath et al., 1997; Tran et al., 2004; Wollenberg et al., 2003; Young et al., 2010). The recurrent mucocutaneous infections associated with HSV are painful and account for the majority of health care utilization, though they are not the most serious manifestation of infection (Shulman, 2005). Primary HSV infection can also be devastating in newborns (Corey and Wald, 2009) and immunocompromised patients, where the virus can be systemically disseminated and cause fatal infection. However, prophylactic antiviral therapy is effective in relieving symptoms in those infected with Human Immunodeficiency Virus (HIV), cancer patients and in patients who have had a bone marrow transplant (Arduino and Porter, 2006) .

Due to the high prevalence of HSV, rare complications of primary HSV-1 infection and reactivation have a considerable medical burden (Khetsuriani et al., 2002). For example, herpes simplex encephalitis is the most common cause of fatal viral encephalitis, and is associated with 70% mortality in untreated patients. Even in patients that receive appropriate treatment, there is a 20 - 30% incidence of mortality, and a high incidence of severe and permanent neurological sequelae (McGrath et al., 1997). Similarly, ocular infection with HSV-1, including herpes simplex keratitis, is also extremely debilitating, and is the most common cause of corneal blindness. This visual loss is not due to the primary HSV infection, but to the corneal thinning, scarring and neovascularisation associated with recurrent disease (as reviewed by Liesegang, 2001). Finally, neonatal HSV infection is

associated with a 60% incidence of mortality in untreated cases, but even with early treatment results in considerable disability amongst the survivors. Most infections result from exposure in the genital tract during delivery, and are usually attributable to HSV-1 infection (Corey and Wald, 2009; Jones et al., 2014). The incidence of genital herpes as a result of HSV-1 infection is rising (Tran et al., 2004), which has implications for the prevention and treatment of neonatal HSV infection.

1.1.3 HSV-1 virion structure and composition

The structure of the HSV-1 virion has been well-characterised, with the capsid structure being resolved to 8.5Å resolution by electron cryomicroscopy and approximately 7 nm resolution for the structure of the virion (Grünewald et al., 2003; Zhou et al., 2000b). The double-stranded DNA genome is found in the centre of the virion as a single densely coiled molecule in a liquid crystalline arrangement (Booy et al., 1991). The folded DNA molecule is enclosed in an icosahedral capsid. This nucleocapsid is composed of 162 capsomers and is approximately 100 nm in diameter (Schrag et al., 1989; Zhou et al., 2000b). Further, the nucleocapsid is composed of at least five different HSV structural proteins (Gibson and Roizman, 1972), and is embedded within the tegument. The tegument is an amorphous, proteinaceous structure (Grünewald et al., 2003) that is surrounded by the viral envelope (van Genderen et al., 1994). The viral envelope is a lipid bilayer membrane of host origin that contains eleven different HSV-1 glycoproteins (Grünewald et al., 2003). More than 50% of recognized HSV-1 genes encode proteins that make up the virion structure (Subak-Sharpe and Dargan, 1998).

1.1.4 The HSV-1 genome

The HSV-1 genome is approximately 152 kb long, and has a G + C content of approximately 68.3%. It is generally accepted that the genome circularises after infection and is maintained during latency in a non-replicating, circular episomal form (Efstathiou et al., 1986; Garber et al., 1993; Mellerick and Fraser, 1987; Rock and Fraser, 1985; Strang and Stow, 2005). Conceptually, the genome is usually divided into two segments, designated unique long (U_L) and unique short (U_S; Figure 1-1). Each segment consists of a unique sequence which is flanked by a pair of inverted repeats, designated as either terminal (T), located at the end of the genome, or internal (I), located at the joint region of the genome. Both the long repeat (R_L) and short repeat (R_S) sequences are distinct (Wadsworth et al., 1975). There is also a terminal redundancy of approximately 400 bp, known as the “a” sequence. One or more copies of this sequence are located internally at the join between the L and S sequences in the opposite orientation to the terminal “a” sequences, and are known as the “a’ ” sequences (Wagner and Summers, 1978).

Figure 1-1. Overview of HSV-1 genome structure. The HSV-1 genome can be divided into two unique linked segments designated U_L and U_S. U_L and U_S are flanked by a pair of inverted repeats, designated TR_L and IR_L, and IR_S and TR_S, respectively. The "a" segment is a 400 bp terminal redundancy found at the genome termini, while the "a' " sequence is an inverted repeat of this sequence found between the two genome segments.

Preparations of HSV-1 DNA consist of a mixture of four possible sequence orientation isomers that differ in the relative orientation of the U_L and U_S sequences (Delius and Clements, 1976). Additionally, as there is a range of copies of each of the repeat regions, the size of the genome can be variable. However, one isomer has been designated as the prototype sequence for the purpose of genomic map representations (Figure 1-1; McGeoch et al., 1988).

More than 74 genes are recognized in the HSV-1 genome, which encode at least 70 distinct proteins. U_L encodes at least 57 genes, and 56 proteins (McGeoch et al., 1988). Likewise, the U_S segment contains at least 12 genes (Watson et al., 2012). Virtually all of those genes identified are unspliced (Roizman, 1982). The most notable examples of HSV-1 genes which are spliced are R_L2 (encoding the protein ICP0), U_S1 (encoding ICP22), U_S12 (encoding ICP47) and the latency associated transcript (LAT; as reveiwed by Rajčáni et al., 2004).

1.1.5 The HSV-1 life cycle: lytic infection, latency and reactivation

The HSV-1 life cycle is very complex, so for conceptual reasons, it is often divided into three distinct phases: lytic infection, latency and reactivation (Figure 1-2). However, to a certain extent these three stages represent a biological continuum (Steiner, 1996).

The primary, lytic infection with HSV-1 is usually initiated in the mucosal membranes or skin. Replication of the virus occurs in the skin, and subsequent death of the host cells occurs (Pellet and Roizman, 2013). The virus quickly gains access to innervating sensory nerves and travels to the cell bodies of the primary sensory neurons via retrograde axonal transport (Antinone and Smith, 2010; Cook and Stevens, 1973). These neurons are collected in the sensory ganglia of the PNS. Within the ganglia, the virus replicates briefly and limited spread of the virus to other neurons may occur. From here virus can also travel back to the skin, infecting additional cells and broadening the geographic area of the initial site of infection. This results in the exposure of additional innervating axonal endings to virus and infection of additional neurons in the ganglia. In this way, viral replication in the ganglia influences the number of neurons infected by both the spread of virus within the PNS and expansion of the area of the surface infection (Shimeld et al., 2001; Simmons and Nash, 1984; Thompson and Sawtell, 2000). Infection will continue at the skin and PNS until it is curtailed by the onset of an adaptive immune response (Nash et al., 1987; Simmons and Nash, 1985; Simmons and Tscharke, 1992; Van Lint et al., 2004).

A portion of neurons that receive the HSV genome survive to establish latency (Bastian et al., 1972; Cook et al., 1974; Shimeld et al., 2001; Stevens and Cook, 1971). Operationally,

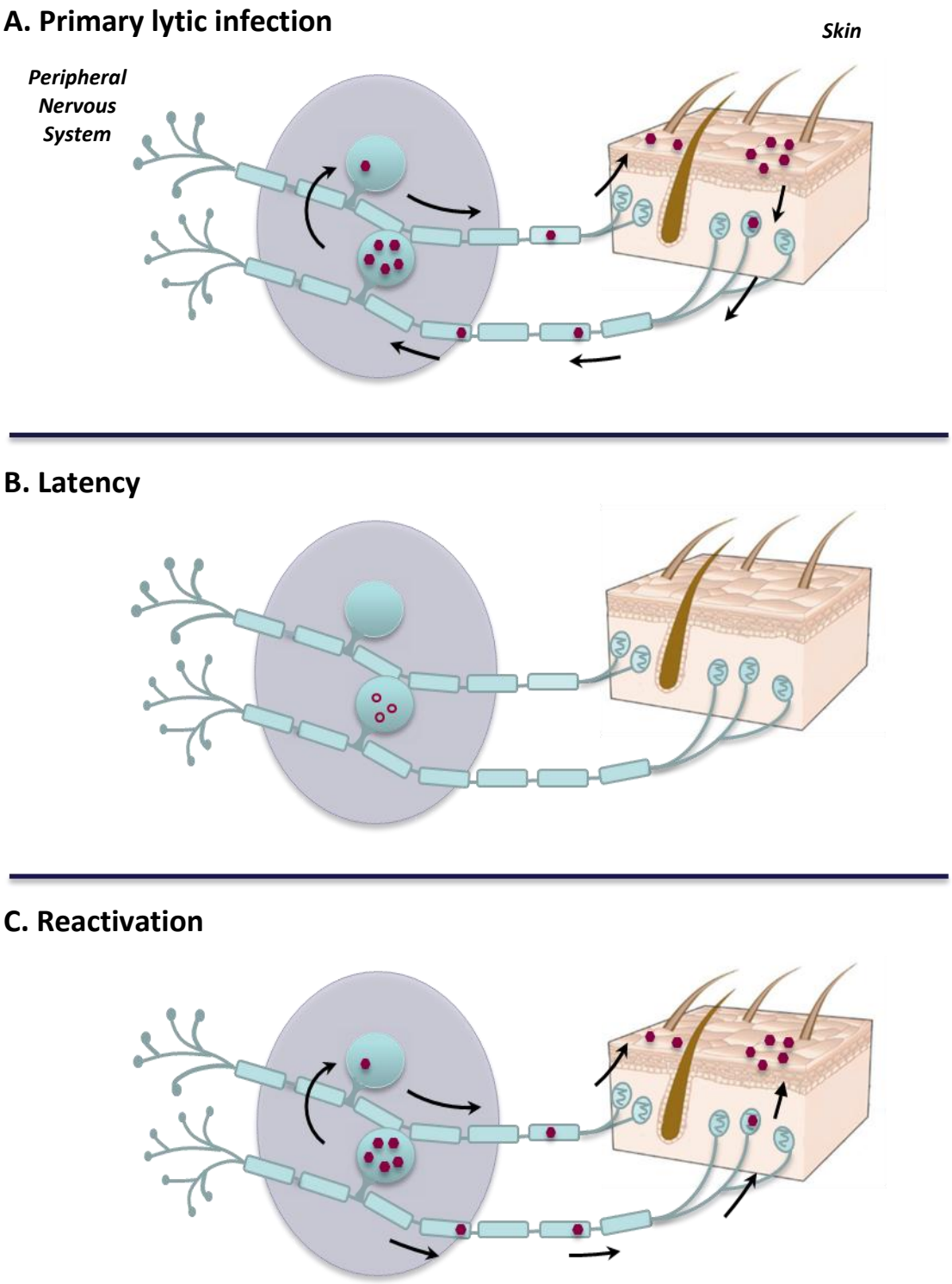

Figure 1-2. Overview of HSV-1 primary lytic infection, latency and reactivation. (A) The primary infection is initiated in the epithelial cells with lytic replication to produce viral progeny. Virus spreads to sensory neurons innervating the primary site of infection, where a productive infection also occurs. The virus can spread to other neurons and also return to the skin by anterograde transport to establish infection in another site. (B) HSV-1 latency is established in the sensory neurons, characterised by the persistence of viral DNA and the lack of infectious virus. (C) Following a stimulus, the virus may reactivation from latency, reestablish a productive infection in both the neurons and the site of primary skin infection.

latency is defined as the persistence of viral DNA in the absence of infectious virus and repression of viral protein production (Decman et al., 2005a; Steiner and Kennedy, 1995; Wagner and Bloom, 1997). The establishment of latency means that there is a stable reservoir of viral DNA that persists for long periods of time (Hill et al., 2008; Hill et al., 1996a; Rock and Fraser, 1983).

The virus can periodically re-emerge from latency in one or a few neurons in response to external stimuli such as stress or immunosuppression (Ecob-Prince and Hassan, 1994; Sawtell et al., 1998). This leads to virion formation, anterograde transport back to the peripheral site and viral shedding, with or without recurrent lesions (Antinone and Smith, 2010; Wisner et al., 2011). When this activity leads to the formation of a lesion it is termed recrudescence (as reviewed by Knipe and Cliffe, 2008).

1.1.6 The immune response elicited by HSV-1 infection

Infection with HSV-1 produces a complex cascade of immune responses, with both the innate and adaptive arms of the immune system recruited. While the exact contribution of different cell subsets to the immune response against HSV is unknown, it appears clear that there is substantial redundancy (Kastrukoff et al., 2010). The immune response is important for restricting the acute infection with HSV-1, but it is unclear to what extent the immune response is responsible for suppressing the virus into latency. Once latency is established, the immune response to HSV-1 plays a vital part in determining the outcome following reactivation (Liu et al., 2000). Therefore, for the sake of clarity, only the immune response to acute primary HSV-1 infection will be discussed in this section, with the role of the host's immune response during latency discussed in greater detail in Section 1.3.7.

Following infection with HSV-1, an innate immune response is induced that is vital for controlling the HSV-1 replication and preventing virus spread to the central nervous system (CNS). This begins with an influx of neutrophils, though these cells probably do not play a key role in controlling infection (Stumpf et al., 2002; Wojtasiak et al., 2010). During this early stage of infection, numerous chemokines and cytokines are produced through induction of pathogen recognition receptors such as toll-like receptors (TLRs) 2, 3 and 9 (Davey et al., 2010; Rasmussen et al., 2007; Sørensen et al., 2008). These factors play an important role in attracting other immune cells to the site of infection that are able to effectively suppress local HSV-1 infection (Cheng et al., 2000; Kastrukoff et al., 2010; Shimeld et al., 1995). This suppression of virus is thought to be mediated by the interferons (IFNs), particularly IFN-α and IFN-β, produced by cells such as plasmacytoid dendritic cells, macrophages and natural killer (NK) cells (Rasmussen et al., 2007). $\gamma\delta^+$ T

cells also infiltrate the trigeminal ganglia (TG) of ocularly infected mice shortly after infection, but it is unknown if they significantly contribute to the control of HSV-1 (Kastrukoff et al., 2010; Kodukula et al., 1999; Liu et al., 1996; Sciammas et al., 1997).

IFN-α and IFN-β have potent antiviral effects, limiting the replication and spread of virus at both the site of infection and within the nervous system, demonstrated by the enhanced virulence of HSV in IFN-receptor deficient mice following corneal infection (Leib et al., 1999). The importance of IFN-α and IFN-β for controlling HSV-1 infection is further underscored by the multiple mechanisms employed by the virus to evade this IFN response (Leib et al., 2000; Lin et al., 2004; Sanchez and Mohr, 2007). In addition, IFN-γ and tumour necrosis factor α (TNF-α) have some role in controlling viral infection, such as through the mediation of leukocyte infiltration and upregulation of major histocompatibility complex class I (MHC-I), but the overall contribution of IFN-γ to controlling HSV-1 infection is controversial (Geiger et al., 1997; Ghiasi et al., 2000; Kastrukoff et al., 2010; Kodukula et al., 1999; Leib et al., 1999; Liu et al., 1996; Tang and Hendricks, 1996; Tigges et al., 1996). Various other cytokines and antimicrobial molecules have been implicated in control of HSV-1 infection, including, but not limited to, interleukin (IL)-6, nitric oxide and IL-12 (Karupiah et al., 1993; Kodukula et al., 1999; Pasieka et al., 2009; Stumpf et al., 2002).

Ultimately it is the adaptive immune response that is required to control the virus infection and for the establishment of latency. Large numbers of $CD8^+$ T cells are recruited and produced, along with the production of large amounts of IFN-γ by $CD4^+$ T cells. This is dependent on the presentation of antigen by primed dendritic cells to $CD4^+$ and $CD8^+$ T cells (Allan et al., 2003; Bedoui et al., 2009; Lee et al., 2009). Using $CD4^+$ T cell deficient mice, it has been shown that $CD4^+$ T cells are important for controlling HSV-1 in the periphery, probably via the recruitment of cells such as macrophages (Manickan and Rouse, 1995). By contrast, in the nervous system $CD8^+$ T cells play a more significant role (Nash et al., 1987; Simmons and Nash, 1985; Simmons and Tscharke, 1992; Valyi-Nagy et al., 1992).

Nonspecific $CD8^+$ T cell recruitment into inflamed and infected tissues occurs shortly after infection, but subsequent accumulation, expansion and maintenance of activated $CD8^+$ T cells is HSV-specific (Stock et al., 2011; Van Lint et al., 2005; Wakim et al., 2008a). By transferring HSV-specific effector $CD8^+$ T cells, Wakim and colleagues (2008b) found that the presence of HSV-specific effector $CD8^+$ T cells during acute infection can attenuate primary infection. These $CD8^+$ T cells do not prevent the establishment of latency within neurons but they can dampen the skin infection and limit skin to nerve transmission,

thereby reducing the average HSV genome copy number in residual latently infected neurons Further, if activated HSV-specific $CD8^+$ T cells are transferred into an immune incompetent $RAG1^{-/-}$ mouse shortly after infection, these same cells can completely clear ongoing lytic replication (Van Lint et al., 2004). Therefore, $CD8^+$ T cells may act to clear replicating virus after infection is well established, as well as limiting the spread of HSV-1 from the primary site of infection or to the CNS to reduce the viral genome copy number within latently infected neurons (Kastrukoff et al., 2010; Van Lint et al., 2004).

Infection with HSV-1 results in the production of a humoral immune response but it does not play a dominant role in controlling infection (Deshpande et al., 2000a). In an ocular model of HSV-1 infection, B-cell deficient mice were found to be more susceptible to herpes-induced encephalitis and keratitis, with increased viral persistence in the eye. However, these mice are also deficient in T cell mediated immune responses, and it is likely that B cells primarily function as regulators of the T cell response in the context of HSV-1 infection by presenting antigen or producing cytokines (Deshpande et al., 2000b). It has also been shown that antibodies against HSV can mediate prophylactic protection in mice, but this is dependent on high concentrations of antibody or sera that far exceed normal physiological levels following HSV-1 infection of mice. For example, it has also been shown that the administration of a monoclonal antibody can protect nude mice against subsequent HSV-1 infection (Sanna et al., 1996). In addition, the administration of subunit vaccines designed to elicit antibody responses directed against HSV-1 glycoproteins resulted in high neutralising antibody titres that were protective against subsequent lethal challenges of HSV-1 in mice (Ghiasi et al., 1994). So, the induction of a strong humoral immune may be able to mediate protection from HSV-1 infection in a vaccine context, but the humoral immune response does not appear to significantly influence the course of a natural HSV-1 infection.

1.2 The cascade of HSV-1 lytic gene expression

In the majority of cell types, including epithelial cells, HSV-1 is a cytolytic virus (Roizman, 2011; Syrjänen et al., 1996). HSV-1 lytic infection is characterised by the expression of an ordered cascade of genes. With the exception of a small family of RNAs known as the latency associated transcripts, or LATs, all HSV-1 genes are classified into one of three main temporal classes: immediate early (also referred to as α), early (β; also sometimes referred to as delayed early) and late (γ; Honess and Roizman, 1974; Stevens et al., 1987). The assignment of genes to specific temporal classes is usually performed based on their

expression in cells *in vitro*, such as fibroblasts, although there may be subtle distinctions in patterns of expression *in vivo*, particularly in neuronal cells (Harkness et al., 2014; Honess and Roizman, 1974; Stingley et al., 2000). All three classes of genes are subject to temporal regulation and recognition by various transcription factors. These transcription factors can bind to the different motifs, such as stimulator protein 1 (SP1) binding motifs and CAAT elements, found within the promoter region, as well as other upstream nucleotide sequences (Jones and Tjian, 1985; Lieu and Wagner, 2000; Pande et al., 1998; as reviewed by Rajčáni et al., 2004). However, all HSV-1 promoters, regardless of their class, require the presence of a TATA element (Homa et al., 1988; Pande et al., 1998; Preston et al., 1984). Despite decades of research, the precise mechanisms of this complex regulatory control are unknown and are under intensive study.

1.2.1 The viral transactivators: expression and function of the immediate early genes

The immediate early genes are the first class of genes expressed following infection of a cell, with these genes being expressed within one or two hours of infection (Harkness et al., 2014; Honess and Roizman, 1974; Stingley et al., 2000). The expression occurs without any HSV-1 protein synthesis in the newly infected cell, using the pre-existing transcription apparatus of the cell (Honess and Roizman, 1974). The expression of the immediate early genes is augmented and stimulated by the viral regulatory transcription factor virion protein (VP) 16, which forms a part of the virion tegument (Campbell et al., 1984).

There are only five IE proteins expressed by HSV-1, of which only two – ICP4 and ICP27 - are considered essential, as they are required for viral replication *in vitro* (Dixon and Schaffer, 1980; Mavromara-Nazos et al., 1986; Sacks et al., 1985; Sears et al., 1985). These genes, which have been identified based on their timing of expression and the failure of repression of expression by protein synthesis inhibitors, such as puromycin or cycloheximide, in cell culture (Honess and Roizman, 1974; Stingley et al., 2000; Summers et al., 2001), are:

1. R_L2 (also known as α0), encoding ICP0
2. R_S1 (also known as α4), encoding ICP4
3. U_S1 (also known as α22), encoding ICP22
4. U_S12 (or α47), encoding ICP47
5. U_L54, encoding ICP27

Given their responsiveness to VP16, these genes are also defined based on the presence of a 'TAATGARAT' VP16 responsiveness element (VRE) in their promoter (Mackem and Roizman, 1982). Briefly, following HSV-1 infection, VP16 binds host cell factor 1 (HCF-1),

enabling nuclear localization, where it then associated with octamer binding protein 1 (OCT-1). OCT-1 binds to the VRE, stimulating transcription of the immediate early genes(Arnosti et al., 1993; Boissière et al., 1999; Preston et al., 1988). In addition, there are other motifs within these promoters that are not as conserved across this class of genes, such as SP1 binding motifs, motifs for binding of the cAMP response element binding protein and F2 transcription factor binding motifs (Jones and Tjian, 1985; O'Rourke and O'Hare, 1993; Wheatley et al., 1992).

Four of the immediate early proteins (with the exception of ICP47) have functions that are related to the control of the HSV-1 gene expression cascade. Two proteins of these proteins, ICP4 and ICP0, are the major transactivators of viral gene expression (DeLuca and Schaffer, 1985; Dixon and Schaffer, 1980; Everett, 1984; O'Hare and Hayward, 1985; Smith et al., 1993). However, most of the proteins encoded by immediate early genes are multifunctional, and have diverse other roles, including regulation of the cell cycle, DNA repair, antiviral responses, cellular transcription, nuclear export of mRNA, and interference with splicing, amongst many others (Früh et al., 1995; Gu et al., 2005; Hardy and Sandri-Goldin, 1994; Hill et al., 1995; Lilley et al., 2011; Orlando et al., 2006a). In this way, they play an important role in creating an environment that is generally permissive for lytic infection (as reviewed by Boutell and Everett, 2013; Smith et al., 2005; Weir, 2001).

1.2.2 Expression and role of the early genes in viral DNA replication

The next class of genes expressed in the HSV-1 gene expression cascade is the early genes. These genes are expressed primarily between four and seven hours after infection (Harkness et al., 2014; Honess and Roizman, 1974). The early genes include seven proteins that are considered essential for DNA replication, namely the DNA polymerase, DNA binding proteins, origin of replication binding protein and members of the helicase/primase complex (Crute et al., 1989; Elias and Lehman, 1988; Lee and Knipe, 1985; Pande et al., 1998; Purifoy et al., 1977; Wu et al., 1988). The remaining proteins encoded by the early genes include other virus-specified enzymes involved in nucleotide metabolism and DNA repair, as well as accessory non-structural proteins (Caradonna and Cheng, 1981; Frame et al., 1985; Jamieson and Subak-Sharpe, 1974; Shao et al., 1993).

Unlike for the immediate early promoters, which are defined based on the presence of the VRE, there is less consensus amongst the required elements for promoters of the E genes. ICP4 is the major transactivator of early gene expression, along with cellular transcription factors like SP1 and CCAAT binding factor (CTF), as well as the Transcription factor II D/TATA Binding Protein (TRIID/TBP) transcription complex (Carrozza and DeLuca, 1996;

Imbalzano et al., 1991). ICP0 also serves to activate transcription of the early genes (Cai and Schaffer, 1992; Chen and Silverstein, 1992; Desai et al., 1993). Of the early genes, the U_L23 (encoding thymidine kinase (TK)), U_L37 and the U_L50 (encoding dUTPase) promoters are the most well studied (Imbalzano et al., 1991; McKnight, 1982; Pande et al., 1998).

1.2.3 Expression and function of the late genes as structural proteins and in immune evasion

The final class of genes in the HSV-1 gene expression cascade is the late genes. These genes are predominantly transcribed after viral DNA synthesis commences, at least four hours after infection, with most expression occurring between six and twelve hours post infection (p.i.; Harkness et al., 2014; Stingley et al., 2000). The late genes are classified into two subclasses, the leaky late (γ_1) and true late (γ_2). The γ_1 genes are transcribed at low levels prior to viral DNA replication, while the transcription of the γ_2 genes is absolutely dependent on prior viral DNA replication (Conley et al., 1981; Holland et al., 1980; Johnson et al., 1986).

Late gene promoters require the presence of a TATA element, and an initiator (INR) element at the cap site, which serves to distinguish them from the early promoters (Huang and Wagner, 1994; Sethna and Weir, 1993; Steffy and Weir, 1991). The distinction between the γ_1 and γ_2 class of genes seems to be dictated by the regulatory elements found within these promoters. Most γ_2 promoters require a downstream activator sequence (DAS) but lack *cis*-acting regulatory elements upstream of the TATA element (Homa et al., 1988; Kibler et al., 1991; Mavromara-Nazos and Roizman, 1989). By contrast, γ_1 promoters do require such elements, similar to those found in the early gene promoters, like SP1 and CAAT binding motifs (Huang et al., 1993a; Huang and Wagner, 1994; Lieu and Wagner, 2000; Sethna and Weir, 1993; Steffy and Weir, 1991). However, there is a complex interplay of factors that regulate expression of this class of genes and as for the early genes, there is less consensus in the common regulatory elements of the late genes (Lieu and Wagner, 2000).

The proper expression of the late genes, both γ_1 and γ_2, requires at least three viral proteins – ICP4, ICP27 and ICP8. ICP4 acts as a transactivator of late gene expression in a similar manner as it does for the early genes (DeLuca and Schaffer, 1985; Watson and Clements, 1980). ICP4 binds to the INR element and DAS found in the promoters of the late genes, especially the γ_2 genes (Guzowski et al., 1994; Kim et al., 2002). Similarly, ICP27 stimulates transcription and translation of the late genes (Fontaine-Rodriguez and Knipe, 2008; Jean et al., 2001). ICP8 has opposing effects on late viral gene expression,

upregulating late gene expression via an association with ICP27 and the cellular RNA polymerase holoenzyme. However, ICP8 can also downregulate expression of the γ_2 genes prior to viral DNA synthesis, possibly through the modulation of the host's chromatin by an ill-defined mechanism (Chen and Knipe, 1996; Gao and Knipe, 1991; Taylor and Knipe, 2004; Zhou and Knipe, 2002). ICP22 and ICP0 also act to upregulate expression of the late genes (Cai and Schaffer, 1992; Chen and Silverstein, 1992; Rice et al., 1995).

Functionally, the late genes can also be divided into two broad categories. The first category includes the structural proteins necessary for the architecture of new virions. More than 30 proteins form a structural part of the virion, and all are expressed with late kinetics (Wagner and Bloom, 1997). The second category concerns the various accessory proteins that are important for HSV-1 infection, many of which form a part of the virion. Examples of these proteins include the immunomodulatory protein ICP34.5, and the virion host shut-off protein, which is responsible for shutting down host protein synthesis (Kwong and Frenkel, 1987; Lubinski et al., 1998; Orvedahl et al., 2007; Suzutani et al., 2000).

1.2.4 Chromatin association with the viral genome and the impact of chromatin modifications on the regulation of lytic viral gene expression

HSV DNA is naked within the virion, and rapidly associates with histones once it enters the nucleus (Muggeridge and Fraser, 1986; Oh and Fraser, 2008; Pignatti and Cassai, 1980). It is likely that this process differs depending on cell type, with a lack of chromatin condensation on the viral genome in epithelial cells relative to in neuronal cells (Knipe and Cliffe, 2008). It was generally thought that there was a lack of chromatin condensation on lytic gene promoters, such as the ICP4 and TK promoters, during acute infection (Herrera and Triezenberg, 2004; Leinbach and Summers, 1980; Lentine and Bachenheimer, 1990; Pignatti and Cassai, 1980; Wang et al., 2005b). However, more recent research suggests that the viral genome is found in unstable nucleosome-like complexes during the lytic infection and replication (Cliffe and Knipe, 2008; Kent et al., 2004; Lacasse and Schang, 2010, 2012). The accessibility of the HSV-1 DNA in these complexes changes over the course of infection (Lacasse and Schang, 2012) but all kinetic classes of promoter become associated with histones (Kent et al., 2004). Following viral DNA replication, new genomes do not become associated with chromatin late in productive infection (Kent et al., 2004; Oh and Fraser, 2008).

Those histones coupled to lytic genes during productive infection are associated with a variety of modifications that largely resemble that of euchromatin. This includes

methylation of lysine 4 of histone H3 (metH3K4) and acetylation of lysines 9 and 14 of histone H3 (acH3K9 and acH3K14, respectively) (Herrera and Triezenberg, 2004; Kent et al., 2004). Although these modifications may stimulate lytic gene expression, the situation is complex. For example, an inhibitor of protein methylation reduced viral gene expression, but specific knockdown of H3K4 methyltransferases using small interference RNA only had a slightly reduced, or no, effect on the expression of some viral genes (Huang et al., 2006).

Several viral proteins are believed to be involved in modulating viral chromatin, such as VP16, ICP0, and ICP8 (Cliffe and Knipe, 2008; Herrera and Triezenberg, 2004; Taylor and Knipe, 2004). These proteins contribute to the lack of chromatin on HSV-1 lytic genes and active modifications on those histones that are assembled on viral DNA, but the details of possible mechanisms remain to be elucidated. For example, VP16 can recruit the chromatin remodeling complexes to viral immediate early promoters, and in the absence of VP16 there are increased levels of H3 on these promoters, as well as decreased amounts of acetylated histones on early gene promoters (Herrera and Triezenberg, 2004; Kutluay and Triezenberg, 2009). Likewise, deletion of ICP0 leads to decreased association of histone 3 with the promoters of the genes encoding ICP4 and ICP8 (Cliffe and Knipe, 2008). This association may be mediated through proteasomal degradation by ICP0 of proteins like Sp100. Sp100 interacts with the heterochromatin binding protein HP1, as well as other proteins involved in the assembly of heterochromatin such as centromere protein (CENP)-A and CENP-C (Chelbi-Alix and de The, 1999; Everett et al., 1999; Lomonte et al., 2001). Further, ICP0 can bind the RE1-silencing transcription factor (REST)/lysine specific demethylase 1 (LSD1)/corepressor element-1 silencing transcription factor (CoREST)/histone deacetylase (HDAC) 1/2 complex, causing the dissociation of HDAC1/2, blocking gene silencing, as well as binding to class II HDACs, reducing their activity (Giordani et al., 2008; Gu et al., 2005; Gu and Roizman, 2007; Lomonte et al., 2004).

1.3 HSV-1 Latency

Definitions of HSV-1 latency vary, but most commonly latency is defined as the presence of the HSV-1 genome in the host's neurons without the production of infectious viral particles. This definition does not preclude viral gene expression, though typically only the LATs can be abundantly detected during latency (Decman et al., 2005a; Steiner and Kennedy, 1995; Stevens and Cook, 1971; Stevens et al., 1987; Wagner and Bloom, 1997). Three stages of latency are recognised, which represent a biological continuum:

establishment, maintenance and reactivation. The suppression, or lack thereof, of viral gene expression is pivotal in all three stages of latency.

Nearly three decades ago, it was hypothesised that the establishment of a lytic or latent HSV-1 infection represents mutually exclusive pathways that diverge early after infection (Kosz-Vnenchak et al., 1993; Margolis et al., 1992; Valyi-Nagy et al., 1991). This hypothesis was based on tissue culture studies that found that the synthesis of immediate early proteins is essential for virus replication and productive lytic infection. Mutants lacking these proteins are not cytotoxic, but are retained in a quiescent state in the cell (Ace et al., 1989; Everett, 1989; Preston and Nicholl, 1997). Further, latency can be established in neurons that did not innervate the area of initial infection and show no evidence of prior immediate early gene expression (Simmons et al., 1992). At some point this state may be disturbed, allowing for reactivation. Unfortunately, such a simplistic view does not explain all facets of latent infection. For example, some neurons survive the expression of genes associated with lytic infection and go on to form part of the latent pool (Proença et al., 2008; Proença et al., 2011; Simmons and Tscharke, 1992). Further, there are numerous biological mechanisms, deriving from the virus and host, which suppress expression from the viral genome and maintain latency, which will be discussed below.

1.3.1 The HSV-1 genome and the impact of viral DNA replication during the acute infection on the establishment of latency

During latency, viral DNA replication does not occur and the viral genome is maintained within the cell as a circular episome (Efstathiou et al., 1986; Rock and Fraser, 1983; Rock and Fraser, 1985). This episome is associated with chromatin and under extensive epigenetic control via histone modifications (Section 1.3.4; as reviewed by Knipe and Cliffe, 2008).

Viral DNA replication is a core feature of the HSV-1 infection and so, at the level of the whole host, precedes the establishment of latency. However, DNA replication is not essential for the establishment of latency, both at the level of the host and within individual cells. Viruses that lack proteins required for viral DNA replication at both the peripheral site of infection, such ICP4, and within the ganglia, such as the viral TK, are able to establish latency (Coen et al., 1989; Dobson et al., 1990; Katz et al., 1990; Sedarati et al., 1993; Steiner et al., 1990; Valyi-Nagy et al., 1991). Further, latency can be established even when viral replication is blocked by acyclovir and cytosine arabinoside treatment (Margolis et al., 1992).

Viral DNA replication is not required for the establishment of latency per se but viral replication in the skin increases the number of virus genomes that can gain access to neurons, and influences the size of the latent HSV-1 reservoir (Ellison et al., 2000; Steiner et al., 1990; Thompson and Sawtell, 2000; Wakim et al., 2008b). Further, based on the expression of LAT and DNA levels in different thoracic segments following flank zosteriform HSV-1 model, it was found that the bulk of DNA detected in latently infected neurons is likely due to replication during the acute infection (Slobedman et al., 1994). While this may be the result of transport of viral genomes from peripheral sites, it may also reflect viral DNA replication in some, but not all, neurons (Simmons et al., 1992). While latently infected neurons must contain at least one copy of the viral genome, contextual analysis (CXA), in which individual neurons are separated and analysed by PCR, has revealed that the viral genome copy number varies between one and 100 copies per infected neuron (Sawtell, 1997). Therefore, there is considerable heterogeneity in the viral DNA content of latently infected cells in both mice and humans, with rare latently-infected neurons harboring thousands of copies of the HSV-1 genome (Chen et al., 2002b; Hill et al., 1996a; Ma et al., 2014; Sawtell, 1997; Wang et al., 2005a). This is likely to be of practical consequence for the progression of the viral infection. Those neurons infected with strains of HSV-1 characterised by higher latent genome copy numbers are more predisposed towards reactivation (Sawtell et al., 1998). Mice infected with different HSV-1 strains differed in their ability to reactivate following transient hyperthermia *in vivo*, which correlated with viral genome copy number distribution, but not the number of neurons harboring latent virus. This suggested that neurons containing large amounts of HSV DNA may be more susceptible to reactivation (Sawtell et al., 1998). Similarly, the rates of reactivation as measured by the detection of cell free virus released from ganglion cells after culture from mice latently infected with HSV-2 were associated with the latent viral load (refer to Section 1.3.7; Hoshino et al., 2007).

1.3.2 The Latency Associated Transcripts

1.3.2.1 Description of the LATs and their expression during latency

The LATs are the only viral transcripts abundantly transcribed during latency and have been the focus of a hefty amount of research. They comprise a series of colinear, predominantly nuclear transcripts. The minor LAT is transcribed antisense to the gene encoding ICP0 and extends to a polyadenylation signal in the short repeat region, making it 8.3 kb long (Zwaagstra et al., 1990). The major LAT is a highly abundant non-polyadenylated species of 2.0 kb and is derived by a splicing event from the less abundant minor LAT. Further splicing of the 2.0 kb major LAT RNA occurs within neurons to

produce the 1.5 kb LAT, which accumulates as a stable lariat and is thought to be important for the establishment of latency (Farrell et al., 1991; Rock et al., 1987; Spivack and Fraser, 1987; Wagner et al., 1988b; Zabolotny et al., 1997). While the LATs can bind to polyribosomes, this probably reflects a structural or regulatory role for the LATs in the ribosomal complex as the major LAT lacks polyadenylation (Ahmed and Fraser, 2001; Goldenberg et al., 1997; Wagner et al., 1988a). The overwhelming consensus is that the LATs do not encode a functional protein, despite some reports to the contrary (Doerig et al., 1991; Drolet et al., 1998; Henderson et al., 2009; Jaber et al., 2009; Lagunoff and Roizman, 1994; Naito et al., 2005; Thomas et al., 1999). One complicating factor in determining the exact role of the LATs during latency is the presence of other ORFs that overlap the LAT region, making the construction of deletion mutants problematic. Proteins that are coded for in the same region as the LATs include ICP34.5, ICP4, and ICP0, as well as other less studied ORFs (Bolovan et al., 1994; Jaber et al., 2009; Lagunoff and Roizman, 1994; Perng et al., 1996a; Perng et al., 1995; Wagner et al., 1988a).

The LATs are first detectable in ganglia during the lytic phase of HSV-1 infection, typically by about 48 to 72 hours p.i. in ocularly infected mice (Kramer et al., 1998). However, much higher transcript levels are detected in ganglia during latency (Margolis et al., 1992). The LATs have been detected in latently infected humans, as well as experimentally infected animal models including the guinea pig, rabbit and mouse (Deatly et al., 1987; Krause et al., 1988; Lyn Burke et al., 1991; Rock et al., 1987; Spivack and Fraser, 1987; Stevens et al., 1988; Stevens et al., 1987; Wang et al., 2005a).

1.3.2.2 The importance of the LATs and their role in the establishment and reactivation from latency

Despite decades of intensive research on the role of the LATs, they are not a critical part of the HSV-1 cycle of latency and reactivation, as the region of the genome encoding the LATs is not absolutely required for either the establishment, maintenance of or reactivation from latency (Fareed and Spivack, 1994; Hill et al., 1990; Izumi et al., 1989; Javier et al., 1988; Leib et al., 1989; Perng et al., 1994; Sedarati et al., 1989; Steiner et al., 1989). Early studies using techniques such as laser capture microdissection (LCM) followed by quantitative reverse-transcriptase PCR (qRT-PCR), *in situ* PCR and direct analyses of individual neurons by CXA found that LATs are transcribed in a fraction of neurons harbouring latent HSV-1 genomes ranging from about five to 30% of latently infected cells (Chen et al., 2002b; Ellison et al., 2000; Maggioncalda et al., 1996; Mehta et al., 1995; Sawtell, 1997; Wang et al., 2005a). However, this has been confounded by the limited sensitivity of these detection methods, the small population of infected neurons, and the

variable expression of the LATs. The variable expression of the LATs proved difficult to account for, as the use of the HSV-2 guinea pig reactivation model revealed that the frequency of spontaneous reactivation is not correlated with the level of LAT production (Bourne et al., 1994). Most recently it has been found that LATs are probably expressed in all latently infected neurons at some point during latency, but the consequences of this transient expression are unknown (Ma et al., 2014; Proença et al., 2008).

Determining the role of the LATs has been problematic, as it is difficult to dissect out the impact of expression during the lytic stage of infection and establishment of latency from the maintenance of and reactivation from latency. A further layer of complexity is added by the different animal models of HSV-1, particularly differences in the rabbit and mouse models of HSV-1 (Perng et al., 2001; as reviewed by Wagner and Bloom, 1997).

The majority of studies using mouse models of HSV-1 infection where the expression of LAT is abrogated conclude these viruses reactivate much less efficiently following explant reactivation or other methods of *in vivo* reactivation (Devi-Rao et al., 1994; Leib et al., 1989; Sawtell and Thompson, 1992a; Steiner et al., 1989). However, reactivation by viruses that fail to express LAT is influenced by the route of infection, the strain of HSV-1 used or the site of latency establishment (Izumi et al., 1989; Nicoll et al., 2012; Perng et al., 2001). A LAT null virus was deficient for reactivation when latency was established in the in the TG but not in the lumbosacral ganglia (Sawtell and Thompson, 1992a). Similarly, a mutant virus lacking the TATA box and promoter function of LAT on the strain 17*syn*+ background was deficient for explant reactivation, but a comparable virus constructed on the less virulent KOS background was not (Devi-Rao et al., 1994; Thompson et al., 1986). In the ocular rabbit model of HSV-1 infection, viruses that lack expression of the LATs establish latency to similar levels but show a reduced frequency of spontaneous reactivation. They also fail to reactivate as efficiently following induced reactivation, in either the iontophoresis-epinephrine or other models of reactivation (Bloom et al., 1994; Hill et al., 1996b; Hill et al., 1990; Perng et al., 1994; Trousdale et al., 1991). Only the first 1.5 kb of the 8.3 kb minor LAT is required for a normal reactivation phenotype (Bloom et al., 1996; Perng et al., 1996b). A smaller 348 bp deletion was shown to be associated with a decrease in spontaneous reactivation frequency (Bloom et al., 1996). However, a similar, though not entirely overlapping, 371 bp deletion in LAT constructed using the McKrae strain had no impact on reactivation in the rabbit ocular model, when the same mutant was constructed using strain 17*syn*+, both spontaneous and induced reactivation were reduced relative to wildtype virus (Hill et al., 1996b; Loutsch et al., 1999; Perng et al., 1996c). Further, this same region is not crucial for the recovery of virus by explant induced reactivation of latently infected mice (Bloom et al., 1996; Maggioncalda et al.,

1994). Given the lack of consistency of the behaviour of LAT mutant viruses in mouse and rabbit models, it is unclear whether any of these findings would be relevant when considering human infection.

The observed reactivation phenotype is based on the assumption that latency is established at equivalent levels in the absence of LAT expression. Most studies show no difference in viral replication during the acute infection or the maintenance of latency, as manifest by the stability of the viral genome over time. Unfortunately, this was often measured by relatively insensitive methods like slot blot hybridisation on whole ganglia (Bloom et al., 1994; Hill et al., 1990). Thompson and Sawtell (1997) found a 75% reduction in the number of cells in which latency is established in mice infected with a mutant lacking either the basal LAT promoter or 5' end of the LAT gene relative to wildtype virus as indicated by the presence of viral DNA detected by CXA. Mice infected with this LAT mutant were impaired for reactivation following hyperthermia. Results from other murine and rabbit models have confirmed that LAT expression seems to dictate the number of neurons in which latency is established, with mutant viruses with reduced LAT expression exhibited a reduce ability to reactive (Devi-Rao et al., 1994; Maggioncalda et al., 1996; Perng et al., 2000a; Sawtell and Thompson, 1992a). However, altering the inoculum dose of the poorly reactivating LAT deletion virus 17ΔPst in rabbit showed that the poor reactivation phenotype cannot be solely accounted for by a failure to establish wildtype levels of latency as evidenced by low viral genome copy number (O'Neil et al., 2004).

It is generally accepted that the abrogation of LAT expression has little impact on the maintenance of latency. However, given the broad viral genome copy number distribution across latently infected cells, qPCR will only reveal substantial differences in the size of the latent reservoir. By using a virus that fails to express LAT due to a deletion in the promoter region in a model that allows for historical marking of all neurons latently infected with HSV-1, it was revealed that the latent reservoir was more unstable in the absence of LAT expression. This was coupled with a slight decrease in the efficiency of latency establishment (Nicoll et al., 2012). Therefore, the LATs may still have an influence on the maintenance of latency.

1.3.2.3 Inhibition of lytic viral gene transcription by the LATs

Since the discovery of the LATs, it has been posited that they serve to inhibit lytic viral gene expression, enhancing the stability of latency (Sawtell and Thompson, 1992a). This was first demonstrated by performing *in situ* hybridisation (ISH) on TG taken from acutely infected mice to show that there is an earlier increase of ICP4, VP16 and glycoprotein H transcripts in the absence of LAT (Garber et al., 1997). Similarly, the detection of rare lytic

transcripts during latency showed that ICP0 transcripts were differentially expressed compared to LAT (Maillet et al., 2006). Further, cultured neuroblastoma cells transformed to express the 2 kb LAT had reduced permissiveness to HSV-1 infection and a reduction in the levels of all immediate early mRNAs, including ICP0 (Farrell et al., 1991; Mador et al., 1998). Further, Chen and colleagues found greater accumulation of ICP4 and TK transcripts during latency following infection with a LAT null virus compared to wildtype virus, suggesting a potential role for LAT in silencing viral gene expression (Chen et al., 1997). By contrast, an opposing phenotype was observed in rabbits ocularly infected with the LAT deletion virus, 17ΔPst, with a significant decrease in accumulation of ICP4, TK or glycoprotein C (gC) transcripts during latency compared to wildtype virus (Giordani et al., 2008). However, despite the palpable differences in the rabbit and mouse models of HSV-1 latency, LAT clearly plays a role in modulating lytic viral gene expression during latency. This was originally thought to be mediated by antisense inhibition of ICP0 or ICP4 by LAT, leading to increased virus shutdown and establishment of latency (Rock et al., 1987; Stevens et al., 1987). However, this is not the case (Burton et al., 2003a; Chen et al., 2002a; Shen et al., 2009; Steiner et al., 1989). This is reinforced by the observation that sequences that are responsible for the spontaneous reactivation of HSV-1 McKrae in the rabbit ocular model do not overlap ICP0 (Perng et al., 1996b). Further, adding the first 1.5 kb of the primary LAT transcript into the dLAT2903 virus at an ectopic locus was able to restore the reactivation phenotype to this virus, despite the absence of expression of the remainder of LAT (Drolet et al., 1999; Perng et al., 1996b).

As an alternative means of regulating viral gene expression, LAT serves as a microRNA (miRNA) precursor (described in greater detail in Section 1.3.3; Umbach et al., 2008). Additionally, two small RNAs that are 62 and 36 nucleotides long have also been identified that are expressed in mice, named LAT sRNA1 and LAT sRNA2 respectively (Peng et al., 2008; Shen et al., 2009). Following cotransfection of sRNA1 or sRNA2 with HSV-1 genomic DNA into Neuro2A cells, they can inhibit cold shock induced apoptosis and the production of infectious virus. They may do this inducing IFN-β promoter activity in the presence of the receptor retinoic acid-inducible gene 1, but they also act by inducing herpes virus entry mediator expression in latently infected mice (Allen et al., 2014; da Silva and Jones, 2013; Peng et al., 2008; Shen et al., 2009).

1.3.2.4 Promotion of cell survival by the anti-apoptotic activity of LAT

LAT has an anti-apoptotic activity that results in increased neuronal survival, increasing the establishment of latency (Perng et al., 2000b; Thompson and Sawtell, 2001). Initial experiments with LAT deletion viruses resulted in increased apoptosis in infected mice

and rabbits during acute infection (Perng et al., 2000b). Subsequent analysis revealed that the region associated with this anti-apoptotic activity *in vivo* mapped to the first 1.5 kb following the LAT promoter, at the 3' end of exon 1 and 5' end of the stable 2kb intron (Ahmed et al., 2002; Branco and Fraser, 2005; Inman et al., 2001; Perng et al., 2000b). Similarly, insertion of other inhibitors of apoptosis into such LAT null viruses is able to restore the ability of these viruses to reactivate in both rabbits and mice, although this was not measured in a highly quantitative way (Jin et al., 2008; Jin et al., 2005; Perng et al., 2002).

Further work, predominantly based on *in vitro* transfection assays with the 2 kb LAT intron, revealed that LAT can block the extrinsic (caspase 8-dependent) apoptosis pathway, as well as less efficiently blocking the intrinsic (caspase 9-dependent) apoptosis pathway, protecting cells from death (Ahmed et al., 2002; Carpenter et al., 2007; Jin et al., 2003; Peng et al., 2004). It has also been shown that the 2 kb LAT can protect neuronal Neuro2A and C1300 cells against granzyme B (gzmB)-mediated caspase3-induced apoptosis and protect against $CD8^+$ T cell killing *in vitro* (Jiang et al., 2011). Using LAT deletion viruses in Neuro2A cells, it was revealed that LATs can prevent apoptosis by inducing preferential accumulation of the anti-apoptotic Bcl-X_L over the pro-apoptotic Bcl-X_S transcripts(Peng et al., 2003). However, the exact mechanism by which LAT mediates protection against apoptosis remains to be fully elucidated.

1.3.3 Role of miRNAs in the regulation of the establishment and maintenance of latency

Briefly, miRNAs are approximately 22 nucleotide RNAs derived from longer primary transcripts that specifically recognize target mRNAs and inhibit their translation or promote their degradation (as reviewed by Bartel, 2009). Given the relatively small coding capacity of viral genomes, miRNAs represented an attractive means for regulating viral gene expression, particularly during latency. Recently, it was determined by deep-sequencing approaches of animal and cell culture based models of HSV-1 infection, as well as latently infected human samples, that HSV-1 encodes a set of 17 miRNAs (Held et al., 2011; Jurak et al., 2014; Umbach et al., 2008; Umbach et al., 2009). Up to 27 miRNAs have been identified based on bioinformatics-based approaches (Cui et al., 2006; Jurak et al., 2010; Munson and Burch, 2012; Pfeffer et al., 2005). Host miRNAs can also play a role in regulating HSV-1 infection. For example, the host miRNA miR-23a binds to the Interferon Regulatory Factor 1 (IRF1), downregulating signaling through the IRF1-mediated innate antiviral signaling pathway and augmenting viral replication (Ru et al., 2014).

Many of these HSV-1 miRNAs accumulate during lytic infection, with at least one miRNA (miR-H1) being expressed only during this time (Cui et al., 2006; Jurak et al., 2010; Munson and Burch, 2012; Umbach et al., 2009). While dispersed across the genome, there is a concentration of miRNAs encoded within the regions around the origin of replication (Jurak et al., 2010). Most of the virally derived miRNAs are persistently expressed throughout latency, with the majority derived from the LAT precursor or encoded in the LAT region (Jurak et al., 2010; Umbach et al., 2008; Umbach et al., 2009). These miRNAs are not essential but they may have some role in regulating the establishment and maintenance of latency in mice, as shown using LAT deletion viruses (Kramer et al., 2011). For example, miR-H2 is found within the LAT region and is antisense to ICP0, and knocking out miR-H2 leads to increased accumulation of ICP0 protein. This virus reactivates slightly faster following explant cultivation, but there was no effect on the establishment of latency as determined by viral DNA load in the TG (Jurak et al., 2014; Umbach et al., 2008). Downregulating this miRNA in transient assays did not have any effect on other immediate early HSV-1 genes (Umbach et al., 2009). Similarly, miR-H6 has been shown to downregulate ICP4 expression, and given its role in stimulating its expression of the viral lytic genes, it has been hypothesised that it may be involved in the maintenance of latency (Umbach et al., 2008).

So far, determining the biological role of most miRNAs during HSV-1 infection has been difficult (Du et al., 2015). An investigation into which of the miRNAs were loaded onto the RNA-induced silencing complex (RISC), and therefore are likely to be biologically relevant, revealed that only a fraction of some of the most abundant viral-encoded miRNAs, such as miR-H1-5p and miR-H6-3p, are associated with RISC. Additionally, some miRNAs were not bound to the RISC at all, and are not likely to be functionally relevant (Du et al., 2015; Flores et al., 2013). Further, while some miRNAs are transcribed on the opposite strand to known viral RNAs that serve as their target, for most miRNAs the target, likely of host cell origin, remains unidentified (Du et al., 2015; Jiang et al., 2015; Jurak et al., 2010; Munson and Burch, 2012). Finally, there are substantial differences in the accumulation of RNAs in animal-based versus cell culture models of HSV-1 latency, making dissection of the role of miRNAs in regulating HSV-1 latency a challenging task (Du et al., 2015; Jurak et al., 2014).

1.3.4 Chromatin control of latency and reactivation

In contrast to lytic infection (refer to Section 1.2.4), the viral genome is stably associated with repressive heterochromatin during latency that is believed to maintain repression of viral gene expression (Deshmane and Fraser, 1989). Using chromatin immunoprecipiation (ChIP) assays, it has been shown that methylation of lysine 9 of histone 3 (metH3K9) and

metH3K4 of the ICP4 and TK promoters occurs during the establishment of latency, and was consistently maintained throughout latency. The modifications metH3K9 and metH3K4 are associated with heterochromatin and euchromatin, respectively. Since there was consistently more metH3K9 than metH3K4, the net result is likely repression of lytic viral gene expression and maintenance of latency (Wang et al., 2005b). Viral lytic gene promoters have also been shown to be associated with methylation of lysine 27 of histone 3 (metH3K27) and macroH2A, markers of facultative heterochromatin. Both facultative and constitutive heterochromatin is thought to be widespread on the viral genome (Cliffe et al., 2009; Kwiatkowski et al., 2009). It should also be noted that methylation of viral DNA probably does not play a role in repressing viral gene expression during latency (Dressler et al., 1987; Kubat et al., 2004b).

ChIP assays have also been used to show that the LAT promoter is enriched with the acetylated histone H3 (K9, K14) during latency, consistent with transcriptionally permissive chromatin (Kubat et al., 2004a; Kubat et al., 2004b). This was confirmed in the rabbit ocular HSV-1 infection model of latency, with the LAT region being more transcriptionally permissive than either of the lytic genes ICP27 and ICP0 (Giordani et al., 2008). A similar study found that there was enrichment during latency of euchromatic markers on the LAT 5' exon region relative to ICP0 and ICP4 promoters, but a significant increase in these markers on the ICP4 promoter region (Creech and Neumann, 2010). Overall, it seems likely that LAT exists in a bivalent chromatin state, with a balance of euchromatic and heterochromatic marks (Cliffe et al., 2009; Kwiatkowski et al., 2009). The boundary between the generally permissive chromatin environment around the LAT region relative to the repressive environment of the rest of the genome is maintained by chromatin insulator elements and silencing by nearby chromatin domains during latency. These candidate insulator elements have CCCTC sites that are bound by the CCCTC-binding factor (CTCF) during latency *in vivo* (Amelio et al., 2006b).

LAT itself has been implicated in maintaining a generally repressive chromatinised genome, with mutants that fail to express LAT exhibiting enrichment of modifications such as metH3K4 on lytic viral promoters (Cliffe et al., 2009; Wang et al., 2005b). Likewise, there was a decrease in enrichment of modifications such as dimethylation of metH3K9 (Wang et al., 2005b). However, this situation is not straightforward, as in the absence of LAT, one study found an enrichment of metH3K27 on the viral genome, which is associated with facultative heterochromatin, while another study found a decrease in metH3K27. This was attributed by the authors of both studies to the differences in the strain of HSV-1 used as well as the site in which latency was established (Cliffe et al., 2009; Kwiatkowski et al., 2009). Also, in the rabbit ocular HSV-1 latency model, the LAT

enhancer region and ICP0 region appeared less transcriptionally permissive in the absence of LAT (Giordani et al., 2008).

As would be expected, a role for chromatin modifications in reactivation from latency has also been found. Following explant induced reactivation of mice, there was a decrease in H3 (K9, K14) acetylation of the LAT enhancer and subsequent decrease in RNA abundance. This is followed by an acetylation of the ICP0 promoter (Amelio et al., 2006a). Likewise, using rabbits ocularly infected with the efficiently reactivation McKrae strain of HSV-1, but not the poorly reactivation KOS strain of HSV-1, chromatin remodeling was shown to be an early and essential step in the process of HSV-1 reactivation by transcorneal iontophoresis of epinephrine. There was decreased enrichment following reactivation of euchromatic markers on the LAT 5' exon region, which could be correlated with a decrease in LAT transcripts. However, there was any increase in metH3K4 modifications on the ICP4, but not ICP0, promoter (Creech and Neumann, 2010).

It has been shown that treatment of latently infected rat dorsal root ganglion (DRG) cultures with trichostatin A, a HDAC inhibitor, resulted in activation of previously silenced lytic gene promoters (Arthur et al., 2001). Similarly, treatment of mice with the HDAC inhibitor sodium butyrate led to reactivation of virus and a rapid decrease in H3 (K9, K14) acetylation of the LAT enhancer. This was correlated with an increase in H3 (K9, K14) acetylation of the ICP0 and ICP4 promoters (Neumann et al., 2007a; Neumann et al., 2007b). It also causes a disruption of the CTCF binding to the CCCTC sites, which act to maintain a boundary between the transcriptionally repressive and permissive areas of the genome (Ertel et al., 2012). Similarly, the inhibition of demethylases that remove repressive marks on the HSV-1 genome reduced levels of induced reactivation in infected TG neuronal cultures by the withdrawal of nerve growth factor (NGF), although no one demethylase is able to completely block reactivation (Messer et al., 2015).

1.3.5 The detection of rare lytic viral gene expression during latency

As described previously, the classical definition of latency often precludes lytic viral gene expression during latency, encompassing both the detection of transcripts and protein. In fact, most, but not all, early reports failed to detect the presence of lytic viral transcripts or proteins during latency (Croen et al., 1988; Deatly et al., 1987; Devi-Rao et al., 1994; Green et al., 1981; Krause et al., 1988; Mitchell et al., 1994; Puga and Notkins, 1987; Speck and Simmons, 1991; Spivack and Fraser, 1987; Steiner et al., 1988; Stevens et al., 1987).

Using more sensitive methods of detecting viral gene expression, including ISH and RT-PCR, transcripts from all classes of lytic genes, namely ICP0, ICP4, gC and TK transcripts,

can be detected in murine TG during latency (Chen et al., 2002a; Chen et al., 1997; Feldman et al., 2002; Kramer and Coen, 1995; Kramer et al., 1998; Ma et al., 2014; Maillet et al., 2006; Pesola et al., 2005; Tal-Singer et al., 1997). The expression of lytic genes during latency is was thought to be associated with a high level of expression of these transcripts in a small fraction of latently infected neurons (Feldman et al., 2002). ICP0 and ICP4, but not glycoprotein B (gB), transcripts have also been detected in latently infected human ganglia (Derfuss et al., 2009; Derfuss et al., 2007). In rare cells, there is also evidence for virus replication or protein expression (Feldman et al., 2002; Green et al., 1981; Margolis et al., 2007a; Sawtell, 2003). Further, recently it has been shown by single cell qRT-PCR-based analysis that transcripts associated with viral lytic genes can be detected in nearly two thirds of all latently infected neurons. More than half of these neurons contain transcripts from more than one HSV-1 kinetic class of lytic gene expression (Ma et al., 2014). Debate still surrounds the consequence of the detection of these transcripts. Namely, do they represent low level transcription of the viral genome, in opposition to the apparent global repression of the viral genome? Alternatively, do they represent aborted reactivation attempts?

1.3.6 Initiation of viral gene expression following reactivation

There are numerous stimuli that lead to reactivation, broadly categorised as stress, which initiate different signaling and gene expression cascades. Reactivation can be initiated following many global stimuli, including, but not limited to, transient hyperthermia, UV light, psychosocial stress, and immune suppression (Djuric et al., 2009; Laycock et al., 1991; Padgett et al., 1998; Sawtell and Thompson, 1992b; Schubert et al., 1990). More specific reactivation stimuli, typically used in conjunction with *in vitro* models of HSV-1 latency, include NGF withdrawal, HDAC inhibitors like trichostatin A and sodium butyrate, forskolin, capsaicin, inducible cAMP early repressor, protein kinase C activation by phorbol myristate acetate, activation of caspase 3 by C2-ceramide, and dexamethasone (Arthur et al., 2001; Camarena et al., 2010; Colgin et al., 2001; Du et al., 2011; Halford et al., 1996b; Hunsperger and Wilcox, 2003a; Hunsperger and Wilcox, 2003b; Neumann et al., 2007b; Smith et al., 1992). The application of these stimuli leads to the expression of viral genes, ultimately leading to an increase in viral genome copy number and, in some cases, the production of infectious virus. Although the characterisation of the subsequent viral gene expression is still largely incomplete, it is broadly organised into two different paradigms.

In the first paradigm, specific viral proteins must be expressed to initiate the HSV-1 gene expression cascade after a reactivation stimulus. The best candidate viral protein is ICP0, a

promiscuous transactivator and the only viral protein known to initiate the production of infectious virus from quiescently infected cultures (Coleman et al., 2008). It has also long been appreciated that mutants that don't express ICP0 fail to reactivate efficiently, although they can initiate the production of lytic proteins (Cai et al., 1993; Thompson and Sawtell, 2006). However, Thompson and Sawtell (2006) showed that if a similar latent load is established in mice by a virus lacking ICP0, then a similar number of antigen positive cells were detected following hyperthermia induced reactivation, suggesting that the primary trigger for reactivation was not ICP0. Other candidates include VP16 and ICP4, whose provision by way of adenoviral vectors is sufficient to reactivate latent HSV-1 primary TG cultures (Halford et al., 2001). This is still a subject of some debate, as viruses which lack these proteins can produce infectious virus akin to wildtype virus following explant-induced reactivation (Steiner et al., 1990). Of particular interest is VP16, due not only to its role as a powerful transactivator, but also to its ability to initiate large scale chromatin remodelling (Arnosti et al., 1993; Herrera and Triezenberg, 2004; Kutluay and Triezenberg, 2009). Shortly after hyperthermic stress-induced reactivation in latently infected mice, VP16 expression can be detected, even in the absence of ICP0 and ICP4 expression, or viral DNA synthesis (Thompson et al., 2009). It is difficult to reconcile the global changes induced by these reactivation stresses that lead to reactivation from only a relatively small population of latently infected neurons.

Alternatively, in the second paradigm, viral gene expression is biphasic following a reactivation stimulus (Kim et al., 2012). Initial viral gene expression is disordered, with HSV-1 lytic genes of all expression classes expressed in the absence of prior protein synthesis (referred to as Phase I expression). There is also decreased expression of LATs and miRNAs during this time (Du et al., 2011; Kim et al., 2012). So, reactivation is initially characterised by a sudden derepression of the whole viral genome. After this time, the expression of viral proteins, such as ICP0, ICP4 and VP16, assists gene expression such that the traditional cascade of viral gene expression is established (referred to as Phase II expression). This is facilitated by VP16 translocating to the nucleus, where VP16 can exert its transactivating functions along with its cellular cofactors HCF-1 and Oct-1 (Kim et al., 2012). The end result is the replication of the viral genome and production of infectious virus.

1.3.7 Role of the host's immune response in the maintenance of latency and prevention of reactivation

The complexity of the intimate relationship between HSV-1 and its host is exemplified by the adaptive immune response to the latent virus. This is most obviously manifested as the

high frequency of reactivation of HSV-1 that results from immunosuppression as a result of cancer treatment or following transplantation (Djuric et al., 2009; Schubert et al., 1990). The interaction between the virus and the immune system is dominated by the $CD8^+$ T cell response.

As described in Section 1.1.4, $CD8^+$ T cells infiltrate the ganglia of mice from five days p.i. where they are retained following the establishment of latency, although some have reported that this infiltrate is cleared over time (Gebhardt and Hill, 1988; Khanna et al., 2003; Liu et al., 1996; Shimeld et al., 1995; Van Lint et al., 2005). Within HSV-1 infected C57Bl/6 mice, a large proportion of these cells are specific for the immunodominant epitope gB_{498}, and non-HSV specific $CD8^+$ T cells are selectively lost during latency (Khanna et al., 2003; Sheridan et al., 2009; St. Leger et al., 2011). Despite the presence of $CD8^+$ T cells, very little neuronal loss or obvious pathology is observed (Tscharke and Simmons, 1999; Verjans et al., 2007).

A newly defined memory $CD8^+$ T cell subset, named resident memory T (T_{RM}) cells, are important for controlling HSV-1 latency. Gebhardt and colleagues (2009) found this population of $CD8^+$ T_{RM} cells are resident in the skin and sensory ganglia during latent HSV-1 infection of mice and are in disequilibrium with the circulating lymphocyte pool (Mackay et al., 2012). Mackay and colleagues (2012) showed that inflammation is sufficient to draw these cells into a highly localised area of skin in the absence of antigen recognition, where they become lodged and provide protection against local challenge with virus. Further, $CD8^+$ T_{RM} cells can mount a proliferative response entirely within DRG following challenge by reactivation (Wakim et al., 2008c).

Nearly all $CD8^+$ T cells within latently infected ganglia express the early activation marker, CD69 and CD103, which functions in the survival and retention of these cells (Mackay et al., 2013). Later, the $CD8^+$ T cells have a $CD44^{hi}$ phenotype, suggesting persistent activation. They also have a slow homeostatic turnover (Gebhardt et al., 2009). These cells have the capacity to produce IFN-γ and are $gzmB^+$, indicating recent activation, with some cells show T cell receptor (TLR) polarization towards infected cells (Jiang et al., 2011; Khanna et al., 2003; Van Lint et al., 2005). By using bone marrow chimeras, it has been shown that the production of gzmB is completely dependent upon antigen presentation by parenchymal cells (Van Lint et al., 2005). IFN-α may also play a role in suppressing reactivation (De Regge et al., 2010). Inflammatory cytokines, including IFN-γ and TNF-α, and transcripts for molecules involved in chemoattraction, such as Chemokine (C-C motif) ligand 5**,** have all been detected during latency in the ganglia of HSV-1 infected mice and

humans (Cantin et al., 1995; Chen et al., 2000; Halford et al., 1996a; Halford et al., 1997; Liu et al., 1996; Shimeld et al., 1997; Stock et al., 2011; Theil et al., 2003a).

It is highly likely that these $CD8^+$ T cells are able to suppress reactivation. In *ex vivo* cultures of latently infected TG, both exogenous HSV-1 specific $CD8^+$ T cells, or alternatively a gB_{498} specific $CD8^+$ T cell clone, were able to suppress viral replication and cytopathic effect (CPE) in an MHC restricted manner (Khanna et al., 2003; Liu et al., 2000). However, viral genomes and some immediate early and early gene transcripts were still detectable in these cultures (Liu et al., 2000). The suppression of viral activity may be mediated in part by the IFN-γ that is produced by these cultures and augments the $CD8^+$ T cell response (Liu et al., 2001). The addition of IFN-γ to *ex vivo* cultures of latently infected TG neurons reduced the frequency of reactivation by at least 50% and reduced the amount of CPE (Carr et al., 2009; Decman et al., 2005b; Liu et al., 2000). The addition of IFN-γ to these cultures was also associated with a reduction in the expression of ICP0 and gC (Decman et al., 2005b). Finally, using IFN-γ or IFN-γ receptor knockout mice in which normal levels of latency are established in the TG, reactivation following hyperthermic stress is enhanced, further implicating IFN-γ in the suppression of reactivation (Cantin et al., 1999).

There is some evidence that gzmB is an important mediator of HSV-1 latency. Firstly, gzmB has been shown to mediate cleavage of ICP4 (Knickelbein et al., 2008). Using mouse neuroblastoma lines infected with HSV, treatment with gzmB decreased cleavage of caspase3 and increased neuronal survival rates. This did not hold in cell lines in which LAT was deleted, linking LAT with protection from gzmB -induced apoptosis (Jiang et al., 2011). Secondly, latency is unstable in HSV-1 infected-perforin and gzmB deficient mice (Knickelbein et al., 2008).

The role of CD8 T cells in regulating HSV-1 latency has been partially verified in humans, with the detection of $CD8^+$ T cells in the trigeminal, geniculate and vestibular ganglia of HSV-1 latently-infected humans (Arbusow et al., 2010; Derfuss et al., 2009; Derfuss et al., 2007; Theil et al., 2003a; Verjans et al., 2007). Some of these cells are found in the vicinity of or surrounding latently infected neurons (Derfuss et al., 2009; Theil et al., 2003a; Verjans et al., 2007). These cells have an activated phenotype, upregulating markers like CD69, gzmB and granzyme A (gzmA), and perforin, but lacked expression of the homing molecules C-C chemokine receptor type 7 and CD62L (Derfuss et al., 2007; Verjans et al., 2007). Further, $CD8\alpha\alpha^+$ T cells, which closely resemble the T_{RM} $CD8^+$ T cells identified in mice, have been found in the skin of humans infected with HSV-2. The presence of these $CD8\alpha\alpha^+$ T cells was found to be correlated with increased virus control (Schiffer et al.,

2010; Zhu et al., 2007; Zhu et al., 2013). These cells have direct cytotoxic action against newly infected cells in the skin, and produce antiviral cytokines (Zhu et al., 2007; Zhu et al., 2013). Therefore, this robust $CD8^+$ T cell response at the skin is likely important for preventing virus reactivation and possible recrudescence.

While there is no direct role for $CD4^+$ T cells in the maintenance of latency, they do infiltrate the DRG and are detectable at low levels throughout latency in both mice and humans (Liu et al., 1996; Shimeld et al., 1995; Theil et al., 2003a). $CD4^+$ T_{RM} cells are also found in the skin, but unlike the $CD8^+$ T_{RM} cells their role requires interplay between macrophages, antigen recognition and the production of IFN-γ and other downstream chemokines (Iijima and Iwasaki, 2014). $CD4^+$ T_{RM} cells also show a different pattern of localisation in the dermis as a part of a wider recirculation, while $CD8^+$ T_{RM} cells are found lodged in the epidermis (Gebhardt et al., 2011; Zhu et al., 2007). Ablation of $CD4^+$ T cells revealed a failure to maintain the latent state, as evidenced by increased viral genome load. There was also a lower frequency of IFN-γ and TNF-α producing $CD8^+$ T cells, suggesting that $CD4^+$ T cell help is required to avert functional compromise of $CD8^+$ T cells (Frank et al., 2010).

It is unlikely that antibody responses play a significant role in maintaining latency. There is a measureable antibody response during latency, with serum antibody levels in ocularly infected mice increasing until 30 days p.i. However, they then plateau throughout latency until at least 125 days p.i. (Halford et al., 1996a). Further, recurring mucocutaneous reactivations are associated with rising serum titers in humans (Zweerink and Stanton, 1981).

Finally, the innate immune response does have some role in regulating HSV reactivation. For example, it has been shown that plasmacytoid dendritic cells infiltrate the dermis of recurrent HSV-2 lesions in humans and are able to stimulate T cell proliferation (Donaghy et al., 2009). However, interaction of the innate immune system with HSV during latency and beyond is largely unexplored.

1.4 Aims of this thesis

The biology of HSV-1 is dominated by its ability to establish a latent infection within the host. However, latency is not established in isolation, and is preceded by a lytic infection that is characterised by viral replication, extensive lytic gene expression and the production of infectious virus. Therefore, the course of HSV-1 infection, both on a per cell

basis and for the entire animal, is dictated not just by current, but also past, events. There is evidence that some viral gene expression, largely limited to the immediate early class of gene expression, can precede the establishment of latency within some neurons, but the expression of on a handful of prototypic HSV-1 lytic genes has been studied so far (Proença et al., 2008; Proença et al., 2011). Additionally, it was recently reported that lytic gene transcription occurs at a low level and sporadic in many neurons, but there is much less evidence to suggest that there is production of viral protein during latency.

Reporter genes such as the green fluorescent protein (GFP) and β-galactosidase (β-gal) have proved invaluable for tracking viral gene expression, particularly when using *in vivo* models of infection. However, as lytic gene promoters are silenced during latency, they are of limited utility for tracking gene expression during latency. More importantly, conventional reporters are unable to reveal prior gene expression that has been suppressed or that is transient or at a low level. Recently, a novel method for tracking viral gene expression was described that utilises ROSA26R reporter mice (Proença et al., 2008; Wakim et al., 2008b). ROSA26R mice contain a *lacZ* reporter gene that is separated from the constitutive ROSA promoter by a large insert containing the neomycin resistance gene as well as multiple stop codons, preventing the expression of *lacZ*. This insert is flanked by *loxP* sites, so the *lacZ* reporter will only be expressed following Cre-mediated recombination. By using HSV-1 to drive expression of *cre*, cells that experience viral promoter activity are able to be permanently marked and identified by this stable reporter gene expression (Figure 1-3). Therefore, this system is ideal for investigating the impact of prior lytic viral gene expression on the establishment of latency and beyond. Therefore, the aims of this thesis are:

1. To develop and optimise methods to construct HSV-1 that express Cre recombinase under different classes of HSV-1 promoters.

2. To determine the proportion of HSV-1 infected neurons that experience lytic viral gene expression and establish latency.

3. To determine if there is an accumulation of neurons that have experienced lytic viral gene expression during latency.

4. To examine ICP47 promoter activity during the establishment of latency that can lead to the production of viral protein, and to investigate whether increasing the level of presentation of a $CD8^+$ T cell epitope can alter the progression of either the acute or latent HSV-1 infection.

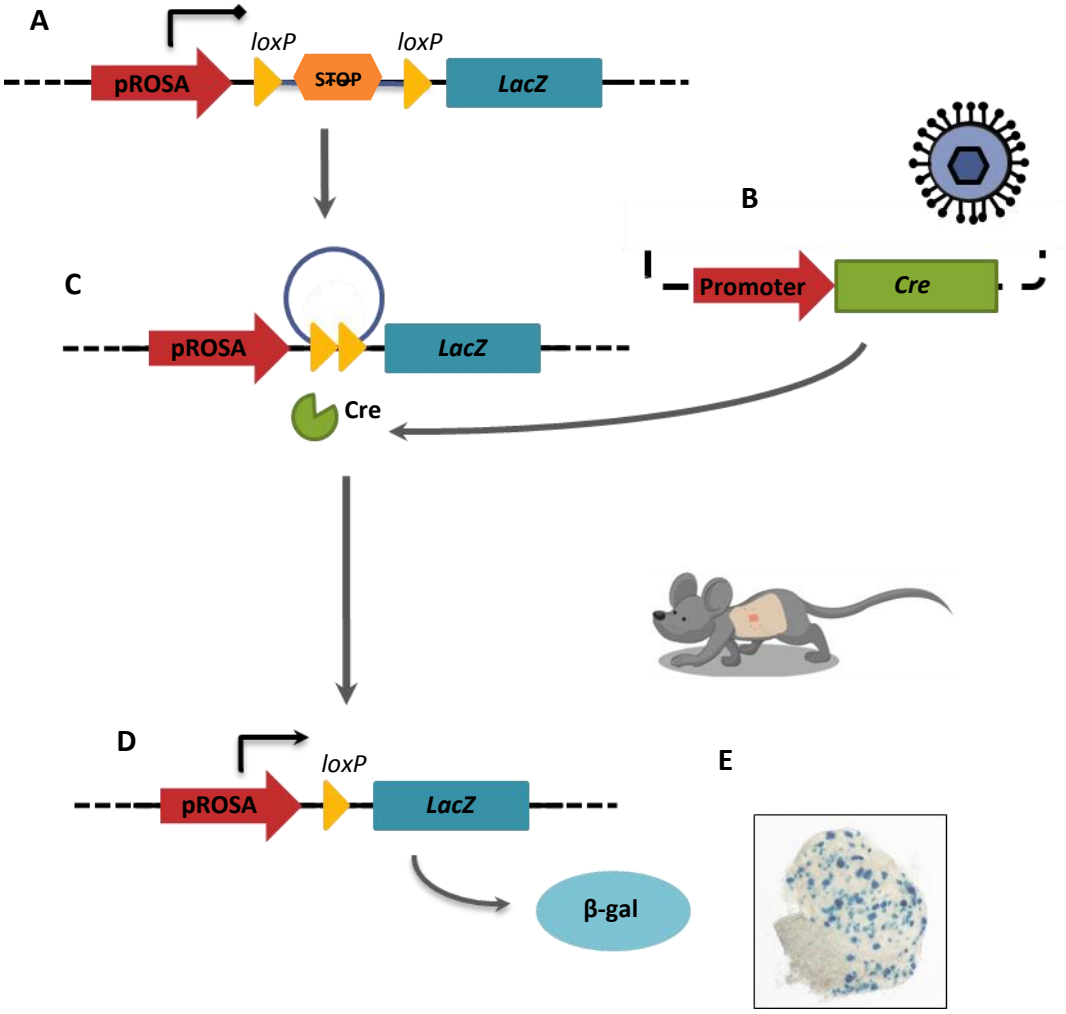

Figure 1-3. ROSA26R mice can be used to permanently mark neurons latently infected with HSV-1. (A) ROSA26R transgenic mice encode the *LacZ* reporter gene under the ROSA26 promoter. Expression of *LacZ* is prevented by the presence of a *loxP*-flanked neomycin insert. (B) Cre recombinase is encoded within the viral genome. (C) Once mice are infected with HSV-1 encoding *Cre*, Cre recombinase can mediate recombination between the *loxP* sites, allowing excision of the insert. (D) This allows for expression of β-gal. (E) A representative DRG taken from a ROSA26R mouse infected with HSV-1 expressing *Cre* that has been stained for the presence of β-gal with the substrate X-gal.

2 | Materials and Methods

2.1 Materials

2.1.1 Solvents

DMSO	Dimethyl sulfoxide
Ethanol	Ethanol (Merck).
Methanol	Methanol (Merck).
***N, N* dimethylformamide**	*N, N* dimethylformamide (DMF; Sigma-Aldrich).
Nuclease free water	Nuclease free water (Ambion).
Sterile water	Sterile water (Baxter healthcare).
RO water	Water purified using Type 3 system (reverse osmosis).
Ultrapure water	Water purified using Type 1 system (analogous to MilliQ water; TKA).

2.1.2 Buffers

Colony cracking buffer	1.5 mM sucrose (Amresco), 0.5% sodium dodecyl sulphate (SDS; Sigma-Aldrich) and 200 mM sodium hydroxide (Sigma-Aldrich) in ultrapure water
EDTA	0.5 M EDTA (Sigma-Aldrich) in ultrapure water, with the pH adjusted to 8.0 with sodium hydroxide pellets (Sigma-Aldrich).
FACS PBS	1× phosphate buffered saline (PBS) supplemented with 2% foetal bovine serum (FBS; refer to Section 2.1.4).
$MgCl_2$ buffer	0.1 M magnesium chloride (Ajax FineChem) and 4.5 M β-mercaptoethanol (Sigma-Aldrich) in ultrapure water.
PBS	10× PBS (Invitrogen) was diluted in ultrapure water to 1× PBS.
Red cell lysis buffer	0.14 M ammonium chloride (Sigma-Aldrich) and 19 mM Trizma base (Sigma-Aldrich) in ultrapure water. The pH was adjusted to 7.2, and the buffer was autoclaved prior to use.

RSB buffer	10 mM Trizma base, 10 mM potassium chloride (Sigma-Aldrich) and 1.5 mM magnesium chloride (Ajax FineChem) in ultrapure water.
Sodium phosphate buffer	0.1 M sodium phosphate buffer is made up of 0.1 M sodium phosphate dibasic dihydrate (Sigma-Aldrich) and 0.1 M sodium phosphate monobasic dihydrate (Merck) in ultrapure water.
1 M Tris-Cl	1 M Trizma base in ultrapure water, adjusted to pH 8.0.
1× T4 DNA ligase buffer	10× T4 DNA ligase buffer (New England Biolabs), diluted as appropriate.
1× TAE buffer	1× Tris-acetate-EDTA (TAE) buffer consists of 40 mM Trizma base, 20 mM glacial acetic acid (Univar) and 1 mM EDTA (pH 8.0) in ultrapure water.
1× TBE buffer	10× Tris-borate-EDTA (TBE) buffer consists of 89 mM Trizma base, 89 mM boric acid (Merck) and 2 mM EDTA in sterile water. This is autoclaved and diluted to 1× stock prior to use.
1× ThermoPol buffer	10× ThermoPol reaction buffer (New England Biolabs), diluted as appropriate.
TE buffer	10 mM Trizma base pH 8.0 and 1 mM EDTA in ultrapure water.

2.1.3 Media for bacterial culture

Antibiotics	Stock solutions were made up in ultrapure water prior to filter sterilisation. 100 µg/L ampicillin (Sigma-Aldrich) or 50 µg/mL kanamycin (Sigma-Aldrich) were added to LB media or agar after autoclaving and cooling when required.
Glycerol	60% (v/v) glycerol (Sigma-Aldrich) in ultrapure water.
Luria-Bertani (LB) broth	10 g/L tryptone (Bacto), 5 g/L yeast extract (Bacto), 10 g/L sodium chloride (Bacto) in deionised water.
LB agar	LB broth with 15 g/L Bacto-agar (Bacto).

Super optimal broth with catabolite repression (SOC) medium	20 g/L tryptone, 5 g/L yeast extract, 0.5 g/L sodium chloride, 2.5 mM potassium chloride, 20 mM glucose (Merck) and 10 mM magnesium chloride in ultrapure water.

2.1.4 Media for cell culture

FBS FBS (Serana).

CMC-MEM 0.4% carboxymethylcellulose (CMC) in Minimum Essential Medium (MEM; no phenol red; Invitrogen) supplemented with 4 mM L-glutamine, 5 mM HEPES, 50 μM 2-mercaptoethanol and 2% (v/v) FBS.

DMEM Dulbecco's Modified Eagle Medium (DMEM; high glucose, with phenol red; Invitrogen) was supplemented with 2 mM L-glutamine and 2% (v/v) or 10% (v/v) of heat-inactivated FBS for cell culture and dilution of virus (DMEM-2 and DMEM-10, respectively).

MEM MEM (phenol red; Invitrogen) was supplemented with 4 mM L-glutamine (Invitrogen), 5 mM HEPES (Invitrogen), 50 μM 2-mercaptoethanol (MEM-0; Invitrogen) and 2% (v/v) or 10% (v/v) heat-inactivated foetal bovine serum (FBS; SAFC Biosciences) was used for cell culture and dilution of virus (MEM-2 and MEM-10, respectively).

2.1.5 Reagents for molecular biology

Acrylamide 40% acrylamide and *bis* Acrylamide (29:1) solution (Bio-Rad).

Agarose 0.8, 1 or 2% (w/v) UltraPure agarose (Life Technologies) in 1× TAE buffer.

Antarctic phosphatase Antarctic phosphatase with 10× reaction buffer (New England Biolabs).

APS 10% (w/v) ammonium persulphate (APS; Bio-Rad) in ultrapure water.

BigDye terminator	BigDye terminator for DNA sequencing (Life Technologies) with 5× reaction buffer was obtained from the Biomolecular Resource Facility, John Curtin School of Medical Research (JCSMR), the Australian National University (ANU).
cDNA synthesis kit	SuperScript VILO cDNA synthesis kit (Life Technologies).
Chloroform	Chloroform (Merck).
Colony cracking marker mix	0.6 mM potassium chloride (Sigma-Aldrich) and 0.1% (w/v) bromophenol blue (Merck) in ultrapure water.
DNase	DNase I recombinant, RNase free (Roche).
6× DNA gel loading buffer	0.25% (w/v) bromophenol blue (Merck) or xylene cyanol (Sigma-Aldrich) in 30% (v/v) glycerol (Sigma-Aldrich) in ultrapure water.
DNA markers	100 bp and 1 kb DNA markers (New England Biolabs), supercoiled DNA ladder (Life Technologies) and 1 kb DNA extension ladder (Life Technologies).
DNA polymerases	*Taq* DNA polymerase with 10× ThermoPol buffer (New England Biolabs), and Phusion DNA polymerase with 5× HF or GC buffer (New England Biolabs).
DNA staining solution	SYBR Safe DNA gel stain solution (Invitrogen), at a 1 in 10 000 dilution in RO water.
dNTP mix	10 mM deoxyribonucleotide triphosphate (dNTP) mix (Bioline).
DTT	100 mM dithioreitol (DTT).
Geneclean spin kit	Geneclean spin kit (MP Biomedicals).
Glycogen	20 µg/µL UltraPure glycogen (Invitrogen).
IGEPAL	IGEPAL CA-630 (Sigma-Aldrich), also known as octyl phenyl-polyethylene glycol, is chemically indistinguishable from Nonidet P-40, which is no longer commercially available.

InFusion HD cloning kit	InFusion HD cloning kit (Clontech).
LigaFast rapid DNA ligation kit	LigaFast rapid DNA ligation kit (Promega).
Phenol	Phenol (Fluka).
Phenol:chloroform	Phenol:chloroform:isoamyl alcohol (25:24:1 ratio; Fluka).
Plasmid MiniPrep kit	Plasmid MiniPrep kit (Axygen).
Plasmid MidiPrep kit	Plasmid MidiPrep kit (Axygen).
Potassium chloride	1 M potassium chloride (Sigma-Aldrich) in ultrapure water.
qPCR mastermix	2× LightCycler480 probes master mix (Roche) for use in Roche LightCycler480 real-time PCR machine.
Qubit assays	Qubit dsDNA HS assay (Life Technologies) and Qubit RNA HS assay (Life Technologies).
Restriction enzymes	Various restriction enzymes (New England Biolabs).
RNase inhibitor	RNasin ribonuclease inhibitor (Promega).
RNA isolation kit	Two RNA isolation kits were used; the total RNA isolation kit (Promega) for medium scale RNA isolation (typically from cultured cells) and the RNAqueous micro kit (Ambion) for small scale RNA isolation from mouse DRG.
RNA polymerase	SP6 RNA polymerase (Promega).
rNTP mix	Ribonucleoside triphosphate (rNTP) mix (500 μM of each rNTP; Promega).
Sodium acetate	3 M sodium acetate (Merck) in ultrapure water.
Sodium carbonate	1 M sodium carbonate (Sigma-Aldrich) in ultrapure water.
Sodium hydroxide	5 M sodium hydroxide (Sigma-Aldrich) in ultrapure water.
10% SDS	10% (w/v) SDS (Sigma-Aldrich).

Sucrose	Sucrose (Amresco).
T4 DNA ligase	400 units/μL T4 DNA ligase (New England Biolabs) or 3 units/μL T4 DNA ligase (Promega).
TEMED	N-N-N'-N'-tetramethylethylenediamine (TEMED; Biorad).

2.1.6 Reagents for cell culture, immunology and virology

Actinomycin D	20 mg/mL actinomycin D (Life Technologies) in methanol.
Acyclovir	22.5 mM acyclovir (Sigma-Aldrich) in DMSO.
Collagenase/DNase solution	1 mg/mL Type IV Collagenase (at least 160 units/mL; Worthington) and 0.03 mg/mL DNase (at least 600 units/mL; Roche) in DMEM-2.
Crystal violet staining solution	2.3% (v/v) crystal violet (Sigma-Aldrich) in 20% (v/v) ethanol.
Cycloheximide	100 mg/mL cycloheximide (Sigma-Aldrich).
DDAO-galactosidase	9*H*-(1,3-dichloro-9,9-dimethylacridin-2-one-7-yl) β-D-galactopyranoside (DDAO-galactosidase; Invitrogen).
Glutaraldehyde	25% glutaraldehyde in water, Grade II (Sigma-Aldrich).
Lipofectamine	Lipofectamine 2000 (Invitrogen).
1× ONPG	4 mg/mL ortho-nitrophenyl-β-galactoside (ONPG; Sigma-Aldrich) in 0.1 M sodium phosphate buffer.
PFA	16% paraformaldehyde (PFA) in water (Electron Microscopy Sciences). This was diluted to 1% (w/v) PFA in PBS as required.
Proteinase K	10 μg/mL proteinase K (Roche).
Saponin	5% (w/v) saponin (Fluka) dissolved in sterile water. This was diluted 1 in 10 in FACS-PBS before use.
Trypan blue	Trypan blue solution, 0.4% (Invitrogen).
Trypsin	0.05% (w/v) trypsin with 0.53 mM EDTA (Invitrogen).

2.1.7 Reagents for infection of mice with HSV-1

Avertin	12.5 mg/mL 2,2,2-tribromoethanol (Sigma-Aldrich) and 2.5% (v/v) 2-methyl-butanol (Sigma-Aldrich) in sterile water. This is then sterilised by filtration through a 0.22 μm filter (Millipore) and stored in the dark at 4°C for no more than 14 days before use.
Veet™ depilatory cream	Veet™ depilatory cream for sensitive skin (Reckitt Benckiser).

2.1.8 Chemicals for removal of DRG and isolation and fixation of cells

50% glycerol	50% (v/v) glycerol in 1× PBS.
Permeabilisation buffer	2 mM magnesium chloride, 0.01% (w/v) sodium deoxycholate (Sigma-Aldrich), 0.02% (v/v) IGEPAL, 5 mM potassium ferrocyanide (Sigma-Aldrich) and 5 mM potassium ferricyanide (Sigma-Aldrich) in ultrapure water.
PFA/glutaraldehyde fixative	2% (v/v) PFA and 0.5% (v/v) glutaraldehyde (Sigma-Aldrich) in 1× PBS.
X-gal	40 mg/mL 5-bromo-4-chloro-indolyl-β-D-galactopyranoside (X-gal; Bio Vectra) in DMF.
X-gal staining buffer	Permeabilisation buffer with 1 mg/ml 5-bromo-4-chloro-indolyl-β-D-galactopyranoside (X-gal).

2.1.9 Plasmid constructs

All plasmid DNA was isolated using the Axygen MiniPrep or MidiPrep kit as described in Section 2.2.2.1. The plasmids used in this thesis are described in Table 2.1. Those plasmids that were produced during this thesis are described in Table 2.2.

Plasmid Name	Description	Source
pTracer-CMV/bsd	Generic mammalian expression vector	Purchased from Invitrogen, Life Technologies
pT 456	Carries the mCherry fluorescent protein coding sequence	Provided by Dr. T. Newsome, the University of Sydney
pIGCN21	Contains the eGFP/Cre (eGC) fusion protein sequence (Lee et al., 2001)	National Cancer Institute (NIH) Biological Resources Branch
pUC57 pLAT eGC	Contains sequences homologous to the LAT region (HSV-1 17 119863 - 120364) with an eGFP/Cre fusion gene inserted behind an encephalomyocarditis virus (ECMV) internal ribosome entry site (IRES) followed by the Simian Virus 40 (SV40) polyA sequence 3at position 120364, cloned into the pUC57 vector	Purchased from GenScript
pUC57 – pICP47 w/o OriS	Contains ICP47 promoter sequence (HSV-1 KOS 145998-146497) with the sequence encoding the OriS (HSV-1 KOS 145533-145577) removed	Purchased from GenScript
pU26/7	Contains sequences homologous to the U_L26/U_L27 region of HSV-1 (HSV-1 KOS 51431 - 54154), with a multiple cloning site (MCS) inserted at position 52809	T. Stefanovic and Dr. D. Tscharke (unpublished)
pCR-Blunt II	Generic expression vector containing the lethal *ccdB* gene fused to C-terminus of *lacZα*	Purchased from Invitrogen, Life Technologies
pUC57 pICP47 Venus	Contains the ICP47 promoter sequence (HSV-1 KOS 145998 - 146497) with the sequence encoding the OriS (HSV-1 KOS 145533 - 145577) removed, followed by the Venus fluorescent protein coding sequence and the bovine growth hormone (BGH) polyA sequence, cloned into the pUC57 vector	Purchased from GenScript
pUC57 pICP0 mC Cre	Contains the ICP0 promoter sequence (HSV-1 KOS 1271 - 2238), followed by an mCherry/Cre fusion gene analogous to the eGFP/Cre fusion gene found in pIGCN21, followed by the BGH polyA sequence, cloned into the pUC57 vector	Purchased from GenScript
pUC57 qICP47	Contains a 64 bp fragment of ICP47 cloned behind the SP6 promoter in the pUC57 vector	Purchased from GenScript

Table 2-1. Description of plasmids used in this thesis. Details of plasmids used in this thesis that were already available or which I designed and purchased from GenScript.

Plasmid Name	Description	Source
pCR-Blunt II Cre (R)	Contains the coding sequence for the eGFP/Cre fusion gene inserted behind the SP6 promoter into the pUC57 vector	S. Smith and Dr. D. Tscharke, unpublished
pX330	Contains the humanised coding sequence for the *S.pyogenes cas9* gene as a part of a CRISPR array (Cong et al., 2013)	Addgene plasmid 42230
pX330-mC	Contains a guide RNA designed to target the mCherry coding sequence inserted into pX330	T. Stefanovic and Dr. D. Tscharke (unpublished)

Table 2-1 cont. Description of plasmids used in this thesis.

Plasmid Name	Description
pT U_L3/U_L4	Transfer vector containing sequences flanking the HSV-1 U_L3/U_L4 intergenic region (HSV-1 KOS 10534 – 12682) with a MCS inserted at the HSV-1 genomic location 11649 (HSV-1 KOS)
pT CMV IE_mC	The vector pT U_L3/U_L4 with the coding sequence of the mCherry fluorescent protein inserted behind the Cytomegalovirus Immediate Early (CMV IE) promoter
pT CMV IE_mC_BGH	pT CMV IE_mC with the BGH polyA inserted in behind the mCherry gene
pT eGC	The vector pT U_L3/U_L4 with the coding sequence of an eGFP/Cre fusion gene followed by the BGH polyA
pT pICP47_ eGC	pT eGC with the ICP47 promoter sequence (HSV-1 KOS 145998 - 146497), with the sequence encoding the OriS (HSV-1 KOS 145533 - 145577) removed, inserted such that it directs expression of eGFP/Cre
pT pICP6_eGC	pT eGC with the ICP6 promoter sequence (HSV-1 KOS 85906 – 86166) inserted such that it directs expression of eGFP/Cre
pT pgB_eGC	pT eGC with the gB promoter sequence (HSV-1 KOS 55985 – 56282) inserted such that it directs expression of eGFP/Cre
pT pC_eGC	pT eGC with the CMV IE promoter sequence inserted such that it directs expression of eGFP/Cre
pU3.0.5kbF	Transfer vector containing ~1 kb total of sequence flanking the HSV-1 UL3/UL4 intergenic region (HSV-1 KOS 11200 - 12179) with a MCS at position 11649 (HSV-1 KOS)
pU3.1kbF	Transfer vector containing ~2 kb total of sequence flanking the HSV-1 UL3/UL4 intergenic region (HSV-1 KOS 10700 - 12722) with a MCS at position 11649 (HSV-1 KOS)

Table 2-2. Description of plasmids constructed for use in this thesis.

Plasmid Name	Description
pU3.2kbF	Transfer vector containing ~4 kb total of sequence flanking the HSV-1 UL3/UL4 intergenic region (HSV-1 KOS 9803 - 13698) with a MCS at position 11649 (HSV-1 KOS)
pU3.3kbF	Transfer vector containing ~5.6 kb total of sequence flanking the HSV-1 UL3/UL4 intergenic region (HSV-1 KOS 8689 - 14663) with a MCS at position 11649 (HSV-1 KOS)
pU3.0.5kbF-Venus	pU3.0.5kbF with the ICP47 promoter sequence (HSV-1 KOS 145998 - 146497), with the sequence encoding the OriS (HSV-1 KOS 145533 - 145577) removed, inserted such that it directs expression of the fluorescent protein Venus, followed by a BGH polyA
pU3.1kbF-Venus	pU3.1kbF with the ICP47 promoter sequence (HSV-1 KOS 145998 - 146497), with the sequence encoding the OriS (HSV-1 KOS 145533 - 145577) removed, inserted such that it directs expression of the fluorescent protein Venus, followed by a BGH polyA
pU3.2kbF-Venus	pU3.2kbF with the ICP47 promoter sequence (HSV-1 KOS 145998 - 146497), with the sequence encoding the OriS (HSV-1 KOS 145533 - 145577) removed, inserted such that it directs expression of the fluorescent protein Venus, followed by a BGH polyA
pU3.3kbF-Venus	pU3.3kbF with the ICP47 promoter sequence (HSV-1 KOS 145998 - 146497), with the sequence encoding the OriS (HSV-1 KOS 145533 - 145577) removed, inserted such that it directs expression of the fluorescent protein Venus, followed by a BGH polyA
pT pICP0 mC Cre	The vector pT U_L3/U_L4 with ICP0 promoter sequence (HSV-1 KOS 1271 - 2238), followed by a mCherry/Cre fusion gene analogous to the eGFP/Cre fusion gene found in pIGCN21, and then the BGH polyA sequence inserted at the SpeI site
pT pICP0_eGC	The vector pT U_L3/U_L4 with ICP0 promoter sequence (HSV-1 KOS 1271 - 2238), followed by an eGFP/Cre fusion gene and then the BGH polyA sequence inserted at the SpeI site
pUC57 LAT pCmC	Contains sequences homologous to the LAT region (HSV-1 17 119863 - 120364) with the mCherry gene inserted behind the CMV IE promoter followed by the SV40 polyA sequence at position 120364, cloned into the pUC57 vector
pU26/7 pICP47	pU26/7 with the ICP47 promoter sequence (HSV-1 KOS 145998 - 146497), with the sequence encoding the OriS (HSV-1 KOS 145533 - 145577) removed, inserted into the centre of U_L26/U_L27 region (HSV-1 KOS 52809)
pU26/7 pICP47/Tdtom	The fluorescent protein Tdtomato was inserted after the ICP47 promoter, followed by the BGH polyA

Table 2-2 cont. Description of plasmids constructed for use in this thesis.

Plasmid Name	Description
pU3.2kbF-ESgBCre	pU3.2kbF vector with an endoplasmic reticulum (ER)-targeted gB minigene under the control of the gB promoter sequence (HSV-1 KOS 55985 – 56282) followed by the SV40 polyA, and in the opposite orientation there is the CMV IE promoter sequence inserted such that it directs expression of eGFP/Cre followed by a BGH polyA
pX330-minigB	Contains a guide RNA designed to target the ER-targeting gB minigene coding sequence inserted into pX330
pU3.2kbF-gBCre	pU3.2kbF vector with a minimal gB epitope sequence under the control of the gB promoter sequence (HSV-1 KOS 55985 – 56282) followed by the SV40 polyA, and in the opposite orientation there is the CMV IE promoter sequence inserted such that it directs expression of eGFP/Cre followed by a BGH polyA

Table 2-2. Description of plasmids constructed for use in this thesis.

2.1.10 Oligodeoxynucleotides

Oligodeoxynucleotides which were used on this study are listed in Table 2.3. All oligodeoxynucleotides were purchased from Sigma Genosys and were used from working stocks diluted to a concentration of 10 μM in sterile water.

Primer Name	Sequence
0.5Lf Fwd	GCTATGCATCAAGCTTACCCTGTTTATGGTGTCGTC
0.5Rf Rev	TGCATGCTCGAGCGGCCCTGTTGGTGATTATCGACTGTC
1Lf Fwd	GCTATGCATCAAGCTTCCTCGGGTCCATTGC
1Rf Rev	TGCATGCTCGAGCGGCCATTGACTCTACGGAGCTGG
2.6Lf Fwd	GCTATGCATCAAGCTTGGAGAGGGGGTATATAAACCAA
2Lf Fwd	GCTATGCATCAAGCTTCCGCCAGCCACACAC
2Lf Seq Rev	GTCCCAACCGATTCTAGAGTG
2Rf Rev	TGCATGCTCGAGCGGCCCACCAACTACTCGCAGAGC
2Rf Seq Fwd	GTAGTCGGCGTTTATGGC
3Lf Seq Fwd	AACACCCAGGAAACAGAAAC
3Lf Seq Fwd	AACACCCAGGAAACAGAAAC
3Lf Seq Rev	ACACACCCAGCCTTCACAGGT
3Rf Rev	TGCATGCTCGAGCGGCCCGACCCATCAACACCATC
3Rf Seq Fwd	ATCTGGCTGTTGAGGACGTAA

Table 2-3. Details of oligodeoxynucleotides used in this thesis.

Primer Name	Sequence
3Rf Seq Rev	CCAGCCCGGCCTGACTAT
BGH Lf	GCGGCCGCAGAATTCCTGTGCCTTCTAGTTGCCAG
BGH Rf II	CCATTAAAGAACTAGCTGCTATTGTCTTCCCAATC
BGH Seq Fwd	AAGCCTTCGACGTGGAGG
BGH Seq Rev	GCCACCACCTGTTCCTGTAC
bla seq	AATAGGGGTTCCGCGCACAT
CMV Fwd	ATATCTGCAGACTAGTCCGTATTACCGCCATGCA
CMV IE Lf	ATATCTGCAGACTAGTGCCAGATATACGCGTTGACA
CMV IE Rf	GACTCGAGCGGCCGCAGTTAGCCAGAGAGCTCTGC
CMV Rev	CGCCCTTGCTCACCATGGTGGCGACCGGTAGC
Consensus Lf Rev	GCGGCCGCTGGTACCCAACAAACAACCAGCCAAAT
Consensus Rf Fwd	GGTACCAGCGGCCGCTCTTTAATGGACCGCCC
Cre F	CGTATAGCCGAAATTGCCAG
Cre Lf Seq	CACGACCAAGTGACAGCAAT
Cre R	CAAAACAGGTAGTTATTCGG
Cre Rf Seq	TGGCAATTTCGGCTATACGT
ef-1 seq	CTTCTCTAGGCACCGGTTCA
eGFP Cre Lf II	ATATCTGCAGACTAGTATGGTGAGCAAGGGCG
eGFP/Cre Lf Seq	TGGGGGTGTTCTGCTGGTAG
eGFP/Cre Rf Seq	CCACAACATCGAGGACGGCA
EGFPnoMet	GTGAGCAAGGGCGAGGAG
ER Rev	AGGTACATGATTTTAGGCTTGC
FwdHSV-gBend	ACACAAGGCCAAGAAGAAGG
gB P Fwd	TTGGATATCTGCAGATCAACGGGCCCCTCTT
gB P Rev	TGCTCACCATACTAGTCGAGCTCCCCGCAC
GFP/Cre F	GTTAACGCGGACTAGTCCGTATTACCGCCAT
GFP/Cre R	CATTAAAGAGCGGCCTGCTATTGTCTTCCCAATCC
LAT CMV Fwd	GCGCTCGCGGCGGCCGCCAGATATACGCGTTGACA
LAT mC Rev	TAAACAAGTTACTAGTTACTTGTACAGCTCGTCCA
LAT R2	ATGGAGCCAGAACCACAGTG
M13 Rev+	CAGGAAACAGCTATGAC
mCfwd	CTACGACGCTGAGGTCAAGA

Table 2-3 cont. Details of oligodeoxynucleotides used in this thesis.

Primer Name	Sequence
mCherry Lf	GCGGCCGCTCGAGTCATGGTGAGCAAGGGCGAGGA
mCherry Rf	CCATTAAAGAACTAGTTTACTTGTACAGCTCGTCCA
mCherry Rf II	GAATTCTGCGGCCGCTTACTTGTACAGCTCGTCCA
mCrev	GTAGATGAACTCGCCGTCC
minigB F	TGCAATAAACAAGTTCTATCACAGCCGGGC
minigB R	GTGCGGGGAGCTCGAATGAGGTACATGATTTTAGG
No ER Rev	AGCTCGAATGTCCTCCAT
noESF1	GGCTGGTTGTTTGTTGG
noESF2	GAACTCGATGGAGGACATTCGAGCTCCCCGC
noESR1	TCCTCCATCGAGTTCGC
noESR2	ATGGCGGTAATACGGACTAG
pgB F	AATCATGTACCTCATTCGAGCTCCCCGCAC
pgB R	ACTAGTCCGCGTTAACTCAACGGGCCCCTCT
pgB R	ACTAGTCCGCGTTAACTCAACGGGCCCCTCT
pICP0 mC Fwd	CATACGACCCCCATGGTGAGCAAGGGCGAGG
pICP0 mC Rev	CAGTAAATTGGAGTTAACTGCAGAATTTTGAGCTCG
pICP0 Seq Fwd	ACTTGCAGAGGCCTTGTTCC
pICP0 Seq Rev	GGCTCCAAGCGTATATATGC
pICP47 Seq Fwd	CGGGACCGCCCCAAGGG
pICP47 Seq Rev	CCCGTTGGTCCCGGCGT
pSC11lacZseq	GTGCTGCAAGGCGATTAAGT
pT Rev Cre-C	AGGAATTCTGCGGCCCTAATCGCCATCTTCCAGCA
pTracer bla	TCTAGGTCTTGAAAGGAGTG
ptracer CMV IE Rf	GGCCATGTTATCCTCCTCGC
ptracer CMV IE Rf	GGCCATGTTATCCTCCTCGC
pTracer EF1	TGTACTGAGAGTGCACCATA
ptracer mC Lf	GTACGGTGGGAGGTCTATAT
ptracer UL3 Lf	TTACACGCGATCTTCGGACG
ptracer UL4 Rf	CGCGGACACCATTTACATCA
pX330 seq_F	TGGACTATCATATGCTTACCG
pX330 seq_R	TAGATGTACTGCCAAGTAGGAA
RevHSVgBend	GACCAACGAGACCATCACG

Table 2-3 cont. Details of oligodeoxynucleotides used in this thesis.

Primer Name	Sequence
RR1 P Fwd	TTGGATATCTGCAGAACTCGTTGTTCGTTGACC
RR1 P Rev	TGCTCACCATACTAGGGCAAGTTTCCAAAGCAC
Seq RevpEGFPN1	CTCGACCAGGATGGGCAC
SeqT7pro	TAATACGACTCACTATAGGG
SV40 F	TTGTTGGGTACCAGCCAGACATGATAAGATACATTG
SV40 R	CCCGGCTGTGATAGAACTTGTTTATTGCAGC
Tdt Fwd	TGATGACGGCCATGTTGT
Tomato BGH Fwd	CGGGAAAGATATCGCCTGCTATTGTCTTCCCAATCC
Tomato BGH Rev	CACTAGTGCGGCCGCATGGTGAGCAAGGGCG
UL26 Left	CGTTAACAACATGATGCTGCG
UL26 Seq Rev	CCCACCTGAGGGCGATAGTG
UL27 Seq Fwd	TTGTTGGGAACTTGGGTGTA
UL27 Seq Rev	ATGACCATGATTACGCCAAGC
UL3 Lf	TGCACTCTCAGTACAGTTACTAAACACGACCCTGA
UL3 Rf	ACTAGTCTGCAGATATCCAACAAACAACCAGCCAAAT
UL3 Seq Fwd	GCCGTCAAGAACTGTTATCC
UL3 Seq Rev	ATTGGCTCGGACGAGACGAA
UL4 Lf	GATATCTGCAGACTAGTTCTTTAATGGACCGCCCGCA
UL4 Rf	CTTTCAAGACCTAGAATTGACTCTACGGAGCTGGC
UL4 Seq Fwd	GTTTGTCTGCGTATTCCAGG
UL4 Seq Rev	CGTCGTCAACACCAACATCA

Table 2-3 cont. Details of oligodeoxynucleotides used in this thesis.

2.1.11 *Escherichia coli* Strains

Three strains of *E. coli* were used in this thesis, namely α-Select Chemically Competent Cells (Gold Efficiency, Bioline), XL10 Gold Chemically Competent Cells (prepared in house) and One Shot Stbl3 Chemically Competent *E. coli* (Invitrogen). α-Select cells were routinely employed, whereas XL10 Gold and Stbl3 cells were used when plasmids were low copy number or were likely to form a complex secondary structure, respectively.

2.1.12 Mice

Female specific pathogen-free C57Bl/6 or B6.129S4-Gt(ROSA)26Sor^{tm1So}/J (ROSA26R; a gift from Dr. Frank Carbone) mice were sourced from the Australian Phenomics Facility (APF; Canberra, Australia; Soriano, 1999). All mice were housed at the Wes Whitten

Animal Facility, Research School of Biology, ANU according to ethical requirements, and were at least eight weeks of age prior to use. Food and water were provided, and cages were changed weekly or upon resolution of infection. All experiments were approved by the ANU Animal Ethics and Experimentation Committee under protocols A2011/001, A2011/015, A2013/037 and A2014/025.

2.1.13 Cell lines

All cell lines used in this study are listed in Table 2-4. Cells were maintained in MEM-10 or DMEM-10 at 37°C with 5% CO_2 in culture flasks, and were subcultured twice a week. The cells were maintained as described in Section 2.2.10.

Cell Line	Origin	Property	Use	Split Ratio
293A	Primary human embryonic kidney cells transformed with human adenovirus 5 DNA	Adherent	For generating recombinant HSV-1 by transfection/ infection	1 in 12
Vero	African green velvet monkey kidney epithelial cells	Adherent	A) For generating recombinant HSV-1 by cotransfection of plasmid and viral DNA B) For plaque purification of recombinant virus C) For growing virus stocks D) HSV-1 titration, plaque morphology and replication analysis	1 in 8
Vero SUA	Vero cells that have been stably transfected to contain the *lacZ* gene preceded by the neomycin phosphotransferase gene which is flanked by *lox P* sites, controlled by the CAG promoter	Adherent	For assessing recombination frequency following provision of Cre recombinase	1 in 8
HSV-2.3.2E2	The $CD8^+$ T cell clone HSV-2.3 fused with the BWZ.36 cell line containing the NFAT-lacZ construct	Semi-adherent	As effectors for use with the *in vitro* antigen presentation assays	1 in 10

Table 2-4. Mammalian cell lines used in this thesis. For further details on Vero, 293A and MC57G cell lines, refer to the American Type Culture Collection (www.atcc.org), USA. Vero SUA, 293-K^b, DC2.4 cell lines and the HSV 2.3.2E2 hybridoma have been described previously (Mueller et al., 2002; Rinaldi et al., 1999; Shen et al., 1997; Tscharke et al., 2005).

Cell Line	Origin	Property	Use	Split Ratio
293-K^b	293A cells that stably express H-$2K^b$ under the control of the CMV IE promoter	Adherent	As stimulators for use with the *in vitro* antigen presentation assays	1 in 12
DC2.4	Dendritic cell-like cell line generated from a C57Bl/6 mouse which expresses H-$2K^b$ and H-$2D^b$	Adherent	As stimulators for use with the *in vitro* antigen presentation assays	1 in 16
MC57G	Fibrosarcoma cell line generated from a tumour arising in a C57Bl/6 mouse treated with methycholanthrene	Adherent	As stimulators for use with the *in vitro* antigen presentation assays	1 in 14

Table 2-4 cont. Mammalian cell lines used in this thesis.

2.1.14 Viruses

The viruses constructed in this study are listed in Table 2-5, and described in more detail in Chapter three. HSV-1 KOS and KOS.6β were kindly provided by Dr. F. R. Carbone (University of Melbourne, Australia). All were titrated prior to use.

Virus	Description	Reference
HSV-1 KOS	Wildtype HSV-1 strain KOS	Smith, 1964
KOS6β	KOS that expresses β-gal under the control of the U_L39 (encoding the protein ICP6) promoter	Summers et al, 2001
HSV-1 pC_mC	KOS expressing mCherry under the control of the CMV IE promoter from the U_L3/U_L4 intergenic region	Unpublished
HSV-1 pICP47_eGC	KOS expressing an eGFP/Cre fusion gene under the control of the ICP47 promoter with the OriS deleted from the U_L3/U_L4 intergenic region	Unpublished
HSV-1 pgB_eGC	KOS expressing an eGFP/Cre fusion gene under the control of the U_L27 (gB) promoter from the U_L3/U_L4 intergenic region	Unpublished
HSV-1 pICP6_eGC	KOS expressing an eGFP/Cre fusion gene under the control of the U_L39 (ICP6) promoter from the U_L3/U_L4 intergenic region	Unpublished
HSV-1 pC_eGC	KOS expressing an eGFP/Cre fusion gene under the control of the CMV IE promoter from the U_L3/U_L4 intergenic region	Russell et al, 2015

Table 2-5. Details of viruses used in this thesis.

Virus	Description	Reference
HSV-1 pICP0_eGC	KOS expressing an eGFP/Cre fusion gene under the control of the α0 (ICP0) promoter from the U_L3/U_L4 intergenic region	Unpublished
HSV-1 LAT pCmC	KOS expressing mCherry gene under the control of the CMV IE promoter from the LAT region	Unpublished
HSV-1 pLAT_eGC	KOS expressing an eGFP/Cre fusion gene under the control of an IRES to dictate expression of this gene from the LAT promoter	Unpublished
HSV-1 pICP47/Tdtom	KOS expressing Tdtomato under the under the control of the ICP47 promoter with the OriS deleted from the U_L26/U_L27 intergenic region	Russell et al, 2015
HSV-1 ESminigB_Cre	KOS expressing an eGFP/Cre fusion gene under the control of the CMV IE promoter. In the opposite direction an ER-targeted gB_{498} minigene is expressed under the gB promoter, from the U_L3/U_L4 intergenic region	Unpublished
HSV-1 minigB_Cre	KOS expressing an eGFP/Cre fusion gene under the control of the CMV IE promoter. In the opposite direction a cytosolic gB_{498} minigene is expressed under the gB promoter, from the U_L3/U_L4 intergenic region	Unpublished

Table 2-5 cont. Details of viruses used in this thesis.

2.1.15 Antibodies and immunological reagents

The antibodies used in this study are listed in Table 2-6. When required, the cell culture supernatant from the 2.4G2 hybridoma cell line, which produces anti-mouse CD16/CD32, was used as a Fc receptor block.

Antibody	Species	Clone
Anti-mouse-CD8α-APC-Cy7[1]	Rat	53-6.7
Anti-mouse-CD62L-FITC[2]	Mouse	MEL-14
Anti-mouse-CD45.2-BV421[3]	Mouse	104
Anti-mouse-CD4-PE-Cy7[4]	Rat	GK1.5
Anti-human/mouse-GzmB-AlexaFluor647	Mouse	GB11

Table 2-6. Details of commercially antibodies used in this thesis. All antibodies were sourced from Biolegend. [1]APC-Cy7: allophycocyanin-cyanine 7. [2]FITC: Fluorescein isothiocyanate. [3]BV421: Brilliant Violet 421. [4]PE-Cy7: phycoerythrin-cyanine 7

A dextramer consists of a dextran backbone with an optimised number of MHC molecules and a fluorochrome bound to it, allowing for the detection of antigen-specific T cell TCRs that bind the MHC-antigen complex (Batard et al., 2006). A dextramer was used in this thesis that was specific for the gB_{498} epitope (amino acid sequence SSIEFARL) in the context of the H-$2K^b$ MHC allele and contained the phycoerythrin (PE) fluorochrome to enable detection by flow cytometry.

2.2 Methods

2.2.1 Growth and maintenance of bacteria

E. coli were grown at 37°C overnight in liquid LB broth in a shaking incubator or on solid LB-agar plates supplemented with antibiotics as appropriate. Bacterial stocks were stored at -80°C as glycerol stocks (400 µL of 60% (v/v) glycerol and 600 µL of overnight culture).

2.2.2 DNA purification

2.2.2.1 Plasmid DNA isolation

For most plasmids, plasmid DNA was isolated from 1.5 to 4 mL of liquid *E. coli* cultures using the Axygen plasmid MiniPrep kit according to the manufacturer's instructions, including the optional W2 washing step. The DNA was eluted in 60 µL of sterile water.

If a plasmid was low copy number, the transformed bacteria grew poorly or a large mass of DNA was required, DNA was extracted from 100 mL of liquid *E. coli* cultures using the Axygen MidiPrep kit according to the manufacturer's instructions. DNA was eluted in 500 µL of sterile water.

2.2.2.2 Purification of PCR products

PCR products were purified using the Gene Clean Spin kit according to the manufacturer's instructions. The DNA was eluted in 15 µL of sterile water.

In some circumstances, DNA was purified from an agarose gel to ensure that DNA of the correct size was isolated. After DNA gel electrophoresis (refer to Section 2.2.5), the agarose gel was stained with DNA staining solution and illuminated using an Invitrogen Safe Imager Blue-Light Transilluminator (Life Technologies). The bands containing the DNA fragment of the appropriate size were excised from the gel. The Gene Clean Spin kit was used to purify the DNA fragments from the gel according to the manufacturer's instructions. The DNA was eluted in 15 µL of sterile water.

2.2.2.3 Crude plasmid isolation for size differentiation (colony cracking)

Colony cracking was used to rapidly screen transformed bacterial colonies to identify clones carrying a plasmid of the correct size. This method was used when the insert was large and there was a substantial size difference between the parent vector and the newly constructed plasmid. Single bacterial colonies were selected from LB-agar plates and spotted onto a fresh LB-agar plate with the appropriate antibiotic, with the remainder resuspended in 40 µL 10 mM EDTA. Next, 50 µL of freshly made cracking buffer was added to each colony and incubated for five minutes at room temperature. Then, 10 µL of marker mix was added and incubated for five minutes on ice. The mixture was centrifuged at 20200 *g* for three minutes, and approximately 30 µL of the supernatant was loaded onto a 1% (w/v) agarose gel and run against the supercoiled DNA ladder (refer to Section 2.2.5).

2.2.2.4 Purification of infectious HSV-1 DNA for transfection

To generate infectious HSV-1 DNA for the cotransfection of viral and plasmid DNA to construct recombinant viruses (refer to Section 2.2.11.1), confluent Vero cell monolayers were infected at a multiplicity of infection (MOI) of 0.1 and incubated at 37°C and 5% CO_2 for 24 hours or until full CPE is evident. The cells were harvested in media and centrifuged at 820 *g* for 10 minutes at 4°C and the supernatant was discarded. The cell pellet was washed with cold PBS, before being resuspended in TE with 0.5% (w/v) SDS and 50 µg/mL proteinase K, and incubated at 37°C overnight. This aqueous mix was then mixed with an equal volume of phenol and inverted carefully to mix the two phases. This mix was then centrifuged at 4300 *g* for 15 minutes to separate the two phases. The aqueous phase was then re-extracted with phenol:chloroform at least twice more. The final aqueous phase was then extracted with chloroform to remove trace phenol, before the DNA is precipitated by mixing the last aqueous phase with 0.1 volume of 3 M sodium acetate and three volumes of 100% ethanol. The DNA was pelleted by centrifugation at 5050 *g* for five minutes. The pellet was gently washed with 70% ethanol before being air dried and then suspended in an appropriate volume of TE and incubated on ice overnight.

2.2.2.5 Crude virus DNA preparation from isolated plaques and viral stocks

Viral DNA was prepared from isolated plaques to serve as the template for diagnostic PCRs (refer to Section 2.2.12). 96 well plates of confluent Vero cells were prepared and 75 µL of the virus from individual isolated plaques was added to each well as appropriate. The cells were incubated for two days at 37°C in 5% CO_2. The media was then removed and the infected cell monolayers were washed with PBS before 100 µL of 10 µg/mL proteinase K in 1× ThermoPol buffer in sterile water was added to each well. The plates were then

frozen in a -80°C freezer and thawed to lyse cell membranes to release the virus. Alternatively, 10 µL of virus was mixed with 1× ThermoPol buffer in sterile water to a total volume of 100 µL. The plates were incubated at 56°C for 20 minutes, and then 85°C for 15 minutes. The undiluted supernatant was used as template for diagnostic PCRs.

2.2.2.6 Purification of HSV-1 DNA for use in whole genome digests

To generate purified HSV-1 DNA for use in whole genome digests (refer to Section 2.2.4), confluent Vero cell monolayers were infected at an MOI of 0.1 and incubated at 37°C and 5% CO_2 for 24 hours or until full CPE is evident. The cells were harvested in media and centrifuged at 820 *g* for 10 minutes at 4°C to separate the supernatant and cellular debris. The supernatant was collected and stored on ice. The cells were then lysed with RSB buffer containing 0.5% (v/v) IGEPAL by incubation for ten minutes on ice. The nuclei are then pelleted by centrifuging this sample at 820 *g* for 10 minutes at 4°C. The supernatant was collected and the cell pellet was extracted again using RSB buffer containing 0.5% (v/v) IGEPAL. All of the supernatants were pooled and pelleted by centrifuging at 17 680 *g* for two hours at 4°C. The pellet was then resuspended in 1.6 mL of TE with 0.5% SDS and 50 µg/mL proteinase K, and incubated at 37°C for 5 minutes. This aqueous mixture was divided into two separate aliquots and was then mixed with an equal volume of phenol:chloroform and carefully inverted until all phases were uniformly mixed. This mix was then centrifuged at 20200 *g* for 10 minutes to separate the two phases. The aqueous phase was then re-extracted with phenol:chloroform at least twice more. The DNA was precipitated by mixing the last aqueous phase with 0.1 volume of 3M sodium acetate and three volumes of 100% ethanol. The DNA was pelleted by centrifugation at 20200 *g* for 20 minutes. The pellet was gently washed with 70% ethanol before being air dried and then resuspended in an appropriate volume of TE and incubated on ice overnight.

2.2.2.7 Purification of nucleic acids by sodium acetate/ethanol precipitation

To purify linearised plasmids prior to transfection (refer to Section 2.2.11), an ethanol/sodium acetate precipitation was performed to purify the DNA in a sterile environment. The DNA was precipitated by the addition of 0.1 volume of 3 M sodium acetate and three volumes of 100% ethanol and vigorous mixing. If the DNA did not immediately form a visible precipitate, it was left to incubate on ice for 15 minutes. The DNA was centrifuged at 20200 *g* for 20 minutes to pellet the DNA, and then washed with 70% ethanol. The ethanol was removed in a clean environment within a biosafety cabinet and allowed to air dry for 15 minutes. The DNA was then resuspended in an appropriate volume of sterile DNA.

2.2.3 Polymerase Chain Reaction

PCR was performed for several purposes, including molecular cloning, screening of recombinant viruses and amplification of viral genomic DNA for sequencing. PCRs were performed in either 20 or 50 µL reaction volumes using either an Eppendorf Mastercycler or ABI Veriti 96-well Thermocycler. PCR using high fidelity Phusion DNA polymerase was performed when the products were used for the production of recombinant viruses or sequencing. For all remaining applications, PCR was carried out using *Taq* DNA polymerase. The template for PCR was either purified plasmid (refer to Section 2.2.2.1) or viral genomic DNA (refer to Section 2.2.2.5), diluted as required in sterile water.

To perform PCR using Phusion DNA polymerase, 1 unit of Phusion DNA polymerase, 1× Phusion HF buffer, 200 µM dNTPs, 0.5 µM of each forward and reverse primer and the appropriate volume (typically between 0.5 – 2 µL; usually about 1 ng) of template DNA were mixed together to a final volume of 20 µL with sterile water. If the desired DNA fragment was predicted to have a high GC content, the Phusion HF buffer was replaced with the Phusion GC buffer and supplemented with 4% DMSO, and the mass of template DNA used was reduced ten-fold. The samples were then run on a PCR machine using the following program, with the appropriate annealing temperature determined using the Thermo Scientific T_m calculator based on Breslauer's thermodynamics1:

Initial denaturation - 98°C for 3 min

Amplification and detection – 30 cycles of:

a. Denaturation - 98°C for 10 s
b. Annealing – the appropriate T_m for 30 s
c. Extension - 72°C for 30 s per kb

Cooling – hold at 4°C

To perform PCR with *Taq* DNA polymerase, 1 unit of *Taq* DNA polymerase was added to 1× ThermoPol buffer, 200 µM dNTPs, 0.5 µM of each forward and reverse primer, and 2 µl of DNA (usually about 1 ng of DNA) in a final volume of 25 µl in sterile water. Samples were then run on a PCR machine, using the following program:

Initial denaturation - 95°C for 30 s

Amplification and detection – 30 cycles of:

a. Denaturation - 95°C for 30 s
b. Annealing – the appropriate T_m for 30 s
c. Extension - 72°C for 1 min per kb

Cooling – hold at 4°C

The appropriate annealing temperature was determined using the formula:

$$T_m = (\#\text{ of A and T bases}) \times 2 + (\#\text{ of G and C bases}) \times 4$$

2.2.4 Restriction enzyme digestion

Restriction enzyme digests were used to linearise plasmids for cloning, diagnostic screening of newly generated plasmids, to linearise plasmids prior to transfection and for confirmation of the genomic structure of newly constructed viruses. Digests were carried out according to the manufacturer's (New England Biolabs) instructions and incubated at the recommended temperature for one to 16 hours. When appropriate, restriction enzymes were inactivated by heating at 65°C, or as recommended, for 15 minutes.

2.2.5 DNA gel electrophoresis

To visualise PCR products or the resulting DNA fragments following restriction enzyme digest, these DNA fragments were separated by gel electrophoresis. To resolve fragments that were larger than 200 bp, a 0.8, 1 or 2% (w/v) TAE agarose gel was cast as appropriate. 0.5 µg of DNA ladder per lane was loaded into a well of each gel as appropriate for use as a molecular size standard. Samples were mixed with the appropriate volume of 6× DNA loading dye and loaded into the wells. Gels were run at 30 to 100 V for 35 min to 6 hours as required in a horizontal electrophoresis apparatus (Bio-Rad) filled with 1× TAE buffer. The gel was then post stained with DNA staining solution for 15 to 20 minutes and the gel was visualised using a UV transilluminator system (Vilber-Lourmat). The size and concentration of the resulting DNA fragments were estimated by comparison to the DNA ladder.

To resolve DNA fragments smaller than 200 bp, 12% polyacrylamide gels were used to separate DNA fragments based on size. Gel plates were washed thoroughly with RO water, followed by 100% ethanol and allowed to air dry. 10 mL of the 12% polyacrylamide gel solution was prepared by mixing together 3.6 mL of acrylamide, 1.2 mL of 10× TBE, 200 µL of 10% (w/v) APS, 10 µL of TEMED and 4.8 mL sterile water. The gels were cast in a Mini PROTEAN casting apparatus (Bio-Rad). Samples were mixed with the appropriate volume of 6× DNA loading dye and 10 µL was loaded to the wells along with 0.5 µg of a low MW DNA ladder per lane for use as a molecular size standard. Samples were electrophoresed in 1× TBE at 60 V for two hours on a Mini PROTEAN Tetra cell apparatus (Bio-Rad). The gel was then post stained with DNA staining solution for 15 minutes before visualisation of the gel using a UV transilluminator system.

2.2.6 Molecular cloning

Two methods were used for the construction of plasmids during this project, namely InFusion cloning (Clontech) and standard ligation of digested or amplified DNA. Those plasmids that were difficult to clone due to troublesome secondary structure were purchased from GenScript.

2.2.6.1 In-Fusion molecular cloning

In-Fusion cloning is a recombination based cloning strategy that was used to insert one or two PCR products into a linearised plasmid in a single reaction. The plasmids that were constructed using the In-Fusion cloning method are described in Table 2-7 and 2-8. Each insert was amplified by PCR using a high fidelity polymerase from HSV-1 or plasmid DNA with the appropriate primers (Tables 2-7 and 2-8). These primers contain 15 nucleotide extensions at their 5' end that are identical to the vector sequence flanking a unique restriction site in the vector or are complementary to a neighbouring PCR product. If more than two inserts were required, they were first joined together by splice overlap PCR to join them together before cloning. In splice overlap PCR, each fragment was amplified such that the overlapping sequences at the end were added. These amplified fragments with regions of homology on the two ends to be joined together, were then used as template DNA for another PCR with the external primers, such that they will knit together.

Plasmid produced	Vector details			Insert(s) details		
	Parental plasmid	Forward primer	Reverse primer	Template DNA	Forward primer	Reverse primer
pT U_L3/U_L4	pTracer-CMV/bsd	pTracer bla	pTracer EF1	HSV-1 KOS	UL3 Lf	UL3 Rf
					UL4 Lf	UL4 Rf

Table 2-7. Description of the strategy used to construct plasmid pT U_L3/U_L4 by In-Fusion cloning. To linearise the pTracer-CMV/bsd, the vector was amplified using the primers described. The U_L3 and U_L4 fragments were amplified with 5' end which are identical to the vector sequence flanking a unique restriction site in the vector or are complementary to the neighbouring PCR product. The three fragments were joined together by In-Fusion cloning.

Plasmid produced	Vector details		Insert details		
	Parental plasmid	Restriction enzyme(s)	Template DNA	Forward primer	Reverse primer
pT CMV IE_mC	pTracer CMV/bsd	SpeI	pTracer CMV/bsd	CMV IE Lf	CMV IE Rf
			pT456	mCherry Lf	mCherry Rf
pT CMV IE_mC_BGH	pT CMV IE_mC	SpeI	pTracer CMV/bsd	CMV IE Lf	mCherry Rf II
			pTracer CMV/bsd	BGH Lf	BGH Rf II
pT eGC	pT U_L3/U_L4	SpeI	pIGCN21	eGFP Cre Lf II	pT Rev Cre C
			pTracer CMV/bsd	BGH Lf	BGH Rf II
pT pgB_eGC	pT eGC	SpeI	HSV-1 KOS	gB P Fwd	gB P Rev
pT pICP6_eGC	pT eGC	SpeI	HSV-1 KOS	RR1 P Fwd	RR1 P Rev
pT pC_eGC	pT eGC	SpeI	pTracer CMV/bsd	CMV Fwd	CMV Rev
pUC57 LAT pCmC	pUC57 pLAT eGC	SpeI and NotI	pTracer CMV IE_mC	LAT CMV Fwd	LAT mC Rev
pU26/7 pICP47/Tdtom	pU26/7 pICP47	NotI	pCIGH3	Tomato BGH Fwd	Tomato BGH Rev
pU3.0.5kbF	pCR-Blunt II	HindIII and NotI	HSV-1 KOS	0.5Lf Fwd	Consensus Lf Rev
			HSV-1 KOS	Consensus Rf Fwd	0.5Rf Rev
pU3.1kbF	pCR-Blunt II	HindIII and NotI	HSV-1 KOS	1Lf Fwd	Consensus Lf Rev
			HSV-1 KOS	Consensus Rf Fwd	1Rf Rev

Table 2-8. Description of the strategy used to construct plasmids using In-Fusion cloning. The cloning strategy used to construct each plasmid is described. The vector was linearised with the indicated restriction endonuclease. The insert(s) were amplified using the primers indicated, with sequences added onto the 5' end that are identical to the vector sequence flanking a unique restriction site in the vector or are complementary to the neighbouring PCR product. If more than two inserts were inserted into the vector, they were first joined by splice overlap PCR.

Plasmid produced	Vector details		Insert details		
	Parental plasmid	Restriction enzyme(s)	Template DNA	Forward primer	Reverse primer
pU3.2kbF	pCR-Blunt II	HindIII and NotI	HSV-1 KOS	2Lf Fwd	Consensus Lf Rev
			HSV-1 KOS	Consensus Rf Fwd	2Rf Rev
pU3.3kbF	pCR-Blunt II	HindIII and NotI	HSV-1 KOS	2.6Lf Fwd	Consensus Lf Rev
			HSV-1 KOS	Consensus Rf Fwd	3Rf Rev
pT pICP0_eGC	pT pICP0 mC Cre	NheI	pT pICP0 mC Cre	pICP0 mC Fwd	pICP0 GFP Rev
pU3.2kbF-gBCre	pU3.2kbF-ESgBCre	KpnI and SpeI	pU3.2kbF-ESgBCre	noESF1	noESR1
				noESF2	noESR2
pU3.2kbF-ESgBCre	pU3.2kbF	NotI	pT pC_eGC	GFP/Cre F	GFP/Cre R
			pT pgB_eGC	pgB F	pgB R
			MVA p7.5 ESmini (gB-498-505)	minigB F	minigB R
			pT U_L3/U_L4	SV40 F	SV40 R

Table 2-8 cont. Description of the strategy used to construct plasmids using In-Fusion cloning.

Prior to cloning, the vector and insert DNA was coprecipitated, with 100 ng of vector DNA and a 2:1 molar ratio of insert to vector DNA. The DNA was precipitated by mixing together 1/10 volume 3 M sodium acetate, three volumes of 100% ethanol and 20 µg of glycogen, followed by vigorous mixing. The DNA was centrifuged at 20200 *g* for 15 minutes to pellet the DNA, and then washed with 70% ethanol. The DNA pellet was allowed to air dry for 15 minutes, and then resuspended in 8 µL of sterile DNA.

The In-Fusion HD cloning kit (Clontech) was used according to the manufacturer's instructions. In general, a 2:1 molar ratio of insert to vector was used, with a final volume of 10 µL. 2.5 µL of the undiluted In-Fusion reaction mix was used for transformation into chemically competent *E. coli* by heat shock (refer to Section 2.2.8).

2.2.6.2 Conventional ligation for molecular cloning

DNA fragments that were unable to be amplified efficiently due to secondary structure were excised from the parental plasmid by restriction digest. The vector was linearised with enzyme such they produce complementary overhanging sequences. These plasmids were constructed using a conventional ligation strategy, with the details shown in Table 2-9.

Plasmid produced	Parental plasmid	Template plasmid	Restriction enzyme (s)
pT pICP47_eGC	pT eGC	pUC57 pICP47 w/o OriS	SpeI
pU26/7 pICP47	pU26/7	pUC57 pICP47 w/o OriS	SpeI
pU3.0.5kbF-Venus	pU3.0.5kbF	pUC57 pICP47 Venus	KpnI
pU3.1kbF-Venus	pU3.1kbF	pUC57 pICP47 Venus	KpnI
pU3.2kbF-Venus	pU3.2kbF	pUC57 pICP47 Venus	KpnI
pU3.3kbF-Venus	pU3.3kbF	pUC57 pICP47 Venus	KpnI
pT pICP0_mC Cre	pT U_L3/U_L4	pUC57-pICP0 mC Cre	SpeI

Table 2-9. Description of the strategy used to construct plasmids by a conventional ligation method. The cloning strategy used to construct each plasmid is described. The vector and insert was linearised with the indicated restriction endonuclease and were cloned together using T4 DNA ligase.

The vector was first dephosphorylated using Antarctic phosphatase according to the manufacturer's instructions (New England Biolabs). Briefly, 1× Antarctic phosphatase reaction buffer, 5 units of Antarctic phosphatase and 1 µg of linearised plasmid DNA were mixed to a final volume of 15 µL in sterile water and incubated for 15 minutes at 37°C. The enzyme was then heat inactivated by incubating at 70°C for five minutes.

Prior to ligation, the insert and vector DNA was coprecipitated as described in Section 2.2.6.1, with 100 ng of vector DNA and a 2:1 molar ratio of insert to vector DNA. This DNA was ligated using the LigaFast rapid DNA ligation system (Promega) according to the manufacturer's instructions with three units of T4 DNA ligase. 2.5 µL of the undiluted ligation reaction was used for transformation into chemically competent *E.coli* by heat shock (refer to Section 2.2.8).

Finally, to construct the plasmid pX330-minigB, single stranded oligodeoxynucleotides were annealed and cloned into the vector pX330 (as described by Cong et al., 2013). The vector pX330 was linearised using the restriction endonuclease BbsI (New England Biolabs) as previously described (refer to Section 2.2.4). The oligodeoxynucleotides S_ER

and AS_ER (sequences CACCGGCCGCGCTGCAGACTGCCGCA and AAACTGCGGCAGTCTGCAGCGCGGCC, respectively) were annealed by mixing together 100 μM of each oligonucleotide and 1× T4 ligation buffer (New England Biolabs) in sterile water, and incubating at 95°C for five minutes, before leaving to cool to room temperature. To ligate the oligodeoxynucleotides into the vector, approximately 25 ng of vector and 20 μM of the annealed oligodeoxynucleotides were mixed with 10 units of BbsI, 4.5 units of T4 DNA ligase (New England Biolabs) and 1× T4 ligation buffer in a final volume of 15 μL in sterile water. This mix was then incubated at 37°C for one hour and 2 μL of the reaction was then used for transformation into Stbl3 competent cells by heat shock (refer to Section 2.2.8).

2.2.7 Nucleic acid quantification

For routine determination of DNA concentration, the DNA quantity was measured in 2 μL samples using a Nanodrop UV/Vis spectrophotometer (Thermo Scientific) or a BioSpec Analyzer (Shimadzu). To quantify nucleic acid concentration more accurately and sensitively for use in qPCR applications, a Qubit fluorometer (Life Technologies) was employed. To detect RNA, the Qubit RNA HS assay kit (Life Technologies) was used according to the manufacturer's instructions. To detect DNA, the Qubit dsDNA HS assay kit (Life Technologies) was used as per the manufacturer's instructions.

2.2.8 Transformation by heat shock

50 μL of α-Select Chemically Competent *E. coli* or XL10 Gold Chemically Competent *E. coli* were aliquoted in 14 mL polypropylene tubes (Falcon) and mixed with 2.5 μL of InFusion or ligation mixture, or 1 μL of purified plasmid. The bacteria were incubated on ice for 30 minutes, and heat shocked at 42°C for 30 seconds. Next, the bacteria were placed on ice for two minutes, before the addition of 950 μL of SOC. The bacteria were allowed to recover at 37°C for one hour with shaking. Between 50 and 200 μL of bacteria were plated onto LB-agar plates with the appropriate antibiotics and incubated at 37°C overnight.

Alternatively, 50 μL of OneShot Stbl3 competent cells (Invitrogen) were mixed together with 2 μL of the DNA ligation and were incubated on ice for 30 minutes. The bacteria were then heat shocked at 42°C for 45 seconds and then left on ice for two minutes. Next, 250 μL of pre-warmed SOC was added to the vial before the bacteria were left to recover at 37°C for one hour with shaking. 25 μL of cells were plated onto LB-agar plates with the appropriate antibiotics and incubated at 37°C overnight.

The transformants were then screened by colony cracking (refer to Section 2.2.2.3), and the insertion was confirmed by restriction digest of isolated plasmid DNA (refer to Section 2.2.4) and DNA gel electrophoresis (refer to Section 2.2.5) followed by sequencing (refer to Section 2.2.9).

2.2.9 DNA sequencing

DNA sequencing reactions were carried out using Big Dye Terminator according to the ACRF Biomolecular Resource Facility (JCSMR, ANU) guidelines. Briefly, up to 20 ng of PCR product or 150 to 300 μg of purified plasmid was added to 1 μL of BigDye terminator, 3.2 pmol of the appropriate primer, and 3.5 μL of reaction buffer, and made up to a total reaction volume of 20 μL with sterile water. The details of the oligonucleotide primers used in the sequencing reactions are found in Table 2-10. The sequencing reaction was then performed as follows:

Initial denaturation - 96°C for 5 min

Amplification and detection – 30 cycles of:

a. Denaturation - 96°C for 10 s
b. Annealing – 50°C for 5 s
c. Extension - 60°C for 4 min

Cooling – hold at 4°C

Primer Name	Used to Sequence
2Lf Seq Rev	pU3.2kbF; pU3.3kbF; HSV-1 ESminigB_Cre; HSV-1 minigB_Cre
2Rf Seq Fwd	pU3.2kbF; pU3.3kbF; HSV-1 ESminigB_Cre; HSV-1 minigB_Cre
3Lf Seq Fwd	pU3.3kbF; HSV-1 ESminigB_Cre; HSV-1 minigB_Cre
3Lf Seq Rev	pU3.3kbF
3Rf Seq Rev	pU3.3kbF; HSV-1 ESminigB_Cre; HSV-1 minigB_Cre
3Rf Seq Fwd	pU3.3kbF
BGH Seq Fwd	pU26/7 pICP47/Tdtom
BGH Seq Rev	pU26/7 pICP47/Tdtom
bla seq	pT U_L3/U_L4; pT eGC; pT pgB_eGC; pT pICP6_eGC
Cre Lf Seq	pT eGC; pT pgB_eGC; pT pICP6_eGC; HSV-1 pICP47_eGC; HSV-1 pICP6_eGC; HSV-1 pgB_eGC; HSV-1 pC_eGC; pT pICP0 mC Cre; pU3.2kbF-minigB_Cre; HSV-1 ESminigB_Cre; pT pICP0_eGC; HSV-1 pICP0_eGC; HSV-1 minigB_Cre

Table 2-10. Details of oligodeoxynucleotides used in sequencing reactions.

Primer Name	Used to Sequence
Cre Rf Seq	pT eGC; pT pgB_eGC; pT pICP6_eGC; HSV-1 pICP47_eGC; HSV-1 pICP6_eGC; HSV-1 pgB_eGC; pT pICP0 mC Cre; pU3.2kbF-minigB_Cre; HSV-1 ESminigB_Cre; pT pICP0_eGC; HSV-1 pICP0_eGC; HSV-1 minigB_Cre
ef-1 seq	pT U_L3/U_L4; pT eGC; pT pgB_eGC; pT pICP6_eGC
eGFP/Cre Lf Seq	pT eGC; pT pgB_eGC; pT pICP6_eGC; HSV-1 pICP47_eGC; HSV-1 pICP6_eGC; HSV-1 pgB_eGC; HSV-1 pC_eGC; pU3.2kbF-minigB_Cre; HSV-1 ESminigB_Cre; pT pICP0_eGC; HSV-1 pICP0_eGC; HSV-1 minigB_Cre
eGFP/Cre Rf Seq	pT eGC; pT pgB_eGC; pT pICP6_eGC; HSV-1 pICP47_eGC; HSV-1 pICP6_eGC; HSV-1 pgB_eGC; HSV-1 pC_eGC; pU3.2kbF-minigB_Cre; HSV-1 ESminigB_Cre; pT pICP0_eGC; HSV-1 pICP0_eGC; HSV-1 minigB_Cre
EGFPnoMet	pU3.0.5kbF-Venus; pU3.1kbF-Venus; pU3.2kbF-Venus; pU3.3kbF-Venus; pU3.2kbF-minigB_Cre; HSV-1 ESminigB_Cre; pT pICP0_eGC; HSV-1 pICP0_eGC; HSV-1 minigB_Cre
ER no Met	HSV-1 minigB_Cre
FwdHSV-gBend	pU26/7 pICP47/Tdtom
m13 Rev+	pU26/7 pICP47/Tdtom
mCfwd	pT pICP0 mC Cre
mCrev	pT pICP0 mC Cre
pgB R	pU3.2kbF-gB_Cre
pICP0 Seq Fwd	HSV-1 pICP0_eGC
pICP0 Seq Rev	HSV-1 pICP0_eGC
pICP47 Seq Fwd	HSV-1 pICP47_eGC; pU26/7 pICP47/Tdtom; pU3.0.5kbF-Venus; pU3.1kbF-Venus; pU3.2kbF-Venus; pU3.3kbF-Venus
pICP47 Seq Rev	HSV-1 pICP47_eGC; pU26/7 pICP47/Tdtom; pU3.0.5kbF-Venus; pU3.1kbF-Venus; pU3.2kbF-Venus; pU3.3kbF-Venus
pSC11lacZseq	pU26/7 pICP47/Tdtom
ptracer CMV IE Rf	pT U_L3/U_L4; pT CMV IE_mC; HSV-1 pC_mC; pT pICP0 mC Cre
ptracer mC Lf	pT U_L3/U_L4; pT eGC; pT pgB_eGC; pT pICP6_eGC; pT CMV IE_mC; HSV-1 pC_mC; pU3.2kbF-minigB_Cre; HSV-1 ESminigB_Cre; HSV-1 minigB_Cre
ptracer UL3 Lf	pT U_L3/U_L4; pT eGC; pT pgB_eGC; pT pICP6_eGC; HSV-1 pC_mC; HSV-1 pICP6_eGC; HSV-1 pgB_eGC; HSV-1 pC_eGC; pU3.0.5kbF; pU3.1kbF; pU3.2kbF; pU3.3kbF; pT pICP0 mC Cre; pU3.0.5kbF-Venus; pU3.1kbF-Venus; pU3.2kbF-Venus; pU3.3kbF-Venus; pU3.2kbF-minigB_Cre; HSV-1 ESminigB_Cre; pU3.2kbF-gB_Cre; HSV-1 minigB_Cre

Table 2-10 cont. Details of oligodeoxynucleotides used in sequencing reactions.

Primer Name	Used to Sequence
ptracer UL4 Rf	pT U_L3/U_L4; pT eGC; pT pgB_eGC; pT pICP6_eGC; HSV-1 pC_mC; HSV-1 pICP47_eGC; HSV-1 pICP6_eGC; HSV-1 pgB_eGC; HSV-1 pC_eGC; pU3.0.5kbF; pU3.1kbF; pU3.2kbF; pU3.3kbF; pT pICP0 mC Cre; pU3.0.5kbF-Venus; pU3.1kbF-Venus; pU3.2kbF-Venus; pU3.3kbF-Venus; pU3.2kbF-minigB_Cre; HSV-1 ESminigB_Cre; pT pICP0_eGC; HSV-1 pICP0_eGC; HSV-1 minigB_Cre
pX330 Seq F	pX330-ER
pX330 Seq R	pX330-ER
Seq RevpEGFPN1	pT eGC; pT pgB_eGC; pT pICP6_eGC; HSV-1 pgB_eGC; pU3.0.5kbF-Venus; pU3.3kbF-Venus; pU3.2kbF-minigB_Cre; HSV-1 ESminigB_Cre; pT pICP0_eGC; HSV-1 pICP0_eGC; pU3.2kbF-gB_Cre; HSV-1 minigB_Cre
Seq T7 Pro	pU3.0.5kbF; pU3.1kbF; pU3.2kbF; pU3.3kbF
SV40 F	pU3.2kbF-gB_Cre
Tdt Fwd	pU26/7 pICP47/Tdtom
UL26 Seq Rev	pU26/7 pICP47/Tdtom
UL27 Seq Fwd	pU26/7 pICP47/Tdtom; pU3.0.5kbF; pU3.1kbF; pU3.2kbF; pU3.3kbF
UL27 Seq Rev	pU26/7 pICP47/Tdtom
UL3 Seq Fwd	HSV-1 pC_mC; HSV-1 pICP47_eGC; HSV-1 pICP6_eGC; HSV-1 pgB_eGC; HSV-1 pC_eGC; HSV-1 ESminigB_Cre; HSV-1 pICP0_eGC; HSV-1 minigB_Cre
UL3 Seq Rev	HSV-1 pC_mC; HSV-1 pICP6_eGC; HSV-1 pgB_eGC; HSV-1 pC_eGC; pU3.0.5kbF; pU3.1kbF; pU3.2kbF; pU3.3kbF; HSV-1 ESminigB_Cre; HSV-1 pICP0_eGC; HSV-1 minigB_Cre
UL4 Seq Fwd	HSV-1 pC_mC; HSV-1 pICP47_eGC; HSV-1 pICP6_eGC; HSV-1 pgB_eGC; HSV-1 pC_eGC; pU3.0.5kbF; pU3.1kbF; pU3.2kbF; pU3.3kbF; HSV-1 ESminigB_Cre; HSV-1 pICP0_eGC
UL4 Seq Rev	HSV-1 pC_mC; HSV-1 pICP47_eGC; HSV-1 pICP6_eGC; HSV-1 pgB_eGC; HSV-1 pC_eGC; HSV-1 ESminigB_Cre; HSV-1 pICP0_eGC; HSV-1 minigB_Cre

Table 2-10 cont. Details of oligodeoxynucleotides used in sequencing reactions.

An ethanol/sodium acetate precipitation was performed to remove excess dye terminators from the sequencing reaction. 80 µL of a solution containing 75 mM sodium acetate, 3.125 mM EDTA and 75% ethanol was added to each 20 µL sequencing reaction and incubated at room temperature for 15 minutes to precipitate the extension products. The solution was centrifuged at 20200 *g* for 20 minutes to pellet the extension products, and then washed with 70% ethanol. Samples were dried and submitted to the ACRF Biomolecular Resource Facility (JCSMR, ANU) for sequencing. Vector NTI (version 11.0;

Life Technologies) and Chromas (Technelysium) were used for DNA sequence analysis. Sequences were analysed by comparison to the published HSV-1 KOS genome sequence (Accession #JQ673480, Macdonald et al., 2012) and the original assembled plasmid sequence.

2.2.10 Preparation of mammalian cell lines

The mammalian cell lines used in this study were described in Table 2-4. All cell culture and *in vitro* HSV-1 infections were incubated at 37°C in the presence of 5% CO_2. Cell lines were subcultured twice per week at a split ratio that ensured cells would grow to form a confluent monolayer within three or four days (Table 2-4). For long-term storage, cells were resuspended in the appropriate media with 10% DMSO, slowly cooled and kept in liquid nitrogen.

To subculture mammalian cells, media was removed and cells were washed gently with PBS to remove excess medium. The cells were then treated with trypsin for three minutes at 37°C or until all the cells detached. Then, the cells were diluted appropriately and transferred into new culturing flasks (Nunc), or 6- or 96- well flat bottomed tissue culture plates (Corning). Plates were incubated at 37°C with 5% CO_2 until grown into a semi-confluent or confluent monolayer as required.

2.2.11 Generation of recombinant viruses

The strategy used to generate recombinant HSV-1 produced in this study relies on homologous DNA recombination between a transfer plasmid containing the sequence of the desired insertion flanked by sequence homologous to the site of insertion in the viral genome, and the viral genome found within HSV-1 infected cells provided by one of two methods: cotransfection of viral and plasmid DNA (refer to Section 2.2.11.1), or transfection of plasmid DNA followed by infection with virus (transfection/infection; refer to Section 2.2.11.2).

2.2.11.1 Cotransfection of viral and plasmid DNA to generate recombinant viruses

In brief, a transfection mix was prepared by gently mixing 5 µg of viral genomic DNA and the appropriate mass of plasmid DNA in the required ratio in the required volume of MEM-0. The appropriate volume of Lipofectamine 2000 was resuspended in the appropriate volume of media as recommended by the manufacturer (Invitrogen) and incubated for five minutes at room temperature. The DNA was then mixed with the Lipofectamine mixture by gentle pipetting. This mix was then incubated at room temperature for 20 minutes. The medium on confluent 293A cell monolayers in six well

plates was replaced with 500 µL of MEM-0 and 500 µL of transfection mix was added to each well dropwise. This was incubated at 37°C with 5% CO_2 for five hours. This inoculum was then replaced with 2 mL of CMC-MEM. The use of phenol red-free MEM avoids the autofluorescence associated with this pH indicator. The cells were then incubated for three days at 37°C with 5% CO_2.

To harvest the recombinant virus generated, the plates were observed using fluorescence microscopy for the formation of plaques (Olympus microscope CKX41, equipped with the reflected fluorescence illuminator CKX-RFA). All plaques were counted and fluorescent plaques marked with a pen on the bottom of the plates. Individual plaques were then selected and collected in 500 µL MEM-0. Alternatively, all cells were harvested. In both cases, the cells were frozen on dry ice and then thawed in a 37°C water bath to lyse the cells and release the virus. This was repeated another two times. This cell lysate was used for the isolation of the recombinant viruses by plaque purification (refer to Section 2.2.12).

2.2.11.2 Infection/transfection method to generate recombinant viruses

A transfection mix was prepared by gently mixing 3 µg of linearised plasmid in 180 µl of MEM-0 with 6 µL of Lipofectamine 2000 in 180 µL of MEM-0. The mixture of DNA and Lipofectamine was then incubated at room temperature for 20 minutes. The medium on confluent 293A cell monolayers in six well plates was replaced with 500 µL of MEM-0 and 500 µL of transfection mix was added to each well dropwise. This was incubated at 37°C with 5% CO_2 for five hours. The transfection mix was then replaced with HSV-1 KOS at a MOI of 0.01 PFU of virus to cells in MEM-0 and incubated at 37°C with 5% CO_2 for a further two hours. The virus inoculum was then replaced with 2 mL of MEM-2 and incubated for three days at 37°C with 5% CO_2.

After two days, the cells were harvested. These cells were frozen on dry ice and then thawed in a 37°C water bath to lyse the cells and release the virus. This was repeated another two times. This cell lysate was used for the isolation of the recombinant viruses by plaque purification.

2.2.12 Plaque purification for the isolation of recombinant viruses

To isolate recombinant HSV-1 from its wildtype virus, plaque purification for the selection of the recombinant viruses was employed. This process was combined with fluorescent marker screening when possible. Briefly, the cell lysate from the transfection process (described in Section 2.2.11.1 and 2.2.11.2) was serially diluted in at least six five-fold steps with MEM-0. This was then added to confluent monolayers of Vero cells in six well

plates and incubated for two hours at 37°C with 5% CO_2. This inoculum was then replaced with 2 mL of CMC-MEM per well so that maintain individual plaques are maintained. The plates were incubated for two days at 37°C with 5% CO_2. Two days later, the plates were observed using an Olympus CKX41 microscope and all plaques were counted. If appropriate, recombinant plaques were identified by fluorescence microscopy, and the fluorescent plaques were marked with a pen on the bottom of the plates. The plaques were collected by scraping the cell monolayer with a 20 µL pipette tip and aspirating cells into the tip, and then transferring the cells into 500 µL MEM-0. Each sample was then frozen and thawed three times. The isolated plaques were then used to infect new plates for another round of plaque purification. After some rounds of plaque purification, the isolated plaques were analysed by diagnostic PCRs for the presence of recombinant and wildtype virus (refer to Section 2.2.3; Table 2-11).

Virus	Forward Primer	Reverse Primer	Amplified viral genome region	Expected size of the PCR product (bp)
HSV-1 pC_mC	pTracer UL3 Lf	pTracer UL4 Rf	U_L3/U_L4 intergenic region	502 (wildtype); 2073 (recombinant)
	pTracer UL3 Lf	pTracer CMV IE Rf	U_L3/U_L4 intergenic region with insertion of mCherry cassette	886
	pTracer mC Lf	pTracer UL4 Rf		1277
HSV-1 pICP6_ eGC	pTracer UL3 Lf	pTracer UL4 Rf	U_L3/U_L4 intergenic region	502 (wildtype); 2757 (recombinant)
	UL3 Seq Fwd	Seq RevpEGFPN1	U_L3/U_L4 intergenic region with insertion of pICP6_eGC cassette	1575
	Cre Lf Seq	UL4 Seq Rev		1991
HSV-1 pgB_ eGC	pTracer UL3 Lf	pTracer UL4 Rf	U_L3/U_L4 intergenic region	502 (wildtype); 2073 (recombinant)
	UL3 Seq Fwd	Seq RevpEGFPN1	U_L3/U_L4 intergenic region with insertion of pgB_eGC cassette	1612
	Cre Lf Seq	UL4 Seq Rev		1991
HSV-1 pC_eGC	pTracer UL3 Lf	pTracer UL4 Rf	U_L3/U_L4 intergenic region	502 (wildtype); 3149 (recombinant)
	UL3 Seq Fwd	Seq RevpEGFPN1	U_L3/U_L4 intergenic region with insertion of pC_eGC cassette	1945
	Cre Lf Seq	UL4 Seq Rev		1991

Table 2-11. Details of diagnostic PCRs used to identify the recombinant viruses constructed in this thesis. The names of the primers used to screen for the presence of recombinant, wildtype or parental viruses used in this thesis, with the expected size of the fragments generated. If only one fragment size is indicated, then wildtype virus would not be expected to amplify with the primers used.

Virus	Forward Primer	Reverse Primer	Amplified viral genome region	Expected size of the PCR product (bp)
HSV-1 pICP0_eGC	pTracer UL3 Lf	pTracer UL4 Rf	U_L3/U_L4 intergenic region	2073 (parent); 3492 (recombinant)
	UL3 Seq Fwd	pTracer CMV IE Rf	U_L3/U_L4 intergenic region with insertion of mCherry cassette	1919
	Cre Lf Seq	UL4 Seq Rev	UL3/UL4 intergenic region with the ICP0 promoter pICP0_eGC cassette	1995
HSV-1 LAT pCmC	ptracer mC Lf	LAT R2	LAT region with insertion of the CMV IE promoter mCherry cassette	928
HSV-1 pLAT_ eGC	eGFP/Cre Rf Seq	Cre Rf Seq	LAT region with insertion of the IRES/eGFP Cre cassette	782
	Cre F	Cre R		203
	ptracer mC Lf	LAT R2	LAT region with insertion of the CMV IE promoter mCherry cassette	928
HSV-1 pICP47/ Tdtom	UL26 Left	BGH Seq Rev	UL26/UL27 intergenic region with the ICP47 promoter Tdtomato cassette	1782
	Rev HSV gBend	Fwd HSV gBend		989 (wildtype); recombinant fails to amplify
HSV-1 ESminigB_ Cre	pTracer UL3 Lf	pTracer UL4 Rf	U_L3/U_L4 intergenic region	502 (wildtype); 3670 (recombinant)
	Cre Lf Seq	3Rf Seq Rev	U_L3/U_L4 intergenic region with the ESminigB_Cre expression cassette	2983
HSV-1 minigB_Cre	3Lf Seq Fwd	ER Rev	U_L3/U_L4 intergenic region with the ESminigB_Cre expression cassette	2298
	UL3 Seq Fwd	No ER Rev	U_L3/U_L4 intergenic region with the minigB_Cre expression cassette	1423

Table 2-11 cont. Details of diagnostic PCRs used to identify the recombinant viruses constructed in this thesis.

When the desired recombinant virus was found to be free of parent virus, a stock was grown (refer to Section 2.2.13). Where possible, the recombination and plaque purification process was performed twice in parallel to isolate two independent recombinant viruses.

2.2.13 Preparation of virus stocks

To prepare the initial seed stock of virus, a 25 cm^2 flask of confluent Vero cells was inoculated with the virus from an isolated plaque in 2 mL of MEM-0 and incubated at 37°C and 5% CO_2 for one hour. The inoculum was then replaced with MEM-2 and incubated at 37°C with 5% CO_2 for three days. The infected cells were then harvested and collected by centrifugation at 820 *g* for 10 minutes at 4°C. The supernatant was removed and cells resuspended in 500 µL of MEM-0. The cells were then subjected to three cycles of freeze/thawing by placing on dry ice until frozen and thawing in a 37°C waterbath to release the virus. If appropriate, a small fraction of this crude viral stock was removed and DNA was prepared (refer to Section 2.2.2.5). The appropriate region of insertion was then amplified and analysed by DNA sequencing to confirm that no errors could be identified in the inserted sequence or in the flanking HSV-1 sequence (refer to Sections 2.2.3, 2.2.5 and 2.2.9). If the sequence of the desired region was confirmed, this virus would be designated as the seed stock.

To prepare a master stock, a 75 cm^2 flask of confluent Vero cells was seeded with approximately one quarter of the seed stock in 5 ml of MEM-2 and incubated at 37°C and 5% CO_2 for one hour. An additional 10 mL of fresh warm MEM-2 was then added to the flask. The cells were then incubated at 37°C with 5% CO_2 for three days. The infected cells were then harvested and collected by centrifugation at 820 *g* for 10 minutes at 4°C. The supernatant was then removed and centrifuged at 17 684 *g* for 90 minutes at 4°C (supernatant-associated virus). The pellet was resuspended in 1 mL of MEM-0. Meanwhile, the cell associated virus was prepared by sonicating the cell pellet for 60 s at ~60% power (Branson 102 cup-horn sonifier). The cells were collected by centrifugation at 820 *g* for 10 minutes at 4°C. The supernatant was reserved, and the disruption and collection of cells was repeated again. The cell- and supernatant-associated virus was then pooled and this master stock was then titrated.

To prepare a working stock, five 175 cm^2 flasks were seeded at an MOI of 0.01 as described for a master stock, and after three days, or when the cells of the flask had reached full CPE, the virus stock was harvested as previously described for the master stock. This working stock was then titrated and transferred into small aliquots. Virus

stocks were stored at -80°C when not in use. Once thawed, any remaining virus that was unused was discarded.

2.2.14 Standard plaque assay for the titration of HSV-1

A standard plaque assay was performed to determine the virus titre of newly prepared virus stocks (refer to Section 2.2.13), samples from growth curves (refer to Section 2.2.16) or homogenates of organs isolated from infected mice (refer to Sections 2.2.21 and 2.2.22). Firstly, duplicate ten-fold dilutions of virus stock were prepared in MEM-0. The medium was removed from two six well plates of confluent Vero cells, and 0.5 mL of the appropriate virus dilutions, typically ranging from 10^{-1} to 10^{-10}, was added to the cells. The cells were incubated at 37°C and 5% CO_2 for 90 minutes, with rocking every 15 minutes to ensure that all cells are evenly infected with virus. The inoculum was then replaced with CMC-MEM and incubated for 48 hours at 37°C and 5% CO_2. The media was then removed and replaced with a crystal violet staining solution. After 15 minutes, excess staining solution was removed and plates were allowed to air dry. The stained plates were then visualised and counted using an Olympus CXK41 light microscope at 40× magnification. The virus concentration is calculated as the number of PFU per mL, and was calculated as an average of duplicate titrations for virus stocks. Duplication titrations that differed by more than two-fold were rejected and repeated.

2.2.15 Quantification of *in vitro* fluorescent protein expression from HSV-1 by flow cytometry

To quantify the expression of fluorescent proteins following transfection or infection of cells with a plasmid or virus designed to express a fluorescent protein, including enhanced GFP (eGFP), mCherry and Venus, a flow cytometry-based approach was used. If appropriate, a cell suspension was prepared via the typsinisation of adherent cells as previously described in Section 2.2.10. Up to 1×10^6 cells were transferred to 96 well round bottomed tissue culture plate (Falcon) and centrifuged at 462 *g* for 5 minutes at 4°C to pellet the cells. The cells were washed with PBS to remove excess media and were then fixed in 1% PFA by incubation at room temperature for 20 minutes. The cells were then centrifuged at 905 *g* for three minutes at 4°C to pellet the cells. They were then washed again with FACS-PBS, before being resuspended in 60 – 100 µL of FACS-PBS for flow cytometric analysis (refer to Section 2.2.30).

2.2.16 Viral *in vitro* growth curves

2.2.16.1 Single step growth curves

Confluent Vero cell monolayers in six-well tissue culture plates were infected with 5×10^6 PFU virus in 1 mL MEM-0 (MOI of 5) for one hour at 37°C with 5% CO_2. The unabsorbed virus was then removed and the cell monolayer was washed once with 1 mL of warm FACS-PBS. Next, 2 mL of MEM-2 was then added to each well. The 0 hour p.i. samples were harvested immediately after the addition of fresh media. The remaining plates were incubated for two, four, six, 12 and 24 hours before the cells were harvested. These cells were harvested by scraping them off the plates using cell lifters (Corning) and collecting them in the existing media. These samples were then subjected to three rounds of freezing and then thawing and titrated as described in Section 2.2.14.

2.2.16.2 Multiple step growth curves

Multiple step growth curves were performed by infecting confluent Vero cell monolayers with 1×10^4 PFU virus in 1 mL MEM-0 (MOI 0.01). The cells were incubated for one hour at 37°C with 5% CO_2. The unabsorbed viruses were then removed and the cell monolayer was washed once with 1 mL of warm FACS-PBS and then replaced with 2 mL of fresh MEM-2. The 0 hour p.i. samples were harvested immediately after the addition of fresh media. At six, 24, 48 and 72 hours p.i. the cells were harvested and titrated as described in Section 2.2.14.

2.2.17 Cycloheximide reversal and acyclovir inhibition assay

Confluent Vero SUA cell monolayers were pre-treated with 100 µg/mL cycloheximide or 50 µM acyclovir, or left untreated, for one hour at 37°C with 5% CO_2. The cells were then infected with 1×10^6 PFU of virus in 500 µL of the appropriate drug (MOI 5). After incubation for one hour at 37°C with 5% CO_2, the unabsorbed virus was removed and replaced with fresh media containing the appropriate drug. The cells were then incubated for six hours at 37°C, 5% CO_2. The media containing cycloheximide was then removed and those cells were washed three times with media containing 5 µg/mL actinomycin D. The washed cells were then overlaid with 2 mL of MEM-2 containing 5 µg/mL actinomycin D. The cells were incubated for a further four hours at 37°C, 5% CO_2. After this time, cell monolayers were photographed for the expression of eGFP at 400× magnification by fluorescence microscopy (Olympus microscope CKX41, equipped with the reflected fluorescence illuminator CKX-RFA, and Olympus DP20 digital microscope camera). The cell monolayers were then washed with PBS before being harvested with trypsin and transferred to a 96 well round bottomed plate (Falcon) for fixation. The cells were washed

with FACS-PBS, followed by PBS only, before being incubated with 1% PFA at room temperature for 20 minutes. The cells were then washed with FACS-PBS before being resuspended in 60 µL FACS-PBS for analysis by flow cytometry (refer to Section 2.2.30).

2.2.18 Staining of infected Vero SUA cell monolayers for detection of β-gal expression

Semi-confluent Vero SUA cell monolayers with approximately 8.2×10^4 cells per well in a 24 well plate were infected with 4.1×10^5 PFU per well in 500 µL MEM-0 (MOI 5). After incubation for one hour at 37°C with 5% CO_2, the unabsorbed virus was removed and the cell monolayer was washed with 500 µL of warm FACS-PBS. Next, 1 mL of MEM-0 was then added to each well. The 0 hour p.i. sample was immediately fixed, while the remaining samples were fixed at four, eight, 12, 16, 20 or 24 hours p.i. To fix cells, cell monolayers were washed with PBS, and overlaid with PFA/glutaraldehyde fixative. The cells were incubated at 4°C for at least one hour. The fixative was washed off with PBS, and cell monolayers were photographed for the expression of eGFP at 400× magnification by fluorescence microscopy (Olympus microscope CKX41, equipped with the reflected fluorescence illuminator CKX-RFA, and Olympus DP20 digital microscope camera). The permeabilisation buffer was then added to the cells and they were incubated at 4°C for 30 minutes. This buffer was then replaced with fresh permeabilisation buffer containing 1 mg/mL X-gal. After 16 hours, the buffer was removed, the cells were washed with PBS and the cell monolayer was overlaid with 50% glycerol. The cell monolayers were then photographed for the expression of β-gal by light microscopy without phase contrast (Olympus microscope CKX41 and DP20 camera).

2.2.19 Infection of mice with HSV-1

Female mice at least eight weeks of age were infected with 1×10^8 PFU of HSV-1 via tattoo on the flank (Russell et al., 2015) as a modification of the method developed by Simmons and Nash (1984). Mice were anesthetised by intraperitoneal (i.p.) injection of Avertin at a dose of approximately 250 mg/kg tribromoethanol using a 1 mL syringe (BD Biosciences) and 26G needle (BD Biosciences). The left flank was clipped from the dorsal to ventral midline, and depilated with Veet™ for sensitive skin to remove all hair. A small area of skin of the left flank (5 mm by 5 mm, or 25 mm^2) situated above the dorsal tip of the spleen was tattooed for ten seconds using Swiss rotary tattoo machine (Pullman Tools) using a ten round shader tattoo needle that had been dipped in a virus solution at a concentration of 1×10^8 PFU/mL in PBS. Excess inoculum was wiped off the skin. Mice were then bundled in tissue until they regained consciousness to maintain adequate core body temperature. Mice were monitored for clinical score, as indicated by ruffled fur,

hunched body and activity levels (see Table 2-12), and for the development of lesions on the day of the infection, and then from day two p.i. until such time as lesions were fully resolved. A total score of less than six was considered mild, a score of between three and five was considered moderate. A score of six was considered severe.

Criteria	Grade 0	Grade 1	Grade 2
Posture	Normal	Hunching noted only at rest	Severe hunching impairs movement
Activity	Normal	Mild to moderately decreased	Stationary unless stimulated
Fur texture	Normal	Mild to moderate ruffling	Severe ruffling/poor grooming

Table 2-12. Scoring scheme used to monitor clinical signs of systemic infection following HSV-1 infection. Symptoms for each of these criterion were categorised into three grades of severity. For symptoms within grades 0, 1 or 2, a mouse receives a score of 0, 1, or 2, respectively, with a possible total of 6 for all three criteria.

2.2.20 Harvesting tissue from mice

Mice were euthanised by asphyxiation with CO_2. All mice were swabbed with 80% ethanol prior to the removal of infected tissue. The DRG found on the ipsilateral side corresponding to spinal levels T5 to L1, located by their relationship to the ribs, were extracted using fine curved forceps DRG used for X-gal staining were placed into 50 µl of PFA/glutaraldehyde fixative for each DRG (refer to Section 2.2.23), while those used for titration or immunology experiments were pooled and placed into 800 µL of MEM-2 (refer to Section 2.2.22). Pooled DRG used for the extraction of nucleic acid were immediately snap frozen in a tube placed on dry ice (refer to Section 2.2.25.2). If required, skin was also excised as a 1 cm^2 region or the entire lesion area and placed into 800 µl of MEM-2 (refer to Section 2.2.22). The spleen may also have been removed and collected in 2 mL of DMEM-2 (refer to Section 2.2.26).

2.2.21 *In vitro* reaction of latent virus

DRGs from spinal levels T5 to L1 were harvested from an infected mouse and pooled together (refer to Section 2.2.20). The pooled DRG were incubated at 37°C and 5% CO_2 for five days. The DRGs were then homogenised in 1 mL glass tissue grinders (Wheaton) and subjected to three cycles of freeze/thawing by placing on dry ice until frozen and thawing in a 37°C waterbath. The titre of virus in DRGs was then quantified by a standard plaque assay (refer to Section 2.2.14).

2.2.22 Titration of virus from skin and DRG

Skin or pooled DRG from spinal levels T5 to L1 from each infected mouse were homogenized in MEM-2 in 1 mL glass tissue grinders. Homogenates were subjected to three cycles of freeze/thawing by placing on dry ice until frozen and thawing in a 37°C waterbath. Infectious virus was quantified by plaque assay on Vero cells (refer to Section 2.2.14).

2.2.23 X-gal staining of whole DRG for detection of β-gal expression

Following removal of DRG from mice (refer to Section 2.2.20) they were placed directly into 50 µL of the PFA/glutaraldehyde fixative for an hour on ice. The DRG were then thoroughly washed with PBS three times to remove the fixative before being placed into the permeabilisation buffer for 30 minutes on ice. This was then replaced with fresh permeabilisation buffer containing 1 mg/mL X-gal added just prior to use. The DRG were stained overnight for 16 hours at 4°C. The DRG were then rinsed in PBS, followed by clarification in 50% glycerol in PBS at 4°C overnight. Then, the individual DRG were placed on slides, dissected to remove unnecessary tissue (with care taken to ensure that this does not disrupt any X-gal stained cells) and a coverslip was mounted carefully above them. DRG were examined and photographed using an Olympus CKX41 light microscope with attached Olympus DP20 digital microscope camera at 40× magnification without phase contrast. The number of β-gal$^+$ cells per DRG was calculated as described in Section 2.2.31.2.

Although highly unlikely, it is possible that there could be expression of β-gal in ROSA26R mice in the absence of Cre expression. This could be either through the failure of the stop cassette to block expression of β-gal, or through recombination between the direct repeats of the *loxP* site that leads to the removal of the stop cassette (refer to Figure 1-3). To determine if this could account for the accumulation of β-gal$^+$ cells during the establishment of latency in ROSA26R mice, groups of ROSA26R mice were infected with either HSV-1 pICP47_eGC (Cre$^+$) or HSV-1 pICP47_Tdtom (Cre$^-$). These mice were then culled at 20 days p.i., their DRG removed and β-gal expression was assessed (Figure 2-1). In the ROSA26R mice infected with HSV-1 pICP47_eGC, a large population of β-gal$^+$ cells was observed. By contrast, for mice infected with the Cre$^-$ virus, HSV-1 pICP47_Tdtom, no β-gal$^+$ cells were detectable. This confirms that β-gal expression is undetectable in ROSA26R mice in the absence of Cre expression.

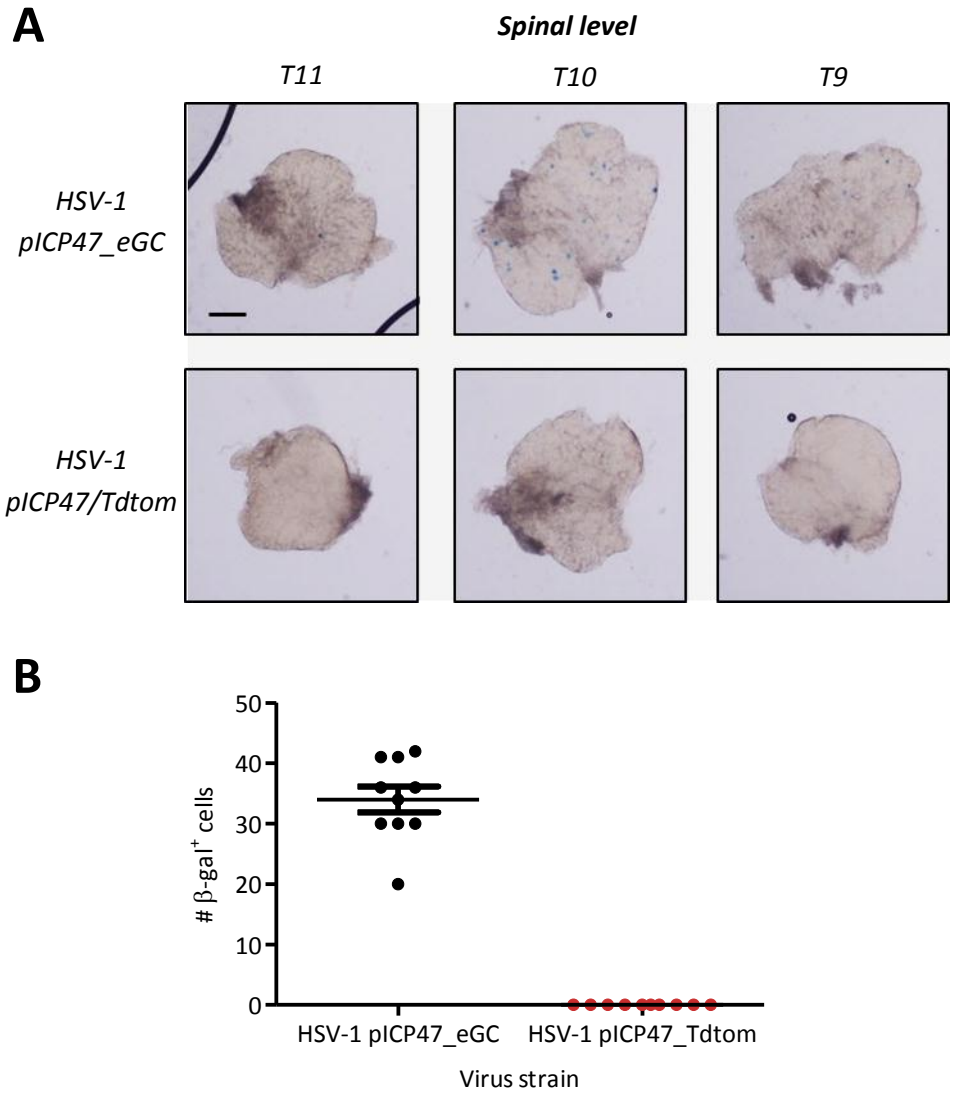

Figure 2-1. β-gal expression is undetectable during latency in the absence of Cre expression. Groups of five ROSA26R mice were infected with 1×10^8 PFU/mL HSV-1 pICP47_eGC or pICP47_Tdtom. At 20 days p.i. mice were culled and innervating DRG (from spinal levels T5 to L1) removed and processed for measurement of β-gal expression. Circles show results for each mouse and bars mean±SEM. Data are pooled from two independent experiments (n = 10 per virus).

2.2.24 Detection of fluorescent protein expression in whole DRG

To determine the number of cells within DRG that express fluorescent proteins like eGFP or Tdtomato, DRG were removed from mice infected with the appropriate virus (refer to Section 2.2.20) and were placed directly into 50 µL each of the PFA/glutaraldehyde fixative per DRG for an hour on ice. The DRG were then thoroughly washed with PBS three times to remove the fixative before being in 50% glycerol in PBS. The individual DRG were then placed on slides, dissected to remove unnecessary tissue and a coverslip was mounted carefully above them. DRG were examined and photographed using a Leica DM5500 light microscope with attached monochrome DFC365FX camera at 50× or 100× magnification. The number of fluorescence^{+} cells per DRG was calculated as described in Section 2.2.31.2.

2.2.25 qPCR analysis

2.2.25.1 Total RNA isolation from whole brain

Immediately following collection of the brain, it was disrupted, quartered and snap frozen in tubes in a dry ice/ethanol bath. Samples were stored at -80°C until required. RNA was isolated using the Promega Total RNA Isolation System. Briefly, samples were homogenised in 1 mL RNA lysis buffer in 1 mL glass tissue grinders. This was divided into 175 µL aliquots and the RNA was isolated as per the manufacturer's instructions with the optional DNase treatment. A further 2 hour DNase treatment was performed on the eluted RNA as described in Section 2.2.25.3, prior to the precipitation of RNA as described for DNA in Section 2.2.2.7. The yield of RNA was then assessed using the Qubit fluorometer as described in Section 2.2.7.

2.2.25.2 Total RNA isolation from pooled DRG

Immediately following collection of DRG from spinal levels T13 to T8 they were snap frozen in tubes in a dry ice/ethanol bath. Samples were stored at -80°C until required. RNA was isolated using the RNAqueous micro kit (Ambion). Briefly, DRG were homogenised in 100 µL of the lysis solution that contains guanidinium thiocyanate using a 1 mL glass tissue grinder on ice. RNA was then isolated from the lysate as per the manufacturer's instructions with the optional post elution DNase treatment.

As this DNase treatment was not sufficient to eliminate all viral DNA from the RNA samples, a further DNase treatment step was performed for 1 h as described in Section 2.2.25.3. Given the very small quantity of RNA (less than 1 µg) that is extracted from these

samples, routine quantification of RNA and assessment of RNA quality by gel electrophoresis was not possible.

2.2.25.3 Additional DNase treatment of RNA to eliminate residual DNA

To completely eliminate DNA from the extracted RNA such that it was undetected by qPCR, a more robust DNase treatment step was required. A reaction mix was prepared containing approximately 0.1 µg RNA, 1× DNase incubation buffer (Roche), 20 U DNase (Roche), 20 U RNasin ribonuclease inhibitor (Promega) and nuclease free water (Ambion) to 30 µL. This reaction was incubated at 37°C for one to four hours, depending upon the quantity of RNA used. The enzyme was then heat inactivated by incubation at 75°C for 10 minutes.

2.2.25.4 cDNA synthesis

cDNA synthesis reactions were performed using the SuperScript VILO cDNA synthesis kit (Invitrogen) according to the manufacturer's instructions. This reverse transcriptase kit uses the SuperScript III reverse transcriptase and a random primer mix, which results in the high cDNA yields (Ståhlberg et al., 2004b). Briefly, 2 µL of RNA was mixed with 1× VILO reaction mix, 1× SuperScript enzyme mix, and made up to 20 µL with nuclease free water (Ambion). This was then incubated at 25°C for 10 minutes, followed by incubation at 42°C for 60 minutes. The reaction was terminated by incubation at 85°C for five minutes and stored at -20°C until it was required.

2.2.25.5 Construction of RNA standards for qPCR assay

Plasmid DNA was isolated and linearised with either HindIII or NotI (refer to Sections 2.2.2.1 and 2.2.4). The resulting DNA fragment was analysed by agarose gel electrophoresis to confirm that the plasmid was fully linearised to prevent long run-on transcripts with multiple copies of the transcript in the same message (refer to Section 2.2.5). To synthesise RNA, 2 µg of linearised plasmid DNA was mixed with 1× transcription optimised reaction buffer (Promega), 10 mM DTT (Promega), 100 U RNasin ribonuclease inhibitor, rNTP mix (500 µM each; Promega), and 40 U SP6 RNA polymerase (Promega). This mix was then incubated at 37°C for two hours. To eliminate plasmid DNA, a DNase treatment was performed as described in Section 2.2.25.3 for four hours. The RNA concentration was then quantified using the Qubit fluorimeter as described in Section 2.2.7.

The RNA was then diluted in ten-fold serial dilutions to the desired concentration for each step of the standard curve (Table 2-13). Using each dilution and 311 ng irrelevant RNA

(refer to Section 2.2.25.1), a series of cDNA synthesis reactions were carried out according to section 2.2.25.4. These standards were then diluted one in five in nuclease free water and 2 µL of each standard was then used in each qPCR reaction.

Input RNA concentration for cDNA synthesis (copies/µL)	Final copy number per qPCR reaction (copies)
2.5×10^7	1×10^6
2.5×10^6	1×10^5
2.5×10^5	1×10^4
2.5×10^4	1×10^3
1.25×10^4	5×10^2
6.25×10^3	2.5×10^2
2.5×10^3	1×10^2

Table 2-13. RNA copy number for qPCR standards. The required input RNA concentration for each cDNA synthesis reaction to construct standards with the final copy number per qPCR reaction shown.

2.2.25.6 Details of qPCR assay design

All gene expression assays were designed by and purchased from Applied Biosystems. They were already optimised and further investigation of annealing temperature was not performed. The *rbfox3* assay was a predesigned assay (assay ID: Mm01248771_m1; UniGene: Mm.341103) and the primer and probe sequence information is not disclosed. The probe was conjugated to the fluorescent reporter molecule VIC.

To design the *Cre* assay, the sequence of the *eGFP/Cre* fusion gene based on the plasmid pIGCN21 was supplied to Applied Biosystems. This assay was also supplied as a predesigned assay (CRE_RECOM; assay ID: A17MR8), and the probe with conjugated to the fluorescent reporter molecule 6-carboxyfluorescein (6-FAM). The details of this assay are found in Table 2-14.

For the detection of U_S12 transcripts (for simplicities sake, now referred to as ICP47 transcripts), previously published primer and probe sequences were selected (Table 2-14; Ma et al., 2014). These probes were conjugated 5' to the fluorescent reporter molecule 6-FAM, with a 3' Minor Groove Binder Non Fluorescent Quencher (MGBNFQ). The MGB

moiety allows more stable binding of the probe to DNA, increasing the melting temperature of the probe (Kutyavin et al., 2000).

Assay	Primer/ probe	Use	Concentration (nM)	Sequence
CRE_ RECOM	Forward primer	Forward primer used to amplify eGFP/Cre	900	CGGCGGATCCGA AAAGAAAA
	Reverse primer	Reverse primer used to amplify eGFP/Cre	900	ACGCTAGAGCCT GTTTTGCA
	Probe	Hydrolysis probe that binds with the amplified eGFP/Cre region	250	**6-FAM-** TTCACCGGCATC AACG-**MGBNFQ**
ICP47	Forward primer	Forward primer used to amplify U_S12	650	GTGCACGGCGGT TCTG
	Reverse primer	Reverse primer used to amplify U_S12	650	CGTACGCGATGA GATCAATAAAAG G
	Probe	Hydrolysis probe that binds with the amplified U_S12 region	250	**6-FAM-** CCGCCTCCCGGT CCT-**MGBNFQ**

Table 2-14. Details of oligodeoxynucleotides used for qPCR analysis. The actual T_m of the probe is unknown due to the addition of the MGB moiety, though an estimate based on the TK-specific sequence is indicated.

2.2.25.7 qPCR analysis of viral transcripts within DRG

When setting up all qPCR experiments, a unidirectional workflow pattern (pre- to post-qPCR) was enforced, with physically separate laboratories utilised for the construction of mastermixes, isolation of RNA from tissues and subsequent processing, and the isolation and handling of plasmid DNA. In order to carry out absolute quantification of viral transcripts within DRG, the following experiment was carried out. The samples from each mouse were used in two assays to detect either *Cre* transcripts or U_S12 transcripts (which will be referred to as ICP47 transcripts hereafter) within the same run. Each reaction was performed in triplicate. The entire standard curve (as described in Section 2.2.25.5) was used in parallel on each plate. Each qPCR reaction to detect *Cre* transcripts contained 1× LightCycler 480 probes master mix (Roche), 2× *rbfox3* gene expression assay, 1× *Cre* gene expression assay, and 3 µL of cDNA in a final volume of 20 µL. Each qPCR reaction to detect ICP47 transcripts contained 1× LightCycler 480 probes master mix, 2× *rbfox3* gene expression assay, 250 nM ICP47 probe, 650 nM each of the ICP47 forward and reverse primers, and 3 µL of cDNA in a final volume of 20 µL. No template controls were included

for all assays on each run. The qPCR assays were performed with the Roche LightCycler480, using the following program:

Preincubation - 95°C for 10 min

Amplification and detection – 50 cycles of:

a. Denaturation - 95°C for 15 s
b. Annealing - 60°C for 30 s
c. Extension - 72°C for 1 s

Cooling – 40°C for 10 s

Threshold cycle (C_T) values were calculated using Roche LightCycler 480 software (version 1.5).

2.2.26 Preparation of splenocytes from mice

At seven days p.i., mice were culled and their spleens harvested (refer to Section 2.2.20). Individual spleens were gently homogenised through cell strainers in DMEM-2. The single cell suspensions of splenocytes were centrifuged at 462 *g* for five minutes at 4°C, and resuspended in red cell lysis buffer for five minutes. Approximately 25 ml of PBS was added to each sample, and cells were centrifuged at 462 *g* for five minutes at 4°C. The splenocytes were then resuspended in DMEM-10and viable splenocytes were counted using trypan blue staining. The concentration of splenocytes was then adjusted for each sample using DMEM-10, typically to 1 x 10^7 cells/mL.

2.2.27 Preparation of cells from DRG for immunological analysis

DRGs were collected from mice from spinal levels T5 to L1 (refer to Section 2.2.20) and placed directly into 1 mL of collagenase/DNase in DMEM-10. The DRG were trimmed using a scalpel blade under a dissecting microscope to remove axons and excess tissue. The DRGs were then incubated at 200 oscillations per minute (opm; Bioline shaking incubator) at 37°C for 60 minutes. The DRG were then gently ground through a 70 µM cell strainer and washed with excess FACS-PBS. The cells were centrifuged at 524 *g* for five minutes at room temperature, and resuspended in 100 µL of FACS-PBS for subsequent analysis.

2.2.28 Surface staining and intracellular cytokine staining for gzmB

For antibody staining of DRG-associated cells, 100 µL of a DRG cell suspension (refer to Section 2.2.27) or 1×10^6 splenocytes (refer to Section 2.2.26) were added to individual wells of a 96 well round bottomed plate as appropriate. The cells were centrifuged at 524

g for five minutes at 4°C and resuspended in 10 µL Fc block and 30 µL FACS-PBS. Then, the cells were incubated on ice for 15 minutes, before being washed with FAC-PBS and resuspended in 3 or 6 µL of the gB_{498}-specific dextramer for the DRG and splenocytes samples, respectively, in a total volume of 40 µL. The mixture of cells and dextramer was incubated at room temperature for 10 minutes in the dark. Next, 40 µL of antibodies, namely anti-CD8α-APC-Cy7, anti-CD62L-FITC, anti-CD45.2-BV421 and anti-CD4-PE-Cy7 (diluted 1 in 75 in FACS-PBS), were added to the cells. The cells were then incubated on ice in the dark for 30 minutes. The stained cells were washed with FACS-PBS, followed by PBS only, before incubation at room temperature for 20 minutes to fix the cells. The fixed cells were then washed repeated with FACS-PBS before staining with 50 µL of anti-gzmB-AlexaFluor647 antibody (1 in 200 dilution in FACS-PBS in 0.25% saponin). The following day, cells were washed twice with FACS-PBS and resuspended in 60 µL FACS-PBS for analysis by flow cytometry (refer to Section 2.2.30).

2.2.29 *In vitro* antigen presentation assay

293-K^b, DC2.4 or MC57G cells (Table 2-4) in single cell suspension were mixed with the appropriate virus at an MOI of 5 in 500 µL of DMEM-0. The cells were gently agitated in a 37°C waterbath for three minutes in a 4.5 mL round bottomed tube (Starstedt) before being incubated at 37°C with shaking at 200 opm for 30 minutes. The cells were then transferred into 10 mL of warm DMEM-10 in a 15 mL Falcon tube and were incubated for a further 5½ hours at 37°C. During the infection period, the cells were either rotated at four rpm using the MACSmix tube rotator (Miltenyi Biotec) or were gently mixed every 20 minutes.

The infected cells were collected by centrifugation at 462 *g* for five minutes at room temperature and adjusted for 1×10^4 (stimulator to effector ratio of 1:5), 5×10^3 (1:10), 1×10^3 (1:50) and 5×10^2 (1:100) cells per well. Then, 100 µL of infected cells were cocultured with 5×10^4 effectors per well in a round-bottomed 96 well plate, in triplicate. In each case, uninfected cells served as stimulators for a negative control, while effectors stimulated with 0.125 µM synthetic gB_{498} peptide (sequence SSIEFARL; GenScript). The cells were incubated at 37°C with 5% CO_2 for 12 hours. The cells were then washed twice with PBS and then resuspended in 100 µL/well 0.1 M sodium phosphate buffer. The plate was subjected to three cycles of freezing and thawing, before being centrifuged at 524 *g* for five minutes at 4°C. 75 µL per well of supernatant was added to a 96 well flat bottomed transparent tissue culture plate (Corning), with 1 µL of $MgCl_2$ buffer and 22 µL of ONPG. This was incubated at 37°C for up to eight hours, before 100 µL 1 M sodium carbonate was added to each well to stop the reaction. The optical density at 420 nm was measured using

a Tecan Infinite M1000 PRO plate reader. The data was analysed as described in Section 2.2.30.5.

2.2.30 Analysis of fluorescence by flow cytometry

Flow cytometry was used in this thesis to detect the expression of fluorescent proteins such as eGFP and mCherry, as well as fluorochrome-conjugated antibodies. In this thesis, a LSR-II Flow Cytometer (BD Biosciences) was used for data acquisition. An appropriate number of events were collected for each experiment, but typically at least 100 000 events were collected. The flow cytometry data was analysed as described in Section 2.2.31.4.

2.2.31 Data analysis

2.2.31.1 Bioinformatic analysis

Vector NTI (Life Technologies) software was used to design cloning strategies and recombinant virus strains. Oligonucleotide primers were designed with the aid of NetPrimer software (Premier Biosoft). Vector NTI and Chromas (Technelysium) was used to analyse newly generated DNA sequences.

2.2.31.2 Determination of the number of β-gal$^+$ or fluorescent cells per DRG

The images of whole DRG for the expression of β-gal or fluorescent proteins were prepared using ImageJ 1.45s software (Rasband, 1997-2012; Schneider et al., 2012). To determine the number of β-gal$^+$ cells or fluorescent$^+$ cells, images were imported in sequence and analysed using the cell counter plugin.

2.2.31.3 Analysis of qPCR data

In all qPCR assays, a standard curve was constructed and included in each run. The C_T values were calculated using the Roche LightCycler 480 software. To account for run to run variation and variation in input RNA quantity, the expression of the transcript of interest was normalised relative to the endogenous *rbfox3* reference gene. Next, to produce a standard curve, the mean C_T values calculated for the standards were plotted against the logarithm of the HSV-1 RNA copy number of each standard. From this, a linear regression equation was obtained. To calculate the amplification efficiency (*E*), the following equation was used:

$$E = 10^{-1/slope}$$

To convert this into a percentage of template that was amplified in each cycle (*% Efficiency*), the following equation was used:

$$\% \, Efficiency = (E - 1) \times 100$$

The linear regression equations were also used to calculate the viral RNA transcript number using the C_T values obtained for each sample.

2.2.31.4 Flow cytometric analysis

Flow cytometry data was analysed with Flowjo 8.7.1 software (Tree Star). For each sample, events were gated to exclude doublets, debris and some dead cells on forward scatter (FSC) versus side scatter (SSC) plots. To analyse the data, the appropriate gates were applied to the samples as follows.

To quantify the expression of fluorescent proteins following transfection or infection of cells with a plasmid or virus designed to express a fluorescent protein, such as eGFP, mCherry and Venus, cells were gated on a plot showing SSC by the fluorescent protein (Figures 2-2 and 2-3). If more appropriate, the results were also analysed as a histogram to illustrate the levels of fluorescent protein expression.

To analyse the immunological data, samples were gated on a plot of SSC by CD45.2 expression to gate the cells that are $CD45.2^+$ (Figure 2-4). These cells were then gated on a plot of CD8 by CD4 expression to identify the cells that are $CD8^+CD45.2^+$. The $CD8^+$ cells were next gated on a plot of gzmB by CD62L to identify the activated $CD8^+$ T cells ($gzmB^{hi}CD62L^{lo}$). They were also gated on a plot of CD8 versus the gB_{498} dextramer to identify the gB_{498}-specific $CD8^+$ T cells (Figure 2-4). Backgrounds were determined using splenocytes isolated from a mock infected mouse, and were either subtracted from the final total or were presented seperately, as appropriate. These cells were then gated on a plot of gzmB by CD62L to identify the activated $CD8^+$ T cells ($gzmB^{hi}CD62L^{lo}$). The number of gB_{498} specific $CD8^+$ T cells (T) was calculated as follows:

$$T = \textit{total splenocyte count} \times \% \; CD45.2^+ \textit{ of all events} \times CD8^+ \textit{ of all } CD45.2^+ \textit{ events} \times \% \; gB_{498}\textit{-specific of } CD45.2^+CD8^+ \textit{ events}$$

2.2.31.5 Analysis of antigen presentation data

To determine the presentation of antigen by the *in vitro* antigen presentation assay, the percentage of maximal stimulation relative to gB_{498} peptide stimulation was determined. From each sample, a background value of either infected effector cells or mock infected cells was subtracted as appropriate. These values were then divided by the average OD_{420} of three wells stimulated with the gB_{498} peptide as described previously and multiplied by 100 to calculate the percentage stimulation.

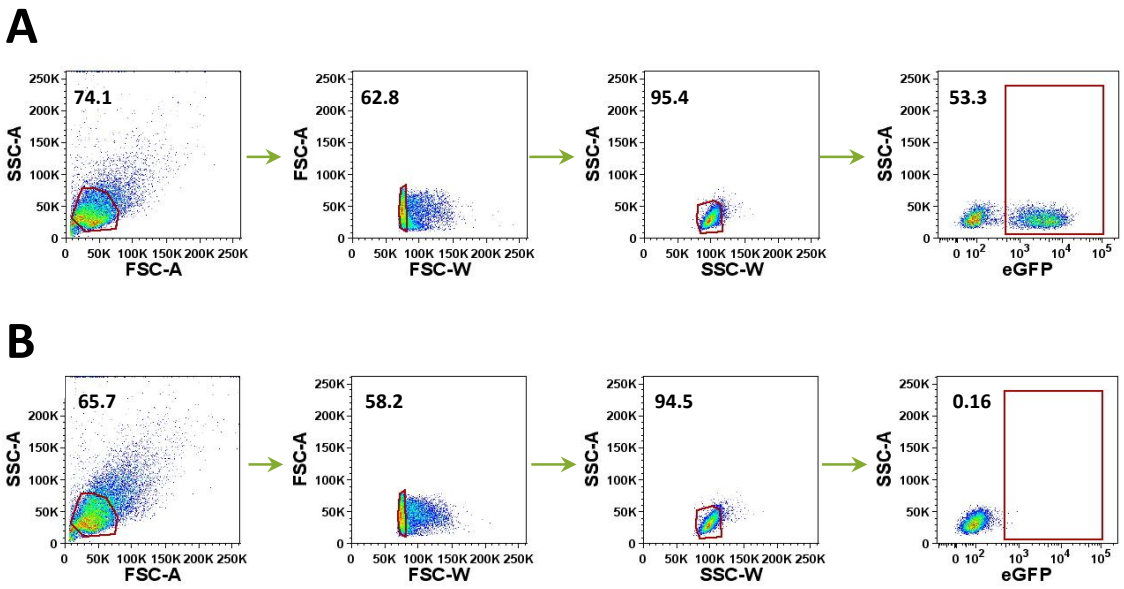

Figure 2-2. The gating strategy used to identify eGFP⁺ cells. 293-K^b cells were infected with (A) HSV-1 pC_eGC or (B) mock infected with PBS, and incubated for six hours at 37°C, 5% CO_2. The cells were then fixed and analysed by flow cytometry. To identify the eGFP⁺ infected cells, events were first gated on a SSC × FSC plot. Singlets were next gated on a plot of FSC (width signal) × FSC (area signal), followed by gating on a plot of SSC (width signal) × FSC (area signal). The eGFP⁺ events were then gated on a eGFP × SSC (area signal). The number in each plot represents the percentage of events of the gated population relative to the population shown in the plot.

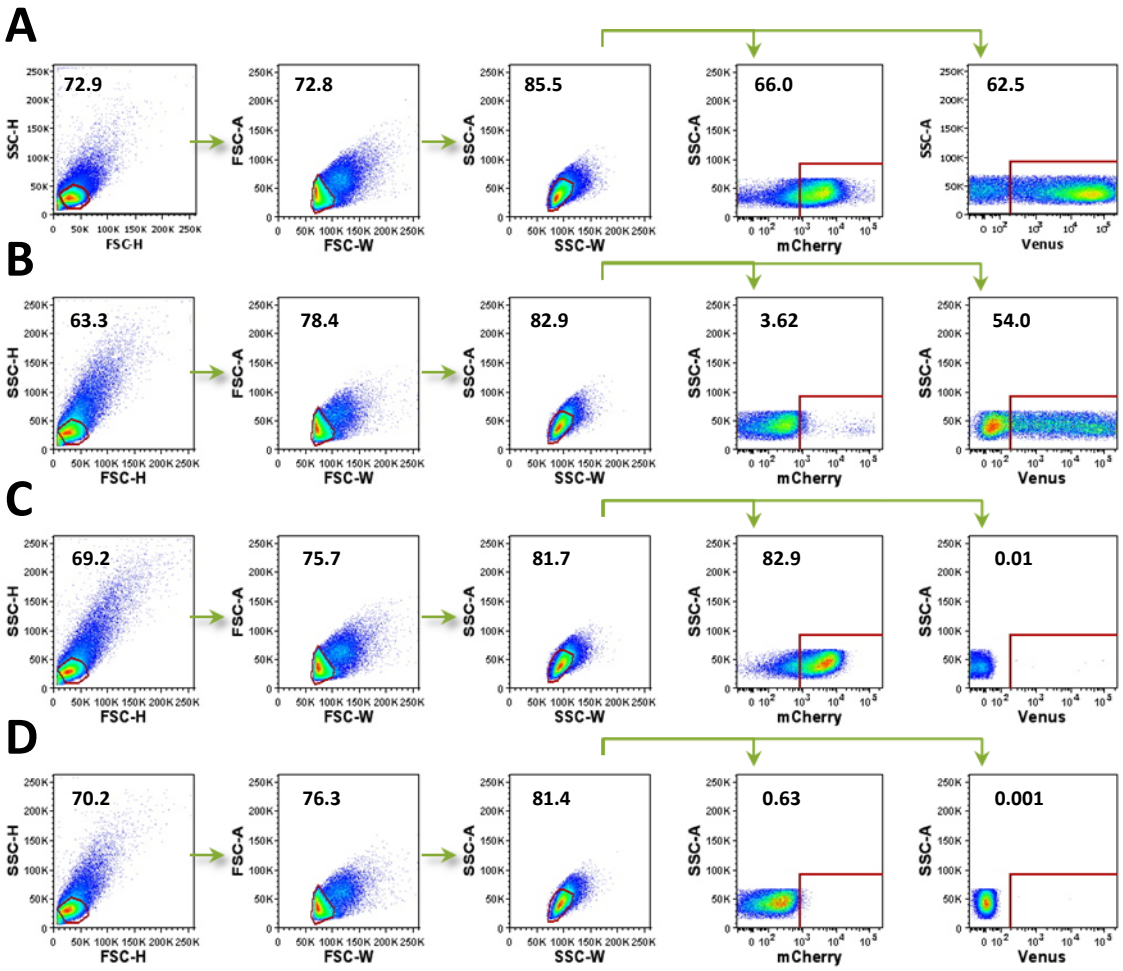

Figure 2-3. The gating strategy used to identify Venus⁺ and mCherry⁺ cells. 293A cells were (A) transfected with pU3.0.5kbF-Venus and pX330 for five hours, followed by infection with infection with HSV-1 pCmC (MOI 0.01), (B) were transfected with the pUC3.0.5kbF-Venus and pX330 plasmids but were not infected, (C) untransfected but were infected with HSV-1 pC_mC (MOI 0.01) or (D) were not transfected or infected. They were incubated for three days at 37°C, 5% CO_2. The cells were then harvested, fixed and analysed by flow cytometry. To identify the fluorescent infected cells, events were first gated on a SSC × FSC plot. Singlets were next gated on a plot of FSC (width signal) × FSC (area signal), followed by gating on a plot of SSC (width signal) × FSC (area signal). The mCherry⁺ events were then gated on a mCherry × SSC (area signal), while the Venus⁺ events were gated on a Venus × SSC (area signal). The number in each plot represents the percentage of events of the gated population relative to the population shown in the plot.

Figure 2-4. The gating strategy used to identify activated $CD8^+$ T cells and activated gB_{498}-specific $CD8^+$ T cells. A C57Bl/6 mouse was mock infected with (A&C) PBS or (B&D) infected by tattoo with 1×10^8 PFU/mL HSV-1 minigB_Cre. After seven days, the $CD8^+$ T cell response in the (A - C) spleen and (D) DRG was measured by gB_{498} dextramer and CD62L surface staining with intracellular staining for gzmB. A&B were stained with 6 µL of dextramer, and C&D were stained with 3 µL of dextramer. To identify the antibody-bound cells, events were first gated on a SSC × FSC plot. Singlets were next gated on a plot of FSC (width signal) × FSC (area signal), followed by gating on a plot of SSC (width signal) × FSC (area signal). The $CD45.2^+$ events were then gated on a CD45.2 × SSC (area signal) plot. The $CD8^+$ events were then gated from the lymphocytes on a CD8 × CD4 plot. The gB_{498} dextramer events were then gated from this population on a CD8 × gB_{498} dextramer plot, while the activated $CD8^+$ T cells were also gated on a gzmB × CD62L plot. For A&B, the activated gB_{498} $CD8^+$ T cells were then identified based on a gzmB × CD62L plot, while for C&D the activated gB_{498} $CD8^+$ T cells were identified based on a gB_{498} dextramer × gzmB plot as all activated cells in the periphery should be $CD62L^{lo}$.

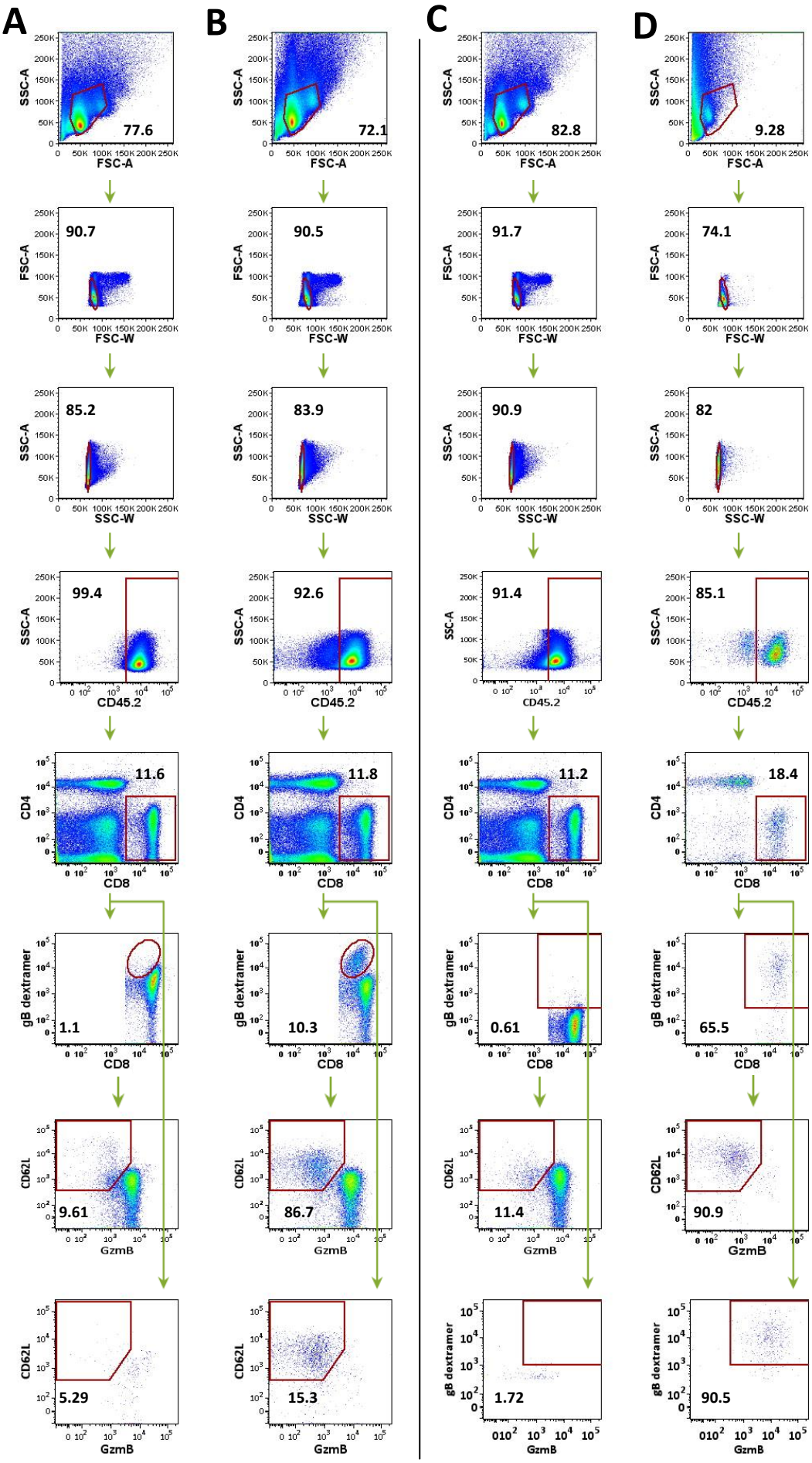
A
B
C
D
SSC-A
FSC-A
77.6
72.1
82.8
9.28
FSC-W
90.7
90.5
91.7
74.1
SSC-W
85.2
83.9
90.9
82
CD45.2
99.4
92.6
91.4
85.1
CD8
CD4
11.6
11.8
11.2
18.4
gB dextramer
1.1
10.3
0.61
65.5
GzmB
CD62L
9.61
86.7
11.4
90.9
5.29
15.3
1.72
90.5

2.2.31.6 Statistical analysis

The statistical approach taken in this thesis was developed in consultation with Dr. Terry Neeman of the Statistical Consulting Unit, ANU. Statistical analyses were performed using GraphPad Prism5 software or GenStat software. In general, when two groups of samples were compared, the unpaired Student's *t* test was used to compare means. A one-way analysis of variance (ANOVA) was performed if more sample groups were to be compared, followed by Newman Kwel's post-test to make pairwise comparisons. However, for the comparisons of the numbers of β-gal$^+$ cells within the DRG of infected mice across different days, several assumptions for the use of an ANOVA are violated. Theoretically, the number of β-gal$^+$ is a discrete variable and strictly should not be analysed using an ANOVA. However, biologically this data does behave as a continuous variable, and so for this reason the violation of this assumption was considered to be trivial. Further, to perform an ANOVA, the dependent variable should be approximately normally distributed, which may not be true. However, an ANOVA is relatively robust to violations of this assumption, and since it is likely that this data is normally distributed, this factor was disregarded (Schmider et al., 2010). Finally, and likely most importantly, an ANOVA assumes homogeneity of variances. Given that the group size is typically unequal in most of the data presented in this thesis, it should not be assumed that the variances are homogenous. To account for this, the data was transformed into logarithmic values and then the fold change was compared relative to the earliest time point using an ANOVA followed by a calculation of the least significant difference of the means (LSD; $p < 0.05$). When this was performed using the transformed data presented in Chapter 4 for analyses using HSV-1 pgB_eGC and HSV-1 pICP47_eGC, those differences identified that were statistically significant ($p < 0.05$) were identical to those found when a one way ANOVA was performed with the untransformed values ($p < 0.05$). However, data transformed in this way can no longer be presented as raw numbers. Therefore, as a compromise, and to ensure that data was presented as collected in its native state, differences between two or more samples groups were compared by an ANOVA with pairwise comparisons made using the more conservative Bonferroni's post-test, with significance denoted if $p < 0.05$. In many cases, the *p* value was less than 0.001, but in order to be more conservative in the data analysis, this was not denoted on the figures. When multiple viruses across different days were compared, a two-way ANOVA was performed followed by Bonferroni's post-test to make pairwise comparisons. The difference between each pair was considered to be statistically significant when $p < 0.05$ overall and also for each pair. Although it is possible that there were some pairwise comparisons that were false negatives, this was deemed less problematic than false positives for the sake of this analysis. Finally, the number of β-

gal$^+$ cells per mouse on the same day p.i. with the same virus were pooled from separate experiments, and a fixed effects model was applied in which the experiment was identified as a block. It was found that there was minimal difference in the variance within each block and within each day. This meant that data across different experiments could be legitimately pooled for the purposes of statistical analysis.

3 Development of methods used for the construction of recombinant HSV

3.1 Introduction

The original method for engineering HSV relies upon homologous recombination between a transfer plasmid that contains viral sequences flanking the desired insertion site and the virus genome in cultured mammalian cells (Roizman and Jenkins, 1985). Recombination between the transfer plasmid and the viral genome occurs at a relatively low rate, so efficient methods are required to select or screen the few recombinant viruses produced (Kolb and Brandt, 2004; Ramachandran et al., 2008; Tanaka et al., 2004). As an alternative, recombineering of HSV genomes propagated as bacterial artificial chromosomes (BACs) has been used as a rapid, efficient method of generating recombinant HSV without the need to plaque purify the resulting virus (Borst et al., 2004; Gierasch et al., 2006; Horsburgh et al., 1999; Saeki et al., 1998; Stavropoulos and Strathdee, 1998; Tanaka et al., 2003). However, viruses recovered from these BACs often contain residual BAC sequences in the viral genome that can lead to a loss of gene function, depending on the site of insertion (Horsburgh et al., 1999; Saeki et al., 1998; Stavropoulos and Strathdee, 1998). Cre/*loxP* recombination can be used to remove these BAC sequences, but a single residual *loxP* site remains at the site of BAC insertion and excision, which might be problematic when the ROSA26R/Cre system is used (Gierasch et al., 2006; Tanaka et al., 2003). Further, the HSV-1 genome contains palindromic sequences that can be unstable in bacteria (Horsburgh et al., 1999; Post et al., 1980). It has been reported that major deletions or rearrangements have not occurred during serial passage of the HSV genome in BACs but more minor changes would probably be overlooked (Gierasch et al., 2006; Horsburgh et al., 1999). As a result, recombinant HSV generated using a BAC based method may have attenuated viral growth, particularly *in vivo*, and altered pathogenesis (Horsburgh et al., 1999; Saeki et al., 1998; Stavropoulos and Strathdee, 1998).

Since it is highly desirable for the viruses used in this thesis to resemble wild type virus, both *in vitro* and *in vivo*, a homologous recombination based method was chosen for the construction of these recombinant viruses. Further, many of the viruses required for use in this thesis are designed to incorporate a selectable marker, typically a fluorescent protein, facilitating the selection of the recombinant virus (Tanaka et al., 2004). The generation of recombinant HSV typically involves cotransfection of high quality HSV-1 genomic DNA and transfer plasmid DNA, followed by plaque purification to obtain the desired recombinant virus (Balliet et al., 2007; Tanaka et al., 2004). Alternatively, another simpler variation of this method relies upon transfecting cells with the transfer plasmid and then infecting these cells with virus as a means of providing the viral genome, referred to as transfection/infection (Orr et al., 2005). However, few details on the use of the latter method have been published. While the transfection/infection method not commonly used

to engineer HSV-1, it is a method often used to engineer poxviruses, which have a non-infectious, large dsDNA genome (Falkner and Moss, 1990; Mackett et al., 1982; Wong et al., 2011).

The recently developed CRISPR/Cas9 system for genome editing exploits the type II prokaryotic clustered regularly spaced palindromic repeats (CRISPR) adaptive immune system that provides acquired immunity for bacteria and most archaea against plasmid DNA and viruses by targeting DNA in a sequence specific manner (as reviewed by Horvath and Barrangou, 2010). The CRISPR/Cas9 system relies on a RNA guide (gRNA) and GG protospacer adjacent motif (PAM) contained within an associated CRISPR RNA transcript and the Cas9 nuclease. These form a complex and cleave double stranded DNA at target sequences matching those of the gRNA (Jinek et al., 2012). These breaks can be repaired by either non-homologous end joining or homologous recombination when a suitable template is provided (Cong et al., 2013; Jinek et al., 2012; Mali et al., 2013). The CRISPR/Cas9 system has been used for genome editing of a range of cell lines and organisms as diverse as human cell lines, *Danio rerio* (zebrafish), Drosophilia, mice and model plants like *Arabidopsis thaliana* (Cong et al., 2013; Gratz et al., 2013; Hwang et al., 2013; Li et al., 2013; Mali et al., 2013). The CRISPR/Cas9 genome editing tools were recently combined with the transfection/infection based method for generating HSV by us and others, greatly facilitating the construction of recombinant HSV-1 (Bi et al., 2014; Russell et al., 2015; Suenaga et al., 2014). We also compared the improvement in recombination frequency associated with CRISPR/Cas9 targeting to optimised transfection/infection methods (refer to Section 3.3.2; Russell et al., 2015).

Therefore, the aim of this chapter was to develop an efficient system based on a homologous-recombination based method for constructing recombinant HSV-1 expressing different proteins, including fluorescent reporter proteins, and Cre recombinase. The results in this chapter are divided into four sections, with the first describing the construction of different recombinant viruses using a traditional cotransfection method. The next section describes the development and optimisation of a transfection/infection based method for engineering HSV, with the addition of the CRISPR/Cas9 tool to further increase the efficiency of HSV genome engineering. Then the use of a second, largely uncharacterised, intergenic region between the U_L26 and U_L27 genes of HSV-1 for the expression of foreign DNA was described. Finally the growth and pathogenesis of these viruses was assessed by a variety of methods.

3.2 Generation of recombinant HSV-1 using a co-transfection method

3.2.1 Verification of the U_L3/U_L4 intergenic region as a suitable site for insertion of foreign genes into HSV-1 KOS

In order to generate recombinant HSV-1 that express Cre, a site in the genome where foreign sequence could be inserted without altering virus growth or pathogenesis was required. The U_L3/U_L4 intergenic region was chosen as it has been previously shown that insertions at this location do not alter virus growth or virulence of engineered HSV compared with wildtype viruses (Morimoto et al., 2009; Tanaka et al., 2004). To verify that this site could be used for insertion of foreign DNA into HSV-1 KOS, a transfer plasmid was constructed that contains approximately 2 kb of sequence from the U_L3/U_L4 region of HSV-1 KOS was constructed (pT $U_L3/4$; refer to Section 2.1.9). These HSV-1 sequences were generated in two PCRs using primer extensions to add EcoRV, PstI and SpeI sites between the two native polyA sequences that are required for the proper termination of U_L3, U_L4 and U_L5 transcription (Figure 3-1; Morimoto et al., 2009). A mCherry expression cassette was then inserted into the SpeI site to construct pT pCmC. This allows strong, constitutive expression of the mCherry fluorescent protein under the control of the CMV IE promoter, which enables the easy identification of the presence of recombinant virus by microscopy.

Two independent, parallel cotransfections of viral HSV-1 and pT pCmC DNA were performed in Vero cells. After three days growth, mCherry$^+$ plaques were able to be identified by fluorescence microscopy. Five plaques were selected directly from each well of transfected cells. All ten plaques were then subjected to up to five rounds of plaque purification. For the majority of these plaques (8 of 10), the frequency of mCherry$^+$ plaques showed an overall decrease over multiple rounds of plaque purification and so they were abandoned (Figure 3-2). For the remaining two plaques the frequency of mCherry$^+$ plaques sharply increased during the second round of plaque purification (lineages 1 and 2 on Figure 3-2). Following three rounds of plaque purification of these two lineages of virus all plaques were mCherry$^+$ as determined by screening more than 200 plaques by microscopy. A further round of plaque purification was required to eliminate parent virus as detected by PCR. Two independently isolated mCherry$^+$ viruses were obtained (named HSV-1 pC_mC 1 and 2, respectively), confirming that I was able to insert a foreign gene into the U_L3/U_L4 region of HSV-1 by a homologous recombination based cotransfection method.

Next, the *in vitro* growth of these two independently isolated viruses, named HSV-1

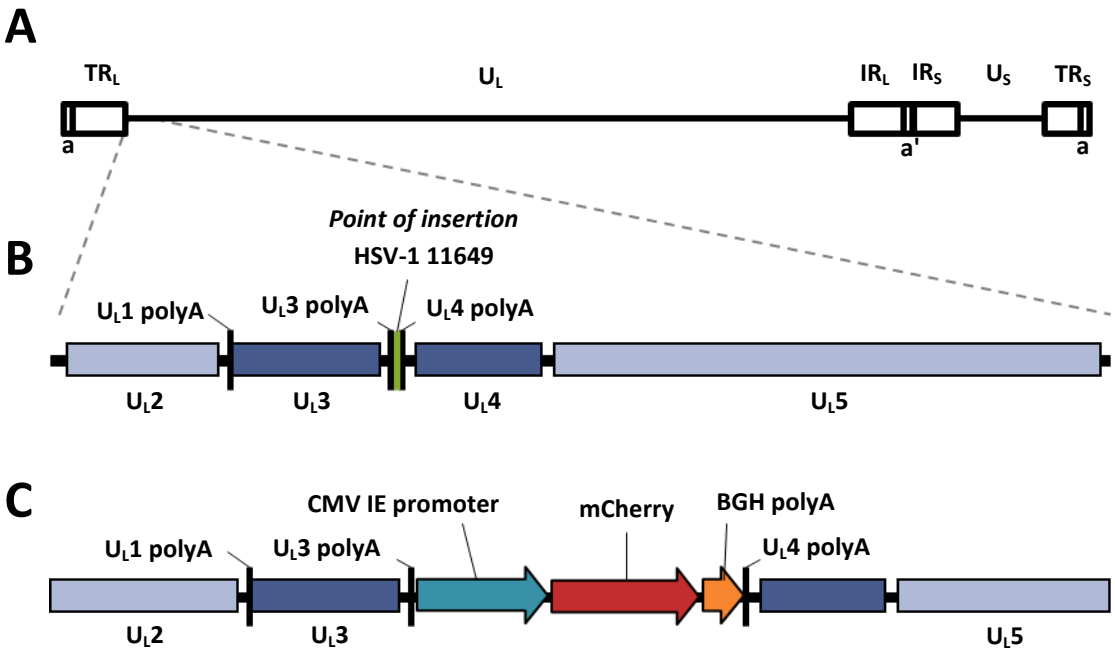

Figure 3-1. Location of the U_L3/U_L3 intergenic region for the insertion of foreign DNA into HSV-1. (A) Schematic representation of the HSV-1 genome with the location of U_L3 and U_L4 indicated (to scale). (B) Schematic representation of the U_L3/U_L4 intergenic region, with the point at which the mCherry cassette is inserted indicated in green and the base pair position indicated using numbers from HSV-1 KOS (JQ673480). (C) Schematic representation of the mCherry expression cassette in the intergenic space between U_L3 and U_L4.

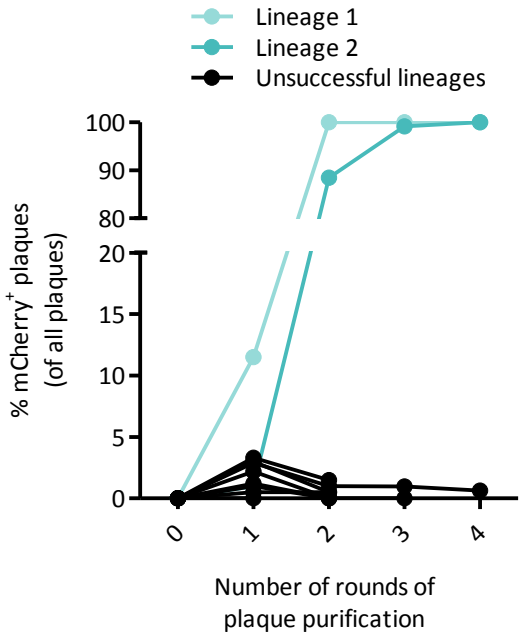

Figure 3-2. Results of plaque purification when using a cotransfection homologous recombination-based method for generating HSV-1 pC_mC. Linearised pT pCmC plasmid DNA and HSV-1 KOS genomic DNA was cotransfected into Vero cells. At 72 hours p.i., individual mCherry$^+$ plaques were identified and the percentage mCherry$^+$ plaques determined (round 0 of plaque purification). Five plaques from each of two independent parallel transfections were identified and plaque purification was attempted. The proportion of mCherry$^+$ progeny for each round of plaque purification is shown, with approximately 200 plaques per lineage examined each round for red fluorescence by microscopy as appropriate. Two lineages out of ten were successfully plaque purified until free from wildtype virus as determined by PCR and sequencing.

pC_mC1 and HSV-1 pC_mC 2, was shown to be unaffected by the addition of mCherry into the U_L3/U_L4 intergenic region. These viruses showed no differences in growth relative to HSV-1 KOS in Vero cells following either high (Figure 3-3A) or low (Figure 3-3B) MOI infection.

In order to verify that the pathogenesis and growth of the recombinant viruses generated in this thesis was similar, a variation on the flank zosteriform infection model of HSV-1 was used (Blyth et al., 1984; Simmons and Nash, 1984; Van Lint et al., 2004). In this model, HSV-1 is introduced into the flank of the mouse by tattoo (Russell et al., 2015). Unlike scarification, the skin is left unbroken by the inoculation, and there is no sign of skin damage the day after infection, paralleling that of natural infection (Simmons and Nash, 1984). The tattoo model also allows the development of a primary lesion to be clearly observed from two days p.i., and zosteriform spread is detectable from five days p.i. (Figure 3-4A1). The size of the lesion can also be estimated, as is shown in Figure 3-4A2. Unfortunately, there is some uncertainty involved in such measurement, due to the active nature of mice and the difficulty in measuring the curved skin surface of the flank using calipers. Further, as with other HSV-1 infection models, including scarification-based methods, tattoo infection does not result in a defined dose of virus being delivered. Many variables can influence the infection process, but by using a defined inoculum titre, controlling the length of time and pressure when tattooing, and randomising mice into experimental groups, the impact of these variables can be managed. Despite these limitations, the infection of mice on the flank by tattoo is a very useful animal model of HSV-1 infection.

One virus was selected (HSV-1 pC_mC 2) and following infection of C57Bl/6 mice with either HSV-1 pC_mC 2 or wildtype HSV-1 KOS, skin lesion development was similar (Figure 3-4B). The growth of this virus in C57Bl/6 mice was also assessed relative to wildtype HSV-1 (Figure 3-4C). Virus growth was unimpaired in the skin. Although the difference in mean virus titre in the DRG of mice infected with HSV-1 KOS or HSV-1 pC_mC 2 was statistically significant, it was less than two-fold, which is at the limit of the resolving power of our plaque assay. For this reason it was deemed likely to be biologically insignificant. This confirms previous observations that the U_L3/U_L4 intergenic region can be used as an insertion site without compromising HSV-1 replication or pathogenesis (Morimoto et al., 2009; Tanaka et al., 2004).

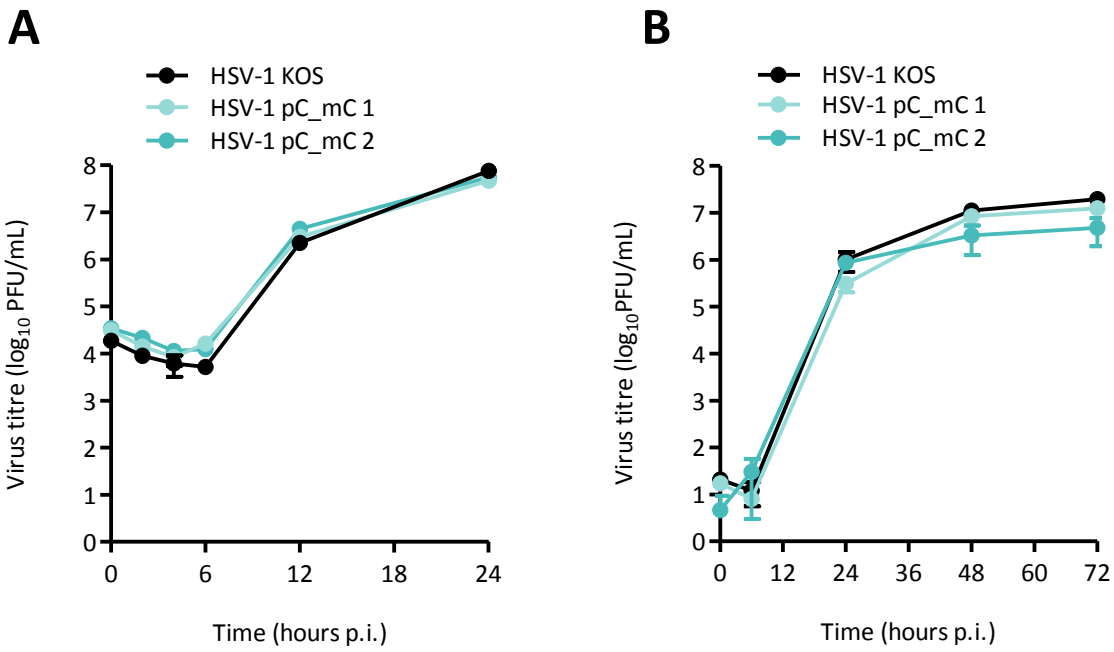

Figure 3-3. Insertion of mCherry into the U_L3/U_L4 intergenic region has no effect on virus growth *in vitro* relative to HSV-1 KOS. The replication of two independent lineages of HSV-1 pC_mC (blue) was compared to the parent wildtype HSV-1 KOS (black) in Vero cells in (A) single and (B) multiple step growth curves. (A) Confluent cell monolayers in 9.6 cm^2 tissue culture wells were infected at a high MOI (5 PFU/cell in 1 mL M0). After one hour, the inoculum was removed, cells washed and 2 mL M2 was added. A 0 hour p.i. sample was collected immediately following the addition of fresh media. The remaining samples were harvested at 2, 4, 6, 12 or 24 hours p.i. (B) Confluent cell monolayers in 9.6 cm^2 tissue culture wells were infected at a low MOI (0.01 PFU/cell in 1 mL M0). After one hour, the inoculum was removed, cells washed and 2 mL M2 was added. A 0 hour p.i. sample was collected immediately following the addition of fresh media. The remaining samples were harvested at 6, 24, 48 or 72 hours p.i. Virus titres were determined by standard plaque assay. Data are mean±SEM of three replicates.

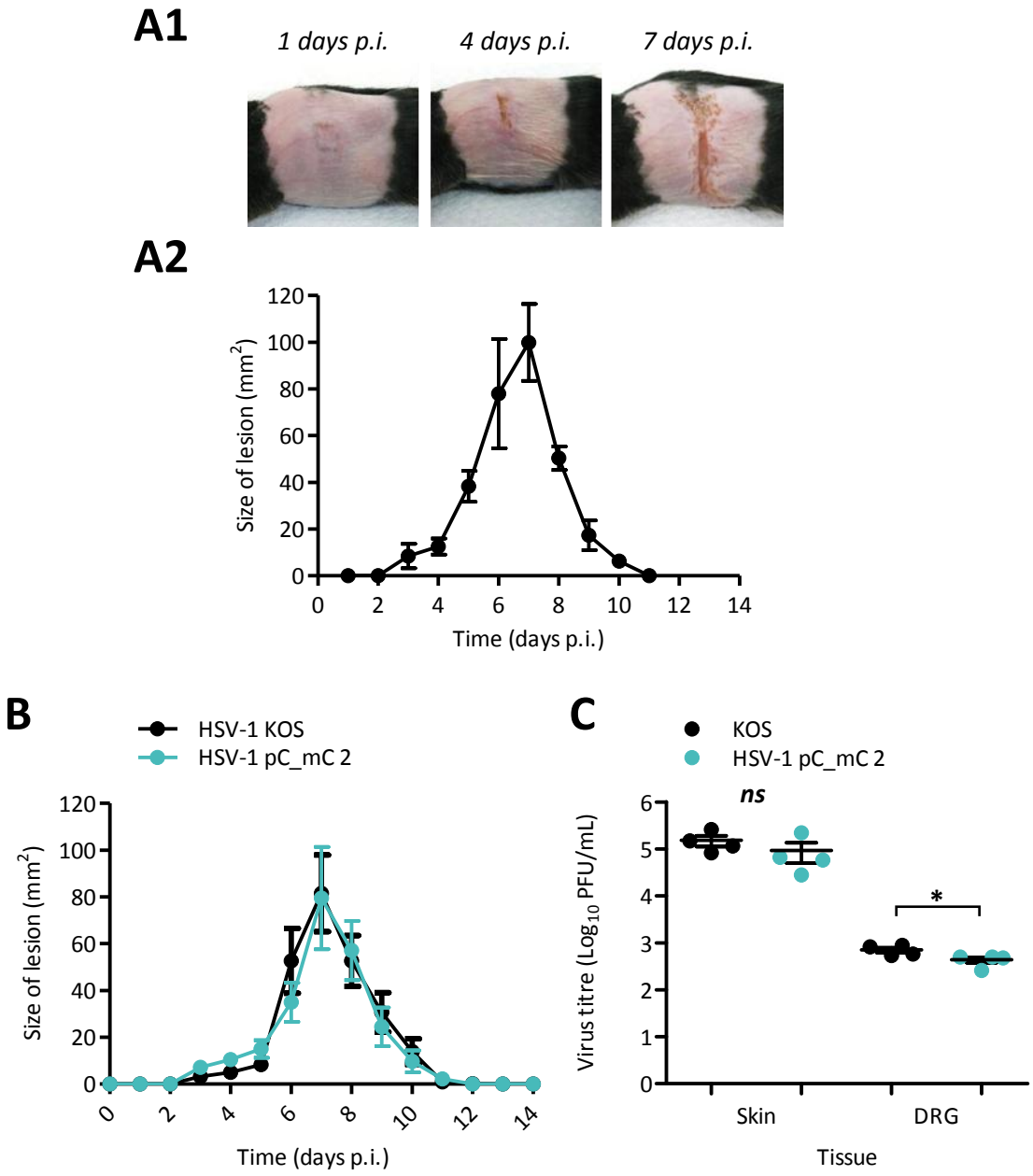

Figure 3-4. Insertion of mCherry into the U_L3/U_L4 intergenic region has no effect on viral pathogenesis or growth *in vivo* relative to HSV-1 KOS. C57Bl/6 mice were infected by tattoo with 1×10^8 PFU/mL with WT HSV-1 KOS. (A1) Photographs of a representative mouse were taken at one, four, and seven days p.i. (A2) To estimate total lesion size over time, lesion size was measured daily using a caliper and clinical score was monitored daily, with mice never displaying any signs of illness other than the herpetic lesion on the flank. Data is mean lesion size±SEM (n = 3). (B) C57Bl/6 mice were infected by tattoo with 1×10^8 PFU/mL with HSV-1 KOS (black) or HSV-1 pC_mC 2 (blue). Lesion size was measured daily and shown as mean lesion size±SEM (n = 5 for HSV-1 KOS, n = 4 for HSV-1 pC_mC 2). Data was analysed by a Kruskal-Wallis test ($p > 0.05$). (C) Amounts of infectious virus in skin and innervating DRG of C57Bl/6 mice five days after flank infection with 1×10^8 PFU/mL HSV-1 KOS (black) and HSV-1 pC_mC 2 (blue). Infectious virus was determined by standard plaque assay from ten DRG (spinal levels T5 to L1) or 1 cm^2 skin located over the inoculation size. Circles show results for each mouse (n=4) and bars represent mean±SEM. The means were compared by an unpaired *t* test, where significance is denoted by * ($p < 0.05$) or as *ns* (not significant).

3.2.2 Cotransfection of plasmid and viral DNA to generate recombinant HSV-1

The construction of another four viruses which express an *eGFP/Cre* recombinase fusion gene (Lee et al., 2001) under the control of different promoters from the U_L3/U_L4 intergenic site was attempted using similar methods. Each HSV-1 promoter was chosen as it had been at least partially defined and was characterised as being from the immediate early, early or late temporal class of HSV gene expression. The U_S1/U_S12 promoter that dictates expression of ICP22 and ICP47, respectively, was chosen as the representative immediate early promoter (and named the ICP47 for the rest of this thesis for the sake of clarity). The promoter for the gene U_L39 encoding ICP6 was chosen as the representative early promoter, while the promoter for the gene U_L27 encoding gB was chosen as the representative late promoter. Finally, the CMV IE promoter was also used to direct expression of the gene encoding *eGFP/Cre* from HSV-1.

3.2.2.1 Construction of recombinant HSV-1 expressing Cre under the control of the ICP47 promoter

One of the two prototypic immediate early promoters chosen for use in this thesis was the ICP47 promoter. The U_S1 and U_S12 genes are located in the U_S region of the HSV-1 genome while the promoters are found in the TR_S and IR_S regions, respectively (see Figure 1-1; Murchie and McGeoch, 1982). As such, both genes are expressed from an identical promoter (Barklie Clements et al., 1977; Gelman and Silverstein, 1987; Murchie and McGeoch, 1982). As the efficiency of Cre-mediated recombination is linked to promoter strength, a high level of Cre expression was essential and so the sequence from -400 to +100 (where +1 is defined as the nucleotide of the mRNA start site) was chosen for use as the ICP47 promoter (Araki et al., 1997; Gelman and Silverstein, 1987). Further, the eGFP/Cre protein used in all constructs is nuclear targeted to increase efficiency of Cre-mediated recombination (Logvinoff and Epstein, 2000). An origin of replication (OriS) is also found within the ICP47 promoter sequence, but to avoid the insertion of a third copy of the OriS into HSV-1 it was omitted from the promoter sequence in this construct. The OriS sequence is not strictly required for the correct temporal class expression of U_S1 or U_S12, but in the absence of this sequence, expression from the ICP47 promoter was enhanced almost 2-3 fold as determined by luciferase expression in mouse embryonic fibroblasts, Vero cells and dissociated TG cultures. However, luciferase expression was similar in the presence or absence of the OriS sequence within the ICP47 promoter in the eye, periocular tissue or TG following infection by corneal scarification (Summers and Leib, 2002). Therefore, the ICP47 promoter and an eGFP/Cre cassette were inserted into pT $U_L3/4$ to construct pT pICP47_eGC (refer to Section 2.2.6.2).

To construct HSV-1 pICP47_eGC, cotransfection of pT pICP47_eGC plasmid and HSV-1 KOS genomic DNA into Vero cells was carried out at a ratio of 2:1, 4:1, 8:1, 16:1 or 32:1. Instead of picking these plaques directly, all cells and media were harvested following three days incubation. This virus was diluted and used to infect new Vero cell monolayers. The rationale was that a further growth step may help eliminate unstable or otherwise defective virus. After two days of growth, $eGFP^+$ plaques were identified and 29 individual plaques picked. Of these 29 plaques, only two plaques showed an overall increase in the number of $eGFP^+$ plaques after two subsequent rounds of purification. After a total of four rounds of plaque purification, two $eGFP^+$ viruses that originated from independent, parallel transfections were identified and found to be free from wildtype virus by fluorescence microscopy (Figure 3-5, lineages 1 and 2) and PCR (data not shown). The first lineage was selected, named HSV-1 pICP47_eGC, and the sequence of the *eGFP/Cre* cassette in the U_L3/U_L4 region was confirmed by PCR and sequencing and the virus phenotype was assessed both *in vitro* and *in vivo* (refer to Section 3.5).

3.2.2.2 Construction of recombinant HSV-1 expressing Cre under the control of the gB promoter

The promoter directing expression of the U_L27 gene, encoding gB, was chosen as a representative γ_1 promoter was chosen for use in this thesis (herein referred to as the gB promoter for simplicity). Transfection assays using promoter-chloramphenicol acetyltransferase (CAT) plasmids that contained various deletions in the gB promoter region have been used to identify a 86 base pair minimal promoter sequence (from -69 to +20 bp). However, U_L27 has a long 5'-transcribed noncoding sequence of 268 nucleotides that was shown to enhance expression, but is not required for correct temporal expression (Pederson et al., 1992). Therefore, to a ensure maximal expression of *Cre* in ROSA26R mice, the 298 bp promoter sequence from -260 to +38 bp was amplified from HSV-1 KOS and cloned into pT $U_L3/4$ to construct pT pgB_eGC (refer to Section 2.2.6.1).

This virus was constructed in a similar manner to HSV-1 pICP47_eGC. An initial cotransfection of pT pgB_eGC plasmid and HSV-1 KOS genomic DNA was carried out at a ratio of 2:1, 4:1 or 7:1 in Vero cells. All cells and media were harvested following three days incubation. This harvested virus was then used to infect new Vero cell monolayers, enabling the identification of $eGFP^+$ plaques. Initially, 21 plaques were selected and subjected to another round of plaque purification, but only four of these showed enrichment for $eGFP^+$ virus. Two of $eGFP^+$ plaques were selected for further plaque purification. Following another round of plaque purification (four rounds in total), two independently isolated $eGFP^+$ virus were generated which was shown to be free from

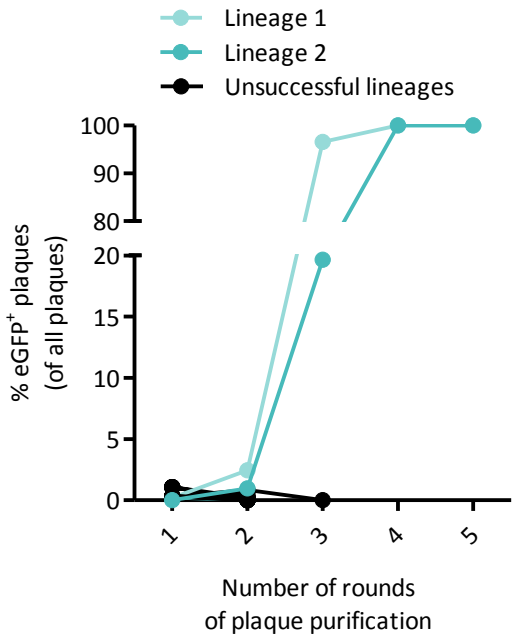

Figure 3-5. Results of plaque purification when using a cotransfection homologous recombination-based method for construction of HSV-1 pICP47_eGC. Linearised pT pICP47_eGC plasmid DNA and HSV-1 KOS genomic DNA was cotransfected into Vero cells (plasmid:viral DNA ratio of 2:1, 4:1, 8:1, 16:1 or 32:1) . After three days, all virus was harvested into the original media. Virus was serially diluted and used to infect fresh cultures of Vero cells, and after two days, individual eGFP$^+$ plaques were identified and counted. The percentage eGFP$^+$ plaques was determined (round 1 of plaque purification). eGFP$^+$ plaques from two independent parallel transfections were identified and plaque purification attempted, with the proportion of eGFP$^+$ progeny for each round of plaque purification shown. Approximately 200 plaques per lineage were examined each round for green fluorescence by microscopy as appropriate. Two lineages out of 29 were successfully plaque purified to be free from wildtype virus as determined by PCR and sequencing.

wildtype virus by microscopy and PCR screening (data not shown). One virus was selected, named HSV-1 pgB_eGC, and the correct insertion of the transgene into the U_L3/U_L4 intergenic region was confirmed by sequencing. The similarity in the phenotype of this virus to wildtype HSV-1 was confirmed both *in vitro* and *in vivo* (refer to Section 3.5).

3.2.2.3 Construction of recombinant HSV-1 expressing Cre under the control of the ICP6 promoter

The large subunit of the ribonucleotide reductase enzyme, known ICP6 or ribonucleotide reductase 1, is encoded by the gene U_L39, which is classed as an early gene, although it is uniquely regulated among the HSV-1 genes. Unlike other early genes, it is weakly responsive to VP16 transactivation due to the presence of a TAATGARAT-like motif. In some circumstances, ICP6 was found to be expressed at a low level in the presence of cycloheximide (Honess and Roizman, 1974; Sze and Herman, 1992). However, ICP0 is the major transactivator of ICP6 expression, and as such it is usually considered to be an early gene (Desai et al., 1993; Sze and Herman, 1992). High levels of U_L39 transcripts accumulate during lytic infection *in vitro*, so the UL39 promoter (now referred to as the ICP6 promoter) was chosen as the early promoter for use in this thesis. A series of CAT plasmids containing different regions of sequence from the ICP6 promoter have been used in transfection assays to identify a region from -217 to +29 that contains the putative transcriptional consensus elements, including those responsible for promoter induction by VP16 and ICP0 (Desai et al., 1993). Therefore, this region was chosen as the ICP6 promoter sequence and amplified from HSV-1 KOS. The ICP6 promoter and *eGFP/cre* fusion were cloned into pT $U_L3/4$ to construct pT pICP6_eGC.

To construct this virus, pT pICP6_eGC plasmid DNA and HSV-1 KOS viral DNA was cotransfected into Vero cells at a ratio of 2:1, 4:1, 8:1, 16:1 or 32:1. Following three days of incubation, all cells and media were harvested. This harvested virus was used to infect new Vero cell monolayers, enabling the identification of $eGFP^+$ plaques. Eight $eGFP^+$ plaques were selected with the aim of purifying the desired virus, but only one could be successfully plaque purified. Following several rounds of plaque purification, an $eGFP^+$ virus was isolated and found to be free from wildtype virus by microscopy (Figure 3-6) and PCR screening (data not shown). This virus was named HSV-1 pICP6_eGC, and the correct insertion of the transgene into the U_L3/U_L4 intergenic region was confirmed by sequencing. The virus phenotype was also assessed relative to wildtype HSV-1 using both *in vitro* and *in vivo* models (refer to Section 3.5).

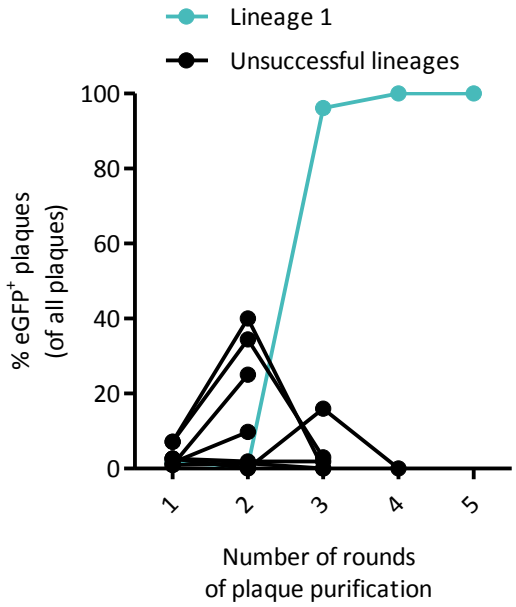

Figure 3-6. Results of plaque purification following a cotransfection homologous recombination- based method for construction of HSV-1 pICP6_eGC. Linearised pT pICP6_eGC plasmid DNA and HSV-1 KOS genomic DNA was cotransfected into Vero cells (plasmid:viral DNA ratio of 2:1, 4:1, 8:1, 16:1 or 32:1) . After three days, all virus and cells were harvested into the original media. The supernatant and cell associated virus was then separated by centrifugation. This cell-associated virus was serially diluted and used to infect fresh cultures of Vero cells. After two days growth, individual eGFP$^+$ plaques were identified and counted. Eight plaques from two independent parallel transfections were identified and plaque purification attempted, with the proportion of eGFP$^+$ progeny for each round of plaque purification shown. Approximately 200 plaques per lineage were examined each round for green fluorescence by microscopy as appropriate. Only one lineage able to be plaque purified to yield a stable recombinant virus free from wildtype virus as determined by microscopy and PCR screening.

3.2.2.4 Construction of recombinant HSV-1 expressing Cre under the control of the CMV IE promoter

The CMV IE promoter is a strong and constitutively active promoter in mammalian cells that has been widely used to drive expression of foreign DNA from HSV-1 (Arthur et al., 2001; Boshart et al., 1985; Ecob-Prince et al., 1995; Nelson et al., 1987). The CMV IE promoter is briefly active in cells infected with HSV-1, even if lytic gene expression does not occur prior to the establishment of latency (Arthur et al., 2001). Further, activity under the CMV IE promoter is also decoupled from the HSV-1 gene expression cascade and is not dependent on the HSV-1 transactivator VP16 (Preston and Nicholl, 1997; Stinski and Roehr, 1985). Therefore, the expression of *eGFP/Cre* under the control of this promoter in ROSA26R mice will result in β-gal expression in the majority of latently infected cells (Proença et al., 2008).

Cotransfection of pT pC_eGC plasmid DNA and HSV-1 KOS genomic DNA was performed as previously described. Again, all virus and media were harvested following three days incubation. This harvested virus was then used to infect new Vero cell monolayers, and after two days growth $eGFP^+$ plaques were identifiable. Of these, 25 plaques were initially selected and up to five rounds of plaque purification attempted, but none were able to be successfully purified to generate the recombinant virus.

3.3 Transfection/infection methods for generating recombinant HSV-1

Having failed to purify a virus expressing *eGFP/Cre* from the CMV IE promoter using a cotransfection-based method, a means of improving either the frequency of recombinant virus generated or stability of virus generated was sought. An alternative method for generating recombinant HSV-1 involves transfecting plasmid DNA into HSV-infected cells, although few details have been published (Foster et al., 1999; Orr et al., 2005). Importantly, the transfection/infection method is not reliant on the isolation of high quality HSV genomic DNA. It has been anecdotally suggested that the quality of genomic DNA used during transfection influences the generation of stable recombinant virus. Unfortunately, in practice the isolation of such high quality DNA can be difficult to achieve. Therefore, a transfection/infection based method was explored as a means of generating the viruses required.

Highly transfectable 293A cells were transfected with linearised pT pC_eGC DNA, five hours prior to infection with HSV-1 KOS. The transfection efficiency was approximately

80% as determined by flow cytometry (data not shown). After three days, all cells and media were harvested. This virus was used to infect new Vero cells monolayers and after two days of growth, the proportion of $eGFP^+$ plaques of all plaques was determined. These $eGFP^+$ plaques were identified at an average frequency of 0.4%. This is lower than that previously observed for other cotransfections (such as described in Figure 3-6) but is within a similar range to that previously published using a cotransfection method (Kolb and Brandt, 2004; Krisky et al., 1997). Despite the slight reduction in the efficiency of the generation of recombinant virus initially, all four of the original plaques selected were able to be plaque purified to yield clean stocks of $eGFP^+$ virus determined by microscopy (Figure 3-7) and PCR (data not shown). Therefore, the lower initial yield of $eGFP^+$ plaques was offset by the higher fraction of $eGFP^+$ plaques that gave rise to pure stocks of virus. One of these virus stocks was selected, named HSV-1 pC_eGC, and was sequenced to confirm the insertion of the *eGFP/Cre* cassette into the U_L3/U_L4 intergenic region. The virus phenotype was assessed both *in vitro* and *in vivo* relative to wildtype HSV-1 (refer to Section 3.5).

3.3.1 Optimisation of variables associated with the transfection/infection method of generating recombinant virus

It was believed that further optimisation would be worthwhile to improve the infection/transfection method for the construction of recombinant HSV. Three parameters associated with the infection/transfection methods were tested to establish those that were important for the generation of recombinant virus, namely:

1. The MOI,
2. Transfection efficiency, and
3. The length of flanking region sequence.

To determine if the amount of virus used to infect cells influenced the frequency of recombination, 293A cells were transfected with linearised pT pC_eGC DNA. Five hours later, these cells were infected with HSV-1 KOS at an MOI of 0.01, 0.001 or 0.0001. All virus and media were harvested after three days. Serial dilutions of this virus were used to infect new cultures of Vero cells, allowing quantification of $eGFP^+$ and $eGFP^-$ progeny. Unsurprisingly, as MOI increased, the total virus yield improved (Figure 3-8). However, the proportion of $eGFP^+$ to $eGFP^-$ plaques remained similar, and so to augment virus yield from transfections a MOI of 0.01 was chosen for subsequent experiments.

To examine the effect of transfection efficiency on the generation of recombinant virus, varied amounts of linearised or circular plasmids were transfected into 293A cells to achieve differing transfection efficiencies, measured by flow cytometry (Figure 3-9A&B).

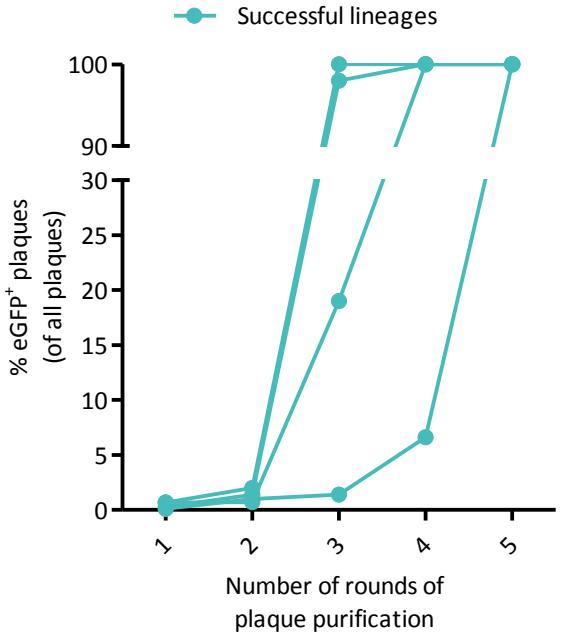

Figure 3-7. Successful plaque purification of all plaques when using a transfection/infection homologous recombination-based method for the construction of HSV-1 pC_eGC. 293A cells were transfected with linearised pT pC_eGC plasmid DNA and 5 hours later were infected with HSV-1 KOS. After three days, all virus was harvested into the original media. Virus was serially diluted and used to infect fresh cultures of Vero cells, allowing individual eGFP$^+$ plaques to be identified after 48 hours growth. The percentage eGFP$^+$ plaques was determined (round 1 of plaque purification) by screening approximately 200 plaques per lineage for green fluorescence by microscopy as appropriate. Four plaques from two independent parallel transfections were identified and plaque purification attempted, with the proportion of eGFP$^+$ progeny for each round of plaque purification shown, all of which

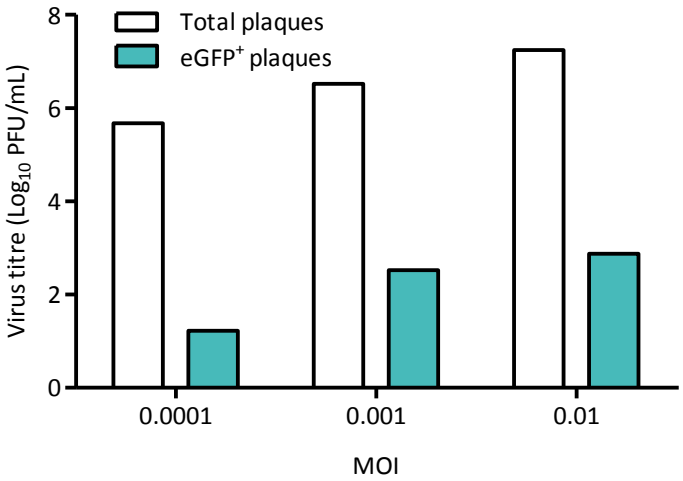

Figure 3-8. Effect of MOI on the virus output following transfection/infection to generate recombinant HSV-1. Confluent 293A cells were transfected with linearised pT pC_eGC DNA and 5 hours later were infected with HSV-1 at the MOIs shown. All virus and cells were harvested at 72 hours p.i. This virus was serially diluted and used to infect monolayers of Vero cells. After two days growth, the total number of plaques (open) and eGFP$^+$ plaques (blue) was determined. Data are representative of two independent experiments.

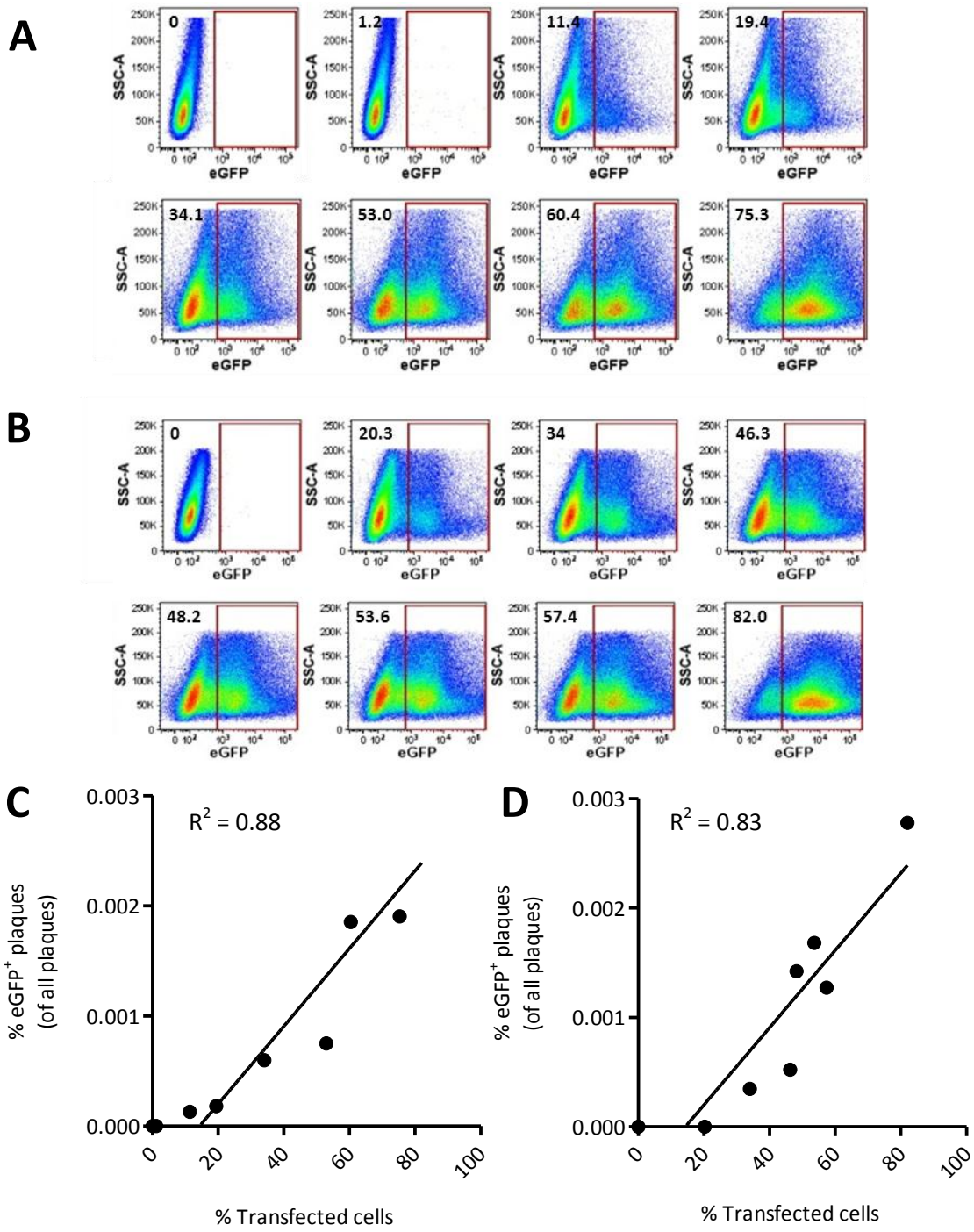

Figure 3-9. Effect of transfection efficiency on the virus output following transfection/infection to generate recombinant HSV-1. 293A cells were transfected with (A) intact or (B) linearised pT pC_eGC DNA such that a range of transfection efficiencies were achieved as determined by flow cytometry to detect eGFP expression. The number in each plot represents the percentage of eGFP+ events of the gated population relative to the population shown in the plot. Five hours later, cells were infected with HSV-1 a MOI of 0.01. All virus and cells were harvested at 72 hours p.i. and serially diluted and used to infect monolayers of Vero cells. This allowed the proportion of eGFP+ plaques to be determined after two days growth. (C) Transfection efficiency versus the proportion of eGFP+ plaques following transfection/infection using (C) intact or (D) linearised DNA. Linear regressions were performed and R^2 values are shown on each graph.

After five hours, cells were infected with HSV-1 KOS at a MOI of 0.01. All virus and media was harvested after three days, and serial dilutions of this virus were used to infect new cultures. The proportion of plaques that were eGFP$^+$ could then be determined. Recombinant progeny were not reliably produced if the frequency of recombination was less than approximately 20% (Figure 3-9D). Higher transfection efficiencies improved the proportion of eGFP$^+$ plaques in a roughly linear manner (Figure 3-9). However, this is unlikely to be relevant in practice, as even with the highest transfection efficiency, hundreds of plaques will need to be screened to identify a single plaque containing the desired recombinant virus.

The final parameter tested was the length of the viral sequences flanking the insertion site used in the transfer plasmid. It has been suggested that the region of sequence homologous to the HSV genome that flanks the insertion site must be at least 0.5 to 1 kb to allow for efficient recombination (Coffin, 2010; Goins et al., 2008). However, the impact the length of this flanking sequence has on the frequency of recombination does not appear to have been systematically examined. Plasmids were generated that contained approximately 0.5, 1, 2 or 3 kb of sequence on either site of the U_L3/U_L4 intergenic region (Figure 3-10A). The yellow fluorescent protein Venus was chosen as a marker so that fluorescence could be used to identify any recombinant plaques while widening the range of foreign genes in our repertoire that can be inserted using the transfection/infection method (Hernandez and Sandri-Goldin, 2010; Morimoto et al., 2009; Nagai et al., 2002). The transfer plasmids were transfected into 293A cells such that the transfection efficiency was similar for all plasmids as determined by flow cytometry for the detection of Venus expression (Figure 3-10B). After five hours, the cells were infected with HSV-1 KOS at a MOI of 0.01. All virus and media was harvested after three days, and serial dilutions of this virus were used to infect new monolayers of Vero cells. After two days of growth, the proportion of Venus$^+$ plaques of total virus was determined by fluorescence microscopy (Figure 3-10C). In two independent experiments, the frequency of Venus$^+$ plaques was directly proportional to the length of the flanking sequence in the transfer plasmids, with the range of efficiency being in the order of 10-fold. Three plaques were selected from a transfection with each of the four transfer plasmids and subjected to a single round of plaque purification. In all cases enrichment of Venus$^+$ virus relative to wildtype virus was observed (data not shown). Two of these plaques were selected and subjected to additional rounds of plaque purification (Figure 3-10D), leading to the production of pure stocks of recombinant virus as determined by microscopy and PCR (data not shown).

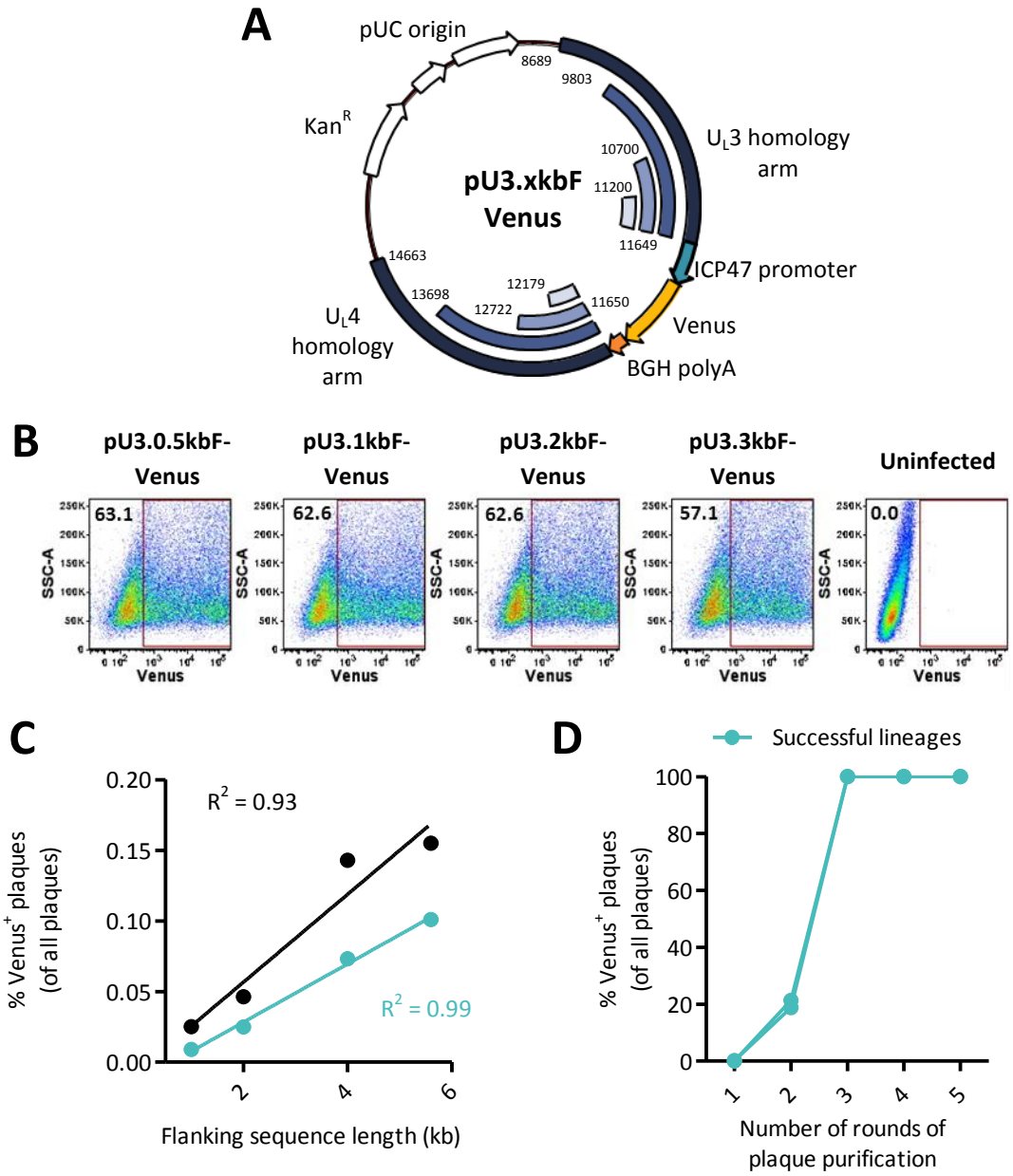

Figure 3-10. Influence of flank sequence length on recombinant HSV generation by transfection/infection. (A) Representative map of plasmids with different lengths of U_L3/U_L4 flanking sequences. Four different lengths were used as depicted by the concentric purple boxes to generate plasmids pU3.0.5kbF-Venus (HSV-1 KOS 11200-12179), pU3.1kbF-Venus (HSV-1 KOS 10700-12722), pU3.2kbF-Venus (HSV-1 KOS 9803-13698) and pU3.3kbF-Venus (HSV-1 KOS 8689-14663). Other features are as marked. (B) 293A monolayers were transfected with the each of the plasmids shown in (A) such that the transfection efficiency was similar for all plasmids as determined by flow cytometry (B). The number in each plot represents the percentage of Venus+ events of the gated population relative to the population shown in the plot. The cells were infected at an MOI of 0.01 5 hours later. All virus and media were harvested at 72 hours p.i. and used to infect monolayers of fresh Vero cells. (C) The percentage of Venus+ plaques of all HSV plaques is shown (round 1 of plaque purification). Two independent experiments are indicated with markers in blue and black. Linear regressions were performed and R^2 values are shown on each graph. (D) Two Venus+ plaques were selected and plaque purified until they were free from wildtype virus as determined by microscopy and PCR screening.

3.3.2 CRISPR/Cas9 targeting of the site of recombination for improving transfection/infection methods

In all the experiments described so far, the frequency of the generation of recombinant virus by transfection/infection was high enough to allow the visual selection of viruses that express a fluorescent marker. However, even with the optimisation of this method described in Section 3.3.1, it would be challenging to identify recombinant virus without the aid of visual selection. Recently, CRISPR/Cas9 genome engineering approaches have been used to improve the efficiency of homologous recombination (Mali et al., 2013), and we believed that it may greatly increase the efficiency of HSV-1 genome engineering. Therefore, we decided to focus on developing this method for the construction of the recombinant HSV-1 required for this thesis (Russell et al., 2015). During the course of this thesis, two reports have also been published that reinforce how promising the CRISPR/Cas9 approach is for engineering the HSV-1 genome (Bi et al., 2014; Suenaga et al., 2014).

3.3.2.1 Generation of HSV-1 pICP0_eGC using CRISPR/Cas9 in combination with a transfection/infection based method

A recombinant virus was designed to determine whether a CRISPR/Cas9 based system could be used to generate recombinant HSV-1. This virus was designed to express *eGFP/Cre* using the ICP0 promoter from the U_L3/U_L4 intergenic space, and was modelled on that used by Proença and colleagues (2008). 293A cells were transfected with linearised pT pICP0_eGC DNA and either pX330 or pX330-mC. The plasmid pX330-mC encodes a gRNA that targets mCherry for cleavage along with the CRISPR machinery. The U6 promoter initiates transcription of the gRNA with guanine and requires the protospacer-adjcaent motif (PAM)-NGG followed by the 20 bp target sequence. The control pX330 plasmid contains only the Cas9 nuclease and the gRNA but lacks the 20 bp target sequence and so is unable to cleave mCherry. Five hours after transfection, the cells were infected with HSV-1 pCmC. After three days growth, all virus and media were harvested. Serial dilutions of this virus were replated on Vero cells, and the proportion of $eGFP^+$, $mCherry^+$ and non-fluorescent plaques was determined (round 1 of plaque purification). The frequency of $eGFP^+$ plaques when the conventional transfection/infection method was used (ie. when the control pX330 plasmid was used) was comparable to that of previous experiments, with a frequency of recombination of 0.03% (Figure 3-11A). By contrast, when the mCherry targeted Cas9 was used to cleave the viral genome, the frequency of recombination was substantially higher (~6%). This is comparable with the frequency of generation of recombinant virus subsequently reported by Bi and colleagues (2014), and Suenaga and colleagues (2014). So, targeting the genome

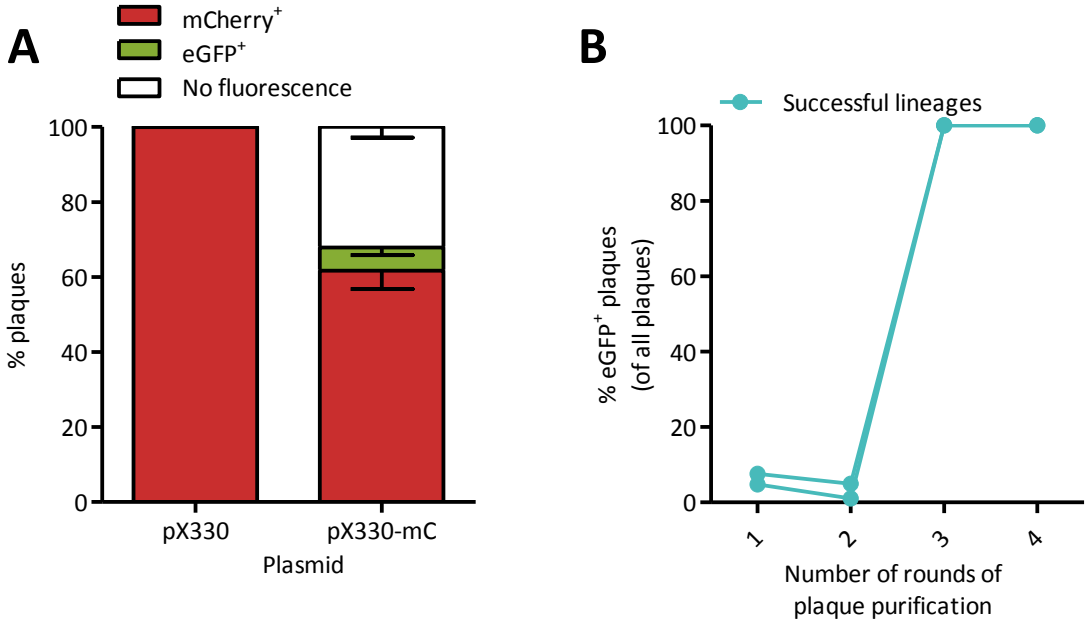

Figure 3-11. Generation of HSV-1 pICP0_eGC by transfection/infection method with the use of CRISPR/Cas9 to target the site of insertion. (A) 293A cell monolayers were cotransfected with 2 µg of the repair plasmid pT pICP0_eGC and either pX330 or pX330-mC. After five hours, cells were infected with HSV-1 pCmC at an MOI of 0.01. All virus and media was harvested after three days and used to infect monolayers of Vero cells (round 1 of plaque purification). The percentage of eGFP+ (green), mCherry+ (red) and non-fluorescent (clear) plaques where mCherry was targeted (with pX330-mC) or not (with pX330) is shown, with up to 200 plaques screened by microscopy for the detection of fluorescence. Two parallel independent transfections were performed and the results shown as mean-SEM. (B) Two plaques from two independent parallel transfections were identified and plaque purified until found to be free from wildtype virus as shown by microscopy and PCR.

for cleavage using the CRISPR/Cas9 system resulted in an almost 200-fold increase in frequency of the desired recombinant virus. Approximately a third of the viral progeny generated did not exhibit detectable fluorescence, indicating the viral genome had likely been cleaved but not repaired with the provided repair plasmid.

Two eGFP$^+$ plaques were identified by microscopy and subjected to a further round of plaque purification, after which time a plaque that was free from wildtype virus was identified (Figure 3-11B). While single-round isolation of recombinant HSV has been reported (Bi et al., 2014), this relied upon selecting a plaque containing recombinant virus only as determined by PCR, which was not used in this case. Following another round of plaque purification to verify the absence of detectable wildtype virus by microscopy (Figure 3-11B) and PCR (data not shown), two independent viruses were isolated, and one, named HSV-1 pICP0_eGC, was selected for future study. This virus was sequenced to verify the insertion of the *eGFP/Cre* cassette into the U_L3/U_L4 intergenic region. Although four single base pair mutations were identified, only two (D61N and R183G) lead to amino acid substitutions, both within the non-essential U_L3 ORF (Baines and Roizman, 1991). The mutations would not be expected to impact upon the nuclear localisation or nuclear export sequences of U_L3, but as there is no identifiable function for the protein encoded by U_L3 it is difficult to hypothesise if there would have an identifiable phenotype *in vivo* (Markovitz, 2007; Zheng et al., 2011). Nonetheless, subsequent characterisation of this virus revealed no differences in growth or pathogenesis relative to wildtype virus (refer to Section 3.5).

Given the high frequency with which recombinant virus was detected and the reduced number of rounds of plaque purification required to isolate this recombinant virus, it was confirmed that it would be feasible to use this method to generate a recombinant virus using PCR screening alone.

3.3.2.2 Generation of non-fluorescent HSV-1 using the CRISPR/Cas9 based method

A virus was required for use in this thesis that expresses the *eGFP/Cre* gene under the control of the LAT promoter. However, the LAT region is transcriptionally complex, with multiple promoters identified, each with different elements that dictate both short and long-term expression of the LATs (Figure 3-12A&B; Berthomme et al., 2000; Chen et al., 1995; Dobson et al., 1995; Dobson et al., 1989; Goins et al., 1994; Lokensgard et al., 1997). Further, expression of reporter genes from putative LAT promoters inserted into an ectopic locus in the genome has not always continued long term throughout latency (Dobson et al., 1995; Goins et al., 1994; Margolis et al., 1993). Alternatively, β-gal has been the control of the LAT promoter by an IRES, resulting in long-term expression of β-gal

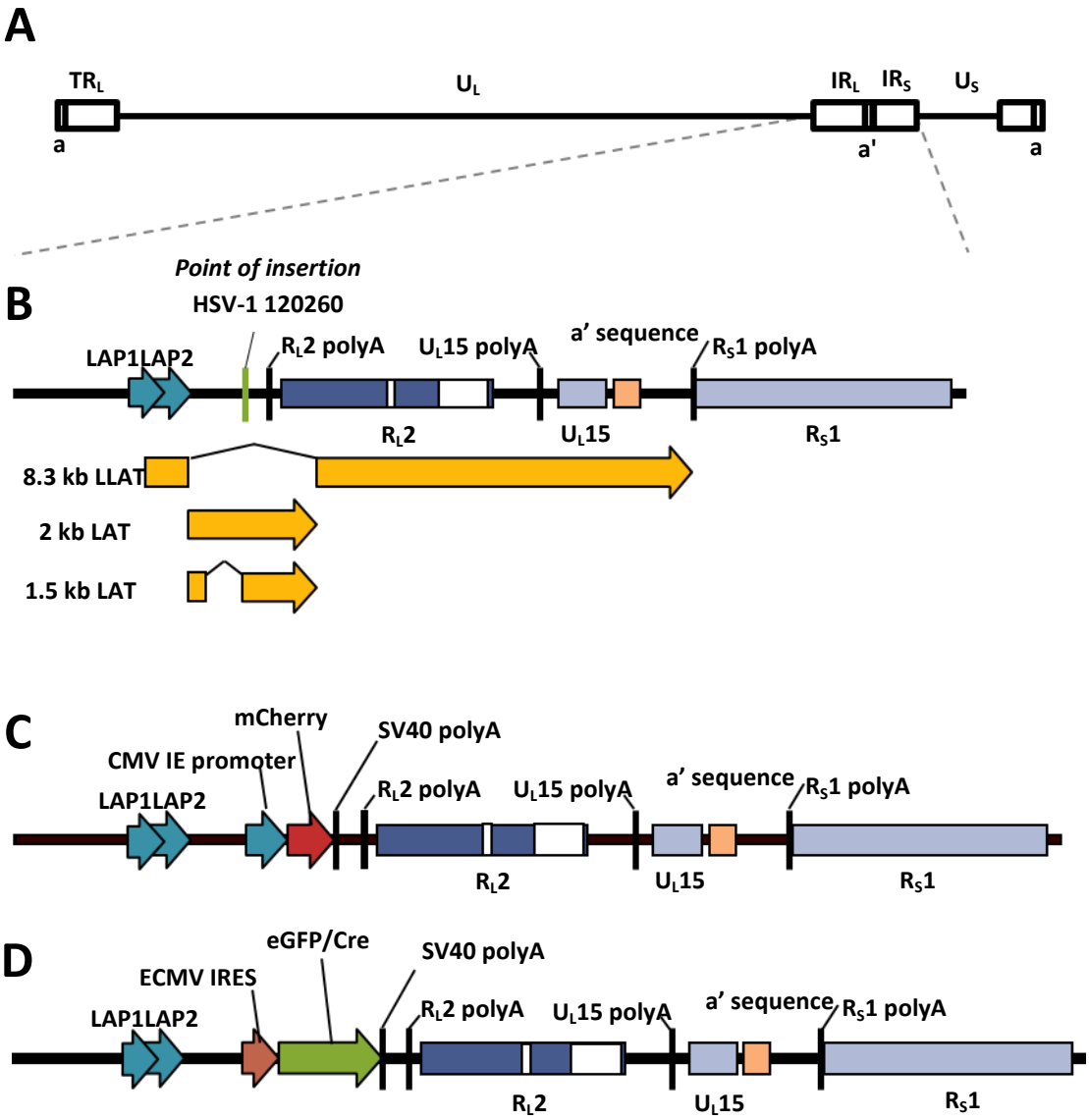

Figure 3-12. The LAT region of HSV-1. (A) Schematic representation of the HSV-1 genome with the location of LAT region indicated (to scale), with the point at which the gene expression cassettes are inserted indicated in green and the base pair position indicated using numbers from HSV-1 KOS (JQ673480). For simplicity, only the LAT region within the IR_L at the left hand side of the prototypic genome is shown. The relevant ORFs are indicated, including the genes RL2, which encodes ICP0, U_L15, which encodes ICP34.5, and RS1, which encodes ICP4. (B) Schematic representation of the LAT region, with the transcription pattern of the LATs indicated. The 8.3kb major LAT, 2 kb minor LAT and 1.5kb LAT are indicated in yellow, and the Latency Associated Promoter (LAPs) are indicated in blue. (C) Schematic representation of the LAT region of HSV-1 LAT pCmC, showing the CMV IE/mCherry cassette. (D) Schematic representation of the LAT region of HSV-1 pLAT_eGC, showing the IRES/eGFP Cre cassette.

inserted approximately 1.5 kb downstream of the LAT transcription site and placed under during latency (Lachmann and Efstathiou, 1997; Lachmann et al., 1996). For these reasons, a CRISPR/Cas9 based approach was used to generate a recombinant virus in which the *eGFP/Cre* is placed under the control of an IRES inserted into the LAT region (Lachmann and Efstathiou, 1997). Insertions at this location do not affect LAT promoter-mediated transcription when a gene under the control of the ECMV IRES was inserted approximately 1.5 kb downstream from the LAT transcription start site.

As the LAT promoter is not typically highly expressed *in vitro*, this virus cannot be selected for and plaque purified based on reporter gene expression in Vero cells (Batchelor and O'Hare, 1990; Zwaagstra et al., 1990). To overcome this, I chose to use the strategy employed by Lachmann and Efstathiou (1997). They constructed a virus whereby β-gal was expressed from the constitutive CMV IE promoter from the desired location in the LAT region of the genome. They then replaced the CMV IE promoter with an IRES that directs expression of β-gal from the LAT promoter, enabling the selection of plaques that are no longer β-gal$^+$. Therefore, I decided to construct a recombinant virus whereby mCherry was expressed under the CMV IE promoter, and so would appear red by fluorescence microscopy. A construct was then introduced such that the mCherry transgene was replaced with an *eGFP/Cre* fusion gene under the control of an IRES, allowing for the screening and purification of this non-fluorescent virus in Vero cells.

A construct was designed that contains 1.2 kb of sequence that is homologous to the LAT region of HSV-1. Into this region, the fluorescent protein mCherry was inserted under the control of the CMV IE promoter (Figure 3-12C). This plasmid was transfected into cells, followed by infection with HSV-1 KOS. After three days, the virus and media was harvested and serially dilutions of virus were used to infect fresh cultures of Vero cells. This allowed for the identification of mCherry$^+$ plaques. Several rounds of plaque purification were then carried out until a mCherry$^+$ virus could be identified that was free from wildtype virus as determined by PCR. This virus was named HSV-1 LAT pCmC. To verify that the mCherry cassette was inserted into the correct location of the genome, genomic HSV-1 LAT pCmC DNA was isolated and digested with PsiI or XhoI before agarose gel electrophoresis. This revealed that the *mCherry* cassette was located at both ends of the IR_L at the desired location and it is unlikely that there have been any gross morphological changes to the viral genome (Figure 3-13A&B).

To generate HSV-1 pLAT_eGC, a plasmid, named pUC57 pLAT_eGC, was designed that contained 1.2 kb of sequence homologous to the LAT region of HSV-1, and an *eGFP/Cre* fusion gene under the control of an IRES was inserted into the middle of this region. This

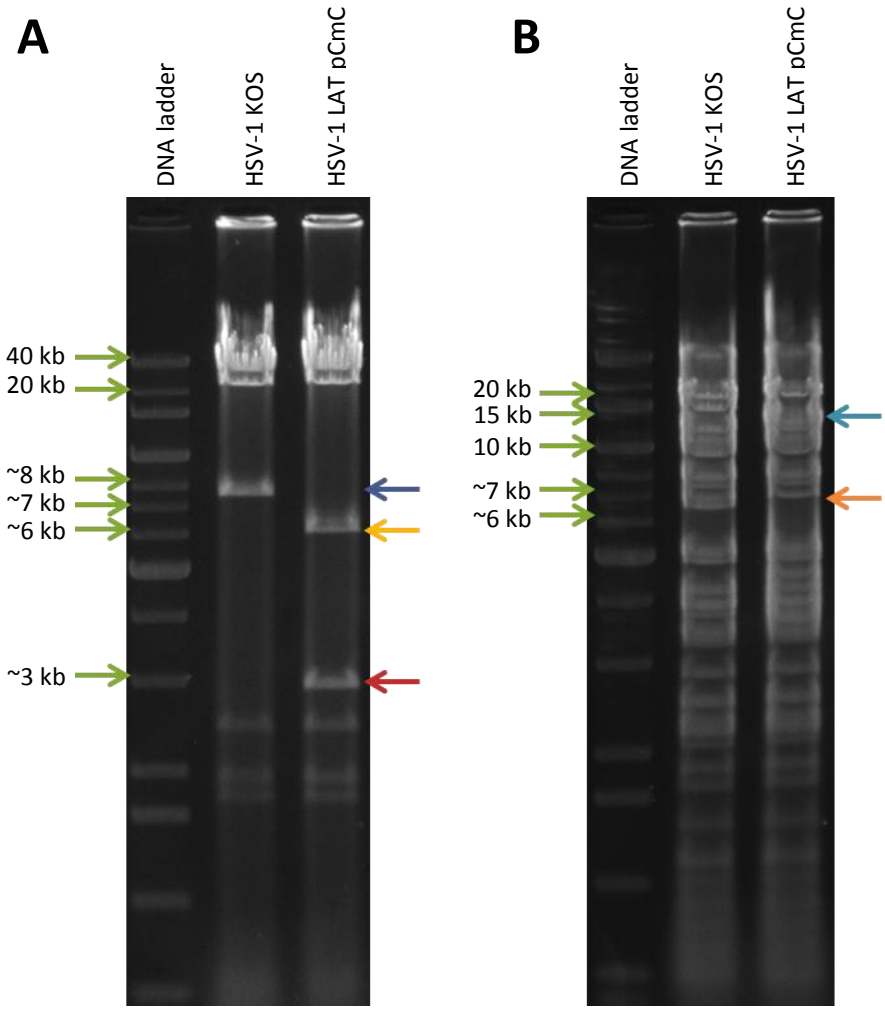

Figure 3-13. Characterisation of HSV-1 with a mCherry expression cassette inserted into the LAT region of HSV-1 KOS by whole genome restriction enzyme digest. The addition of the mCherry cassette into both ends of the genome results in an extra 2948 bp of sequence total. (A) DNA of HSV-1 KOS and HSV-1 pLAT pCmC was digested with PsiI overnight and analysed by agarose gel electrophoresis. This leads to the cleavage of the 33.4 kb and 7.6 kb (the approximate size is indicated by the purple arrow) PsiI fragments of wildtype HSV-1 KOS into 2.9 kb (the approximate size is indicated by the red arrow) and 31.9 kb, and 6.1 (the approximate size is indicated by the yellow arrow) and 3.0 kb (the approximate size is indicated by the red arrow) fragments respectively. (B) DNA of HSV-1 KOS and HSV-1 LAT pCmC was digested with XhoI overnight and analysed by gel electrophoresis. This leads to the cleavage of the 6.1 kb (the approximate size is indicated by the orange arrow) and 14.3 kb (the approximate size is indicated by the blue arrow) XhoI fragments of wildtype HSV-1 KOS into 3.5 kb and 4.0 kb, and 12.2 kb and 3.5 kb fragments respectively. The sizes of relevant fragments of the 1 kb DNA extension ladder are indicated using green arrows.

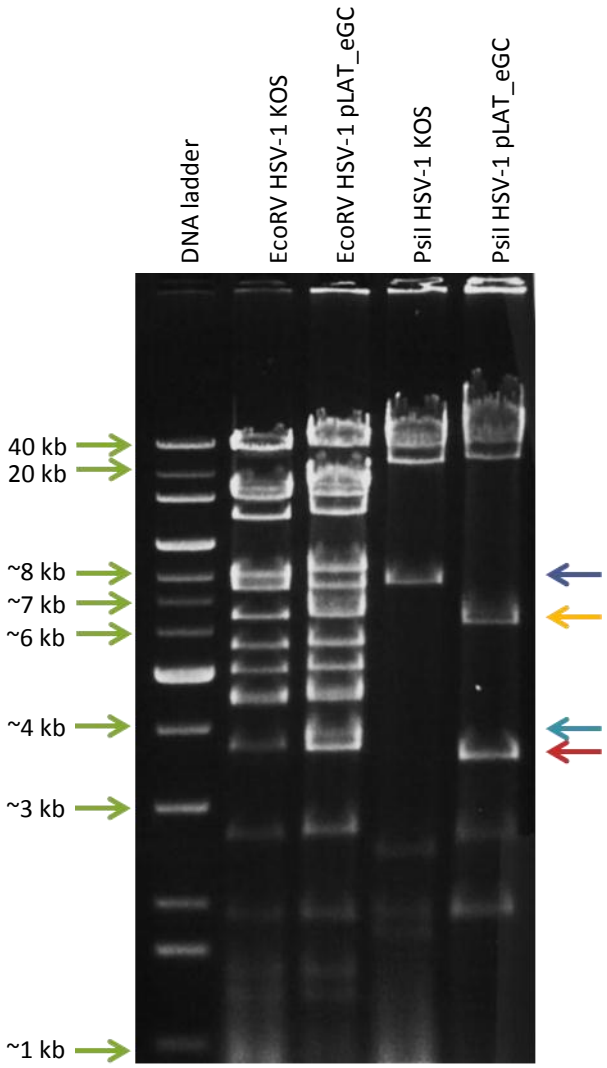

Figure 3-14. Characterisation of HSV-1 with an eGFP expression cassette inserted into the LAT region of HSV-1 KOS by whole genome restriction enzyme digest. The addition of the mCherry cassette into both ends of the genome results in an extra 2513 bp of sequence total. DNA of HSV-1 KOS and HSV-1 pLAT pCmC was digested with EcoRV or PsiI overnight and analysed by agarose gel electrophoresis. This leads to the cleavage of the 33.4 kb and 7.7 kb EcoRV fragments of wildtype HSV-1 KOS into 3.6 kb (the approximate size is indicated by the blue arrow) and 32.4 kb, and 6.6 kb and 3.6 kb (the approximate size is indicated by the blue arrow) fragments respectively. This leads to the cleavage of the 33.4 kb and 7.6 kb (the approximate size is indicated by the purple arrow) PsiI fragments of wildtype HSV-1 KOS into 0.5 kb, 3.5 kb (indicated by the red arrow) and 31.9 kb fragments, and 0.5 kb, 6.1 kb (the approximate size is indicated by the yellow arrow) and 3.4 kb (the approximate size is indicated by the red arrow) fragments respectively. The sizes of relevant fragments of the 1 kb DNA extension ladder are indicated using green arrows.

plasmid was cotransfected with either pX330 or pX330-mC into 293A cells, followed by infection with HSV-1 LAT pCmC after five hours. After three days, the virus and cells were harvested and this virus was serially diluted and used to infect fresh cultures of Vero cells. Fluorescence negative plaques could be identified after two days growth. PCR screening was then used to identify plaques that were positive for the *eGFP/Cre* fusion gene (data not shown). Once the desired recombinant virus was identified, three rounds of plaque purification were carried out to isolate pure recombinant virus that did not express mCherry and so was free from the parent HSV-1 LAT pCmC virus. Sequencing of this region was not performed due to the difficulties associated with the high average 'GC' content of 66%, up to 97.5% in some areas, and complex secondary structure of the LAT region of the genome. To verify that the *eGFP/Cre* cassette was inserted the correct location, genomic DNA was isolated and digested with PsiI or EcoRV before agarose gel electrophoresis. As far as the resolution of this gel allows, this confirmed that the cassette was located in the LAT region at both ends of the IR_L, and that there had not been any gross morphological changes to the viral genome (Figure 3-14).

3.3.2.3 Investigation of variables that influence the frequency of generation of recombinant virus when using the CRISPR/Cas9 based method

To improve the efficiency of the construction of recombinant HSV-1 by CRISPR/Cas9 technology, the impact of two parameters associated with the CRISPR/Cas9 method of generating recombinant virus were considered:

1. The length of flanking region sequence, as increasing the length of the sequence homologous to the site of insertion in the genome was resulted in an increase in the frequency of the generation of recombinant virus when using the conventional infection/transfection method (refer to Section 3.3.1).
2. The DNA ratio of CRISPR/Cas9 targeting plasmid to repair plasmid. It was previously shown that following cleavage of the HSV-1 pC_mC genome by Cas9 with a gRNA designed to cleave mCherry, almost of a third of viral progeny did not exhibit detectable fluorescence. It is likely that the viral genome had been cleaved by Cas9, but was not repaired with the plasmid DNA template provided (refer to Section 3.3.2.1). The failure to correctly repair the viral genome may have been due to a limited amount of repair template provided, particularly as each cell is likely infected with more than one copy of the viral genome. Therefore, increasing the amount of repair template may result in an increase in the frequency of the desired recombinant virus.

The Venus transfer plasmids with different sizes of flanking sequence (Figure 3-11A)

were transfected into 293A cells such that the transfection efficiency was similar (as determined by flow cytometry, data not shown) with either pX330 or pX330-mC in a 1:1 ratio. The cells were then infected with HSV-1 pCmC at a MOI of 0.01. After three days growth, the virus and media were harvested and then used to infect new Vero cells. The proportion of Venus$^+$, mCherry$^+$ and fluorescence negative plaques could then be determined by microscopy after another two days growth. Regardless of the repair plasmid used, the use of mCherry-targeting pX330-mC had a dramatic effect, improving the frequency of Venus$^+$ plaques by more than 100-fold compared to the control pX330 plasmid. Therefore, increasing the length of sequence flanking the Venus insert from 1 to 5.6 kb made only a marginal difference in the generation of recombinant virus (Figure 3-15A). The use of the transfer plasmid with a total flanking sequence of 5.6 kb appeared to facilitate a slightly higher frequency of recombination but this was not observed in a second independent experiment.

To examine the impact of altering the ratio of the repair plasmid DNA to pX330-mC, 293A cells were transfected with 2 µg of the repair plasmid pU3.1kbF-Venus and either pX330 or pX330-mC in a molar ratio of 4:1, 2:1, 1:1 or 1:2. The cells were then infected with HSV-1 pCmC at an MOI of 0.01. All virus was harvested after three days and fresh monolayers of Vero cells were infected with serial dilutions of the progeny of these transfection/infections. After two days of growth the proportion of Venus$^+$, mCherry$^+$ and fluorescence negative plaques was determined. Altering the ratio of the CRISPR/Cas9 plasmid to the repair plasmid had only a modest impact on the proportion of Venus$^+$ virus generated. Further, there was almost no impact on the proportion of non-fluorescent plaques observed (Figure 3-15B). As such, altering the proportion of CRISPR/Cas9 plasmid to repair plasmid is likely to be of little consequence for the optimisation of this method of generating recombinant HSV.

3.4 Identification of a second intergenic region for the expression of foreign genes

A variety of different locations have been identified in the HSV-1 genome that may be appropriate for the insertion of foreign DNA. A suitable site is flanked by genes that are convergently transcribed (Morimoto et al., 2009). Additionally, there should be enough sequence between the two polyA sites of these genes to allow an insertion to be made without disrupting either transcription unit. This includes locations such as the U_L50/U_L51 or U_S1/U_S2 intergenic regions, and the extensively characterised U_L3/U_L4 intergenic

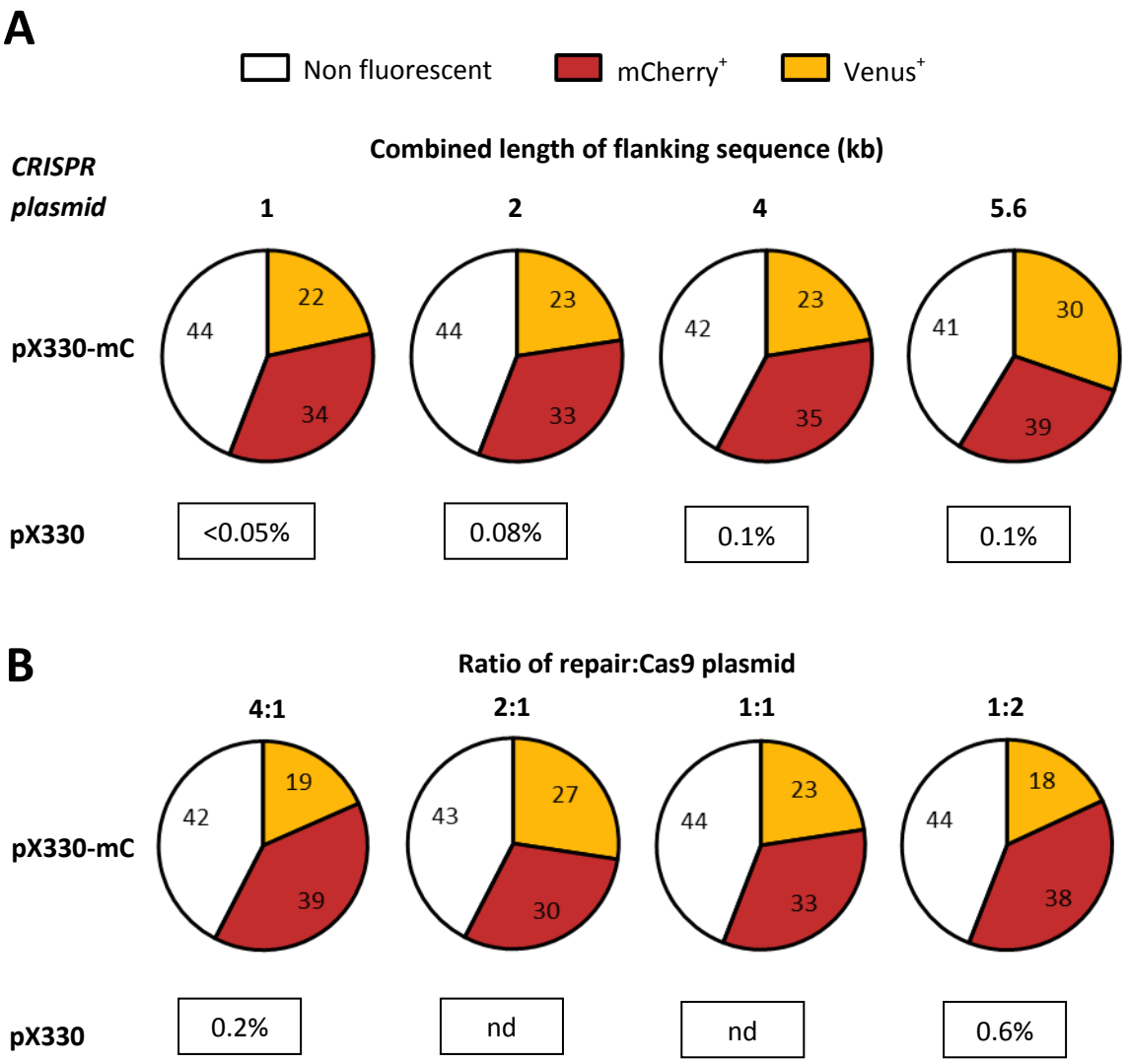

Figure 3-15. Targeting the site of insertion using CRISPR-Cas9 has an overriding effect on recombination frequency. (A) 293A cell monolayers were cotransfected with 2 µg of one of the plasmids shown in Fig. 3-11A and either pX330 or pX330-mC in a 1:1 ratio, and infected with HSV-1 pCmC at an MOI of 0.01 5 hours later. All virus and media was harvested after three days and used to infect monolayers of Vero cells. Pie charts show the percentage of Venus+, mCherry+ and non-fluorescent plaques where mCherry was targeted (with pX330-mC) and boxes below are the approximate percent of Venus+ plaques found when the control (pX330) plasmid was used. (B) 293A monolayers were cotransfected with 2 µg pU3.1kbF-Venus and the appropriate mass of either pX330 or pX330-mC so the ratio of these plasmids was 4:1, 2:1, 1:1 or 1:2, and infected with HSV-1 pCmC at an MOI of 0.01 5 hours later. All virus and media was harvested after three days and used to infect monolayers of Vero cells. The pie charts and boxes show data as for panel A, and nd = not determined. These experiments were repeated with similar results (data not shown).

region (refer to Section 3.2.1; Morimoto et al., 2009; Tanaka et al., 2004). Most other common sites of insertion, such as the U_S5/U_S6 region and *tk* locus, invariably lead to some loss of viral sequence or disruption of some ORFs (Mocarski and Roizman, 1982; Proença et al., 2008; Rinaldi et al., 1999). These sites are then less desirable locations for insertion into the HSV genome when wildtype virulence is desired.

The space between U_L26 and U_L27 genes has the ideal structure for the insertion of foreign genes, and has had a limited history of genetic manipulation (Balliet et al., 2007; Bzik et al., 1984; Cai et al., 1993; Holland et al., 1984; Morimoto et al., 2009; Potel et al., 2002). The U_L27 region has been engineered to introduce mutations into gB for structural and functional analyses (Desai et al., 1994). Foreign DNA has also been inserted into the U_L26/U_L27 site previously, but in some cases the resultant viruses showed reduced virulence in mice relative to wildtype virus (Balliet et al., 2007; Cai et al., 1993; Orr et al., 2005). For one virus, the insertion disrupted the native polyA signal of U_L26, so this was replaced with the SV40 polyA (Orr et al., 2005). It was not clear why the phenotype of this virus was altered. Given the previous use of the U_L26/U_L27 intergenic region as a site of insertion, this region was chosen for use as a second site of insertion, with care taken to leave the two transcription units intact (Figure 3-16).

3.4.1 Design and construction of the transfer plasmid pU26/7 for insertion of DNA into the $U_L26/27$ intergenic site

The location of the shared U_L24 and U_L26 putative polyA signal and the U_L27 polyA signal was identified based on an analyses of polyA sites of HSV-1 by McGregor and colleagues (1996). Approximately 2 kb of the U_L26/U_L27 region was amplified and cloned into the pUC vector with the insertion of an MCS between these putative polyA sites. This meant that an ICP47 promoter (as described in Section 3.2.2.1) Tdtomato expression cassette could be inserted into a position midway between the U_L26 and U_L27 polyA sites to generate pU26/7 pICP47_Tdtom (Figure 3-16).

3.4.2 Generation of HSV-1 expressing Tdtomato from the U_L26/U_L27 intergenic region

To determine if the U_L26/U_L27 region would be suitable for the expression of foreign genes from HSV-1, a virus was constructed that expressed the fluorescent reporter Tdtomato from this site under the control of the ICP47 promoter. Linearised pU26/7 pICP47/Tdtom plasmid DNA was transfected into 293A cells followed by infection with HSV-1 KOS for two hours. After 72 hours, all cells and media were harvested, and used to infect new Vero cell monolayers. After 2 days of growth, the proportion of Tdtomato$^+$

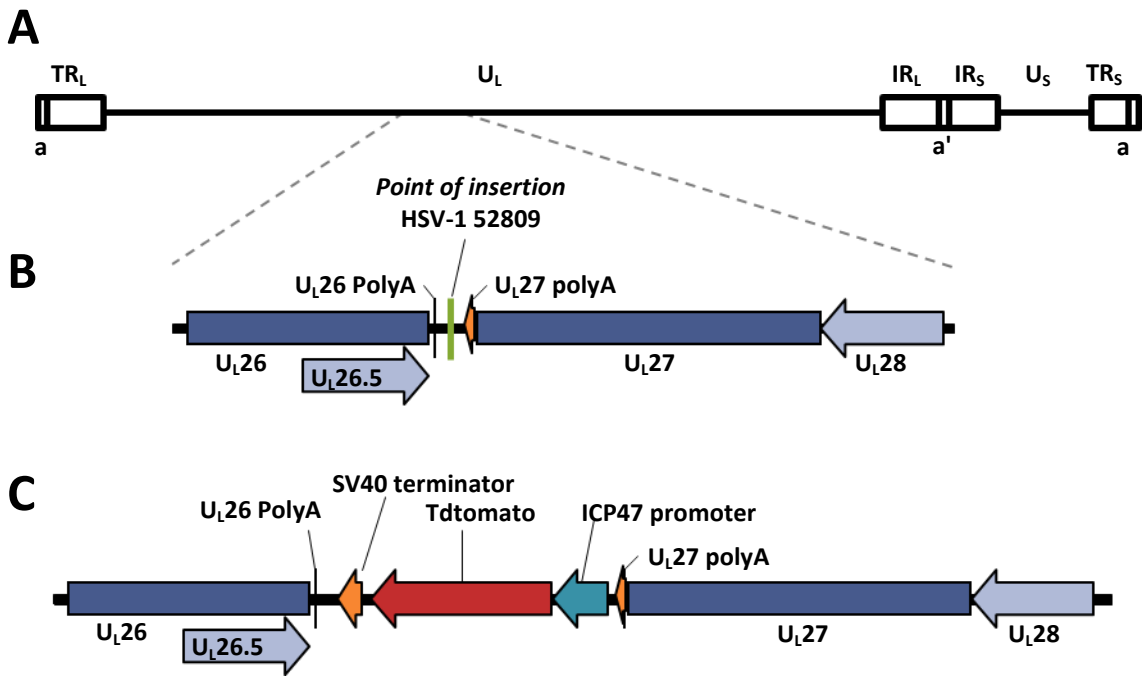

Figure 3-16. Identification of the U_L26/U_L27 intergenic region for the insertion of foreign DNA into HSV-1. (A) Schematic representation of the HSV-1 genome with the location of U_L26 and U_L27 indicated (to scale). (B) Schematic representation of the U_L26/U_L27 intergenic region, with the point at which the Tdtomato cassette is inserted indicated in green and the base pair position indicated using numbers from HSV-1 KOS (JQ673480).(C) Schematic representation of the Tdtomato expression cassette in the intergenic space between U_L26 and U_L27.

plaques was determined. A Tdtomato$^+$ plaque was selected from each of two independent, parallel transfections and plaque purified to yield pure recombinant virus (Figure 3-17), which was free from wildtype virus as determined by microscopy and PCR. One of these viruses was chosen for further examination and named HSV-1 pICP47/Tdtom.

Secondary structure within the ICP47 promoter meant that amplifying the entire Tdtomato cassette by PCR was very difficult, so a restriction digest of the viral genome was performed to demonstrate that the Tdtomato had been inserted as expected into the U_L26/U_L27 intergenic region (Figure 3-18). Unfortunately, there was not sufficient resolution to allow confirmation that gross morphological changes to the viral genome had not occurred. To further characterise HSV-1 pICP47/Tdtom, its replication ability was assessed relative to HSV-1 KOS by a multiple step growth curve (MOI 0.01) in Vero cells. Both viruses grew with similar kinetics *in vitro* (Figure 3-19). Both viruses replicated to similar titres to HSV-1 KOS *in vivo* (refer to Section 3.5.3). Overall, this data suggests that this U_L26/U_L27 site can be used to construct recombinant HSV-1 without the disruption of genes, growth defects or any attenuation *in vivo*.

3.5 Characterisation of recombinant HSV-1 designed to express *eGFP/Cre* from the U_L3/U_L4 intergenic region

In this thesis, a number of viruses were designed and constructed that express *eGFP/Cre* under the control of various promoters. It is important that these viruses are similar to wildtype HSV-1 KOS when used both *in vitro* and *in vivo*.

3.5.1 Assessment of replicative ability of recombinant viruses *in vitro*

To verify that these viruses exhibit similar growth to wildtype HSV-1 *in vitro*, multiple step growth curves (MOI 0.01) were performed in Vero cells. The growth of the parental virus KOS was assessed relative to one of the recombinant viruses generated. HSV-1 pICP47_eGC, HSV-1 pICP6_eGC, HSV-1 pICP0_eGC, HSV-1 pgB_eGC or HSV-1 pC_eGC did not exhibit any change in kinetics compared to wildtype virus *in vitro*, suggesting that the replication ability of these viruses was similar to HSV-1 KOS (Figure 3-20).

In order to assess the replication ability of HSV-1 pLAT_eGC, first the growth of the parent virus HSV-1 LAT pCmC was assessed in Vero cells by a multiple step growth curve (MOI 0.01). This demonstrated that the wildtype HSV-1 KOS and HSV-1 LAT pCmC grew with similar kinetics (Figure 3-21A). Once the recombinant virus HSV-1 pLAT_eGC was constructed, the growth of HSV-1 pLAT_eGC was assessed in comparison to HSV-1 LAT

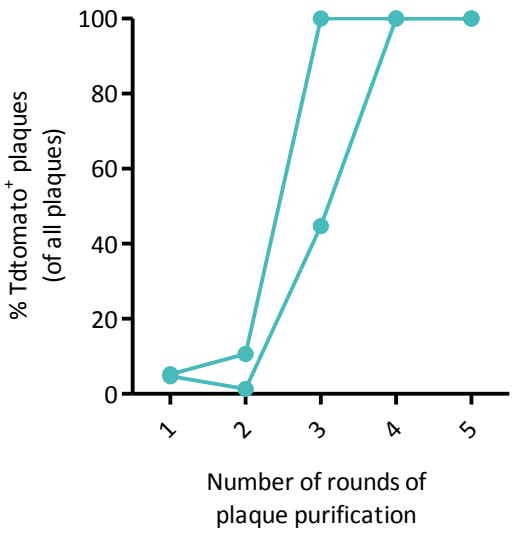

Figure 3-17. Generation of recombinant HSV-1 containing a Tdtomato expression cassette inserted into the U_L26/U_L27 intergenic region. 293A cell monolayers were transfected with pU26/7 pICP47_Tdtom and after 5 hours were infected with HSV-1 KOS at an MOI of 0.01. After 72 hours, all virus and media was harvested and used to infect monolayers of Vero cells (round 1 of plaque purification). After two days growth, the frequency of Tdtomato+ plaques was determined as a percentage of total plaques (round 1 of plaque purification). Two parallel, independent transfections were carried out and a plaque was selected from each transfection. Multiple rounds of plaque purification were performed and the percentage of Tdtomato+ plaques was determined until they were found to be free from wildtype virus as shown by microscopy and PCR.

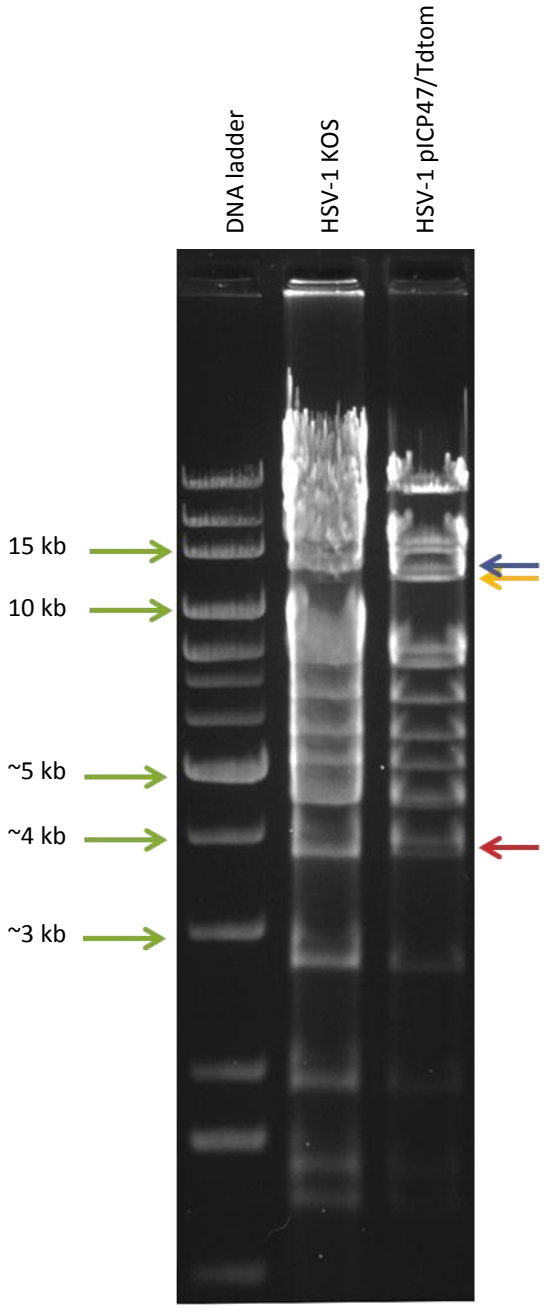

Figure 3-18. Confirmation of the U_L26/27 intergenic region as the site of insertion of Tdtomato cassette in HSV-1 pICP47/Tdtom. (A) DNA of HSV-1 KOS and HSV-1 pICP47_Tdtom was digested with *EcoR*V overnight and analysed by agarose gel electrophoresis. The Tdtomato expression cassette contains an additional *Eco*RV site. This results in the addition of an extra 2.155 kb sequence into the ~14.9 found in wt KOS (likely to be the unresolved doublet indicated by the purple arrow), which will be cleaved by digestion with *Eco*RV into ~3.9 kb and 13.1 kb fragments (the approximate size is indicated using red and yellow arrows, respectively). The sizes of relevant fragments of the 1 kb DNA extension ladder are indicated using green arrows.

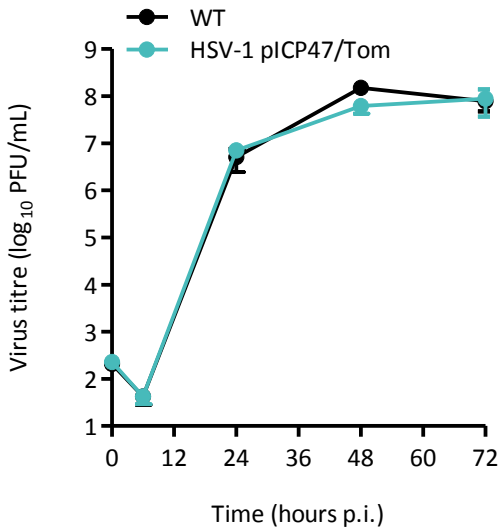

Figure 3-19. Insertion of Tdtomato into the U_L26/U_L27 intergenic region has no effect on replication kinetics either *in vitro* or *in vivo* relative to HSV-1 KOS. The replication of HSV-1 pICP47/Tdtom (blue) was compared to parent wildtype HSV-1 KOS (black) in Vero cells in a multiple step growth curve. Confluent cell monolayers in 9.6 cm^2 tissue culture wells were infected at a low MOI (0.01 PFU/cell in 1 mL M0). After one hour, the inoculum was removed, cells washed and 2 mL M2 added. A 0 hour p.i. sample was collected immediately after the addition of fresh media. The remaining samples were harvested at 6, 24, 48 or 72 hours p.i. Virus titres were determined by standard plaque assay. Data are mean±SEM of three replicates.

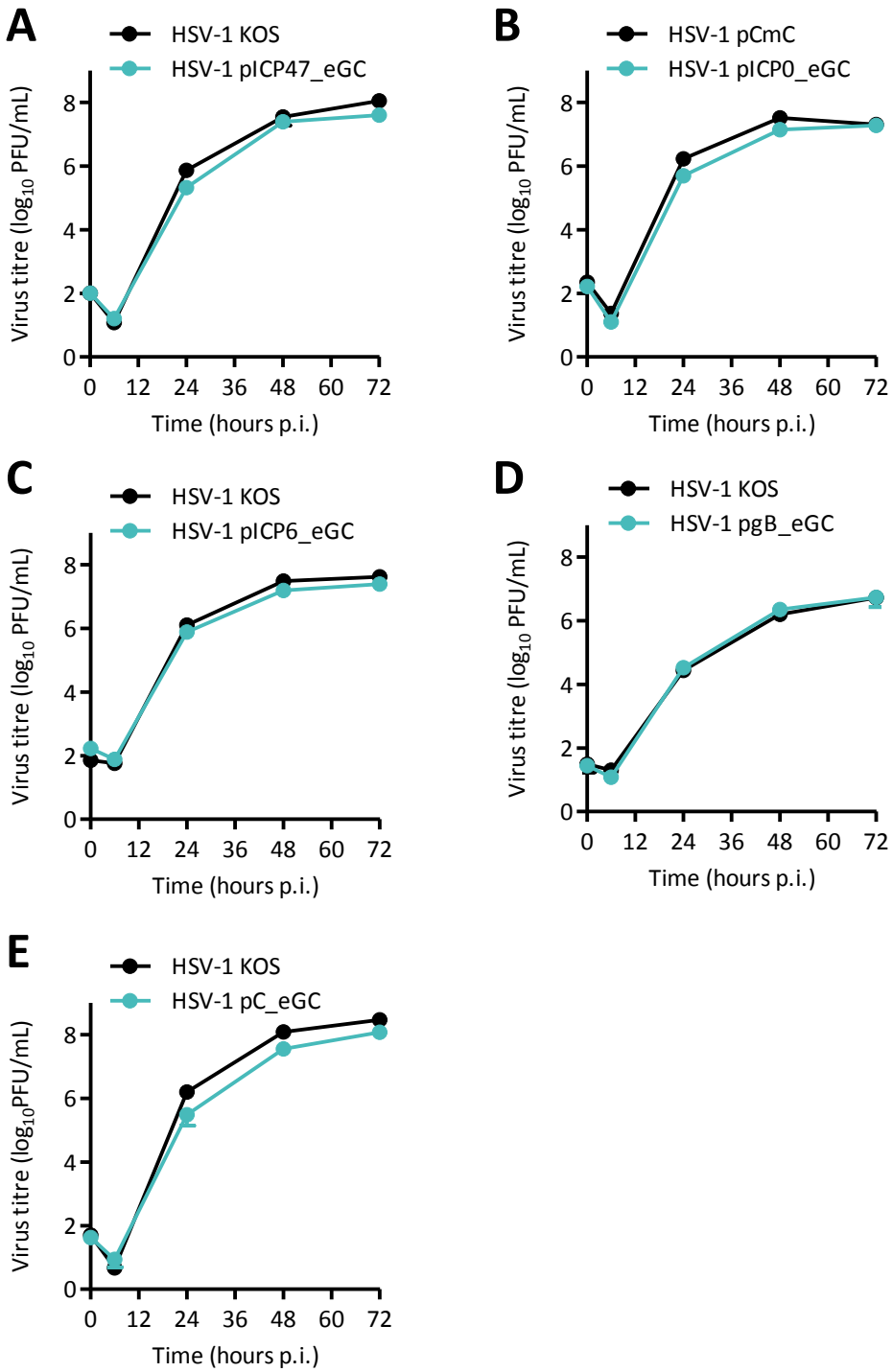

Figure 3-20. Insertion of eGFP/Cre under various HSV-1 promoters into the U_L3/U_L4 intergenic region has no effect on virus growth *in vitro* relative to HSV-1 KOS. The replication of (A) HSV-1 pICP47_eGC, (B) HSV-1 pICP0_eGC, (C) HSV-1 pICP6_eGC, (D) HSV-1 pgB_eGC or (E) HSV-1 pC_eGC (blue) was compared to the parent wildtype HSV-1 KOS or HSV-1 pCmC (black) in Vero cells in multiple step growth curves. Confluent cell monolayers in 9.6 cm^2 tissue culture wells were infected at a low MOI (0.01 PFU/cell in 1 mL M0). After one hour, the inoculum was removed, cells washed and 2 mL M2 was added. A 0 hour p.i. sample was collected immediately following the addition of fresh media. The remaining samples were harvested at 6, 24, 48 or 72 hours p.i. Virus titres were determined by standard plaque assay. Data are mean±SEM of three replicates.

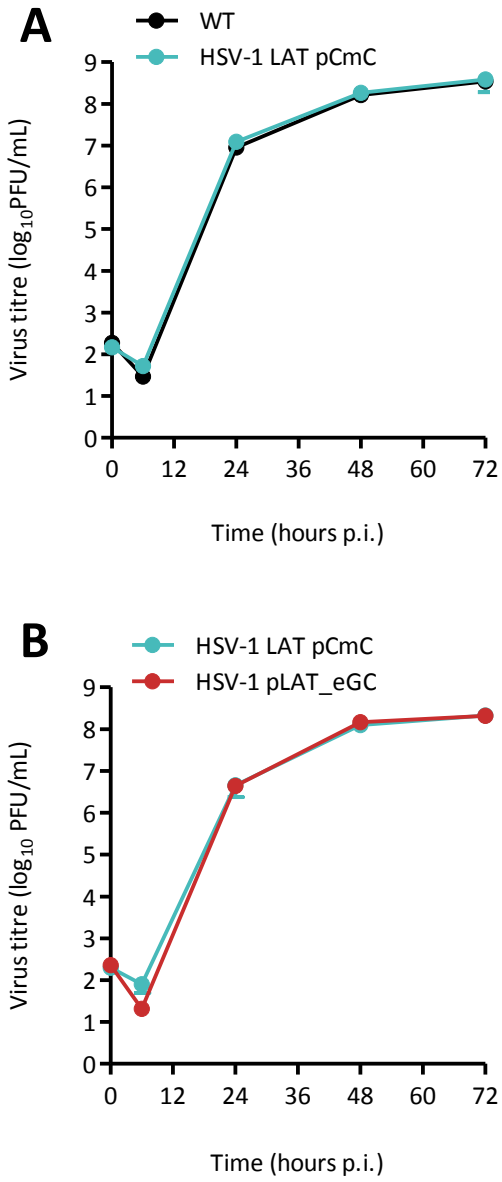

Figure 3-21. Insertion of eGFP/Cre under the control of an IRES into the LAT region has no effect on virus growth *in vitro* relative to HSV-1 KOS. (A) The replication of HSV-1 LAT pCmC (blue) was compared to the parent wildtype HSV-1 KOS (black) in Vero cells in a multiple step growth curve. (B) The replication of HSV-1 pLAT_eGC (red) was compared to the parent wildtype HSV-1 LAT pCmC (blue) and wildtype HSV-1 KOS (black) in Vero cells in a multiple step growth curve. Confluent cell monolayers in 9.6 cm^2 tissue culture wells were infected at a low MOI (0.01 PFU/cell in 1 mL M0). After one, the inoculum was removed, cells washed and 2 mL M2 was added. A 0 hour p.i. sample was collected immediately following the addition of fresh media. The remaining samples were harvested at 6, 24, 48 or 72 hours p.i. Virus titres were determined by standard plaque assay. Data are mean±SEM of three replicates.

pCmC by another multiple step growth curve (MOI 0.01; Figure 3-21B). This confirmed that HSV-1 pLAT_eGC, HSV-1 LAT pCmC and HSV-1 KOS have a similar replicative ability *in vitro*.

3.5.2 Confirmation of expression kinetics of ectopic promoters

One way to distinguish the three major classes of HSV-1 genes is by their expression following the treatment of infected cells with different drugs. Cycloheximide inhibits translation, and so viral genes will only be transcribed in the presence of this drug if their expression is not dependent on viral transactivators synthesised after HSV-1 infection. In other words, cycloheximide inhibits the expression of the early and late genes, but not the immediate genes (Honess and Roizman, 1974). Another drug, acyclovir, blocks HSV-1 DNA replication, and so prevents the expression of the γ_2 genes, but not the immediate early, early and γ_1 genes (Nichol et al., 1996; Summers and Leib, 2002).

In order to confirm that the expression under the ectopic promoters used in this thesis is as predicted based on their kinetic class the expression of the *eGFP/Cre* cassette following drug inhibition was tested. A cycloheximide reversal experiment was performed in which Vero cell monolayers were infected with each recombinant virus in the presence or absence of cycloheximide. After six hours, the cycloheximide block is reversed and replaced with actinomycin D, which blocks transcription, allowing only the accumulated mRNA to be translated into protein (Honess and Roizman, 1974; Honess and Roizman, 1975; Summers and Leib, 2002). In addition, separate Vero cell monolayers were infected with each recombinant virus in the presence of acyclovir. The concentration of acyclovir used was able to prevent transcription of the γ_2 gene encoding gC, but not the other genes expressed with immediate early or early kinetics, such as U_S12, as detected by semi-quantitative RT-PCR (data not shown).

As shown in Figure 3-22A&D, detectable eGFP expression was observed in the absence of any treatment as expected for all recombinant viruses that contain the *eGFP/Cre* cassette, with the exception of HSV-1 pLAT_eGC. However, the LAT promoter is not expressed in Vero cells, so this result was expected (refer to Section 3.3.2.2). Neither cycloheximide nor acyclovir inhibition prevented expression of eGFP in cells infected with HSV-1 pICP0_eGC or HSV-1 pICP47_eGC, confirming that eGFP is expressed as would be expected when under the control of an immediate early promoter. Similarly, expression of eGFP by HSV-1 pC_eGC was not prevented by either of these drugs. In this case it likely reflects that the CMV IE promoter is largely independent of the cascade of HSV-1 gene expression (Arthur et al., 2001; Preston and Nicholl, 1997; Stinski and Roehr, 1985). Although cycloheximide

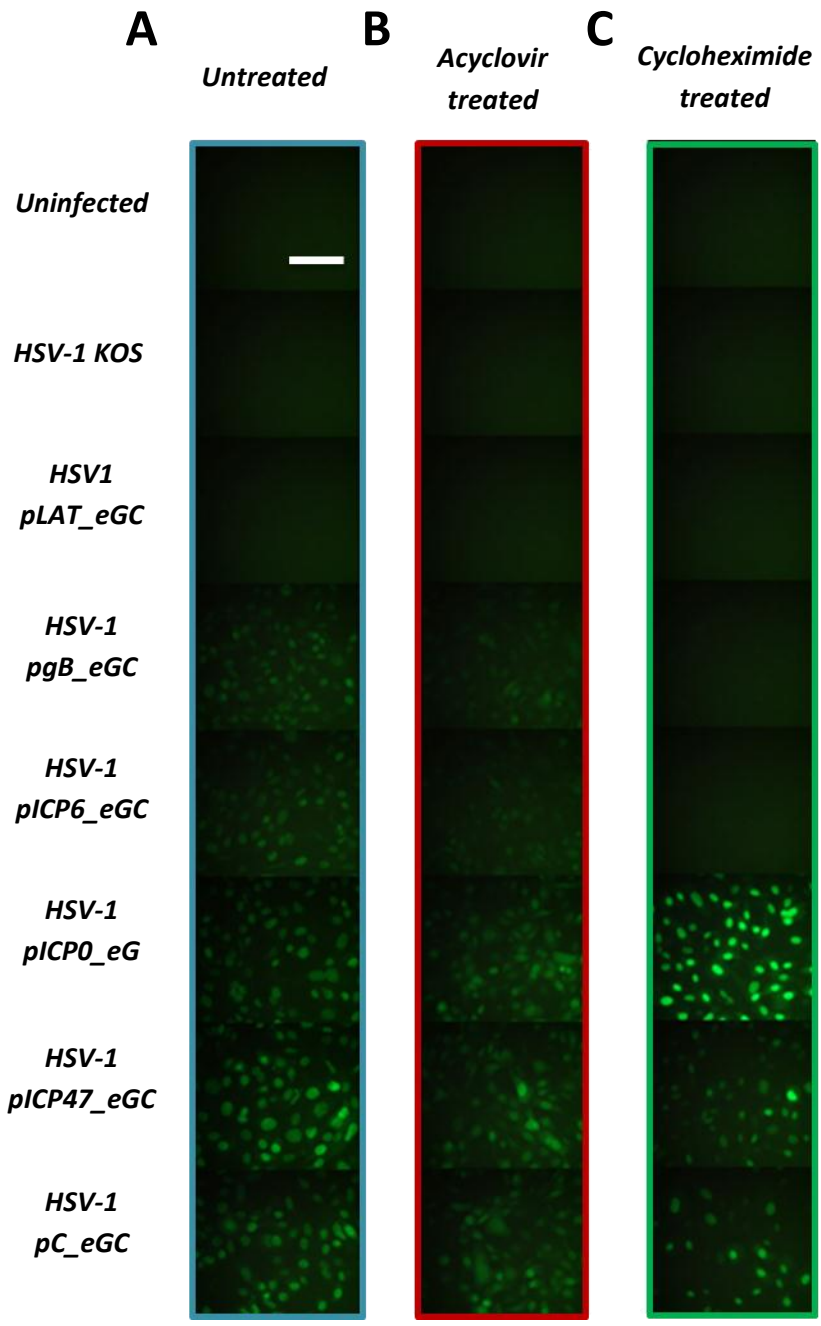

Figure 3-22. Characterisation of promoter class *in vitro*. Confluent Vero cell monolayers in 2 cm^2 tissue culture wells were pretreated with either (C&F) cycloheximide or (B&E) 50 µM acyclovir, or left untreated (A&D) for one hour. Cells were then infected at a high MOI (5 PFU/cell in 500 µL M0 with appropriate drug) with HSV-1 KOS, HSV-1 pLAT_eGC, HSV-1 pgB_eGC, HSV-1 pICP6_eGC, HSV-1 pICP0_eGC, HSV-1 pICP47_eGC or HSV-1 pC_eGC, or left uninfected. After one hour, the inoculum was removed, and 1 mL M2 was added, with appropriate drug if required. Cells were incubated for six hours at 37°C, 5% CO_2 before cycloheximide was removed and actinomycin D added to these wells. Cells were incubated for a further four hours at 37°C, 5% CO_2. (A-C) Cells were photographed for eGFP expression at 400× magnification (scale bar = 50 µm, as indicated on top left photograph). (D-F) Cells were then fixed and eGFP expression assessed by flow cytometry. The shaded grey area represents the eGFP expression of uninfected cells for the top panels, and the eGFP expression of HSV-1 KOS infected cells for all remaining figures. The expression of eGFP by the infected cells is shown in either blue (untreated), red (acyclovir treated) or green (cycloheximide treated).

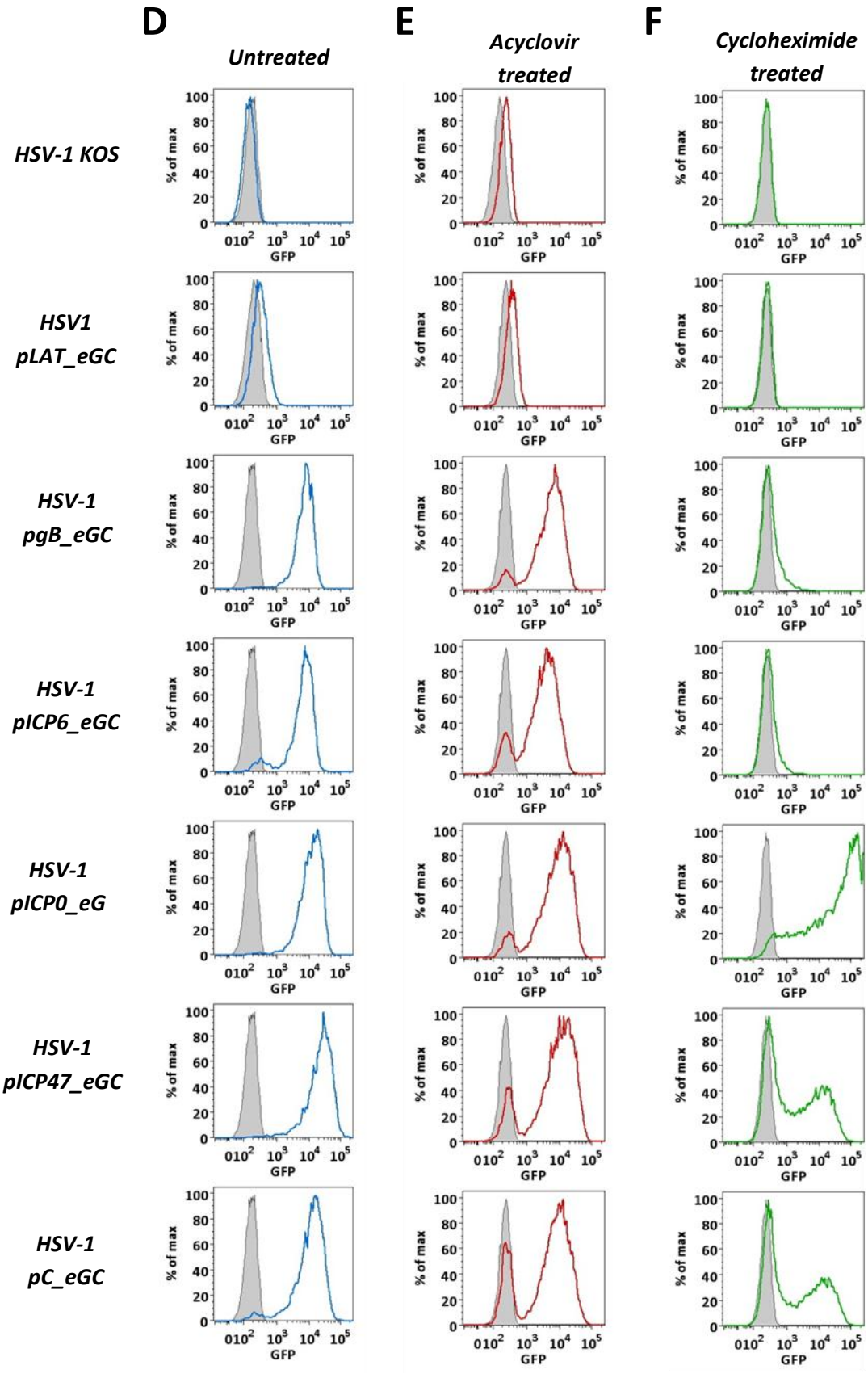
D
E
F
Untreated
Acyclovir treated
Cycloheximide treated
HSV-1 KOS
HSV1 pLAT_eGC
HSV-1 pgB_eGC
HSV-1 pICP6_eGC
HSV-1 pICP0_eG
HSV-1 pICP47_eGC
HSV-1 pC_eGC
% of max
GFP

was able to prevent eGFP expression from HSV-1 pICP6_eGC and HSV-1 pgB_eGC, acyclovir was not able to block eGFP expression, as would be expected for an early or γ_1 promoter (Figure 3-22).

Treatment with acyclovir did slightly decrease the expression of eGFP in all cells infected with a virus expected to express eGFP (Figure 3-22C&F). This has previously been observed by Nichol and colleagues (1996) in infected cultures of superior cervical ganglion neurons but not Vero cells, although the semi-quantitative RT-PCR assay used was relatively insensitive to transcript levels. Viral replication and secondary spread may have occurred in the cells that were untreated compared to those treated with acyclovir, but they found that this was unlikely to be the case (Nichol et al., 1996). Similarly, in this experiment, the high MOI used and short timeframe in which this experiment was conducted mean that the slight inhibition of eGFP expression by acyclovir is very unlikely to be accounted for by viral replication and secondary spread of virus. However, it does remain difficult to account for this observation. In conclusion, based on the cycloheximide reversal assay and acyclovir inhibition assay, all the defined promoters used in this thesis were expressed as would be expected based on their kinetic class.

3.5.3 Assessment of pathogenesis and growth of recombinant viruses *in vivo*

To confirm that the pathogenesis of recombinant HSV-1 containing an *eGFP/Cre* marker gene was comparable to HSV-1 KOS *in vivo*, C57Bl/6 mice were infected with either HSV-1 KOS or a recombinant HSV-1, and lesion size was monitored daily. All mice developed a zosteriform lesion, indicating that the virus was able to spread within the PNS back to the skin. For all viruses tested, namely HSV-1 pICP47_eGC, HSV-1 pICP6_eGC and HSV-1 pgB_eGC, a similar lesion progression to HSV-1 KOS was observed (Figure 3-23).

To determine if these viruses had a similar replicative ability to HSV-1 KOS *in vivo*, C57Bl/6 mice were infected with either HSV-1 KOS, HSV-1 pICP47_eGC, HSV- 1pICP6_eGC or HSV-1 pgB_eGC and the amount of virus in the skin and DRG at five days p.i. was determined. Although the size of the lesions on these mice was not measured, mice were checked daily to confirm that they developed lesions as would be expected. All mice developed primary lesions by day three p.i. and showed signs of zosteriform spread of virus on day five p.i. The amount of virus found in the skin or DRG was similar for all viruses relative to HSV-1 KOS for all viruses tested (Figure 3-24).

The flank tattoo infection method for assessing viral growth and pathogenesis has several advantages. While lesions are not measured, mice are checked daily to ensure they

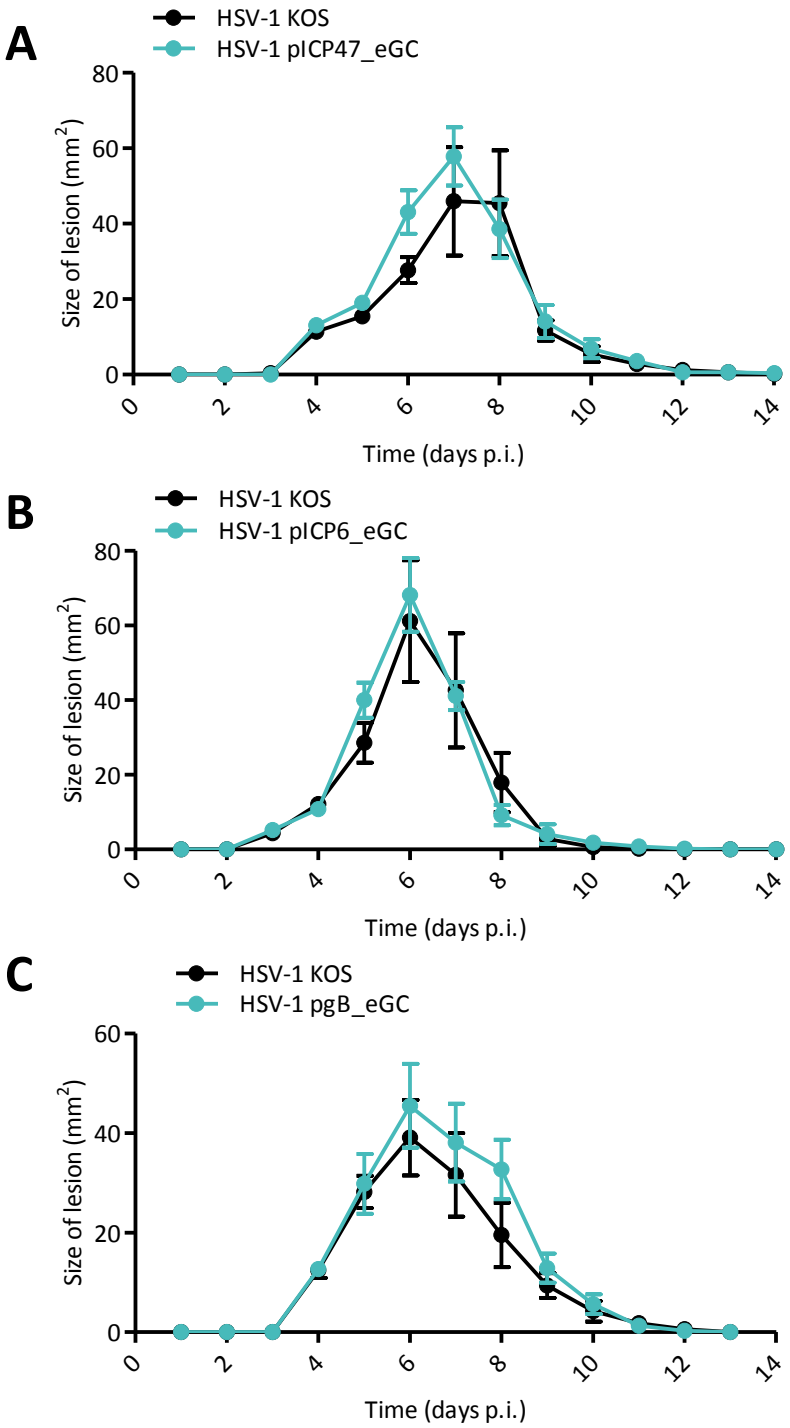

Figure 3-23. Insertion of eGFP/Cre under various HSV-1 promoters into the U_L3/U_L4 intergenic region has no effect on lesion development in mice relative to HSV-1 KOS. C57Bl/6 mice were infected by tattoo with 1×10^8 PFU/mL with HSV-1 KOS or the appropriate recombinant virus. Lesion size was measured daily using a caliper and clinical score was monitored daily, with mice never displaying any signs of illness other than the herpetic lesion on the flank. (A) Comparison of mean lesion size of C57Bl/6 mice infected with 1×10^8 PFU/mL HSV-1 KOS (black) or HSV-1 pICP47_eGC (blue). (B) Comparison of mean lesion size of C57Bl/6 mice infected with 1×10^8 PFU/mL HSV-1 KOS (black) or HSV-1 pICP6_eGC. (C) Comparison of mean lesion size of C57Bl/6 mice infected with 1×10^8 PFU/mL HSV-1 KOS (black) or HSV-1 pgB_eGC (blue). Data is mean lesion size±SEM (n = 5). Data was analysed by a Kruskal-Wallis test, but in all cases the differences in the median lesion size was insignificant ($p > 0.05$).

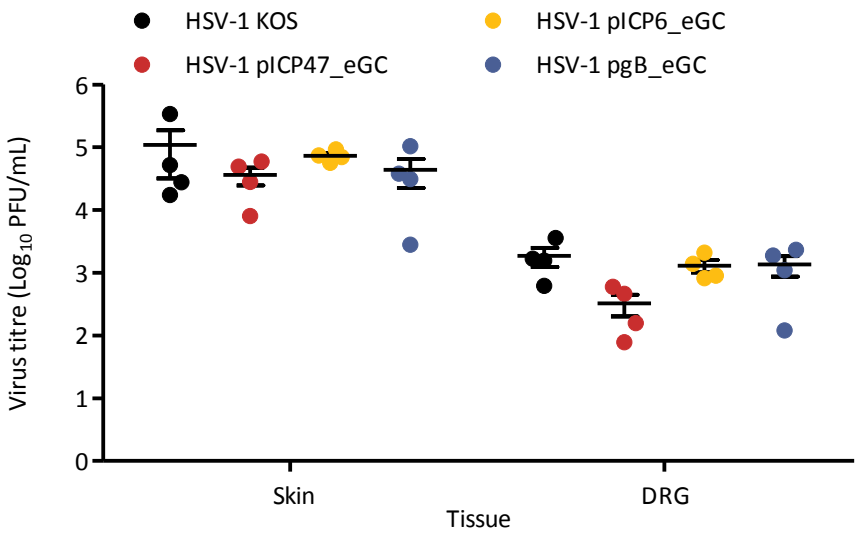

Figure 3-24. Insertion of eGFP/Cre under various HSV-1 promoters into the U_L3/U_L4 intergenic region has no effect on virus growth *in vivo* relative to HSV-1 KOS. Groups of four C57Bl/6 mice were infected by tattoo with 1×10^8 PFU/mL with HSV-1 KOS (black), HSV-1 pICP47_eGC (red), HSV-1 pICP6_eGC (yellow) or HSV-1 pgB_eGC (purple). At five days p.i. mice were culled and infectious virus was determined by standard plaque assay from ten DRG (spinal levels L1 to T5) or 1 cm^2 skin located over the inoculation size. The limit of detection is two PFU per sample. Circles show results for each mouse (n=4) and bars represent mean±SEM. The amount of virus in the skin or DRG of mice infected with each recombinant virus was compared to that of HSV-1 KOS using an ANOVA, but the difference in means was not statistically significant.

develop a primary lesion, typically on day three p.i., and demonstrate signs of secondary spread, typically on day five p.i. As secondary, or zosteriform, spread is dependent on HSV-1 gaining access to the PNS to allow for spread of virus, the observation of secondary lesions provides an easy, quick visual means of confirming that the pathogenesis of the virus is as expected. It also allows the measurement of virus growth in both the skin and DRG. Finally, using this method alone minimises the numbers of mice required to confirm the pathogenesis and growth of the recombinant viruses generated in this thesis, and therefore was now used exclusively for this purpose.

Given this, the growth of HSV-1 pC_eGC was assessed relative to HSV-1 KOS in C57Bl/6 mice. All mice developed primary lesions by day three p.i. and showed signs of zosteriform spread of virus on day five p.i. Again, the amount of virus in the skin and DRG was measured at day five p.i. (Figure 3-25). The amount of virus in both the skin and DRG was similar in both the HSV-1 KOS and HSV-1 pC_eGC infected mice.

To assess the growth of HSV-1 pICP47/Tdtom, C57Bl/6 mice were infected on the flank with either HSV-1 KOS or HSV-1 pICP47/Tdtom. All mice developed a primary lesion on day three p.i. and zosteriform spread could be identified on day five p.i. On day five p.i., mice were culled and growth of virus in the DRG and skin was determined by standard plaque assay. The growth of HSV-1 pICP47/Tdtom was not compromised relative to HSV-1 KOS (Figure 3-26). There was a statistically significant difference in growth of HSV-1 pICP47/Tdtom in the skin compared to HSV-1 KOS, but this increase was only just over three-fold and is unlikely to be biologically significant.

Similarly, the growth of HSV-1 pICP0_eGC was determined compared to HSV-1 KOS in C57Bl/6 mice by quantifying the amount of virus in the skin and DRG at five days p.i. (Figure 3-27). Again, the amount of virus in the skin and DRG was comparable for HSV-1 KOS and HSV-1 pICP0_eGC infected mice. All mice developed primary and zosteriform lesions as expected.

Finally, to verify that HSV-1 pLAT_eGC demonstrates similar growth *in vivo* compared to HSV-1 KOS, first the growth of the parent HSV-1 LAT pCmC was assessed relative to HSV-1 KOS in C57Bl/6 mice. At five days p.i. there was a similar titre of virus in both the skin and DRG (Figure 3-28). Then, the growth of HSV-1 pLAT_eGC was compared to HSV-1 KOS in C57Bl/6 mice at five days p.i., with a similar amount of virus in both the skin and DRG (Figure 3-28). In both cases, all mice showed a normal progression of lesion development.

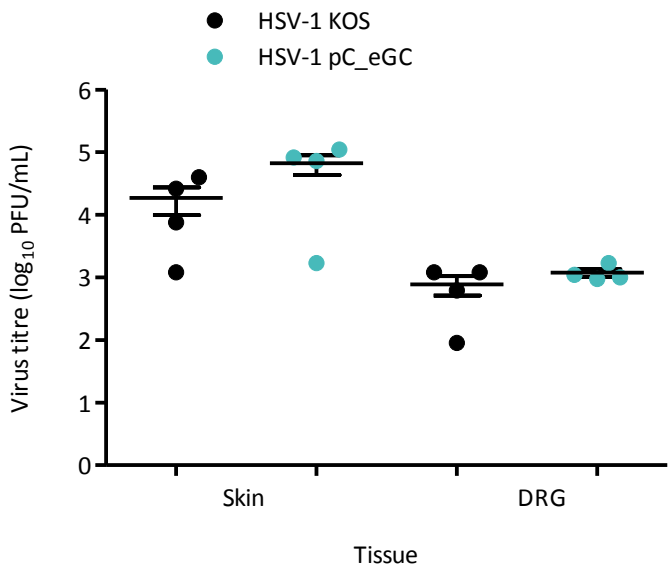

Figure 3-25. HSV-1 pC_eGC has no defect in virus growth *in vivo* relative to HSV-1 KOS. Groups of four C57Bl/6 mice were infected by tattoo with 1×10^8 PFU/mL with HSV-1 KOS (black) or HSV-1 pC_eGC (blue). At five days p.i. mice were culled and infectious virus was determined by standard plaque assay from ten DRG (spinal levels L1 to T5) or 1 cm^2 skin located over the inoculation size. The limit of detection was two PFU per tissue. Circles show results for each mouse (n=4) and bars represent mean±SEM. The means were compared in each tissue by an unpaired *t* test, but in both cases the difference was not statistically significant ($p > 0.05$).

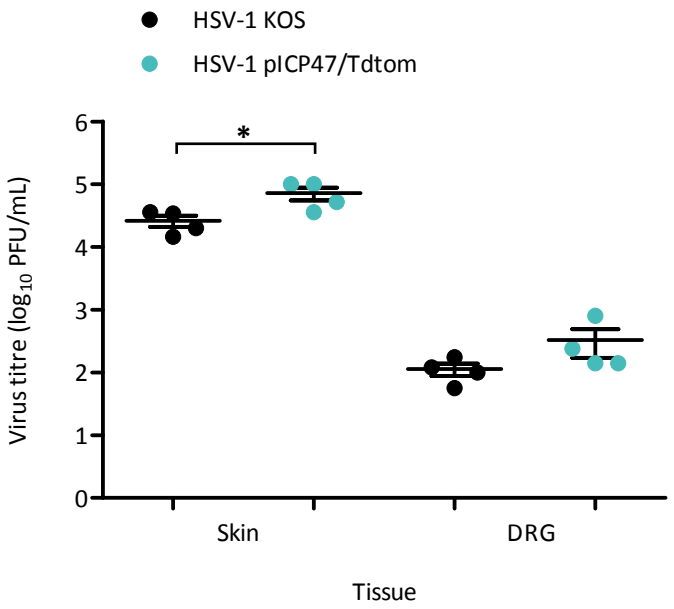

Figure 3-26. Insertion of Tdtomato into the U_L26/U_L27 intergenic region has no effect on replication kinetics *in vivo* relative to HSV-1 KOS. Groups of four C57Bl/6 mice were infected by tattoo with 1×10^8 PFU/mL with HSV-1 KOS (black) or HSV-1 pICP47/Tdtom (blue). Infectious virus was determined by standard plaque assay from ten DRG (spinal levels L1 to T5) or 1 cm^2 skin located over the inoculation size five days after infection. The limit of detection was two PFU for each tissue. Circles show results for each mouse (n=4) and bars represent mean±SEM. The means were compared by an unpaired *t* test, where significance is denoted by * ($p < 0.05$) or as *ns* (not significant).

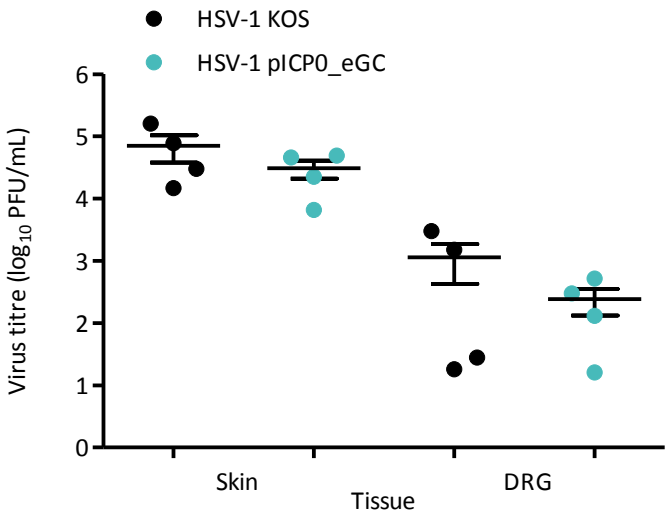

Figure 3-27. HSV-1 pICP0_eGC has no defect in virus growth *in vivo* relative to the HSV-1 KOS. Groups of four C57Bl/6 mice were infected by tattoo with 1×10^8 PFU/mL with HSV-1 KOS (black) or HSV-1 pC_eGC (blue). At five days p.i. mice were culled and infectious virus was determined by standard plaque assay from ten DRG (spinal levels L1 to T5) or 1 cm^2 skin located over the inoculation size. The limit of detection was two PFU per tissue. Circles show results for each mouse (n=4) and bars represent mean±SEM. The means were compared in each tissue by an unpaired *t* test, but in both cases the difference was not statistically significant ($p > 0.05$).

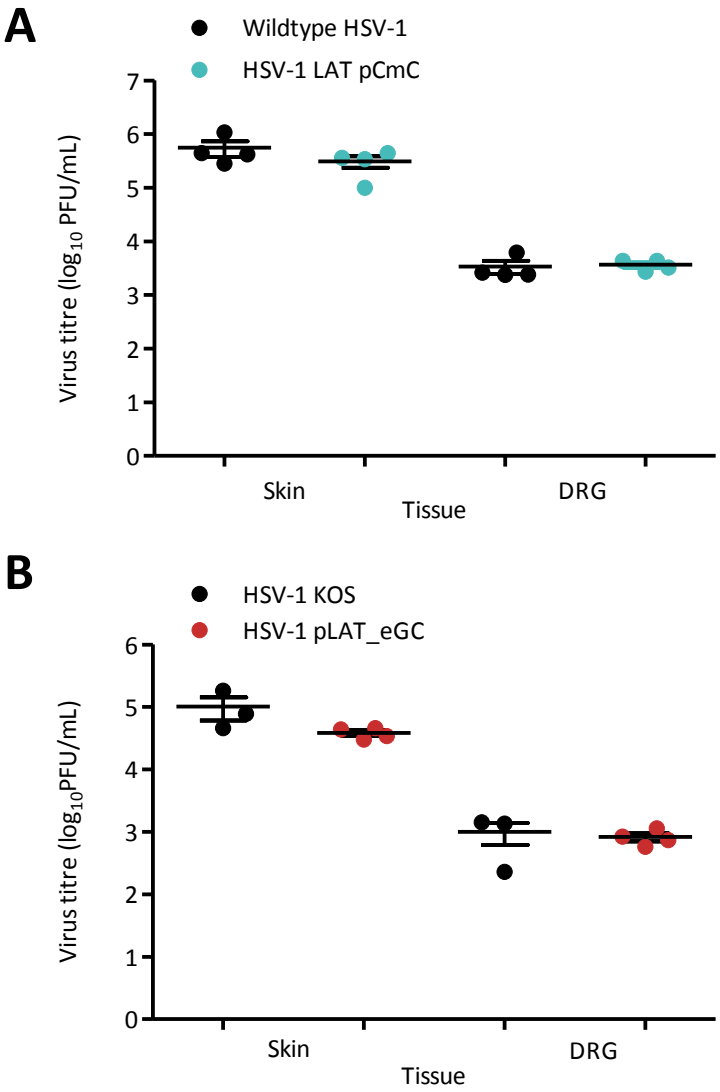

Figure 3-28. Insertion of eGFP/Cre under the control of an IRES into the LAT region has no effect on virus growth *in vivo* relative to HSV-1 KOS. Groups of three or four C57Bl/6 mice were infected with 1×10^8 PFU/mL HSV-1 by tattoo. At five days p.i., mice were culled and the amount of infectious virus was determined by standard plaque assay from ten DRG (spinal levels L1 to T5), or 1 cm^2 skin located over the site of infection. Circles show results for each mouse and bars represent mean±SEM. The limit of detection was two PFU per tissue. The means were compared in each tissue by an unpaired *t* test, but in all cases the difference was not statistically significant ($p > 0.05$). (A) Comparison of amount of virus in C57Bl/6 mice infected with HSV-1 KOS (black) or HSV-1 LAT pCmC (blue). (B) Comparison of amount of virus in C57Bl/6 mice infected with HSV-1 KOS (black) or HSV-1 pLAT_eGC (red).

3.5.4 Ability of recombinant viruses to reactivate from latency to produce infectious virus

Finally, given that the viruses tested can replicate comparably to HSV-1 KOS *in vivo* and show a similar pattern of lesion development, it was important to verify that these viruses could reactivate from latency. C57Bl/6 mice were infected by tattoo with HSV-1 KOS, HSV-1 pICP0_eGC, HSV-1 pICP47_eGC, HSV-1 pICP6_eGC, HSV-1 pgB_eGC, HSV-1 pC_eGC or HSV-1 pICP47_Tdtom. The infection was allowed to proceed for 30 days to establish latency. The DRG were then explanted and incubated for five days, during which time the virus should reactivate. The DRG were then homogenised and the presence of infectious virus was then confirmed by infecting Vero cell monolayers with these homogenates. The ability of the viruses to express a fluorescent protein as appropriate was also assessed, to confirm that the eGFP/Cre or Tdtomato expression cassette was not lost over time. All plaques were either $eGFP^+$, $Tdtomato^+$ or, in the case of HSV-1 KOS, non-fluorescent as appropriate (Figure 3-29). All mice contained reactivatable virus as determined by this assay. A similar experiment was performed to confirm that HSV-1 pLAT_eGC can reactivate from latency. C57Bl/6 mice were infected with either HSV-1 KOS, the parent virus HSV-1 LAT pCmC or HSV-1 pLAT_eGC. At 30 days p.i. the DRG were explanted and incubated for five days to assess reactivation. The DRG were then homogenised and the homogenates were used to infect Vero cell monolayers. Retrievable infectious virus detected from all mice, indicated all viruses can reactivate. As expected, only those cells which were infected with the explanted homogenised DRG from mice infected with HSV-1 LAT pCmC had observable mCherry fluorescence, and no eGFP fluorescence was detectable for any sample (Figure 3-30).

3.6 Discussion

This chapter focused on the development of homologous recombination-based strategies for engineering HSV. Initially, a conventional approach was used that relied upon cotransfection of viral genomic and transfer plasmid DNA. While the cotransfection-based method is widely used, when employed to construct the viruses required for this thesis, it was not always reliable and was time consuming. The efficiency of recombination when the cotransfection method was used to generate recombinant virus was comparable to that previously reported in the literature, typically 0.1 – 5% (Kolb and Brandt, 2004; Krisky et al., 1997), but most of the plaques selected were unable to be plaque purified to yield pure recombinant virus. Anecdotally, the lack of success achieved when using this method to construct recombinant virus is probably due to the poor quality of the genomic

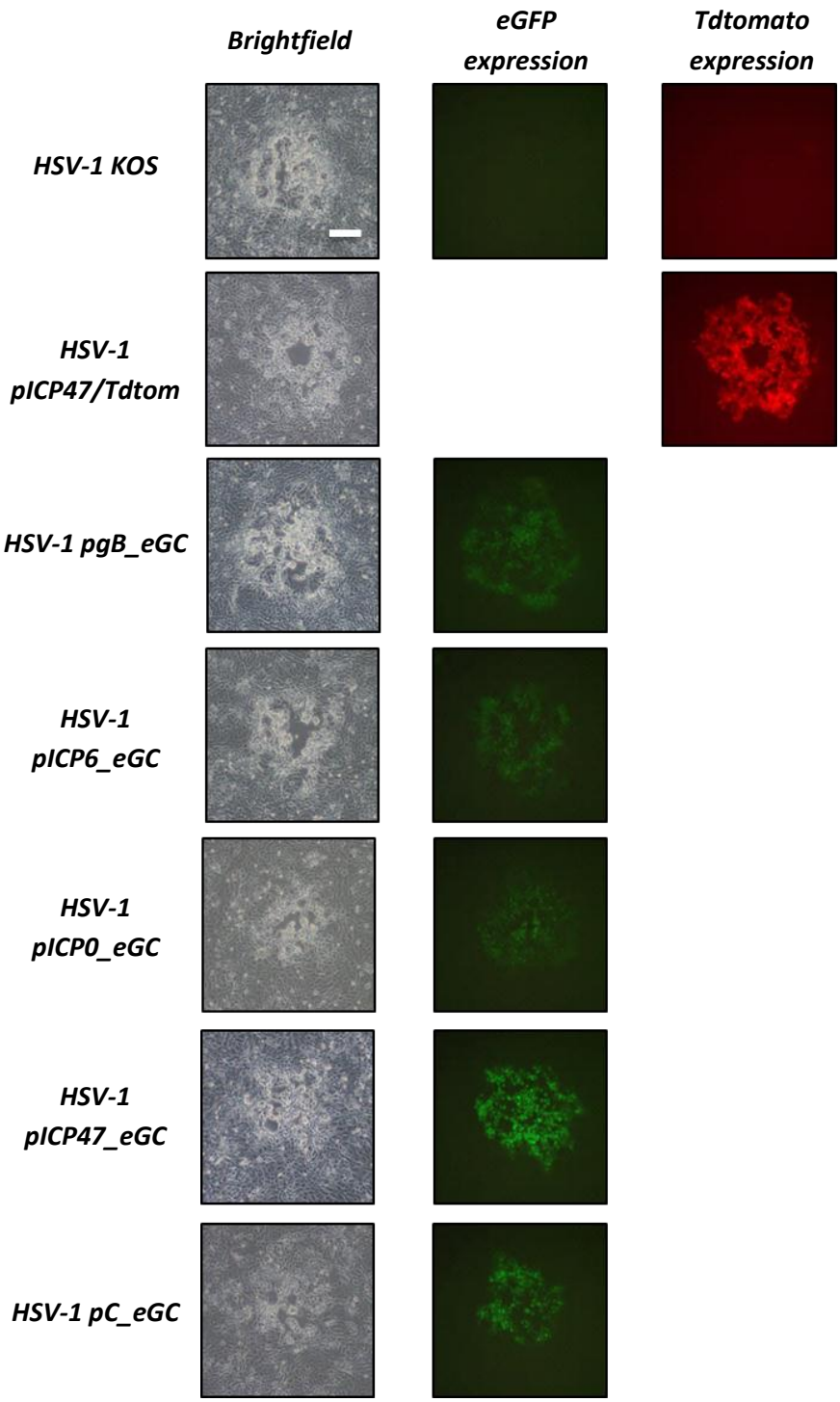

Figure 3-29. Fluorescent reporter genes inserted into the U_L3/U_L4 or U_L26/U_L27 intergenic region are not lost and maintain function during infection of mice. Groups of two C57Bl/6 mice were infected by tattoo with 1×10^8 PFU/mL of one of the viruses listed. At 30 days pi, DRG from spinal levels T5 to L1 were removed and incubated at 37°C for reactivation by explant. After five days DRG were homogenised, and the homogenates were titrated on Vero cells. Representative plaques formed by the parent virus HSV-1 KOS and the recombinant viruses on Vero cells under semi-solid M2-CMC as shown by phase contrast microscopy or fluorescence microscopy for the detection of eGFP or Tdtomato at 100× magnification (scale bar = 150 µm, as indicated on top left photograph).

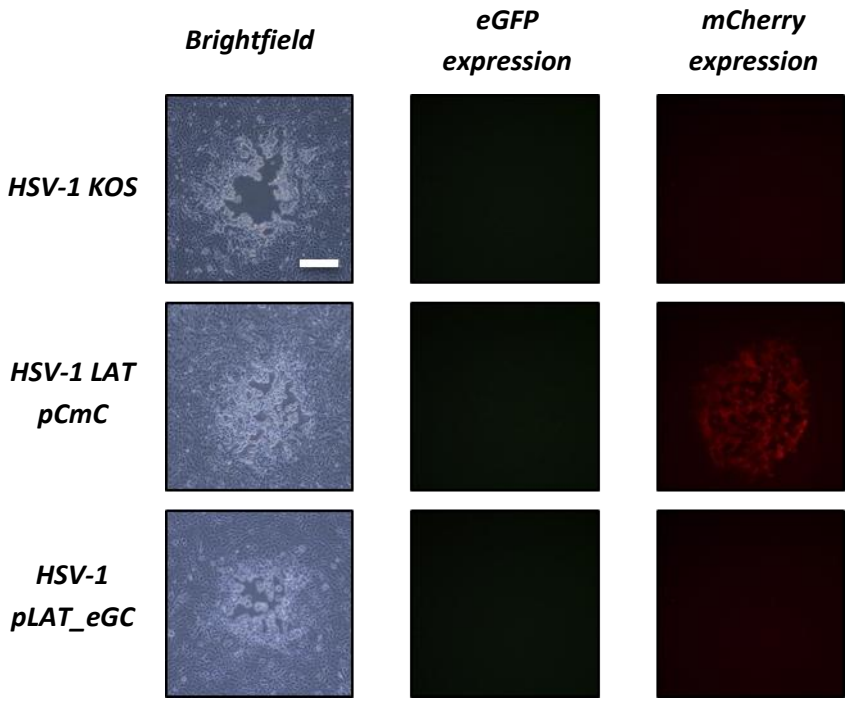

Figure 3-30. Fluorescent reporter genes inserted into the LAT region under the control of the CMV IE, but not LAT, promoter of HSV-1 are expressed *in vitro* following reactivation. Groups of two C57Bl/6 mice were infected by tattoo with 1×10^8 PFU/mL of one of the viruses listed. At 30 days pi, DRG from spinal levels T5 to L1 were removed and incubated at 37°C for reactivation by explant. After five days DRG were homogenised, and the homogenates were titrated on Vero cells. Representative plaques formed by the parent virus HSV-1 KOS and the recombinant viruses on Vero cells under semi-solid M2-CMC as shown by phase contrast microscopy or fluorescence microscopy for the detection of eGFP or mCherry at 100× magnification (scale bar = 200 μm, as indicated on the top left image).

DNA isolated. The infectivity of the whole viral genome preparation used was approximately 61 plaques per μg of DNA (data not shown), less than the 100-1000 plaques per μg of viral DNA recommended for the generation of recombinant HSV-1 vectors (Burton et al., 2003b; Goins et al., 2008). Methods were pursued to improve HSV-1 DNA quality, such as the dialysis rather than sodium acetate/ethanol precipitation of genomic DNA following phenol/chloroform extraction to prevent shearing of DNA, but were ultimately abandoned. In the meantime, the transfection/infection method for the generation of recombinant HSV-1 was investigated as it is not dependent upon isolating high quality DNA (Foster et al., 1999; Orr et al., 2005). Although the initial frequency of recombination was slightly lower when the transfection/infection method was used compared to the traditional cotransfection method, in all cases the desired recombinant virus was able to be isolated. This method was efficient enough to reliably generate recombinant HSV using a strong marker for screening, in this case a fluorescent protein. While the impact of several variables on this process was examined, it was found that a transfection efficiency of more than 20% was crucial. Further, higher efficiencies of transfection efficiency improved the proportion of recombinant progeny. Similarly, increasing the length of flanking sequence used in the transfer plasmids improved the generation of recombinant virus. This supports the recommendation that more than 500 bp of homologous sequence that flanks the desired site of infection is required in the transfer vector, although this was not systematically examined (Coffin, 2010; Goins et al., 2008). However, the slight increase in the frequency of recombinant virus should be weighed against the lower transfection efficiencies typically achieved with larger plasmids (data not shown; McLenachan et al., 2007). Although the efficiency could be altered by up to 10-fold, the optimisation of this method did not improve efficiency to such an extent that PCR screening alone would be viable for the identification of recombinant virus without the aid of a selectable marker.

The impact of the recently described CRISPR/Cas9-based genome editing technology on the ability to alter genomes of a variety of organisms is considerable (Cong et al., 2013; Gratz et al., 2013; Hwang et al., 2013; Li et al., 2013; Mali et al., 2013). So far, the majority of interest in the application of this technology in the field of virology has focused on disrupting viral DNA as a potential therapeutic treatment (Ebina et al., 2013; Hu et al., 2014; Kennedy et al., 2015a; Kennedy et al., 2014; Wang and Quake, 2014; Zhen et al., 2015). For example, the use of a Cas9 system targeting the HIV-1 long terminal repeats can disrupt HIV-1 provirus in Jurkat cell and microglial cell lines (Ebina et al., 2013; Hu et al., 2014). Similarly, a Cas9-based approach targeting the Hepatitis B surface antigen, core and reverse transcriptase proteins was able to suppress viral replication and dramatically

reduced viral DNA levels in an *in vitro* HepAD38 chronic Hepatitis B infection model and HepaRG model, which mimics the early phases of infection (Kennedy et al., 2015a). Overall, however, there has been less published on the application of Cas9-based technologies for constructing mutant or recombinant viruses. Cas9-based technologies have the potential to greatly facilitate this process, particularly when considering large, double-stranded DNA viruses that have proved less amenable to manipulation than smaller viruses (Bi et al., 2014). Recently, the manipulation of the vaccinia virus and adenovirus genomes using a Cas9-based approach was performed, with a high frequency of recombination that was advantageous over previous methods used to engineer these viruses (Bi et al., 2014; Yuan et al., 2015). Cas9-based targeting has been used to engineer HSV in a limited number of publications, with a dramatic improvement in the frequency of recombination identified (Bi et al., 2014; Suenaga et al., 2014). In this thesis and as we published (Russell et al., 2015), the incorporation of a mCherry-targeting Cas9 plasmid into the transfection/infection method used led to a large improvement in the initial frequency of recombination. The adoption of a CRISPR/Cas9-based approach also facilitated the construction of recombinant viruses without the use of a fluorescent marker screening.

Consistent with previously published results (Bi et al., 2014; Suenaga et al., 2014), not all the virus obtained following Cas9 cleavage of the mCherry sequence in HSV-1 pC_mC during transfection/infection contained the desired modification. Since the Cas9/gRNA complex is efficiently expressed, many complexes can accumulate within a cell to cleave the viral genome. It was speculated that the failure to modify the viral genome as desired is caused not by inefficient cleavage of the viral genome, but a failure to repair it correctly. Given the multiple viral genome copies per cell, the repair template may have been limiting, but altering the ratio of repair to Cas9-containing plasmid did not alter the proportion of fluorescent progeny produced. Therefore, the presence of multiple copies of the viral genome within the cell may exhaust the limited ability of the cellular mechanisms to repair such double-stranded breaks, particularly in light of HSV-1's ability to shut down host protein synthesis via various mechanisms (Hardy and Sandri-Goldin, 1994; Read and Frenkel, 1983; Spencer et al., 1997).

In this thesis, it was found that the use of transfer plasmids with long homology sequences flanking the insertion site is of less importance when Cas9 is used to cleave the viral genome compared to the conventional transfection/infection method. This is not surprising, given that Suenaga and colleagues (2014) used a 150 bp single-stranded oligonucleotide as a repair template when restoring a gE deletion virus to wildtype, which would be technically difficult using a conventional homologous recombination-based

method for generating HSV-1 mutants (Kolb and Brandt, 2004; Krisky et al., 1997). Although the generation of this revertant virus was less efficient than the generation of the original gE deletion virus using the Cas9-based system, it proved feasible (Suenaga et al., 2014). Further, the Cas9-based system seems relatively insensitive to alterations in protocol when using the same gRNA. The two main determinants of the efficiency of the Cas9 system are thought to be the expression levels of the CRISPR RNA and the target sequence used (Jinek et al., 2013). For example, a gRNA targeting the gene encoding gE was substantially more effective than those gRNAs used to target U_L23 (Bi et al., 2014; Suenaga et al., 2014).

One of the major sources for concern when using a genome editing methodology such as CRISPR/Cas9 is the potential for off-target effects, in which a mutation, typically a small insertion or deletion, occurs at an undesired location in the genome. The gRNA recognises a 22-bp target DNA sequence that can tolerate mismatches at several nucleotide positions, suggesting that in the context of the human genome there may be thousands of off target sites (Cong et al., 2013; Fu et al., 2013; Hsu et al., 2013; Jinek et al., 2012; Pattanayak et al., 2013). To date though, there are conflicting reports of the frequency of off-target effects as determined by various methodologies including whole genome or exome sequencing and deep sequencing, amongst others (Cho et al., 2014; Fu et al., 2013; Hsu et al., 2013; Kim et al., 2015; Pattanayak et al., 2013; Veres et al., 2014). There are a number of bioinformatics-based approaches for the design of gRNAs to try and minimise off target effects that account for the small size of the gRNA, but the *in vitro* or *in vivo* effectiveness of these remains to be seen (Bae et al., 2014; Xiao et al., 2014; Xie et al., 2014; Zhu et al., 2014). One strategy that reduces the frequency of off-target effects by at least fifty fold is the use of paired Cas9-nickases that introduce two individual nicks in the genome. These nicks are repaired with high fidelity through the base excision or homologous recombination repair pathways. Unfortunately, the nickase-based approach does require two highly active gRNAs, which can limit targetable sites (Cho et al., 2014; Mali et al., 2013; Ran et al., 2013).

Generally, off-target effects will always be of less concern when considering using a CRISPR/Cas9-based approach to edit the comparatively small viral genome, and there is evidence that in the context of viral genome engineering they can be avoided entirely (Bi et al., 2014). While several single base pair mutations were identified in the U_L3 gene of HSV-1 pICP0_eGC that was constructed using a CRISPR/Cas9-based approach (refer to Section 3.3.2.1), other viruses were constructed where mCherry was targeted and no mutations were identified in U_L3 (refer to Section 5.4.1). Furthermore, at best the mCherry targeting sequences will bind to U_L3 with eight mismatches, none of which are located near the site of the single base pair mutations observed. So, it is unlikely the gRNA used

could have bound to the sites were the mutations occurred. Previous attempts to construct this virus without the aid of Cas9 failed to yield eGFP$^+$ plaques, suggesting that the insertion of the ICP0 promoter sequence at this location may cause instability in the viral genome, which may be compensated for by mutations in U_L3. When constructing recombinant viruses, it is always possible that undesirable mutations to the viral genome occur, regardless of whether Cas9 is employed to facilitate this process or not (Gierasch et al., 2006).

While the use of the U_L26/U_L27 insertion site is not novel, in this thesis a position between the polyA signals associated with these two transcription units was chosen and care was taken that no HSV sequence was deleted. It is unclear why previous attempts to add genes into this region led to attenuation, but it may be related to the failure to maintain the native polyA of U_L26 or U_L27 (Balliet et al., 2007; Foster et al., 1999; Orr et al., 2005). All the elements associated with transcription in the U_L26/U_L27 region may not be able to be easily replaced, with outcomes that may not be able to be well predicted, which is important to consider when designing recombinant HSV-1.

The use of recombinant HSV that express marker genes, such as fluorescent proteins like eGFP, for examining viral pathogenesis cannot be underestimated. However, some of those viruses previously described in the literature have alterations in virus growth or pathogenesis (Balliet et al., 2007; Orr et al., 2005). In at least one case, there was instability of the insert in the genome and loss of eGFP expression, presumably due to the presence of direct sequence repeats flanking the insert (Balliet et al., 2007). In another case, loss of eGFP expression occurred over time, possibly by repression of eGFP expression as the eGFP cassette was retained in the genome (Balliet et al., 2007; Foster et al., 1999). Many HSV-1 engineered to express foreign genes contain deletions of some of the viral genome, albeit often in genes that are deemed non-essential or whose function has not been identified (Mocarski et al., 1980; Potel et al., 2002; Proença et al., 2008; Ramachandran et al., 2008; Wakim et al., 2008b). Therefore, the characterisation of the recombinant viruses used in this thesis was of critical importance. For all viruses generated for use in this thesis, there were no obviously discernible changes in virus growth or pathogenesis, and all were constructed such that there would be no loss of viral sequence and minimal disruption to the genome.

Overall, several methods for the generation of recombinant viruses were explored in this chapter, with the use of the CRISPR/Cas9 based method providing the single greatest increase in efficiency. These methods have been used to construct ten different

recombinant HSV, which express a range of fluorescent proteins under the control of several promoters from three different locations in the genome.

4 | HSV-1 lytic gene expression during the establishment and maintenance of latency

4.1 Introduction

One of the hallmarks of HSV-1 latency is the marked repression of viral gene transcription, with only the LATs able to be abundantly detected (Bastian et al., 1972; Cook et al., 1974; Shimeld et al., 2001; Stevens and Cook, 1971). A few early studies found evidence of low level, likely transient, transcription of lytic genes during latency, but there is even less evidence that detectable viral protein is produced. This activity was typically either deemed biologically irrelevant, or a consequence of low level reactivation that does not result in detectable infectious virus or symptoms (Chen et al., 2002a; Chen et al., 1997; Du et al., 2011; Feldman et al., 2002; Giordani et al., 2008; Green et al., 1981; Kramer and Coen, 1995; Kramer et al., 1998; Maillet et al., 2006; Margolis et al., 2007a; Pesola et al., 2005; Preston, 2000; Sawtell, 2003; Tal-Singer et al., 1997). However, the retention of activated $CD8^+$ T cells within the sensory ganglia of latently infected mice and humans argues for the production of viral protein during latency (Halford et al., 1996a; Khanna et al., 2003; Van Lint et al., 2005; van Velzen et al., 2013). The $CD8^+$ T cell response is highly focused, with at least half of those cells retained in the DRG of latently infected C57Bl/6 mice being specific for the gB_{498} epitope, derived from the late protein gB (Khanna et al., 2003; St. Leger et al., 2011). However, there is no direct evidence for detectable gB protein expression during latency. More recently, using a sensitive approach based on single cell analysis of transcription in latently infected mouse DRG, Ma and colleagues (2014) found a more extensive pattern of viral gene transcription during latency, with more than two thirds of all latently infected neurons containing transcripts of at least one lytic gene. Additionally, host antiviral and survival gene transcription was modulated in response to the presence of lytic viral transcripts. This clearly indicates that the viral transcription observed is likely to be biologically relevant.

The use of conventional reporter genes has proved invaluable for tracking viral gene expression during the acute HSV-1 infection (Balliet et al., 2007; Lachmann et al., 1999; Margolis et al., 1993; Summers et al., 2001). Unfortunately, such reporters are ill suited to the detection of the low level or transient expression of HSV-1 lytic genes that may occur during latency. The ROSA26R/Cre mouse system is ideal for examining HSV-1 promoter activity during latency as it allows the examination of historic gene expression and is not dependent on continual promoter activity (refer to Section 1.4). This system has been used previously to reveal that a large population of neurons that experience immediate early, but not early or late, classes of viral promoter expression are able to survive the lytic infection and establish latency. To date, no promoter activity associated with lytic gene expression was detectable during latency, as demonstrated by an increased number of β-gal^+ cells. However, only a small number of well-characterised HSV-1 promoters of each

class of the viral gene expression cascade have been employed thus far (Nicoll et al., 2012; Proença et al., 2008; Proença et al., 2011; Wakim et al., 2008b).

The first aim of this chapter is to define further the kinetics of acute infection and size of the latent viral reservoir. This relies on the use of both the ROSA26R/Cre reporter system as well as conventional methods for tracking the acute HSV-1 infection. The next two sections focus on the primary aim of this chapter, which is to measure the accumulation of β-gal marked cells in ROSA26R mice infected with HSV-1 as dictated by different HSV-1 lytic gene promoters. This involves examining historic viral gene expression during the acute infection, as well as the establishment and maintenance of latency. In particular, the focus is on the promoters of those viral genes that are associated with the antigen recognised by the host's $CD8^+$ T cell response, including gB. The third section is closely related and examines whether all lytic gene promoters of the same class of viral gene expression are historically expressed with similar kinetics *in vivo*. Finally, the fourth section examines the historical expression of LAT throughout the establishment and maintenance of latency in the ROSA26R mouse model.

4.2 HSV-1 continues to spread after the acute infection is curtailed

4.2.1 Historical analysis of HSV-1 infection reveals continued spread of virus beyond the peak of infection

Coupling *cre* expression with the strong constitutive CMV IE promoter allows the population of latently infected neurons to be easily tracked. It has been shown that the CMV IE promoter is briefly active in cultured sensory neurons prior to the establishment of a latent infection (Arthur et al., 2001), suggesting it is likely active in all HSV-1 infected cells *in vivo*, regardless of the outcome of infection. This was confirmed by Ma and colleagues (2014), who used single-cell qPCR for the detection of HSV-1 genomes in ROSA-YFP mice, which are analogous to the ROSA26R mice used in this thesis, infected with a virus expressing *cre* under the CMV IE promoter. They demonstrated that less than 20% of cells that fail to express YFP contain HSV-1 genomes. Since the limit of detection was 10 genome copies, it is reasonable to assume that the use of the CMV IE promoter in the ROSA26R/Cre mouse system allows for the marking of the overwhelming majority of infected cells, regardless of whether a lytic or latent infection is established (Ma et al., 2014). Therefore, the verification of the kinetics of HSV-1 infection was attempted using the ROSA26R mouse model as previously described (Proença et al., 2008; Wakim et al.,

2008b). This was combined with the zosteriform model of HSV-1 infection, which exploits the segmental cutaneous innervation of vertebrates to track the anatomical spread of viral gene expression within the PNS (refer to Section 3.2.1 for a more detailed description of this model; Speck and Simmons, 1991). In addition, more time points were included compared to previous studies (Proença et al., 2008; Wakim et al., 2008b), to enable the progression of infection to be closely monitored, particularly between the acute and latent infection.

In order to quantify the progression of infection, ROSA26R mice were infected with HSV-1 pC_eGC, and culled at various times p.i. to allow quantification of the number of β-gal$^+$ cells in DRG. As expected, HSV-1 pC_eGC related β-gal expression was readily detectable in a sizeable population of cells across multiple ganglia (Figure 4-1). There was a substantial rise in the number of β-gal$^+$ cells between five and 10 days p.i. (Figure 4-2), an unexpected finding as the peak in the acute infection is usually around day four p.i. as defined by the presence of detectable infectious virus (Van Lint et al., 2004). Further spread of virus to other distal sensory ganglia was found at this later time, as shown by the number of DRG that contain at least one β-gal marked cell (Figure 4-2B). This extends to an average of more than seven and up to 10 DRG. Many of the distal DRG contain sensory neurons that do not directly innervate the site of infection, even allowing for the overlap in adjacent dermatomes (Speck and Simmons, 1991). The number of β-gal$^+$ cells declined between days 10 and 20 p.i., presumably as neurons die as either a consequence of lytic infection or the host's immune response. The number of β-gal$^+$ cells plateaued during latency until day 40 p.i., supporting the hypothesis that little, in any, virus spread or loss of neurons occurs during latency in mice.

To more thoroughly characterise the kinetics of neuronal marking, ROSA26R mice were infected with HSV-1 pC_eGC and culled at two-day intervals from day three to day 15 p.i. (Figure 4-3). This revealed that the peak in the number of β-gal$^+$ cells was around day nine p.i. (Figure 4-3A). The spread of virus to distal DRG also increased up until approximately day nine p.i., after which time it plateaued (Figure 4-3B). This suggests that HSV-1 is entering new neurons beyond the peak of the acute infection as defined by conventional means and establishing a latent infection.

4.2.2 The kinetics of the acute HSV-1 infection

Given the unexpected finding that the peak size of the reservoir of infected cells as defined using HSV-1 pC_eGC in the ROSA26R mouse system was at day nine p.i., it was important to confirm that the kinetics of acute infection were normal in this model using a

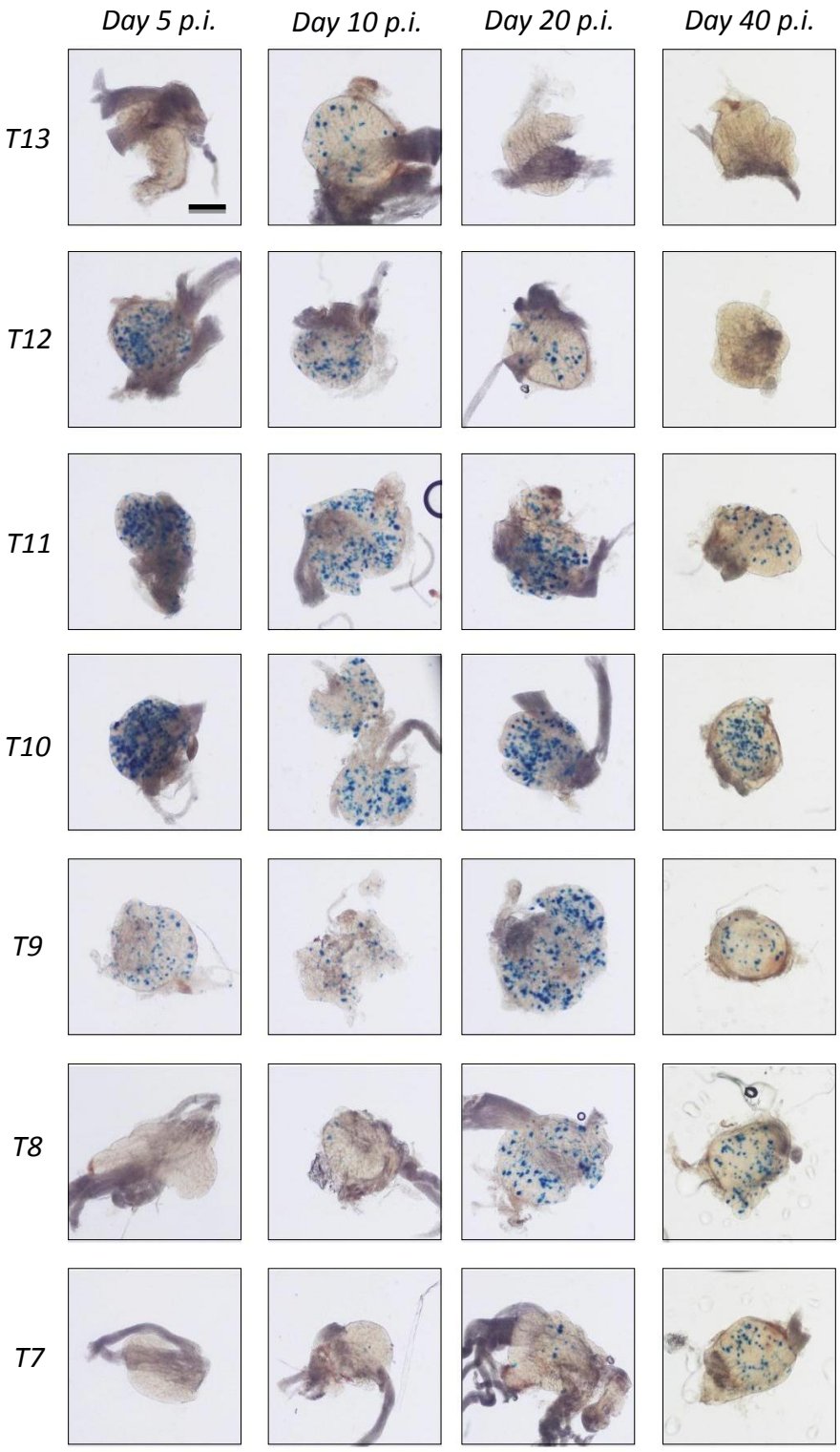

Figure 4-1. Photomicrographs of DRG from ROSA26R mice infected with HSV-1 pC_eGC over time. ROSA26R mice were infected with 1×10^8 PFU/mL HSV-1 pC_eGC. At the indicated times mice were culled and DRG (from spinal levels T5 to L1) were removed and processed for the detection of β-gal activity. Photomicrographs were taken of each DRG at 40× magnification (scale bar = 300 μm, as indicated on top left image). The images of DRG from spinal levels T13 to T7 from an individual mouse are shown for each time point, and are representative of two experiments (n = 9; refer to Figure 4-2). β-gal$^+$ cells were still detectable in spinal levels L1, T6 and T5 for mice on days 10, 20 and 40 p.i.

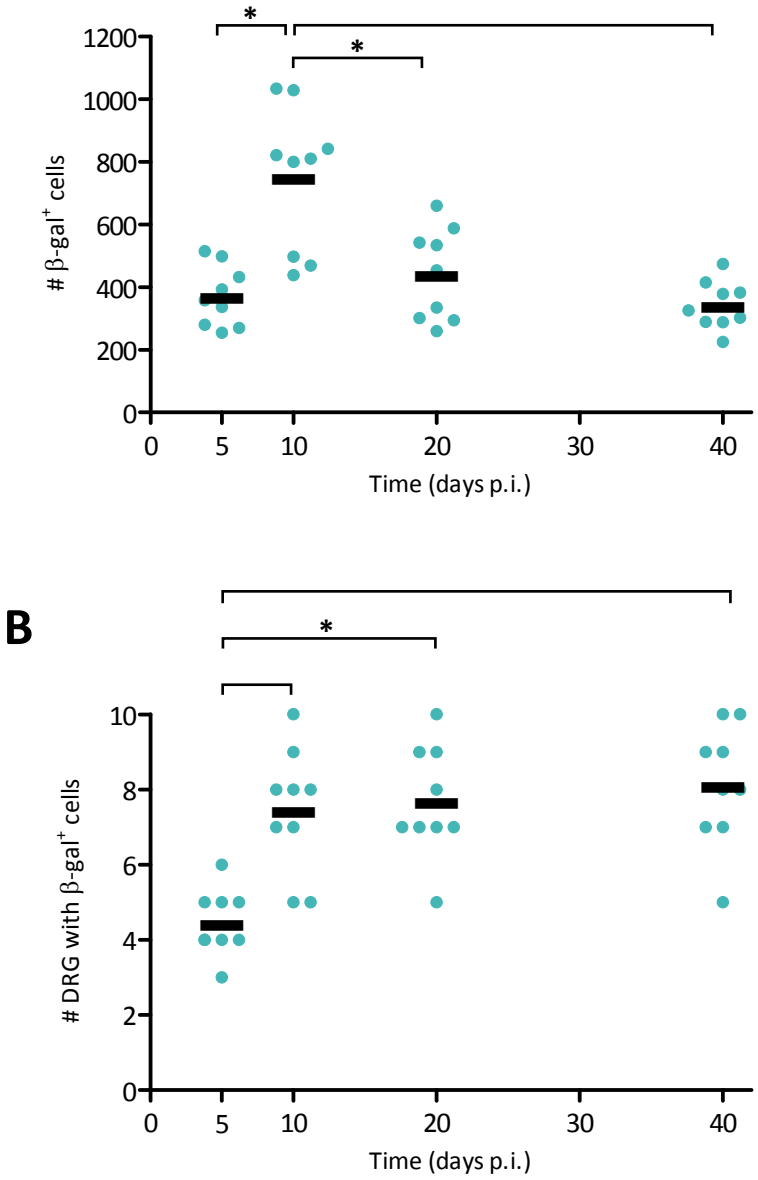

Figure 4-2. Measuring the kinetics of HSV-1 infection using the ROSA26R/Cre mouse system reveals that the peak in the size of the infected cell population is later than the peak of acute infection as defined by conventional means. Groups of four or five ROSA26R mice were infected with 1×10^8 PFU/mL HSV-1 pC_eGC. At 5, 10, 20 or 40 days p.i. mice were culled and DRG (from spinal levels T5 to L1) removed and processed for the detection of β-gal activity. Both (A) the total number of β-gal$^+$ cells per mouse and (B) the number of DRG per mouse containing at least one β-gal$^+$ cell are shown. Each circle represents one mouse and the black bar represents the mean value for all mice at each time point. The results are pooled from two independent experiments (n = 9 per time point). Statistical significance was determined by a one way ANOVA ($p < 0.001$) with Bonferroni's post-test to make pairwise comparisons (*$p < 0.05$).

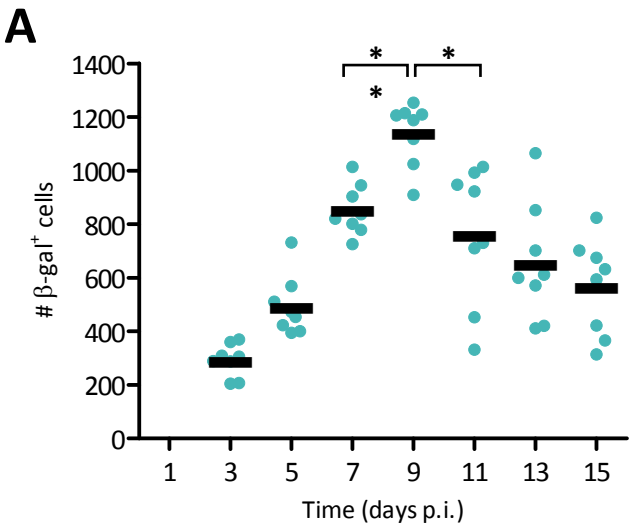

B

Pairwise comparisons from (A)						
Day	3	5	7	9	11	13
5	ns					
7	*	*				
9	*	*	*			
11	*	*	ns	*		
13	*	ns	ns	*	ns	
15	*	ns	ns	*	ns	ns

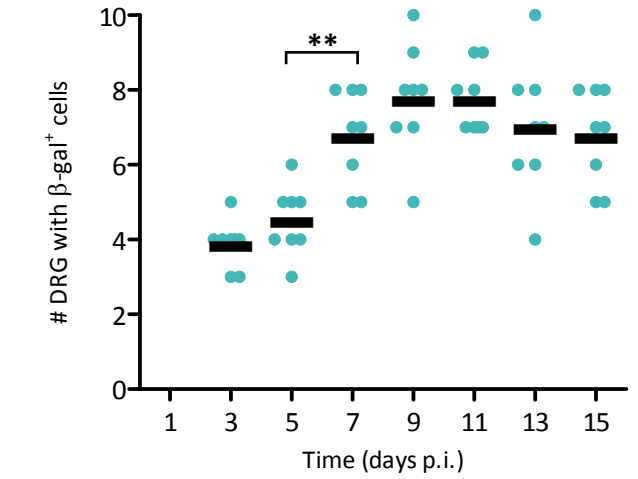

D

Pairwise comparisons from (C)						
Day	3	5	7	9	11	13
5	ns					
7	*	*				
9	*	*	ns			
11	*	*	ns	ns		
13	*	*	ns	ns	ns	
15	*	*	ns	ns	ns	ns

Figure 4-3. A finer time course reveals that the peak in the accumulation of β-gal marked neurons in ROSA26R mice infected with HSV-1 pC_eGC is at 9 days p.i. Groups of three to five ROSA26R mice were infected with 1×10^8 PFU/mL HSV-1 pC_eGC. At 3, 5, 7, 9, 11, 13 or 15 days p.i. mice were culled and the DRG (from spinal levels T5 to L1) were removed and processed for determination of β-gal activity. Both (A) the total number of β-gal+ cells per mouse and (C) the number of DRG per mouse containing at least one β-gal+ cell are shown. Each circle represents one mouse and the black bar represents the mean value for all mice at each time point. The results are pooled from two independent experiments (n = 8 per time point). (B&D) Statistical significance was determined by a one way ANOVA ($p < 0.001$) with Bonferroni's post-test to make pairwise comparisons, with the key statistical differences indicated on (A) and (C) (*$p < 0.05$).

conventional method such as the detection of infectious virus. Therefore, ROSA26R mice were infected with HSV-1 pC_eGC and culled daily from one until eight days p.i. The innervating DRG ranging from T5 to L1 and the skin around the site of the lesion was collected. The amount of virus in these tissues was determined by standard plaque assay (Figure 4-4). The peak in viral titre in the DRG occurred on day three p.i., plateauing on days four and five p.i., before decreasing until day seven p.i. (Figure 4-4A&B). The viral titre in the skin was very high initially, and there was a similar titre of virus in the skin until day six p.i. (Figure 4-4C&D). There was a slight drop in the titre of virus measured on day four p.i. but only the skin surrounding the visible lesion was collected. However, infectious virus may be present in areas of skin where a visible lesion has yet to form, and it is likely that the titre of virus in the skin was underestimated on day four. Detectable infectious virus was cleared by day eight p.i. Therefore, consistent with previous reports, the acute infection as defined by the presence of infectious virus is resolved by day eight p.i. (Sawtell et al., 1998; Sedarati et al., 1989; Speck and Simmons, 1998; Van Lint et al., 2004).

The detection of the presence of infectious virus may not be sensitive to the presence of small amounts of viral activity, and so is not an ideal method for determining when the acute infection is resolved. Therefore, the expression of the reporter gene β-gal was monitored over the course of the acute infection as an alternate method. The virus KOS6β expresses β-gal under the control of the ICP6 promoter. KOS6β has previously been used to monitor the progression of infection in the mouse corneal scarification model of HSV-1 infection. It was found that β-gal activity rose proportionally and concomitantly with the detection of infectious virus (Summers et al., 2001). However, this report focused on the period shortly after infection, namely the first four days p.i. Therefore, C57Bl/6 mice were infected with HSV-1 KOS6β on the flank. Groups of mice were culled at three-day intervals from day one p.i. until day 16 p.i., as well as during latency at day 30 p.i. The innervating DRG were then removed and the number of β-gal$^+$ cells was estimated. The β-gal activity as measured by X-gal staining was not well localised (Figure 4-5), but as I was interested in comparing the extent of lytic gene expression on different days p.i., an absolute measure of the number of neurons that were expressing β-gal was not essential. To ensure that estimates of the number of β-gal$^+$ cells were consistently performed, data from mice culled on different days were randomised and counted in a single sitting. Individual mice from different experiments were then compared to ensure that the counting of cells was similar.

The number of β-gal$^+$ cells peaked on day four p.i., and declined significantly by day seven p.i. (Figure 4-6). The detection of β-gal expression in a few cells was observable up until 16 days p.i. in some mice, suggesting continued low level viral gene expression. There are

A

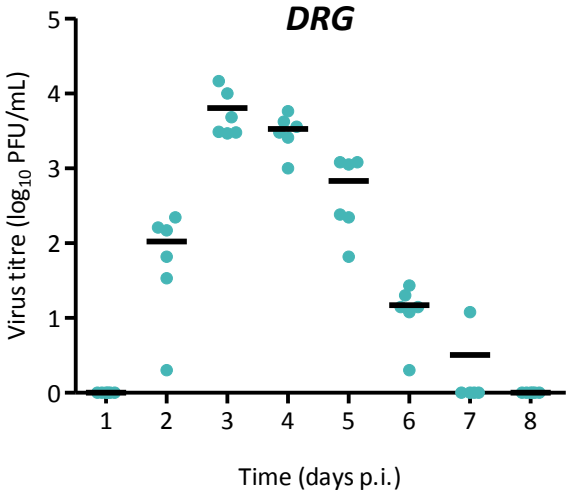

B

Pairwise comparisons from (A)							
Day	1	2	3	4	5	6	7
2	ns						
3	***	***					
4	*	*	**				
5	ns	ns	***	*			
6	ns	ns	***	*	ns		
7	ns	ns	***	*	ns	ns	
8	ns	ns	***	*	ns	ns	ns

C

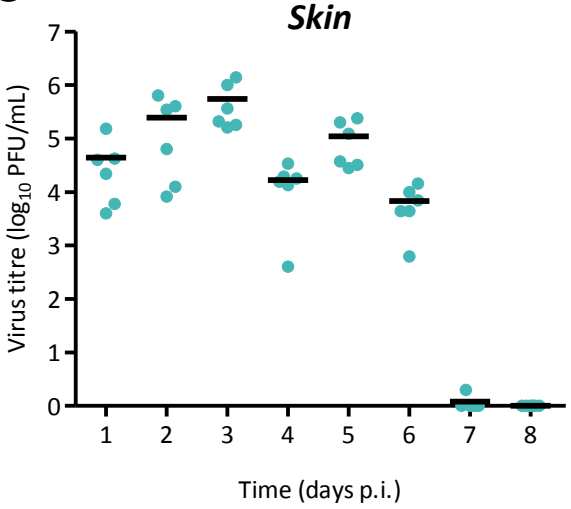

D

Pairwise comparisons from (C)							
Day	1	2	3	4	5	6	7
2	ns						
3	**	ns					
4	ns	ns	**				
5	ns	ns	*	ns			
6	ns	ns	**	ns	ns		
7	ns	ns	**	ns	ns	ns	
8	ns	ns	**	ns	ns	ns	ns

Figure 4-4. Growth of HSV-1 pC_eGC in ROSA26R mice. Groups of two or three ROSA26R mice were infected with 1×10^8 PFU/mL HSV-1 pC_eGC. Mice were culled every 24 hours from one to eight days p.i. and (A) ten DRG (from spinal levels T5 to L1) and (C) the skin encompassing the lesion were taken and the amount of virus in each tissue determined by standard plaque assay. Each circle represents one mouse and the black bar represents the mean value for all mice at that time point. The results are pooled from two independent experiments *(n* = 5 – 6 per time point). (B&D) Statistical significance was determined by a one way ANOVA followed by Newman Kwel's post-test to make pairwise comparisons (*$p < 0.05$, **$p < 0.01$, ***$p < 0.001$).

many possible explanations for this continued β-gal expression, such as a prolonged lytic infection within a small subset of neurons. It may also represent a resumption of lytic gene expression within latently infected neurons. It has been shown that reactivation can occur shortly after infection, even at day nine p.i., as shown using the *in vivo* transient hyperthermia model of reactivation (Sawtell, 2003). Alternatively, it is possible that this may reflect the spread of virus into new neurons beyond the traditionally defined acute infection, described in Section 4.2.1. Finally, the stability of the β-gal protein means that it may not well reflect low level or persistent gene expression, particularly following a peak in expression (Margolis et al., 1993).

4.2.3 Identification of a population of neurons that experience HSV-1 gene expression prior to the establishment of latency

The use of the HSV-1 Cre/ROSA26R reporter system suggested that the activity of HSV-1 may continue beyond the acute infection, but the CMV IE promoter is not a typical native HSV-1 promoter. To determine if this increase in the number of β-gal$^+$ cells between five and 10 days p.i. could be seen when a bona fide HSV-1 promoter is used to drive expression of Cre, ROSA26R mice were infected with HSV-1 expressing Cre under the control of the immediate early promoter for ICP0. This virus uses a similar promoter sequence to the virus ICP0 Cre used by Proença and colleagues (2008) in the ROSA26R model (refer to Section 3.3.2.1).

Mice were then culled at various times p.i., and their DRG removed and β-gal expression was assayed (Figure 4-7). Although a smaller population of cells were β-gal$^+$ than was observed when the CMV IE promoter was used to direct expression of *Cre* (Figure 4-2), the peak in the number of β-gal$^+$ cells was at 10 days p.i., concurrent with an increase in the spread of virus to distal DRG (Figure 4-8). There was a decrease in the number of β-gal$^+$ cells until 20 days p.i., with more than half the number of β-gal marked neurons surviving into latency. However, from 20 days p.i. and into latency the number of β-gal$^+$ cells remained stable, suggesting little, if any, activity of the ICP0 promoter during latency. These results are consistent with the findings previously reported by Proença and colleagues (2008) when they employed ICP0 Cre in the ROSA26R model.

It is believed that the expression of the immediate early genes does not necessarily mark the engagement of the full cascade of lytic viral gene expression. Therefore, looking at historical expression of other classes of viral gene expression may reveal differences in the survival of different populations of infected cells. Therefore, ROSA26R mice were infected with HSV-1 pICP6_eGC, as this directs the expression of Cre from a prototypical early HSV-1 promoter. Mice were culled at different times p.i., their DRG removed and the

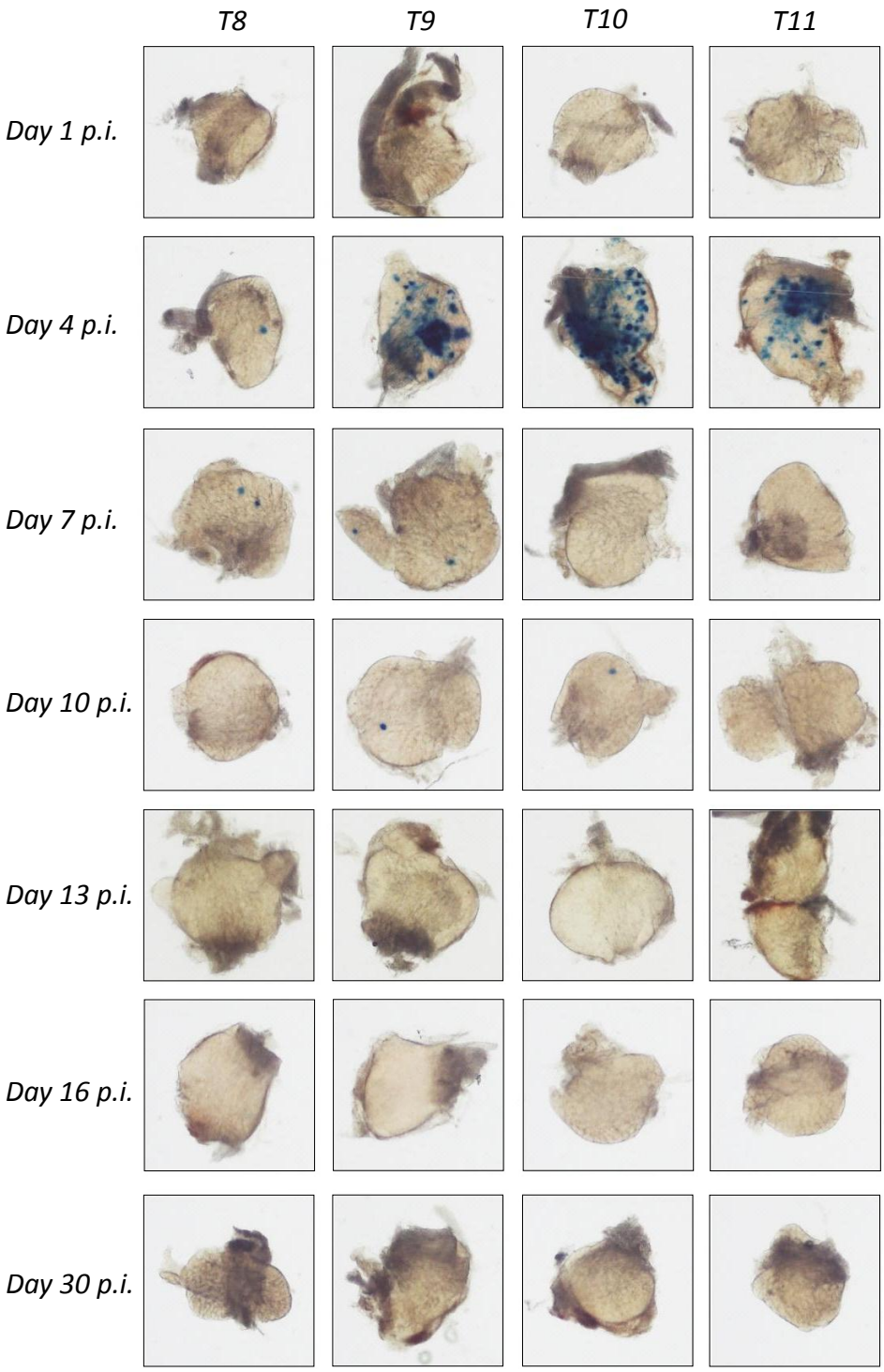

Figure 4-5. Photomicrographs of DRG from C57Bl/6 mice infected with KOS6β over time. C57Bl/6 mice were infected with 1×10^8 PFU/mL KOS6β. At 1, 4, 7, 10, 13, 16 or 30 days p.i. mice were culled and DRG (from spinal levels T5 to L1) were removed and processed for the detection of β-gal activity. Photomicrographs were taken of each DRG at 40× magnification (scale bar = 300 μm, as indicated on the top left image). The images of DRG from spinal levels T8 to T11 from an individual mouse are shown for each time point, and are representative of two independent experiments (*n* = 8, refer to Figure 4-6). No β-gal$^+$ cells were observed in the DRG from those spinal levels not shown.

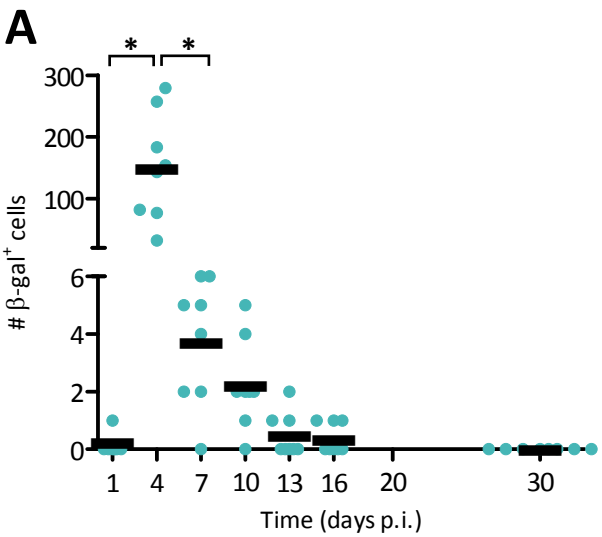

B

Pairwise comparisons from (A)						
Day	1	4	7	10	13	16
4	*					
7	ns	*				
10	ns	*	ns			
13	ns	*	ns	ns		
16	ns	*	ns	ns	ns	
30	ns	*	ns	ns	ns	ns

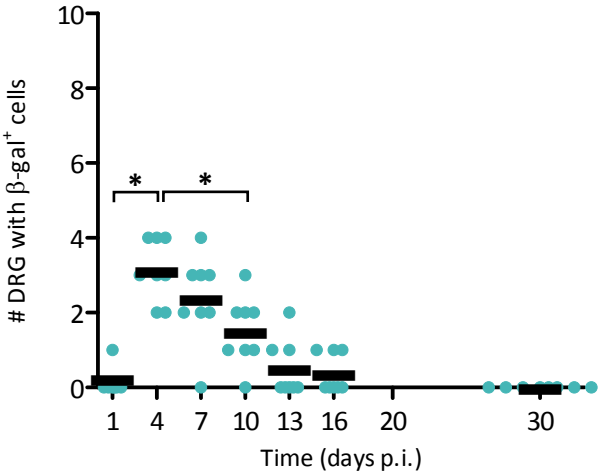

D

Pairwise comparisons from (C)						
Day	1	4	7	10	13	16
4	*					
7	*	ns				
10	*	*	ns			
13	ns	*	*	ns		
16	ns	*	*	ns	ns	
30	ns	*	*	*	ns	ns

Figure 4-6. Kinetics of lytic gene expression during HSV-1 infection of C57Bl/6 mice. Groups of four C57Bl/6 mice were infected with 1×10^8 PFU/mL KOS6β. At 1, 4, 7, 10, 13, 16 or 30 days p.i. mice were culled and DRG (from spinal levels T5 to L1) were removed and processed for the detection of β-gal activity. Both (A) the total number of β-gal$^+$ cells per mouse and (C) the number of DRG per mouse containing at least one β-gal$^+$ cell are shown. Each circle represents one mouse and the black bar represents the mean value for all mice at each time point (n = 8 per time point). The results are pooled from two independent experiments. (B&D) Statistical significance was determined by an one way ANOVA ($p < 0.001$) with Bonferroni's post-test to make pairwise comparisons, with the key statistical differences indicated on (A) and (C) (*$p < 0.05$).

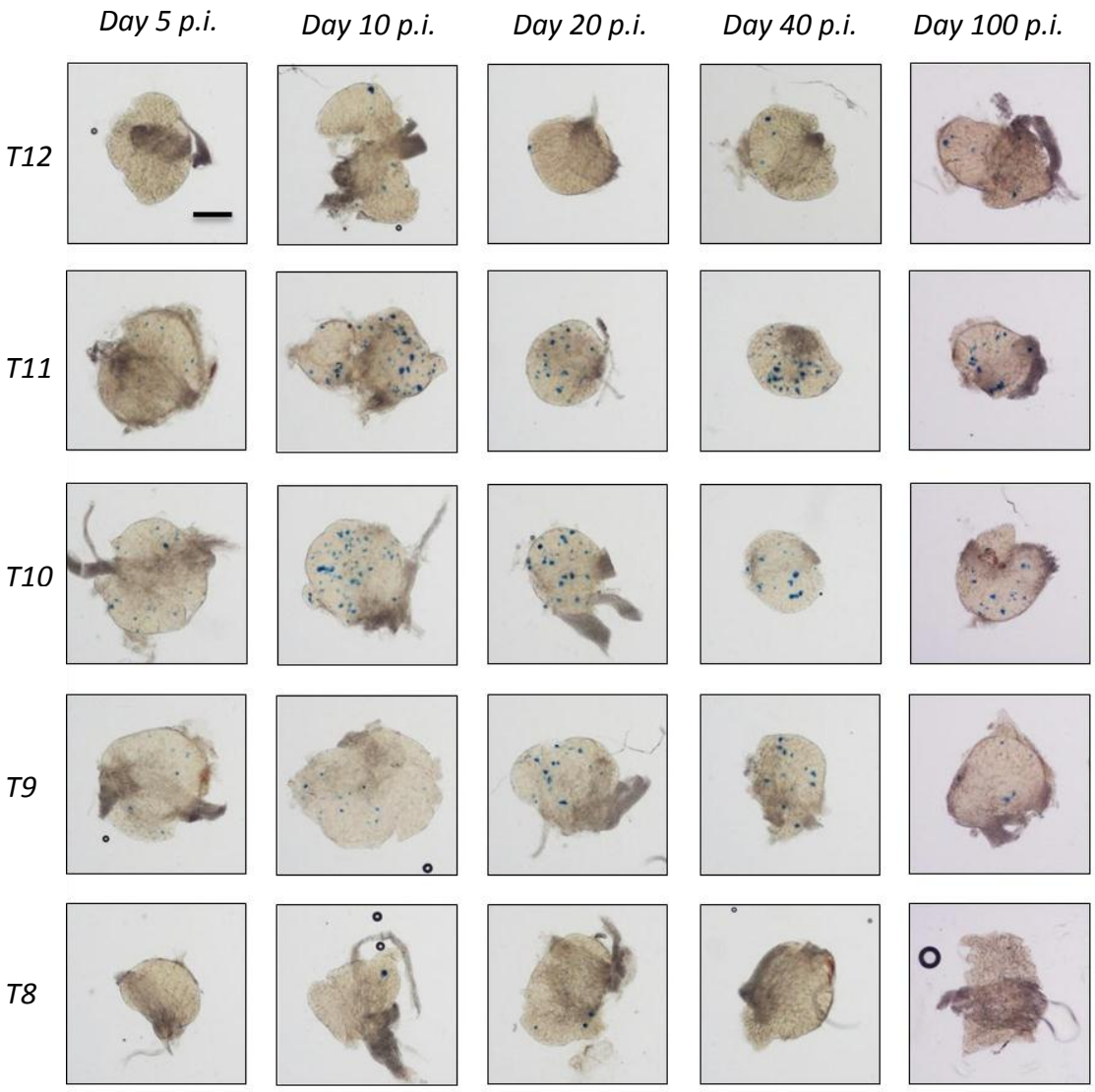

Figure 4-7. Photomicrographs of DRG from ROSA26R mice infected with HSV-1 pICP0_eGC over time. ROSA26R mice were infected with 1×10^8 PFU/mL HSV-1 pICP0_eGC. At the indicated times mice were culled and DRG (from spinal levels T5 to L1) were removed and processed for the detection of β-gal activity. Photomicrographs were taken of each DRG at 40× magnification (scale bar = 300 μm, as indicated on the top left image). The images of DRG from spinal levels T8 to T12 from an individual mouse are shown for each time point, and are representative of three independent experiments (n = 10 – 11, refer to Figure 4-8). β-gal$^+$ cells were not observed in the DRG of those spinal levels not shown.

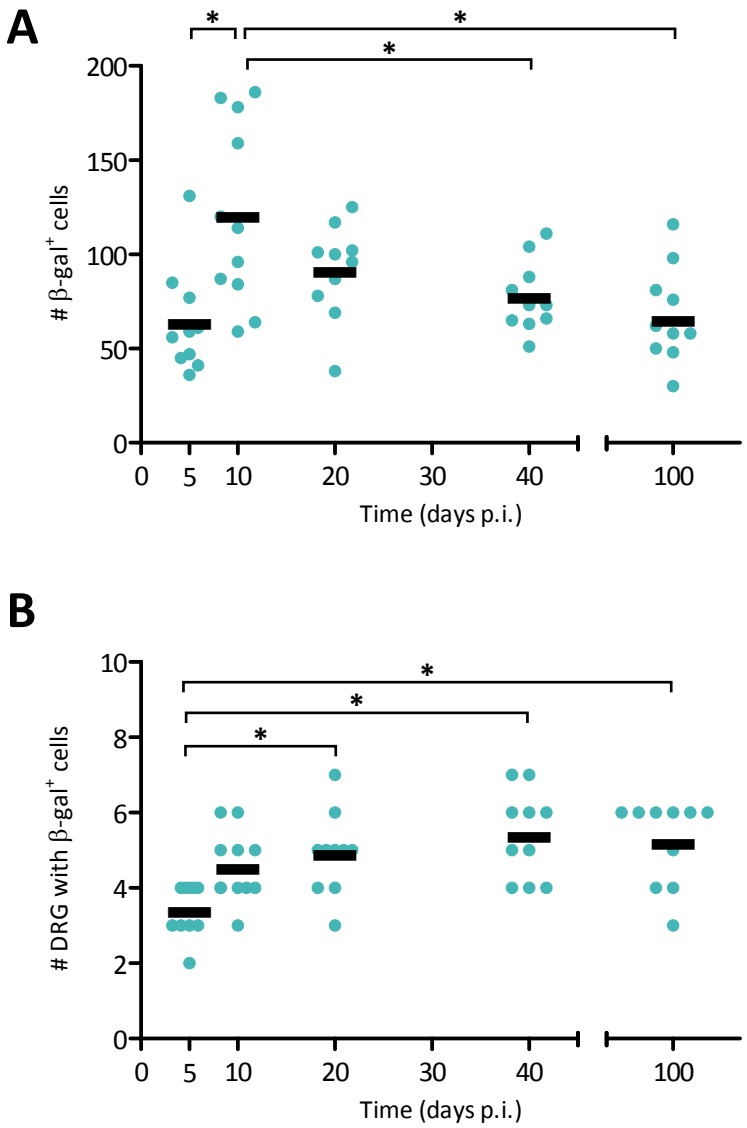

Figure 4-8. The number of β-gal marked cells in ROSA26R mice infected with HSV-1 pICP0_eGC remains stable throughout latency. Groups of two to five ROSA26R mice were infected with 1×10^8 PFU/mL HSV-1 pICP0_eGC. At 5, 10, 20, 40 or 100 days p.i. mice were culled and the DRG (from spinal levels T5 to L1) were removed and processed for the detection of β-gal activity. Both (A) the total number of β-gal$^+$ cells per mouse and (B) the number of DRG per mouse containing at least one β-gal$^+$ cell are shown. Each circle represents one mouse and the black bar represents the mean value for all mice at each time point. The results are pooled from three independent experiments (n = 10 – 11 per time point). Statistical significance was determined by a one way ANOVA ($p < 0.001$) with Bonferroni's post-test to make pairwise comparisons (*$p < 0.05$).

number of β-gal+ cells was determined. The most striking observation is that only a relatively small population of cells were β-gal+ (Figure 4-9). However, in contrast to previous observations, the number of β-gal+ cells and the distribution of β-gal marked cells across different spinal levels was more consistent over time (Figure 4-10).

To look at expression of the late HSV-1 genes, mice were infected with HSV-1 pgB_eGC, culled at various times p.i. and β-gal expression was assayed in DRG (Figure 4-11). Even fewer cells were β-gal marked following infection of ROSA26R mice with HSV-1 pgB_eGC compared to HSV-1 pICP6_eGC. An increase was also observed in the number of β-gal+ cells between five and 10 days p.i. (Figure 4-12). This was associated with an increase in the number of DRG in which β-gal+ cells were detectable, likely reflecting the spread of virus to distal spinal levels described in Section 4.2.1. The number of β-gal+ cells declined between days 10 and 20 p.i., again consistent with previous observations (refer to Section 4.2.1). However, there was an almost two fold increase in the number of β-gal+ cells between days 20 and 40. This is well within the period operationally accepted as latency. This suggested activity under the gB promoter may occur during latency that could lead to protein production.

4.2.4 An estimation of the delay between Cre expression from HSV-1 and detectable β-gal activity

It is possible that the delay in the peak of the acute infection as determined by conventional methods compared to the marking of cells in the ROSA26R/Cre model may simply be due to a delay in *lacZ* expression leading to detectable β-gal activity. The timing of β-gal activity in ROSA26R mice is contingent upon sufficient expression of the *eGFP/Cre* fusion gene from HSV-1 following the infection of a cell, followed by recombination between the *loxP* sites in the mouse genome by eGFP/Cre and finally accumulation of sufficient β-gal protein to be detectable following X-gal staining. The Vero SUA cell line contains a similar *loxP*-flanked insert that prevents expression of β-gal before the provision of the Cre recombinase (Rinaldi et al., 1999). Therefore, the detection of expression of eGFP, which is directly under the control of the viral promoter, can be compared with β-gal activity from the Vero SUA cells, which is dependent upon Cre mediated recombination.

The expression of eGFP and β-gal was not able to be directly compared within the same cell. While fluorogenic substrates do exist for β-gal, the most commonly used substrate fluorescein-di-β-D-galactopyranoside emits light in a similar region of the spectrum as eGFP (Nolan et al., 1988). An alternate substrate for β-gal, DDAO-galactosidase, which emits in the far red shifted region of the spectrum, was tested but was not retained well in

the cells and exhibited substantial non-specific staining (data not shown; Gong et al., 2009).

Therefore, semi-confluent Vero SUA cell monolayers were infected with HSV-1 KOS, HSV-1 pC_eGC, HSV-1 pICP0_eGC, HSV-1 pICP6_eGC or HSV-1 pgB_eGC (MOI of 5), or were left uninfected. Following one hour absorption, the virus inoculum was replaced with fresh media (this was called 0 hours p.i.). At four hour intervals from 0 until 24 hours p.i., the monolayers were fixed and then photographed for expression of eGFP. The cells were then stained with X-gal and photographed for visualisation of β-gal activity. Expression of eGFP was detectable at four hours p.i. in cells infected with HSV-1 expressing eGFP/Cre under either the CMV IE promoter, or the immediate early ICP0 promoter (Figure 4-13). By contrast, in cells infected with HSV-1 expressing eGFP/Cre from an early promoter (ICP6) or late promoter (gB), eGFP expression was first detectable at eight hours p.i. In all cases, detectable β-gal expression was first evident from 12 hours after expression of eGFP. As previously reported, the longer it takes for eGFP/Cre to be expressed following infection, the fewer cells become β-gal$^+$. This is probably attributable to virus induced host cell shut off and cell death prior to *lacZ* expression (Proença et al., 2008). However, these results are caveated by the biggest limitation of this experiment, which is that it was performed using a Vero cell-based culture system, as opposed to the infection of neurons within ROSA26R mice, and so may not faithfully model the ROSA26R/Cre system *in vivo*.

Cre-mediated recombination is rapid, taking only a few minutes in the context of *in vitro* systems (Abremski and Hoess, 1985). Further, consistent with the results presented here, it has been shown that recombination frequency between *loxP* sites in a murine cell line paralleled the accumulation of Cre, peaking at 15 hours post-delivery (Sauer and Henderson, 1988). It is not possible to definitively determine the delay between the initial expression of *cre* and the detection of β-gal activity by X-gal staining within an infected cell within a HSV-1 infected ROSA26R mouse. However, it is highly unlikely that this 12 hour delay is solely responsible for the disparity between the peak of β-gal activity at nine days p.i. in ROSA26R mice infected with HSV-1 pC_eGC as compared to the peak in β-gal activity at four days p.i. observed in KOS6β-infected C57Bl/6 mice.

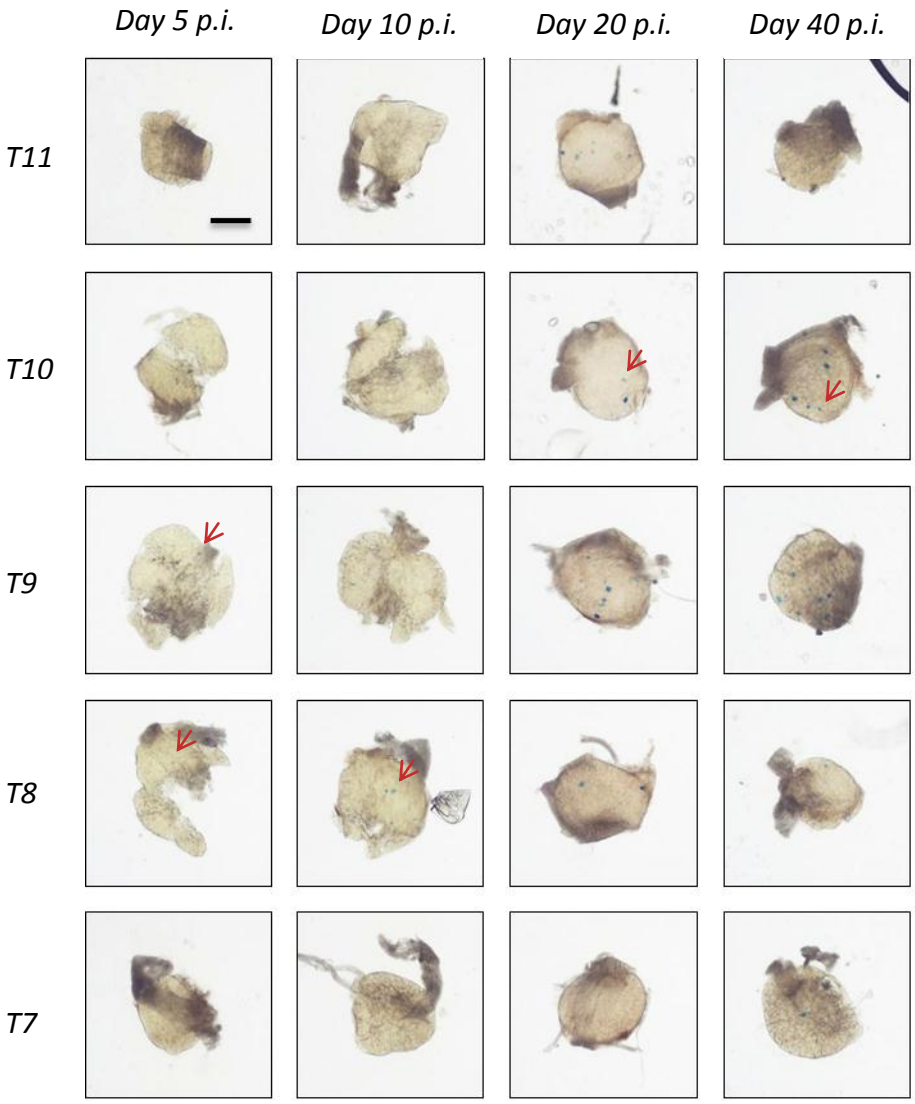

Figure 4-9. Photomicrographs of DRG from ROSA26R mice infected with HSV-1 pICP6_eGC over time. Groups of ROSA26R mice were infected with 1×10^8 PFU/mL HSV-1 pICP6_eGC. At the indicated times mice were culled and the DRG (from spinal levels T5 to L1) were removed and processed for the detection of β-gal activity. Photomicrographs were taken of each DRG at 40× magnification (scale bar = 300 µm, as indicated on the top left image). The images of DRG from spinal levels T7 to T12 from an individual mouse are shown for each time point and are representative of three independent experiments (n = 13 – 14, refer to Figure 4-10). Some example β-gal$^+$ cells are indicated by the red arrows. No β-gal$^+$ cells were seen in spinal levels T5, T6, T7, T13 or L1.

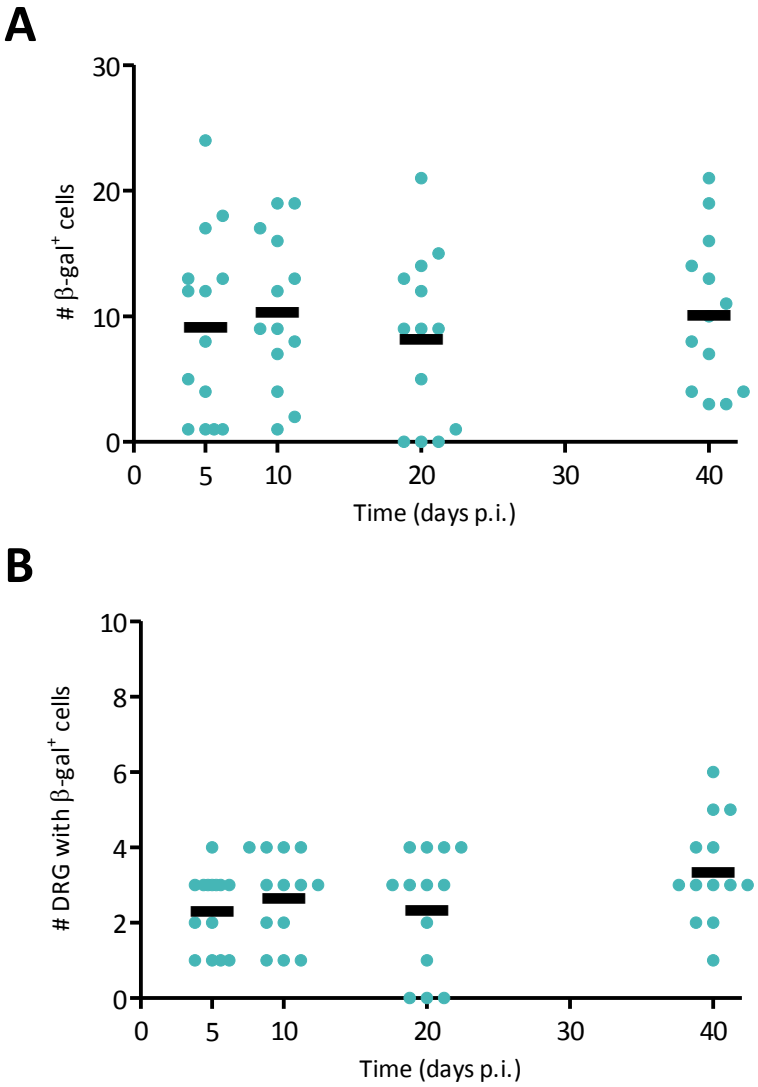

Figure 4-10. Very few cells become marked during infection with HSV-1 pICP6_eGC within ROSA26R mice. Groups of four or five ROSA26R mice were infected with 1×10^8 PFU/mL HSV-1 pICP6_eGC. At 5, 10, 20 or 40 days p.i. mice were culled and the DRG (from spinal levels T5 to L1) were removed and processed for the detection of β-gal activity. Both (A) the total number of β-gal$^+$ cells per mouse and (B) the number of DRG per mouse containing at least one β-gal$^+$ cell are shown. Each circle represents one mouse and the black bar represents the mean value for all mice at each time point. The results are pooled from three independent experiments (n = 13 – 14 per time point). A one way ANOVA was performed, but the means are not significantly different (p > 0.05).

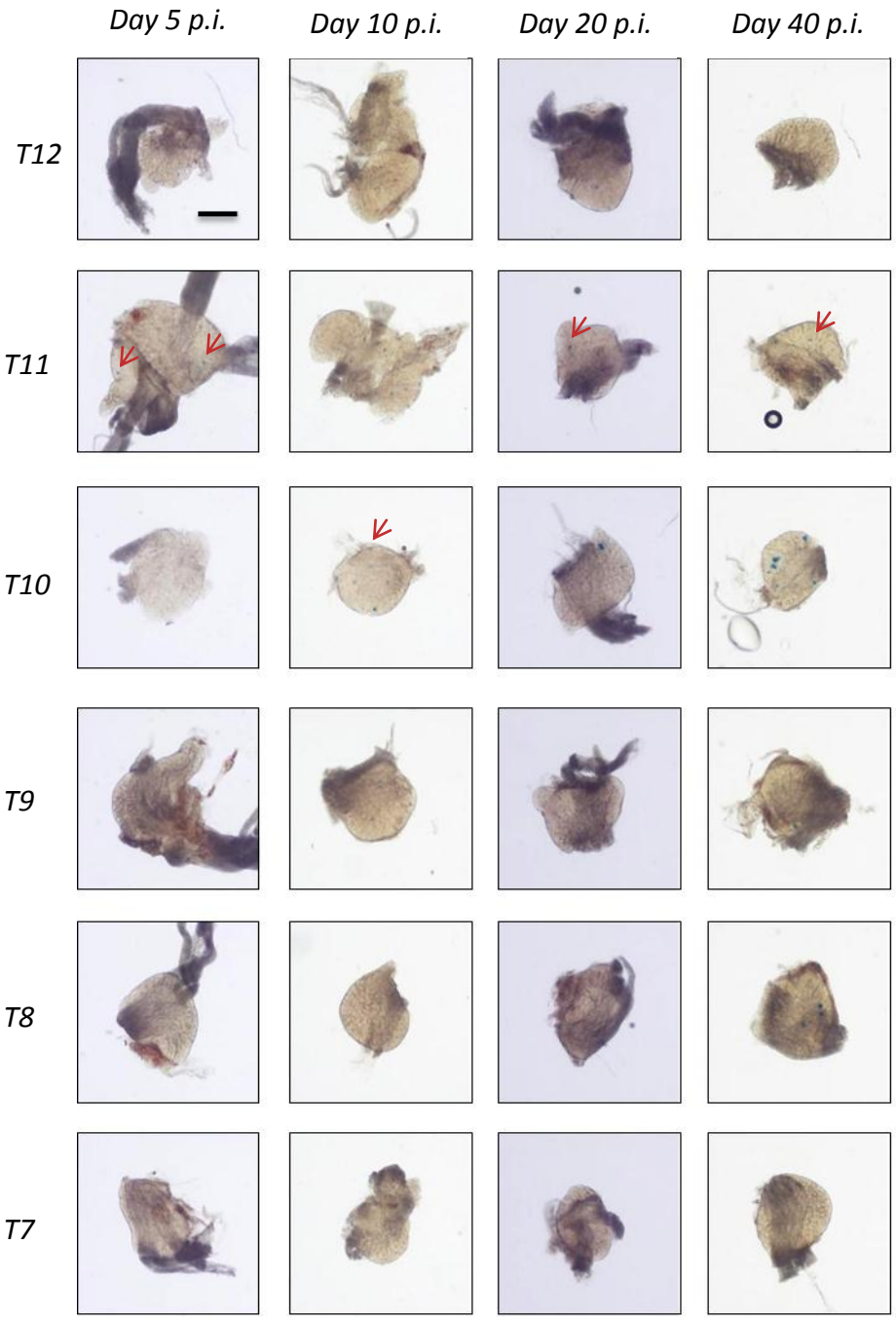

Figure 4-11. Photomicrographs of DRG from ROSA26R mice infected with HSV-1 pgB_eGC over time. ROSA26R mice were infected with 1×10^8 PFU/mL HSV-1 pgB_eGC. At the indicated times mice were culled and the DRG (from spinal levels T5 to L1) were removed and processed for the detection of β-gal activity. Photomicrographs were taken of each DRG at 40× magnification (scale bar = 300 μm, as indicated on the top left image). The images of DRG from spinal levels T7 to T12 from an individual mouse are shown for each time point, and are representative of five independent experiments (n = 16 – 20, refer to Figure 4-12). Some example β-gal$^+$ cells are indicated by the red arrows. No β-gal$^+$ cells were detectable in spinal levels T5, T6, T13 or L1.

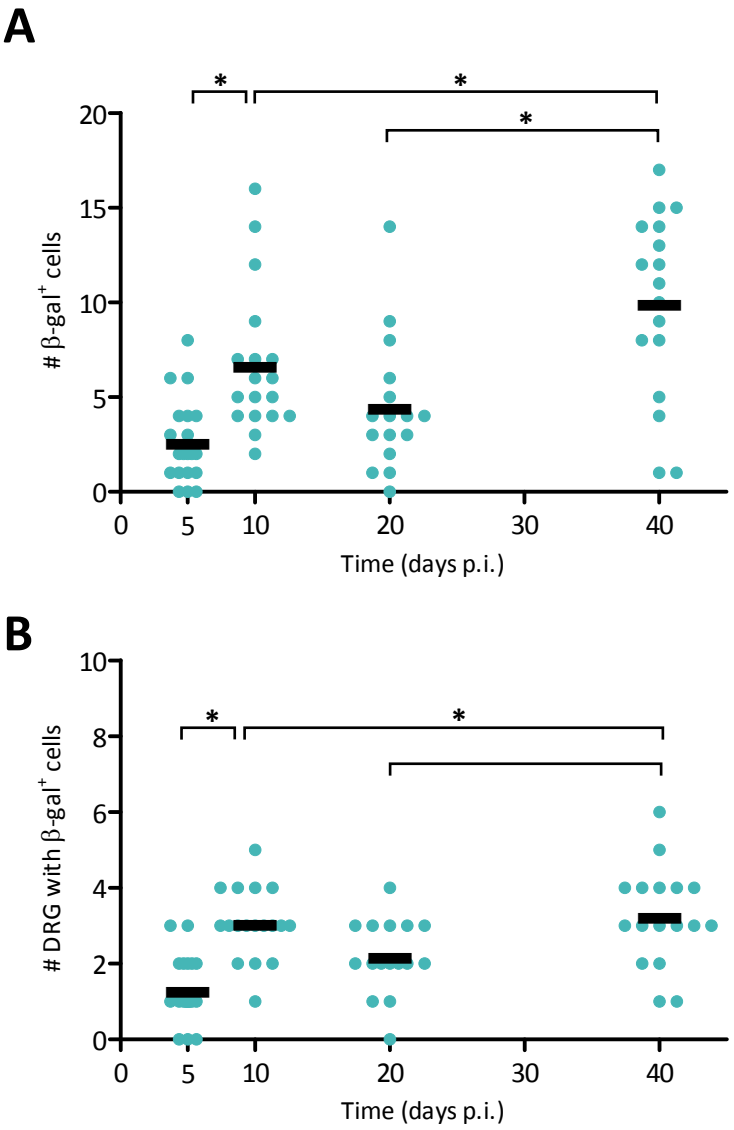

Figure 4-12. Accumulation of β-gal marked cells in ROSA26R mice infected with HSV-1 pgB_eGC throughout latency. Groups of two to six ROSA26R mice were infected with 1×10^8 PFU/mL HSV-1 pgB_eGC. At 5, 10, 20 or 40 days p.i. mice were culled and DRG (from spinal levels T5 to L1) were removed and processed for the detection of β-gal activity. Both (A) the total number of β-gal$^+$ cells per mouse and (B) the number of DRG per mouse containing at least one β-gal$^+$ cell are shown. Each circle represents one mouse and the black bar represents the mean value for all mice at each time point. The results are pooled from five independent experiments (n = 16 – 20 per time point). Statistical significance was determined by a one way ANOVA ($p < 0.001$) with Bonferroni's post-test to make pairwise comparisons (*$p < 0.05$).

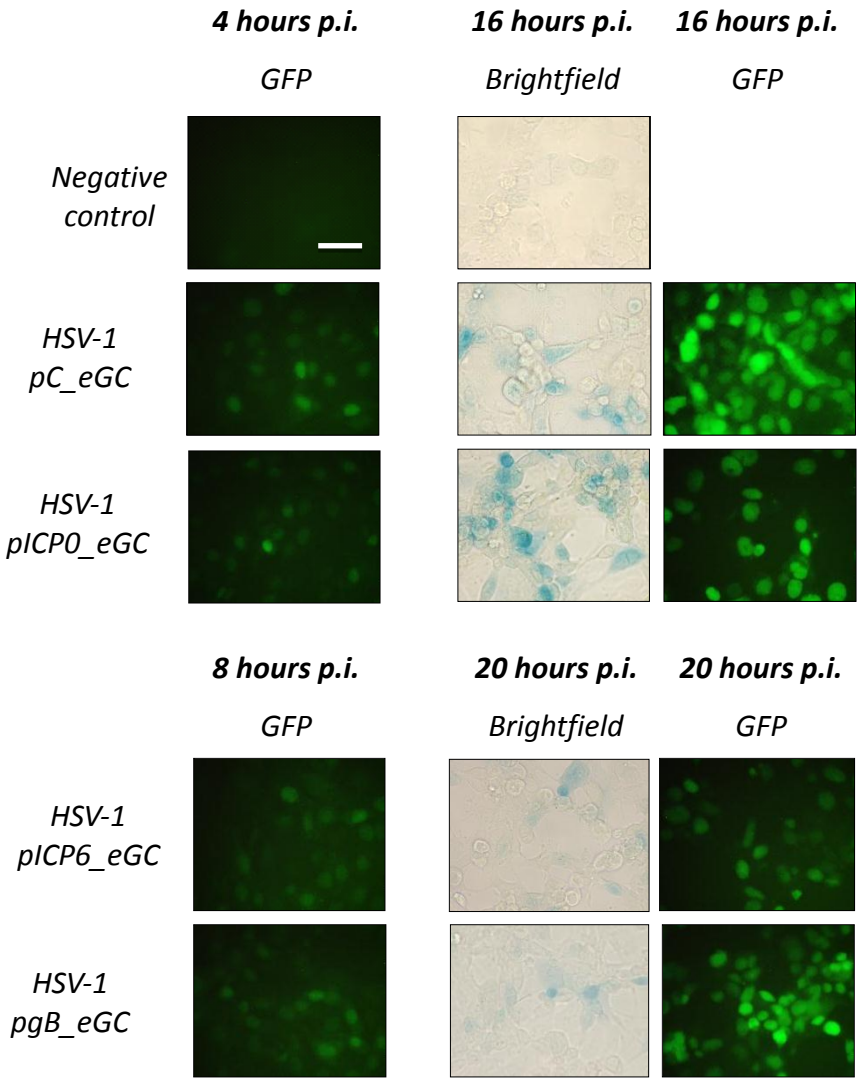

Figure 4-13. Detection of β-gal activity lags twelve hours behind expression of eGFP/Cre in Vero SUA cells. Semi-confluent Vero SUA cell monolayers (~8.2 × 104 cells per well of a 24 well plate) were infected with HSV-1 KOS, HSV-1 pC_eGC, HSV-1 pICP0_eGC, HSV-1 pICP6_eGC or HSV-1 pgB_eGC at an MOI of five. The cell monolayers were fixed at four hour intervals from 0 to 24 hours p.i. and examined for eGFP expression. The monolayers were then stained and examined for β-gal activity. Photomicrographs are shown taken at 400× magnification, with images showing a representative image of the same monolayer before and after staining to detect eGFP and β-gal expression, respectively (scale bar = 50 μm, shown on the top left image). Data are representative of two independent experiments.

4.3 Activity under HSV-1 promoters can give rise to protein expression during latency

To date, there have been no published reports that find an accumulation of β-gal marked cells in ROSA26R mice that are infected with HSV-1 that expresses Cre from a lytic promoter. So, there is no evidence from the ROSA26R/Cre system indicating that lytic viral promoter activity could lead to protein production during latency (Proença et al., 2008; Proença et al., 2011). Notably, lytic viral promoters tested in this system include those that direct expression of key transactivator proteins, which may initiate gene expression leading to reactivation, including ICP4, ICP0 and VP16 (Cai et al., 1993; Halford et al., 2001; Thompson et al., 2009). The observation that β-gal marked neurons do not accumulate during latency in ROSA26R mice infected with a virus expressing *Cre* from the ICP0 promoter was confirmed in Section 4.2.3. However, the increase in the number of β-gal$^+$ cells in ROSA26R mice infected with HSV-1 pgB_eGC during days 20 and 40 p.i. (Figure 4-12) suggested that expression from the gB promoter during latency may lead to low level protein expression. The difference between the mean number of β-gal$^+$ cells per mouse on days 20 and 40 p.i. was statistically significant, although the low number of β-gal$^+$ cells makes this result less convincing. Therefore, the number of β-gal$^+$ cells was assessed at day 10, 21 and 100 p.i. to allow continued accumulation of gB promoter-marked cells during latency over a long timeframe.

ROSA26R mice were infected with HSV-1 pgB_eGC and culled at days 10, 21 and 100 p.i., their DRG were removed and the number of β-gal$^+$ cells was determined. The number of β-gal marked cells detected on days 10 and 21 p.i. was not significantly different when compared to the previous experiment (Figure 4-11). The number of β-gal$^+$ cells continued to rise throughout latency between days 21 and 100 p.i., with an almost three-fold average increase in the number of β-gal$^+$ cells over this time (Figure 4-14A). There was also an increased number of DRG that contain at least one β-gal$^+$ cell during this time (Figure 4-14B). This increase is unlikely to be due to the spread of virus to previously uninfected neurons during latency, as it was shown in Section 4.2.1. that HSV-1 is able to spread to distal DRG by day 10 p.i.. Rather, the increase in the number of DRG that contain at least one β-gal$^+$ cell probably reflects gB promoter activity in neurons that were infected during the course of the acute infection but did not become β-gal marked. So, even neurons that do not directly innervate the site of infection can experience gB promoter activity during latency.

Next, β-gal activity in ROSA26R mice infected with HSV-1 pICP6_eGC was assessed. Groups of ROSA26R mice were infected with HSV-1 pICP6_eGC and culled at days 10, 20 and 100

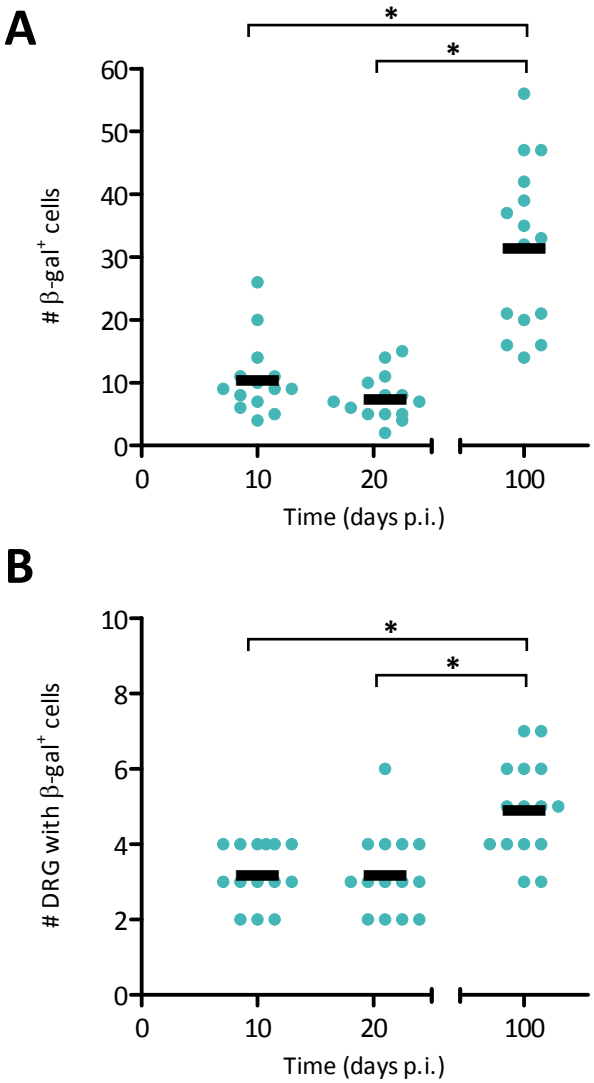

Figure 4-14. Accumulation of β-gal marked cells in ROSA26R mice infected with HSV-1 pgB_eGC throughout latency. Groups of four to five ROSA26R mice were infected with 1×10^8 PFU/mL HSV-1 pgB_eGC. At 10, 21 or 100 days p.i. mice were culled and the DRG (from spinal levels T5 to L1) were removed and processed for the detection of β-gal activity. Both (A) the total number of β-gal$^+$ cells per mouse and (B) the number of DRG per mouse containing at least one β-gal$^+$ cell are shown. Each circle represents one mouse and the black bar represents the mean value for all mice at each time point. The results are pooled from three independent experiments (n = 14 – 15 per time point). Statistical significance was determined by a one way ANOVA (p < 0.001) with Bonferroni's post-test to make pairwise comparisons (*p < 0.05).

p.i., their DRG were removed and the number of β-gal$^+$ cells was determined. This virus also showed a significant increase in the number of β-gal$^+$ cells between days 10 and 100 p.i. (Figure 4-15A). Again, there was an increased number of DRG that contain at least a single β-gal$^+$ cell during this time (Figure 4-15B). As for the accumulation of β-gal marked cells during infection of ROSA26R mice with HSV-1 pgB_eGC (Figure 4-14), this observation likely reflects activity under the ICP6 promoter in DRG that were infected during the acute infection but whose neurons do not directly innervate the site of infection.

The increase in the number of β-gal$^+$ cells in mice infected with either HSV-1 pICP6_eGC or HSV-1 pgB_eGC during latency may be a result of sporadic reactivation and resultant spread of virus when the ROSA26R/Cre system was employed. However, the failure to observe an accumulation of β-gal marked neurons during latency in ROSA26R mice infected with HSV-1 pICP0_eGC also argues against this possibility. This possibility did remain to be addressed. Therefore, ROSA26R mice were infected with HSV-1 pC_eGC, and mice were culled at 10, 20 and 100 dpi, when the expression of β-gal in DRG was assayed. There was an initial decline in the number of β-gal$^+$ cells between 10 and 20 days p.i. (Figure 4-16) and the loss of infected neurons during the establishment of latency, consistent with that previously described (Section 4.2.1). However, latency itself was remarkably stable, with the number of β-gal$^+$ cells remaining similar between 20 and 100 days p.i. Further, the number of DRG that contain β-gal$^+$ cells was similar between days 20 and 100 p.i., suggesting there is little, if any, spread of virus during this time.

It is possible that any increase in the number of β-gal marked cells due to the spread of virus to previously uninfected cells may be precisely balanced by the loss of β-gal$^+$ cells due to reactivation. Based on the data presented in Figure 4-16, to theoretically observe a statistically significant net change in the size of the viral reservoir over the 80 days of latency measured, a minimum of at least 50 β-gal$^+$ neurons must be lost, or approximately two β-gal$^+$ neurons every three days. This places a limit on the ability of this system to detect reactivation and new infection, especially as reactivation probably occurs from only a few neurons. However, the failure to detect an increase in the number of β-gal marked cells in ROSA26R mice infected with HSV-1 pICP0_eGC indicates that there is not substantial reactivation and spread of virus in this system (refer to Section 4.2.3). So, it is reasonable to conclude that latency is stable in our mouse model and is comparable with other murine models of HSV-1 latency (Gebhardt and Halford, 2005; Laycock et al., 1991). Given this, there is likely gB and ICP6 promoter activity during latency, albeit at a low level or of a transient nature, which can lead to the expression of viral protein.

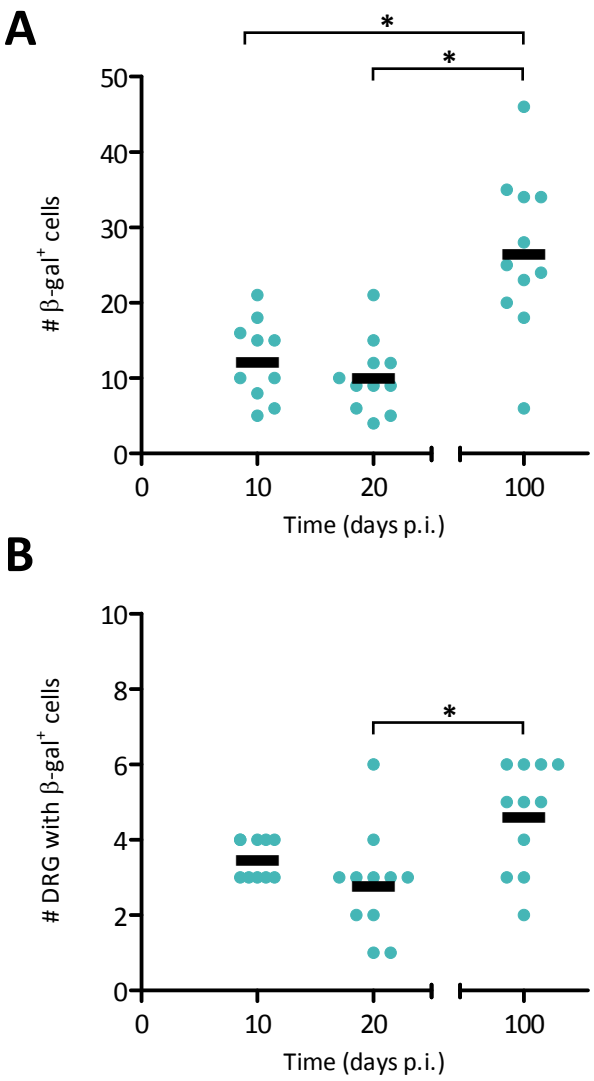

Figure 4-15. Following infection with HSV-1 pICP6_eGC, β-gal marked cells slowly accumulate throughout latency, indicating viral protein production. Groups of three or four ROSA26R mice were infected with 1×10^8 PFU/mL HSV-1 pICP6_eGC. At 10, 20 or 100 days p.i. mice were culled and the DRG (from spinal levels T5 to L1) were removed and processed for the detection of β-gal activity. Both (A) the total number of β-gal$^+$ cells per mouse and (B) the number of DRG per mouse containing at least one β-gal$^+$ cell are shown. Each circle represents one mouse and the black bar represents the mean value for all mice at each time point (n = 10 – 11 per time point). The results are pooled from three independent experiments. Statistical significance was determined by a one way ANOVA ($p < 0.05$) with Bonferroni's post-test to make pairwise comparisons (*$p < 0.05$).

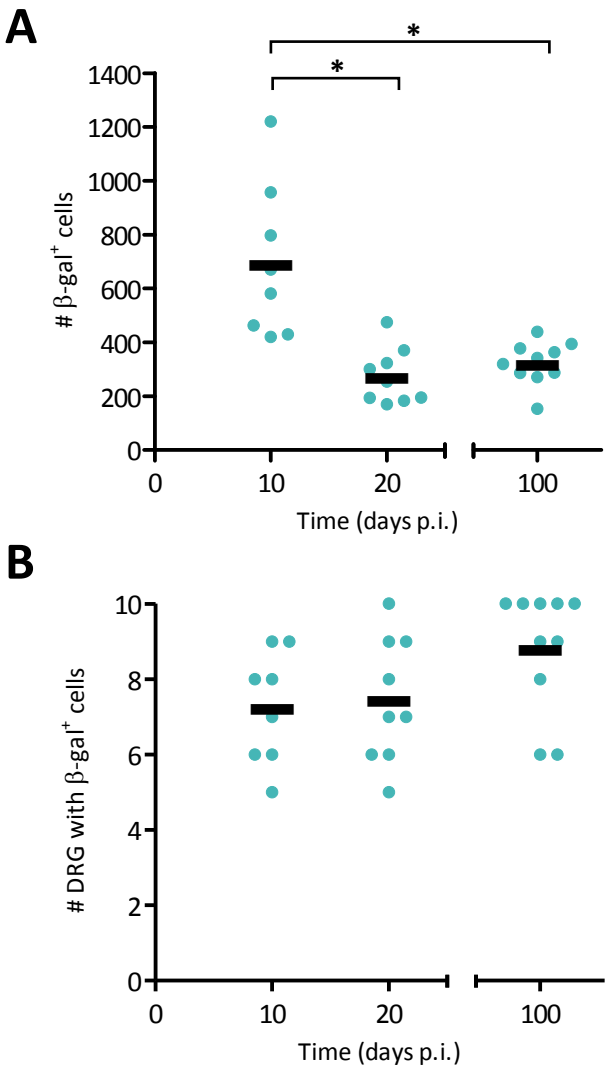

Figure 4-16. There is no significant gain or loss of β-gal marked neurons after the establishment of latency, indicating latency in ROSA26R mice is stable. Groups of four or five ROSA26R mice were infected with 1×10^8 PFU/mL HSV-1 pC_eGC. At 10, 20 or 100 days p.i. mice were culled and DRG (from spinal levels T5 to L1) were removed and processed for the detection of β-gal activity. Both (A) the total number of β-gal$^+$ cells per mouse and (B) the number of DRG per mouse containing at least one β-gal$^+$ cell are shown. Each circle represents one mouse and the black bar represents the mean value for all mice at each time point. The results are pooled from 3 independent experiments (n = 8 – 10 per time point). Statistical significance was determined by a one way ANOVA ($p < 0.001$) with Bonferroni's post-test to make pairwise comparisons (*$p < 0.05$).

4.4 The expression of Cre under different HSV-1 promoters *in vivo* may not be well predicted by kinetic class

Thus far, only a single representative promoter of each kinetic class was chosen for the examination of historical gene expression during the establishment and maintenance of latency. However, HSV-1 is a large virus with many genes within each kinetic class (Pellet and Roizman, 2013). Although there are consensus promoter elements that dictate expression, especially in epithelial cells, there are known differences in the regulatory control of genes within the same kinetic class (Homa et al., 1988; Honess and Roizman, 1974; Pande et al., 1998; Sze and Herman, 1992). These differences remain largely unexplored in the context of *in vivo* infection models and, in particular, during latency. There are five immediate early genes, but only the activity of two immediate early gene promoters, namely ICP0 and ICP4, have been examined in the ROSA26R/Cre model (refer to Section 4.2.3; Proença et al., 2008; Proença et al., 2011). Additionally, two of the remaining immediate early genes, encoding ICP22 and ICP47, share promoter sequences (Barklie Clements et al., 1977; Gelman and Silverstein, 1987; Murchie and McGeoch, 1982).

To further extend this study, a virus was used in which a gene encoding an eGFP/Cre protein was placed under the control of the ICP47/22 promoter at an ectopic locus (refer to Section 3.2.2.1). Groups of ROSA26R mice were infected with HSV-1 pICP47_eGC, and culled at various times p.i. and the number of β-gal$^+$ cells per DRG determined (Figure 4-17). A distinct trend in the number of β-gal$^+$ cells was observed, with a substantial, significant increase in the number of β-gal$^+$ cells seen between days five and 20 p.i. (Figure 4-18A). This was associated with an increased number of DRG that contain at least one β-gal$^+$ cell between days 20 and 40 p.i. (Figure 4-18B), indicating activity of this promoter may occur in neurons that did not directly innervate the site of the initial skin infection. The accumulation of β-gal marked cells in ROSA26R mice infected with HSV-1 pICP47_eGC contrasts with the pattern observed when historical expression under the ICP0 promoter was observed in this model (Figure 4-8) and that previously observed when Proença and colleagues (2008; 2011) used the ICP0 and ICP4 promoters in this system. It more closely resembles the trend in the marking of neurons in ROSA26R mice when Cre is expressed from the LAT promoter published by Proença and colleagues (2008). Given this unexpected finding, the activity of the ICP47/22 promoter during latency will be explored further in Chapter 5.

4.5 Expression of Cre under the LAT promoter in ROSA26R mice leads to the β-gal marking of a substantial population of cells

It was shown that the activity of the ICP47 promoter leads to the continued marking of a reasonable sized population of cells during latency. This surprising trend is similar to that reported by Proença and colleagues (2008), for a virus designed to express Cre under the LAT promoter, named LAT Cre. However, LAT Cre was constructed on a different genetic background, SC16, and a different route of infection was used. Therefore, a virus was constructed using the KOS strain of virus which contains an *eGFP/Cre* fusion gene under the control of an IRES inserted into the LAT locus (refer to Section 3.4).

As would be expected, it was previously shown that there was no expression of eGFP from HSV-1 pLAT_eGC following infection of Vero cells (refer to Section 3.5), but this does not verify that eGFP expression will be observed during latency *in vivo*. Therefore, C57Bl/6 mice were infected with HSV-1 pLAT_eGC. There mice were culled at either four or 30 days p.i. to assess expression of eGFP within the DRG during either acute or latent infection, respectively (Figure 4-19). A small population of $eGFP^+$ cells was detectable at four days p.i., with clear nuclear localisation of eGFP (Figure 4-19B). The expression of eGFP was detected in DRG of multiple spinal levels in each mouse (Figure 4-19D). Further, there was a similar number of $eGFP^+$ cells detectable during latency and the acute infection (Figure 4-19C). This confirms that expression of the eGFP/Cre cassette from an IRES inserted into the LAT locus in HSV-1 pLAT_eGC is possible.

To test if there was historical expression under the LAT promoter in ROSA26R mice, groups of mice were infected with HSV-1 pLAT_eGC. Mice were culled at various times p.i., and the number of $\beta\text{-gal}^+$ cells in the DRG was determined (Figure 4-20). As observed by Proença and colleagues (2008), the initial population of cells that becomes $\beta\text{-gal}^+$ during the acute infection (at five and 10 days p.i.) was substantial, and comparable to that of ROSA26R mice infected with HSV-1 pC_eGC (Figure 4-2, and 4-21). The spread of virus to distal DRG was greater, with an average of nine DRG containing at least one β-gal marked cell on day 10 p.i., as compared to HSV-1 pC_eGC where an average of seven DRG contain at least one β-gal marked cell. However, the population of $\beta\text{-gal}^+$ cells continued to increase until 20 days p.i., by which time latency should be largely established. The population of β-gal marked cells remained largely stable throughout latency. This observation was unexpected, as it implies that the population of β-gal marked cells in ROSA26R mice infected with HSV-1 pLAT_eGC is more than twice that of ROSA26R mice infected with HSV-1 pC_eGC. Given that results presented in this chapter indicate that the ROSA26R/Cre system is more sensitive to the activity under viral promoters than a

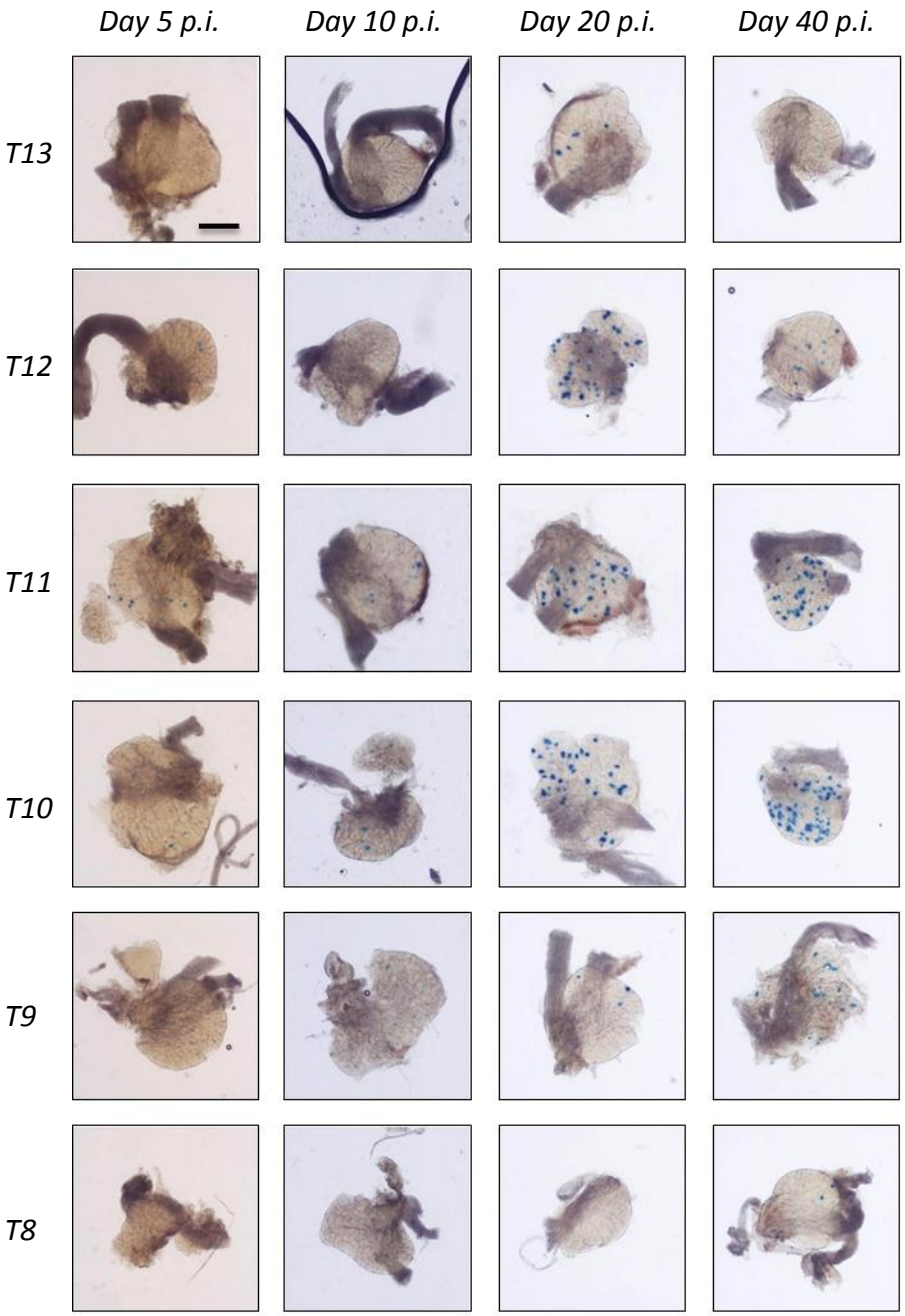

Figure 4-17. Representative photomicrographs of DRG from ROSA26R mice infected with HSV-1 pICP47_eGC over time. ROSA26R mice were infected with 1×10^8 PFU/mL HSV-1 pICP47_eGC. At the indicated times mice were culled and the DRG (from spinal levels T5 to L1) were removed and processed for the detection of β-gal activity. Photomicrographs were taken of each DRG at 40× magnification (scale bar = 300 μm, as indicated on the top left image). The images of DRG from spinal levels T7 to T12 from an individual mouse are shown for each time point, and are representative of three independent experiments (n = 11, refer to Figure 4-18). β-gal$^+$ cells were undetectable in spinal levels T5, T6, T7, or L1.

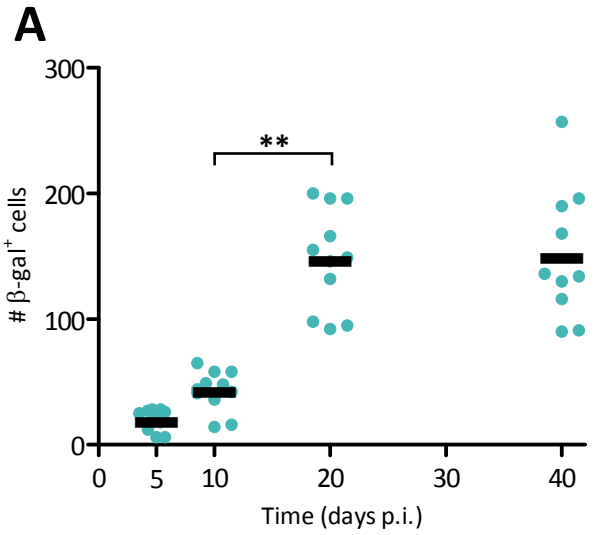

B

Pairwise comparisons from (A)			
Day	5	10	20
10	ns		
20	*	*	
40	*	*	ns

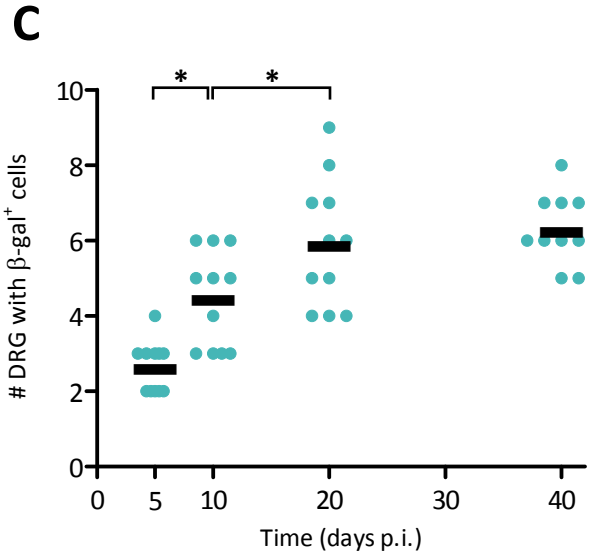

D

Pairwise comparisons from (C)			
Day	5	10	20
10	*		
20	*	*	
40	*	*	ns

Figure 4-18. Activity under the ICP47 promoter leading to viral protein production occurs during the establishment of latency and throughout latency. Groups of two to five ROSA26R mice were infected with 1×10^8 PFU/mL HSV-1 pICP47_eGC. At 5, 10, 20 or 40 days p.i. mice were culled and the DRG (from spinal levels L1 to T5) were removed and processed for the detection of β-gal activity. Both (A) the total number of β-gal+ cells per mouse and (C) the number of DRG per mouse containing at least one β-gal+ cell are shown. Each circle represents one mouse and the black bar represents the mean value for all mice at each time point. The results are pooled from three independent experiments (n = 11 per time point). (B&D) Statistical significance was determined by a one way ANOVA ($p < 0.001$) with Bonferroni's post-test to make pairwise comparisons, with key statistical differences indicated on (A) and (C), where * represents that $p < 0.05$.

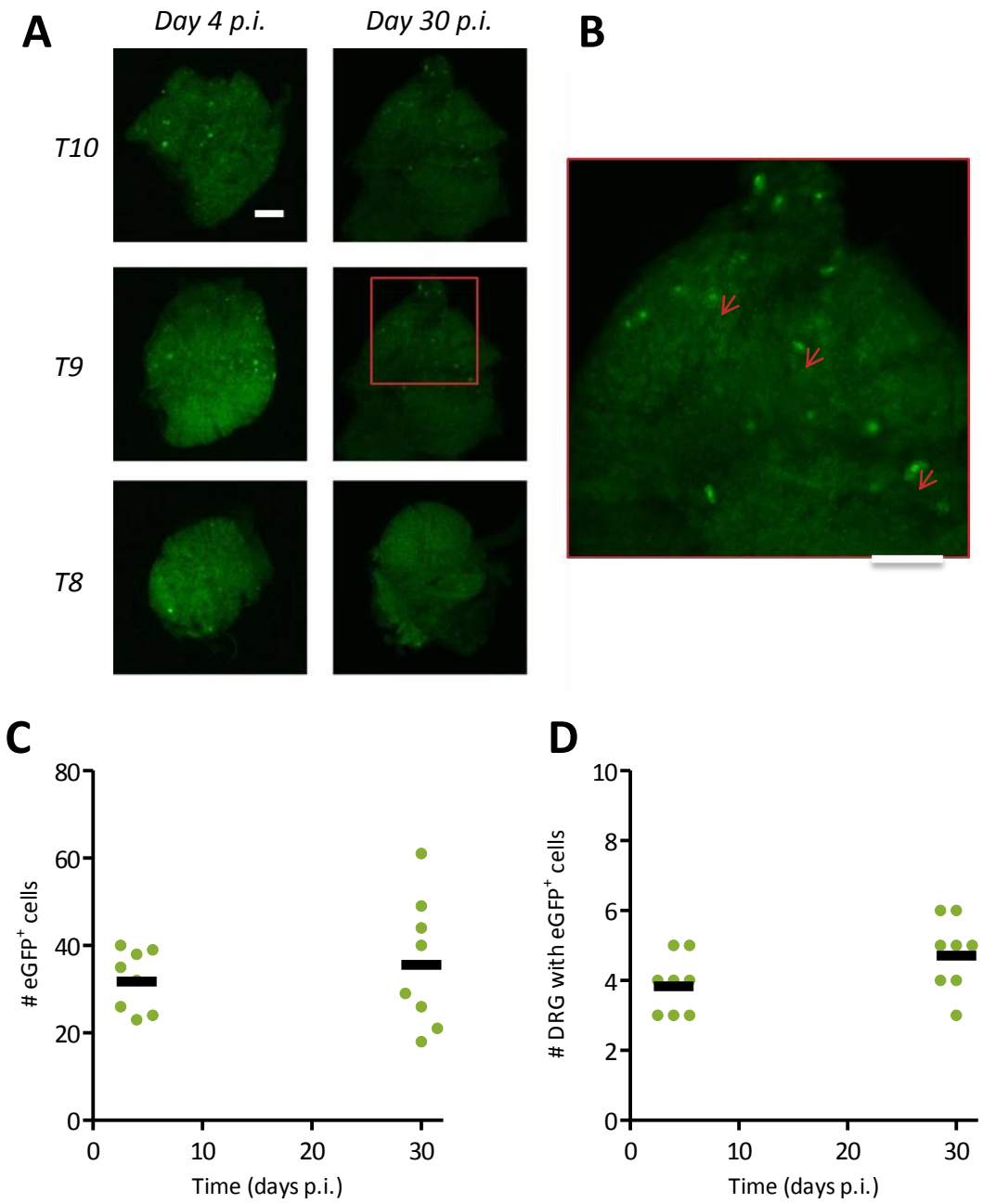

Figure 4-19. Expression of eGFP in C57Bl/6 mice infected with HSV-1 pLAT_eGC. Groups of four C57Bl/6 mice were infected with 1×10^8 PFU/mL HSV-1 pLAT_eGC. At 4 or 30 days p.i. mice were culled and the DRG (from spinal levels T5 to L1) were removed and processed for the detection of eGFP expression. (A) Photomicrographs are representative of a single mouse taken at 50× magnification (scale bar = 250 µm, as indicated on top left image), with photos showing spinal levels T10 to T8, with eGFP$^+$ cells still detectable in the remaining DRG. (B) A magnified view of the red box at 100× magnification, where the red arrows indicate the localisation of eGFP/Cre (scale bar = 300 µm). Both (C) the total number of eGFP$^+$ cells per mouse and (D) the number of DRG per mouse containing at least one eGFP$^+$ cell are shown. Each circle represents one mouse and the black bar represents the mean value for all mice at each time point. The results are pooled from two independent experiments. An unpaired *t* test with Welch's correction was performed but no statistically significant difference between means was found ($p > 0.05$).

traditional plaque assay, it is highly likely that this virus has an undesired secondary site mutation that has resulted in a subtle alteration in its growth or pathogenesis *in vivo*. Alternatively, the LAT region is transcriptionally complex (refer to Figure 3-12), and the insertion of this expression cassette may have affected gene expression from this region. Therefore, to make any conclusions based on this data, it is important that a revertant virus is constructed to begin to resolve these concerns.

4.6 Discussion

This chapter began with a historical analysis of HSV-1 infection using ROSA26R mice infected with HSV-1 pC_eGC to reveal the entire population of live infected cells. Surprisingly, continued spread of virus beyond the peak of infection was observed. By contrast, the presence of infectious virus peaks at four days p.i., as does the expression of *lacZ* from KOS6β-infected mice. Therefore, the maximal viral load occurs much earlier during the acute infection (these results are summarised in Figure 4-22), consistent with previous reports using similar models of HSV-1 infection (Luker et al., 2002; Sawtell et al., 1998; Sedarati et al., 1989; Simmons and Nash, 1984; Speck and Simmons, 1998; Van Lint et al., 2004). HSV-1 is a highly cytolytic virus, and during the peak of viral activity it is likely that many neurons are infected and are dying, so would not undergo *lacZ* expression in the ROSA26R/Cre mouse model. Therefore, it is likely that the peak in the historical β-gal marking of neurons in ROSA26R/Cre mice at day 10 p.i. compared to the maximal virus load at day four p.i. can be explained by a bias towards the establishment of a latent infection in cells that first receive viral genomes later in infection (after day five p.i.). Such an explanation could also account for the much slower decline in viral genome copy number during the resolution of the acute infection (Chen et al., 2000; Wakim et al., 2008b), when compared to infectious virus (refer to Section 4.2.2; Van Lint et al., 2004). The viral genome copy number reflects acutely infected neurons, including those that are dying, and those in which latency has been established, while the marking of cells in the ROSA26R/Cre mouse model likely does not reflect viral activity during acute infection very well. The net result of the resolution of the acute infection is likely to be the loss of viral genomes due to lytic infection, but later times p.i. this may be partially balanced by the slow spread of virus and the establishment of a latent infection in previously uninfected neurons. The establishment phase of latency occurs in the context of a rapidly developing adaptive immune response, with the development of a strong $CD8^+$ T cell

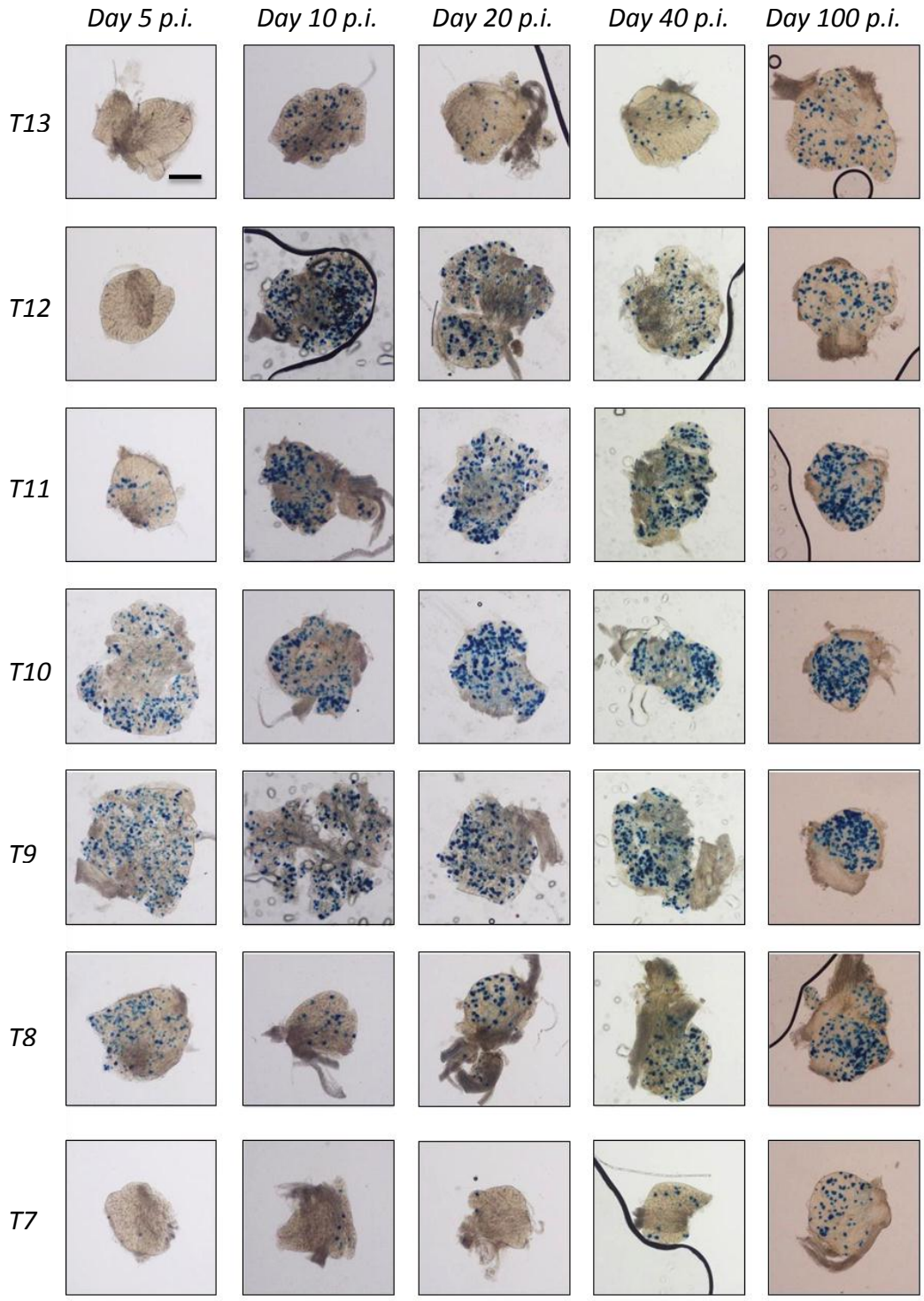

Figure 4-20. Photomicrographs of DRG from ROSA26R mice infected with HSV-1 pLAT_eGC over time. Groups of ROSA26R mice were infected with 1×10^8 PFU/mL HSV-1 pLAT_eGC. At the indicated times mice were culled and the DRG (from spinal levels T5 to L1) were removed and processed for the detection of β-gal activity (see Figure 4-21). Photomicrographs were taken of each DRG at 40× magnification (scale bar = 300 μm, as indicated on the top left image). The images of DRG from spinal levels T7 to T13 from an individual mouse are shown for each time point and are representative of three independent experiments (n = 8, refer to Figure 4-21). β-gal$^+$ cells were still detectable in spinal levels L1, T6 and T5 for mice on days 10, 20 and 40 p.i.

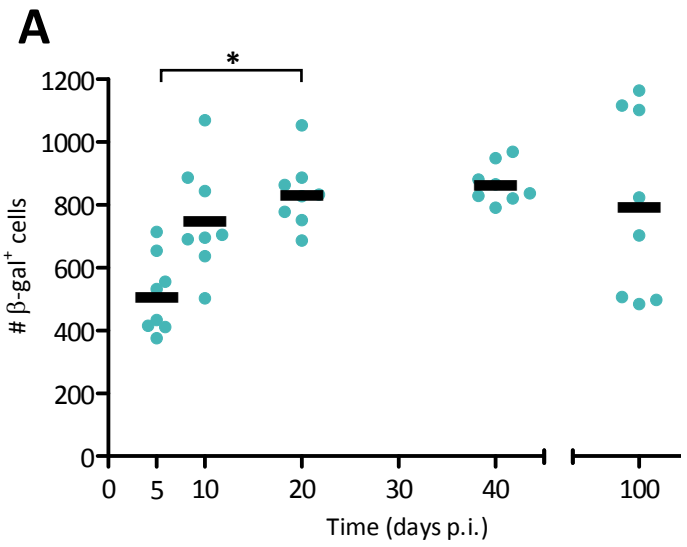

B

Pairwise comparisons from (A)				
Day	5	10	20	40
10	ns			
20	*	ns		
40	*	ns	ns	
100	*	ns	ns	ns

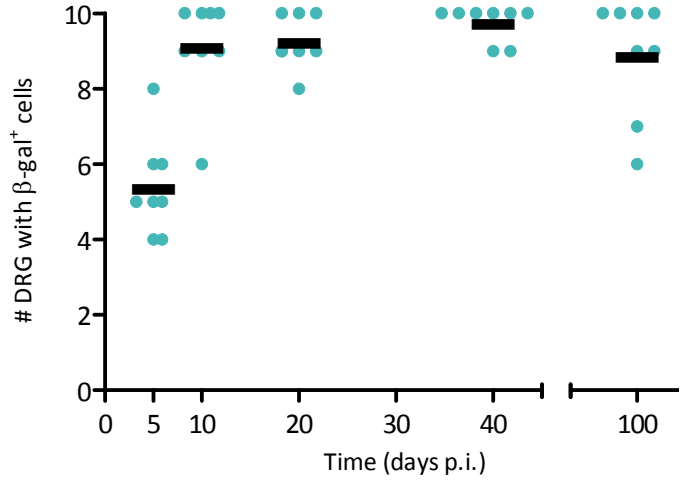

D

Pairwise comparisons from (C)				
Day	5	10	20	40
10	*			
20	*	ns		
40	*	ns	ns	
100	*	ns	ns	ns

Figure 4-21. Accumulation of β-gal marked cells indicates continued activity under the LAT promoter during latency. Groups of three to five ROSA26R mice were infected with 1×10^8 PFU/mL HSV-1 pLAT_eGC. At 5, 10, 20, 40 or 100 days p.i. mice were culled and the DRG (from spinal levels T5 to L1) were removed and processed for the detection of β-gal activity. Both (A) the total number of β-gal$^+$ cells per mouse and (C) the number of DRG per mouse containing at least one β-gal$^+$ cell are shown. Each circle represents one mouse and the black bar represents the mean value for all mice at each time point. The results are pooled from three independent experiments (n = 8 for each time point). (B&D) Statistical significance was determined by a one way ANOVA ($p < 0.01$) with Dunn's post-test to make pairwise comparisons, with key statistical differences indicated on (A) and (C) (*$p < 0.05$).

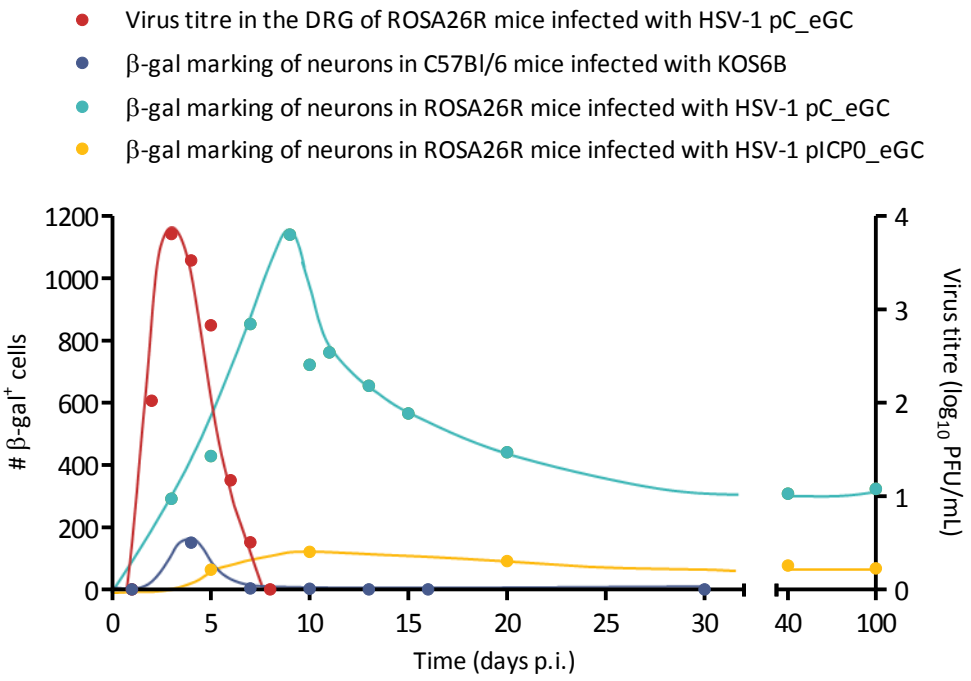

Figure 4-22. Summary of trends in historical marking of neurons in ROSA26R mice during acute infection compared to conventional means of tracking the acute HSV-1 infection. The mean titre of virus within the DRG of ROSA26R mice infected with HSV-1 pC_eGC from Figure 4-4 is shown in red, and plotted on the X-axis versus the Y-axis on the left hand side. Reporter gene activity throughout the acute infection is shown in purple as the mean number of β-gal+ cells in KOS6β infected C57Bl/6 mice. The means of data from Figures 4-2, 4-3 and 4-16 is shown in blue, indicating the accumulation of β-gal marked cells in ROSA26R mice infected with HSV-1 pC_eGC over time. Finally, the means of the data from Figure 4-8 is shown in yellow indicating the accumulation of β-gal marked cells in ROSA26R mice infected with HSV-1

response that peaks at day seven p.i. (Coles et al., 2002), and will be discussed in more detail in Chapter 6.

The observation made using the ROSA26R/Cre system that the spread of virus continues beyond the peak of the acute infection at day four p.i. was not restricted to those mice infected with HSV-1 pC_eGC. Rather, it also extends to include historical marking of neurons by Cre expressed from bona fide HSV-1 lytic promoters. This is exemplified by ROSA26R mice infected with HSV-1 pICP0_eGC, with the peak in the number of β-gal$^+$ cells at day 10 p.i. Both HSV-1 pICP47_eGC and HSV-1 pICP0_eGC were able to mark a substantial population of neurons in acutely infected ROSA26R mice. These observations are consistent with those observations by Proença and colleagues when other viruses that express *cre* from an immediate early promoter were employed in the ROSA26R mouse model (2008; 2011). Even though the number of β-gal$^+$ cells detected is clearly different, in both cases about one third of all latently infected cells likely experienced prior ICP0 expression prior to the establishment of latency (Proença et al., 2008). The simplistic, phage λ-like model of latency implies that cells experiencing lytic gene expression inevitably die, but the β-gal marking of cells in ROSA26R mice infected with HSV-1 pICP0_eGC or HSV-1 pICP47_eGC is more consistent with other studies suggesting latency establishment can be preceded by immediate gene expression (Kosz-Vnenchak et al., 1993; Kramer et al., 1998; Margolis et al., 1992; Nichol et al., 1996; Speck and Simmons, 1991; Steiner et al., 1990; Valyi-Nagy et al., 1991).

It is likely that the outcome for those cells in which the full cascade of lytic gene expression is completed is death (Pellet and Roizman, 2013). This likely accounts for why very few cells became β-gal marked following expression of *cre* under the early ICP6 or leaky late gB promoters. These results are consistent with similar observations made by Proença and colleagues (2008; 2011) when either the early *tk*, or late gC or VP16 promoters were used to drive expression of *cre*. However, there is a large, vital population of neurons during the acute infection that experience expression of the early and late genes required for viral DNA replication and the production of infectious virus to drive the spread of virus between about days two and five p.i. (Kramer et al., 1998; Pellet and Roizman, 2013; Speck and Simmons, 1991). There are several possibilities to explain the failure to detect large numbers of β-gal$^+$ cells in ROSA26R mice infected with either HSV-1 pICP6_eGC or HSV-1 pgB_eGC. Cells may fail to express sufficient Cre protein before viral shutdown of the host cell transcription occurs. So, the modification to the genome necessary for the expression of β-gal does not occur, even if the cell survives (Laurent et al., 1998; Smiley, 2004). Alternately, neurons may survive expression of early or late genes prior to establishment of latency, but not express sufficient Cre or β-gal for the detection of β-gal activity,

although this is inconsistent with models of HSV-1 latency establishment. Finally, and most likely, latency is not established in neurons which experience early or late gene expression and so they die, likely before they are able to express sufficient β-gal to be detected by X-gal staining (Proença et al., 2008; Proença et al., 2011). This is consistent with most models of HSV-1 latency establishment in neurons (Kosz-Vnenchak et al., 1993; Kramer et al., 1998; Margolis et al., 1992; Nichol et al., 1996; Speck and Simmons, 1991; Steiner et al., 1990; Valyi-Nagy et al., 1991). One way to investigate this further would be to look for expression of eGFP in ROSA26R mice infected with HSV-1 expressing eGFP/Cre from a lytic gene promoter, which would reflect current gene expression, even in cells in which a lytic infection is established. This could then be compared with β-gal expression in the same sample, ideally within the same cell, but there are currently no fluorescent substrates for β-gal available that can be used in combination with eGFP detection. Overall, it is clear that the ROSA26R/Cre mouse model will fail to reveal the considerable population of neurons that undergo a lytic infection leading to cell death early during infection and account for the bulk viral load during the acute infection.

There have been some reports that describe the detection of a low level of virus activity beyond day seven p.i. In this thesis, β-gal expression was detectable in a small population of cells until 16 days p.i. in C57Bl/6 mice infected with KOS6β (refer to Section 4.2.2). Unfortunately, the β-gal protein is extremely stable, a limitation when monitoring viral gene expression over time (Margolis et al., 1993). However, using immunohistochemistry with a polyclonal HSV-1 antibody to study gene expression in the TG of HSV-1 infected mice, Shimeld and colleagues (1995) were able to detect the presence of viral antigen until day 10 p.i. Using a similar method, Sawtell (2003) was also able to detect antigen in DRG from ocularly infected mice on days nine and 17 p.i. Further, when examining the viral transcript copy number relative to host RNA levels, Zhou and colleagues (2013) found that ICP27, TK and VP16 transcripts were detectable at similar levels or even higher on day seven compared to day three p.i. Further, although infectious virus is not usually reliably detected beyond day seven p.i. in murine models of HSV-1 infection (Sedarati et al., 1989), Sawtell (2003) was able to detect low levels of infectious virus in DRG in a subset of ocularly infected mice on both days nine and 17 p.i., although not day 14 p.i. There are also multiple reports of low level detection of infectious virus as determined by plaque assay on infected mice on day eight or nine p.i., but in this thesis infectious virus could not be detected at this time (refer to Figure 4-4; Ramachandran et al., 2008; Sawtell et al., 1998; Steiner et al., 1989; Thompson et al., 1986). In summary, there are multiple lines of evidence that indicate viral activity beyond the peak of the acute infection, but it is always at an exceptionally low level. This is consistent with the peak of historical marking of

neurons in the ROSA26R/Cre mouse system resulting from a decrease in the intensity of infected cell death as a result of lytic infection, rather than an increase in the number of neurons becoming infected at later times p.i.

The biological relevance of continued viral activity beyond day seven p.i. and during the establishment of latency is most clearly demonstrated by the increase in the number of DRG that contain β-gal marked cells between day five and 10 p.i. in ROSA26R mice infected with HSV-1 pC_eGC. Since β-gal activity can be detected in distal DRG that do not directly innervate the site of infection during latency (at 100 days p.i.; see Figure 4-16), the increased spread of virus between days five and 10 p.i. likely results in an increase in the number of neurons that harbour latent HSV-1. Further, the increased spread of virus to distal DRG in ROSA26R mice infected with HSV-1 pICP0_eGC, HSV-1 pICP47_eGC or HSV-1 pgB_eGC indicates that lytic promoter expression can occur in those neurons that do not directly innervate the site of infection. Speck and Simmons (1991) have previously shown productive infection, characterised by the presence of infectious virus during the acute infection and viral antigen, was restricted to the ganglia that innervate the site of infection, namely T6 to L1. By contrast, they found that latent infection is much more widespread, as assessed by the presence of LAT^+ neurons and the retrieval of virus following reactivation from ganglia from spinal levels T6 to L1. Given their methods were insensitive to low level or transient expression of viral proteins or transcripts (Speck and Simmons, 1991), their results are consistent with those presented in this thesis. Further, the DRG that directly innervate the site of infection had relatively more copies of viral DNA per LAT^+ cell, compared to those DRG that were distal to the site of infection (Simmons et al., 1992). Therefore, there is less amplification of DNA during the productive phase of infection in the DRG that do not directly innervate the site of infection. This is consistent with the findings in this thesis that virus spreads to more distal DRG at a time when productive infection is limited. While there is a caveat – namely, that the analysis of whole ganglia can mask variability between individually infected cells – the extent of lytic infection and entry into latency differs with direct innervation of the site of infection.

It is not entirely clear how the virus spreads to the DRG that do not directly innervate the site of infection. In the flank zosteriform model of HSV-1 infection, the virus spreads from the site of infection in the skin to the DRG. Further spread occurs in the PNS, allowing the virus to reach axons that do not directly innervate the inoculation site, but belong to the same dermatome. The overlapping nature of the dermatomes facilitates virus spread across different spinal levels to a certain extent, with neurons from thoracic levels T8 and T12 likely innervating the site of infection above T10 (Speck and Simmons, 1991). However, the spread of virus to distal DRG between days five and 10 p.i. occurs when

infectious virus appears absent from the skin or DRG (refer to Section 4.2.2). Therefore, an alternative explanation is that at later times p.i. virus transmission may occur in an anatomical structure other than the DRG or skin. The dorsal horn of the spinal cord is organised into overlapping cell columns that receive inputs from DRG. The transmission of virus through the cell column may lead to transneuronal spread of virus to the sensory neurons of DRG that enter and terminate at other segmental levels (Smith et al., 2000). This is believed to account for the detection of latently infected neurons at spinal levels distal to the site of primary infection (Lachmann et al., 1999; Speck and Simmons, 1991), and likely occurs at later times after infection (beyond day five p.i.). It has been shown that the neurovirulent HSV-1 strain SC16 can pass trans-synaptically in the spinal cord using a CMV IE-*lacZ* reporter, which labels motor neurons that do not connect with the site of skin infection (Smith et al., 2000). Further, there is a similar level of detectable viral genomes relative to cellular DNA in the spinal cord and DRG following footpad inoculation of guinea pigs with HSV-1 strain 17 (Ohashi et al., 2011). However, the spread of HSV-1 to the CNS, including the spinal cord, is believed to occur only in mice infected with the more neurovirulent HSV-1 strains, while the strain of HSV-1 used in this thesis, KOS, is poorly neurovirulent (Blyth et al., 1984; Thompson et al., 1986). Following footpad inoculation with HSV-1 KOS, infectious virus has been detected in the feet, sciatic nerve trunk, and lumbosacral ganglia. KOS can be detected in the CNS, but this is limited to the detection of small amounts of virus in the spinal cord that is cleared before day four p.i. (Thompson et al., 1986). Although traditional plaques assays can be extremely sensitive, stochastic variation means that they may not be able to detect low levels of infectious virus reliably (Margolis et al., 2007a). Therefore, virus spread within the spinal cord is the most probable explanation for the detection of β-gal marked cells in distal DRG.

Not all immediate early promoters used in this thesis resulted in a similar trend in historical expression in ROSA26R mice. When the ICP47 promoter was used to regulate the expression of *cre* in ROSA26R mice, a substantial population of cells became marked during the course of the acute infection. A surprising and novel finding was that there was a more than threefold increase in the number of β-gal$^+$ cells during the establishment phase of latency, and continued accumulation of marked β-gal$^+$ cells throughout latency. As previously described, this promoter is found in the inverted U_S genomic repeats and so a similar promoter controls expression of both the IE genes U_S1 (encoding ICP22) and U_S12 (encoding ICP47; Barklie Clements et al., 1977; Gelman and Silverstein, 1987; Murchie and McGeoch, 1982). The possible role that ICP47 may play in the establishment of latency will be investigated in greater detail in Chapter 5.

Like ICP47, the multifunctional ICP22 protein has received relatively little attention compared to the other immediate early proteins. ICP22 was initially identified as a viral transactivator for some late genes (Bowman et al., 2009; Long et al., 1999; Rice et al., 1995; Sears et al., 1985). It is not considered essential for virus growth *in vitro* but studies using ICP22 mutant viruses have revealed a replication defect in certain cell lines and mouse models (Orlando et al., 2006b; Sears et al., 1985). ICP22 may regulate late viral gene expression by altering cyclin dependent kinase 1, a critical cell cycle factor, and can also modulate neurovirulence (Advani et al., 2000b; Orlando et al., 2006b; Poffenberger et al., 1994; Sears et al., 1985). ICP22 is also important for regulating host cell functions, such as regulating phosphorylation of RNA polymerase II, which has been hypothesised to suppress transcription of host genes (Bowman et al., 2009; Fraser and Rice, 2005; Rice et al., 1995). It can also cause a relocalisation of host cell chaperones and can change the expression of key cell cycle regulatory proteins (Advani et al., 2000a; Bastian et al., 2010; Orlando et al., 2006a). Mutant viruses lacking ICP22 expression are deficient for reactivation, but this is likely to be caused by a failure to establish wildtype levels of latency due to their replication defect (Orlando et al., 2006b; Poffenberger et al., 1994; Sears et al., 1985). It has been suggested that ICP22 may play an important role in the establishment of latency by repressing viral gene transcription shortly after the infection of primary neurons (Bowman et al., 2009). Therefore, it is possible that this accumulation of β-gal$^+$ cells during the establishment of latency may reflect ICP22 expression that serves to repress viral gene expression and prevent reactivation events, but as yet there is little evidence to support this. Given the limited characterisation of the role of ICP22 *in vivo*, a re-examination of the phenotype of ICP22 mutants, potentially in conjunction with a highly sensitive means of determining the extent of the establishment of latency like the ROSA26R/Cre mouse model, would be advantageous to further illuminate the role of this protein in HSV-1 infection.

The similarity in the number of β-gal$^+$ cells on days 20, 40 and 100 days p.i. in ROSA26R mice infected with HSV-1 pC_eGC and HSV-1 pICP0_eGC suggests that, unless precisely balanced, cells are not being lost during latency, or alternatively, the size of the latent reservoir is not increasing. Therefore, the latent state is extremely stable in this model, and provides further evidence supporting the consensus that spontaneous reactivation does not generally occur in mice (Gebhardt and Halford, 2005; Laycock et al., 1991). However, there was a gradual accumulation of β-gal marked cells in ROSA26R mice infected with HSV-1 pICP6_eGC or HSV-1 pgB_eGC over the course of latency, suggesting that expression under these promoters leading to protein production occurs. At face value, this activity may be attributable to low level spontaneous reactivation, which has been

described previously (Margolis et al., 2007a; Sawtell, 2003; Shimeld et al., 1990; Tullo et al., 1982; Willey et al., 1984). Studies of spontaneous reactivation, as evidenced by the shedding of virus in the tear film of rabbits latently infected with HSV-1 McKrae, revealed that reactivation does not alter the quantity of DNA and expression of LAT in the trigeminal ganglia as measured over 360 days (Hill et al., 1996a). Further, studies using *in vivo* reactivation models, such as transient hyperthermia or UV irradiation of latently infected mice, suggest that very little infectious virus is produced in the ganglia following reactivation (Fawl and Roizman, 1993; Sawtell, 1998; Shimeld et al., 1996a; Shimomura et al., 1985). Therefore, reactivation likely originates from a very small population of neurons, and has little impact on the latent reservoir of virus (Bloom et al., 1994; Sawtell, 2003; Sawtell and Thompson, 1992b; Shimeld et al., 1996b). In addition, the general consensus is that reactivation does not lead to replication and spread of virus to large populations of previously uninfected neurons (Wagner and Bloom, 1997). Finally, the number of β-gal marked neurons did not accumulate in ROSA26R mice infected with HSV-1 pICP0_eGC. Taken together, these considerations suggest that any accumulation of β-gal marked neurons in the ROSA26R/Cre mouse model infected with HSV-1 pICP6_eGC or HSV-1 pgB_eGC is unlikely to reflect spontaneous reactivation leading to the production of infectious virus. As the expression of β-gal in ROSA26R mice is dependent on the activity of functional Cre protein, HSV-1 lytic promoter activity can lead to protein production during latency, albeit at likely at very low levels and/or sporadically in very few cells.

The expression of viral protein during latency is not unprecedented, as there have been at least three reports of the detection of HSV-1 proteins by ISH with polyclonal HSV-1 antisera, and one report of ICP4 expression during latency in mice (Feldman et al., 2002; Green et al., 1981; Margolis et al., 2007a; Sawtell, 2003). Further, there has been a slow accumulation of reports over the last few decades that suggest that lytic gene transcripts, namely transcripts for the ICP4, TK and gC proteins, may be synthesised occasionally during latency as detected using conventional methods like ISH or RT-PCR. However, the detection of ICP6 transcripts has not been attempted (Chen et al., 2002a; Chen et al., 1997; Feldman et al., 2002; Kramer and Coen, 1995; Kramer et al., 1998; Ma et al., 2014; Pesola et al., 2005; Tal-Singer et al., 1997). Further, Derfuss and colleagues (2007) failed to detect gB transcripts by RT-qPCR on single cells isolated by LCM from latently infected human trigeminal ganglia. Despite this, other studies have failed to detect any accumulation of β-gal$^+$ cells in ROSA26R mice infected with viruses where *Cre* is expressed from the *tk* or gC promoters (Proença et al., 2008; Proença et al., 2011). This argues that the presence of detectable transcripts by ISH does not correlate with the accumulation of β-gal marked neurons in latently infected ROSA26R mice. Further, Ma and colleagues (2014) used the

ROSA-YFP mice, which are analogous to the ROSA26R mice used in this thesis, infected with a virus expressing *cre* under the CMV IE promoter to identify every cell latently infected with HSV-1, and combined this with LCM and single-cell qRT-PCR to assess viral gene transcription during latency. They showed that there is low level transcription of HSV-1 lytic genes in two thirds of latently infected cells, although they did not quantify transcript levels within individual cells. Cre mediated recombination is correlated with promoter strength, so this accumulation of β-gal$^+$ cells may simply reflect the amount of gB or ICP6 transcripts generated within the latently infected cell (Araki et al., 1997; Pasparakis, 2007). Therefore, we suggest that these results presented in this thesis reflect the choice of viral promoters used. This is confirmed by the overall similarity in the pattern of accumulation of β-gal marked cells in ROSA26R mice infected with HSV-1 pICP0_eGC (refer to Section 4.2.3), with that of the trend observed by Proença and colleagues (2008) when they employed their virus ICP0 Cre in the ROSA26R model.

The results presented in this chapter provide support for the argument that the retention and activation of CD8$^+$ T cells means that viral antigen, and more specifically gB protein, is present in latently infected mice (Decman et al., 2005a; Divito et al., 2006). The protein gB includes an immunodominant epitope that is recognised by more than 50% of CD8$^+$ T cells during the acute infection, as well as those retained within the DRG of C57Bl/6 mice during latency (Khanna et al., 2003; Sheridan et al., 2006; St. Leger et al., 2013; St. Leger et al., 2011). ICP6 also encodes a number of subdominant epitopes that are recognised by CD8$^+$ T cells, although unlike gB-specific CD8$^+$ T cells retained in the DRG, the ICP6-specific CD8$^+$ cells seem to lose functionality during latency as shown by IFN-γ production (Frank et al., 2010; Khanna et al., 2003; St. Leger et al., 2013; St. Leger et al., 2011). CD8$^+$ T_{RM} cells in the DRG, but not the skin, show signs of continuous antigen stimulation, such as the detection of gzmB (Gebhardt et al., 2009; Khanna et al., 2003; Mintern et al., 2007). Further, van Lint and colleagues (2005) found that the detection of gzmB within gB_{498}-specific CD8$^+$ T cells during latency is dependent upon antigen presentation by cells of the parenchyma, most likely neurons. The findings presented in this thesis provide the first virological evidence that protein can be produced from the gB promoter during latency. Although this antigen is probably expressed at very low levels and sporadically, CD8$^+$ T cells are exquisitely sensitive to antigen and are able to recognize as few as one peptide:MHC-I complex (Purbhoo et al., 2004). Therefore, the low level, likely sporadic, expression of gB antigen is likely to be of a sufficient level to explain the activation of CD8$^+$ T cells. It has been suggested that the primary function of these CD8$^+$ T cells is to prevent reactivation, possibly through an IFN-γ dependent mechanism (Campbell et al., 1984). This has mainly been demonstrated using reactivated *in vitro* cultures of latently infected

TG (Carr et al., 2009; Decman et al., 2005b; Khanna et al., 2003; Liu et al., 2000). Further, Ramachandran and colleagues (2010) examined the effect of delaying the expression of gB on the $CD8^+$ T cell response to HSV-1 by placing gB under the control of the gC promoter. This virus had a replication defect *in vivo*, but by using a low dose for infection with the control rescue virus in which gB is expressed under its native promoter to establish a similar latent viral load, they were able to show that the $CD8^+$ T cell response in the lymph nodes is similar, indicating that priming was not impaired. Interestingly, there ws a significant reduction in the number of activated ($gzmB^+$) $CD8^+$ T cells within the DRG during latency. Proença and colleagues (2008) have shown that gC promoter activity does not result in an accumulation of β-gal marked during latency in ROSA26R mice, unlike that observed for the gB promoter in this chapter. It can be speculated that the low level gB promoter activity observed in the ROSA26R system is important for the retention of activated gB-specific $CD8^+$ T cells within the ganglia. These $CD8^+$ T cells may engage neurons expressing significant levels of ICP6 or gB, suppressing reactivation and subsequent cell death, which serves to increase the population of cells in ROSA26R mice that become β-gal marked during latency.

One disadvantage of this system is that it is impossible to reveal subsequent promoter activity within an already infected, β-gal marked cell. As such, it is possible that promoter activity as inferred from the accumulation of β-gal marked cells in the ROSA26R/Cre mouse system is underestimated, and may explain why there is no accumulation of β-gal marked cells during latency in ROSA26R mice infected with HSV-1 pICP0_eGC. However, the accumulation of β-gal marked cells during latency in ROSA26R mice infected with HSV-1 pICP6_eGC or HSV-1 pgB_eGC, as well as the comparable virus that utilises an immediate early promoter, HSV-1 pICP47_eGC (refer to Section 5.2.1), argues against this. None-the-less, an alternative strategy to overcome this would be to use an inducible Cre system. In these systems, Cre is been fused to mutated hormone-binding domains of the estrogen receptor (CreER; Metzger et al., 1995). CreER is inactive until the synthetic ligand 4-hydroxytamoxifen (OHT) is provided. Then, CreER is able to localise to the nucleus and mediate *loxP* recombination in ROSA26R mice, allowing for expression of β-gal (Feil et al., 1996; Feil et al., 1997; Metzger et al., 1995; Soriano, 1999). CreER could be placed under the control of the ICP0 promoter expressed from HSV-1, and if OHT is not administered until after the resolution of the acute infection, then the ICP0 promoter-dependent marking of cells during latency can be dissected from that which occurs during the primary lytic infection.

It is often assumed that genes within the same class of viral gene expression will be expressed with similar kinetics, but this is likely to be an oversimplification (Harkness et

al., 2014). For example, transcripts accumulate to different levels based on infection *in vitro* using MRC5 and HeLa cells as well as primary adult TG neuronal cultures (Harkness et al., 2014; Stingley et al., 2000). It has even been suggested that the early and late classes of viral gene expression should not really be considered to be distinct as in reality they exist as a biological continuum. In particular, the distinction between different classes of viral genes may not be clear during latency due to the almost global suppression of viral lytic gene expression (Pellet and Roizman, 2013). The suppression of lytic viral gene expression is principally mediated by the prevention of transcription through chromatin control of the genome, with some contribution to regulation by miRNAs and other LAT encoded RNAs (Knipe and Cliffe, 2008; Kramer et al., 2011; Peng et al., 2008; Shen et al., 2009; Umbach et al., 2008). The genes encoding ICP6 and gB are located in the U_L region of the genome that is broadly associated with repressive heterochromatin, with metH3K9 and metH3K27, although this exists in balance across the genome (Cliffe et al., 2009; Deshmane and Fraser, 1989; Kwiatkowski et al., 2009; Wang et al., 2005b). It is also possible that miRNAs are able to prevent the expression of specific viral proteins. For example, the miR-H2-3p is expressed in latency and is able to mediate a reduction of ICP0 protein, but not transcripts (Umbach et al., 2008). However, to date, no miRNA has been identified that is able to inhibit ICP6 or gB expression (Cui et al., 2006; Jurak et al., 2010; Munson and Burch, 2012; Umbach et al., 2009). It is also probable that other mammalian post-transcriptional control mechanisms are co-opted to regulate the expression of different viral genes. However, beyond the role of the viral protein ICP27 in the area of post transcriptional regulation (as reviewed by Sandri-Goldin, 2011), such as the regulation of translation of VP16 (Ellison et al., 2005), the post-transcriptional regulation of HSV-1 gene expression remains an underexplored area (Weir, 2001).

Another caveat to the interpretation of the results presented in this chapter is that RNA structure within the coding sequence might regulate translation of viral proteins. This layer of regulation will be lost when the promoter sequence is used to direct expression of an alternate gene, namely *eGFP/Cre*. Such an issue would be compounded by the use of an ectopic location for the insertion of *eGFP/Cre.* All viruses constructed in this thesis that express *eGFP/Cre* under the control of a lytic gene promoter used the U_L3/U_L4 intergenic location without the disruption of any genes. By contrast, the viruses used by Proença and colleagues (2008; 2011) contained disruptions of the gene encoding U_S5, which is required for maximal inhibition of the cell's apoptosis machinery as well as the modulation of other cellular processes (Aubert et al., 2008; Jerome et al., 2001; Jerome et al., 1999). However, insertions into the U_S5 location do not alter virus growth *in vitro* or *in vivo*, or the establishment of latency, and to a certain extent U_S5 exhibits functional redundancy with

other HSV-1 proteins (Aubert et al., 2006; Balan et al., 1994; Roizman and Whitley, 2001; Zhou et al., 2000a). Further, the accumulation of β-gal marked cells in ROSA26R mice infected with CMV Cre and ICP0 Cre observed by Proença and colleagues (2008; 2011) is similar to that of the viruses HSV-1 pC_eGC and HSV-1 pICP0_eGC as described in this thesis.

The frequency of Cre mediated recombination *in vitro* is correlated with promoter activity (Araki et al., 1997). Therefore, the promoter sequences used were based on published *in vitro* deletion based analysis using CAT plasmids to identify the maximal promoter, while still maintaining correct temporal expression (Desai et al., 1993; Pederson et al., 1992; Preston et al., 1984; Summers and Leib, 2002). However, repressive elements associated with each promoter may not have been included in the modified version inserted into the ectopic locus. In particular, there is cluster of binding motifs for the CTCF protein located between the ICP47 promoter and U_S12, and another downstream of U_S10 (Amelio et al., 2006b), but this motif was not included in the ICP47 promoter used in this thesis. These motifs become enriched with the CTCF protein during latency, having enhancer blocking and silencing activities and acting as a barrier between the transcriptionally permissive LAT region and the remainder of the HSV-1 genome (Amelio et al., 2006b). Therefore, it cannot be ruled out that the insertion of the ICP47 promoter in the potentially more repressive U_L3/U_L4 region may alter the expression kinetics relative to the native promoter. However, it seems paradoxical that this would account for the striking accumulation of β-gal$^+$ cells during the establishment of latency in ROSA26R mice infected with HSV-1 pICP47_eGC.

The viruses used in this thesis were constructed on the relatively avirulent KOS genetic background, as opposed to the more virulent SC16 strain of HSV-1 used by Proença and colleagues (Blyth et al., 1984; Dix et al., 1983; Hill et al., 1975; Proença et al., 2008). The most cited difference between HSV-1 strains is that the virulence of different strains of HSV-1 correlates with an increased frequency of reactivation in mice as measuring using induced *in vivo* reactivation models, and a higher genome copy number per neuron (Sawtell et al., 1998; Sawtell and Thompson, 1992b; Strelow et al., 1994; Thompson et al., 1986). SC16 is substantially more neurovirulent than KOS, and some mice may die as a result of acute infection (Blyth et al., 1984), which may shape the latent viral reservoir in the surviving mice. However, both SC16 and KOS are able to efficiently establish latency in both mice and rabbits, and both exhibit a low rate of virus shedding following adrenergic induction of reactivation in latently infected rabbits (Blyth et al., 1984; Hill et al., 1987). Further, both the HSV-1 KOS and SC16 strains are considered to be low phenotypic reactivators (Hill et al., 1987; Toma et al., 2008; Webre et al., 2012). Therefore, it is

difficult to determine how the use of different HSV-1 strains would account for the differences in protein expression inferred using the ROSA26R model.

A different method and route of infection was used in this thesis compared to that utilised by Proença and colleagues (2008). HSV-1, and in particular HSV-1 LAT deletion mutants, can behave differently following infection via different routes with latency established in either the TG or DRG (Nicoll et al., 2012; Sawtell and Thompson, 1992a). Moreover, HSV-1 and HSV-2 show a preference for establishment in different neuronal subtypes following ocular infection of mice, namely $A5^+$ and $KH10^+$ neurons respectively, indicating that HSV may behave differently in sensory ganglia at different anatomical sites (Margolis et al., 2007b). The site of latency establishment is unlikely to account for differences in cell marking observed in this thesis relative to that published by Proença and colleagues (2008; 2011), as latency was established in a similar site, namely the cervical ganglia versus the DRG. Further, they found that there was no difference in the trend of cell marking of latently neurons with HSV-1 expressing Cre under the control of the CMV IE, VP16 or ICP0 promoters when mice were inoculated by scarification of the ear, leading to latency establishment in the DRG, or whisker-pad, leading to latency establishment in the TG (Proença et al., 2011).

The trend in the accumulation of $\beta\text{-gal}^+$ cells in ROSA26R mice infected with HSV-1 expressing Cre from an IRES in the LAT locus was very different to that observed by Proença and colleagues (2008) when they examined the accumulation of β-gal marked neurons in ROSA26R mice infected with HSV LAT Cre. The number of $\beta\text{-gal}^+$ cells in ROSA26R mice infected with HSV-1 pLAT_eGC at 10 days p.i. was comparable to that of those mice infected with HSV-1 pC_eGC, and remained stable throughout latency (refer to Section 4.2.3 and 4.5). As such, at 100 days p.i., more than twice as many cells were β-gal marked when ROSA26R mice were infected with HSV-1 pLAT_eGC compared to HSV-1 pC_eGC. At first, this may be taken to suggest that the CMV IE promoter is not expressed in all infected cells prior to the establishment of latency and so may not mark the entire population of latently infected cells. However, the CMV IE promoter has been shown to be expressed in a constitutive manner in all cells infected with HSV-1 in a primary neuronal culture model of latency (Arthur et al., 2001). Further, Proença and colleagues observed a slow accumulation of β-gal marked neurons between days five and 30 p.i. in ROSA26R mice infected with HSV LAT Cre, which stabilised thereafter. Therefore, it is more likely that HSV-1 pLAT_eGC has an unanticipated genomic alteration that is causing the observed phenotype. To determine if this is the case, a revertant virus should be constructed.

It is difficult to introduce any foreign transgenes into the LAT region of HSV-1 without disrupting any coding or regulatory regions (Bolovan et al., 1994; Jaber et al., 2009; Lagunoff and Roizman, 1994; Perng et al., 1996a; Perng et al., 1995; Wagner et al., 1988a). Such disruptions may impact on the stability of latency, enabling the virus to spread and increase the number of infected cells, even during latency. It has been demonstrated that even a small decrease in the viral genome copy number per cell in mice infected with HSV-1 LAT mutants can alter their reactivation phenotype, and so may alter the efficiency of cell marking in ROSA26R mice (Devi-Rao et al., 1994; Maggioncalda et al., 1996; Perng et al., 2000a; Sawtell and Thompson, 1992a). Therefore, the viral genome copy number by qPCR during latency should be used to confirm that the latent reservoir was similar to wildtype virus. Given that the spread of virus to different sensory ganglia appears greater following infection with HSV-1 pLAT_eGC compared to HSV-1 pC_eGC, it would be of interest to examine this on a per ganglion basis. This could also be paired with an examination of the ability of HSV-1 pLAT_eGC to reactivate to produce infectious virus based on the spinal level of the ganglion. Finally, a virus in which Cre is under the control of the CMV IE promoter from the same location of the genome within the LATs could be used to directly compare the accumulation of marked β-gal$^+$ cells in ROSA26R mice during latency.

In summary, in this chapter the accumulation of β-gal marked cells in ROSA26R mice infected with HSV-1 expressing Cre as dictated by different promoters was characterised. This revealed that the establishment of latency is characterised by a period of slow spread of virus. It was also found that lytic promoter activity can lead to protein expression during latency, suggesting that some lytic proteins may be expressed during latency. The pattern of β-gal$^+$ cell accumulation in ROSA26R mice infected with HSV-1 expressing Cre under the ICP47/22 promoter was starkly different from that previously observed, and qualitatively appeared similar to that of LAT, than other lytic gene promoters. This intriguing finding will be investigated in more detail in chapter 5.

5 | An analysis of the expression of ICP47 during latency establishment and maintenance: a role for viral immune evasion and the $CD8^+$ T cell response during the establishment of latency

5.1 Introduction

The pattern of accumulation of marked β-gal$^+$ cells during the establishment of latency was starkly different in ROSA26R mice infected with HSV-1 pICP47_eGC compared to other HSV-1 lytic promoters (refer to Section 4.4). This indicates that ICP47 and ICP22 may be more highly expressed during the establishment of latency. ICP47 is unique as it is encoded by the only immediate early gene that does not act as a transactivator of viral gene expression (DeLuca and Schaffer, 1985; Dixon and Schaffer, 1980; Everett, 1984; O'Hare and Hayward, 1985; Smith et al., 1993). Instead, it has only one known function, which is to inhibit the transporter associated with antigen presentation (TAP), and so hamper the host's CD8$^+$ T cell response to HSV-1 (Früh et al., 1995; Goldsmith et al., 1998; Hill et al., 1995; Orr et al., 2007; York et al., 1994). While not discounting a possible role for ICP22 expression during the establishment of latency, this chapter will focus on ICP47 and its role in evasion of the CD8$^+$ T cell response during HSV-1 infection.

CD8$^+$ T cells form an important part of the host's immune response to many pathogens, including HSV-1 (as described in Sections 1.1.5 and 1.3.6). CD8$^+$ T cells recognize short peptides that are presented on the cell surface by MHC-I, via an interaction with its TCR (Bjorkman et al., 1987). There are two main pathways by which peptides are presented on MHC-I, namely direct and cross presentation. In direct presentation, these peptides are derived from intracellular proteins, including virus-derived proteins, which are processed endogenously with cells. Antigens are first cleaved into shorter fragments, a process that occurs mainly by proteasomes (Bennink et al., 1984; Gooding and O'Connell, 1983; Niedermann et al., 1995; Rock et al., 1994; Townsend et al., 1989). The peptides generated are transported into the endoplasmic reticulum by TAP, where they bind partially assembled MHC-I molecules associated with β_2-microglobulin, with the aid of several accessory proteins (Antoniou et al., 2002; Bahram et al., 1991; Gao et al., 2002; Ortmann et al., 1997; Peterson et al., 1974). The peptide:MHC-I complex is then transported to the cell surface (Figure 5-1; Cox et al., 1990; Grey et al., 1973; Jackson et al., 1994; Nuchtern et al., 1989; Peterson et al., 1974; Yewdell and Bennink, 1989). Alternatively, some cell types, predominantly dendritic cell subsets, are able to present exogenous proteins that are acquired through the endocytic pathway on their MHC-I, a process known as cross presentation (Bevan, 1976a; Bevan, 1976b; Heath et al., 1998; Joffre et al., 2012; Jung et al., 2002; Kurts et al., 2001).

Naïve CD8$^+$ T cells circulate within the host, and in the case of an infection, become primed (or activated), a process that mainly occurs within the secondary lymphoid organs such as the lymph nodes (Mueller et al., 2002). Priming occurs when naïve CD8$^+$ T cells encounter

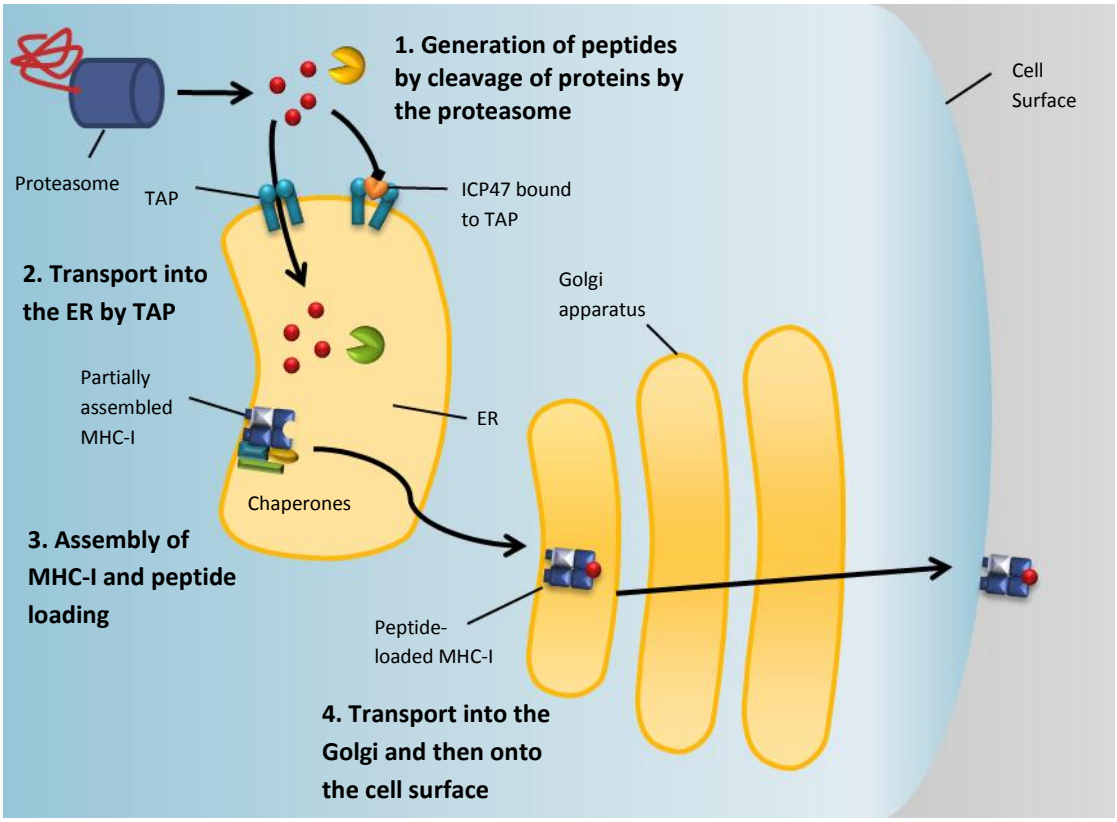

Figure 5-1. Basic overview of antigen presentation. 1. The proteasome cleaves cytosolic proteins to produce polypeptides, which may be trimmed further in the cytoplasm. 2. Polypeptides are transported into the ER by TAP. Alternatively, ICP47 may bind to TAP, preventing the transport of peptides into the ER. 3. Partially assembled MHC-I molecules in ER will bind peptide, stabilising the MHC-I, with the aid of a number of chaperones. 4. The peptide-loaded MHC-I molecules are transported through the Golgi apparatus and to the cell surface.

activated professional antigen presenting cells (APCs), such as dendritic cells, displaying the appropriate peptide:MHC-I complex. Priming also requires costimulatory signals to promote the survival, acquisition of function and expansion of the $CD8^+$ T cell population (Curtsinger et al., 2005; Thompson et al., 1989). HSV-1 can infect APCs, but only poorly, so cross presentation is the primary means by which HSV-1 antigens are presented by professional APCs to $CD8^+$ T cells to prime them following infection (Bosnjak et al., 2005; Jirmo et al., 2009; Mueller et al., 2002). The primed $CD8^+$ T cells are able to differentiate and expand into effector cells, and then migrate to the site of infection where they can recognise virus infected cells. Primed $CD8^+$ T cells then typically either kill the infected cells directly or secrete antiviral factors like cytokines (Huang et al., 1993b; Kägi et al., 1994; Lowin et al., 1994; Morris et al., 1982; Slifka and Whitton, 2000; Zinkernagel and Doherty, 1974).

ICP47 inhibits endogenous presentation on MHC-I by binding directly to the TAP1/2 heterodimer, preventing the loading of peptides onto MHC-I (Figure 5-1; Ahn et al., 1996; Früh et al., 1995; Galocha et al., 1997; Hill et al., 1995; Tomazin et al., 1996). This leads to a reduction in the lysis of fibroblast cells by $CD8^+$ T cells *in vitro* (York et al., 1994). However, ICP47 has a low affinity for murine TAP, and peptide transport in these cells is not substantially inhibited (Ahn et al., 1996; Tomazin et al., 1996). ICP47 does this by binding to TAP, blocking the ATP hydrolysis of the nucleotide binding domain of TAP, likely locking TAP in the inward facing conformation (Chen et al., 2003; Lacaille and Androlewicz, 1998; Verweij et al., 2015). This limits the availability of peptides in the ER to load onto MHC-I, and hence results in the retention of MHC-I within the ER (York et al., 1994). Functionally, the poor binding of ICP47 to mouse, but not human, TAP can be correlated with the relative resistance of HSV-1 infected mouse, but not human, fibroblasts to cytotoxic T cells (Koelle et al., 1993; Pfizenmaier et al., 1977; Posavad and Rosenthal, 1992; Tigges et al., 1996; York et al., 1994). While the usefulness of mouse models of HSV-1 to study ICP47 is limited, it has been found that viruses that lack ICP47 expression are still able to replicate *in vivo* but are less neurovirulent, a phenotype that is dependent on the presence of $CD8^+$ T cells (Goldsmith et al., 1998).

Overall, ICP47 is a critical immune evasion molecule, helping the virus to subvert the host's $CD8^+$ T cell response. The aim of this chapter is to further investigate the expression of ICP47 during latency using the ROSA26R/Cre mouse model. Then, results are presented that confirm that the continued accumulation of $\beta\text{-gal}^+$ cells during the establishment of latency in ROSA26R mice infected with HSV-1 pICP47_eGC is likely due to bona fide expression of ICP47. Finally, a method of increasing antigen presentation on MHC-I in an

effort to overwhelm ICP47 mediated inhibition of the $CD8^+$ T cell response will be used to further investigate the role of ICP47 during HSV-1 latency establishment.

5.2 Continued historical marking of neurons by expression of Cre from the ICP47/22 promoter in ROSA26R mice infected with HSV-1

5.2.1 Further characterisation of historical marking under the ICP47/22 promoter in ROSA26R mice

As described in Chapter four, historical activity of the ICP47/22 promoter in ROSA26R mice was strikingly different from that observed when other lytic promoters were used in the ROSA26R/Cre system. Notably, there was continued activity under this promoter beyond the resolution of the acute infection, as defined by conventional means, and into the establishment of latency. Such a broad time course may fail to detect peak in the β-gal marking of cells, masking the more subtle variations in ICP47 promoter activity that may occur. Therefore, a more comprehensive analysis of the accumulation of β-gal marked cells in ROSA26R mice infected with HSV-1 pICP47_eGC was performed, focusing on the establishment phase of latency.

Groups of ROSA26R mice were infected with HSV-1 pICP47_eGC. They were culled at 5, 10, 30 and 40 days p.i., as well as at three day intervals from 15 to 21 days p.i. The β-gal marking of cells was measured as previously described (Figure 5-2). This analysis of the historic marking of cells in mice infected with HSV-1 pICP47_eGC revealed a gradual accumulation of marked $\beta\text{-gal}^+$ cells during the establishment of latency that largely plateaued by day 24 p.i. There was no peak in the number of β-gal marked cells during the lytic infection. The historic marking of such a large number of β-gal cells marked is inconsistent with the sporadic dysregulated viral gene expression that has been reported to occur after the acute infection has resolved, as discussed in Section 4.6, and to date is limited to this lytic promoter. Additionally, the number of DRG containing at least one β-gal marked cell increased until day 15 p.i., and then plateaued thereafter. This is likely to reflect the continued spread of virus beyond the acute infection that was described in Chapter 4.

Given the accumulation in $\beta\text{-gal}^+$ cells during the establishment of latency, it was of interest to determine if the β-gal marking of cells continued once latency was stably established. Therefore, groups of ROSA26R mice were infected with HSV-1 pICP47_eGC and culled at 10, 20 and 100 days p.i. The expression of β-gal was then assessed in the

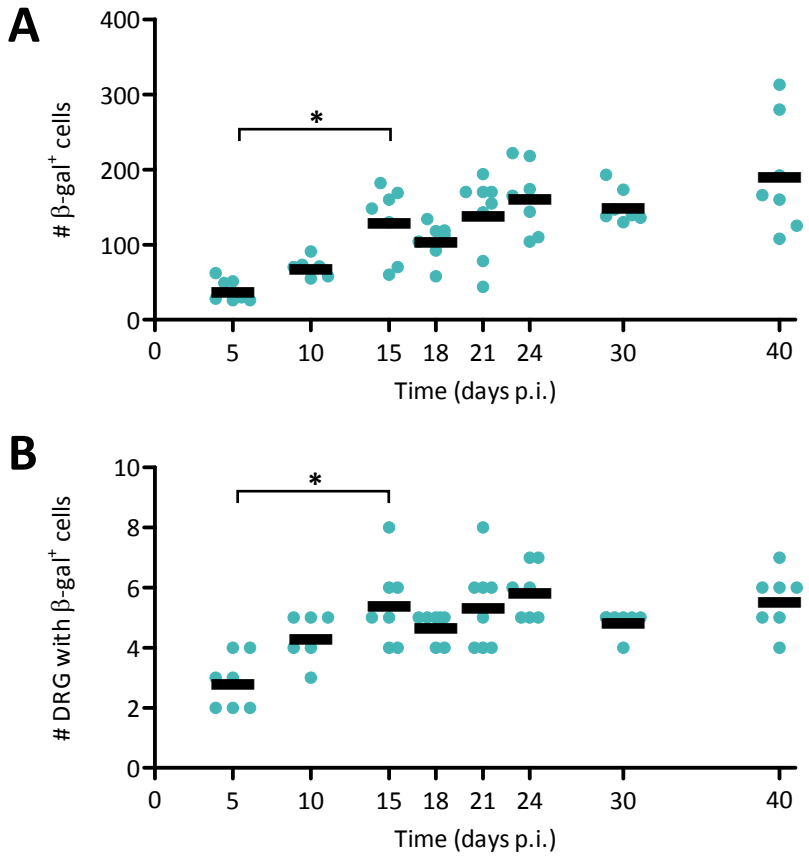

C

Pairwise comparisons from (A)							
Day	5	10	15	18	21	24	30
10	ns						
15	*	ns					
18	ns	ns	ns				
21	*	ns	ns	ns			
24	*	*	ns	ns	ns		
30	*	*	ns	ns	ns	ns	
40	*	*	ns	*	ns	ns	ns

D

Pairwise comparisons from (B)							
Day	5	10	15	18	21	24	30
10	ns						
15	*	ns					
18	*	ns	ns				
21	*	ns	ns	ns			
24	*	ns	ns	ns	ns		
30	*	ns	ns	ns	ns	ns	
40	*	ns	ns	ns	ns	ns	ns

Figure 5-2. Gradual accumulation of β-gal marked cells during the establishment of latency in ROSA26R mice infected with HSV-1 pICP47_eGC. Groups of three to five ROSA26R mice were infected with 1×10^8 PFU/mL HSV-1 pICP47_eGC. At the indicated days p.i. mice were culled and the DRG (from spinal levels T5 to L1) were removed and processed for determination of β-gal activity. Both (A) the total number of β-gal+ cells per mouse and (B) the number of DRG per mouse containing at least one β-gal+ cell are shown. Each circle represents one mouse and the black bar represents the mean value for all mice at each time point. The results are pooled from two independent experiments (n = 6 – 8 per time point). (C&D) Statistical significance was determined by a one way ANOVA ($p < 0.001$) with Bonferroni's post-test to make pairwise comparisons, with key statistical differences indicated on (A) and (B) (*$p < 0.05$).

DRG. There was a statistically significant increase in the number of β-gal+ cells during the establishment of latency between days 10 to 20 p.i. (Figure 5-3). Further, there was also a statistically significant increase in the number of β-gal+ cells throughout latency (i.e. between days 20 and 100 post infection). This confirmed the results presented in Figure 4-17 that suggested the accumulation of β-gal+ cells during latency in ROSA26R mice infected with HSV-1 pICP47_eGC. There was also a minor, but statistically significant, increase in the spread of virus between days 10 and 100 p.i. as shown by the number of DRG with at least one β-gal+ cell. This increase probably reflects expression of ICP47 during latency in cells that had become infected during the period of the acute infection but did not experience ICP47 expression, rather than reactivation and infection of new cells during latency. If reactivation was responsible for the accumulation of β-gal marked cells in ROSA26R mice infected with HSV-1 pICP47_eGC, then the number of β-gal marked cells in ROSA26R mice infected with HSV-1 pC_eGC or HSV-1 pICP0_eGC should increase during latency.

Overall, the accumulation of β-gal marked cells, particularly during the establishment phase of latency, in ROSA26R mice infected with HSV-1 pICP47_eGC is starkly different to every lytic HSV-1 promoter studied to date (refer to Chapter 4; Proença et al., 2008; Proença et al., 2011). In qualitative terms, it most closely correspond to that the activity of the LAT promoter as described by Proença and colleagues, and suggests that this promoter may be regulated in a manner that is unlike other HSV-1 lytic gene promoters. Based on the current paradigm of a largely global repression of viral protein synthesis during latency, and a historic failure to detect such protein expression at a substantial level, it seems reasonable to speculate that this ICP47 expression is likely transient and at a low level (Croen et al., 1988; Deatly et al., 1987; Devi-Rao et al., 1994; Krause et al., 1988; Mitchell et al., 1994; Puga and Notkins, 1987; Speck and Simmons, 1991; Spivack and Fraser, 1987; Steiner et al., 1988; Stevens et al., 1987).

5.3 Verification of the behaviour of the ICP47/22 promoter as a lytic promoter in ROSA26R mice

In this thesis, the expression of Cre in HSV-1 pICP47_eGC was from an ectopic locus using a modified ICP47/22 promoter. It was believed that expression under this promoter would be similar to that of native ICP47 protein, although this assumption may be erroneous. In particular, there are regulatory elements found in the U_S region of the HSV-1 genome, such as CTCF domains, and while these are not primarily responsible for regulating

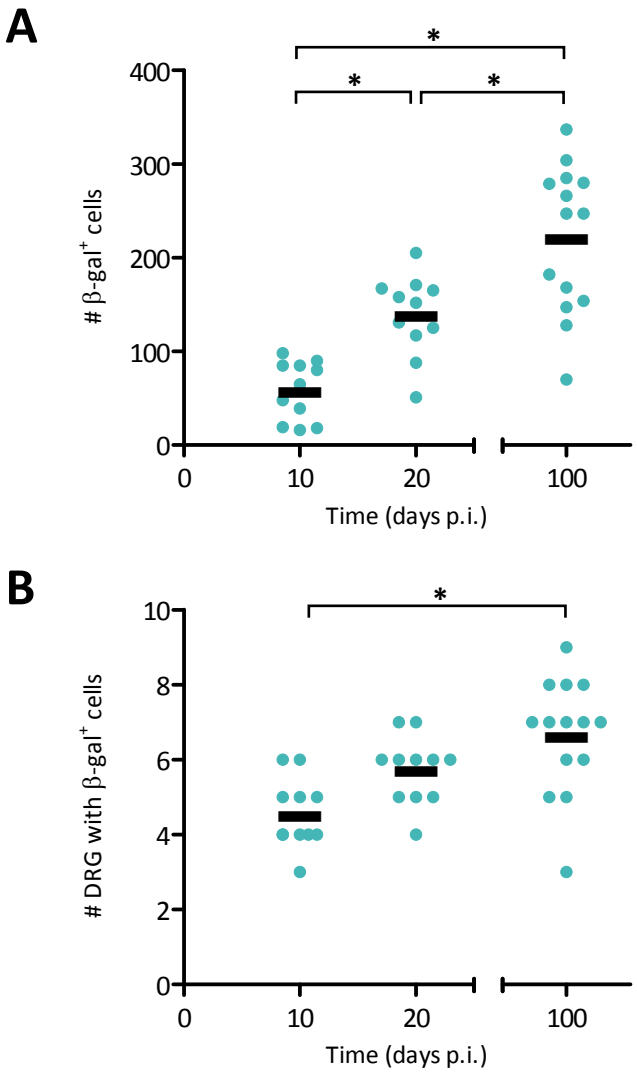

Figure 5-3. Continued accumulation of β-gal marked cells in ROSA26R mice infected with HSV-1 pICP47_eGC in which latency has been stably established. Groups of three to six ROSA26R mice were infected with 1×10^8 PFU/mL HSV-1 pICP47_eGC. At 10, 20 or 100 days p.i. mice were culled and the DRG (from spinal levels T5 to L1) were removed and processed for determination of β-gal activity. Both (A) the total number of β-gal$^+$ cells per mouse and (B) the number of DRG per mouse containing at least one β-gal$^+$ cell are shown. Each circle represents one mouse and the black bar represents the mean value for all mice at each time point. The results are pooled from three independent experiments (n = 11 – 14 per time point). Statistical significance was determined by a one way ANOVA ($p < 0.001$) with Bonferroni's post-test to make pairwise comparisons (*$p < 0.05$).

transcription of U_S12 during the lytic infection, they likely play some role in expression during latency (refer to Section 4.6; Amelio et al., 2006b). Ideally then, it would be desirable to be able to directly detect ICP47 protein during the establishment or maintenance phases of latency. Recent studies that detect rare viral protein expression during latency or following induced reactivation have relied upon the use of immunohistochemical staining of serial sections (Feldman et al., 2002; Green et al., 1981; Margolis et al., 2007a; Sawtell, 2003; Sawtell and Thompson, 1992a, b). ISH for the detection of ICP47 RNA could also be performed. ISH is an exquisitely sensitive method that has previously been exploited to detect rare lytic transcripts within latently infected ganglia (Carter et al., 2010; Feldman et al., 2002; Femino et al., 1998; Maillet et al., 2006). However, all of these methods rely on the detection of ICP47 expression at the point of measurement, and so will be confounded by an intermittent expression profile. This will be exacerbated by stochastic variation associated with the small population of neurons that is potentially infected and expressing ICP47 at any point in time (Kaern et al., 2005; Marinov et al., 2014). It is probable that even if these methods were employed they may fail to detect transient/low level ICP47 expression, and may still prove inconclusive. So, for the purposes of this thesis it was decided that the focus would be on verifying that the modified ICP47 promoter inserted into the ectopic locus is able to faithfully model ICP47 expression *in vivo*.

5.3.1 A failure to properly establish latency cannot account for the accumulation of β-gal marked cells in ROSA26R mice infected with HSV-1 pICP47_eGC

It is possible that the continued accumulation of β-gal$^+$ cells in ROSA26R mice infected with HSV-1 could be due to a failure to establish or maintain latency. To confirm that latency is established in this system, groups of ROSA26R mice were infected with HSV-1 pICP47_eGC. The mice were then culled at four days p.i., at the peak of the acute infection, as well at 20 and 40 days p.i., by which time a latent infection should be established. The amount of infectious virus in the DRG was then assessed by standard plaque assay using the homogenised tissue. As shown in Figure 5-4, infectious virus was detectable at four days p.i. The amount of virus detected at this time was similar to that detected in ROSA26R mice infected with HSV-1 pC_eGC and is comparable with that previously reported in the literature (see Figure 4-3; Van Lint et al., 2004). Further, infectious virus was undetectable at 20 and 40 days p.i. This confirms that, at least operationally, latency is established in ROSA26R mice infected with HSV-1 pICP47_eGC as would be expected.

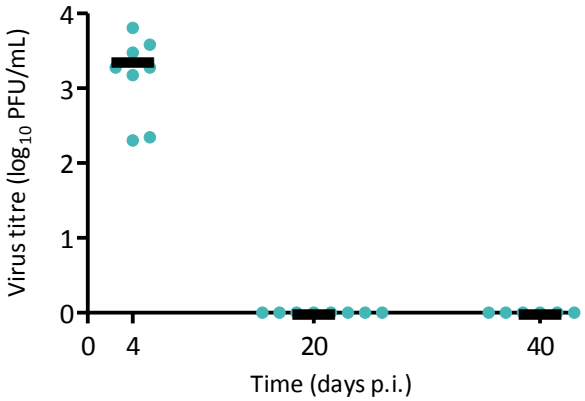

Figure 5-4. Infectious HSV-1 pICP47_eGC virus is undetectable during latency. Groups of four C57Bl/6 mice were infected with 1×10^8 PFU/mL HSV-1 pICP47_eGC. At 4, 20 or 40 days p.i. mice were culled and innervating DRG (from spinal levels T5 to L1) removed and infectious virus determined by standard plaque assay. Circles show results for each mouse and bars mean±SEM, and data are pooled from two independent experiments (n = 8 per time point). The limit of detection was two PFU per mouse.

5.3.2 Correlation of ICP47 and Cre expression by RT-qPCR in mice infected with HSV-1 pICP47_eGC

One way of confirming that native and ectopic ICP47 promoters regulate gene expression in a similar temporal manner is to correlate the expression of the native ICP47 transcripts with eGFP/Cre transcripts, which are expressed from the ectopic ICP47 promoter. A fluorescence based RT-qPCR assay is one of the most widely used methods for detecting even low copy number transcripts in a range of biological settings. Therefore, a qRT-PCR based assay was developed to quantify the levels of ICP47 and eGFP/Cre transcripts within the DRG of HSV-1 infected mice. These assays were designed to conform to the minimum information for the publication of quantitative PCR experiments guidelines (Bustin, 2010; Bustin et al., 2009).

5.3.2.1 Design of a RT-qPCR assay for detection of ICP47 and Cre transcripts within HSV-1 infected DRG

There are two principle methods of quantification of RNA transcripts – absolute, in which the number of transcripts is determined in relation to a specific unit, and relative quantification, where the expression of a transcript of interest is expressed relative to a reference gene. Relative quantification is a more commonly used method due to the comparative ease of assay development. However, in the context of monitoring viral gene expression over time, relative quantification is not ideal as it is difficult to demonstrate the absence of a given transcript. When the amount of mRNA is such that it is just above the limit of a threshold of detection, reproducibility can become an issue and when expressed as fold change it can lead to misleading results (Mackay, 2004; Mackay et al., 2002). Given these potential pitfalls, it was decided that an approach based on the absolute quantification of viral DNA would be used to quantify viral transcript levels *in vivo*.

A hydrolysis probe-based qPCR method was chosen due to its potential for high specificity and sensitivity (Broberg et al., 2003). Many conventional reference genes, such as β-actin or GAPDH, can vary widely in expression, and so are unsuitable for use (Dheda et al., 2004; Radonić et al., 2004; Tricarico et al., 2002). Pertinently, both GAPDH and β-actin mRNA levels decrease within cells as HSV-1 infection progresses (Greco et al., 1997). Additionally, there is an influx of inflammatory and other immune cells into the site of infection that changes throughout the course of infection (Liu et al., 1996; Shimeld et al., 1995), which would be expected to alter certain transcript levels (Kodukula et al., 1999). It was reasoned that since infected neurons in which the virus would be expected to modulate gene expression make up a very small population within a DRG, a neuron-specific reference gene would be an appropriate choice. Therefore, the highly specific

neuronal marker *Rbfox3*, more commonly known as *NeuN*, was chosen for use as a reference gene (Kim et al., 2009; Mullen et al., 1992).

An experiment was performed to validate that the ICP47 or Cre assay can be duplexed with the *Rbfox3* assay without affecting the reaction efficiency. A standard curve was constructed using cDNA synthesised based on RNA isolated from mice infected with HSV-1 pICP47_eGC four days previously. Reactions were performed either singly or were duplexed, and for each reaction the C_T values of each dilution were plotted against the log of dilution factor (Figure 5-5). The efficiency of each reaction was calculated based on the slope of the linear regression line, with the results summarised in Table 5-1. In all cases, the R^2 values were greater than 0.99. For both the ICP47 and Cre assays the reaction efficiency ranged between 95 and 99%, whether it was performed singly or duplexed. Although the efficiency of the *Rbfox3* assay was less than the conventionally accepted 90%, the amplification efficiency was similar when this assay was duplexed or performed singly. A titration of the amount of the premixed assay used, or in other words changing the amount of primer and probe, did not alter the efficiency of this assay (data not shown). Given that in this context the purpose of the *Rbfox3* reference gene is primarily to control for the normalisation of sample input, the reaction efficiency was deemed sufficient for the purposes required. Overall, it was concluded that it is valid to duplex either of these assays with the reference gene *Rbfox3*, which in turn can be used to normalise the levels of input RNA used in these assays.

Reaction	R^2 value	Gradient	Reaction efficiency (%)
Cre only	0.996	-3.36±0.063	98.4±2.62
Cre and NeuN duplexed (Cre detection)	0.999	-3.42±0.033	96.0±1.29
Cre and NeuN duplexed (NeuN detection)	0.998	-3.81±0.047	83.0±1.39
NeuN only	0.991	-3.90±0.10	80.5±0.27
ICP47 and NeuN duplexed (NeuN detection)	0.997	-3.71±0.073	86.0±2.33
ICP47 and NeuN duplexed (ICP47 detection)	0.997	-3.44±0.054	95.3±2.10
ICP47 only	0.990	-3.38±0.093	97.6±3.85

Table 5-1. Assessment of reaction efficiency when duplexing reactions. Summary of results of standard curve assessing the reaction efficiency when duplexing ICP47 and NeuN or Cre and NeuN as shown in Figure 5-5. The R^2 value, gradient of the standard curve and reaction efficiency is shown.

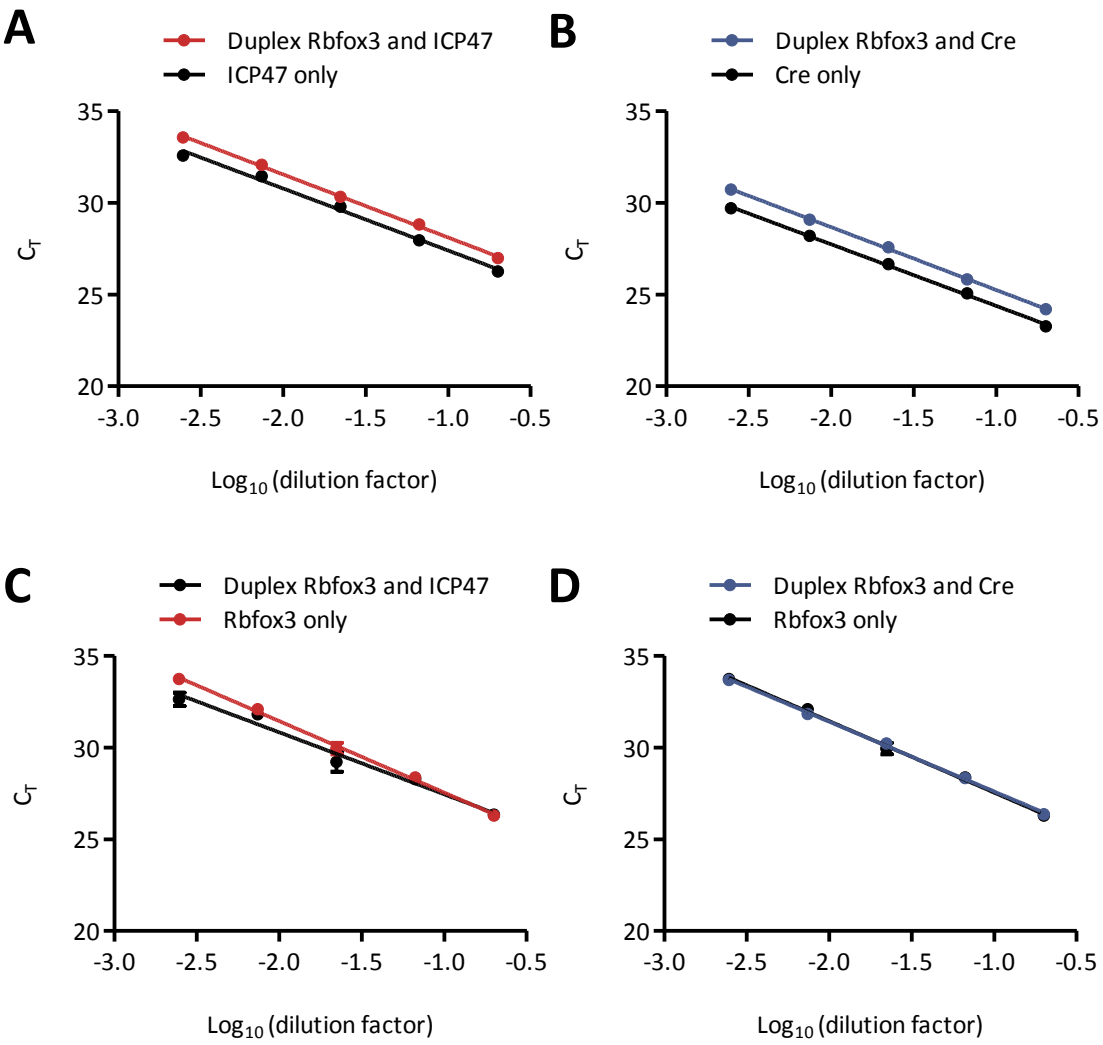

Figure 5-5. Assessment of reaction efficiency when duplexing ICP47 or Cre assays with the reference *Rbfox3* assay. Four C57Bl/6 mice were infected with 1×10^8 PFU/mL HSV-1 pICP47_eGC and at five days p.i. mice were culled, and the innervating DRG (spinal levels T8 to T13) were removed and snap frozen. RNA was extracted and cDNA synthesis performed. Five three-fold serial dilutions of cDNA were used to construct the standard curve. A qPCR reaction was performed to assess the reaction efficiency when reactions were either performed singly or duplexing assays. Each reaction was performed in triplicate with mean±SEM shown and a least square linear regression performed using C_T values from each dilution. (A) Assessment of reaction efficiency by qPCR for detection of Cre only, NeuN only or duplexing Cre and NeuN (C_T values for Cre shown). (B) Assessment of reaction efficiency by qPCR for detection of Cre only, NeuN only or duplexing Cre and NeuN (C_T values for NeuN shown). (C) Assessment of reaction efficiency by qPCR for detection of ICP47 only, NeuN only or duplexing ICP47 and NeuN (C_T values for ICP47 shown). (B) Assessment of reaction efficiency by qPCR for detection of Cre only, NeuN only or duplexing Cre and NeuN (C_T values for NeuN shown).

5.3.2.2 Design and construction of an RNA-based standard curve for the absolute quantification of ICP47 and Cre transcripts

In order to perform absolute quantification of RNA copy number, a suitable standard curve is required. Although standard curves can be based on DNA, they only undergo PCR amplification, and not reverse transcription, a step that can introduce a major source of transcript-dependent variability (Ståhlberg et al., 2004a). Therefore, the accurate absolute quantification of mRNA levels by RT-qPCR depends on the construction of an RNA-based standard curve. To do this, the DNA containing the area of interest was cloned into plasmids containing the SP6 promoter. The SP6 RNA polymerase was used to synthesise ICP47 and Cre RNA transcripts using linearised plasmid as a template. To confirm that the desired product was being detected following amplification of the cDNA, a cDNA synthesis was carried out using 1 x 10^6 copies of the appropriate RNA sample, including a –RT control, and qPCR reaction was carried out. The resulting products were then analysed by PAGE (Figure 5-6). The resulting DNA fragments were each approximately 60 bp as desired, and given the high specificity of the primer/hydrolysis probe approach used, this RNA was found to be appropriate for the construction of the standard curves.

To construct the RNA standard curve, the appropriate RNA transcript was diluted to the desired concentration in a pool of irrelevant RNA taken from an uninfected mouse. This RNA was then used in cDNA synthesis reaction. Therefore, in the final qPCR reaction, the desired quantity of template RNA was diluted in the equivalent amount of RNA from a single mouse. In order to determine the linearity and reproducibility of this standard curve, a qPCR assay was performed (Figure 5-7). The R^2 values were both greater than 0.99, indicating a high level of reproducibility. The efficiency of the ICP47 assay was calculated to be 100.7% based on this assay, while the efficiency of the Cre assay was 99.3%, with a limit of detection of 250 copies per reaction.

5.3.2.3 Comparison of the expression of ICP47 and Cre transcripts over time in mice infected with HSV-1 pICP47_eGC

In order to compare the activity of the native and ectopic ICP47 promoter, groups of three or four C57Bl/6 mice were infected with HSV-1 pICP47_eGC. A single mouse was culled on either day 1, 4, 7, 10 or 15 p.i., and the DRG immediately removed and snap frozen as rapidly as possible (within five minutes of the death of the mouse). This was repeated another five times, so in this way there were at least two independent biological replicates per time point. A single mouse was mock infected with PBS to serve as a control and was treated as per the infected mice. RNA was isolated and cDNA synthesis performed. The number of each transcript was quantified by qPCR assay, with each reaction performed in triplicate and so containing one sixth of the RNA isolated from each mouse. In the majority

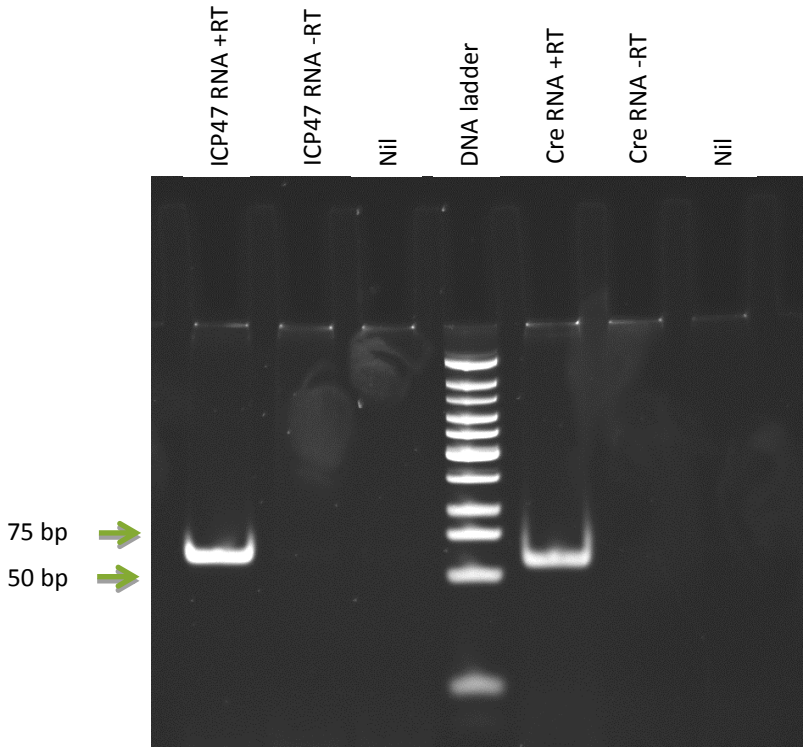

Figure 5-6. Verification of detection of ICP47 and Cre transcripts by qPCR. 1 x 10^6 copies of ICP47 or Cre RNA was reverse transcribed and a qPCR reaction carried out. The resulting DNA fragments were analysed by PAGE and showed fragments of the expected size were detected. The arrows indicate the size of the corresponding DNA fragments of the low weight molecular DNA ladder used.

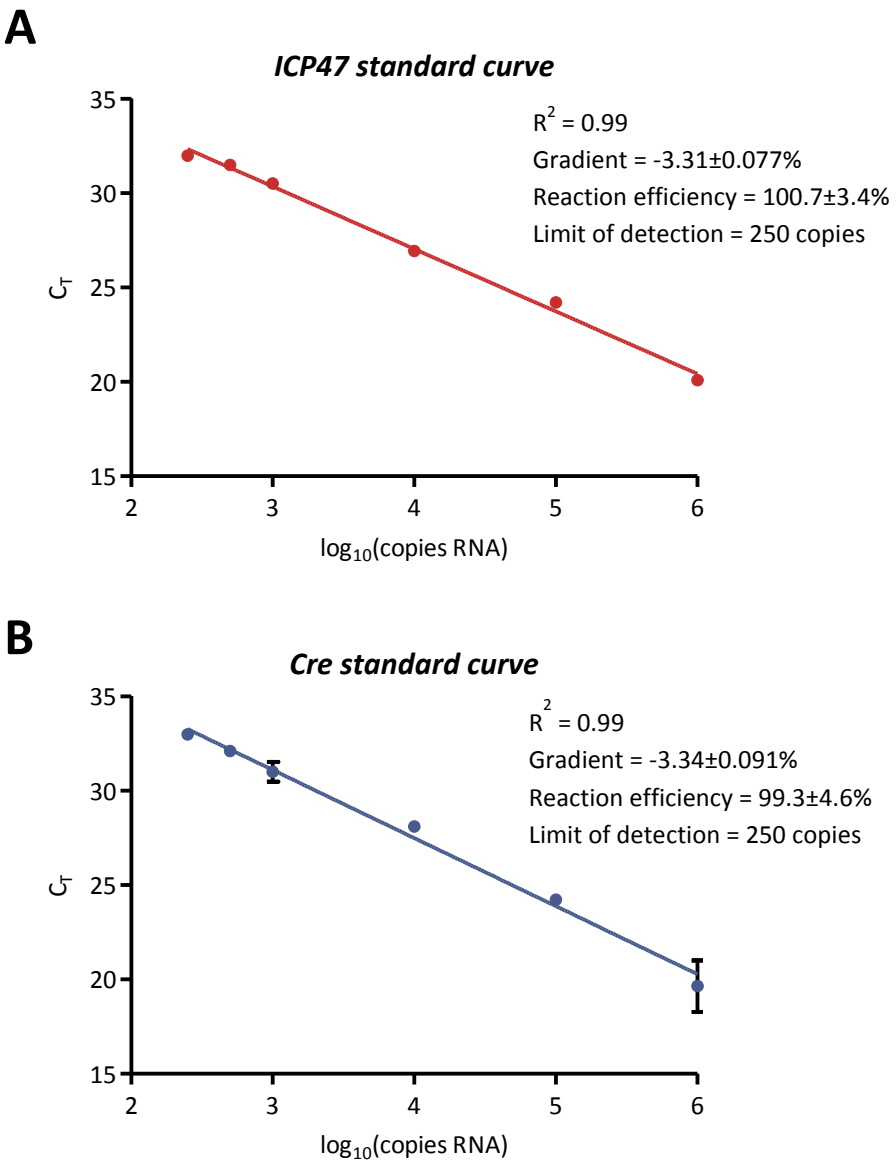

Figure 5-7. RNA-based standard curves for absolute quantification of ICP47 and Cre transcripts in DRG taken from HSV-1 infected mice. ICP47 or Cre RNA transcripts were synthesised from either pUC57 qICP47, or pCR bluntII Cre(R) using SP6 RNA polymerase, and serially diluted to the appropriate copy number in an equal quantity of irrelevant neuronal RNA. For each point on the standard curve, a separate cDNA synthesis reaction was performed. This was followed by a qPCR reaction performed in triplicate, with the standard curve for detection of (A) ICP47 and (B) Cre transcripts shown, where n = 3 and each point represent mean±SEM. The least square linear regression line is calculated using the C_T values from each dilution and the R^2 value, the gradient of the line and the resulting reaction efficiency and the limit of detection are reported on each graph.

of cases, no amplification was detected in the –RT control, but for four mice there was possibly some amplification at the limit of detection with a C_T of more than 31. Given that this represents in each case less than 1% of the nucleic acid amplified from the +RT samples, it was deemed irrelevant for the purposes of this analysis.

As expected, the peak in the detection of both ICP47 and Cre transcripts was at day four p.i., corresponding to the peak of the acute infection (Figure 5-8). Transcript levels then declined, with ICP47 and Cre transcripts levels being similar, with no statistically significant differences observed between the amount of Cre or ICP47 transcripts per day. Somewhat surprisingly, Cre transcripts were detectable in a single mouse at day one p.i. By day 10 p.i., the number of ICP47 transcripts had mostly fallen below the limit of detection, while the number of Cre transcripts was slightly above the limit of detection. This is likely to reflect increased stability of Cre over ICP47 transcripts, or slightly increased expression of eGFP/Cre compared to ICP47. By day 15 p.i. no Cre or ICP47 transcripts were detectable in either mouse. Given that the accumulation of β-gal marked cells in ROSA26R mice infected with HSV-1 pICP47_eGC is gradual and occurs over relatively long time period, from days 10 to 30 p.i. (Figure 5-1), it is unlikely that this can be accounted for simply by the persistence of a low level Cre transcripts. However, the caveat remains that transcript and protein abundance are not directly proportional and may not be well correlated. In addition to varying efficiencies in the translation of mRNA, protein abundance can also be influenced by stability or degradation of the protein. Therefore, to determine if protein continues to be expressed during latency establishment when regulated by the ectopic ICP47 promoter, a different approach was required.

5.3.3 Activity of the ICP47/22 promoter during HSV-1 infection as defined using a conventional fluorescent reporter

Generally, the expression of HSV-1 genes *in vivo* follows a characteristic pattern exemplified in Figure 4-6. To confirm that the expression of eGFP/Cre from the ectopic ICP47 promoter is similar to other HSV-1 lytic genes, C57Bl/6 mice were infected with HSV-1 pICP47_eGC. The mice were then culled at 1, 4, 7 or 14 days post infection, their DRG removed and fixed, and the expression of eGFP was assessed using fluorescent microscopy of whole mounts of DRG (Figure 5-9). The use of whole DRG is advantageous for the detection of reporter genes or viral antigen as it is feasible to examine the entire tissue and determine absolute numbers of positive cells, which is impractical and difficult with serially sectioned tissues (Margolis et al., 1992; Marshall et al., 2000; Sawtell et al., 1998; Simmons and Tscharke, 1992). While visualisation of fluorescence in whole DRG can be problematic due to the thickness and autofluorescence associated with these tissues, recent advances in microscopy and image processing, such as improvements in

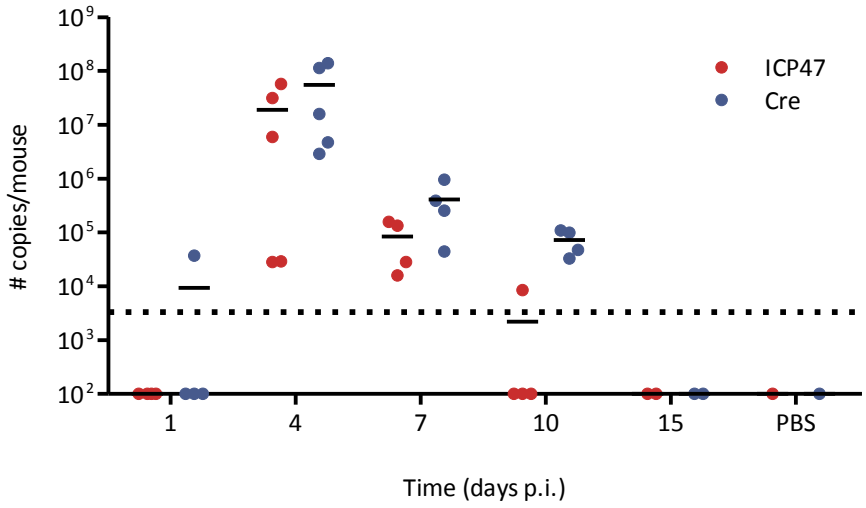

Figure 5-8. Detection of ICP47 and Cre transcripts over time in C57Bl/6 mice infected with HSV-1 pICP47_eGC. Groups of three or four C57Bl/6 mice were infected with 1×10^8 PFU/mL HSV-1 pICP47_eGC and at the 1, 4, 7, 10 or 15 days p.i. a mouse was culled, and the DRG (spinal levels T8 to T13) were removed and snap frozen. This was repeated a further five times. RNA was extracted and cDNA synthesis performed before a qPCR assay was set up to determine ICP47 (red) and Cre (purple) transcript levels in each sample. Each point represents a single mouse, where the mean of triplicate reactions is shown. The limit of detection was 3333 copies of RNA per mouse as indicated by the broken line. The data was analysed using a two way ANOVA, but no statistically significant differences were found ($p > 0.05$).

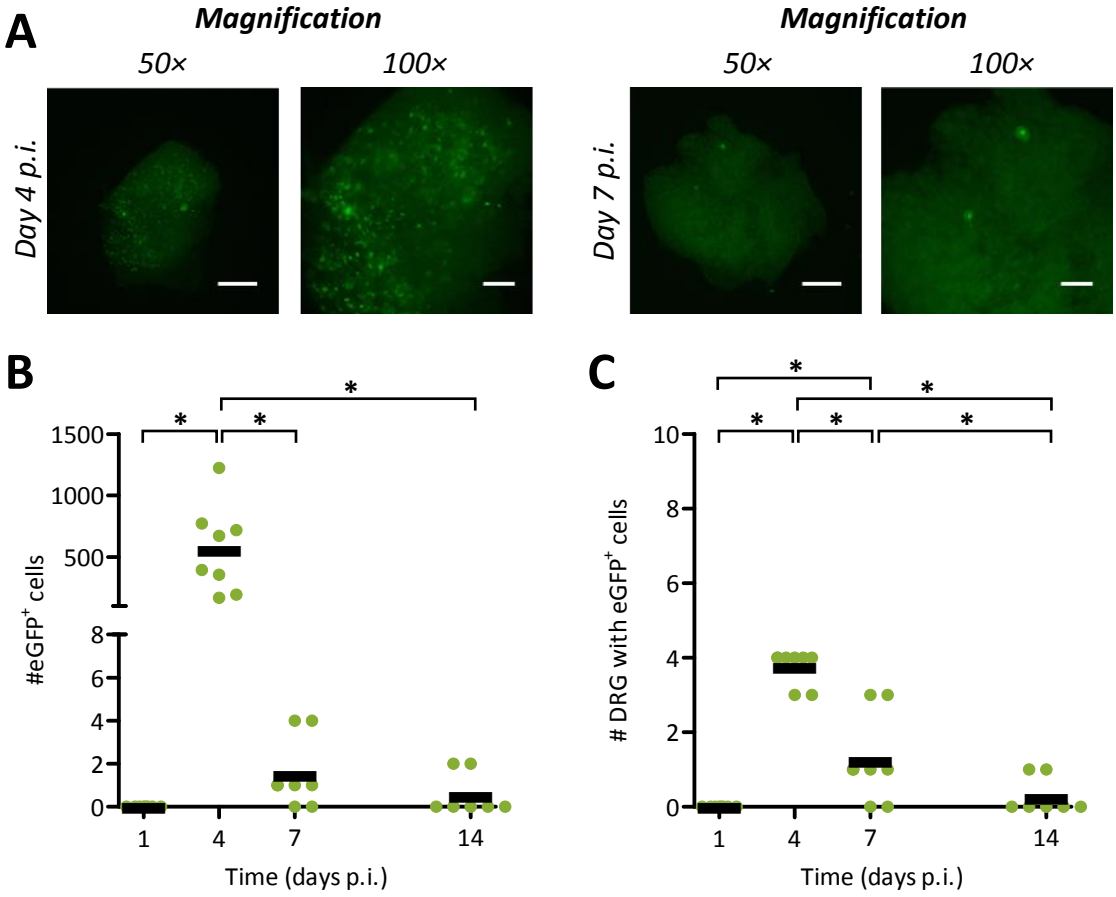

Figure 5-9. Expression of eGFP in C57Bl/6 mice infected with HSV-1 pICP47_eGC. Groups of four C57Bl/6 mice were infected with 1×10^8 PFU/mL HSV-1 pICP47_eGC. At 1, 4, 7, or 14 days p.i. mice were culled and innervating DRG (from spinal levels T5 to L1) removed and processed for determination of eGFP expression. (A) Representative photomicrographs showing eGFP associated fluorescence in a single DRG at days 4 or 7 p.i. at either 50× (scale bar = 250 µm) or 100× magnification (scale bar = 100 µm). Both (B) the total number of eGFP$^+$ cells per mouse and (C) the number of DRG per mouse containing at least one eGFP$^+$ cell are shown. Each circle represents one mouse and the black bar represents the mean value for all mice at each time point. The results are pooled from 2 independent experiments (n = 8 for each time point). Statistical significance was determined by a one way ANOVA ($p < 0.001$) and pairwise comparisons were performed using the Bonferroni's post-test (*$p < 0.05$).

apochromatic correction to provide high contrast images, mean that this is now a feasible approach for the visualisation of fluorescent reporter proteins like eGFP expressed *in vivo* (Spitzer et al., 2011).

The peak in the number of $eGFP^+$ cells was at four days p.i. (Figure 5-9). Some eGFP expression was detectable at 14 days p.i. but this was restricted to a small population of cells, consistent with the observable β-gal expression in mice infected with KOS6β (Figure 4-6). Therefore, it is unlikely that the expression of the eGFP/Cre protein from this modified ICP47 is regulated in a substantially different manner to the native ICP47 which contains a copy of the OriS sequence.

The U_L3/U_L4 intergenic region is found within the U_L region of the genome, in closer proximity to the CTRL1 CTCF motif found near the TR_L/U_L junction (Figure 1-1). CTCF binds to these motifs, and act as a barrier to partition the genome into the transcriptionally permissive chromatin around the LAT region and repressive areas of chromatin across the remainder of the genome (Amelio et al., 2006b). Therefore, expression of eGFP/Cre from the intergenic U_L3/U_L4 region may be typical of a lytic HSV-1 gene, but this may not hold for the expression under the ICP47 promoter from other locations in the genome. To attempt to verify that expression from the ICP47 promoter is not altered by its location in the genome, the expression of Tdtomato was measured in C57Bl/6 mice infected with HSV-1 pICP47/Tdtom, a virus constructed to express Tdtomato from the U_L26/U_L27 intergenic region of HSV-1 (refer to Section 3.4). Unlike the U_L3/U_L4 region, the U_L26/U_L27 region is not found near any of these CTCF motifs. Furthermore, the fluorescent reporter Tdtomato is one of the brightest fluorescent reporter proteins available (Shaner et al., 2004). The emission maximum of Tdtomato is at 581 nm, which is less affected by the autofluorescence typically observed in the green spectrum close to that of eGFP, an issue of particular concern in neuronal tissue (Shaner et al., 2004; Spitzer et al., 2011). As such, there should be less background fluorescence compared to HSV-1 pICP47_eGC, possibly allowing greater sensitivity. Groups of C57Bl/6 mice were infected with HSV-1 pICP47/Tdtom, and were culled at three day intervals from day one to 16 p.i. Mice were also culled at 30 days p.i. to allow for the assessment of ICP47 promoter activity during latency. Expression of Tdtomato was assessed by fluorescent microscopy of whole mounts of fixed DRG (Figure 5-10).

A peak in the number of $Tdtomato^+$ cells was observed at 4 days p.i., with a decline in the number of $Tdtomato^+$ cells until 13 days p.i. No $Tdtomato^+$ cells were detectable during latency at day 30 p.i. The pattern in the number of $Tdtomato^+$ cells resembles that of β-gal expression in C57Bl/6 mice infected with KOS6β (Figure 4-6). This is more consistent with

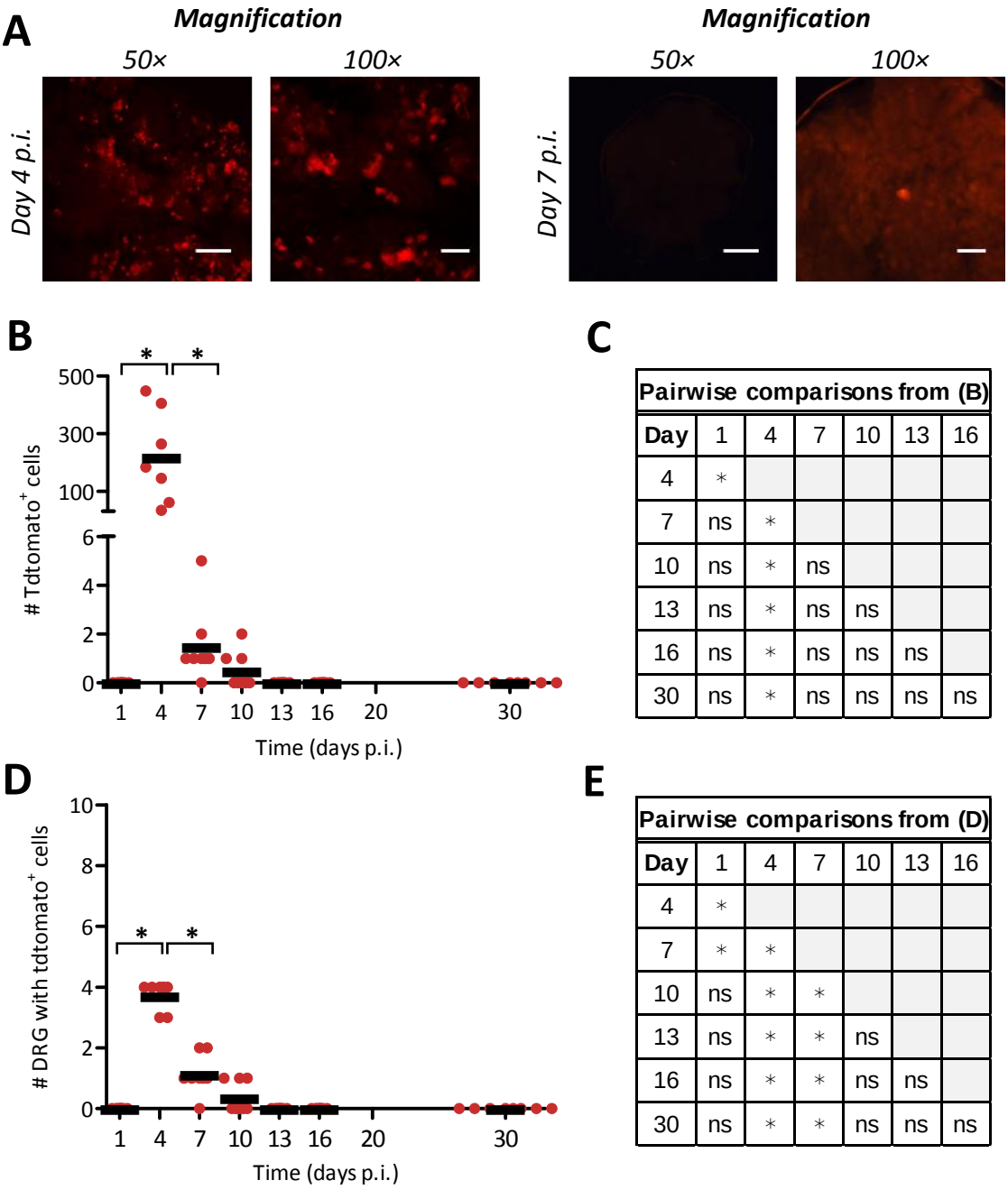

C

Pairwise comparisons from (B)						
Day	1	4	7	10	13	16
4	*					
7	ns	*				
10	ns	*	ns			
13	ns	*	ns	ns		
16	ns	*	ns	ns	ns	
30	ns	*	ns	ns	ns	ns

E

Pairwise comparisons from (D)						
Day	1	4	7	10	13	16
4	*					
7	*	*				
10	ns	*	*			
13	ns	*	*	ns		
16	ns	*	*	ns	ns	
30	ns	*	*	ns	ns	ns

Figure 5-10. Expression of Tdtomato in C57Bl/6 mice infected with HSV-1 pICP47/Tdtom. Groups of three or four C57Bl/6 mice were infected with 1×10^8 PFU/mL HSV-1 pICP47/Tdtom. At 1, 4, 7, 10, 13, 16 or 30 days p.i. mice were culled and innervating DRG (from spinal levels T5 to L1) removed and processed for determination of Tdtomato expression. (A) Representative photomicrographs showing Tdtomato associated fluorescence in a single DRG at days 4 or 7 p.i. at either 50× (scale bar = 250 µm) or 100× magnification (scale bar = 100 µm). Both (B) the total number of Tdtomato$^+$ cells per mouse and (C) the number of DRG per mouse containing at least one Tdtomato$^+$ cell are shown. Each circle represents one mouse and the black bar represents the mean value for all mice at each time point. The results are pooled from two independent experiments (n = 7 – 8 per time point). (C&E) Statistical significance was determined by a one way ANOVA ($p < 0.001$) with Bonferroni's post-test to make pairwise comparisons, with key statistical differences indicated on (B) and (D) (*$p < 0.05$).

the conventional view of the activity of lytic promoters during latency, and confirms that this modified ICP47 promoter is likely still behaving as a lytic HSV-1 promoter.

5.3.4 Despite some caveats, the ectopic modified ICP47 promoter behaves in a similar manner as the native HSV-1 ICP47 promoter

In summary, in this thesis the virus HSV-1 pICP47_eGC has been extensively characterised. It replicates comparably to wildtype HSV-1 *in vitro* in Vero cells (refer to Section 3.5.1). The expression of eGFP from this ectopic promoter was not inhibited by either cycloheximide or acyclovir, as would be expected for the native ICP47 promoter (refer to Section 3.5.2). HSV-1 pICP47_eGC also shows similar pathogenesis to wildtype HSV-1 as evidenced by lesion progression and size as assessed using the zosteriform C57Bl/6 mouse model of HSV-1 infection (refer to Section 3.5.3). Further, similar amounts of infectious virus are found in the skin and DRG of C57Bl/6 mice infected with either HSV-1 pICP47_eGC or wildtype HSV-1 KOS (refer to Section 3.5.3). Fluorescence reporter gene expression from either the $U_L3/4$ or $U_L26/27$ locus is as would be expected of the native ICP47 protein during the lytic infection, with a failure to detect fluorescence during latency. Further, a RT-qPCR based assay demonstrated that the expression of Cre and ICP47 transcripts was reasonably well correlated, even given the caveats outlined in Section 5.3.4, with both transcripts undetectable by day 15 p.i. HSV-1 pICP47_eGC also establishes latency normally, with a failure to detect infectious virus in latently infected DRG (refer to Section 5.3.2). It also has a normal reactivation phenotype as demonstrated by explant reactivation, and maintains the eGFP/Cre expression cassette long-term (refer to Section 3.5.4). Therefore, even though there are inherent disadvantages to inferring gene expression through reporter gene expression from an ectopic locus, the use of these viruses in the ROSA26R model enabled the detection of ICP47 expression during the establishment and maintenance of latency that has not been revealed previously.

The expression of ICP47 during the establishment of latency is probably transient and/or at a low level, but does occur in a substantial population of cells. Furthermore, the use of the ROSA26R model means that these cells are able to survive ICP47 expression. This is of interest given the role for this protein in evasion of the $CD8^+$ T cell response (Früh et al., 1995; Goldsmith et al., 1998; Hill et al., 1995; Orr et al., 2007; York et al., 1994), as it has been shown that the survival of HSV-1 antigen positive neurons is dependent on the presence of $CD8^+$ T cells (Simmons and Tscharke, 1992). However, to date investigations into the ICP47 have been limited to its impact upon the acute HSV-1 immune response (Goldsmith et al., 1998). Since latency is established normally by viruses that lack ICP47 expression in mouse models of infection (Thilaga Velusamy and David Tscharke,

unpublished data), this suggested a more nuanced approach is needed to dissect the role of ICP47 expression during latency.

5.4 Investigating the role of TAP inhibition by ICP47 during latency in mice

The inhibition of TAP in mouse fibroblasts requires concentrations of ICP47 that are 50-100 fold higher than those needed to inhibit peptide transport through TAP in human fibroblasts (Ahn et al., 1996; Tomazin et al., 1996). So, while the prevention of expression of ICP47 should increase the efficiency of antigen presentation on MHC-I, in practice the poor affinity of ICP47 to murine TAP means that very large differences in phenotype are not observed in murine models of HSV-1 infection (Ahn et al., 1996; Goldsmith et al., 1998; Tomazin et al., 1996). Therefore, enhancing antigen presentation on MHC-I may be a more effective approach for investigating the role of ICP47 in mice. Minigenes are small genes consisting of a start codon followed by the minimal sequence required to encode an immunogenic peptide that is able to bind to MHC-I (referred to as epitopes). Minigenes can be synthesised in vast quantities and are very efficiently presented by MHC-I on the cell surface because they do not have to be processed by the proteasomes or other cytosolic enzymes (Antón et al., 1997; Porgador et al., 1997; Princiotta et al., 2003). In this way, it was hypothesised that the expression of a minigene from HSV-1 would enhance presentation on MHC-I and better approximate the behaviour of a virus that lacks ICP47 expression in humans. There is a caveat, that the likely comparatively high level expression of ICP47 (Harkness et al., 2014) means that ICP47 may still be able to exert some degree of inhibition on the presentation of a cytosolic minigene. However, the inclusion of an ER-targeting motif can result in the transport of these peptides directly into the ER, eliminating the requirement for TAP transport prior to binding of peptide to MHC-I (Bacik et al., 1994). Therefore, to adopt a conservative approach, an additional virus was constructed in which an ER-targeted minigene, which should be presented independently of ICP47, was introduced into HSV-1.

Given that the aim is to investigate ICP47 activity during latency, when expression under most promoters is silenced, the continued expression of antigen during latency is problematic. Fortunately, results presented in this thesis indicate that there is low level activity of the gB promoter during latency (refer to Section 4.3), and a peptide encoded within gB (gB_{498}) elicits a strong $CD8^+$ T cell response during latency in C57Bl/6 mice (Sheridan et al., 2009; St. Leger et al., 2011). Therefore, a cytosolic or ER-targeted gB_{498} minigene were chosen for insertion into the virus to further investigate the role of antigen presentation on MHC-I and ICP47 during HSV-1 infection.

5.4.1 Generation of recombinant HSV-1 containing a gB_{498} minigene

The first virus was constructed to contain an additional copy of the gB_{498} epitope with an ER-targeting motif. An *eGFP/Cre* fusion gene under the control of the CMV IE promoter was also introduced into this virus simultaneously. This virus was named HSV-1 ESminigB_Cre (Figure 5-11). HSV-1 ESminigB_Cre was then modified to remove the ER-targeting motif – in other words, to construct a virus that expressed a cytosolic gB_{498} epitope. This virus was named HSV-1 minigB_Cre (Figure 5-11). The expression of eGFP by microscopy, as well as PCR and sequencing of the insert and surrounding regions of the genome, was then performed to verify the construction of these viruses and the absence of wildtype virus. In both cases, two independently plaque purified viruses were isolated.

To confirm that these viruses resemble wildtype virus, a multiple step growth curve was performed in Vero cells following low MOI infection (MOI 0.01; Figure 5-12). The growth of HSV-1 ESminigB_Cre was similar to that of the parent, wildtype HSV-1 KOS, and the control virus HSV-1 pC_eGC, which contains the *eGFP/Cre* fusion gene but lacks the additional copy of the gB_{498} epitope (Figure 5-12A). Similarly, the growth of HSV-1 minigB_Cre was not compromised relative to the parent virus, HSV-1 ESminigB_Cre (Figure 5-12B).

5.4.2 Addition of a cytosolic or ER-targeted gB_{498} minigene to HSV-1 enhances presentation of gB_{498}

To confirm that the gB_{498} minigene is expressed and is able to enhance presentation on MHC-I, an indirect *in vitro* antigen presentation was established as there is no reagent that allows the direct detection of gB_{498}:H-$2K^b$ complexes. This assay utilises a gB hybridoma (HSV-2.3.2E2) that recognises the gB_{498} epitope in the context of H-$2K^b$ and has been engineered to contain the *lacZ* gene under the control of the IL-2 promoter (Mueller et al., 2002). Therefore, following co-culture of infected target cells with the hybridoma, the hybridoma becomes activated and IL-2 promoter induction occurs, leading to the production of β-gal that can be assayed using the ONPG substrate. The relative absorbance of each sample can then be calculated relative to maximal peptide simulation with synthetic peptides, as opposed to target cells. This should reflect the direct presentation of antigen on the surface of the target cells (Karttunen et al., 1992; Mueller et al., 2002).

Initially, the dendritic cell-like cell line derived from C57Bl/6 mice, DC2.4, was infected with the control HSV-1 pC_eGC, HSV-1 ESminigB_Cre or HSV-1 minigB_Cre.

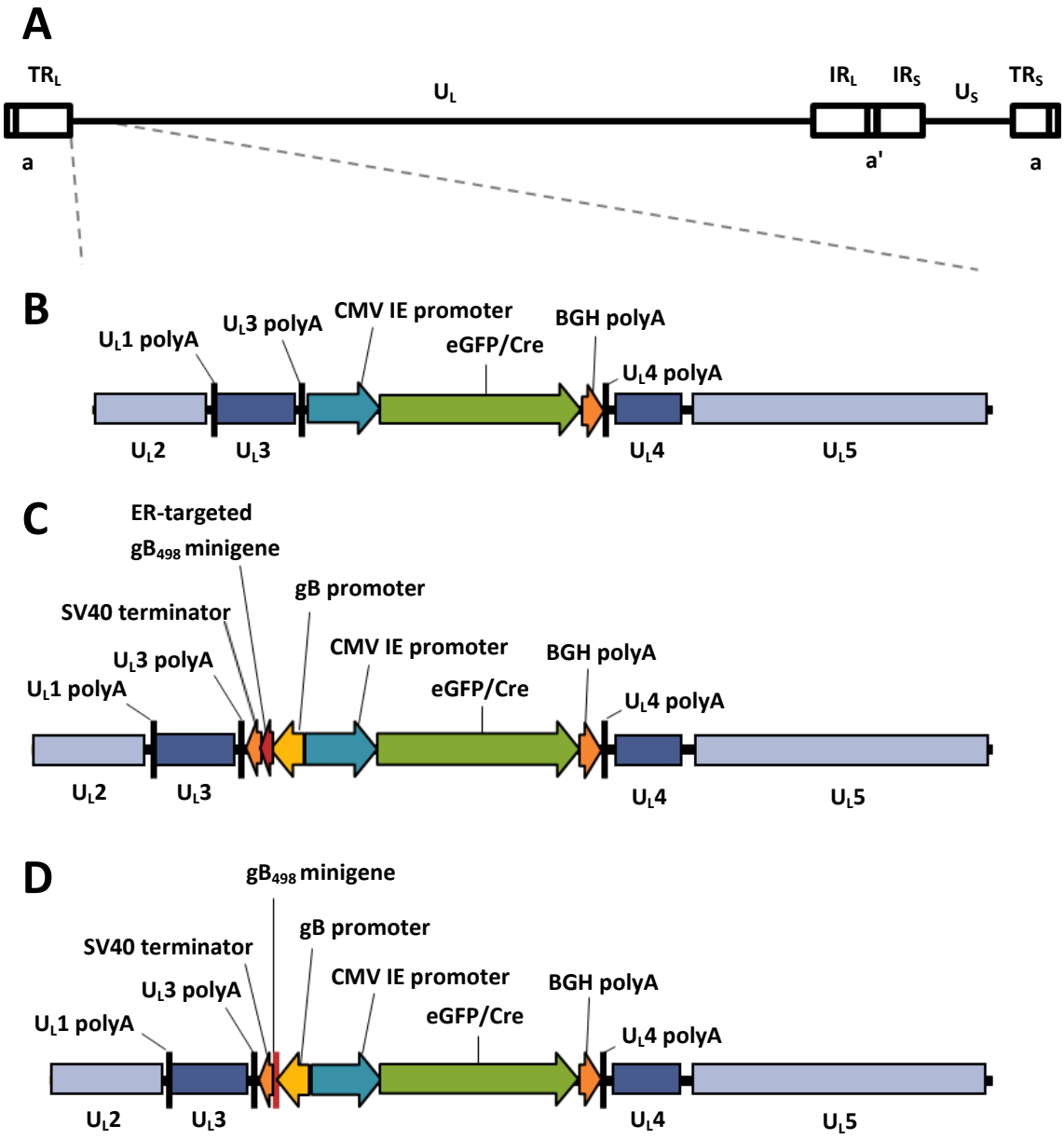

Figure 5-11. Design of recombinant viruses HSV-1 ESminigB_Cre and HSV-1 minigB_Cre. (A) Schematic representation of the HSV-1 genome with the location of U_L3 and U_L4 indicated (to scale). (B) Schematic representation of the CMV IE promoter eGFP/Cre expression cassette inserted the intergenic space between U_L3 and U_L4 in HSV-1 pC_eGC. (C) Schematic representation of HSV-1 ESminigB_Cre, showing the eGFP/Cre expression cassette and the ER-targeted gB_{498} minigene which are divergently transcribed, inserted into the intergenic space between U_L3 and U_L4. (D) Schematic representation of HSV-1 minigB_Cre, showing the eGFP/Cre expression cassette and the minimal gB498 minigene which are divergently transcribed, inserted into the intergenic space between U_L3 and U_L4.

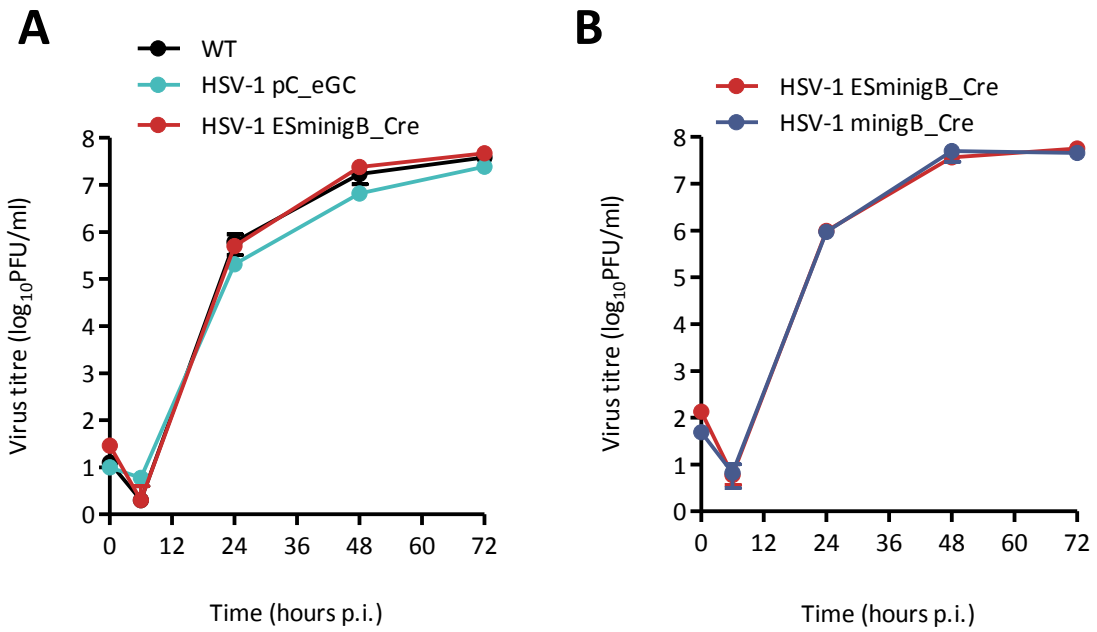

Figure 5-12. Insertion of a gB$_{498\text{-}505}$ minigene has no effect on viral replication *in vitro*. (A) The replication of HSV-1 ESminigB_Cre (red) was compared to wildtype HSV-1 KOS (black) and HSV-1 pC_eGC (blue) in Vero cells in a multiple step growth curve. (B) The replication of HSV-1 minigB_Cre (purple) was compared to the parent HSV-1 ESminigB_Cre (red) in Vero cells in a multiple step growth curve. Confluent cell monolayers in 9.6 cm^2 tissue culture wells were infected at a low MOI (0.01 PFU/cell in 1 mL M0). After one hour, the inoculum was removed, cells washed and 2 mL M2 was added. A 0 hour p.i. sample was collected immediately following the addition of fresh media. The remaining samples were harvested at 6, 24, 48 or 72 hpi. Virus titres were determined by standard plaque assay. Data are mean±SEM of three replicates.

Although only 50 – 60% of cells were infected as determined by flow cytometry for the detection of eGFP (data not shown), these cells were able to efficiently present the gB_{498} epitope, as inferred by stimulation of the gB hybridoma (Figure 5-13A). HSV-1 minigB_Cre infected cells may be able to better stimulate the hybridoma than HSV-1 ESminigB_Cre infected cells, but this trend was not replicated in all experiments. Both HSV-1 minigB_Cre and ESminigB_Cre infected cells were able to stimulate the gB hybridoma slightly more effectively than HSV-1 pC_eGC infected cells. However, the DC2.4 cell line is highly efficient at presenting antigen and is often considered to be less physiologically relevant. Therefore, the antigen presentation assay was repeated, but with infected MC57G mouse fibroblasts as the serving as the stimulator (Figure 5-21B). The level of stimulation was much lower, probably because of the relatively inefficiency of antigen presentation by this cell line. A similar trend was observed in which HSV-1 minigB_Cre infected cells were able to stimulate the gB hybridoma marginally more efficiently than HSV-1 ESminigB_Cre infected cells. Both were slightly more effective at stimulating the hybridoma than HSV-1 pC_eGC infected cells.

It has been well characterised that ICP47 is much less effective at inhibiting TAP in murine compared to human cells, so it was of interest to determine if similar levels of antigen presentation would be observed in human cells infected with HSV-1 minigB_Cre or HSV-1 ESminigB_Cre. Therefore, the human derived $293K^b$ cell line was infected with HSV-1 pC_eGC, HSV-1 ESminigB_Cre or HSV-1 minigB_Cre. $293K^b$ cells have been engineered to stably express the murine H-$2K^b$ MHC-I allele and so are able to present the gB_{498} epitope on their cell surface. Infected $293K^b$ cells were then used to stimulate the gB hybridoma. Both HSV-1 ESminigB_Cre and HSV-1 minigB_Cre infected cells were better able to stimulate the gB hybridoma than HSV-1 pC_eGC, suggesting that the incorporation of an additional minimal gB_{498} epitope results in efficient antigen presentation, regardless of whether or not this epitope is ER targeted or not.

5.4.3 The pathogenesis and *in vivo* growth of recombinant HSV-1 containing a gB_{498} minigene

To assess the pathogenicity of these viruses, the flank zosteriform model of HSV-1 infection was employed as described previously (refer to Section 3.2.1). Groups of ROSA26R mice were infected with either of these viruses. Lesion size was measured and clinical score monitored daily. Mice did not develop any clinical signs of illness other than their lesion, indicating that these viruses were not more neurovirulent than the parent virus KOS. The lesions on mice infected with HSV-1 ESminigB_Cre or minigB_Cre were significantly larger compared to the mice infected with the control virus (Figure 5-14A).

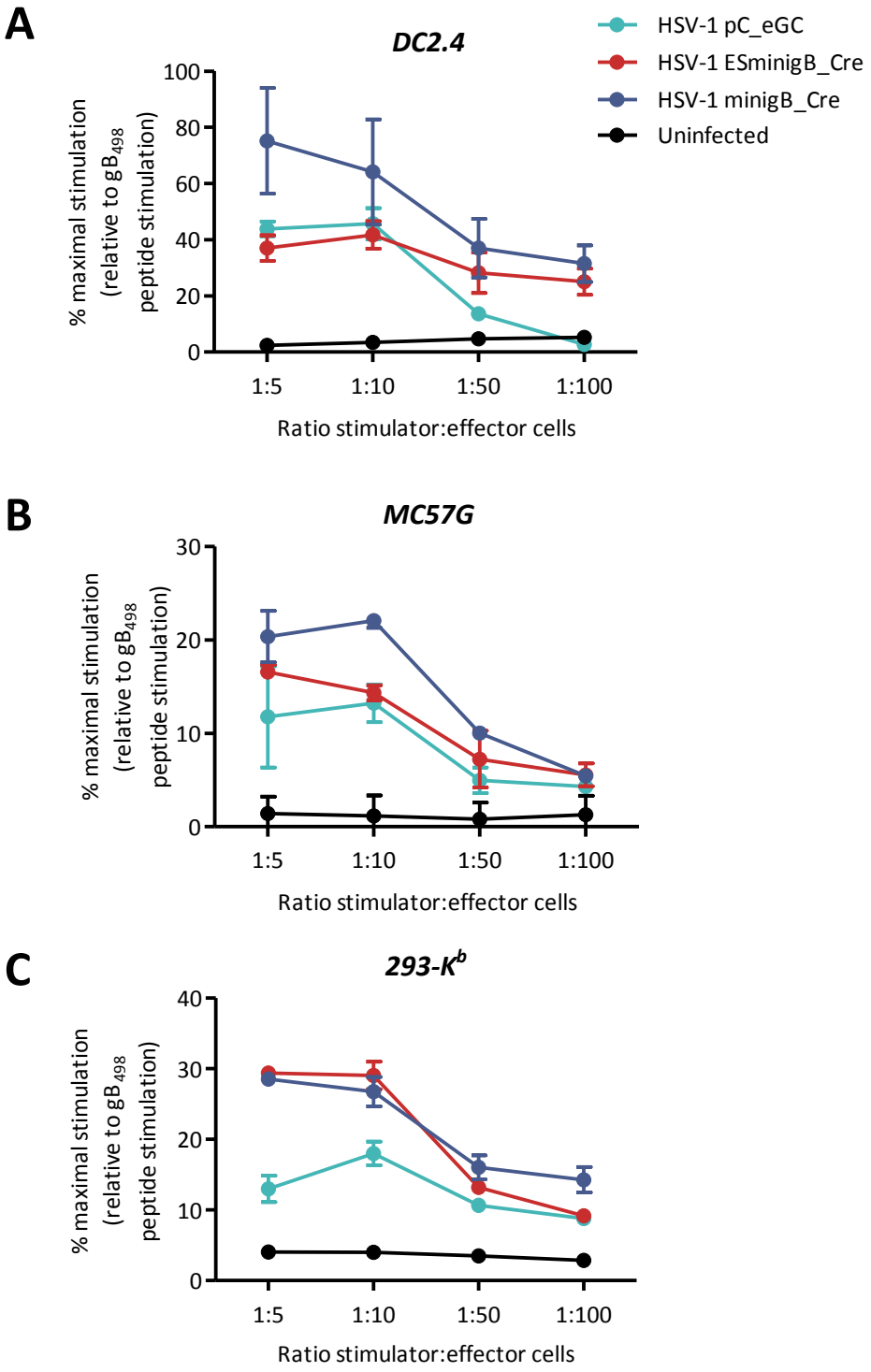

Figure 5-13. Enhancement of antigen presentation *in vitro* with the addition of a gB_{498} minigene to HSV-1. (A) DC2.4, (B) MC57G or (C) 293-K^b were infected with HSV-1 pC_eGC, HSV-1 ESminigB_Cre or HSV-1 minigB_Cre for six hours. The infected cells or 0.125 µM gB_{498} peptide were then cocultured with the gB_{498} specific hybridoma at the indicated stimulator:effector ratio for twelve hours. Cells were lysed and assayed for β-gal expression using ONPG. Absorbance was measured at 420 nm, and the % stimulation was calculated relative to maximal gB_{498} peptide stimulation. Each stimulation was performed in triplicate and results are presented at mean±SEM. Each cell line was tested seperately and the results shown are representative of at least two independent experiments.

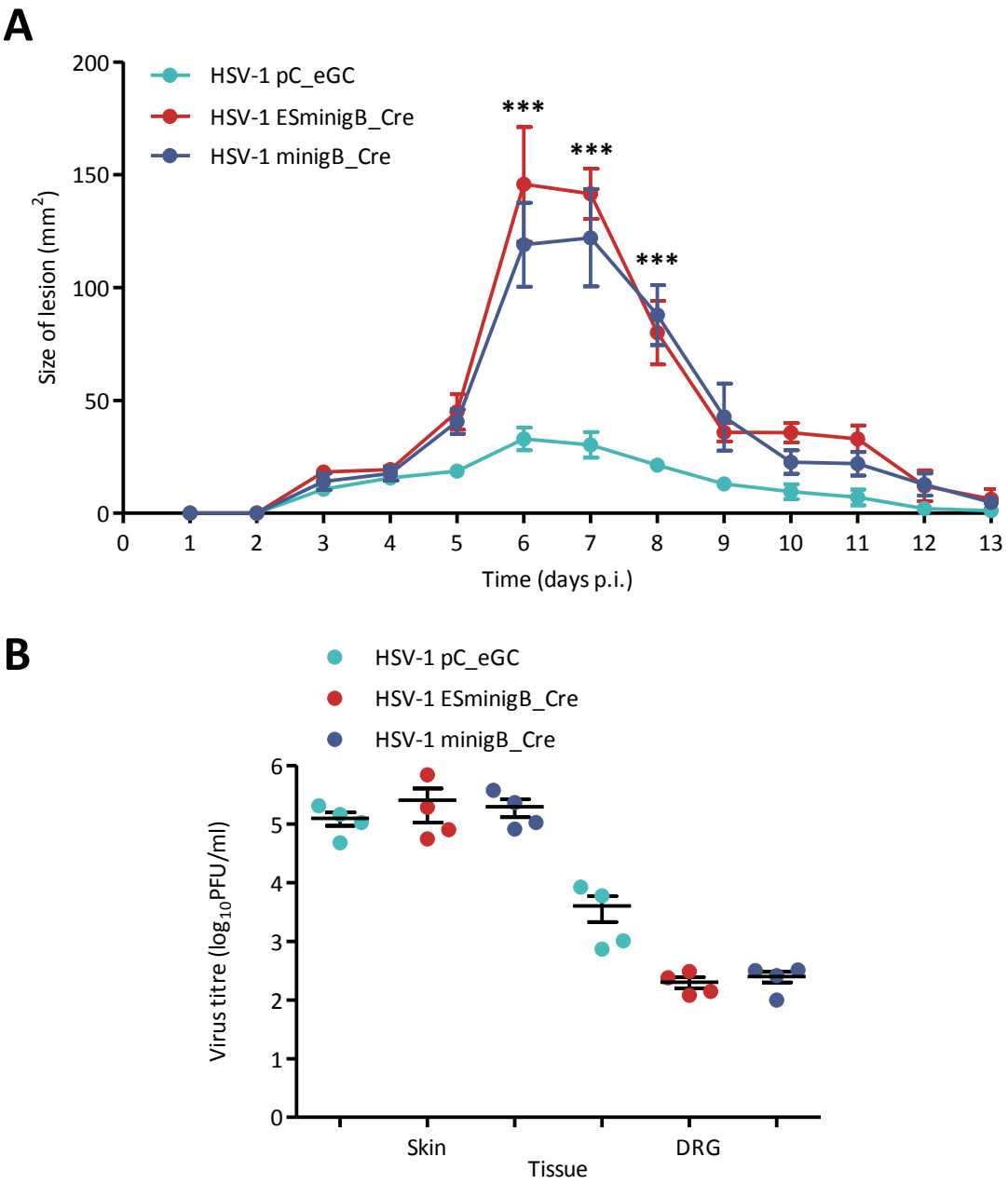

Figure 5-14. Insertion of a $gB_{498\text{-}505}$ minigene into HSV-1 results in larger lesions in C57Bl/6 mice following infection. (A) C57Bl/6 mice were infected by tattoo with 1×10^8 PFU/mL with HSV-1 pC_eGC (blue), HSV-1 ESminigB_Cre (red) or HSV-1 minigB_Cre (purple). Lesion size was measured daily using a caliper and clinical score was monitored daily, with mice never displaying any signs of illness other than the herpetic lesion on the flank. Data is mean lesion size±SEM (n = 3). Data were compared using a one way ANOVA and were found to be significant ($p < 0.01$), and the means of lesion size on each day were compared using a Bonferroni's post-test (***$p < 0.001$). (B) The growth of HSV-1 ESminigB_Cre (red) and HSV-1 minigB_Cre (purple) was compared to HSV-1 pC_eGC (blue) *in vivo*. Groups of four C57Bl/6 mice were infected by tattoo with 1×10^8 PFU/mL. Mice were culled at five days p.i., and infectious virus was determined by standard plaque assay from 10 DRG (spinal levels T5 to L1) or 1 cm^2 skin located over the inoculation size. Circles show results for each mouse (n = 4) and bars represent mean±SEM. The means for each tissue were compared by a one way ANOVA, but no statistically significant differences were observed ($p > 0.05$).

The growth of these viruses was also assessed in both the skin and DRG. Groups of C57Bl/6 mice were infected with either of the HSV-1 pC_eGC, ESminigB_Cre or minigB_Cre viruses. On day five p.i., mice were culled and the amount of virus in the skin and innervating DRG was determined. The growth of the virus in the skin was similar in mice infected with each virus (Figure 5-14B). However, mice infected with each of the viruses containing an additional copy of the gB_{498} epitope had approximately ten-fold less virus in the DRG compared to HSV-1 pC_eGC infected mice. Although this was not a statistically significant difference, it is greater than that which has been previously observed for any other recombinant virus compared to wildtype virus used in this thesis. This suggests that there may be a relevant, but marginal, decease in the amount of virus within the DRG, reflecting either reduced spread of virus or less replication within the DRG.

To confirm that these viruses are able to reactivate from latency, groups of two C57Bl/6 mice were infected with HSV-1 KOS, HSV-1 pC_eGC, HSV-1 ESminigB_Cre or HSV-1 minigB_Cre. At 30 days p.i. the DRG were explanted and incubated for five days to assess reactivation. The DRG were then homogenised and the homogenates were used to infect Vero cell monolayers. Retrievable infectious virus was detected from all mice. As expected, all plaques from virus reactivated from all mice, bar those infected with HSV-1 KOS, were $eGFP^+$, confirming the stability of this insert (Figure 5-15).

5.4.4 No enhancement of the $CD8^+$ T cell response to HSV-1 with the addition of an extra copy of the gB_{498} epitope

It has been demonstrated that deletion of ICP47 does not alter the size of the $CD8^+$ T cell response to HSV-1 (Goldsmith et al., 1998). This is consistent with reports that HSV-1 antigen is largely cross presented by professional APCs, where ICP47 would not expressed, to prime $CD8^+$ T cells (Bosnjak et al., 2005; Jirmo et al., 2009; Mueller et al., 2002). Further, most minigenes are unable to be cross presented (Norbury et al., 2004; Serna et al., 2003). Given that the direct presentation of antigen by infected APCs does not contribute substantially to priming of the $CD8^+$ T cell response, the addition of a gB_{498} minigene to these viruses should not alter the size of the CD8+ T cell response elicited by them, but this should be formally tested. Therefore, the size of the $CD8^+$ T cell response in mice infected with a virus expressing either a cytosolic or ER-targeted gB_{498} minigene was measured.

Seven days after infection, the $CD8^+$ T cell response to HSV-1 pC_eGC, HSV-1 ESminigB_Cre or HSV-1 minigB_Cre in C57Bl/6 mice was assessed both in the DRG (Figure 5-16) and the spleen (Figure 5-17). As expected, very few $CD8^+$ T cells were detected in the DRG of the mock infected control mouse (Figure 5-16A&B, left panel). By contrast, mice infected with

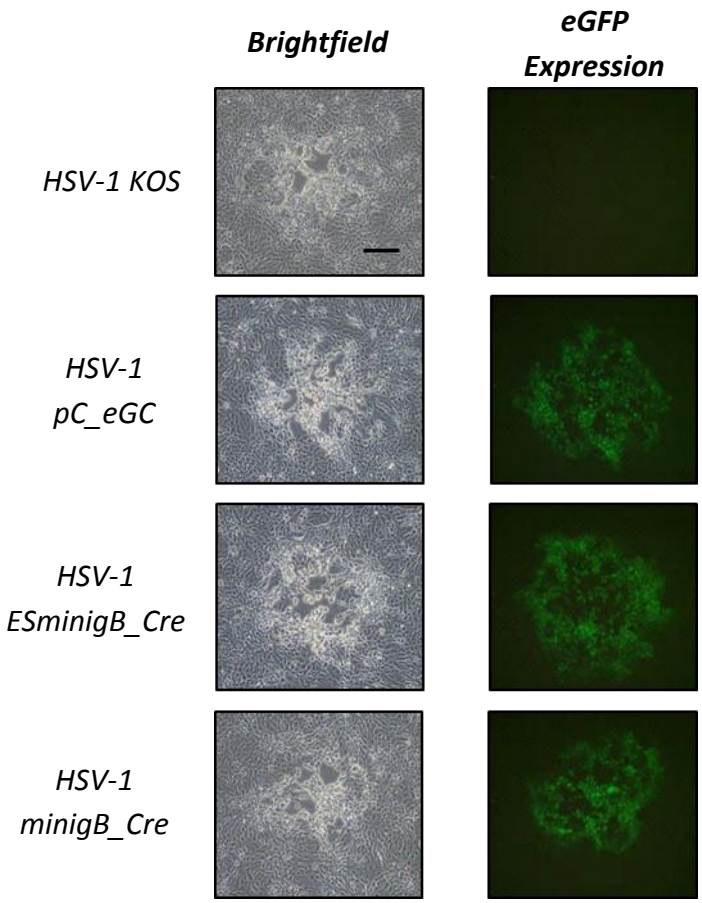

Figure 5-15. HSV-1 ESminigB_Cre and minigB_Cre express eGFP following explant reactivation. Groups of two C57Bl/6 mice were infected by tattoo with 1×10^8 PFU/mL of one of the viruses listed. At 30 days p.i., DRG from spinal levels T5 to L1 were removed and incubated at 37°C for reactivation by explant. After 5 days DRG were homogenised, and the homogenates were titrated on Vero cells. Representative plaques formed by the parent virus HSV-1 KOS and the recombinant viruses on Vero cells under semi-solid M2-CMC as shown by phase contrast microscopy or fluorescence microscopy for the detection of eGFP at 100× magnification (scale bar = 150 μm, as indicated on the top left photograph).

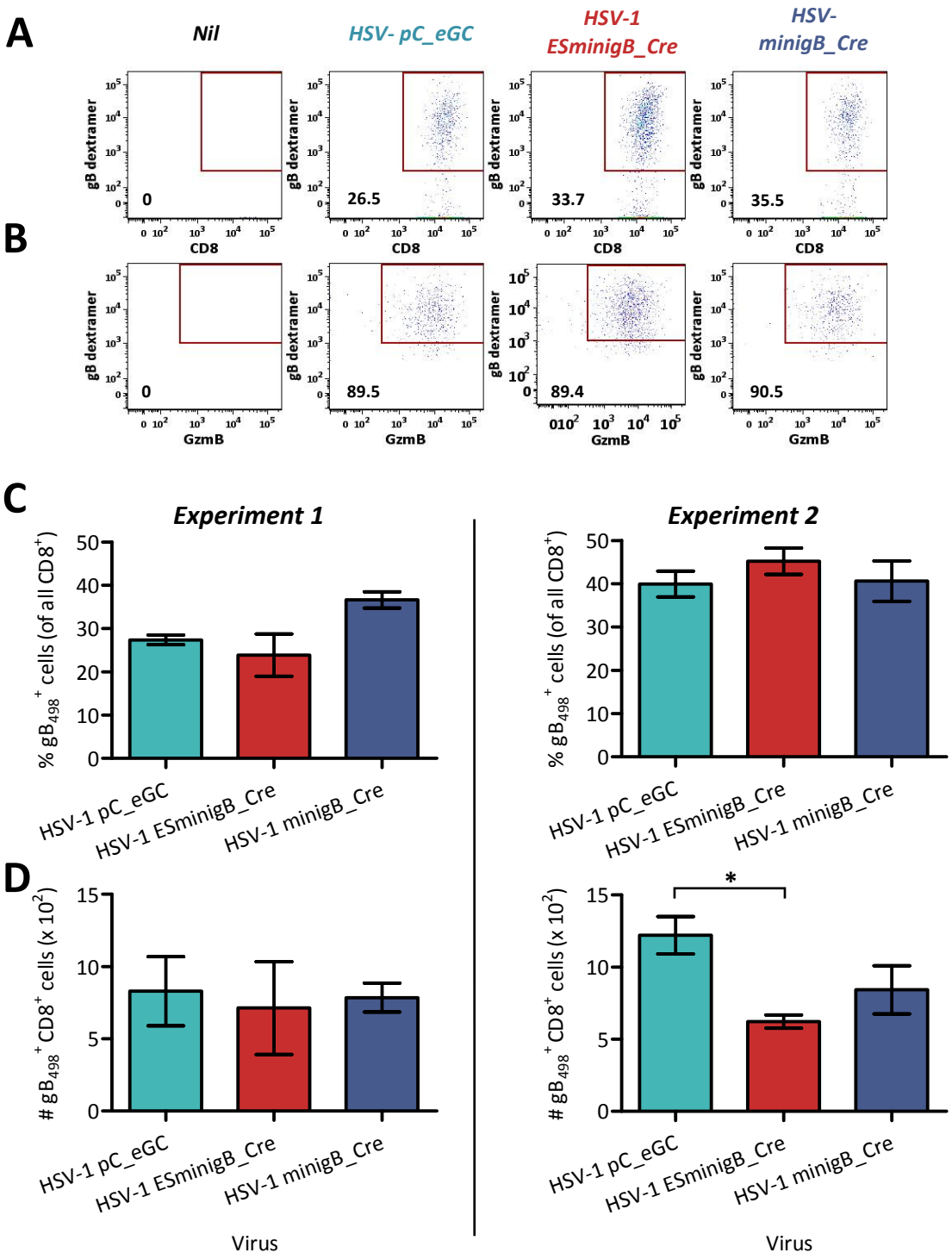

Figure 5-16. The addition of a gB_{498} minigene to HSV-1 does not alter the size of the $CD8^+$ T cell response in the DRG. The $CD8^+$ T cell response in the DRG (from thoracic levels T8 to T13) was measured in the experiments described in Figure 5-17. Representative flow cytometry plots for mice either mock infected (nil), or with HSV-1 pC_eGC, HSV-1 ESminigB_Cre or minigB_Cre showing (A) the percentage gB_{498}-specific CD8+ T cells of all $CD8^+$ T cells within the DRG or (B) the percentage of activated gB_{498}-specific $CD8^+$ T cells of all CD8+ T cells within the DRG, as indicated by the detection of gzmB. The (A) percentage and (B) number gB_{498}-specific CD8+ T cells of all CD8+ T cells within the DRG where n = 3 and mean±SEM. The results of two independent experiments are shown as the left and right panels. The means were compared for each graph by a one way ANOVA with Newman Kwels post test (*$p < 0.05$).

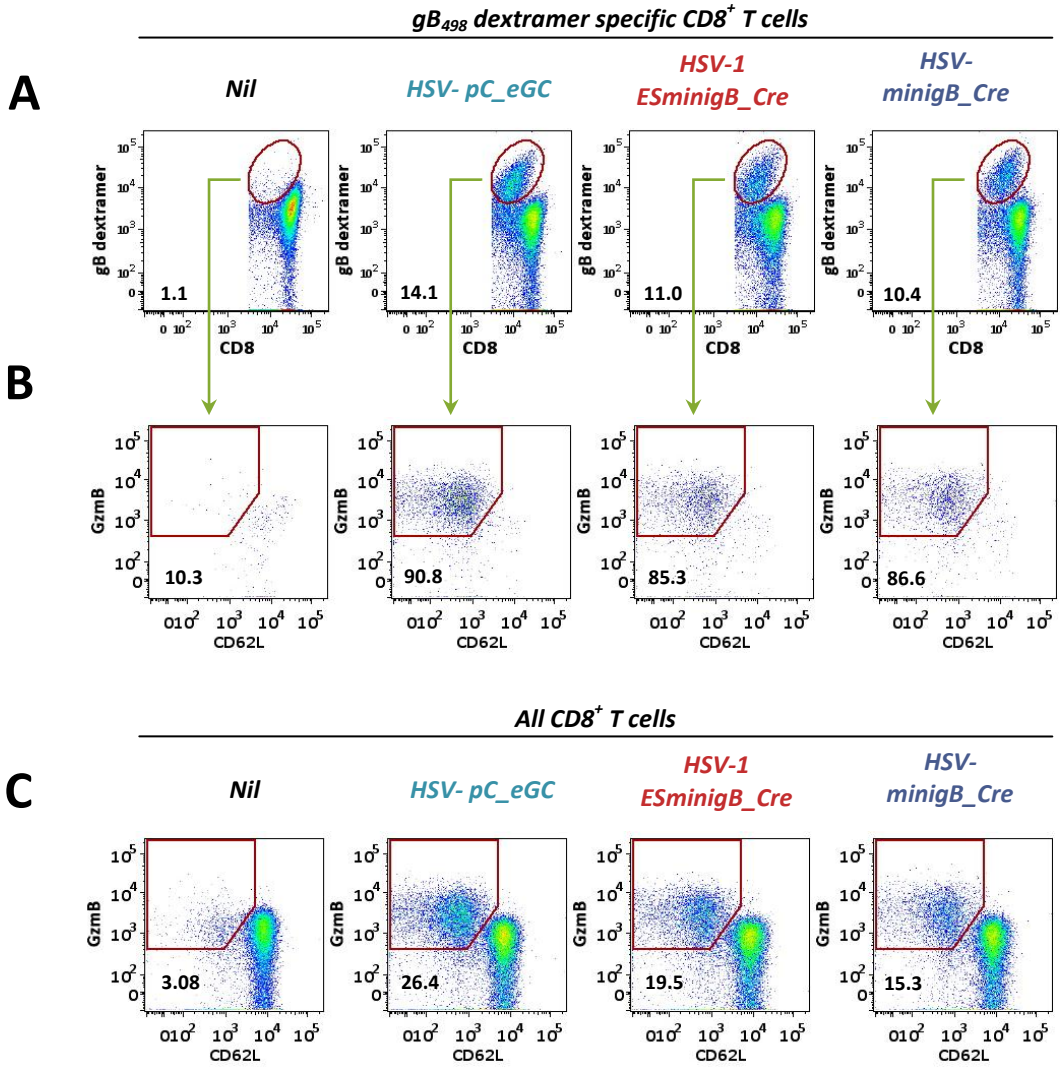

Figure 5-17. The addition of a gB_{498} minigene to HSV-1 does not alter the size of the $CD8^+$ T cell response in the spleen. Groups of two or three C57Bl/6 mice were tattoo infected with 1×10^8 PFU/mL HSV-1 pC_eGC (blue), HSV-1 ESminigB_Cre (red) or HSV-1 minigB_Cre (purple), with one C57Bl/6 control mouse mock infected with PBS. At 7 days p.i. the $CD8^+$ T cell response in the spleen and DRG (shown in Figure 5-17) was measured by gB_{498} dextramer and CD62L surface staining with intracellular staining for gzmB. Representative flow cytometry plots for a mouse infected with each mouse or mock infected (nil) showing (A) the percentage of gB_{498}-specific $CD8^+$ T cells of all $CD8^+$ T cells within the spleen, (B) the percentage of activated gB_{498}-specific $CD8^+$ T cells of all $CD8^+$ T cells within the spleen or (C) the percentage activated $CD8^+$ T cells within the spleen. The (D) the percentage and (E) number of gB_{498}-specific $CD8^+$ T cells of all $CD8^+$ T cells within the spleen where n = 3 and mean±SEM is shown. (F) The percentage of activated gB_{498}-specific $CD8^+$ T cells of all $CD8^+$ T cells within the spleen is shown were n = 2 - 3 and the mean±SEM is shown. (G) The percentage of activated $CD8^+$ T cells within the spleen where n = 2 - 3 and the mean±SEM is shown. The results of two independent experiments are shown by the left and right panels. The means were compared for the data presented in each graph by a one way ANOVA with Newman Kwels post test, but in all cases the difference was not statistically significant ($p > 0.05$).

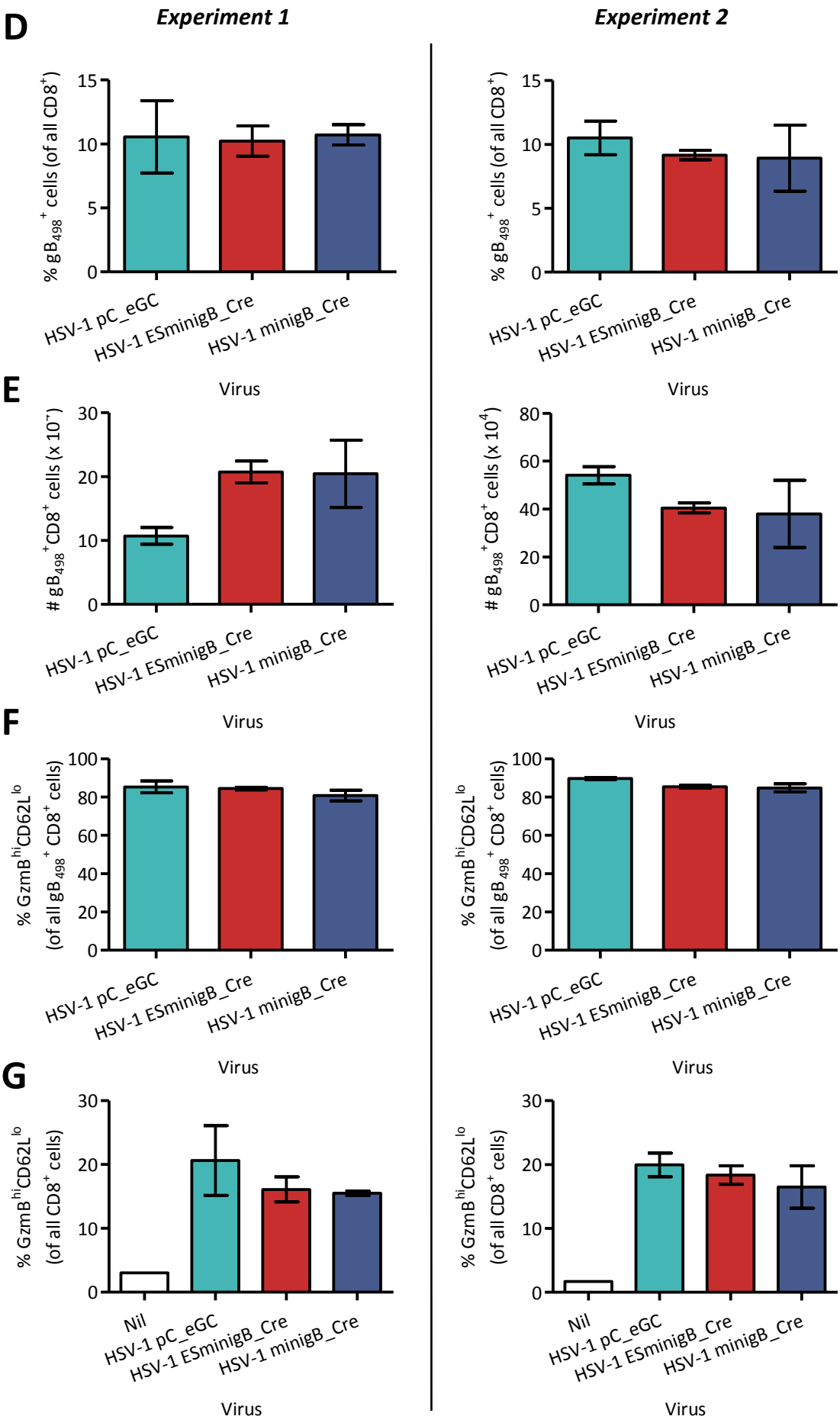
D
Experiment 1
Experiment 2
% gB498+ cells (of all CD8+)
15
10
5
0
HSV-1 pC_eGC
HSV-1 ESminigB_Cre
HSV-1 minigB_Cre
Virus
E
gB498+CD8+ cells (x 10-4)
30
20
10
0
80
60
40
20
F
% GzmBhiCD62Llo (of all gB498+ CD8+ cells)
100
80
60
40
20
G
% GzmBhiCD62Llo (of all CD8+ cells)
Nil

HSV-1 showed an infiltration of approximately 1×10^2 gB_{498} $CD8^+$ T cells (Figure 5-16D). Again, there was no difference in the size of the $CD8^+$ T cell response in the DRG with mice infected with HSV-1 pC_eGC, ESminigB_Cre or minigB_Cre (Figure 5-16). There was a statistically significant increase in the number of gB_{498}-specific $CD8^+$ T cells in the DRG of mice infected with HSV-1 pC_eGC compared to HSV-1 ESminigB_Cre in the second experiment, but such a difference was not observed in the first experiment, and so is not considered to be important.

The gB_{498}-specific $CD8^+$ T cell response in mice infected with HSV-1 pC_eGC, ESminigB_Cre or minigB_Cre was similar as measured in the spleen, with approximately 10% of $CD8^+$ T cells in the spleen being gB_{498} specific (Figure 5-17A&D). This is also reflected in the total number of gB_{498}-specific $CD8^+$ T cells (Figure 5-17E). The majority of the gB_{498}-specific $CD8^+$ T cells exhibited an activated phenotype, with high levels of gzmB and low levels of CD62L (Figure 5-17B&F). The proportion of all $CD8^+$ T cells in the spleen responding to HSV-1 was determined as measured by a $gzmB^{hi}CD62L^{lo}$ phenotype, regardless of specificity (Yuen et al., 2010). Using the gzmB/CD62L method, the total $CD8^+$ T cell response to each of the viruses tested was also found to be very similar (Figure 5-15C&G). Therefore, the insertion of an additional copy of the gB_{498} epitope to HSV-1 does not alter the size of the $CD8^+$ T cell response to HSV-1 in either the spleen, or a site of infection, the DRG innervating the infected skin.

5.4.5 Survival of neurons in mice infected with HSV-1 expressing an immunogenic gB_{498} epitope that is able to evade ICP47-mediated inhibition of TAP

The addition of an additional epitope that evades ICP47-mediated inhibition of TAP should lead to an increase in antigen presentation on the surface of infected neurons. This could lead to an increased engagement of the $CD8^+$ T cell response and a subsequent loss of neurons. The ROSA26R/Cre mouse system can be used to assess the survival of neurons, particularly throughout latency, as both viruses constructed contain an eGFP/Cre cassette under the control of the CMV IE promoter. Therefore, to determine if there is additional loss of neurons in mice infected with a virus that includes a gB_{498} minigene, groups of ROSA26R mice were infected with HSV-1 minigB_Cre and culled at 5, 10, 20, 40 or 100 days p.i. The innervating DRG were removed and the number of β-gal^+ cells determined (Figure 5-18).

The peak in the number of β-gal^+ cells was between 5 and 10 days p.i., but the difference in the number of β-gal^+ cells on these two days was not statistically significant. By contrast, when ROSA26R mice were infected with HSV-1 pC_eGC, where there are significantly more

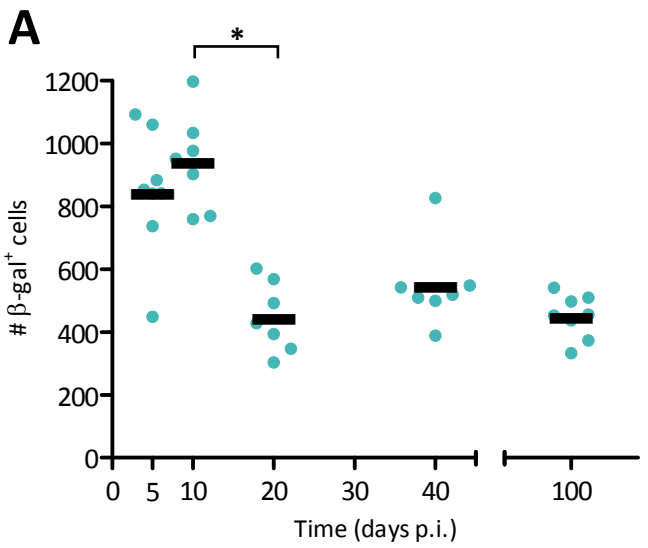

B

Pairwise comparisons from (A)				
Day	5	10	20	40
10	ns			
20	*	*		
40	*	*	ns	
100	*	*	ns	ns

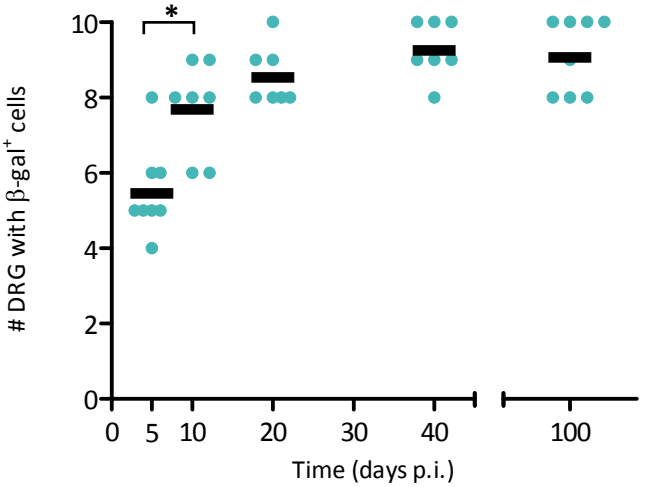

D

Pairwise comparisons from (C)				
Day	5	10	20	40
10	*			
20	*	ns		
40	*	ns	ns	
100	*	ns	ns	ns

Figure 5-18. Expression of β-gal in ROSA26R mice infected with HSV-1 minigB_Cre. Groups of three to five ROSA26R mice were infected with 1×10^8 PFU/mL HSV-1 minigB_Cre. At 5, 10, 20, 40 or 100 days p.i. mice were culled and innervating DRG (from spinal levels T5 to L1) removed and processed for determination of β-gal expression. Both (A) the total number of β-gal+ cells per mouse and (B) the number of DRG per mouse containing at least one β-gal+ cell are shown. Each circle represents one mouse and the black bar represents the mean value for all mice at each time point. The results are pooled from two independent experiments (n = 8 per time point). (B&D) Statistical significance was determined by a one way ANOVA ($p < 0.001$) with Bonferroni's post-test to make pairwise comparisons, with key statistical differences indicated on (A) and (C) (*$p < 0.05$).

β-gal marked cells on day 10 p.i. compared to day five p.i. (Figure 5-18). There was also an increased spread of virus to additional DRG during this time, consistent with that observed for HSV-1 pC_eGC. The number of β-gal$^+$ cells declined as latency was established and remained constant throughout latency, between 20 and 100 days p.i. Therefore, there does not appear to be a significant loss in the number of infected neurons throughout latency in mice infected with HSV-1 engineered to express a cytosolic gB_{498} minigene, or alternatively, increased spread of virus during this time. However, the observation that there may be an increased number of β-gal$^+$ cells in ROSA26R mice infected with HSV-1 minigB_Cre on day five p.i. remained, so to further extend this, the survival of cells in ROSA26R mice infected with HSV-1 ESminigB_Cre was performed as this virus may be expected to have a stronger phenotype in mice.

To assess this, groups of ROSA26R mice were infected with HSV-1 ESminigB_Cre, culled at various times post infection and their DRG removed and the number of β-gal$^+$ cells measured (Figure 5-19). Again, there was an increased number of β-gal marked cells on day 5 p.i., such that there was not a statistically significant increase in the number of β-gal marked cells between days 5 and 10 p.i. However, there was increased spread of virus to different spinal levels at this time, which stabilised after day 10 p.i. The number of β-gal$^+$ cells then declined as latency was established. Latency appeared stable, with the number of β-gal$^+$ cells remaining constant between 20 and 100 days p.i. There was no statistically significant difference in the spread of virus as indicated by the number of DRG that contained at least one β-gal$^+$ cell during latency. Therefore, as far as can be determined within the limits of this assay (discussed in Section 4.6), there was no spread of virus or loss of neurons during latency that occurs with the addition of an ER-targeted gB_{498} minigene to HSV-1.

So, the only difference in the number of infected cells over time for HSV-1 ESminigB_Cre or HSV-1 minigB_Cre was an increased number of β-gal$^+$ cells at 5 days p.i. compared to that typically observed following infection with HSV-1 pC_eGC (refer to Figure 4-2). Therefore, to confirm this observation and directly compare the survival of neurons mice infected with HSV-1 with either an ER-targeted or cytosolic minigene to the HSV-1 pC_eGC, groups of ROSA26R mice were infected with HSV-1 pC_eGC, ESminigB_Cre or minigB_Cre. Mice were culled at four, seven, 10 or 13 days p.i., their innervating DRG removed and the number of β-gal$^+$ cells was counted (Figure 5-20).

For all viruses, the number of β-gal$^+$ cells the increase in the number of β-gal marked cells between four and seven days p.i. was statistically significant. When comparing the number of β-gal marked cells on day four p.i. between the three different viruses, there was no

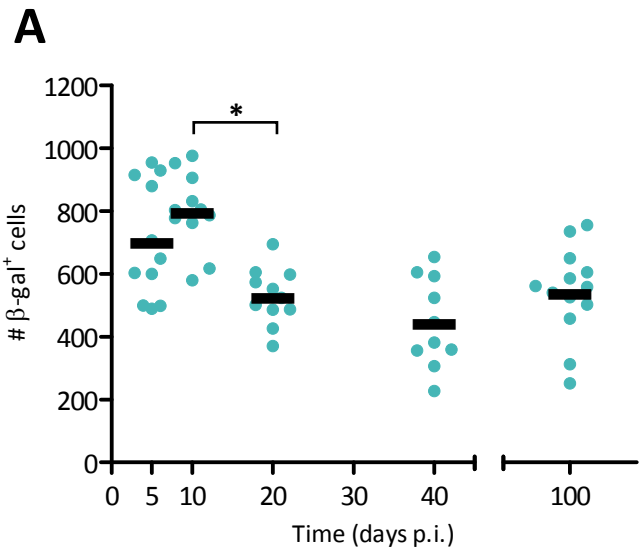

B

Pairwise comparisons from (A)				
Day	5	10	20	40
10	ns			
20	ns	*		
40	*	*	ns	
100	*	*	ns	ns

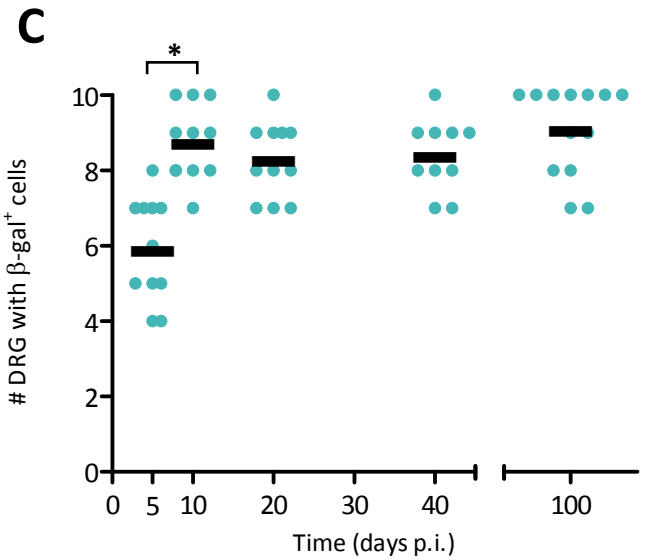

D

Pairwise comparisons from (C)				
Day	5	10	20	40
10	*			
20	*	ns		
40	*	ns	ns	
100	*	ns	ns	ns

Figure 5-19. Expression of β-gal in ROSA26R mice infected with HSV-1 ESminigB_Cre. Groups of three to five ROSA26R mice were infected with 1×10^8 PFU/mL HSV-1 ESminigB_Cre. At 5, 10, 20, 40 or 100 days p.i. mice were culled and innervating DRG (from spinal levels T5 to L1) removed and processed for determination of β-gal expression. Both (A) the total number of β-gal+ cells per mouse and (B) the number of DRG per mouse containing at least one β-gal+ cell are shown. Each circle represents one mouse and the black bar represents the mean value for all mice at each time point. The results are pooled from three independent experiments (n = 10 – 13 per time point). (B&D) Statistical significance was determined by a one way ANOVA ($p < 0.001$) with Bonferroni's post-test to make pairwise comparisons, with key statistical differences indicated on (A) and (C) (*$p < 0.05$).

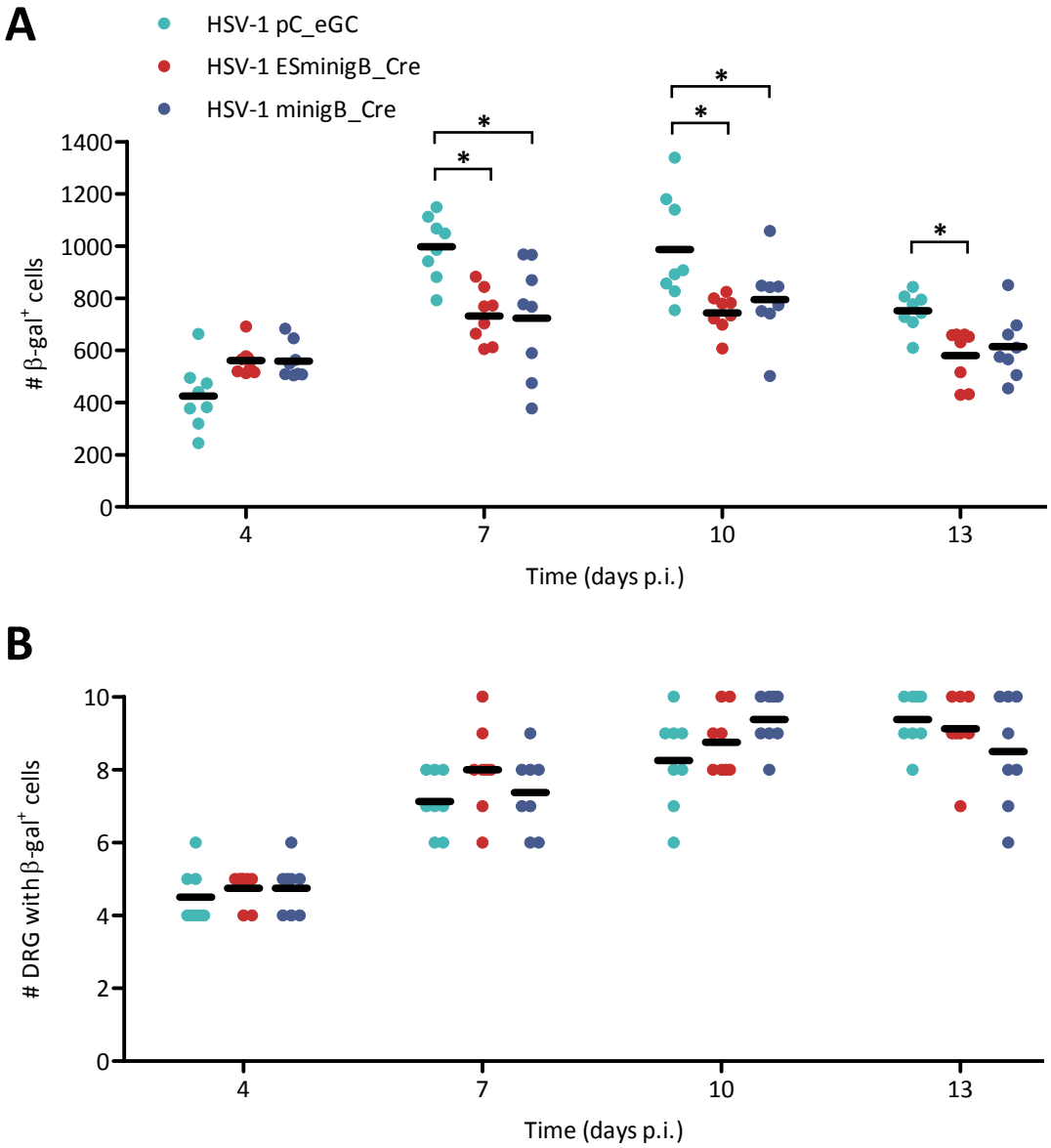

Figure 5-20. Expression of β-gal in ROSA26R mice infected with HSV-1 ESminigB_Cre in direct comparison to minigB_Cre. Groups of two or three ROSA26R mice were infected with 1×10^8 PFU/mL HSV-1 pC_eGC (blue), ESminigB_Cre (red) or minigB_Cre (purple). At 4, 7, 10, or 13 days p.i. mice were culled and innervating DRG (from spinal levels L1 to T5) removed and processed for determination of β-gal expression. Both (A) the total number of β-gal$^+$ cells per mouse and (B) the number of DRG per mouse containing at least one β-gal$^+$ cell are shown. Each circle represents one mouse and the black bar represents the mean value for all mice at each time point. The results are pooled from 3 independent experiments (n = 8 per virus per time point). Statistical significance was determined by a two way ANOVA ($p < 0.001$ for (A) and $p > 0.05$ for (B) with Bonferroni's post-test to make pairwise comparisons (*$p < 0.05$).

statistically significant differences. However, there was significantly more β-gal$^+$ cells in mice infected with HSV-1 pC_eGC, compared to either virus containing an additional copy of the $gB_{498\text{-}505}$ epitope on both seven and 10 days p.i. Therefore, there may be an increased loss of neurons in mice infected with these viruses that occurs around the peak of the CD8$^+$ T cell response (Coles et al., 2002). By day 13 p.i. the difference in the number of β-gal marked cells is largely abrogated, with only a slight, though still significant, difference in the number of β-gal$^+$ cells in mice infected with HSV-1 ESminigB_Cre. Mice infected with all viruses had significantly less β-gal marked cells on day 13 compared to day 10 p.i., consistent with previous results following infection of ROSA26R mice with HSV-1 pC_eGC (Figure 5-20A; refer to Figure 4-3).

For all viruses, there was a statistically significant increase in spread between days four and seven p.i., as shown by the number of DRG that contain at least a single β-gal cell. For HSV-1 minigB_Cre there was also a significant increase in the spread of virus between days seven and 10 p.i., while for HSV-1 pC_eGC there was significantly more spread of virus between days seven and 13 p.i. However, on each day, there was no significant difference in the number of DRG containing at least one β-gal$^+$ cell, indicating that there was no difference in the spread of virus with the addition of a gB_{498} minigene (Figure 5-20B).

Overall, there was no discernible difference in the loss of neurons in mice infected with a virus containing either a cytosolic or ER-targeted minigene. The subtle decrease in the number of β-gal$^+$ neurons relative to HSV-1 pC_eGC is attributable to the addition of an extra copy of the gB_{498} epitope (Figure 5-19). However, there is the very important caveat that HSV-1 minigB_Cre was derived from HSV-1 ESminigB_Cre, and a revertant virus was not constructed. Therefore, it is formally possible that any differences in the accumulation of β-gal marked cells following infection of ROSA26R mice may reflect the effect of an unintended secondary site mutation.

5.5 Discussion

This chapter began with the finding that marked β-gal$^+$ cells continued to accumulate during latency in ROSA26 mice infected with HSV-1 pICP47_eGC, in addition to the substantial cell marking that takes place during latency establishment. This is indicative that ICP47 expression continues to occur in additional neurons during latency. However, examining the temporal expression of eGFP or Tdtomato as regulated by this promoter during the establishment phase of latency and beyond did not lead to the detection of any

reporter gene activity (refer to Section 5.3.4). Therefore, this led to the conclusion that any expression of ICP47 during this time is likely to be at a low level and transient.

There are disadvantages to using an ectopic locus to express *cre* under the ICP47 promoter, but it was felt that this virus design would be most likely to faithfully model ICP47 expression. Often proteins are tagged with reporter genes to ensure they are expressed with identical kinetics, but in this case it was unfeasible. ICP47 is a small, approximately 12 kDa, protein (88 amino acids long), and the fusion of an additional 146 kDa eGFP/Cre or 35 kDa Cre protein would be likely to disrupt its function and prevent it from binding TAP (Abremski and Hoess, 1984; Phillips, 2001; Rixon and McGeoch, 1984). Alternatively, the *eGFP/Cre* gene could be inserted in place of U_S12 so that eGFP/Cre is expressed under the native ICP47 promoter. However, ICP47 function would need to be restored to HSV-1, probably by inserting it into an ectopic location under its native promoter, which has similar limitations to the virus constructed in this thesis. Further, the replacement of ICP47 may disrupt other regulatory elements in this region. The U_S10, U_S11 and U_S12 genes are encoded by three mRNAs that have distinct 5' termini but a common 3' terminus. As such, the U_S12 transcript has a long untranslated region. Further, the ORFs of the U_S10 and U_S11 genes overlap each other out-of-frame (Rixon and McGeoch, 1984). Finally, insertion of *eGFP/Cre* under the control of an IRES behind the U_S12 gene could be performed, such that eGFP/Cre is expressed under the native U_S12 promoter (Adam et al., 1991; Ghattas et al., 1991; as reviewed by Ngoi et al., 2004). However, genes under the control of an IRES are not always expressed as abundantly as the gene under direct promoter control, and the addition of such a large sequence may result in a significant disruption to this area of the genome (Hennecke et al., 2001; Mizuguchi et al., 2000; Rixon and McGeoch, 1984). Despite their limitations, the construction of these viruses and the investigation of their behaviour *in vivo*, particularly using the ROSA26R mouse system, represents an important future direction for the confirmation of the results presented in this chapter.

By using the ICP47/22 promoter, the data presented in this thesis indicates that ICP47 and/or ICP22 may be expressed during the establishment of latency. While the focus of this thesis has been on ICP47, ICP22 plays an important role during HSV-1 infection. As described previously, ICP47 has been demonstrated to have an immunomodulatory role in HSV-1 infection, inhibiting the transport of antigen, and thus plays a role in protecting cells from the $CD8^+$ T cell response (Früh et al., 1995; Goldsmith et al., 1998; Hill et al., 1995; Orr et al., 2007; York et al., 1994). Further, a recent analysis of the HSV-1 transcriptome by RNAseq revealed that ICP47 is one of the most abundantly transcribed genes in productively infected TG neuronal cultures, suggesting it may be highly expressed

in the PNS *in vivo* (Harkness et al., 2014). Despite this, a mutant virus that fails to express ICP47 showed that ICP47 expression has little impact on corneal and skin disease severity following ocular infection. This observation is typically attributed to the poor binding of ICP47 to mouse TAP. This virus lacking ICP47 expression also replicated normally in the skin, possibly because IFN-γ is able to stimulate upregulation of MHC-I, balancing the poor inhibition of murine TAP by ICP47 (Ahn et al., 1996; Goldsmith et al., 1998; Tigges et al., 1996; Tomazin et al., 1996; Wallach et al., 1982).

ICP47 is just one of many HSV-1 immune modulators that are expressed during the course of the acute infection, targeting all facets of the antiviral response. For example, the virion host shutoff protein has been shown to be an important immunomodulator that counteracts the innate immune response through multiple mechanisms, including the shutdown of the host cell's protein synthesis, leading to down-regulation of MHC-I expression (Kwong and Frenkel, 1987; Pasieka et al., 2009; Suzutani et al., 2000; Tigges et al., 1996). Likewise, the γ34.5, ICP0 and U_S11 proteins all help HSV to evade type I IFN activity via a number of different mechanisms (Leib et al., 2000; Lin et al., 2004; as reviewed by Paladino and Mossman, 2009; Sanchez and Mohr, 2007). The HSV-1 glycoproteins also play important roles in immunoevasion. Glycoprotein L and gE bind antibody on the surface of infected cells and virions, forming bipolar bridges that allow them to escape neutralisation by complement and antibody dependent killer cells (Frank and Friedman, 1989; Lubinski et al., 2011; Nagashunmugam et al., 1998). Further, gC acts as a C3B receptor, blocking activation of both the alternative and classical complement pathways (Hung et al., 1994; Kostavasili et al., 1997; Lubinski et al., 1998). In summary, HSV-1 does express other immune modulators, but ICP47 is unique as it is expressed early in the gene expression cascade, and targets the $CD8^+$ T cell response (Goldsmith et al., 1998; Harkness et al., 2014).

It was originally believed that neurons do not express MHC-I, suggesting that this was a site where the virus could reside that helps it to evade the immune response (Joly et al., 1991; Lampson and Fisher, 1984; Wong et al., 1984). However, it was shown in 1992 (Simmons and Tscharke) that $CD8^+$ T cells play an important role in controlling the acute infection in ganglia. Moreover, more recent, sensitive analyses have revealed that neurons are able to express MHC-I (Goddard et al., 2007). The expression of MHC-I is usually upregulated in response to stimuli such as cytokines, direct injury and, in particular, viral infection, such as during acute HSV-1 infection (Lampson and Fisher, 1984; Maehlen et al., 1988; as reviewed by Neumann, 2001; O'Malley and MacLeish, 1993; Pereira and Simmons, 1999; Pereira et al., 1994; Wallach et al., 1982). There is little evidence to suggest that latently infected neurons express MHC-I, but it is likely to be upregulated

during reactivation, possibly in response to IFN-γ production (Lampson and Fisher, 1984; Pereira et al., 1994; Wallach et al., 1982). Therefore, given the exquisite sensitivity of $CD8^+$ T cells to even very low levels of antigen, the low level of MHC-I expression and the results presented in this thesis suggesting continued expression of ICP47 during latency, it is likely ICP47 could have a significant impact on the $CD8^+$ T cell response to HSV-1 in the PNS by restricting antigen presentation on MHC-I (Purbhoo et al., 2004). This is reinforced by the increased neurovirulence of HSV-1 that lacks ICP47 expression (Goldsmith et al., 1998).

ICP47 could help HSV-1 to avoid $CD8^+$ T cell surveillance in the ganglia during latency and thereby facilitate reactivation, but the frequency of reactivation or the stability of latency has not been measured using any of the mutant viruses available which lack ICP47 (Goldsmith et al., 1998; Mavromara-Nazos et al., 1986). The general consensus is that neurons fail to survive reactivation, but results presented in this thesis suggest that those cells that experience ICP47 expression during latency survive and continue to accumulate. This seeming paradox may be explained by the ability of ICP47 to prevent transport by human TAP far more efficiently than mouse TAP (Ahn et al., 1996; Früh et al., 1995; Jugovic et al., 1998; Tomazin et al., 1996; York et al., 1994). In an effort to address this issue, Orr and colleagues (2005) introduced inhibitors of antigen presentation from other herpesviruses which block MHC-I expression on mouse cells in an effort to mimic the inhibition of antigen presentation by HSV-1 observed in humans. This included US11 from human Cytomegalovirus (CMV), which binds the MHC-I heavy chain in the ER and translocates it to the cytoplasm for degradation, and m152 from murine CMV, which retains MHC-I complexes in the ER/*cis* Golgi intermediate compartment (Ameres et al., 2014; Wiertz et al., 1996; Ziegler et al., 2000; Ziegler et al., 1997). They found that murine fibroblasts were more susceptible to $CD8^+$ T cell mediated lysis. This translated into a loss of $CD8^+$ T cell mediated control of the acute infection and increased virulence (Orr et al., 2005; Orr et al., 2007). Further, the frequency of induced reactivation *in vivo* following UV irradiation was increased in mice infected with HSV-1 containing the genes encoding either US11 or m152 in a $CD8^+$ T cell dependent manner (Orr et al., 2007). However, both US11 and m152 inhibit different stages of MHC-I presentation, which may not be as effective as that of ICP47 in human cells. For example, US11 is just one of four genes encoded by human CMV that is able to inhibit MHC-I presentation, and its effectiveness in preventing antigen presentation is restricted by factors like MHC allotype (Ameres et al., 2014). Further, although m152 effectively blocks presentation *in vitro*, it has less effect on the $CD8^+$ T cell response *in vivo* (Gold et al., 2002). Alternatively, a more relevant approach to examining the role of ICP47 is to develop a transgenic mouse in which murine TAP is

replaced with human TAP, also known as a humanised TAP mouse. This model would most likely be viable as it is known that human TAP can interact with mouse MHC molecules, loading them with viral peptides (Tscharke et al., 2005). Further, the expression of mouse, but not human, TAP in a stable HeLa cell line designed to express ICP47 allowed for the transport of peptide (Früh et al., 1995). In this mouse model, ICP47 would bind more efficiently to TAP, and this confounding variable could then be removed, and the importance of ICP47 truly explored.

In an attempt to determine the functional relevance of ICP47, two viruses that incorporate a gB_{498} minigene designed to enhance presentation on MHC-I were constructed and studied. The gB_{498} peptide was presented as efficiently as both an ER targeted or cytosolic minigene in both murine or human derived cell lines (refer to Section 5.4.4). Both ER-targeted and cytosolic minigenes are generally presented much more efficiently than antigen that is processed from full length protein, which is typically an inefficient process at physiological levels (Antón et al., 1997; Porgador et al., 1997; Princiotta et al., 2003). Therefore, these results confirm that the efficiency of presentation of the gB_{498} minigene is able to overwhelm any potential inhibition by TAP (Ahn et al., 1996; Früh et al., 1995; Jugovic et al., 1998; Tomazin et al., 1996). However, this result could be due to methodological differences, as the effect of ICP47 inhibition of TAP on the presentation of antigen on MHC-I on the cell surface was not directly measured. Instead, the ability of cytotoxic T cells to lyse infected human or mouse fibroblasts was used as a surrogate measure of inhibition of MHC-I presentation (Karttunen et al., 1992; Mueller et al., 2002; York et al., 1994), whereas in this chapter the activation of a gB_{498} specific hybridoma following stimulation with infected cells was used to infer gB_{498} presentation. Overall, the most reasonable interpretation is that the expression of the gB_{498} minigene effectively swamps the antigen presentation pathways and is able to overcome any effect ICP47 inhibition may have on antigen presentation.

No differences were observed in the stability of latency within ROSA26 mice infected with HSV-1 pC_eGC, HSV-1 ESminigB_Cre or minigB_Cre but given the limited sensitivity of this system, the ineffectiveness of ICP47 in mice and their lack of spontaneous reactivation, this was not unexpected (Ahn et al., 1996; Deatly et al., 1987; Früh et al., 1995; Gebhardt and Halford, 2005; Jugovic et al., 1998; Laycock et al., 1991; Tomazin et al., 1996). Further, the results presented by Orr and colleagues (2007), who found an increased rate of reactivation following UV irradiation, suggest that the impact of ICP47 may be greatest on reactivation. In this thesis, induced reactivation was assessed by explant, a less physiological method of reactivation that is largely independent of the host's immune response, and is not very sensitive (Sawtell and Thompson, 2004; Stevens and Cook,

1971). The assessment of the ability of the virus to reactivate in each individual ganglion by explant is more sensitive, and reflects not just the ability of the virus to reactivate but also the spread of virus during the acute infection and beyond. Further, it may be of interest to investigate the frequency of reactivation in a more relevant model, such as UV induced reactivation, which can be used in mice with an intact immune system (Shimeld et al., 1996b; Wakim et al., 2008c).

The only differences in phenotype of these viruses were observed during the acute infection, contrary to what was hypothesised based on the continued accumulation of β-gal marked cells in ROSA26R mice infected with HSV-1 pICP47 during latency establishment and beyond. On days four and seven p.i. there were significantly fewer β-gal marked cells in ROSA26 mice. Given how small this difference was and the lack of a revertant virus to control for secondary site mutations, the importance of these findings is unclear. There was less virus in the DRG of those mice infected with viruses containing a gB minigene, although this difference was not found to be statistically significant. The most striking difference was the increased lesion size in mice infected with either HSV-1 ESminigB_Cre or minigB_Cre relative to the control virus HSV-1 pC_eGC, peaking at days four to six p.i. The disease severity of herpes labialis is correlated with viral load (Rytel et al., 1978; Spruance et al., 1977), but the amount of virus in the skin at five days p.i. was similar for HSV-1 pC_eGC, ESminigB_Cre and minigB_Cre. It would be of interest to see if there is continued persistence of infectious virus beyond day five p.i. Despite this marked difference in lesion size, there did not appear any difference in the day when the lesions healed. There is the caveat that a proper revertant control virus was not constructed, but the insertion of an extra copy of the gB_{498} epitope under the control of different promoters into two independently derived HSV-1 resulted in a similar increase in lesion size following tattoo infection (Tijana Stefanovic and David Tscharke, unpublished data). Overall, the insertion of a copy of the gB_{498} minigene into HSV-1 suggested that the larger lesion size may be due to increased immunopathology.

The timing of the difference in lesion size implicates $CD8^+$ T cells, as well as suggesting a role for cells of the innate immune response in this phenomenon, such as NK cells or macrophages, likely mediated by altered cytokine production (Coles et al., 2002; Kodukula et al., 1999; Liu et al., 1996; Stumpf et al., 2002; Van Lint et al., 2004). Recently, the role of proinflammatory processes on the progression and resolution of HSV skin lesions has begun to be appreciated, with two clinical trials showing an increased efficacy of topical acyclovir when combined with a hydrocortisone cream (as reviewed by Hull et al., 2011; Hull et al., 2014). Further, it is believed that the proinflammatory cytokines like TNF-α,

IFN-γ and IL-6 can play an important role in mediating HSV-1 infection (Geiger et al., 1997; Kodukula et al., 1999; Liu et al., 1996; Pasieka et al., 2009; Stumpf et al., 2002). For example, mice lacking IL-6 are more likely to succumb to lethal HSV-1 ocular infection following infection with the McKrae strain. Further, there were no observable differences in viral replication, spread to the nervous system, establishment of latency or reactivation relative to wildtype mice, suggesting that this is mediated by immunopathology (LeBlanc et al., 1999). Consistent with this, mice lacking IL-6 have also been shown to exhibit less corneal inflammation than control mice following infection with the RE strain of HSV-1 (Fenton et al., 2002). As expected, the addition of a gB_{498} minigene had little impact on the generation of the $CD8^+$ T cell response towards HSV-1 (Goldsmith et al., 1998; Orr et al., 2005). As minigenes, including the gB_{498} minigene, are only able to be presented via direct presentation, the only effect should be on antigen presentation by infected cells, and not on cross presentation, which is carried out by APCs that prime the $CD8^+$ T cell response (Wong and Tscharke, unpublished data; Bosnjak et al., 2005; Jirmo et al., 2009; Mueller et al., 2002). It is likely that the increased expression of the immunodominant gB_{498} epitope on infected cells leads to a more effective $CD8^+$ T cell response, especially in the PNS where MHC-I expression is lower (Pereira et al., 1994). Therefore, it would be of interest to examine the production of IFN-γ and other proinflammatory cytokines in mice infected with these viruses. Further, as these cytokines mediate the influx of other immune cells which could potentially mediate the skin pathology observed, it would be of interest to measure infiltration of NK cells, macrophages or γδ $CD8^+$ T cells.

The discovery that ICP47 may be expressed during the establishment phase of latency and beyond further confirms the role of ICP47 in the intersection between the host's immune response and viral reactivation. In light of the stability of latency in mice, the relatively poor ability of ICP47 to bind to murine TAP, and the results presented in this chapter, ICP47 warrants further investigation, particularly when considering latency. This coincides with an increasing appreciation for the role $CD8^+$ T cells play in mediating the maintenance of and reactivation from latency (recently reviewed by Egan et al., 2013).

6 | Final discussion

Herpesviruses are ubiquitous, connected by their central defining characteristic, which is their ability to establish latency. Historically, HSV latency was believed to be especially profound, a paradigm that has shaped HSV research. However, despite decades of research, the role of disparate biological factors, both virus and host, in regulating latency remains enigmatic. Although approximately one third of those infected with HSV will experience a symptomatic episode (reviewed by Whitley et al., 1998), there is no vaccine against HSV-1 (McAllister and Schleiss, 2014) and only limited, often ineffective, options for antiviral drug treatment available. There is currently no treatment available that targets the virus during latency, or enables clearance of the latent reservoir of viral DNA (reviewed by James and Prichard, 2014). Further, recurrent ocular infection is responsible for most of the morbidity associated with HSV-1 (Rolinski and Hus, 2014). As such it is critical that we develop a greater understanding of HSV-1 latency and reactivation to address this significant health issue. This final discussion will draw together the important themes of this thesis, beginning with the need to continually develop and improve upon models to investigate HSV. Next, the establishment phase of latency will be considered, with particular emphasis on the implications of low level viral activity during this time in the context of a strong $CD8^+$ T cell response. Finally, a model for viral reactivation during latency will be elaborated upon, which discusses the multiple barriers that the virus must overcome prior to reactivation, viral dissemination and recrudescence.

In this thesis, the ROSA26R/Cre mouse system was employed to track viral gene expression, allowing permanent marking of cells that have experienced promoter activity, even if this activity is not ongoing. Central to the use of this model was the development of methods for the generation of recombinant HSV that express Cre recombinase with minimal disruption to the viral genome, described in Chapter three. By optimising the transfection/infection method for generating recombinant virus, as well as incorporating the CRISPR/Cas9 technology, the efficiency by which these viruses could be constructed was greatly improved, with a more 200-fold increase in efficiency of recombination when CRISPR/Cas9 is employed in conjunction with the optimised transfection/infection method compared to the transfection/infection based method alone (Russell et al., 2015). These improvements facilitated the construction of the viruses required to investigate lytic viral gene expression during both the lytic infection and latency, as described in chapters four and five. This also included several viruses that proved too difficult to construct before the adoption of the CRISPR/Cas9 system. In the future, this system will likely prove invaluable for generating recombinant HSV-1 more efficiently with minimal unintended disruptions of the viral genome, particularly small changes such as single point mutations or deletions of protein domains (Bi et al., 2014; Russell et al., 2015;

Suenaga et al., 2014). Given the current advances in genome engineering using CRISPR/Cas9 technology (Doudna and Charpentier, 2014), these advances will aid in the development of more effective models for the study of HSV-1, including both animal and tissue culture systems.

The acute HSV-1 infection has been relatively well characterised, but the absence of infectious virus, coinciding with the peak in the CD8 T cell response, at day seven p.i. is often considered to mark the resolution of this stage of infection (Coles et al., 2002; Luker et al., 2002; Sawtell et al., 1998; Sedarati et al., 1989; Simmons and Nash, 1984; Simmons and Tscharke, 1992; Speck and Simmons, 1998; Van Lint et al., 2004). One of the most striking findings of this thesis was that the peak in the number of β-gal marked neurons in ROSA26R mice infected with HSV-1 pC_eGC, HSV-1 pgB_eGC or HSV-1 pICP0_eGC was at 10 days p.i., beyond the resolution of the acute infection as conventionally determined. This large disparity is unlikely to be accounted for by the low level viral activity that has been detected during this time (Ramachandran et al., 2008; Sawtell, 2003; Sawtell et al., 1998; Sedarati et al., 1989; Shimeld et al., 1995; Steiner et al., 1989; Thompson et al., 1986). It is clear some cells that become β-gal marked will not go on to establish latency, as the number of β-gal marked neurons decreases between days 10 and 20 p.i. in ROSA26R infected mice. However, β-gal marked neurons are detectable during latency in distal DRG like L1 and T5 that were not detectable in ROSA26R mice infected five days previously. Therefore, latency must be established in at least some neurons that are marked between days five and 10 p.i. and there is value in examining this typically ignored stage of the HSV-1 infection.

The antiviral immune response is dramatically different later during the acute infection (between days five and 10 p.i.), with a strong proinflammatory cytokine environment, and the development of a primed $CD8^+$ T cell response, which is believed to be responsible for the cessation of the lytic infection (Coles et al., 2002; Halford et al., 1996a; Shimeld et al., 1997; Simmons and Tscharke, 1992; Van Lint et al., 2004). The presence of these $CD8^+$ T cells may serve to rescue neurons infected with HSV-1, so a latent, rather than lytic, infection may be established in a larger proportion of neurons at this later time p.i. This would be consistent with the observation that, despite the development of a strong $CD8^+$ T cell response during acute HSV-1 infection, there is very little destruction of neuronal tissue in either mice, rabbits or humans, especially in non-ocular models that are associated with lower levels of inflammation (Himmelein et al., 2015; Perng et al., 2000b; Simmons and Tscharke, 1992; Theil et al., 2003a).

A number of non-cytolytic mechanisms have already been identified by which $CD8^+$ T cells may be able to play such a role. For example, Knickelbein and colleagues (2008) proposed that $CD8^+$ T cells may act by a non-cytotoxic mechanism to help maintain latency, in which gzmB cleaves ICP4, presumably to prevent viral gene transcription that could lead to reactivation. GzmA, which is not directly cytolytic, may also play a role in restricting the viral load in ganglia, particularly at later times p.i. (Pereira et al., 2000). Similarly, IFN-γ may also be able to play such a role. In IFN-γ knockout mice, infectious virus is shed for longer after the resolution of the acute infection compared to wildtype mice, although most studies find no difference in the titre of virus within the ganglia during the acute infection (Bouley et al., 1995; Cantin et al., 1999; Leib et al., 1999; Minami et al., 2002). Despite this, there were increased numbers of apoptotic cells in the brains of transgenic mice that are unable to express IFN-γ compared to wildtype mice following intravitreal inoculation with HSV-1 strain F (Geiger et al., 1997). It is also known that IFN-γ can block ICP0 and gC promoter activity as well as reactivation in some neurons in latently infected *ex vivo* TG cultures without an observable cytolytic effect (Decman et al., 2005b; Liu et al., 2001). Likewise, IFN-α can induce a quiescent infection similar to latency following infection of porcine TG neurons (De Regge et al., 2010). There has even been the suggestion that the abundant TNF-α produced at later times p.i. may play some role in viral latency due to its role in protecting neurons against excitogenic and oxidative damage (Shimeld et al., 1997).

Central to this is the other noteworthy finding presented in this thesis is that, unlike for all other HSV-1 that express Cre from a lytic promoter, the number of β-gal marked cells in ROSA26R mice infected with HSV-1 pICP47_eGC continues to rise throughout the establishment of latency and beyond, a finding explored in chapter five. This suggests ICP47 and/or ICP22 may be expressed especially frequently during the establishment of latency. ICP47 acts to inhibit antigen presentation on MHC-I and evade the $CD8^+$ T cell response (York et al., 1994), which may not be cytolytic but instead acts to promote the establishment of latency. Therefore, expression of ICP47 during latency establishment may represent a time of infrequent, abortive attempts at reactivation. ICP22 was first identified as a transactivator of viral gene expression, and so activity under this promoter seems compatible with reactivation, but ICP22 is only required for the expression of some late genes, such as U_S11, U_L44 and U_L48 (Long et al., 1999; Rice et al., 1995; Sears et al., 1985). Rather, ICP22 seems to serve more to limit viral gene expression and modulate the host's transcription machinery (reviewed by Rice and Davido, 2013). As such, the expression of a more promiscuous transactivator like ICP4 (DeLuca and Schaffer, 1985; Dixon and Schaffer, 1980; Smith et al., 1993), or the multifunctional ICP0 proteins

(Everett, 1984; O'Hare and Hayward, 1985), may be more compatible with such a hypothesis. However, such a trend was not observed when Proença and colleagues (2008; 2011) examined the historical activity of the ICP4 and ICP0 promoters in the ROSA26R/Cre mouse model. Therefore, it seems that the establishment phase of latency is a time of conflicting factors, with some promoting viral infection and even reactivation, and others promoting suppression of the viral genome. Further, this phase of infection is also influenced by the host's $CD8^+$ T cell response.

While the establishment and maintenance of latency is a critical part of the HSV-1 life cycle, in order to disseminate the virus to new hosts, reactivation must occur to produce and shed infectious virus. Overcoming this initial inhibition that serves to maintain latency is important for the progression to productive infection, with reactivation on a neuronal level likely to be frequent, but partial (Schiffer et al., 2009). However, there are many hurdles that must be surmounted before reactivation occurs. This includes repression of viral gene expression by the host, downregulation of viral RNAs such as the LATs, and overcoming the various aspects of the host's immune response, ranging from the intrinsic antiviral response through to the role of $CD8^+$ T_{RM} cells in the skin.

Chromatin-mediated repression of the viral genome is generally effective, but there is low level transcription of some viral genes from all regions of the genome in approximately two thirds of latently infected neurons (Ma et al., 2014). Therefore, rather than an impregnable epigenetic barrier to viral gene expression, there exists a balance of more permissive and repressive epigenetic marks that generally favours a repressive environment of facultative chromatin in the majority of latently infected neurons (Cliffe et al., 2009; Wang et al., 2005b). This is particularly true of the LAT region of the genome, which appears to exist in a bivalent state (Kubat et al., 2004a; Kubat et al., 2004b; Kwiatkowski et al., 2009). Given that generally a pool of neuronal tissue is used for a ChIP assay, it is believed that different viral genomes are associated with different epigenetic marks, potentially regulated by the expression of the LATs by an as yet undefined mechanism (reviewed by Bloom et al., 2010). However, for productive reactivation to occur, chromatin remodelling of the viral genome is an essential early step. Reactivation in animal models is followed by a decrease in permissive euchromatic marks on the LAT region and a subsequent increase in RNA abundance and euchromatic marks on other areas of the viral genome (Amelio et al., 2006a; Creech and Neumann, 2010; Neumann et al., 2007a).

The removal of repressive epigenetic marks on the histones associated with the viral genome is closely linked with the initiation of productive viral gene expression following

reactivation. The actions of one or more transactivators have been implicated in initiating the cascade of viral lytic gene expression after reactivation is triggered (Halford et al., 2001), but the importance of different proteins is unknown. Of particular interest are VP16 and ICP0, due to their dual roles in the transactivation of lytic gene expression and in chromatin remodelling (Coleman et al., 2008; Ferenczy and DeLuca, 2011; Herrera and Triezenberg, 2004; Thompson et al., 2009), providing an attractive link between epigenetic derepression of the viral genome and activation of gene expression. However, as yet no clear mechanism has been elucidated. The most likely explanation is that viral gene expression is biphasic, with an initial disordered stage of viral lytic gene expression (Du et al., 2015; Kim et al., 2012). This disordered expression is likely to be ongoing, corresponding to the low level viral gene transcription detected throughout latency (Ma et al., 2014). This is followed by more widespread derepression of the viral genome that leads to the expression of the viral lytic gene expression cascade (Kim et al., 2012), possibly facilitated by key transactivators like VP16.

Concurrent with the initiation of viral lytic gene expression following reactivation is the downregulation of LATs and the short non-coding RNAs encoded within, as well as the various miRNAs associated with the latent infection (Du et al., 2015; Du et al., 2011). Although a mechanism remains to be defined, LATs play a role in regulating the expression of lytic viral genes throughout latency (Chen et al., 1997; Garber et al., 1997; Giordani et al., 2008; Maillet et al., 2006), probably by modulating chromatin (Cliffe et al., 2009; Kwiatkowski et al., 2009; Wang et al., 2005b). LATs also contain short noncoding RNAs that can inhibit apoptosis and the production of infectious virus, thereby mediating reactivation (Peng et al., 2008; Perng et al., 2002; Perng et al., 2000b; Shen et al., 2009). Likewise, although miRNA expression is not essential for the maintenance of latency, they may still have an important role (Du et al., 2015; Kramer et al., 2011). It has been shown that the abrogation of miR-H2 expression leads to an increase in ICP0 expression and a slightly increased rate of reactivation, while stimulating miR-H6 can downregulate ICP4 expression (Jurak et al., 2014; Umbach et al., 2008; Umbach et al., 2009).

It is probable that the expression of viral genes and the modulation of chromatin occurs frequently as the virus attempts to reactivate, but this viral activity is not undetectable by neurons. Intrinsic antiviral immune responses occur during the acute HSV-1 infection, but they are generally insufficient to counter viral replication (Lilley et al., 2011; Rosato and Leib, 2014). These responses includes cellular innate immune mechanisms, such as autophagy, and mechanisms to repression of viral replication and transcription, mainly mediated through nuclear domain 10 proteins (Everett et al., 2006; Lilley et al., 2011; Lukashchuk and Everett, 2010; Yordy et al., 2012). Further, latent infection alters the

transcriptional profile of the ganglia as a whole, with alterations in expression level of multiple genes involved in immune responses in particular, but also cellular metabolism and neuronal physiology (Clement et al., 2008; Kent and Fraser, 2005; Kramer et al., 2003). Similarly, changes in cellular gene expression also occur in induced reactivation models of HSV-1 infection (Higaki et al., 2004; Hill et al., 2001; Kent and Fraser, 2005), although in both cases the interpretation of these results is difficult due to the relatively small population of neurons within the ganglia that are infected. Finally, there is also evidence that neuronal functions may help to maintain latency, such as by NGF signaling through receptor tyrosine kinases (Camarena et al., 2010; Kristie et al., 1999). Therefore, it is reasonable that an intrinsic antiviral response may act to counter reactivation and maintain latency. Some of the first evidence of this was provided by Ma and colleagues (2014), who found evidence that the expression of even low numbers of lytic viral transcripts during latency resulted in a modulation of the host cell's gene expression associated with antiviral activity and cell survival. The neuron seems to be acting to block these reactivation attempts (Ma et al., 2014), and therefore overwhelming this intrinsic antiviral response is likely to be important an important step towards reactivation.

Beyond the cell intrinsic immune response, activated $CD8^+$ T cells are retained within the DRG of both humans and mice, and are able to control virion release within a localised area (Khanna et al., 2003; Theil et al., 2003a; Verjans et al., 2007). The retention of these cells within DRG in an activated state suggests the expression of antigen (Van Lint et al., 2005). This antigen is likely to be expressed only at a low level, especially compared to the frequency by which viral transcription occurs during latency. The level of antigen is likely too low for the activation and recruitment of circulating $CD8^+$ T cells (Kurts et al., 1999), but sufficient to maintain activation of those cells retained within the DRG. Although this could represent an aborted reactivation attempt, it may also be an integral part of HSV-1 latency. Evidence presented in this thesis shows that activity of the ICP6 and gB promoters occurs during latency that can lead to protein production, which the neuron is able to survive, despite the retention of ICP6 and gB-specific $CD8^+$ T cells in the DRG (Khanna et al., 2003; Sheridan et al., 2009; St. Leger et al., 2013; St. Leger et al., 2011). The failure to detect this accumulation of β-gal marked neurons in the ROSA26R/Cre mouse model when promoters for the viral transactivators like ICP0, ICP4 or VP16 were used (Proença et al., 2008; Proença et al., 2011) argues against this activity representing attempted reactivation by the virus that is aborted by responding cytotoxic $CD8^+$ T cells leading to the death of the neuron. It is more consistent with the model proposed by Liu and colleagues (2001; 2000) where $CD8^+$ T cells act to prevent possible reactivation without the death of the latently infected neuron to help maintain latency. They showed that withdrawal of

$CD8^+$ T cells, and the IFN-γ they produce, from latently infected TG cultures can mediate reactivation. Conversely, the addition of exogenous HSV-1 or gB_{498} specific $CD8^+$ T cells can restrict viral replication and cytopathic effect, although viral DNA, and immediate early and early transcripts were still detectable (Liu et al., 2001; Liu et al., 2000). Related to this is the model described by Knickelbein and colleagues (2008) where $CD8^+$ T cells act by a non-cytotoxic, but at least partially gzmB-dependent, mechanism to help maintain latency. Similarly, it has been found that $gzmB^+$ $CD8^+$ T cells are found within the TG of HSV-1 infected humans in the absence of detectable neuronal damage (Theil et al., 2003a; Verjans et al., 2007). Evidence is also presented in this thesis showing that ICP47 promoter activity leading to the production of viral protein can occur during latency. Given the role of ICP47 in inhibiting TAP (Früh et al., 1995; Hill et al., 1995) expression of this protein during latency may be critical for progression to reactivation, especially in the context of the low MHC-I expression on neurons. Overall, this suggests that the expression of low levels of antigen may be a part of a non-progressing latent infection, but overcoming this $CD8^+$ T cell response at the neuron, possibly through ICP47, is an important hurdle that must be overcome on the path to reactivation.

If the virus manages to derepress the viral genome and initiate viral gene expression, downregulate expression of the LATs and miRNAs, evade the localised $CD8^+$ T cell response within the ganglion and produce virions within the neuron, it will still face a robust immune response at the skin surface, with emerging lesions often controlled within 24 hours as shown by the presence of viral shedding from the skin (Mark et al., 2008). $CD8^+$ T_{RM} cells found lodged in the skin play a crucial role in preventing reactivation, acting as a form of immune surveillance (Gebhardt et al., 2009; Gebhardt et al., 2011; Mackay et al., 2012). This is most clearly demonstrated by the presence of $CD8\alpha\alpha^+$ T cells in the skin of humans infected with HSV-2, which closely resemble the T_{RM} $CD8^+$ T cells identified in mice. The presence of these $CD8\alpha\alpha^+$ T cells was found to be correlated with increased virus control (Schiffer et al., 2010; Zhu et al., 2007; Zhu et al., 2013). Other $CD8^+$ T_{EM} cells can also be recruited from circulation to counter viral reactivation, in addition to $CD4^+$ T cells, innate effectors and APCs (Donaghy et al., 2009; Zhu et al., 2007). These cells have direct cytotoxic action against newly infected cells in the skin, and produce antiviral cytokines (Zhu et al., 2007; Zhu et al., 2013). Finally, if this peripheral immunity is overcome, the neuronal infection of the epithelial cells will lead to productive, potentially symptomatic, reactivation (Schiffer et al., 2010). Given the multiple hurdles HSV-1 has to overcome before reactivation occurs, it is unsurprising that recrudescence is relatively infrequent.

More than a decade ago now, Wagner and Bloom (1997) asked the question of whether HSV-1 latency provides a complete model for alphaherpesvirus latent infection and reactivation. HSV-1 was long been viewed as the prototypic latent virus, with an almost-quiescent infection established. However, lately, less restrictive, more complex models are gaining favour, which consider the many factors that drive HSV-1 latency. The absence of lytic viral transcription is no longer considered to be a hallmark of HSV-1 latency, with multiple reports detailing the detection of lytic transcripts from all regions of the genome during latency of both mice and humans (Chen et al., 2002a; Chen et al., 1997; Derfuss et al., 2009; Derfuss et al., 2007; Feldman et al., 2002; Kramer and Coen, 1995; Kramer et al., 1998; Ma et al., 2014; Maillet et al., 2006; Pesola et al., 2005; Tal-Singer et al., 1997). This correlates better with the paradigm of VZV latency, in which viral transcripts for up to 12 genes are detectable in human tissue, usually TG, as detected by ISH or RT-qPCR (Cohrs et al., 1996; Cohrs et al., 2003; Kennedy et al., 2000; Nagel et al., 2011). Interestingly, while the explant of human TG results in reactivation of HSV-1 but not VZV (Baringer and Swoveland, 1973; Plotkin et al., 1977), only IE63 transcripts are detectable in tissue removed and processed from nine hours of death, suggesting that these transcripts are expressed during latency (Ouwendijk et al., 2012). To extend this even further by considering all *herpesviruses*, the role of viral transcription during latency is considered necessary to ensure the genome is maintained in dividing cells, while evading the host's immune response and preventing apoptosis (as reviewed by Speck and Ganem, 2010; Wagner and Bloom, 1997). It has long been assumed that the site of HSV-1 latency within the nucleus of non-dividing sensory neurons precluded the need for such viral activity (Wagner and Bloom, 1997). However, HSV-1 may act to both evade the host's immune response, potentially through the action of ICP47 as discussed in this thesis, and can prevent apoptosis during latency through the action of the LATs (Perng et al., 2000b). While clearly the herpesviruses are a diverse group of viruses with many unique strategies that they employ for latency establishment, maintenance and reactivation, in a broader sense, HSV-1 can no longer be considered unique due to the almost global repression of its genome and lack of transcription – rather, at least in regards to transcriptional activity during latency, it exists on the more repressive end of the spectrum of the *herpesviruses.*

As such, parallels may be able to be drawn between viral transcription and protein production during VZV latency and HSV-1 latency. In the context of HSV-1, such activity is thought to maintain the host's virus specific $CD8^+$ T cell response within the DRG, so a similar mechanism may be responsible for the maintenance of latency operates in those latently infected with VZV. Clearly there is an important role for the cell-mediated immune response in controlling both viral infections, but the nature of this interaction is different

in the context of these two infections (Mori and Nishiyama, 2005). The host's immune response is thought to be important for maintaining VZV latency, with clinical disease resulting from a failure of this immunity with age (Kinchington, 1999; Levin et al., 2003). By contrast, episodes of HSV-1 recrudescence tend to decrease with age (Benedetti et al., 1999). Similarly, VZV-reactive T cells are not retained within ganglia (Verjans et al., 2007), but activated HSV-reactive T cells are retained within latently infected sensory ganglia and act to control HSV-1 virion release within the ganglia and prevent viral reactivation (Khanna et al., 2003; Liu et al., 2001; Liu et al., 2000). Further, despite often infecting the same sensory ganglia or even the same neuron in humans (Cohrs et al., 2005; Cohrs et al., 2000; Theil et al., 2003b; Verjans et al., 2007), reactivation results from different stimuli through different molecular pathways (Kinchington, 1999). Clearly then, there are still notable differences between VZV and HSV-1 infection. Others also include substantial differences in pathogenesis of these viruses, the lack of conservation of the LATs, and the severe host range restriction of VZV (Cohen, 2010; as reviewed by Kennedy et al., 2015b; as reviewed by Kinchington, 1999; Weller and Stoddard, 1952). Therefore, although the concept that HSV-1 is unique as the prototypic silent herpesvirus is clearly outdated, there is still value in comparing the mechanistic basis of latency for different *herpesviruses*.

To summarise, this thesis investigated the spread of virus during the establishment of latency using the ROSA26R/Cre mouse model, finding evidence that the spread of virus occurs beyond the acute infection as defined by the presence of infectious virus, an often neglected phase of infection. Results presented in this thesis indicate viral lytic promoter activity during latency occurs that can lead to viral protein production, and implicate a means by which the virus interacts with the host's immune response during latency. Since the neuron, host immune response and HSV-1 are inextricably linked (Divito et al., 2006), multiple, apparently conflicting, hypotheses mask the fact that it is likely that no one factor is responsible for establishing, maintaining or reactivating from latency. Rather, there are multiple layers of reactivation that must be overcome to facilitate reactivation, but the final outcome, namely viral shedding at the surface and disease presence, is relatively rare. Given this complexity, further research is required, particularly at the interface between the immune response and the virus during latency, to further understand HSV-1 and α-herpesvirus latency, hopefully leading to better therapeutic outcomes.

References

Abremski, K., and Hoess, R. (1984). Bacteriophage P1 site-specific recombination. Purification and properties of the Cre recombinase protein. Journal of Biological Chemistry *259*, 1509-1514.

Abremski, K., and Hoess, R. (1985). Phage P1 Cre-loxP site-specific recombination: Effects of DNA supercoiling on catenation and knotting of recombinant products. Journal of Molecular Biology *184*, 211-220.

Ace, C. I., McKee, T. A., Ryan, J. M., Cameron, J. M., and Preston, C. M. (1989). Construction and characterization of a Herpes Simplex Virus type 1 mutant unable to transinduce immediate-early gene expression. Journal of Virology *63*, 2260-2269.

Adam, M. A., Ramesh, N., Miller, A. D., and Osborne, W. R. (1991). Internal initiation of translation in retroviral vectors carrying picornavirus 5' nontranslated regions. Journal of Virology *65*, 4985-4990.

Advani, S. J., Brandimarti, R., Weichselbaum, R. R., and Roizman, B. (2000a). The disappearance of cyclins A and B and the increase in activity of the G_2/M-phase cellular kinase cdc2 in Herpes Simplex Virus 1-infected cells require expression of the α22/US1.5 and UL13 viral genes. Journal of Virology *74*, 8-15.

Advani, S. J., Weichselbaum, R. R., and Roizman, B. (2000b). The role of cdc2 in the expression of Herpes Simplex Virus genes. Proceedings of the National Academy of Sciences *97*, 10996-11001.

Ahmed, M., and Fraser, N. W. (2001). Herpes Simplex Virus type 1 2-kilobase latency-associated transcript intron associates with ribosomal proteins and splicing factors. Journal of Virology *75*, 12070-12080.

Ahmed, M., Lock, M., Miller, C. G., and Fraser, N. W. (2002). Regions of the Herpes Simplex Virus type 1 Latency-Associated Transcript that protect cells from apoptosis *in vitro* and protect neuronal cells *in vivo*. Journal of Virology *76*, 717-729.

Ahn, K., Meyer, T. H., Uebel, S., Sempé, P., Djaballah, H., Yang, Y., Peterson, P. A., Früh, K., and Tampé, R. (1996). Molecular mechanism and species specificity of TAP inhibition by Herpes Simplex Virus ICP47. The EMBO Journal *15*, 3247-3255.

Allan, R. S., Smith, C. M., Belz, G. T., van Lint, A. L., Wakim, L. M., Heath, W. R., and Carbone, F. R. (2003). Epidermal viral immunity induced by CD8α$^+$ dendritic cells but not by langerhans cells. Science *301*, 1925-1928.

Allen, S. J., Rhode-Kurnow, A., Mott, K. R., Jiang, X., Carpenter, D., Rodriguez-Barbosa, J. I., Jones, C., Wechsler, S. L., Ware, C. F., and Ghiasi, H. (2014). Interactions between Herpesvirus Entry Mediator (TNFRSF14) and Latency-Associated Transcript during Herpes Simplex Virus 1 latency. Journal of Virology *88*, 1961-1971.

Amelio, A. L., Giordani, N. V., Kubat, N. J., O'Neil, J. E., and Bloom, D. C. (2006a). Deacetylation of the Herpes Simplex Virus type 1 Latency-Associated Transcript (LAT) enhancer and a decrease in LAT abundance precede an increase in ICP0 transcriptional permissiveness at early times postexplant. Journal of Virology *80*, 2063-2068.

Amelio, A. L., McAnany, P. K., and Bloom, D. C. (2006b). A chromatin insulator-like element in the Herpes Simplex Virus type 1 Latency-Associated Transcript region binds CCCTC-binding factor and displays enhancer-blocking and silencing activities. Journal of Virology *80*, 2358-2368.

Ameres, S., Besold, K., Plachter, B., and Moosmann, A. (2014). CD8 T cell–evasive functions of Human Cytomegalovirus display pervasive MHC allele specificity, complementarity, and cooperativity. The Journal of Immunology *192*, 5894-5905.

Antinone, S. E., and Smith, G. A. (2010). Retrograde axon transport of Herpes Simplex Virus and Pseudorabies Virus: A live-cell comparative analysis. Journal of Virology *84*, 1504-1512.

Antón, L. C., Yewdell, J. W., and Bennink, J. R. (1997). MHC class I-associated peptides produced from endogenous gene products with vastly different efficiencies. The Journal of Immunology *158*, 2535-2542.

Antoniou, A. N., Ford, S., Alphey, M., Osborne, A., Elliott, T., and Powis, S. J. (2002). The oxidoreductase ERp57 efficiently reduces partially folded in preference to fully folded MHC class I molecules. The EMBO Journal *21*, 2655-2663.

Araki, K., Imaizumi, T., Okuyama, K., Oike, Y., and Yamamura, K.-i. (1997). Efficiency of recombination by Cre transient expression in embryonic stem cells: Comparison of various promoters. Journal of Biochemistry *122*, 977-982.

Arbusow, V., Derfuss, T., Held, K., Himmelein, S., Strupp, M., Gurkov, R., Brandt, T., and Theil, D. (2010). Latency of Herpes Simplex Virus type-1 in human geniculate and vestibular ganglia is associated with infiltration of $CD8^+$ T cells. Journal of Medical Virology *82*, 1917-1920.

Arduino, P. G., and Porter, S. R. (2006). Oral and perioral Herpes Simplex Virus type 1 (HSV-1) infection: Review of its management. Oral Diseases *12*, 254-270.

Arnosti, D. N., Preston, C. M., Hagmann, M., Schaffner, W., Hope, R. G., Laughlan, G., and Luisi, B. F. (1993). Specific transcriptional activation *in vitro* by the Herpes Simplex Virus protein VP16. Nucleic Acids Research *21*, 5570-5576.

Arthur, J. L., Scarpini, C. G., Connor, V., Lachmann, R. H., Tolkovsky, A. M., and Efstathiou, S. (2001). Herpes Simplex Virus type 1 promoter activity during latency establishment, maintenance, and reactivation in primary dorsal root neurons *in vitro*. Journal of Virology *75*, 3885-3895.

Aubert, M., Chen, Z., Lang, R., Dang, C. H., Fowler, C., Sloan, D. D., and Jerome, K. R. (2008). The antiapoptotic Herpes Simplex Virus glycoprotein J localizes to multiple cellular organelles and induces reactive oxygen species formation. Journal of Virology *82*, 617-629.

Aubert, M., Krantz, E. M., and Jerome, K. R. (2006). Herpes Simplex Virus genes U_S3, U_S5, and U_S12 differentially regulate cytotoxic T lymphocyte-induced cytotoxicity. Viral Immunology *19*, 391-408.

Bacik, I., Cox, J. H., Anderson, R., Yewdell, J. W., and Bennink, J. R. (1994). TAP (Transporter associated with Antigen Processing)-independent presentation of endogenously synthesized peptides is enhanced by endoplasmic reticulum insertion sequences located at the amino- but not carboxyl-terminus of the peptide. The Journal of Immunology *152*, 381-387.

Bader, C., Crumpacker, C. S., Schnipper, L. E., Ransil, B., Clark, J. E., Arndt, K., and Freedberg, I. M. (1978). The natural history of recurrent facial-oral infection with Herpes Simplex Virus. The Journal of Infectious Diseases *138*, 897-965.

Bae, S., Park, J., and Kim, J.-S. (2014). Cas-OFFinder: A fast and versatile algorithm that searches for potential off-target sites of Cas9 RNA-guided endonucleases. Bioinformatics *30*, 1473-1475.

Baer, R., Bankier, A. T., and Biggin, M. D. (1984). DNA sequence and expression of the B95-8 Epstein-Barr virus genome. Nature *310*, 207-211.

Bahram, S., Arnold, D., Bresnahan, M., Strominger, J. L., and Spies, T. (1991). Two putative subunits of a peptide pump encoded in the human Major Histocompatibility Complex class II region. Proceedings of the National Academy of Sciences *88*, 10094-10098.

Baines, J. D., and Roizman, B. (1991). The open reading frames U_L3, U_L4, U_L10, and U_L16 are dispensable for the replication of Herpes Simplex Virus 1 in cell culture. Journal of Virology *65*, 938-944.

Balan, P., Davis-Poynter, N., Bell, S., Atkinson, H., Browne, H., and Minson, T. (1994). An analysis of the *in vitro* and *in vivo* phenotypes of mutants of Herpes Simplex Virus type 1 lacking glycoproteins gG, gE, gI or the putative gJ. Journal of General Virology *75*, 1245-1258.

Balliet, J. W., Kushnir, A. S., and Schaffer, P. A. (2007). Construction and characterization of a Herpes Simplex Virus type I recombinant expressing green fluorescent protein: Acute phase replication and reactivation in mice. Virology *361*, 372-383.

Baringer, J. R., and Swoveland, P. (1973). Recovery of Herpes-Simplex Virus from human trigeminal ganglions. New England Journal of Medicine *288*, 648-650.

Barklie Clements, J., Watson, R. J., and Wilkie, N. M. (1977). Temporal regulation of Herpes Simplex Virus type 1 transcription: Location of transcripts on the viral genome. Cell *12*, 275-285.

Bartel, D. P. (2009). MicroRNAs: Target recognition and regulatory functions. Cell *136*, 215-233.

Bastian, F. O., Rabson, A. S., Yee, C. L., and Tralka, T. S. (1972). Herpesvirus hominis: Isolation from human trigeminal ganglion. Science *178*, 306-307.

Bastian, T. W., Livingston, C. M., Weller, S. K., and Rice, S. A. (2010). Herpes Simplex Virus type 1 immediate-early protein ICP22 is required for VICE domain formation during productive viral infection. Journal of Virology *84*, 2384-2394.

Batard, P., Peterson, D. A., Devêvre, E., Guillaume, P., Cerottini, J.-C., Rimoldi, D., Speiser, D. E., Winther, L., and Romero, P. (2006). Dextramers: New generation of fluorescent MHC class I/peptide multimers for visualization of antigen-specific CD8+ T cells. Journal of Immunological Methods *310*, 136-148.

Batchelor, A. H., and O'Hare, P. (1990). Regulation and cell-type-specific activity of a promoter located upstream of the Latency-Associated Transcript of Herpes Simplex Virus type 1. Journal of Virology *64*, 3269-3279.

Bedoui, S., Whitney, P. G., Waithman, J., Eidsmo, L., Wakim, L., Caminschi, I., Allan, R. S., Wojtasiak, M., Shortman, K., Carbone, F. R., *et al.* (2009). Cross-presentation of viral and self antigens by skin-derived $CD103^+$ dendritic cells. Nature Immunology *10*, 488-495.

Benedetti, J. K., Zeh, J., and Corey, L. (1999). Clinical reactivation of genital Herpes Simplex Virus infection decreases in frequency over time. Annals of Internal Medicine *131*, 14-20.

Bennink, J. R., Yewdell, J. W., Smith, G. L., Moller, C., and Moss, B. (1984). Recombinant Vaccinia Virus primes and stimulates Influenza haemagglutinin-specific cytotoxic T cells. Nature *311*, 578-579.

Berthomme, H., Lokensgard, J., Yang, L., Margolis, T., and Feldman, L. T. (2000). Evidence for a bidirectional element located downstream from the Herpes Simplex Virus type 1 Latency-Associated Promoter that increases its activity during latency. Journal of Virology *74*, 3613-3622.

Bevan, M. J. (1976a). Cross priming for a secondary cytotoxic response to minor H antigens with H2 congenic cells which do not cross react in the cytotoxic assay. Journal of Experimental Medicine *143*, 1283-1288.

Bevan, M. J. (1976b). Minor H antigens introduced on H-2 different stimulating cells cross-react at the cytotoxic T cell level during *in vivo* priming. The Journal of Immunology *117*, 2233-2238.

Bi, Y., Sun, L., Gao, D., Ding, C., Li, Z., Li, Y., Cun, W., and Li, Q. (2014). High-efficiency targeted editing of large viral genomes by RNA-guided nucleases. PLoS Pathogens *10*, e1004090.

Bjorkman, P. J., Saper, M. A., Samraoui, B., Bennett, W. S., Strominger, J. L., and Wiley, D. C. (1987). The foreign antigen binding site and T cell recognition regions of class I histocompatibility antigens. Nature *329*, 512-518.

Bloom, D. C., Devi-Rao, G. B., Hill, J. M., Stevens, J. G., and Wagner, E. K. (1994). Molecular analysis of Herpes Simplex Virus type 1 during epinephrine-induced reactivation of latently infected rabbits *in vivo*. Journal of Virology *68*, 1283-1292.

Bloom, D. C., Giordani, N. V., and Kwiatkowski, D. L. (2010). Epigenetic regulation of latent HSV-1 gene expression. Biochimica et Biophysica Acta (BBA) - Gene Regulatory Mechanisms *1799*, 246-256.

Bloom, D. C., Hill, J. M., Devi-Rao, G., Wagner, E. K., Feldman, L. T., and Stevens, J. G. (1996). A 348-base-pair region in the Latency-Associated Transcript facilitates Herpes Simplex Virus type 1 reactivation. Journal of Virology *70*, 2449-2459.

Blyth, W. A., Harbour, D. A., and Hill, T. J. (1984). Pathogenesis of zosteriform spread of Herpes Simplex virus in the mouse. Journal of General Virology *65*, 1477-1486.

Boissière, S. L., Hughes, T., and O'Hare, P. (1999). HCF-dependent nuclear import of VP16. The EMBO Journal *18*, 480-489.

Bolovan, C. A., Sawtell, N. M., and Thompson, R. L. (1994). ICP34.5 mutants of Herpes Simplex Virus type 1 strain 17^{syn+} are attenuated for neurovirulence in mice and for replication in confluent primary mouse embryo cell cultures. Journal of Virology *68*, 48-55.

Booy, F. P., Newcomb, W. W., Trus, B. L., Brown, J. C., Baker, T. S., and Steven, A. C. (1991). Liquid-crystalline, phage-like packing of encapsidated DNA in Herpes Simplex Virus. Cell *64*, 1007-1015.

Borst, E. M., Posfai, G., Pogoda, F., and Messerle, M. (2004). Mutagenesis of herpesvirus BACs by allele replacement. Methods in molecular biology *256*, 269-279.

Boshart, M., Weber, F., Jahn, G., Dorsch-Hasler, K., Fleckenstein, B., and Schaffner, W. (1985). A very strong enhancer is located upstream of an immediate early gene of human cytomegalovirus. Cell *41*, 521-530.

Bosnjak, L., Miranda-Saksena, M., Koelle, D. M., Boadle, R. A., Jones, C. A., and Cunningham, A. L. (2005). Herpes simplex virus infection of human dendritic cells induces apoptosis and allows cross-presentation via uninfected dendritic cells. The Journal of Immunology *174*, 2220-2227.

Bouley, D. M., Kanangat, S., Wire, W., and Rouse, B. T. (1995). Characterization of Herpes Simplex Virus type-1 infection and herpetic stromal keratitis development in IFN-γ knockout mice. The Journal of Immunology *155*, 3964-3971.

Bourne, N., Stanberry, L. R., Connelly, B. L., Kurawadwala, J., Straus, S. E., and Krause, P. R. (1994). Quantity of Latency-Associated Transcript produced by Herpes Simplex Virus is

not predictive of the frequency of experimental recurrent genital herpes. The Journal of Infectious Diseases *169*, 1084-1087.

Boutell, C., and Everett, R. D. (2013). Regulation of alphaherpesvirus infections by the ICP0 family of proteins. Journal of General Virology *94*, 465-481.

Bowman, J. J., Orlando, J. S., Davido, D. J., Kushnir, A. S., and Schaffer, P. A. (2009). Transient expression of Herpes Simplex Virus type 1 ICP22 represses viral promoter activity and complements the replication of an ICP22 null virus. Journal of Virology *83*, 8733-8743.

Branco, F. J., and Fraser, N. W. (2005). Herpes Simplex Virus type 1 Latency-Associated Transcript expression protects trigeminal ganglion neurons from apoptosis. Journal of Virology *79*, 9019-9025.

Broberg, E. K., Nygårdas, M., Salmi, A. A., and Hukkanen, V. (2003). Low copy number detection of Herpes Simplex Virus type 1 mRNA and mouse Th1 type cytokine mRNAs by light cycler quantitative real-time PCR. Journal of Virological Methods *112*, 53-65.

Burton, E. A., Hong, C.-S., and Glorioso, J. C. (2003a). The stable 2.0-kilobase intron of the Herpes Simplex Virus type 1 Latency-Associated Transcript does not function as an antisense repressor of ICP0 in nonneuronal cells. Journal of Virology *77*, 3516-3530.

Burton, E. A., Huang, S., Goins, W. F., and Glorioso, J. C. (2003b). Use of the Herpes Simplex Virus genome to construct gene therapy vectors. In Viral Vectors for Gene Therapy, C.A. Machida, ed. (Totowa, Springer Science & Business Media).

Bustin, S. A. (2010). Why the need for qPCR publication guidelines?—The case for MIQE. Methods *50*, 217-226.

Bustin, S. A., Benes, V., Garson, J. A., Hellemans, J., Huggett, J., Kubista, M., Mueller, R., Nolan, T., Pfaffl, M. W., Shipley, G. L.*, et al.* (2009). The MIQE Guidelines: Minimum information for publication of quantitative real-time PCR experiments. Clinical Chemistry *55*, 611-622.

Bzik, D. J., Fox, B. A., DeLuca, N. A., and Person, S. (1984). Nucleotide sequence specifying the glycoprotein gene, gB, of Herpes Simplex Virus type 1. Virology *133*, 301-314.

Cai, W., Astor, T. L., Liptak, L. M., Cho, C., Coen, D. M., and Schaffer, P. A. (1993). The Herpes Simplex Virus type 1 regulatory protein ICP0 enhances virus replication during acute infection and reactivation from latency. Journal of Virology *67*, 7501-7512.

Cai, W., and Schaffer, P. A. (1992). Herpes Simplex Virus type 1 ICP0 regulates expression of immediate-early, early, and late genes in productively infected cells. Journal of Virology *66*, 2904-2915.

Camarena, V., Kobayashi, M., Kim, J. Y., Roehm, P., Perez, R., Gardner, J., Wilson, A. C., Mohr, I., and Chao, M. V. (2010). Nature and duration of growth factor signaling through receptor tyrosine kinases regulates HSV-1 latency in neurons. Cell Host and Microbe *8*, 320-330.

Campbell, M. E. M., Palfreyman, J. W., and Preston, C. M. (1984). Identification of Herpes Simplex Virus DNA sequences which encode a *trans*-acting polypeptide responsible for stimulation of immediate early transcription. Journal of Molecular Biology *180*, 1-19.

Cantin, E., Tanamachi, B., and Openshaw, H. (1999). Role for gamma interferon in control of Herpes Simplex Virus type 1 reactivation. Journal of Virology *73*, 3418-3423.

Cantin, E. M., Hinton, D. R., Chen, J., and Openshaw, H. (1995). Gamma interferon expression during acute and latent nervous system infection by Herpes Simplex Virus type 1. Journal of Virology *69*, 4898-4905.

Caradonna, S. J., and Cheng, Y. C. (1981). Induction of uracil-DNA glycosylase and dUTP nucleotidohydrolase activity in Herpes Simplex Virus-infected human cells. Journal of Biological Chemistry *256*, 9834-9837.

Carpenter, D., Hsiang, C., Brown, D. J., Jin, L., Osorio, N., BenMohamed, L., Jones, C., and Wechsler, S. L. (2007). Stable cell lines expressing high levels of the Herpes Simplex Virus type 1 LAT are refractory to caspase 3 activation and DNA laddering following cold shock induced apoptosis. Virology *369*, 12-18.

Carr, D. J. J., Austin, B. A., Halford, W. P., and Stuart, P. M. (2009). Delivery of interferon-γ by an adenovirus vector blocks Herpes Simplex Virus type 1 reactivation *in vitro* and *in vivo* independent of RNase L and double-stranded RNA-dependent protein kinase pathways. Journal of Neuroimmunology *206*, 39-43.

Carrozza, M. J., and DeLuca, N. A. (1996). Interaction of the viral activator protein ICP4 with TFIID through TAF250. Molecular and Cellular Biology *16*, 3085-3093.

Carter, B. S., Fletcher, J. S., and Thompson, R. C. (2010). Analysis of messenger RNA expression by *in situ* hybridization using RNA probes synthesized via *in vitro* transcription. Methods *52*, 322-331.

Cha, T., Tom, E., Kemble, G., Duke, G., Mocarski, E., and Spaete, R. (1996). Human Cytomegalovirus clinical isolates carry at least 19 genes not found in laboratory strains. Journal of Virology *70*, 78-83.

Chelbi-Alix, M. K., and de The, H. (1999). Herpes virus induced proteasome-dependent degradation of the nuclear bodies-associated PML and Sp100 proteins. Oncogene *18*, 935-941.

Chen, J., and Silverstein, S. (1992). Herpes Simplex Virus with mutations in the gene encoding ICP0 are defective in gene expression. Journal of Virology *66*, 2916-2927.

Chen, M., Abele, R., and Tampé, R. (2003). Peptides induce ATP hydrolysis at both subunits of the Transporter associated with Antigen Processing. Journal of Biological Chemistry *278*, 29686-29692.

Chen, S.-H., Lee, L. Y., Garber, D. A., Schaffer, P. A., Knipe, D. M., and Coen, D. M. (2002a). Neither LAT nor Open Reading Frame P mutations increase expression of spliced or intron-containing ICP0 transcripts in mouse ganglia latently infected with Herpes Simplex Virus. Journal of Virology *76*, 4764-4772.

Chen, S., Kramer, M., Schaffer, P., and Coen, D. (1997). A viral function represses accumulation of transcripts from productive-cycle genes in mouse ganglia latently infected with Herpes Simplex Virus. Journal of Virology *71*, 5878-5884.

Chen, S. H., Garber, D. A., Schaffer, P. A., Knipe, D. M., and Coen, D. M. (2000). Persistent elevated expression of cytokine transcripts in ganglia latently infected with Herpes Simplex Virus in the absence of ganglionic replication or reactivation. Virology *278*, 207-216.

Chen, X.-P., Mata, M., Kelley, M., Glorioso, J., and Fink, D. (2002b). The relationship of Herpes Simplex Virus Latency Associated Transcript expression to genome copy number: A quantitative study using laser capture microdissection. Journal of NeuroVirology *8*, 204-210.

Chen, X., Schmidt, M. C., Goins, W. F., and Glorioso, J. C. (1995). Two Herpes Simplex Virus type 1 latency-active promoters differ in their contributions to Latency-Associated Transcript expression during lytic and latent infections. Journal of Virology *69*, 7899-7908.

Chen, Y.-M., and Knipe, D. M. (1996). A dominant mutant form of the Herpes Simplex Virus ICP8 protein decreases viral late gene transcription. Virology *221*, 281-290.

Cheng, H., Tumpey, T. M., Staats, H. F., van Rooijen, N., Oakes, J. E., and Lausch, R. N. (2000). Role of macrophages in restricting Herpes Simplex Virus type 1 growth after ocular infection. Investigative Ophthalmology and Visual Science *41*, 1402-1409.

Cho, S. W., Kim, S., Kim, Y., Kweon, J., Kim, H. S., Bae, S., and Kim, J.-S. (2014). Analysis of off-target effects of CRISPR/Cas-derived RNA-guided endonucleases and nickases. Genome Research *24*, 132-141.

Clement, C., Popp, M. P., Bloom, D. C., Schultz, G., Liu, L., Neumann, D. M., Bhattachrjee, P. S., and Hill, J. M. (2008). Microarray analysis of host gene expression for comparison between naïve and HSV-1 latent rabbit trigeminal ganglia. Molecular Vision *14*, 1209-1221.

Cliffe, A. R., Garber, D. A., and Knipe, D. M. (2009). Transcription of the Herpes Simplex Virus Latency-Associated Transcript promotes the formation of facultative heterochromatin on lytic promoters. Journal of Virology *83*, 8182-8190.

Cliffe, A. R., and Knipe, D. M. (2008). Herpes Simplex Virus ICP0 promotes both histone removal and acetylation on viral DNA during lytic infection. Journal of Virology *82*, 12030-12038.

Coen, D. M., Kosz-Vnenchak, M., Jacobson, J. G., Leib, D. A., Bogard, C. L., Schaffer, P. A., Tyler, K. L., and Knipe, D. M. (1989). Thymidine kinase-negative Herpes Simplex Virus mutants establish latency in mouse trigeminal ganglia but do not reactivate. Proceedings of the National Academy of Sciences *86*, 4736-4740.

Coffin, R. S. (2010). Herpes Simplex Virus Protocols (Totowa, New Jersey, Humana Press).

Cohen, J. I. (2010). The Varicella-Zoster Virus genome. Current topics in microbiology and immunology *342*, 1-14.

Cohrs, R. J., Barbour, M., and Gilden, D. H. (1996). Varicella-zoster virus (VZV) transcription during latency in human ganglia: Detection of transcripts mapping to genes 21, 29, 62, and 63 in a cDNA library enriched for VZV RNA. Journal of Virology *70*, 2789-2796.

Cohrs, R. J., Gilden, D. H., Kinchington, P. R., Grinfeld, E., and Kennedy, P. G. E. (2003). Varicella-Zoster Virus gene 66 transcription and translation in latently infected human ganglia. Journal of Virology *77*, 6660-6665.

Cohrs, R. J., Laguardia, J. J., and Gilden, D. (2005). Distribution of latent Herpes Simplex Virus type-1 and Varicella Zoster Virus DNA in human trigeminal ganglia. Virus Genes *31*, 223-227.

Cohrs, R. J., Randall, J., Smith, J., Gilden, D. H., Dabrowski, C., van der Keyl, H., and Tal-Singer, R. (2000). Analysis of individual human trigeminal ganglia for latent Herpes Simplex Virus type 1 and Varicella-Zoster Virus nucleic acids using real-time PCR. Journal of Virology *74*, 11464-11471.

Coleman, H. M., Connor, V., Cheng, Z. S. C., Grey, F., Preston, C. M., and Efstathiou, S. (2008). Histone modifications associated with Herpes Simplex Virus type 1 genomes during quiescence and following ICP0-mediated de-repression. Journal of General Virology *89*, 68-77.

Coles, R. M., Mueller, S. N., Heath, W. R., Carbone, F. R., and Brooks, A. G. (2002). Progression of armed CTL from draining lymph node to spleen shortly after localized infection with Herpes Simplex Virus 1. The Journal of Immunology *168*, 834-838.

Colgin, M. A., Smith, R. L., and Wilcox, C. L. (2001). Inducible cyclic AMP early repressor produces reactivation of latent Herpes Simplex Virus type 1 in neurons *in vitro*. Journal of Virology *75*, 2912-2920.

Cong, L., Ran, F. A., Cox, D., Lin, S., Barretto, R., Habib, N., Hsu, P. D., Wu, X., Jiang, W., Marraffini, L. A.*, et al.* (2013). Multiplex genome engineering using CRISPR/Cas systems. Science *339*, 819-823.

Conley, A. J., Knipe, D. M., Jones, P. C., and Roizman, B. (1981). Molecular genetics of Herpes Simplex Virus. VII. Characterization of a temperature-sensitive mutant produced by *in vitro* mutagenesis and defective in DNA synthesis and accumulation of γ polypeptides. Journal of Virology *37*, 191-206.

Cook, M. L., Bastone, V. B., and Stevens, J. G. (1974). Evidence that neurons harbor latent Herpes Simplex Virus. Infection and Immunity *9*, 946-951.

Cook, M. L., and Stevens, J. G. (1973). Pathogenesis of herpetic neuritis and ganglionitis in mice: Evidence for intra-axonal transport of infection. Infection and Immunity *7*, 272-288.

Corey, L., and Wald, A. (2009). Maternal and neonatal Herpes Simplex Virus infections. New England Journal of Medicine *361*.

Cox, J., Yewdell, J., Eisenlohr, L., Johnson, P., and Bennink, J. (1990). Antigen presentation requires transport of MHC class I molecules from the endoplasmic reticulum. Science *247*, 715-718.

Creech, C. C., and Neumann, D. M. (2010). Changes to euchromatin on LAT and ICP4 following reactivation are more prevalent in an efficiently reactivating strain of HSV-1. PLoS ONE *5*.

Croen, K. D., Ostrove, J. M., Dragovic, L. J., and Straus, S. E. (1988). Patterns of gene expression and sites of latency in human nerve ganglia are different for Varicella-Zoster and Herpes Simplex Virus. Proceedings of the National Academy of Sciences *85*, 9773-9777.

Crute, J. J., Tsurumi, T., Zhu, L. A., Weller, S. K., Olivo, P. D., Challberg, M. D., Mocarski, E. S., and Lehman, I. R. (1989). Herpes Simplex Virus 1 helicase-primase: A complex of three herpes-encoded gene products. Proceedings of the National Academy of Sciences *86*, 2186-2189.

Cui, C., Griffiths, A., Li, G., Silva, L. M., Kramer, M. F., Gaasterland, T., Wang, X.-J., and Coen, D. M. (2006). Prediction and identification of Herpes Simplex Virus 1-encoded microRNAs. Journal of Virology *80*, 5499-5508.

Cunningham, A. L., Taylor, R., Taylor, J., Marks, C., Shaw, J., and Mindel, A. (2006). Prevalence of infection with Herpes Simplex Virus types 1 and 2 in Australia: A nationwide population based survey. Sexually Transmitted Infections *82*, 164-168.

Curtsinger, J. M., Valenzuela, J. O., Agarwal, P., Lins, D., and Mescher, M. F. (2005). Cutting edge: Type I IFNs provide a third signal to CD8 T cells to stimulate clonal expansion and differentiation. The Journal of Immunology *174*, 4465-4469.

da Silva, L. F., and Jones, C. (2013). Small non-coding RNAs encoded within the Herpes Simplex Virus type 1 Latency Associated Transcript (LAT) cooperate with the Retinoic acid Inducible Gene I (RIG-I) to induce β-interferon promoter activity and promote cell survival. Virus Research *175*, 101-109.

Davey, G. M., Wojtasiak, M., Proietto, A. I., Carbone, F. R., Heath, W. R., and Bedoui, S. (2010). Cutting edge: Priming of CD8 T cell immunity to Herpes Simplex Virus type 1 requires cognate TLR3 expression *in vivo*. The Journal of Immunology *184*, 2243-2246.

Davison, A., Eberle, R., Ehlers, B., Hayward, G., McGeoch, D., Minson, A., Pellett, P., Roizman, B., Studdert, M., and Thiry, E. (2009). The order Herpesvirales. Archives of Virology *154*, 171-177.

Davison, A. J. (2007). Human herpesviruses: Biology, therapy, and immunoprophylaxis (Cambridge, Cambridge University Press).

Davison, A. J., and Scott, J. E. (1986). The complete DNA sequence of Varicella-Zoster Virus. Journal of General Virology *67*, 1759-1816.

De Regge, N., Van Opdenbosch, N., Nauwynck, H. J., Efstathiou, S., and Favoreel, H. W. (2010). Interferon alpha induces establishment of alphaherpesvirus latency in sensory neurons *in vitro*. PLoS ONE *5*.

Deatly, A. M., Spivack, J. G., Lavi, E., and Fraser, N. W. (1987). RNA from an immediate early region of the type 1 Herpes Simplex Virus genome is present in the trigeminal ganglia of latently infected mice. Proceedings of the National Academy of Sciences *84*, 3204-3208.

Decman, V., Freeman, M. L., Kinchington, P. R., and Hendricks, R. L. (2005a). Immune control of HSV-1 latency. Viral Immunology *18*, 466-473.

Decman, V., Kinchington, P. R., Harvey, S. A. K., and Hendricks, R. L. (2005b). Gamma interferon can block Herpes Simplex Virus type 1 reactivation from latency, even in the presence of late gene expression. Journal of Virology *79*, 10339-10347.

Delius, H., and Clements, J. B. (1976). A partial denaturation map of Herpes Simplex Virus type 1 DNA: Evidence for inversions of the unique DNA regions. Journal of General Virology *33*, 125-133.

DeLuca, N. A., and Schaffer, P. A. (1985). Activation of immediate-early, early, and late promoters by temperature-sensitive and wild-type forms of Herpes Simplex Virus type 1 protein ICP4. Molecular and Cellular Biology *5*, 1997-2008.

Derfuss, T., Arbusow, V., Strupp, M., Brandt, T., and Theil, D. (2009). The presence of lytic HSV-1 transcripts and clonally expanded T cells with a memory effector phenotype in human sensory ganglia. In Annals of the New York Academy of Sciences, pp. 300-304.

Derfuss, T., Segerer, S., Herberger, S., Sinicina, I., Hüfner, K., Ebelt, K., Knaus, H.-G., Steiner, I., Meinl, E., Dornmair, K.*, et al.* (2007). Presence of HSV-1 immediate early genes and clonally expanded T-cells with a memory effector phenotype in human trigeminal ganglia. Brain Pathology *17*, 389-398.

Desai, P., Homa, F. L., Person, S., and Glorioso, J. C. (1994). A genetic selection method for the transfer of HSV-1 glycoprotein B mutations from plasmid to the viral genome:

Preliminary characterization of transdominance and entry kinetics of mutant viruses. Virology *204*, 312-322.

Desai, P., Ramakrishnan, R., Lin, Z. W., Osak, B., Glorioso, J. C., and Levine, M. (1993). The RR1 gene of Herpes Simplex Virus type 1 is uniquely *trans* activated by ICP0 during infection. Journal of Virology *67*, 6125-6135.

Deshmane, S. L., and Fraser, N. W. (1989). During latency, Herpes Simplex Virus type 1 DNA is associated with nucleosomes in a chromatin structure. Journal of Virology *63*, 943-947.

Deshpande, S. P., Kumaraguru, U., and Rouse, B. T. (2000a). Dual role of B cells in mediating innate and acquired immunity to Herpes Simplex Virus infections. Cellular Immunology *202*, 79-87.

Deshpande, S. P., Zheng, M., Daheshia, M., and Rouse, B. T. (2000b). Pathogenesis of Herpes Simplex Virus-induced ocular immunoinflammatory lesions in B-cell-deficient mice. Journal of Virology *74*, 3517-3524.

Devi-Rao, G. B., Bloom, D. C., Stevens, J. G., and Wagner, E. K. (1994). Herpes Simplex Virus type 1 DNA replication and gene expression during explant-induced reactivation of latently infected murine sensory ganglia. Journal of Virology *68*, 1271-1282.

Dheda, K., Huggett, J. F., Bustin, S. A., Johnson, M. A., Rook, G., and Zumla, A. (2004). Validation of housekeeping genes for normalizing RNA expression in real-time PCR. BioTechniques *37*, 112-114, 116, 118-119.

Divito, S., Cherpes, T. L., and Hendricks, R. L. (2006). A triple entente: Virus, neurons, and $CD8^+$ T cells maintain HSV-1 latency. Immunologic Research *36*, 119-126.

Dix, R. D., McKendall, R. R., and Baringer, J. R. (1983). Comparative neurovirulence of Herpes Simplex Virus type 1 strains after peripheral or intracerebral inoculation of BALB/c mice. Infection and Immunity *40*, 103-112.

Dixon, R. A., and Schaffer, P. A. (1980). Fine-structure mapping and functional analysis of temperature-sensitive mutants in the gene encoding the Herpes Simplex Virus type 1 immediate early protein VP175. Journal of Virology *36*, 189-203.

Djuric, M., Jankovic, L., Jovanovic, T., Pavlica, D., Brkic, S., Knezevic, A., Markovic, D., and Milasin, J. (2009). Prevalence of oral Herpes Simplex Virus reactivation in cancer patients:

A comparison of different techniques of viral detection. Journal of Oral Pathology and Medicine *38*, 167-173.

Dobson, A. T., Margolis, T. P., Gomes, W. A., and Feldman, L. T. (1995). *In vivo* deletion analysis of the Herpes Simplex Virus type 1 Latency-Associated Transcript promoter. Journal of Virology *69*, 2264-2270.

Dobson, A. T., Margolis, T. P., Sedarati, F., Stevens, J. G., and Feldman, L. T. (1990). A latent, nonpathogenic HSV-1-derived vector stably expresses β-galactosidase in mouse neurons. Neuron *5*, 353-360.

Dobson, A. T., Sederati, F., Devi-Rao, G., Flanagan, W. M., Farrell, M. J., Stevens, J. G., Wagner, E. K., and Feldman, L. T. (1989). Identification of the Latency-Associated Transcript promoter by expression of rabbit β-globin mRNA in mouse sensory nerve ganglia latently infected with a recombinant Herpes Simplex Virus. Journal of Virology *63*, 3844-3851.

Doerig, C., Pizer, L. I., and Wilcox, C. L. (1991). An antigen encoded by the Latency-Associated Transcript in neuronal cell cultures latently infected with Herpes Simplex Virus type 1. Journal of Virology *65*, 2724-2727.

Dolan, A., Jamieson, F. E., Cunningham, C., Barnett, B. C., and McGeoch, D. J. (1998). The genome sequence of Herpes Simplex Virus type 2. Journal of Virology *72*, 2010-2021.

Donaghy, H., Bosnjak, L., Harman, A. N., Marsden, V., Tyring, S. K., Meng, T.-C., and Cunningham, A. L. (2009). Role for plasmacytoid dendritic cells in the immune control of recurrent human Herpes Simplex Virus infection. Journal of Virology *83*, 1952-1961.

Doudna, J. A., and Charpentier, E. (2014). The new frontier of genome engineering with CRISPR-Cas9. Science *346*.

Dressler, G. R., Rock, D. L., and Fraser, N. W. (1987). Latent Herpes Simplex Virus type 1 DNA is not extensively methylated *in vivo*. Journal of General Virology *68*, 1761-1765.

Drolet, B. S., Perng, G. C., Cohen, J., Slanina, S. M., Yukht, A., Nesburn, A. B., and Wechsler, S. L. (1998). The region of the Herpes Simplex Virus type 1 LAT gene involved in spontaneous reactivation does not encode a functional protein. Virology *242*, 221-232.

Drolet, B. S., Perng, G. C., Villosis, R. J., Slanina, S. M., Nesburn, A. B., and Wechsler, S. L. (1999). Expression of the first 811 nucleotides of the Herpes Simplex Virus type 1 Latency-Associated Transcript (LAT) partially restores wild-type spontaneous reactivation to a LAT-null mutant. Virology *253*, 96-106.

Du, T., Han, Z., Zhou, G., and Roizman, B. (2015). Patterns of accumulation of miRNAs encoded by Herpes Simplex Virus during productive infection, latency, and on reactivation. Proceedings of the National Academy of Sciences *112*, E49-E55.

Du, T., Zhou, G., and Roizman, B. (2011). HSV-1 gene expression from reactivated ganglia is disordered and concurrent with suppression of latency-associated transcript and miRNAs. Proceedings of the National Academy of Sciences of the United States of America *108*, 18820-18824.

Ebina, H., Misawa, N., Kanemura, Y., and Koyanagi, Y. (2013). Harnessing the CRISPR/Cas9 system to disrupt latent HIV-1 provirus. Scientific Reports *3*, 2510.

Ecob-Prince, M., and Hassan, K. (1994). Reactivation of latent Herpes Simplex Virus from explanted dorsal root ganglia. Journal of General Virology *75*, 2017-2028.

Ecob-Prince, M. S., Hassan, K., Denheen, M. T., and Preston, C. M. (1995). Expression of β-galactosidase in neurons of dorsal root ganglia which are latently infected with Herpes Simplex Virus type 1. Journal of General Virology *76*, 1527-1532.

Efstathiou, S., Minson, A. C., Field, H. J., Anderson, J. R., and Wildy, P. (1986). Detection of Herpes Simplex Virus-specific DNA sequences in latently infected mice and in humans. Journal of Virology *57*, 446-455.

Egan, K. P., Wu, S., Wigdahl, B., and Jennings, S. R. (2013). Immunological control of Herpes Simplex Virus infections. Journal of NeuroVirology *19*, 328-345.

Elias, P., and Lehman, I. R. (1988). Interaction of origin binding protein with an origin of replication of Herpes Simplex Virus 1. Proceedings of the National Academy of Sciences *85*, 2959-2963.

Ellison, A. R., Yang, L., Voytek, C., and Margolis, T. P. (2000). Establishment of latent Herpes Simplex Virus type 1 infection in resistant, sensitive, and immunodeficient mouse strains. Virology *268*, 17-28.

Ellison, K. S., Maranchuk, R. A., Mottet, K. L., and Smiley, J. R. (2005). Control of VP16 translation by the Herpes Simplex Virus type 1 immediate-early protein ICP27. Journal of Virology *79*, 4120-4131.

Ertel, M. K., Cammarata, A. L., Hron, R. J., and Neumann, D. M. (2012). CTCF occupation of the Herpes Simplex Virus 1 genome is disrupted at early times postreactivation in a transcription-dependent manner. Journal of Virology *86*, 12741-12759.

Everett, R. D. (1984). *Trans* activation of transcription by herpes virus products: Requirement for two HSV-1 immediate-early polypeptides for maximum activity. The EMBO Journal *3*, 3135-3141.

Everett, R. D. (1989). Construction and characterization of Herpes Simplex Virus type 1 mutants with defined lesions in immediate early gene 1. Journal of General Virology *70*, 1185-1202.

Everett, R. D., Earnshaw, W. C., Findlay, J., and Lomonte, P. (1999). Specific destruction of kinetochore protein CENP-C and disruption of cell division by herpes simplex virus immediate-early protein Vmw110, Vol 18.

Everett, R. D., Rechter, S., Papior, P., Tavalai, N., Stamminger, T., and Orr, A. (2006). PML contributes to a cellular mechanism of repression of Herpes Simplex Virus type 1 infection that is inactivated by ICP0. Journal of Virology *80*, 7995-8005.

Falkner, F. G., and Moss, B. (1990). Transient dominant selection of recombinant Vaccinia Viruses. Journal of Virology *64*, 3108-3111.

Fareed, M. U., and Spivack, J. G. (1994). Two open reading frames (ORF1 and ORF2) within the 2.0-kilobase Latency-Associated Transcript of Herpes Simplex Virus type 1 are not essential for reactivation from latency. Journal of Virology *68*, 8071-8081.

Farrell, M. J., Dobson, A. T., and Feldman, L. T. (1991). Herpes Simplex Virus latency-associated transcript is a stable intron. Proceedings of the National Academy of Sciences of the United States of America *88*, 790-794.

Fawl, R. L., and Roizman, B. (1993). Induction of reactivation of Herpes Simplex Virus in murine sensory ganglia *in vivo* by cadmium. Journal of Virology *67*, 7025-7031.

Feil, R., Brocard, J., Mascrez, B., Lemeur, M., Metzger, D., and Chambon, P. (1996). Ligand-activated site-specific recombination in mice. Proceedings of the National Academy of Sciences of the United States of America *93*, 10887-10890.

Feil, R., Wagner, J., Metzger, D., and Chambon, P. (1997). Regulation of Cre recombinase activity by mutated estrogen receptor ligand-binding domains. Biochemical and Biophysical Research Communications *237*, 752-757.

Feldman, L. T., Ellison, A. R., Voytek, C. C., Yang, L., Krause, P., and Margolis, T. P. (2002). Spontaneous molecular reactivation of Herpes Simplex Virus type 1 latency in mice.

Proceedings of the National Academy of Sciences of the United States of America *99*, 978-983.

Femino, A. M., Fay, F. S., Fogarty, K., and Singer, R. H. (1998). Visualization of single RNA transcripts *in situ*. Science *280*, 585-590.

Fenton, R. R., Molesworth-Kenyon, S., Oakes, J. E., and Lausch, R. N. (2002). Linkage of IL-6 with neutrophil chemoattractant expression in virus-induced ocular inflammation. Investigative Ophthalmology and Visual Science *43*, 737-743.

Ferenczy, M. W., and DeLuca, N. A. (2011). Reversal of heterochromatic silencing of quiescent Herpes Simplex Virus type 1 by ICP0. Journal of Virology *85*, 3424-3435.

Flores, O., Nakayama, S., Whisnant, A. W., Javanbakht, H., Cullen, B. R., and Bloom, D. C. (2013). Mutational inactivation of Herpes Simplex Virus 1 microRNAs identifies viral mRNA targets and reveals phenotypic effects in culture. Journal of Virology *87*, 6589-6603.

Fontaine-Rodriguez, E. C., and Knipe, D. M. (2008). Herpes Simplex Virus ICP27 increases translation of a subset of viral late mRNAs. Journal of Virology *82*, 3538-3545.

Foster, T. P., Chouljenko, V. N., and Kousoulas, K. G. (1999). Functional characterization of the HveA homolog specified by African Green monkey kidney cells with a Herpes Simplex Virus expressing the green fluorescence protein. Virology *258*, 365-374.

Frame, M. C., Marsden, H. S., and Dutia, B. M. (1985). The ribonucleotide reductase induced by Herpes Simplex Virus type 1 involves minimally a complex of two polypeptides (136K and 38K). Journal of General Virology *66*, 1581-1587.

Frank, G. M., Lepisto, A. J., Freeman, M. L., Sheridan, B. S., Cherpes, T. L., and Hendricks, R. L. (2010). Early $CD4^+$ T cell help prevents partial $CD8^+$ T cell exhaustion and promotes maintenance of Herpes Simplex Virus type 1 latency. The Journal of Immunology *184*, 277-286.

Frank, I., and Friedman, H. M. (1989). A novel function of the herpes simplex virus type 1 Fc receptor: Participation in bipolar bridging of antiviral immunoglobulin G. Journal of Virology *63*, 4479-4488.

Fraser, K. A., and Rice, S. A. (2005). Herpes Simplex Virus type 1 infection leads to loss of serine-2 phosphorylation on the carboxyl-terminal domain of RNA polymerase II. Journal of Virology *79*, 11323-11334.

Früh, K., Ahn, K., Djaballah, H., Sempé, P., van Endert, P. M., Tampé, R., Peterson, P. A., and Yang, Y. (1995). A viral inhibitor of peptide transporters for antigen presentation. Nature *375*, 415-418.

Fu, Y., Foden, J. A., Khayter, C., Maeder, M. L., Reyon, D., Joung, J. K., and Sander, J. D. (2013). High-frequency off-target mutagenesis induced by CRISPR-Cas nucleases in human cells. Nature Biotechnology *31*, 822-826.

Galocha, B., Hill, A., Barnett, B. C., Dolan, A., Raimondi, A., Cook, R. F., Brunner, J., McGeoch, D. J., and Ploegh, H. L. (1997). The active site of ICP47, a Herpes Simplex Virus–encoded inhibitor of the Major Histocompatibility Complex (MHC)-encoded peptide Transporter associated with Antigen Processing (TAP), maps to the NH_2-terminal 35 residues. The Journal of Experimental Medicine *185*, 1565-1572.

Gao, B., Adhikari, R., Howarth, M., Nakamura, K., Gold, M. C., Hill, A. B., Knee, R., Michalak, M., and Elliott, T. (2002). Assembly and antigen-presenting function of MHC class I molecules in cells lacking the ER chaperone calreticulin. Immunity *16*, 99-109.

Gao, M., and Knipe, D. M. (1991). Potential role for Herpes Simplex Virus ICP8 DNA replication protein in stimulation of late gene expression. Journal of Virology *65*, 2666-2675.

Garber, D. A., Beverley, S. M., and Coen, D. M. (1993). Demonstration of circularization of Herpes Simplex Virus DNA following infection using pulsed field gel electrophoresis. Virology *197*, 459-462.

Garber, D. A., Schaffer, P. A., and Knipe, D. M. (1997). A LAT-associated function reduces productive-cycle gene expression during acute infection of murine sensory neurons with Herpes Simplex Virus type 1. Journal of Virology *71*, 5885-5893.

Gebhardt, B. M., and Halford, W. P. (2005). Evidence that spontaneous reactivation of herpes virus does not occur in mice. Virology Journal *2*.

Gebhardt, B. M., and Hill, J. M. (1988). T lymphocytes in the trigeminal ganglia of rabbits during corneal HSV infection. Investigative Ophthalmology and Visual Science *29*, 1683-1691.

Gebhardt, T., Wakim, L. M., Eidsmo, L., Reading, P. C., Heath, W. R., and Carbone, F. R. (2009). Memory T cells in nonlymphoid tissue that provide enhanced local immunity during infection with Herpes Simplex Virus. Nature Immunology *10*, 524-530.

Gebhardt, T., Whitney, P. G., Zaid, A., Mackay, L. K., Brooks, A. G., Heath, W. R., Carbone, F. R., and Mueller, S. N. (2011). Different patterns of peripheral migration by memory $CD4^+$ and $CD8^+$ T cells. Nature *477*, 216-219.

Geiger, K. D., Nash, T. C., Sawyer, S., Krahl, T., Patstone, G., Reed, J. C., Krajewski, S., Dalton, D., Buchmeier, M. J., and Sarvetnick, N. (1997). Interferon-γ protects against Herpes Simplex Virus type 1-mediated neuronal death. Virology *238*, 189-197.

Gelman, I. H., and Silverstein, S. (1987). Herpes Simplex Virus immediate-early promoters are responsive to virus and cell *trans*-acting factors. Journal of Virology *61*, 2286-2296.

Ghattas, I. R., Sanes, J. R., and Majors, J. E. (1991). The encephalomyocarditis virus internal ribosome entry site allows efficient coexpression of two genes from a recombinant provirus in cultured cells and in embryos. Molecular and Cellular Biology *11*, 5848-5859.

Ghiasi, H., Cai, S., Perng, G.-C., Nesburn, A. B., and Wechsler, S. L. (2000). The role of natural killer cells in protection of mice against death and corneal scarring following ocular HSV-1 infection. Antiviral Research *45*, 33-45.

Ghiasi, H., Kaiwar, R., Nesburn, A. B., Slanina, S., and Wechsler, S. L. (1994). Expression of seven Herpes Simplex Virus type 1 glycoproteins (gB, gC, gD, gE, gG, gH, and gI): comparative protection against lethal challenge in mice. Journal of Virology *68*, 2118-2126.

Gibson, W., and Roizman, B. (1972). Proteins specified by Herpes Simplex Virus VIII. Characterization and composition of multiple capsid forms of subtypes 1 and 2. Journal of Virology *10*, 1044-1052.

Gierasch, W. W., Zimmerman, D. L., Ward, S. L., Van Heyningen, T. K., Romine, J. D., and Leib, D. A. (2006). Construction and characterization of Bacterial Artificial Chromosomes containing HSV-1 strains 17 and KOS. Journal of Virological Methods *135*, 197-206.

Giordani, N. V., Neumann, D. M., Kwiatkowski, D. L., Bhattacharjee, P. S., McAnany, P. K., Hill, J. M., and Bloom, D. C. (2008). During Herpes Simplex Virus type 1 infection of rabbits, the ability to express the Latency-Associated Transcript increases latent-phase transcription of lytic genes. Journal of Virology *82*, 6056-6060.

Goddard, C. A., Butts, D. A., and Shatz, C. J. (2007). Regulation of CNS synapses by neuronal MHC class I. Proceedings of the National Academy of Sciences *104*, 6828-6833.

Goins, W. F., Krisky, D. M., Wechuck, J. B., Huang, S., and Glorioso, J. C. (2008). Construction and production of recombinant Herpes Simplex Virus vectors. In Methods in molecular biology, pp. 97-113.

Goins, W. F., Sternberg, L. R., Croen, K. D., Krause, P. R., Hendricks, R. L., Fink, D. J., Straus, S. E., Levine, M., and Glorioso, J. C. (1994). A novel latency-active promoter is contained within the Herpes Simplex Virus type 1 U_L flanking repeats. Journal of Virology *68*, 2239-2252.

Gold, M. C., Munks, M. W., Wagner, M., Koszinowski, U. H., Hill, A. B., and Fling, S. P. (2002). The murine Cytomegalovirus immunomodulatory gene m152 prevents recognition of infected cells by M45-specific CTL but does not alter the immunodominance of the M45-specific CD8 T cell response *in vivo*. The Journal of Immunology *169*, 359-365.

Goldenberg, D., Mador, N., Ball, M., Panet, A., and Steiner, I. (1997). The abundant Latency-Associated Transcripts of Herpes Simplex Virus type 1 are bound to polyribosomes in cultured neuronal cells and during latent infection in mouse trigeminal ganglia. Journal of Virology *71*, 2897-2904.

Goldsmith, K., Chen, W., Johnson, D. C., and Hendricks, R. L. (1998). Infected cell protein (ICP) 47 enhances Herpes Simplex Virus neurovirulence by blocking the $CD8^+$ T cell response. The Journal of Experimental Medicine *187*, 341-348.

Gompels, U. A., Nicholas, J., Lawrence, G., Jones, M., Thomson, B. J., Martin, M. E. D., Efstathiou, S., Craxton, M., and Macaulay, H. A. (1995). The DNA sequence of human herpesvirus-6: Structure, coding content, and genome evolution. Virology *209*, 29-51.

Gong, H., Zhang, B., Little, G., Kovar, J., Chen, H., Xie, W., Schutz-Geschwender, A., and Olive, D. M. (2009). β-Galactosidase activity assay using far-red-shifted fluorescent substrate DDAOG. Analytical Biochemistry *386*, 59-64.

Gooding, L. R., and O'Connell, K. A. (1983). Recognition by cytotoxic T lymphocytes of cells expressing fragments of the SV40 tumor antigen. The Journal of Immunology *131*, 2580-2586.

Gratz, S. J., Cummings, A. M., Nguyen, J. N., Hamm, D. C., Donohue, L. K., Harrison, M. M., Wildonger, J., and O'Connor-Giles, K. M. (2013). Genome engineering of Drosophila with the CRISPR RNA-guided Cas9 nuclease. Genetics *194*, 1029-1035.

Greco, A., Laurent, A. M., and Madjar, J. J. (1997). Repression of β-actin synthesis and persistence of ribosomal protein synthesis after infection of HeLa cells by Herpes Simplex Virus type 1 infection are under translational control. Molecular and General Genetics MGG *256*, 320-327.

Green, M. T., Courtney, R. J., and Dunkel, E. C. (1981). Detection of an immediate early Herpes Simplex Virus type 1 polypeptide in trigeminal ganglia from latently infected animals. Infection and Immunity *34*, 987-992.

Grey, H. M., Kubo, R. T., Colon, S. M., Poulik, M. D., Cresswell, P., Springer, T., Turner, M., and Strominger, J. L. (1973). The small subunit of HL-A antigens is β_2-microglobulin. The Journal of Experimental Medicine *138*, 1608-1612.

Grünewald, K., Desai, P., Winkler, D. C., Heymann, J. B., Belnap, D. M., Baumeister, W., and Steven, A. C. (2003). Three-dimensional structure of Herpes Simplex Virus from cryo-electron tomography. Science *302*, 1396-1398.

Gu, H., Liang, Y., Mandel, G., and Roizman, B. (2005). Components of the REST/CoREST/histone deacetylase repressor complex are disrupted, modified, and translocated in HSV-1-infected cells. Proceedings of the National Academy of Sciences of the United States of America *102*, 7571-7576.

Gu, H., and Roizman, B. (2007). Herpes simplex virus-infected cell protein 0 blocks the silencing of viral DNA by dissociating histone deacetylases from the CoREST–REST complex. Proceedings of the National Academy of Sciences of the United States of America *104*, 17134-17139.

Guzowski, J. F., Singh, J., and Wagner, E. K. (1994). Transcriptional activation of the Herpes Simplex Virus type 1 U_L38 promoter conferred by the *cis*-acting downstream activation sequence is mediated by a cellular transcription factor. Journal of Virology *68*, 7774-7789.

Halford, W., Gebhardt, B., and Carr, D. (1996a). Persistent cytokine expression in trigeminal ganglion latently infected with Herpes Simplex Virus type 1. The Journal of Immunology *157*, 3542-3549.

Halford, W. P., Gebhardt, B. M., and Carr, D. J. (1996b). Mechanisms of Herpes Simplex Virus type 1 reactivation. Journal of Virology *70*, 5051-5060.

Halford, W. P., Gebhardt, B. M., and Carr, D. J. J. (1997). Acyclovir blocks cytokine gene expression in trigeminal ganglia latently infected with Herpes Simplex Virus type 1. Virology *238*, 53-63.

Halford, W. P., Kemp, C. D., Isler, J. A., Davido, D. J., and Schaffer, P. A. (2001). ICP0, ICP4, or VP16 expressed from Adenovirus vectors induces reactivation of latent Herpes Simplex Virus type 1 in primary cultures of latently infected trigeminal ganglion cells. Journal of Virology *75*, 6143-6153.

Hardy, W. R., and Sandri-Goldin, R. M. (1994). Herpes simplex virus inhibits host cell splicing, and regulatory protein ICP27 is required for this effect. Journal of Virology *68*, 7790-7799.

Harkness, J. M., Kader, M., and DeLuca, N. A. (2014). Transcription of the Herpes Simplex Virus 1 genome during productive and quiescent infection of neuronal and nonneuronal cells. Journal of Virology *88*, 6847-6861.

Heath, W. R., Kurts, C., Miller, J. F. A. P., and Carbone, F. R. (1998). Cross-tolerance: A pathway for inducing tolerance to peripheral tissue antigens. The Journal of Experimental Medicine *187*, 1549-1553.

Held, K., Junker, A., Dornmair, K., Meinl, E., Sinicina, I., Brandt, T., Theil, D., and Derfuss, T. (2011). Expression of Herpes Simplex Virus 1-encoded microRNAs in human trigeminal ganglia and their relation to local T-cell infiltrates. Journal of Virology *85*, 9680-9685.

Henderson, G., Jaber, T., Carpenter, D., Wechsler, S., and Jones, C. (2009). Identification of Herpes Simplex Virus type 1 proteins encoded within the first 1.5 kb of the latency-associated transcript. Journal of NeuroVirology *15*, 439-448.

Hennecke, M., Kwissa, M., Metzger, K., Oumard, A., Kröger, A., Schirmbeck, R., Reimann, J., and Hauser, H. (2001). Composition and arrangement of genes define the strength of IRES-driven translation in bicistronic mRNAs. Nucleic Acids Research *29*, 3327-3334.

Hernandez, F. P., and Sandri-Goldin, R. M. (2010). Herpes Simplex Virus 1 regulatory protein ICP27 undergoes a head-to-tail intramolecular interaction. Journal of Virology *84*, 4124-4135.

Herrera, F. J., and Triezenberg, S. J. (2004). VP16-dependent association of chromatin-modifying coactivators and underrepresentation of histones at immediate-early gene promoters during Herpes Simplex Virus infection. Journal of Virology *78*, 9689-9696.

Higaki, S., Deal, T., Fukuda, M., and Shimomura, Y. (2004). Microarray analysis in the HSV-1 latently infected mouse trigeminal ganglion. Cornea *23*, S42-S47.

Hill, A., Juovic, P., York, I., Russ, G., Bennink, J., Yewdell, J., Ploegh, H., and Johnson, D. (1995). Herpes Simplex Virus turns off the TAP to evade host immunity. Nature *375*, 411-415.

Hill, J. M., Ball, M. J., Neumann, D. M., Azcuy, A. M., Bhattacharjee, P. S., Bouhanik, S., Clement, C., Lukiw, W. J., Foster, T. P., Kumar, M.*, et al.* (2008). The high prevalence of Herpes Simplex Virus type 1 DNA in human trigeminal ganglia is not a function of age or gender. Journal of Virology *82*, 8230-8234.

Hill, J. M., Field, M. A. R., and Haruta, Y. (1987). Strain specificity of spontaneous and adrenergically induced HSV-1 ocular reactivation in latently infected rabbits. Current Eye Research *6*, 91-97.

Hill, J. M., Gebhardt, B. M., Wen, R., Bouterie, A. M., Thompson, H. W., O'Callaghan, R. J., Halford, W. P., and Kaufman, H. E. (1996a). Quantitation of Herpes Simplex Virus type 1 DNA and Latency-Associated Transcripts in rabbit trigeminal ganglia demonstrates a stable reservoir of viral nucleic acids during latency. Journal of Virology *70*, 3137-3141.

Hill, J. M., Lukiw, W. J., Gebhardt, B. M., Higaki, S., Loutsch, J. M., Myles, M. E., Thompson, H. W., Kwon, B. S., Bazan, N. G., and Kaufman, H. E. (2001). Gene expression analyzed by microarrays in HSV-1 latent mouse trigeminal ganglion following heat stress. Virus Genes *23*, 273-280.

Hill, J. M., Maggioncalda, J. B., Garza, H. H., Su, Y. H., Fraser, N. W., and Block, T. M. (1996b). *In vivo* epinephrine reactivation of ocular Herpes Simplex Virus type 1 in the rabbit is correlated to a 370-base-pair region located between the promoter and the 5' end of the 2.0 kilobase latency-associated transcript. Journal of Virology *70*, 7270-7274.

Hill, J. M., Sedarati, F., Javier, R. T., Wagner, E. K., and Stevens, J. G. (1990). Herpes simplex virus latent phase transcription facilitates *in vivo* reactivation. Virology *174*, 117-125.

Hill, T. J., Field, H. J., and Blyth, W. A. (1975). Acute and recurrent infection with Herpes Simplex Virus in the mouse: A model for studying latency and recurrent disease. Journal of General Virology *28*, 341-353.

Himmelein, S., Lindemann, A., Sinicina, I., Strupp, M., Brandt, T., and Hüfner, K. (2015). Latent Herpes Simplex Virus 1 infection does not induce apoptosis in human trigeminal ganglia. Journal of Virology *89*, 5747-5750.

Holland, L. E., Anderson, K. P., Shipman Jr, C., and Wagner, E. K. (1980). Viral DNA synthesis is required for the efficient expression of specific Herpes Simplex Virus type 1 mRNA species. Virology *101*, 10-24.

Holland, L. E., Sandri-Goldin, R. M., Goldin, A. L., Glorioso, J. C., and Levine, M. (1984). Transcriptional and genetic analyses of the Herpes Simplex Virus type 1 genome: Coordinates 0.29 to 0.45. Journal of Virology *49*, 947-959.

Homa, F. L., Glorioso, J. C., and Levine, M. (1988). A specific 15-bp TATA box promoter element is required for expression of a Herpes Simplex Virus type 1 late gene. Genes and Development *2*, 40-53.

Honess, R. W., and Roizman, B. (1974). Regulation of Herpesvirus macromolecular synthesis I. Cascade regulation of the synthesis of three groups of viral proteins. Journal of Virology *14*, 8-19.

Honess, R. W., and Roizman, B. (1975). Regulation of herpesvirus macromolecular synthesis: Sequential transition of polypeptide synthesis requires functional viral polypeptides. Proceedings of the National Academy of Sciences *72*, 1276-1280.

Horsburgh, B. C., Hubinette, M. M., Qiang, D., MacDonald, M. L., and Tufaro, F. (1999). Allele replacement: An application that permits rapid manipulation of Herpes Simplex Virus type 1 genomes. Gene Therapy *6*, 922-930.

Horvath, P., and Barrangou, R. (2010). CRISPR/Cas, the immune system of bacteria and archaea. Science *327*, 167-170.

Hoshino, Y., Pesnicak, L., Cohen, J. I., and Straus, S. E. (2007). Rates of reactivation of latent Herpes Simplex Virus from mouse trigeminal ganglia *ex vivo* correlate directly with viral load and inversely with number of infiltrating $CD8^+$ T cells. Journal of Virology *81*, 8157-8164.

Hsu, P. D., Scott, D. A., Weinstein, J. A., Ran, F. A., Konermann, S., Agarwala, V., Li, Y., Fine, E. J., Wu, X., Shalem, O*., et al.* (2013). DNA targeting specificity of RNA-guided Cas9 nucleases. Nature Biotechnology *31*, 827-832.

Hu, W., Kaminski, R., Yang, F., Zhang, Y., Cosentino, L., Li, F., Luo, B., Alvarez-Carbonell, D., Garcia-Mesa, Y., Karn, J.*, et al.* (2014). RNA-directed gene editing specifically eradicates latent and prevents new HIV-1 infection. Proceedings of the National Academy of Sciences of the United States of America *111*, 11461-11466.

Huang, C. J., Goodart, S. A., Rice, M. K., Guzowski, J. F., and Wagner, E. K. (1993a). Mutational analysis of sequences downstream of the TATA box of the Herpes Simplex Virus type 1 major capsid protein (VP5/U_L19) promoter. Journal of Virology *67*, 5109-5116.

Huang, C. J., and Wagner, E. K. (1994). The Herpes Simplex Virus type 1 major capsid protein (VP5-U_L19) promoter contains two *cis*-acting elements influencing late expression. Journal of Virology *68*, 5738-5747.

Huang, J., Kent, J. R., Placek, B., Whelan, K. A., Hollow, C. M., Zeng, P.-Y., Fraser, N. W., and Berger, S. L. (2006). Trimethylation of histone H3 lysine 4 by Set1 in the lytic Infection of human Herpes Simplex Virus 1. Journal of Virology *80*, 5740-5746.

Huang, S., Hendriks, W., Althage, A., Hemmi, S., Bluethmann, H., Kamijo, R., Vilcek, J., Zinkernagel, R. M., and Aguet, M. (1993b). Immune response in mice that lack the interferon-γ receptor. Science *259*, 1742-1745.

Hull, C. M., Harmenberg, J., Arlander, E., Aoki, F., Bring, J., Darpö, B., Levin, M. J., Tyring, S., and Spruance, S. L. (2011). Early treatment of cold sores with topical ME-609 decreases the frequency of ulcerative lesions: A randomized, double-blind, placebo-controlled, patient-initiated clinical trial. Journal of the American Academy of Dermatology *64*, 696.e691-696.e611.

Hull, C. M., Levin, M. J., Tyring, S. K., and Spruance, S. L. (2014). Novel composite efficacy measure to demonstrate the rationale and efficacy of combination antiviral–anti-inflammatory treatment for recurrent Herpes Simplex labialis. Antimicrobial Agents and Chemotherapy *58*, 1273-1278.

Hung, S.-L., Peng, C., Kostavasili, I., Friedman, H. M., Lambris, J. D., Eisenberg, R. J., and Cohen, G. H. (1994). The interaction of glycoprotein C of Herpes Simplex Virus types 1 and 2 with the alternative complement pathway. Virology *203*, 299-312.

Hunsperger, E., and Wilcox, C. (2003a). Caspase-3-dependent reactivation of latent Herpes Simplex Virus type 1 in sensory neuronal cultures. Journal of NeuroVirology *9*, 390-398.

Hunsperger, E. A., and Wilcox, C. L. (2003b). Capsaicin-induced reactivation of latent Herpes Simplex Virus type 1 in sensory neurons in culture. Journal of General Virology *84*, 1071-1078.

Hwang, W. Y., Fu, Y., Reyon, D., Maeder, M. L., Tsai, S. Q., Sander, J. D., Peterson, R. T., Yeh, J. R. J., and Joung, J. K. (2013). Efficient genome editing in zebrafish using a CRISPR-Cas system. Nature Biotechnology *31*, 227-229.

Iijima, N., and Iwasaki, A. (2014). A local macrophage chemokine network sustains protective tissue-resident memory CD4 T cells. Science *346*, 93-98.

Imbalzano, A. N., Coen, D. M., and DeLuca, N. A. (1991). Herpes simplex virus transactivator ICP4 operationally substitutes for the cellular transcription factor Sp1 for efficient expression of the viral thymidine kinase gene. Journal of Virology *65*, 565-574.

Inman, M., Perng, G.-C., Henderson, G., Ghiasi, H., Nesburn, A. B., Wechsler, S. L., and Jones, C. (2001). Region of Herpes Simplex Virus type 1 Latency-Associated Transcript sufficient for wild-type spontaneous reactivation promotes cell survival in tissue culture. Journal of Virology *75*, 3636-3646.

Izumi, K. M., McKelvey, A. M., Devi-Rao, G., Wagner, E. K., and Stevens, J. G. (1989). Molecular and biological characterization of a type 1 Herpes Simplex Virus (HSV-1) specifically deleted for expression of the Latency-Associated Transcript (LAT). Microbial Pathogenesis *7*, 121-134.

Jaber, T., Henderson, G., Li, S., Perng, G.-C., Carpenter, D., Wechsler, S. L., and Jones, C. (2009). Identification of a novel Herpes Simplex Virus type 1 transcript and protein (AL3) expressed during latency. Journal of General Virology *90*, 2342-2352.

Jackson, M. R., Cohen-Doyle, M. F., Peterson, P. A., and Williams, D. B. (1994). Regulation of MHC class I transport by the molecular chaperone, calnexin (p88, IP90). Science *263*, 384-387.

James, S. H., and Prichard, M. N. (2014). Current and future therapies for Herpes Simplex Virus infections: Mechanism of action and drug resistance. Current Opinion in Virology *8*, 54-61.

Jamieson, A. T., and Subak-Sharpe, J. H. (1974). Biochemical studies on the Herpes Simplex Virus-specified deoxypyrimidine kinase activity. Journal of General Virology *24*, 481-492.

Javier, R. T., Stevens, J. G., Dissette, V. B., and Wagner, E. K. (1988). A Herpes Simplex Virus transcript abundant in latently infected neurons is dispensable for for establishment of the latent state. Virology *166*, 254-257.

Jean, S., LeVan, K. M., Song, B., Levine, M., and Knipe, D. M. (2001). Herpes Simplex Virus 1 ICP27 is required for transcription of two viral late (γ2) genes in infected cells. Virology *283*, 273-284.

Jerome, K. R., Chen, Z., Lang, R., Torres, M. R., Hofmeister, J., Smith, S., Fox, R., Froelich, C. J., and Corey, L. (2001). HSV and glycoprotein J inhibit caspase activation and apoptosis induced by granzyme B or Fas. The Journal of Immunology *167*, 3928-3935.

Jerome, K. R., Fox, R., Chen, Z., Sears, A. E., Lee, H.-y., and Corey, L. (1999). Herpes Simplex Virus inhibits apoptosis through the action of two genes, U_S5 and U_S3. Journal of Virology *73*, 8950-8957.

Jiang, X., Alami Chentoufi, A., Hsiang, C., Carpenter, D., Osorio, N., BenMohamed, L., Fraser, N. W., Jones, C., and Wechsler, S. L. (2011). The Herpes Simplex Virus type 1 Latency-Associated Transcript can protect neuron-derived C1300 and Neuro2A cells from granzyme B-induced apoptosis and CD8 T-cell killing. Journal of Virology *85*, 2325-2332.

Jiang, X., Brown, D., Osorio, N., Hsiang, C., Li, L., Chan, L., BenMohamed, L., and Wechsler, S. L. (2015). A Herpes Simplex Virus type 1 mutant disrupted for microRNA H2 with increased neurovirulence and rate of reactivation. Journal of NeuroVirology *21*, 199-209.

Jin, L., Carpenter, D., Moerdyk-Schauwecker, M., Vanarsdall, A., Osorio, N., Hsiang, C., Jones, C., and Wechsler, S. (2008). Cellular FLIP can substitute for the Herpes Simplex Virus type 1 Latency-Associated Transcript gene to support a wild-type virus reactivation phenotype in mice. Journal of NeuroVirology *14*, 389-400.

Jin, L., Peng, W., Perng, G.-C., Brick, D. J., Nesburn, A. B., Jones, C., and Wechsler, S. L. (2003). Identification of Herpes Simplex Virus Type 1 Latency-Associated Transcript sequences that both inhibit apoptosis and enhance the spontaneous reactivation phenotype. Journal of Virology *77*, 6556-6561.

Jin, L., Perng, G.-C., Mott, K. R., Osorio, N., Naito, J., Brick, D. J., Carpenter, D., Jones, C., and Wechsler, S. L. (2005). A Herpes Simplex Virus type 1 mutant expressing a Baculovirus inhibitor of apoptosis gene in place of Latency-Associated Transcript has a wild-type reactivation phenotype in the mouse. Journal of Virology *79*, 12286-12295.

Jinek, M., Chylinski, K., Fonfara, I., Hauer, M., Doudna, J. A., and Charpentier, E. (2012). A programmable dual-RNA–guided DNA endonuclease in adaptive bacterial immunity. Science *337*, 816-821.

Jinek, M., East, A., Cheng, A., Lin, S., Ma, E., and Doudna, J. (2013). RNA-programmed genome editing in human cells. eLife *2*.

Jirmo, A. C., Nagel, C.-H., Bohnen, C., Sodeik, B., and Behrens, G. M. N. (2009). Contribution of direct and cross-presentation to CTL immunity against Herpes Simplex Virus 1. The Journal of Immunology *182*, 283-292.

Joffre, O. P., Segura, E., Savina, A., and Amigorena, S. (2012). Cross-presentation by dendritic cells. Nature Reviews Immunology *12*, 557-569.

Johnson, P. A., MacLean, C., Marsden, H. S., Dalziel, R. G., and Everett, R. D. (1986). The product of gene US11 of Herpes Simplex Virus type 1 is expressed as a true late gene. Journal of General Virology *67*, 871-883.

Joly, E., Mucke, L., and Oldstone, M. (1991). Viral persistence in neurons explained by lack of Major Histocompatibility Class I expression. Science *253*, 1283-1285.

Jones, C. A., Raynes-Greenow, C., and Isaacs, D. (2014). Population-based surveillance of neonatal HSV infection in Australia (1997-2011). Clinical Infectious Diseases.

Jones, K. A., and Tjian, R. (1985). Sp1 binds to promoter sequences and activates Herpes Simplex Virus `immediate-early' gene transcription *in vitro*. Nature *317*, 179-182.

Jugovic, P., Hill, A. M., Tomazin, R., Ploegh, H., and Johnson, D. C. (1998). Inhibition of Major Histocompatibility Complex class I antigen presentation in pig and primate cells by Herpes Simplex Virus type 1 and 2 ICP47. Journal of Virology *72*, 5076-5084.

Jung, S., Unutmaz, D., Wong, P., Sano, G.-I., De los Santos, K., Sparwasser, T., Wu, S., Vuthoori, S., Ko, K., Zavala, F.*, et al.* (2002). *In vivo* depletion of $CD11c^+$ dendritic cells abrogates priming of $CD8^+$ T cells by exogenous cell-associated antigens. Immunity *17*, 211-220.

Jurak, I., Hackenberg, M., Kim, J. Y., Pesola, J. M., Everett, R. D., Preston, C. M., Wilson, A. C., and Coen, D. M. (2014). Expression of Herpes Simplex Virus 1 microRNAs in cell culture models of quiescent and latent infection. Journal of Virology *88*, 2337-2339.

Jurak, I., Kramer, M. F., Mellor, J. C., van Lint, A. L., Roth, F. P., Knipe, D. M., and Coen, D. M. (2010). Numerous conserved and divergent microRNAs expressed by Herpes Simplex Viruses 1 and 2. Journal of Virology *84*, 4659-4672.

Kaern, M., Elston, T. C., Blake, W. J., and Collins, J. J. (2005). Stochasticity in gene expression: from theories to phenotypes. Nature Reviews Genetics *6*, 451-464.

Kägi, D., Ledermann, B., Bürki, K., Seiler, P., Odermatt, B., Olsen, K. J., Podack, E. R., Zinkernagel, R. M., and Hengartner, H. (1994). Cytotoxicity mediated by T cells and natural killer cells is greatly impaired in perforin-deficient mice. Nature *369*, 31-37.

Karttunen, J., Sanderson, S., and Shastri, N. (1992). Detection of rare antigen-presenting cells by the lacZ T-cell activation assay suggests an expression cloning strategy for T-cell antigens. Proceedings of the National Academy of Sciences *89*, 6020-6024.

Karupiah, G., Xie, Q., Buller, R., Nathan, C., Duarte, C., and MacMicking, J. (1993). Inhibition of viral replication by interferon-γ-induced nitric oxide synthase. Science *261*, 1445-1448.

Kastrukoff, L. F., Lau, A. S., Takei, F., Smyth, M. J., Jones, C. M., Clarke, S. R. M., and Carbone, F. R. (2010). Redundancy in the immune system restricts the spread of HSV-1 in the central nervous system (CNS) of C57BL/6 mice. Virology *400*, 248-258.

Katz, J. P., Bodin, E. T., and Coen, D. M. (1990). Quantitative polymerase chain reaction analysis of Herpes Simplex Virus DNA in ganglia of mice infected with replication-incompetent mutants. Journal of Virology *64*, 4288-4295.

Kennedy, E. M., Bassit, L. C., Mueller, H., Kornepati, A. V. R., Bogerd, H. P., Nie, T., Chatterjee, P., Javanbakht, H., Schinazi, R. F., and Cullen, B. R. (2015a). Suppression of Hepatitis B virus DNA accumulation in chronically infected cells using a bacterial CRISPR/Cas RNA-guided DNA endonuclease. Virology *476*, 196-205.

Kennedy, E. M., Kornepati, A. V. R., Goldstein, M., Bogerd, H. P., Poling, B. C., Whisnant, A. W., Kastan, M. B., and Cullen, B. R. (2014). Inactivation of the Human Papillomavirus E6 or E7 gene in cervical carcinoma cells by using a bacterial CRISPR/Cas RNA-guided endonuclease. Journal of Virology *88*, 11965-11972.

Kennedy, P. G., Rovnak, J., Badani, H., and Cohrs, R. J. (2015b). A comparison of HSV-1 and VZV latency and reactivation. Journal of General Virology.

Kennedy, P. G. E., Grinfeld, E., and Bell, J. E. (2000). Varicella-Zoster Virus gene expression in latently infected and explanted human ganglia. Journal of Virology *74*, 11893-11898.

Kent, J. R., and Fraser, N. W. (2005). The cellular response to Herpes Simplex Virus type 1 (HSV-1) during latency and reactivation. Journal of NeuroVirology *11*, 376-383.

Kent, J. R., Zeng, P.-Y., Atanasiu, D., Gardner, J., Fraser, N. W., and Berger, S. L. (2004). During lytic infection Herpes Simplex Virus type 1 is associated with histones bearing modifications that correlate with active transcription. Journal of Virology *78*, 10178-10186.

Khanna, K. M., Bonneau, R. H., Kinchington, P. R., and Hendricks, R. L. (2003). Herpes Simplex Virus-specific memory $CD8^+$ T cells are selectively activated and retained in latently infected sensory ganglia. Immunity *18*, 593-603.

Khetsuriani, N., Holman, R. C., and Anderson, L. J. (2002). Burden of encephalitis-associated hospitalizations in the United States, 1988–1997. Clinical Infectious Diseases *35*, 175-182.

Kibler, P. K., Duncan, J., Keith, B. D., Hupel, T., and Smiley, J. R. (1991). Regulation of Herpes Simplex Virus true late gene expression: Sequences downstream from the U_S11 TATA box inhibit expression from an unreplicated template. Journal of Virology *65*, 6749-6760.

Kim, D., Bae, S., Park, J., Kim, E., Kim, S., Yu, H. R., Hwang, J., Kim, J.-I., and Kim, J.-S. (2015). Digenome-seq: Genome-wide profiling of CRISPR-Cas9 off-target effects in human cells. Nature Methods *12*, 237-243.

Kim, D. B., Zabierowski, S., and DeLuca, N. A. (2002). The initiator element in a Herpes Simplex Virus type 1 late-gene promoter enhances activation by ICP4, resulting in abundant late-gene expression. Journal of Virology *76*, 1548-1558.

Kim, J. Y., Mandarino, A., Chao, M. V., Mohr, I., and Wilson, A. C. (2012). Transient reversal of episome silencing precedes VP16-dependent transcription during reactivation of latent HSV-1 in neurons. PLoS Pathogens *8*, e1002540.

Kim, K. K., Adelstein, R. S., and Kawamoto, S. (2009). Identification of Neuronal Nuclei (NeuN) as Fox-3, a new member of the Fox-1 gene family of splicing factors. Journal of Biological Chemistry *284*, 31052-31061.

Kinchington, P. R. (1999). Latency of Varicella Zoster Virus; a persistently perplexing state. Frontiers in Bioscience *4*, 200 - 211.

Knaup, B., Schünemann, S., and Wolff, M. H. (2000). Subclinical reactivation of Herpes Simplex Virus type 1 in the oral cavity. Oral Microbiology and Immunology *15*, 281-283.

Knickelbein, J. E., Khanna, K. M., Yee, M. B., Baty, C. J., Kinchington, P. R., and Hendricks, R. L. (2008). Noncytotoxic lytic granule-mediated $CD8^+$ T cell inhibition of HSV-1 reactivation from neuronal latency. Science *322*, 268-271.

Knipe, D. M., and Cliffe, A. (2008). Chromatin control of Herpes Simplex Virus lytic and latent infection. Nature Reviews Microbiology *6*, 211-221.

Kodukula, P., Liu, T., Van Rooijen, N., Jager, M. J., and Hendricks, R. L. (1999). Macrophage control of Herpes Simplex Virus type 1 replication in the peripheral nervous system. The Journal of Immunology *162*, 2895-2905.

Koelle, D. M., Tigges, M. A., Burke, R. L., Symington, F. W., Riddell, S. R., Abbo, H., and Corey, L. (1993). Herpes Simplex Virus infection of human fibroblasts and keratinocytes inhibits recognition by cloned CD8+ cytotoxic T lymphocytes. J Clin Invest *91*, 961-968.

Kolb, A. W., and Brandt, C. R. (2004). Enhanced isolation of low frequency Herpes Simplex Virus recombinants using green-fluorescent protein and FACS. Journal of Virological Methods *115*, 73-81.

Kostavasili, I., Sahu, A., Friedman, H., Eisenberg, R., Cohen, G., and Lambris, J. (1997). Mechanism of complement inactivation by glycoprotein C of Herpes Simplex Virus. The Journal of Immunology *158*, 1763-1771.

Kosz-Vnenchak, M., Jacobson, J., Coen, D. M., and Knipe, D. M. (1993). Evidence for a novel regulatory pathway for Herpes Simplex Virus gene expression in trigeminal ganglion neurons. Journal of Virology *67*, 5383-5393.

Kramer, M., and Coen, D. (1995). Quantification of transcripts from the ICP4 and thymidine kinase genes in mouse ganglia latently infected with Herpes Simplex Virus. Journal of Virology *69*, 1389-1399.

Kramer, M. F., Chen, S.-H., Knipe, D. M., and Coen, D. M. (1998). Accumulation of viral transcripts and DNA during establishment of latency by Herpes Simplex Virus. Journal of Virology *72*, 1177-1185.

Kramer, M. F., Cook, W. J., Roth, F. P., Zhu, J., Holman, H., Knipe, D. M., and Coen, D. M. (2003). Latent Herpes Simplex Virus infection of sensory neurons alters neuronal gene expression. Journal of Virology *77*, 9533-9541.

Kramer, M. F., Jurak, I., Pesola, J. M., Boissel, S., Knipe, D. M., and Coen, D. M. (2011). Herpes Simplex Virus 1 microRNAs expressed abundantly during latent infection are not essential for latency in mouse trigeminal ganglia. Virology *417*, 239-247.

Krause, P. R., Croen, K. D., Straus, S. E., and Ostrove, J. M. (1988). Detection and preliminary characterization of Herpes Simplex Virus type 1 transcripts in latently infected human trigeminal ganglia. Journal of Virology *62*, 4819-4823.

Krisky, D. M., Marconi, P. C., Oligino, T., Rouse, R. J. D., Fink, D. J., and Glorioso, J. C. (1997). Rapid method for construction of recombinant HSV gene transfer vectors. Gene Therapy *4*, 1120-1125.

Kristie, T. M., Vogel, J. L., and Sears, A. E. (1999). Nuclear localization of the C1 factor (host cell factor) in sensory neurons correlates with reactivation of Herpes Simplex Virus from latency. Proceedings of the National Academy of Sciences *96*, 1229-1233.

Kubat, N. J., Amelio, A. L., Giordani, N. V., and Bloom, D. C. (2004a). The Herpes Simplex Virus type 1 Latency-Associated Transcript (LAT) enhancer/rcr is hyperacetylated during latency independently of LAT transcription. Journal of Virology *78*, 12508-12518.

Kubat, N. J., Tran, R. K., McAnany, P., and Bloom, D. C. (2004b). Specific histone tail modification and not DNA methylation is a determinant of Herpes Simplex Virus type 1 latent gene expression. Journal of Virology *78*, 1139-1149.

Kurts, C., Cannarile, M., Klebba, I., and Brocker, T. (2001). Cutting edge: Dendritic cells are sufficient to cross-present self-antigens to CD8 T cells *in vivo*. The Journal of Immunology *166*, 1439-1442.

Kurts, C., Sutherland, R. M., Davey, G., Li, M., Lew, A. M., Blanas, E., Carbone, F. R., Miller, J. F. A. P., and Heath, W. R. (1999). CD8 T cell ignorance or tolerance to islet antigens depends on antigen dose. Proceedings of the National Academy of Sciences of the United States of America *96*, 12703-12707.

Kutluay, S. B., and Triezenberg, S. J. (2009). Regulation of histone deposition on the Herpes Simplex Virus type 1 genome during lytic infection. Journal of Virology *83*, 5835-5845.

Kutyavin, I. V., Afonina, I. A., Mills, A., Gorn, V. V., Lukhtanov, E. A., Belousov, E. S., Singer, M. J., Walburger, D. K., Lokhov, S. G., Gall, A. A.*, et al.* (2000). 3′-Minor groove binder-DNA probes increase sequence specificity at PCR extension temperatures. Nucleic Acids Research *28*, 655-661.

Kwiatkowski, D. L., Thompson, H. W., and Bloom, D. C. (2009). The polycomb group protein Bmi1 binds to the Herpes Simplex Virus 1 latent genome and maintains repressive histone marks during latency. Journal of Virology *83*, 8173-8181.

Kwong, A. D., and Frenkel, N. (1987). Herpes simplex virus-infected cells contain a function(s) that destabilizes both host and viral mRNAs. Proceedings of the National Academy of Sciences *84*, 1926-1930.

Lacaille, V. G., and Androlewicz, M. J. (1998). Herpes Simplex Virus inhibitor ICP47 destabilizes the Transporter associated with Antigen Processing (TAP) heterodimer. Journal of Biological Chemistry *273*, 17386-17390.

Lacasse, J. J., and Schang, L. M. (2010). During lytic infections, Herpes Simplex Virus type 1 DNA is in complexes with the properties of unstable nucleosomes. Journal of Virology *84*, 1920-1933.

Lacasse, J. J., and Schang, L. M. (2012). Herpes Simplex Virus 1 DNA is in unstable nucleosomes throughout the lytic infection cycle, and the instability of the nucleosomes is independent of DNA replication. Journal of Virology *86*, 11287-11300.

Lachmann, R., and Efstathiou, S. (1997). Utilization of the Herpes Simplex Virus type 1 latency-associated regulatory region to drive stable reporter gene expression in the nervous system. Journal of Virology *71*, 3197-3207.

Lachmann, R. H., Brown, C., and Efstathiou, S. (1996). A murine RNA polymerase I promoter inserted into the Herpes Simplex Virus type 1 genome is functional during lytic, but not latent, infection. Journal of General Virology *77*, 2575-2582.

Lachmann, R. H., Sadarangani, M., Atkinson, H. R., and Efstathiou, S. (1999). An analysis of Herpes Simplex Virus gene expression during latency establishment and reactivation. Journal of General Virology *80*, 1271-1282.

Lagunoff, M., and Roizman, B. (1994). Expression of a Herpes Simplex Virus 1 open reading frame antisense to the χ34.5 gene and transcribed by an RNA 3' coterminal with the unspliced Latency-Associated Transcript. Journal of Virology *68*, 6021-6028.

Lampson, L. A., and Fisher, C. A. (1984). Weak HLA and β_2-microglobulin expression of neuronal cell lines can be modulated by interferon. Proceedings of the National Academy of Sciences *81*, 6476-6480.

Laurent, A. M., Madjar, J. J., and Greco, A. (1998). Translational control of viral and host protein synthesis during the course of Herpes Simplex Virus type 1 infection: Evidence that initiation of translation is the limiting step. Journal of General Virology *79 (Pt 11)*, 2765-2775.

Laycock, K. A., Lee, S. F., Brady, R. H., and Pepose, J. S. (1991). Characterization of a murine model of recurrent Herpes Simplex viral keratitis induced by ultraviolet B radiation. Investigative Ophthalmology and Visual Science *32*, 2741-2746.

LeBlanc, R. A., Pesnicak, L., Cabral, E. S., Godleski, M., and Straus, S. E. (1999). Lack of Interleukin-6 (IL-6) enhances susceptibility to infection but does not alter latency or reactivation of Herpes Simplex Virus type 1 in IL-6 knockout mice. Journal of Virology *73*, 8145-8151.

Lee, C. K., and Knipe, D. M. (1985). An immunoassay for the study of DNA-binding activities of Herpes Simplex Virus protein ICP8. Journal of Virology *54*, 731-738.

Lee, E. C., Yu, D., Martinez de Velasco, J., Tessarollo, L., Swing, D. A., Court, D. L., Jenkins, N. A., and Copeland, N. G. (2001). A highly efficient *Escherichia coli*-based chromosome engineering system adapted for recombinogenic targeting and subcloning of BAC DNA. Genomics *73*, 56-65.

Lee, H. K., Zamora, M., Linehan, M. M., Iijima, N., Gonzalez, D., Haberman, A., and Iwasaki, A. (2009). Differential roles of migratory and resident DCs in T cell priming after mucosal or skin HSV-1 infection. The Journal of Experimental Medicine *206*, 359-370.

Leib, D. A., Bogard, C. L., Kosz-Vnenchak, M., Hicks, K. A., Coen, D. M., Knipe, D. M., and Schaffer, P. A. (1989). A deletion mutant of the Latency-Associated Transcript of Herpes Simplex Virus type 1 reactivates from the latent state with reduced frequency. Journal of Virology *63*, 2893-2900.

Leib, D. A., Harrison, T. E., Laslo, K. M., Machalek, M. A., Moorman, N. J., and Virgin, H. W. (1999). Interferons regulate the phenotype of wild-type and mutant Herpes Simplex Viruses *in vivo*. The Journal of Experimental Medicine *189*, 663-672.

Leib, D. A., Machalek, M. A., Williams, B. R. G., Silverman, R. H., and Virgin, H. W. (2000). Specific phenotypic restoration of an attenuated virus by knockout of a host resistance gene. Proceedings of the National Academy of Sciences *97*, 6097-6101.

Leinbach, S. S., and Summers, W. C. (1980). The structure of Herpes Simplex Virus type 1 DNA as probed by micrococcal nuclease digestion. Journal of General Virology *51*, 45-59.

Lentine, A. F., and Bachenheimer, S. L. (1990). Intracellular organization of Herpes Simplex Virus type 1 DNA assayed by staphylococcal nuclease sensitivity. Virus Research *16*, 275-292.

Levin, M. J., Smith, J. G., Kaufhold, R. M., Barber, D., Hayward, A. R., Chan, C. Y., Chan, I. S. F., Li, D. J. J., Wang, W., Keller, P. M.*, et al.* (2003). Decline in Varicella-Zoster Virus (VZV)–specific cell-mediated immunity with increasing age and boosting with a high-dose VZV vaccine. The Journal of Infectious Diseases *188*, 1336-1344.

Li, J.-F., Norville, J. E., Aach, J., McCormack, M., Zhang, D., Bush, J., Church, G. M., and Sheen, J. (2013). Multiplex and homologous recombination-mediated genome editing in *Arabidopsis* and *Nicotiana benthamiana* using guide RNA and Cas9. Nature Biotechnology *31*, 688-691.

Liesegang, T. J. (2001). Herpes Simplex Virus epidemiology and ocular importance. Cornea *20*, 1-13.

Lieu, P. T., and Wagner, E. K. (2000). Two leaky-late HSV-1 promoters differ significantly in structural architecture. Virology *272*, 191-203.

Lilley, C. E., Chaurushiya, M. S., Boutell, C., Everett, R. D., and Weitzman, M. D. (2011). The intrinsic antiviral defense to incoming HSV-1 genomes includes specific DNA repair proteins and is counteracted by the viral protein ICP0. PLoS Pathogens *7*, e1002084.

Lin, R., Noyce, R. S., Collins, S. E., Everett, R. D., and Mossman, K. L. (2004). The Herpes Simplex Virus ICP0 RING finger domain inhibits IRF3- and IRF7-mediated activation of interferon-stimulated genes. Journal of Virology *78*, 1675-1684.

Liu, T., Khanna, K. M., Carriere, B. N., and Hendricks, R. L. (2001). Gamma interferon can prevent Herpes Simplex Virus type 1 reactivation from latency in sensory neurons. Journal of Virology *75*, 11178-11184.

Liu, T., Khanna, K. M., Chen, X., Fink, D. J., and Hendricks, R. L. (2000). $CD8^+$ T cells can block Herpes Simplex Virus type 1 (HSV-1) reactivation from latency in sensory neurons. The Journal of Experimental Medicine *191*, 1459-1466.

Liu, T., Tang, Q., and Hendricks, R. (1996). Inflammatory infiltration of the trigeminal ganglion after Herpes Simplex Virus type 1 corneal infection. Journal of Virology *70*, 264-271.

Logvinoff, C., and Epstein, A. L. (2000). Genetic engineering of Herpes Simplex Virus and vector genomes carrying *loxP* sites in cells expressing Cre recombinase. Virology *267*, 102-110.

Lokensgard, J. R., Berthomme, H., and Feldman, L. T. (1997). The latency-associated promoter of Herpes Simplex Virus type 1 requires a region downstream of the transcription start site for long-term expression during latency. Journal of Virology *71*, 6714-6719.

Lomonte, P., Sullivan, K. F., and Everett, R. D. (2001). Degradation of nucleosome-associated Centromeric Histone H3-like Protein CENP-A induced by Herpes Simplex Virus type 1 Protein ICP0. Journal of Biological Chemistry *276*, 5829-5835.

Lomonte, P., Thomas, J., Texier, P., Caron, C., Khochbin, S., and Epstein, A. L. (2004). Functional interaction between class II histone deacetylases and ICP0 of Herpes Simplex Virus type 1. Journal of Virology *78*, 6744-6757.

Long, M. C., Leong, V., Schaffer, P. A., Spencer, C. A., and Rice, S. A. (1999). ICP22 and the U_L13 protein kinase are both required for Herpes Simplex Virus-induced modification of the large subunit of RNA polymerase II. Journal of Virology *73*, 5593-5604.

Loutsch, J. M., Perng, G.-C., Hill, J. M., Zheng, X., Marquart, M. E., Block, T. M., Ghiasi, H., Nesburn, A. B., and Wechsler, S. L. (1999). Identical 371-base-pair deletion mutations in the LAT genes of Herpes Simplex Virus type 1 McKrae and 17^{syn+} result in different *in vivo* reactivation phenotypes. Journal of Virology *73*, 767-771.

Lowin, B., Hahne, M., Mattmann, C., and Tschopp, J. (1994). Cytolytic T-cell cytotoxicity is mediated through perforin and Fas lytic pathways. Nature *370*, 650-652.

Lubinski, J. M., Lazear, H. M., Awasthi, S., Wang, F., and Friedman, H. M. (2011). The Herpes Simplex Virus 1 IgG Fc receptor blocks antibody-mediated complement activation and antibody-dependent cellular cytotoxicity *in vivo*. Journal of Virology *85*, 3239-3249.

Lubinski, J. M., Wang, L., Soulika, A. M., Burger, R., Wetsel, R. A., Colten, H., Cohen, G. H., Eisenberg, R. J., Lambris, J. D., and Friedman, H. M. (1998). Herpes Simplex Virus type 1 glycoprotein gC mediates immune evasion *in vivo*. Journal of Virology *72*, 8257-8263.

Lukashchuk, V., and Everett, R. D. (2010). Regulation of ICP0-null mutant Herpes Simplex Virus type 1 infection by ND10 components ATRX and hDaxx. Journal of Virology *84*, 4026-4040.

Luker, G. D., Bardill, J. P., Prior, J. L., Pica, C. M., Piwnica-Worms, D., and Leib, D. A. (2002). Noninvasive bioluminescence imaging of Herpes Simplex Virus type 1 infection and therapy in living mice. Journal of Virology *76*, 12149-12161.

Lyn Burke, R., Hartog, K., Croen, K. D., and Ostrove, J. M. (1991). Detection and characterization of latent HSV RNA by *in situ* and northern blot hybridization in guinea pigs. Virology *181*, 793-797.

Ma, J. Z., Russell, T. A., Spelman, T., Carbone, F. R., and Tscharke, D. C. (2014). Lytic gene expression is frequent in HSV-1 latent infection and correlates with the engagement of a cell-intrinsic transcriptional response. PLoS Pathogens *10*, e1004237.

Macdonald, S. J., Mostafa, H. H., Morrison, L. A., and Davido, D. J. (2012). Genome sequence of Herpes Simplex Virus 1 strain KOS. Journal of Virology *86*, 6371-6372.

Mackay, I. M. (2004). Real-time PCR in the microbiology laboratory. Clinical Microbiology and Infection *10*, 190-212.

Mackay, I. M., Arden, K. E., and Nitsche, A. (2002). Real-time PCR in virology. Nucleic Acids Research *30*, 1292-1305.

Mackay, L. K., Rahimpour, A., Ma, J. Z., Collins, N., Stock, A. T., Hafon, M.-L., Vega-Ramos, J., Lauzurica, P., Mueller, S. N., Stefanovic, T.*, et al.* (2013). The developmental pathway for $CD103^{+}CD8^{+}$ tissue-resident memory T cells of skin. Nature Immunology *14*, 1294-1301.

Mackay, L. K., Stock, A. T., Ma, J. Z., Jones, C. M., Kent, S. J., Mueller, S. N., Heath, W. R., Carbone, F. R., and Gebhardt, T. (2012). Long-lived epithelial immunity by tissue-resident memory T (T_{RM}) cells in the absence of persisting local antigen presentation. Proceedings of the National Academy of Sciences *109*, 7037-7042.

Mackem, S., and Roizman, B. (1982). Structural features of the Herpes Simplex Virus α gene 4, 0, and 27 promoter-regulatory sequences which confer α regulation on chimeric thymidine kinase genes. Journal of Virology *44*, 939-949.

Mackett, M., Smith, G. L., and Moss, B. (1982). Vaccinia Virus: A selectable eukaryotic cloning and expression vector. Proceedings of the National Academy of Sciences *79*, 7415-7419.

Mador, N., Goldenberg, D., Cohen, O., Panet, A., and Steiner, I. (1998). Herpes Simplex Virus type 1 Latency-Associated Transcripts suppress viral replication and reduce immediate-early gene mRNA levels in a neuronal cell line. Journal of Virology *72*, 5067-5075.

Maehlen, J., Schröder, H. D., Klareskog, L., Olsson, T., and Kristensson, K. (1988). Axotomy induces MHC class I antigen expression on rat nerve cells. Neuroscience letters *92*, 8-13.

Maggioncalda, J., Mehta, A., Fraser, N. W., and Block, T. M. (1994). Analysis of a Herpes Simplex Virus type 1 LAT mutant with a deletion between the putative promoter and the 5' end of the 2.0-kilobase transcript. Journal of Virology *68*, 7816-7824.

Maggioncalda, J., Mehta, A., Su, Y. H., Fraser, N. W., and Block, T. M. (1996). Correlation between Herpes Simplex Virus type 1 rate of reactivation from latent infection and the number of infected neurons in trigeminal ganglia. Virology *225*, 72-81.

Maillet, S., Naas, T., Crepin, S., Roque-Afonso, A. M., Lafay, F., Efstathiou, S., and Labetoulle, M. (2006). Herpes Simplex Virus type 1 latently infected neurons differentially express latency-associated and ICP0 transcripts. Journal of Virology *80*, 9310-9321.

Mali, P., Yang, L., Esvelt, K. M., Aach, J., Guell, M., DiCarlo, J. E., Norville, J. E., and Church, G. M. (2013). RNA-guided human genome engineering via Cas9. Science *339*, 823-826.

Manickan, E., and Rouse, B. T. (1995). Roles of different T-cell subsets in control of Herpes Simplex Virus infection determined by using T-cell-deficient mouse models. Journal of Virology *69*, 8178-8179.

Margolis, T. P., Bloom, D. C., Dobson, A. T., Feldman, L. T., and Stevens, J. G. (1993). Decreased reporter gene expression during latent infection with HSV LAT promoter constructs. Virology *197*, 585-592.

Margolis, T. P., Elfman, F. L., Leib, D., Pakpour, N., Apakupakul, K., Imai, Y., and Voytek, C. (2007a). Spontaneous reactivation of Herpes Simplex Virus type 1 in latently infected murine sensory ganglia. Journal of Virology *81*, 11069-11074.

Margolis, T. P., Imai, Y., Yang, L., Vallas, V., and Krause, P. R. (2007b). Herpes Simplex Virus type 2 (HSV-2) establishes latent infection in a different population of ganglionic neurons than HSV-1: Role of Latency-Associated Transcripts. Journal of Virology *81*, 1872-1878.

Margolis, T. P., Sedarati, F., Dobson, A. T., Feldman, L. T., and Stevens, J. G. (1992). Pathways of viral gene expression during acute neuronal infection with HSV-1. Virology *189*, 150-160.

Marinov, G. K., Williams, B. A., McCue, K., Schroth, G. P., Gertz, J., Myers, R. M., and Wold, B. J. (2014). From single-cell to cell-pool transcriptomes: Stochasticity in gene expression and RNA splicing. Genome Research *24*, 496-510.

Mark, K. E., Wald, A., Magaret, A. S., Selke, S., Olin, L., Huang, M.-L., and Corey, L. (2008). Rapidly cleared episodes of Herpes Simplex Virus reactivation in immunocompetent adults. The Journal of Infectious Diseases *198*, 1141-1149.

Markovitz, N. S. (2007). The Herpes Simplex Virus Type 1 U_L3 transcript starts within the U_L3 Open Reading Frame and encodes a 224-amino-acid protein. Journal of Virology *81*, 10524-10531.

Marshall, K. R., Lachmann, R. H., Efstathiou, S., Rinaldi, A., and Preston, C. M. (2000). Long-term transgene expression in mice infected with a Herpes Simplex Virus type 1 mutant severely impaired for immediate-early gene expression. Journal of Virology *74*, 956-964.

Mavromara-Nazos, P., Ackermann, M., and Roizman, B. (1986). Construction and properties of a viable Herpes Simplex Virus 1 recombinant lacking coding sequences of the α47 gene. Journal of Virology *60*, 807-812.

Mavromara-Nazos, P., and Roizman, B. (1989). Delineation of regulatory domains of early (β) and late (γ_2) genes by construction of chimeric genes expressed in Herpes Simplex Virus 1 genomes. Proceedings of the National Academy of Sciences of the United States of America *86*, 4071-4075.

McAllister, S. C., and Schleiss, M. R. (2014). Prospects and perspectives for development of a vaccine against Herpes Simplex Virus infections. Expert Review of Vaccines *13*, 1349-1360.

McGeoch, D. J., Dalrymple, M. A., Davison, A. J., Dolan, A., Frame, M. C., McNab, D., Perry, L. J., Scott, J. E., and Taylor, P. (1988). The complete DNA sequence of the Long Unique region in the genome of Herpes Simplex Virus type 1. Journal of General Virology *69*, 1531-1574.

McGeoch, D. J., Dolan, A., Donald, S., and Brauer, D. H. K. (1986). Complete DNA sequence of the short repeat region in the genome of Herpes Simplex Virus type 1. Nucleic Acids Research *14*, 1727-1745.

McGrath, N., Anderson, N. E., Croxson, M. C., and Powell, K. F. (1997). Herpes Simplex encephalitis treated with acyclovir: Diagnosis and long term outcome. Journal of Neurology, Neurosurgery and Psychiatry *63*, 321-326.

McGregor, F., Phelan, A., Dunlop, J., and Clements, J. (1996). Regulation of Herpes Simplex Virus poly (A) site usage and the action of immediate-early protein IE63 in the early-late switch. Journal of Virology *70*, 1931-1940.

McKnight, S. L. (1982). Functional relationships between transcriptional control signals of the thymidine kinase gene of Herpes Simplex Virus. Cell *31*, 355-365.

McLenachan, S., Sarsero, J. P., and Ioannou, P. A. (2007). Flow-cytometric analysis of mouse embryonic stem cell lipofection using small and large DNA constructs. Genomics *89*, 708-720.

Mehta, A., Maggioncalda, J., Bagasra, O., Thikkavarapu, S., Saikumari, P., Valyi-Nagy, T., Fraser, N. W., and Block, T. M. (1995). *In situ* DNA PCR and RNA hybridization detection of herpes simplex virus sequences in trigeminal gangliaof latently infected mice. Virology *206*, 633-640.

Mellerick, D. M., and Fraser, N. W. (1987). Physical state of the latent herpes simplex virus genome in a mouse model system: Evidence suggesting an episomal state. Virology *158*, 265-275.

Messer, H. G. P., Jacobs, D., Dhummakupt, A., and Bloom, D. C. (2015). Inhibition of H3K27me3-specific histone demethylases JMJD3 and UTX blocks reactivation of Herpes Simplex Virus 1 in trigeminal ganglion neurons. Journal of Virology *89*, 3417-3420.

Metzger, D., Clifford, J., Chiba, H., and Chambon, P. (1995). Conditional site-specific recombination in mammalian cells using a ligand-dependent chimeric Cre recombinase. Proceedings of the National Academy of Sciences *92*, 6991-6995.

Minami, M., Kita, M., Yan, X.-Q., Yamamoto, T., Iida, T., Sekikawa, K., Iwakura, Y., and Imanishi, J. (2002). Role of IFN-γ and Tumor Necrosis Factor-α in Herpes Simplex Virus type 1 infection. Journal of Interferon and Cytokine Research *22*, 671-676.

Mintern, J. D., Guillonneau, C., Carbone, F. R., Doherty, P. C., and Turner, S. J. (2007). Cutting edge: Tissue-resident memory CTL down-regulate cytolytic molecule expression following virus clearance. The Journal of Immunology *179*, 7220-7224.

Mitchell, W. J., Gressens, P., Martin, J. R., and DeSanto, R. (1994). Herpes simplex virus type 1 DNA persistence, progressive disease and transgenic immediate early gene promoter activity in chronic corneal infections in mice. Journal of General Virology *75*, 1201-1210.

Mizuguchi, H., Xu, Z., Ishii-Watabe, A., Uchida, E., and Hayakawa, T. (2000). IRES-dependent second gene expression is significantly lower than cap-dependent first gene expression in a bicistronic vector. Molecular Therapy *1*, 376-382.

Mocarski, E. S., Post, L. E., and Roizman, B. (1980). Molecular engineering of the Herpes Simplex Virus genome: Insertion of a second L-S junction into the genome causes additional genome inversions. Cell *22*, 243-255.

Mocarski, E. S., and Roizman, B. (1982). Structure and role of the Herpes Simplex Virus DNA termini in inversion, circularization and generation of virion DNA. Cell *31*, 89-97.

Mori, I., and Nishiyama, Y. (2005). Herpes Simplex Virus and Varicella-Zoster Virus: Why do these human alphaherpesviruses behave so differently from one another? Reviews in Medical Virology *15*, 393-406.

Morimoto, T., Arii, J., Akashi, H., and Kawaguchi, Y. (2009). Identification of multiple sites suitable for insertion of foreign genes in Herpes Simplex Virus genomes. Microbiology and Immunology *53*, 155-161.

Morris, A. G., Lin, Y.-L., and Askonas, B. A. (1982). Immune interferon release when a cloned cytotoxic T-cell line meets its correct influenza-infected target cell. Nature *295*, 150-152.

Mueller, S. N., Jones, C. M., Smith, C. M., Heath, W. R., and Carbone, F. R. (2002). Rapid cytotoxic T lymphocyte activation occurs in the draining lymph nodes after cutaneous Herpes Simplex Virus infection as a result of early antigen presentation and not the presence of virus. The Journal of Experimental Medicine *195*, 651-656.

Muggeridge, M. I., and Fraser, N. W. (1986). Chromosomal organization of the Herpes Simplex Virus genome during acute infection of the mouse central nervous system. Journal of Virology *59*, 764-767.

Mullen, R. J., Buck, C. R., and Smith, A. M. (1992). NeuN, a neuronal specific nuclear protein in vertebrates. Development *116*, 201-211.

Munson, D. J., and Burch, A. D. (2012). A novel miRNA produced during lytic HSV-1 infection is important for efficient replication in tissue culture. Archives of Virology *157*, 1677-1688.

Murchie, M. J., and McGeoch, D. J. (1982). DNA sequence analysis of an immediate-early gene region of the Herpes Simplex Virus type 1 genome (map coordinates 0.950 to 0.978). Journal of General Virology *62*, 1-15.

Nagai, T., Ibata, K., Park, E. S., Kubota, M., Mikoshiba, K., and Miyawaki, A. (2002). A variant of yellow fluorescent protein with fast and efficient maturation for cell-biological applications. Nature Biotechnology *20*, 87-90.

Nagashunmugam, T., Lubinski, J., Wang, L., Goldstein, L. T., Weeks, B. S., Sundaresan, P., Kang, E. H., Dubin, G., and Friedman, H. M. (1998). *In vivo* immune evasion mediated by the Herpes Simplex Virus type 1 immunoglobulin G Fc receptor. Journal of Virology *72*, 5351-5359.

Nagel, M. A., Choe, A., Traktinskiy, I., Cordery-Cotter, R., Gilden, D., and Cohrs, R. J. (2011). Varicella-Zoster Virus transcriptome in latently infected human ganglia. Journal of Virology *85*, 2276-2287.

Naito, J., Mukerjee, R., Mott, K. R., Kang, W., Osorio, N., Fraser, N. W., and Perng, G.-C. (2005). Identification of a protein encoded in the herpes simplex virus type 1 latency associated transcript promoter region. Virus Research *108*, 101-110.

Nash, A. A., Jayasuriya, A., Phelan, J., Cobbold, S. P., Waldmann, H., and Prospero, T. (1987). Different roles for $L3T4^+$ and $Lyt\ 2^+$ T cell subsets in the control of an acute Herpes Simplex Virus infection of the skin and nervous system. Journal of General Virology *68*, 825-833.

Nelson, J. A., Reynolds-Kohler, C., and Smith, B. A. (1987). Negative and positive regulation by a short segment in the 5'-flanking region of the human Cytomegalovirus major immediate-early gene. Molecular and Cellular Biology *7*, 4125-4129.

Neumann, D. M., Bhattacharjee, P. S., Giordani, N. V., Bloom, D. C., and Hill, J. M. (2007a). *In vivo* changes in the patterns of chromatin structure associated with the latent Herpes Simplex Virus type 1 genome in mouse trigeminal ganglia can be detected at early times after butyrate treatment. Journal of Virology *81*, 13248-13253.

Neumann, D. M., Bhattacharjee, P. S., and Hill, J. M. (2007b). Sodium butyrate: A chemical inducer of *in vivo* reactivation of Herpes Simplex Virus type 1 in the ocular mouse model. Journal of Virology *81*, 6106-6110.

Neumann, H. (2001). Control of glial immune function by neurons. Glia *36*, 191-199.

Ngoi, S. M., Chien, A. C., and Lee, C. G. (2004). Exploiting internal ribosome entry sites in gene therapy vector design. Current Gene Therapy *4*, 15-31.

Nichol, P. F., Chang, J. Y., Johnson, E. M., and Olivo, P. D. (1996). Herpes Simplex Virus gene expression in neurons: Viral DNA synthesis is a critical regulatory event in the branch point between the lytic and latent pathways. Journal of Virology *70*, 5476-5486.

Nicholas, J. (1996). Determination and analysis of the complete nucleotide sequence of human herpesvirus. Journal of Virology *70*, 5975-5989.

Nicoll, M. P., Proença, J. T., Connor, V., and Efstathiou, S. (2012). Influence of Herpes Simplex Virus 1 Latency-Associated Transcripts on the establishment and maintenance of latency in the ROSA26R reporter mouse model. Journal of Virology *86*, 8848-8858.

Niedermann, G., Butz, S., Ihlenfeldt, H. G., Grimm, R., Lucchiari, M., Hoschutzky, H., Jung, G., Maier, B., and Eichmann, K. (1995). Contribution of proteasome-mediated proteolysis to the hierarchy of epitopes presented by Major Histocompatibility Complex class I molecules. Immunity *2*, 289-299.

Nolan, G. P., Fiering, S., Nicolas, J. F., and Herzenberg, L. A. (1988). Fluorescence-activated cell analysis and sorting of viable mammalian cells based on β-D-galactosidase activity after transduction of *Escherichia coli lacZ*. Proceedings of the National Academy of Sciences *85*, 2603-2607.

Norbury, C. C., Basta, S., Donohue, K. B., Tscharke, D. C., Princiotta, M. F., Berglund, P., Gibbs, J., Bennink, J. R., and Yewdell, J. W. (2004). $CD8^+$ T cell cross-priming via transfer of proteasome substrates. Science *304*, 1318-1321.

Nuchtern, J. G., Bonifacino, J. S., Biddison, W. E., and Klausner, R. D. (1989). Brefeldin A implicates egress from endoplasmic reticulum in class I restricted antigen presentation. Nature *339*, 223-226.

O'Hare, P., and Hayward, G. S. (1985). Three *trans*-acting regulatory proteins of Herpes Simplex Virus modulate immediate-early gene expression in a pathway involving positive and negative feedback regulation. Journal of Virology *56*, 723-733.

O'Malley, M. B., and MacLeish, P. R. (1993). Induction of class I Major Histocompatibility Complex antigens on adult primate retinal neurons. Journal of Neuroimmunology *43*, 45-57.

O'Neil, J. E., Loutsch, J. M., Aguilar, J. S., Hill, J. M., Wagner, E. K., and Bloom, D. C. (2004). Wide variations in Herpes Simplex Virus type 1 inoculum dose and Latency-Associated Transcript expression phenotype do not alter the establishment of latency in the rabbit eye model. Journal of Virology *78*, 5038-5044.

O'Rourke, D., and O'Hare, P. (1993). Mutually exclusive binding of two cellular factors within a critical promoter region of the gene for the IE110k protein of Herpes Simplex Virus. Journal of Virology *67*, 7201-7214.

Oh, J., and Fraser, N. W. (2008). Temporal association of the Herpes Simplex Virus genome with histone proteins during a lytic infection. Journal of Virology *82*, 3530-3537.

Ohashi, M., Bertke, A. S., Patel, A., and Krause, P. R. (2011). Spread of Herpes Simplex Virus to the spinal cord is independent of spread to dorsal root ganglia. Journal of Virology *85*, 3030-3032.

Orlando, J. S., Astor, T. L., Rundle, S. A., and Schaffer, P. A. (2006a). The products of the Herpes Simplex Virus type 1 immediate-early $U_S1/U_S1.5$ genes downregulate levels of S-phase-specific cyclins and facilitate virus replication in S-phase Vero cells. Journal of Virology *80*, 4005-4016.

Orlando, J. S., Balliet, J. W., Kushnir, A. S., Astor, T. L., Kosz-Vnenchak, M., Rice, S. A., Knipe, D. M., and Schaffer, P. A. (2006b). ICP22 is required for wild-type composition and infectivity of Herpes Simplex Virus type 1 virions. Journal of Virology *80*, 9381-9390.

Orr, M. T., Edelmann, K. H., Vieira, J., Corey, L., Raulet, D. H., and Wilson, C. B. (2005). Inhibition of MHC class I is a virulence factor in Herpes Simplex Virus infection of mice. PLoS Pathogens *1*, 0062-0071.

Orr, M. T., Mathis, M. A., Lagunoff, M., Sacks, J. A., and Wilson, C. B. (2007). CD8 T cell control of HSV reactivation from latency is abrogated by viral inhibition of MHC class I. Cell Host and Microbe *2*, 172-180.

Ortmann, B., Copeman, J., Lehner, P. J., Sadasivan, B., Herberg, J. A., Grandea, A. G., Riddell, S. R., Tampe, R., Spies, T., Trowsdale, J.*, et al.* (1997). A critical role for tapasin in the assembly and function of multimeric MHC class I-TAP complexes. Science *277*, 1306-1309.

Orvedahl, A., Alexander, D., Tallóczy, Z., Sun, Q., Wei, Y., Zhang, W., Burns, D., Leib, D. A., and Levine, B. (2007). HSV-1 ICP34.5 confers neurovirulence by targeting the Beclin 1 autophagy protein. Cell Host and Microbe *1*, 23-35.

Ouwendijk, W. J. D., Choe, A., Nagel, M. A., Gilden, D., Osterhaus, A. D. M. E., Cohrs, R. J., and Verjans, G. M. G. M. (2012). Restricted Varicella-Zoster Virus transcription in human trigeminal ganglia obtained soon after death. Journal of Virology *86*, 10203-10206.

Padgett, D. A., Sheridan, J. F., Dorne, J., Berntson, G. G., Candelora, J., and Glaser, R. (1998). Social stress and the reactivation of latent Herpes Simplex Virus type 1. Proceedings of the National Academy of Sciences *95*, 7231-7235.

Paladino, P., and Mossman, K. L. (2009). Mechanisms employed by Herpes Simplex Virus 1 to inhibit the interferon response. Journal of Interferon and Cytokine Research *29*, 599-608.

Pande, N. T., Petroski, M. D., and Wagner, E. K. (1998). Functional modules important for activated expression of early genes of Herpes Simplex Virus type 1 are clustered upstream of the TATA box. Virology *246*, 145-157.

Pasieka, T. J., Cilloniz, C., Lu, B., Teal, T. H., Proll, S. C., Katze, M. G., and Leib, D. A. (2009). Host responses to wild-type and attenuated Herpes Simplex Virus infection in the absence of STAT1. Journal of Virology *83*, 2075-2087.

Pasparakis, M. (2007). Animal models of T cell-mediated skin diseases, T. Zollner, H. Renz, and K. Asadullah, eds. (Heidelberg, Springer Science & Business Media).

Pattanayak, V., Lin, S., Guilinger, J. P., Ma, E., Doudna, J. A., and Liu, D. R. (2013). High-throughput profiling of off-target DNA cleavage reveals RNA-programmed Cas9 nuclease specificity. Nature Biotechnology *31*, 839-843.

Pederson, N. E., Person, S., and Homa, F. L. (1992). Analysis of the gB promoter of Herpes Simplex Virus type 1: High-level expression requires both an 89-base-pair promoter fragment and a nontranslated leader sequence. Journal of Virology *66*, 6226-6232.

Pellet, P., and Roizman, B. (2013). Fields virology, 6th Edition edn (Philadelphia, Lippincott Williams & Wilkins).

Peng, W., Henderson, G., Perng, G.-C., Nesburn, A. B., Wechsler, S. L., and Jones, C. (2003). The gene that encodes the Herpes Simplex Virus type 1 Latency-Associated Transcript influences the accumulation of transcripts (Bcl-xL and Bcl-xS) that encode apoptotic regulatory proteins. Journal of Virology *77*, 10714-10718.

Peng, W., Jin, L., Henderson, G., Perng, G. C., Brick, D. J., Nesburn, A. B., Wechsler, S. L., and Jones, C. (2004). Mapping Herpes Simplex Virus type 1 Latency-Associated Transcript

sequences that protect from apoptosis mediated by a plasmid expressing caspase-8. Journal of NeuroVirology *10*, 260-265.

Peng, W., Vitvitskaia, O., Carpenter, D., Wechsler, S., and Jones, C. (2008). Identification of two small RNAs within the first 1.5-kb of the Herpes Simplex Virus type 1-encoded Latency-Associated Transcript. Journal of NeuroVirology *14*, 41-52.

Pereira, R. A., and Simmons, A. (1999). Cell surface expression of H2 antigens on primary sensory neurons in response to acute but not latent Herpes Simplex Virus infection *in vivo*. Journal of Virology *73*, 6484-6489.

Pereira, R. A., Simon, M. M., and Simmons, A. (2000). Granzyme A, a noncytolytic component of $CD8^+$ cell granules, restricts the spread of Herpes Simplex Virus in the peripheral nervous systems of experimentally infected mice. Journal of Virology *74*, 1029-1032.

Pereira, R. A., Tscharke, D. C., and Simmons, A. (1994). Upregulation of class I Major Histocompatibility Complex gene expression in primary sensory neurons, satellite cells, and Schwann cells of mice in response to acute but not latent Herpes Simplex Virus infection *in vivo*. The Journal of Experimental Medicine *180*, 841-850.

Perng, G.-C., Maguen, B., Jin, L., Mott, K. R., Osorio, N., Slanina, S. M., Yukht, A., Ghiasi, H., Nesburn, A. B., Inman, M.*, et al.* (2002). A gene capable of blocking apoptosis can substitute for the Herpes Simplex Virus type 1 Latency-Associated Transcript gene and restore wild-type reactivation levels. Journal of Virology *76*, 1224-1235.

Perng, G.-C., Slanina, S. M., Ghiasi, H., Nesburn, A. B., and Wechsler, S. L. (2001). The effect of Latency-Associated Transcript on the Herpes Simplex Virus type 1 latency-reactivation phenotype is mouse strain-dependent. Journal of General Virology *82*, 1117-1122.

Perng, G.-C., Slanina, S. M., Yukht, A., Ghiasi, H., Nesburn, A. B., and Wechsler, S. L. (2000a). The Latency-Associated Transcript gene enhances establishment of Herpes Simplex Virus type 1 latency in rabbits. Journal of Virology *74*, 1885-1891.

Perng, G. C., Chokephaibulkit, K., Thompson, R. L., Sawtell, N. M., Slanina, S. M., Ghiasi, H., Nesburn, A. B., and Wechsler, S. L. (1996a). The region of the Herpes Simplex Virus type 1 LAT gene that is colinear with the ICP34.5 gene is not involved in spontaneous reactivation. Journal of Virology *70*, 282-291.

Perng, G. C., Dunkel, E. C., Geary, P. A., Slanina, S. M., Ghiasi, H., Kaiwar, R., Nesburn, A. B., and Wechsler, S. L. (1994). The Latency-Associated Transcript gene of Herpes Simplex Virus type 1 (HSV-1) is required for efficient *in vivo* spontaneous reactivation of HSV-1 from latency. Journal of Virology *68*, 8045-8055.

Perng, G. C., Ghiasi, H., Slanina, S. M., Nesburn, A. B., and Wechsler, S. L. (1996b). The spontaneous reactivation function of the Herpes Simplex Virus type 1 LAT gene resides completely within the first 1.5 kilobases of the 8.3-kilobase primary transcript. Journal of Virology *70*, 976-984.

Perng, G. C., Jones, C., Ciacci-Zanella, J., Stone, M., Henderson, G., Yukht, A., Slanina, S. M., Hofman, F. M., Ghiasi, H., Nesburn, A. B.*, et al.* (2000b). Virus-induced neuronal apoptosis blocked by the Herpes Simplex Virus Latency-Associated Transcript. Science *287*, 1500-1503.

Perng, G. C., Slanina, S. M., Ghiasi, H., Nesburn, A. B., and Wechsler, S. L. (1996c). A 371-nucleotide region between the Herpes Simplex Virus type 1 (HSV-1) LAT promoter and the 2-kilobase LAT is not essential for efficient spontaneous reactivation of latent HSV-1. Journal of Virology *70*, 2014-2018.

Perng, G. C., Thompson, R. L., Sawtell, N. M., Taylor, W. E., Slanina, S. M., Ghiasi, H., Kaiwar, R., Nesburn, A. B., and Wechsler, S. L. (1995). An avirulent ICP34.5 deletion mutant of Herpes Simplex Virus type 1 is capable of *in vivo* spontaneous reactivation. Journal of Virology *69*, 3033-3041.

Pesola, J. M., Zhu, J., Knipe, D. M., and Coen, D. M. (2005). Herpes Simplex Virus 1 immediate-early and early gene expression during reactivation from latency under conditions that prevent infectious virus production. Journal of Virology *79*, 14516-14525.

Peterson, P. A., Rask, L., and Lindblom, J. B. (1974). Highly purified papain-solubilized HL-A antigens contain β_2-microglobulin. Proceedings of the National Academy of Sciences *71*, 35-39.

Pfeffer, S., Sewer, A., Lagos-Quintana, M., Sheridan, R., Sander, C., Grasser, F. A., van Dyk, L. F., Ho, C. K., Shuman, S., Chien, M.*, et al.* (2005). Identification of microRNAs of the herpesvirus family. Nature Methods *2*, 269-276.

Pfizenmaier, K., Jung, H., Starzinski-Powitz, A., Röllinghoff, M., and Wagner, H. (1977). The role of T Cells in anti-Herpes Simplex Virus immunity: I. Induction of antigen-specific cytotoxic T lymphocytes. The Journal of Immunology *119*, 939-944.

Phillips, G. J. (2001). Green fluorescent protein – a bright idea for the study of bacterial protein localization. FEMS Microbiology Letters *204*, 9-18.

Pignatti, P. F., and Cassai, E. (1980). Analysis of Herpes Simplex Virus nucleoprotein complexes extracted from infected cells. Journal of Virology *36*, 816-828.

Plotkin, S. A., Stein, S., Snyder, M., and Immesoete, P. (1977). Attempts to recover Varicella Virus from ganglia. Annals of Neurology *2*, 249-249.

Poffenberger, K. L., Idowu, A. D., Fraser-Smith, E. B., Raichlen, P. E., and Herman, R. C. (1994). A Herpes Simplex Virus type 1 ICP22 deletion mutant is altered for virulence and latency *in vivo*. Archives of Virology *139*, 111-119.

Porgador, A., Yewdell, J. W., Deng, Y., Bennink, J. R., and Germain, R. N. (1997). Localization, quantitation, and *in situ* detection of specific peptide–MHC class I complexes using a monoclonal antibody. Immunity *6*, 715-726.

Posavad, C. M., and Rosenthal, K. L. (1992). Herpes Simplex Virus-infected human fibroblasts are resistant to and inhibit cytotoxic T-lymphocyte activity. Journal of Virology *66*, 6264-6272.

Post, L. E., Conley, A. J., Mocarski, E. S., and Roizman, B. (1980). Cloning of reiterated and nonreiterated Herpes Simplex Virus 1 sequences as BamHI fragments. Proceedings of the National Academy of Sciences of the United States of America *77*, 4201-4205.

Potel, C., Kaelin, K., Gautier, I., Lebon, P., Coppey, J., and Rozenberg, F. (2002). Incorporation of green fluorescent protein into the essential envelope glycoprotein B of Herpes Simplex Virus type 1. Journal of Virological Methods *105*, 13-23.

Preston, C., and Nicholl, M. (1997). Repression of gene expression upon infection of cells with Herpes Simplex Virus type 1 mutants impaired for immediate-early protein synthesis. Journal of Virology *71*, 7807-7813.

Preston, C. M. (2000). Repression of viral transcription during Herpes Simplex Virus latency. Journal of General Virology *81*, 1-19.

Preston, C. M., Cordingley, M. G., and Stow, N. D. (1984). Analysis of DNA sequences which regulate the transcription of a Herpes Simplex Virus immediate early gene. Journal of Virology *50*, 708-716.

Preston, C. M., Frame, M. C., and Campbell, M. E. M. (1988). A complex formed between cell components and an HSV structural polypeptide binds to a viral immediate early gene regulatory DNA sequence. Cell *52*, 425-434.

Princiotta, M. F., Finzi, D., Qian, S.-B., Gibbs, J., Schuchmann, S., Buttgereit, F., Bennink, J. R., and Yewdell, J. W. (2003). Quantitating protein synthesis, degradation, and endogenous antigen processing. Immunity *18*, 343-354.

Proença, J. T., Coleman, H. M., Connor, V., Winton, D. J., and Efstathiou, S. (2008). A historical analysis of Herpes Simplex Virus promoter activation *in vivo* reveals distinct populations of latently infected neurones. Journal of General Virology *89*, 2965-2974.

Proença, J. T., Coleman, H. M., Nicoll, M. P., Connor, V., Preston, C. M., Arthur, J., and Efstathiou, S. (2011). An investigation of Herpes Simplex Virus promoter activity compatible with latency establishment reveals VP16-independent activation of immediate-early promoters in sensory neurones. Journal of General Virology *92*, 2575-2585.

Puga, A., and Notkins, A. L. (1987). Continued expression of a poly(A)+ transcript of Herpes Simplex Virus type 1 in trigeminal ganglia of latently infected mice. Journal of Virology *61*, 1700-1703.

Purbhoo, M. A., Irvine, D. J., Huppa, J. B., and Davis, M. M. (2004). T cell killing does not require the formation of a stable mature immunological synapse. Nature Immunology *5*, 524-530.

Purifoy, D. J. M., Lewis, R. B., and Powell, K. L. (1977). Identification of the Herpes Simplex Virus DNA polymerase gene. Nature *269*, 621-623.

Radonić, A., Thulke, S., Mackay, I. M., Landt, O., Siegert, W., and Nitsche, A. (2004). Guideline to reference gene selection for quantitative real-time PCR. Biochemical and Biophysical Research Communications *313*, 856-862.

Rajčáni, J., Andrea, V., and Ingeborg, R. (2004). Peculiarities of Herpes Simplex Virus (HSV) Transcription: An overview. Virus Genes *28*, 293-310.

Ramachandran, S., Davoli, K. A., Yee, M. B., Hendricks, R. L., and Kinchington, P. R. (2010). Delaying the expression of Herpes Simplex Virus type 1 glycoprotein B (gB) to a true late gene alters neurovirulence and inhibits the gB-$CD8^+$ T-cell response in the trigeminal ganglion. Journal of Virology *84*, 8811-8820.

Ramachandran, S., Knickelbein, J. E., Ferko, C., Hendricks, R. L., and Kinchington, P. R. (2008). Development and pathogenic evaluation of recombinant Herpes Simplex Virus type 1 expressing two fluorescent reporter genes from different lytic promoters. Virology *378*, 254-264.

Ran, F. A., Hsu, Patrick D., Lin, C.-Y., Gootenberg, Jonathan S., Konermann, S., Trevino, A. E., Scott, David A., Inoue, A., Matoba, S., Zhang, Y.*, et al.* (2013). Double nicking by RNA-guided CRISPR Cas9 for enhanced genome editing specificity. Cell *154*, 1380-1389.

Rasband, W. S. (1997-2012). Image J (Bethesda, Maryland, USA, U.S. National Institutes of Health).

Rasmussen, S. B., Sorensen, L. N., Malmgaard, L., Ank, N., Baines, J. D., Chen, Z. J., and Paludan, S. R. (2007). Type I interferon production during Herpes Simplex Virus infection is controlled by cell-type-specific viral recognition through Toll-Like Receptor 9, the mitochondrial antiviral signaling protein pathway, and novel recognition systems. Journal of Virology *81*, 13315-13324.

Read, G. S., and Frenkel, N. (1983). Herpes Simplex Virus mutants defective in the virion-associated shutoff of host polypeptide synthesis and exhibiting abnormal synthesis of α (immediate early) viral polypeptides. Journal of Virology *46*, 498-512.

Rice, S. A., and Davido, D. J. (2013). HSV-1 ICP22: Hijacking host nuclear functions to enhance viral infection. Future microbiology *8*, 311-321.

Rice, S. A., Long, M. C., Lam, V., Schaffer, P. A., and Spencer, C. A. (1995). Herpes Simplex Virus immediate-early protein ICP22 is required for viral modification of host RNA polymerase II and establishment of the normal viral transcription program. Journal of Virology *69*, 5550-5559.

Rinaldi, A., Marshall, K. R., and Preston, C. M. (1999). A non-cytotoxic Herpes Simplex Virus vector which expresses Cre recombinase directs efficient site specific recombination. Virus Research *65*, 11-20.

Rixon, F. J., and McGeoch, D. J. (1984). A 3' co-terminal family of mRNAs from the Herpes Simplex Virus type 1 short region: Two overlapping reading frames encode unrelated polypeptide one of which has highly reiterated amino acid sequence. Nucleic Acids Research *12*, 2473-2487.

Rock, D. L., and Fraser, N. W. (1983). Detection of HSV-1 genome in central nervous system of latently infected mice. Nature *302*, 523-525.

Rock, D. L., and Fraser, N. W. (1985). Latent Herpes Simplex Virus type 1 DNA contains two copies of the virion DNA joint region. Journal of Virology *55*, 849-852.

Rock, D. L., Nesburn, A. B., Ghiasi, H., Ong, J., Lewis, T. L., Lokensgard, J. R., and Wechsler, S. L. (1987). Detection of latency-related viral RNAs in trigeminal ganglia of rabbits latently infected with Herpes Simplex Virus type 1. Journal of Virology *61*, 3820-3826.

Rock, K. L., Gramm, C., Rothstein, L., Clark, K., Stein, R., Dick, L., Hwang, D., and Goldberg, A. L. (1994). Inhibitors of the proteasome block the degradation of most cell proteins and the generation of peptides presented on MHC class I molecules. Cell *78*, 761-771.

Roizman, B. (1982). The Herpesviruses, Vol 3.

Roizman, B. (2011). The checkpoints of viral gene expression in productive and latent infection: The role of the HDAC/CoREST/LSD1/REST repressor complex. Journal of Virology *85*, 7474-7482.

Roizman, B., Carmichael, L. E., Deinhardt, F., de-The, G., Nahmias, A. J., Plowright, W., Rapp, F., Sheldrick, P., Takahashi, M., and Wolf, K. (1981). Herpesviridae. Definition, provisional nomenclature, and taxonomy. The Herpesvirus Study Group, the International Committee on Taxonomy of Viruses. Intervirology *16*, 201-217.

Roizman, B., and Jenkins, F. (1985). Genetic engineering of novel genomes of large DNA viruses. Science *229*, 1208-1214.

Roizman, B., and Whitley, R. J. (2001). The nine ages of Herpes Simplex Virus. Herpes *8*, 23-27.

Roizmann, B., Desrosiers, R. C., Fleckenstein, B., Lopez, C., Minson, A. C., and Studdert, M. J. (1992). The family *Herpesviridae*: an update. The Herpesvirus Study Group of the International Committee on Taxonomy of Viruses. Archives of Virology *123*, 425-449.

Rolinski, J., and Hus, I. (2014). Immunological aspects of acute and recurrent Herpes Simplex Keratitis. Journal of Immunology Research *2014*, 513560.

Rosato, P. C., and Leib, D. A. (2014). Intrinsic innate immunity fails to control Herpes Simplex Virus and Vesicular Stomatitis Virus replication in sensory neurons and fibroblasts. Journal of Virology *88*, 9991-10001.

Ru, J., Sun, H., Fan, H., Wang, C., Li, Y., Liu, M., and Tang, H. (2014). MiR-23a facilitates the replication of HSV-1 through the suppression of Interferon Regulatory Factor 1. PLoS ONE *9*, e114021.

Russell, T. A., Stefanovic, T., and Tscharke, D. C. (2015). Engineering Herpes Simplex Virus by infection–transfection methods including recombination site targeting by CRISPR/Cas9 nucleases. Journal of Virological Methods *213*, 18-25.

Rytel, M. W., Niebojewski, R. A., Aguilar-Torres, F. G., and Russell, T. J. (1978). Recurrent Herpes Simplex labialis: Viral replication and clinical course. The American Journal of the Medical Sciences *276*, 319-323.

Sacks, W. R., Greene, C. C., Aschman, D. P., and Schaffer, P. A. (1985). Herpes simplex virus type 1 ICP27 is an essential regulatory protein. Journal of Virology *55*, 796-805.

Saeki, Y., Ichikawa, T., Saeki, A., Chiocca, E. A., Tobler, K., Ackermann, M., Breakefield, X. O., and Fraefel, C. (1998). Herpes simplex virus type 1 DNA amplified as Bacterial Artificial Chromosome in *Escherichia coli*: Rescue of replication-competent virus progeny and packaging of amplicon vectors. Human Gene Therapy *9*, 2787-2794.

Sanchez, R., and Mohr, I. (2007). Inhibition of cellular 2'-5' oligoadenylate synthetase by the Herpes Simplex Virus Type 1 U_S11 protein. Journal of Virology *81*, 3455-3464.

Sandri-Goldin, R. M. (2011). The many roles of the highly interactive HSV protein ICP27, a key regulator of infection. Future microbiology *6*, 1261-1277.

Sanna, P. P., De Logu, A., Williamson, R. A., Hom, Y.-L., Straus, S. E., Bloom, F. E., and Burton, D. R. (1996). Protection of nude mice by passive immunization with a type-common human recombinant monoclonal antibody against HSV. Virology *215*, 101-106.

Sauer, B., and Henderson, N. (1988). Site-specific DNA recombination in mammalian cells by the Cre recombinase of bacteriophage P1. Proceedings of the National Academy of Sciences *85*, 5166-5170.

Sawtell, N. M. (1997). Comprehensive quantification of Herpes Simplex Virus latency at the single-cell level. Journal of Virology *71*, 5423-5431.

Sawtell, N. M. (1998). The probability of *in vivo* reactivation of Herpes Simplex Virus type 1 increases with the number of latently infected neurons in the ganglia. Journal of Virology *72*, 6888-6892.

Sawtell, N. M. (2003). Quantitative analysis of Herpes Simplex Virus reactivation *in vivo* demonstrates that reactivation in the nervous system is not inhibited at early times postinoculation. Journal of Virology *77*, 4127-4138.

Sawtell, N. M., Poon, D. K., Tansky, C. S., and Thompson, R. L. (1998). The latent Herpes Simplex Virus type 1 genome copy number in individual neurons is virus strain specific and correlates with reactivation. Journal of Virology *72*, 5343-5350.

Sawtell, N. M., and Thompson, R. L. (1992a). Herpes Simplex Virus type 1 Latency-Associated Transcription unit promotes anatomical site-dependent establishment and reactivation from latency. Journal of Virology *66*, 2157-2169.

Sawtell, N. M., and Thompson, R. L. (1992b). Rapid *in vivo* reactivation of Herpes Simplex Virus in latently infected murine ganglionic neurons after transient hyperthermia. Journal of Virology *66*, 2150-2156.

Sawtell, N. M., and Thompson, R. L. (2004). Comparison of Herpes Simplex Virus reactivation in ganglia *in vivo* and in explants demonstrates quantitative and qualitative differences. Journal of Virology *78*, 7784-7794.

Schiffer, J. T., Abu-Raddad, L., Mark, K. E., Zhu, J., Selke, S., Koelle, D. M., Wald, A., and Corey, L. (2010). Mucosal host immune response predicts the severity and duration of Herpes Simplex Virus-2 genital tract shedding episodes. Proceedings of the National Academy of Sciences *107*, 18973-18978.

Schiffer, J. T., Abu-Raddad, L., Mark, K. E., Zhu, J., Selke, S., Magaret, A., Wald, A., and Corey, L. (2009). Frequent release of low amounts of Herpes Simplex Virus from neurons: Results of a mathematical model, Vol 1.

Schmider, E., Ziegler, M., Danay, E., Beyer, L., and Bühner, M. (2010). Is it really robust? Reinvestigating the robustness of ANOVA against violations of the normal distribution assumption. Methodology European Journal of Research Methods for the Behavioral and Social Sciences *6*, 147-151.

Schneider, C. A., Rasband, W. S., and Eliceiri, K. W. (2012). NIH Image to ImageJ: 25 years of image analysis. Nature Methods *9*, 671-675.

Schrag, J. D., Prasad, B. V. V., Rixon, F. J., and Chiu, W. (1989). Three-dimensional structure of the HSV1 nucleocapsid. Cell *56*, 651-660.

Schubert, M. M., Peterson, D. E., Flournoy, N., Meyers, J. D., and Truelove, E. L. (1990). Oral and pharyngeal Herpes Simplex Virus infection after allogeneic bone marrow transplantation: Analysis of factors associated with infection. Oral Surgery, Oral Medicine, Oral Pathology *70*, 286-293.

Sciammas, R., Kodukula, P., Tang, Q., Hendricks, R. L., and Bluestone, J. A. (1997). T cell receptor–γ/δ cells protect mice from Herpes Simplex Virus type 1–induced lethal encephalitis. The Journal of Experimental Medicine *185*, 1969-1975.

Sears, A. E., Halliburton, I. W., Meignier, B., Silver, S., and Roizman, B. (1985). Herpes Simplex Virus 1 mutant deleted in the α22 gene: Growth and gene expression in permissive and restrictive cells and establishment of latency in mice. Journal of Virology *55*, 338-346.

Sedarati, F., Izumi, K. M., Wagner, E. K., and Stevens, J. G. (1989). Herpes Simplex Virus type 1 Latency-Associated Transcription plays no role in establishment or maintenance of a latent infection in murine sensory neurons. Journal of Virology *63*, 4455-4458.

Sedarati, F., Margolis, T. P., and Stevens, J. G. (1993). Latent Infection can be established with drastically restricted transcription and replication of the HSV-1 genome. Virology *192*, 687-691.

Serna, A., Ramirez, M. C., Soukhanova, A., and Sigal, L. J. (2003). Cutting edge: Efficient MHC class I cross-presentation during early Vaccinia infection requires the transfer of proteasomal intermediates between antigen donor and presenting cells. The Journal of Immunology *171*, 5668-5672.

Sethna, M., and Weir, J. P. (1993). Mutational analysis of the Herpes Simplex Virus type 1 glycoprotein E promoter. Virology *196*, 532-540.

Shaner, N. C., Campbell, R. E., Steinbach, P. A., Giepmans, B. N. G., Palmer, A. E., and Tsien, R. Y. (2004). Improved monomeric red, orange and yellow fluorescent proteins derived from *Discosoma* sp. red fluorescent protein. Nature Biotechnology *22*, 1567-1572.

Shao, L., Rapp, L. M., and Weller, S. K. (1993). Herpes Simplex Virus 1 alkaline nuclease is required for efficient egress of capsids from the nucleus. Virology *196*, 146-162.

Shen, W., Sa e Silva, M., Jaber, T., Vitvitskaia, O., Li, S., Henderson, G., and Jones, C. (2009). Two small RNAs encoded within the first 1.5 kilobases of the Herpes Simplex Virus type 1

Latency-Associated Transcript can inhibit productive infection and cooperate to inhibit apoptosis. Journal of Virology *83*, 9131-9139.

Shen, Z., Reznikoff, G., Dranoff, G., and Rock, K. L. (1997). Cloned dendritic cells can present exogenous antigens on both MHC class I and class II molecules. The Journal of Immunology *158*, 2723-2730.

Sheridan, B. S., Cherpes, T. L., Urban, J., Kalinski, P., and Hendricks, R. L. (2009). Reevaluating the $CD8^+$ T cell response to Herpes Simplex Virus type 1: Involvement of $CD8^+$ T cells reactive to subdominant epitopes. Journal of Virology *83*, 2237-2245.

Sheridan, B. S., Khanna, K. M., Frank, G. M., and Hendricks, R. L. (2006). Latent virus influences the generation and maintenance of $CD8^+$ T cell memory. The Journal of Immunology *177*, 8356-8364.

Shimeld, C., Efstathiou, S., and Hill, T. (2001). Tracking the spread of a *lacZ*-tagged Herpes Simplex Virus type 1 between the eye and the nervous system of the mouse: Comparison of primary and recurrent infection. Journal of Virology *75*, 5252-5262.

Shimeld, C., Hill, T. J., Blyth, W. A., and Easty, D. L. (1990). Reactivation of latent infection and induction of recurrent herpetic eye disease in mice. Journal of General Virology *71*, 397-404.

Shimeld, C., Whiteland, J. L., Nicholls, S. M., Easty, D. L., and Hill, T. J. (1996a). Immune cell infiltration in corneas of mice with recurrent Herpes Simplex Virus disease. Journal of General Virology *77*, 977-985.

Shimeld, C., Whiteland, J. L., Nicholls, S. M., Grinfeld, E., Easty, D. L., Gao, H., and Hill, T. J. (1995). Immune cell infiltration and persistence in the mouse trigeminal ganglion after infection of the cornea with Herpes Simplex Virus type 1. Journal of Neuroimmunology *61*, 7-16.

Shimeld, C., Whiteland, J. L., Williams, N. A., Easty, D. L., and Hill, T. J. (1996b). Reactivation of Herpes Simplex Virus type 1 in the mouse trigeminal ganglion: An *in vivo* study of virus antigen and immune cell infiltration. Journal of General Virology *77*, 2583-2590.

Shimeld, C., Whiteland, J. L., Williams, N. A., Easty, D. L., and Hill, T. J. (1997). Cytokine production in the nervous system of mice during acute and latent infection with Herpes Simplex Virus type 1. Journal of General Virology *78*, 3317-3325.

Shimomura, Y., Dudley, J. B., Gongarosa Sr, L. P., and Hill, J. M. (1985). HSV-1 quantitation from rabbit neural tissues after epinephrine-induced reactivation. Investigative Ophthalmology and Visual Science *26*, 121-125.

Shulman, J. D. (2005). Prevalence of oral mucosal lesions in children and youths in the USA. International Journal of Paediatric Dentistry *15*, 89-97.

Simmons, A., and Nash, A. A. (1984). Zosteriform spread of Herpes Simplex Virus as a model of recrudescence and its use to investigate the role of immune cells in prevention of recurrent disease. Journal of Virology *52*, 816-821.

Simmons, A., and Nash, A. A. (1985). Role of antibody in primary and recurrent Herpes Simplex Virus infection. Journal of Virology *53*, 944-948.

Simmons, A., Slobedman, B., Speck, P., Arthur, J., and Efstathiou, S. (1992). Two patterns of persistence of Herpes Simplex Virus DNA sequences in the nervous systems of latently infected mice. Journal of General Virology *73*, 1287-1291.

Simmons, A., and Tscharke, D. C. (1992). Anti-CD8 impairs clearance of Herpes Simplex Virus from the nervous system: Implications for the fate of virally infected neurons. The Journal of Experimental Medicine *175*, 1337-1344.

Slifka, M. K., and Whitton, J. L. (2000). Activated and memory $CD8^+$ T cells can be distinguished by their cytokine profiles and phenotypic markers. The Journal of Immunology *164*, 208-216.

Slobedman, B., Efstathiou, S., and Simmons, A. (1994). Quantitative analysis of Herpes Simplex Virus DNA and transcriptional activity in ganglia of mice latently infected with wild-type and thymidine kinase-deficient viral strains. Journal of General Virology *75*, 2469-2474.

Smiley, J. R. (2004). Herpes Simplex Virus virion host shutoff protein: Immune evasion mediated by a viral RNase? Journal of Virology *78*, 1063-1068.

Smith, C., Lachmann, R. H., and Efstathiou, S. (2000). Expression from the Herpes Simplex Virus type 1 Latency-Associated promoter in the murine central nervous system. Journal of General Virology *81*, 649-662.

Smith, C. A., Bates, P., Rivera-Gonzalez, R., Gu, B., and DeLuca, N. A. (1993). ICP4, the major transcriptional regulatory protein of Herpes Simplex Virus type 1, forms a tripartite complex with TATA-binding protein and TFIIB. Journal of Virology *67*, 4676-4687.

Smith, J. S., and Robinson, N. J. (2002). Age-specific prevalence of infection with Herpes Simplex Virus types 2 and 1: A global review. The Journal of Infectious Diseases *186*, S3-S28.

Smith, R. L., Pizer, L. I., Johnson Jr, E. M., and Wilcox, C. L. (1992). Activation of second-messenger pathways reactivates latent Herpes Simplex Virus in neuronal cultures. Virology *188*, 311-318.

Smith, R. W., Malik, P., and Clements, J. B. (2005). The herpes simplex virus ICP27 protein: A multifunctional post-transcriptional regulator of gene expression. Biochemical Society Transactions *33*, 499-501.

Sørensen, L. N., Reinert, L. S., Malmgaard, L., Bartholdy, C., Thomsen, A. R., and Paludan, S. R. (2008). TLR2 and TLR9 synergistically control Herpes Simplex Virus infection in the brain. The Journal of Immunology *181*, 8604-8612.

Soriano, P. (1999). Generalized *lacZ* expression with the ROSA26 Cre reporter strain. Nature Genetics *21*, 70-71.

Speck, P., and Simmons, A. (1998). Precipitous clearance of Herpes Simplex Virus antigens from the peripheral nervous systems of experimentally infected C57BL/10 mice. Journal of General Virology *79*, 561-564.

Speck, P. G., and Simmons, A. (1991). Divergent molecular pathways of productive and latent infection with a virulent strain of Herpes Simplex Virus type 1. Journal of Virology *65*, 4001-4005.

Speck, S. H., and Ganem, D. (2010). Viral latency and its regulation: Lessons from the γ-Herpesviruses. Cell Host and Microbe *8*, 100-115.

Spencer, C. A., Dahmus, M. E., and Rice, S. A. (1997). Repression of host RNA polymerase II transcription by Herpes Simplex Virus type 1. Journal of Virology *71*, 2031-2040.

Spitzer, N., Sammons, G. S., and Price, E. M. (2011). Autofluorescent cells in rat brain can be convincing impostors in green fluorescent reporter studies. Journal of Neuroscience Methods *197*, 48-55.

Spivack, J. G., and Fraser, N. W. (1987). Detection of Herpes Simplex Virus type 1 transcripts during latent infection in mice. Journal of Virology *61*, 3841-3847.

Spruance, S. L., Overall, J. C., Kern, E. R., Krueger, G. G., Pliam, V., and Miller, W. (1977). The natural history of recurrent Herpes Simplex labialis. New England Journal of Medicine *297*, 69-75.

St. Leger, A. J., Jeon, S., and Hendricks, R. L. (2013). Broadening the repertoire of functional Herpes Simplex Virus type 1–specific $CD8^+$ T cells reduces viral reactivation from latency in sensory ganglia. The Journal of Immunology *191*, 2258-2265.

St. Leger, A. J., Peters, B., Sidney, J., Sette, A., and Hendricks, R. L. (2011). Defining the Herpes Simplex Virus-specific $CD8^+$ T cell repertoire in C57Bl/6 mice. The Journal of Immunology *186*, 3927-3933.

Ståhlberg, A., Håkansson, J., Xian, X., Semb, H., and Kubista, M. (2004a). Properties of the reverse transcription reaction in mRNA quantification. Clinical Chemistry *50*, 509-515.

Ståhlberg, A., Kubista, M., and Pfaffl, M. (2004b). Comparison of reverse transcriptases in gene expression analysis. Clinical Chemistry *50*, 1678-1680.

Stavropoulos, T. A., and Strathdee, C. A. (1998). An enhanced packaging system for helper-dependent Herpes Simplex Virus vectors. Journal of Virology *72*, 7137-7143.

Steffy, K. R., and Weir, J. P. (1991). Upstream promoter elements of the Herpes Simplex Virus type 1 glycoprotein H gene. Journal of Virology *65*, 972-975.

Steiner, I. (1996). Human herpes viruses latent infection in the nervous system. Immunological Reviews *152*, 157-173.

Steiner, I., and Kennedy, P. G. (1995). Herpes Simplex Virus latent infection in the nervous system. Journal of NeuroVirology *1*, 19-29.

Steiner, I., Spivack, J. G., Deshmane, S. L., Ace, C. I., Preston, C. M., and Fraser, N. W. (1990). A Herpes Simplex Virus type 1 mutant containing a nontransducing Vmw65 protein establishes latent infection *in vivo* in the absence of viral replication and reactivates efficiently from explanted trigeminal ganglia. Journal of Virology *64*, 1630-1638.

Steiner, I., Spivack, J. G., Lirette, R. P., Brown, S. M., MacLean, A. R., Subak-Sharpe, J. H., and Fraser, N. W. (1989). Herpes Simplex Virus type 1 Latency-Associated Transcripts are evidently not essential for latent infection. The EMBO Journal *8*, 505-511.

Steiner, I., Spivack, J. G., O'Boyle, D. R., Lavi, E., and Fraser, N. W. (1988). Latent Herpes Simplex Virus type 1 transcription in human trigeminal ganglia. Journal of Virology *62*, 3493-3496.

Stevens, J. G., and Cook, M. L. (1971). Latent Herpes Simplex Virus in spinal ganglia of mice. Science *173*, 843-845.

Stevens, J. G., Haarr, L., Porter, D. D., Cook, M. L., and Wagner, E. K. (1988). Prominence of the Herpes Simplex Virus Latency-Associated Transcript in trigeminal ganglia from seropositive humans. The Journal of Infectious Diseases *158*, 117-123.

Stevens, J. G., Wagner, E. K., and Devi-Rao, G. B. (1987). RNA complementary to a herpesvirus α gene mRNA is prominent in latently infected neurons. Science *235*, 1056-1059.

Stingley, S. W., Ramirez, J. J. G., Aguilar, S. A., Simmen, K., Sandri-Goldin, R. M., Ghazal, P., and Wagner, E. K. (2000). Global analysis of Herpes Simplex Virus type 1 transcription using an oligonucleotide-based DNA microarray. Journal of Virology *74*, 9916-9927.

Stinski, M. F., and Roehr, T. J. (1985). Activation of the major immediate early gene of Human Cytomegalovirus by *cis*-acting elements in the promoter-regulatory sequence and by virus-specific *trans*-acting components. Journal of Virology *55*, 431-441.

Stock, A. T., Jones, C. M., Heath, W. R., and Carbone, F. R. (2011). Rapid recruitment and activation of $CD8^+$ T cells after Herpes Simplex Virus type 1 skin infection. Immunology and Cell Biology *89*, 143-148.

Strang, B. L., and Stow, N. D. (2005). Circularization of the Herpes Simplex Virus type 1 genome upon lytic infection. Journal of Virology *79*, 12487-12494.

Strelow, L. I., Laycock, K. A., Jun, P. Y., Rader, K. A., Brady, R. H., Miller, J. K., Pepose, J. S., and Leib, D. A. (1994). A structural and functional comparison of the Latency-Associated Transcript promoters of Herpes Simplex Virus type 1 strains KOS and McKrae. Journal of General Virology *75*, 2475-2480.

Stumpf, T. H., Case, R., Shimeld, C., Easty, D. L., and Hill, T. J. (2002). Primary Herpes Simplex Virus type 1 infection of the eye triggers similar immune responses in the cornea and the skin of the eyelids. Journal of General Virology *83*, 1579-1590.

Subak-Sharpe, J. H., and Dargan, D. J. (1998). HSV molecular biology: General aspects of Herpes Simplex Virus molecular biology. Virus Genes *16*, 239-251.

Suenaga, T., Kohyama, M., Hirayasu, K., and Arase, H. (2014). Engineering large viral DNA genomes using the CRISPR-Cas9 system. Microbiol Immunol *58*, 513-522.

Summers, B. C., and Leib, D. A. (2002). Herpes Simplex Virus type 1 origins of DNA replication play no role in the regulation of flanking promoters. Journal of Virology *76*, 7020-7029.

Summers, B. C., Margolis, T. P., and Leib, D. A. (2001). Herpes Simplex Virus type 1 corneal infection results in periocular disease by zosteriform spread. Journal of Virology *75*, 5069-5075.

Suzutani, T., Nagamine, M., Shibaki, T., Ogasawara, M., Yoshida, I., Daikoku, T., Nishiyama, Y., and Azuma, M. (2000). The role of the UL41 gene of Herpes Simplex Virus type 1 in evasion of non-specific host defence mechanisms during primary infection. Journal of General Virology *81*, 1763-1771.

Syrjänen, S., Mikola, H., Nykänen, M., and Hukkanen, V. (1996). *In vitro* establishment of lytic and nonproductive infection by Herpes Simplex Virus type 1 in three-dimensional keratinocyte culture. Journal of Virology *70*, 6524-6528.

Sze, P., and Herman, R. C. (1992). The Herpes Simplex Virus type 1 ICP6 gene is regulated by a 'leaky' early promoter. Virus Research *26*, 141-152.

Tal-Singer, R., Lasner, T. M., Podrzucki, W., Skokotas, A., Leary, J. J., Berger, S. L., and Fraser, N. W. (1997). Gene expression during reactivation of Herpes Simplex Virus type 1 from latency in the peripheral nervous system is different from that during lytic infection of tissue cultures. Journal of Virology *71*, 5268-5276.

Tanaka, M., Kagawa, H., Yamanashi, Y., Sata, T., and Kawaguchi, Y. (2003). Construction of an excisable bacterial artificial chromosome containing a full-length infectious clone of Herpes Simplex Virus Type 1: Viruses reconstituted from the clone exhibit wild-type properties *in vitro* and *in vivo*. Journal of Virology *77*, 1382-1391.

Tanaka, M., Kodaira, H., Nishiyama, Y., Sata, T., and Kawaguchi, Y. (2004). Construction of recombinant Herpes Simplex Virus type I expressing green fluorescent protein without loss of any viral genes. Microbes and Infection *6*, 485-493.

Tang, Q., and Hendricks, R. L. (1996). Interferon γ regulates platelet endothelial cell adhesion molecule 1 expression and neutrophil infiltration into Herpes Simplex Virus-infected mouse corneas. The Journal of Experimental Medicine *184*, 1435-1447.

Taylor, T. J., and Knipe, D. M. (2004). Proteomics of Herpes Simplex Virus replication compartments: Association of cellular DNA replication, repair, recombination, and chromatin remodeling proteins with ICP8. Journal of Virology *78*, 5856-5866.

Theil, D., Derfuss, T., Paripovic, I., Herberger, S., Meinl, E., Schueler, O., Strupp, M., Arbusow, V., and Brandt, T. (2003a). Latent herpesvirus infection in human trigeminal ganglia causes chronic immune response. The American Journal of Pathology *163*, 2179-2184.

Theil, D., Paripovic, I., Derfuss, T., Herberger, S., Strupp, M., Arbusow, V., and Brandt, T. (2003b). Dually infected (HSV-1/VZV) single neurons in human trigeminal ganglia. Annals of Neurology *54*, 678-682.

Thomas, S. K., Gough, G., Latchman, D. S., S., R., and Coffin (1999). Herpes Simplex Virus Latency-Associated Transcript encodes a protein which greatly enhances virus growth, can compensate for deficiencies in immediate-early gene expression, and is likely to function during reactivation from virus latency. Journal of Virology *73*, 6618-6625.

Thompson, C. B., Lindsten, T., Ledbetter, J. A., Kunkel, S. L., Young, H. A., Emerson, S. G., Leiden, J. M., and June, C. H. (1989). CD28 activation pathway regulates the production of multiple T-cell-derived lymphokines/cytokines. Proceedings of the National Academy of Sciences of the United States of America *86*, 1333-1337.

Thompson, R. L., Cook, M. L., Devi-Rao, G. B., Wagner, E. K., and Stevens, J. G. (1986). Functional and molecular analyses of the avirulent wild-type Herpes Simplex Virus type 1 strain KOS. Journal of Virology *58*, 203-211.

Thompson, R. L., Preston, C. M., and Sawtell, N. M. (2009). De novo synthesis of VP16 coordinates the exit from HSV latency *in vivo*. PLoS Pathogens *5*.

Thompson, R. L., and Sawtell, N. M. (1997). The Herpes Simplex Virus type 1 Latency-Associated Transcript gene regulates the establishment of latency. Journal of Virology *71*, 5432-5440.

Thompson, R. L., and Sawtell, N. M. (2000). Replication of Herpes Simplex Virus type 1 within trigeminal ganglia is required for high frequency but not high viral genome copy number latency. Journal of Virology *74*, 965-974.

Thompson, R. L., and Sawtell, N. M. (2001). Herpes Simplex Virus Type 1 Latency-Associated Transcript gene promotes neuronal survival. Journal of Virology *75*, 6660-6675.

Thompson, R. L., and Sawtell, N. M. (2006). Evidence that the Herpes Simplex Virus type 1 ICP0 protein does not initiate reactivation from latency *in vivo*. Journal of Virology *80*, 10919-10930.

Tigges, M. A., Leng, S., Johnson, D. C., and Burke, R. L. (1996). Human Herpes Simplex Virus (HSV)-specific $CD8^+$ CTL clones recognize HSV-2-infected fibroblasts after treatment with IFN-γ or when virion host shutoff functions are disabled. The Journal of Immunology *156*, 3901-3910.

Toma, H. S., Murina, A. T., Areaux, R. G., Neumann, D. M., Bhattacharjee, P. S., Foster, T. P., Kaufman, H. E., and Hill, J. M. (2008). Ocular HSV-1 latency, reactivation and recurrent disease. Seminars in Ophthalmology *23*, 249-273.

Tomazin, R., Hill, A. B., Jugovic, P., York, I., van Endert, P., Ploegh, H. L., Andrews, D. W., and Johnson, D. C. (1996). Stable binding of the Herpes Simplex Virus ICP47 protein to the peptide binding site of TAP. The EMBO Journal *15*, 3256-3266.

Townsend, A., Ohlen, C., Bastin, J., Ljunggren, H. G., Foster, L., and Karre, K. (1989). Association of class I major histocompatibility heavy and light chains induced by viral peptides. Nature *340*, 443-448.

Tran, T., Druce, J. D., Catton, M. C., Kelly, H., and Birch, C. J. (2004). Changing epidemiology of genital Herpes Simplex Virus infection in Melbourne, Australia, between 1980 and 2003. Sexually Transmitted Infections *80*, 277-279.

Tricarico, C., Pinzani, P., Bianchi, S., Paglierani, M., Distante, V., Pazzagli, M., Bustin, S. A., and Orlando, C. (2002). Quantitative real-time reverse transcription polymerase chain reaction: Normalization to rRNA or single housekeeping genes is inappropriate for human tissue biopsies. Analytical Biochemistry *309*, 293-300.

Trousdale, M. D., Steiner, I., Spivack, J. G., Deshmane, S. L., Brown, S. M., MacLean, A. R., Subak-Sharpe, J. H., and Fraser, N. W. (1991). *In vivo* and *in vitro* reactivation impairment of a Herpes Simplex Virus type 1 Latency-Associated Transcript variant in a rabbit eye model. Journal of Virology *65*, 6989-6993.

Tscharke, D. C., Karupiah, G., Zhou, J., Palmore, T., Irvine, K. R., Haeryfar, S. M. M., Williams, S., Sidney, J., Sette, A., Bennink, J. R., *et al.* (2005). Identification of poxvirus $CD8^+$ T cell determinants to enable rational design and characterization of smallpox vaccines. The Journal of Experimental Medicine *201*, 95-104.

Tscharke, D. C., and Simmons, A. (1999). Anti-CD8 treatment alters interleukin-4 but not interferon-γ mRNA levels in murine sensory ganglia during Herpes Simplex Virus infection. Archives of Virology *144*, 2229-2238.

Tullo, A. B., Shimeld, C., Blyth, W. A., Hill, T. J., and Easty, D. L. (1982). Spread of virus and distribution of latent infection following ocular Herpes Simplex in the non-immune and immune mouse. Journal of General Virology *63*, 95-101.

Umbach, J. L., Kramer, M. F., Jurak, I., Karnowski, H. W., Coen, D. M., and Cullen, B. R. (2008). MicroRNAs expressed by Herpes Simplex Virus 1 during latent infection regulate viral mRNAs. Nature *454*, 780-783.

Umbach, J. L., Nagel, M. A., Cohrs, R. J., Gilden, D. H., and Cullen, B. R. (2009). Analysis of human Alphaherpesvirus microRNA expression in latently infected human trigeminal ganglia. Journal of Virology *83*, 10677-10683.

Valyi-Nagy, T., Deshmane, S. L., Raengsakulrach, B., Nicosia, M., Gesser, R. M., Wysocka, M., Dillner, A., and Fraser, N. W. (1992). Herpes Simplex Virus type 1 mutant strain *in*1814 establishes a unique, slowly progressing infection in SCID mice. Journal of Virology *66*, 7336-7345.

Valyi-Nagy, T., Deshmane, S. L., Spivack, J. G., Steiner, I., Ace, C. I., Preston, C. M., and Fraser, N. W. (1991). Investigation of Herpes Simplex Virus type 1 (HSV-1) gene expression and DNA synthesis during the establishment of latent infection by an HSV-1 mutant, in1814, that does not replicate in mouse trigeminal ganglia. Journal of General Virology *72*, 641-649.

van Genderen, I. L., Brandimarti, R., Torrisi, M. R., Campadelli, G., and van Meer, G. (1994). The phospholipid composition of extracellular Herpes Simplex virions differs from that of host cell nuclei. Virology *200*, 831-836.

Van Lint, A., Ayers, M., Brooks, A. G., Coles, R. M., Heath, W. R., and Carbone, F. R. (2004). Herpes Simplex Virus-specific $CD8^+$ T cells can clear established lytic infections from skin and nerves and can partially limit the early spread of virus after cutaneous inoculation. The Journal of Immunology *172*, 392-397.

Van Lint, A. L., Kleinert, L., Clarke, S. R. M., Stock, A., Heath, W. R., and Carbone, F. R. (2005). Latent infection with Herpes Simplex Virus is associated with ongoing $CD8^+$ T-cell stimulation by parenchymal cells within sensory ganglia. Journal of Virology *79*, 14843-14851.

van Velzen, M., Jing, L., Osterhaus, A. D. M. E., Sette, A., Koelle, D. M., and Verjans, G. M. G. M. (2013). Local CD4 and CD8 T-cell reactivity to HSV-1 antigens documents broad viral protein expression and immune competence in latently infected human trigeminal ganglia. PLoS Pathogens *9*, e1003547.

Veres, A., Gosis, Bridget S., Ding, Q., Collins, R., Ragavendran, A., Brand, H., Erdin, S., Cowan, C. A., Talkowski, Michael E., and Musunuru, K. (2014). Low incidence of off-target mutations in individual CRISPR-Cas9 and TALEN targeted human stem cell clones detected by whole-genome sequencing. Cell Stem Cell *15*, 27-30.

Verjans, G. M. G. M., Hintzen, R. Q., van Dun, J. M., Poot, A., Milikan, J. C., Laman, J. D., Langerak, A. W., Kinchington, P. R., and Osterhaus, A. D. M. E. (2007). Selective retention of Herpes Simplex Virus-specific T cells in latently infected human trigeminal ganglia. Proceedings of the National Academy of Sciences *104*, 3496-3501.

Verweij, M. C., Horst, D., Griffin, B. D., Luteijn, R. D., Davison, A. J., Ressing, M. E., and Wiertz, E. J. H. J. (2015). Viral inhibition of the Transporter associated with Antigen Processing (TAP): A striking example of functional convergent evolution. PLoS Pathogens *11*, e1004743.

Wadsworth, S., Jacob, R. J., and Roizman, B. (1975). Anatomy of Herpes Simplex Virus DNA. II. Size, composition, and arrangement of inverted terminal repetitions. Journal of Virology *15*, 1487-1497.

Wagner, E. K., and Bloom, D. C. (1997). Experimental investigation of Herpes Simplex Virus latency. Clinical Microbiology Reviews *10*, 419-443.

Wagner, E. K., Devi-Rao, G., Feldman, L. T., Dobson, A. T., Zhang, Y. F., Flanagan, W. M., and Stevens, J. G. (1988a). Physical characterization of the Herpes Simplex Virus Latency-Associated Transcript in neurons. Journal of Virology *62*, 1194-1202.

Wagner, E. K., Flanagan, W. M., Devi-Rao, G., Zhang, Y. F., Hill, J. M., Anderson, K. P., and Stevens, J. G. (1988b). The Herpes Simplex Virus Latency-Associated Transcript is spliced during the latent phase of infection. Journal of Virology *62*, 4577-4585.

Wagner, M. J., and Summers, W. C. (1978). Structure of the joint region and the termini of the DNA of Herpes Simplex Virus type 1. Journal of Virology *27*, 374-387.

Wakim, L. M., Gebhardt, T., Heath, W. R., and Carbone, F. R. (2008a). Cutting edge: Local recall responses by memory T cells newly recruited to peripheral nonlymphoid tissues. The Journal of Immunology *181*, 5837-5841.

Wakim, L. M., Jones, C. M., Gebhardt, T., Preston, C. M., and Carbone, F. R. (2008b). $CD8^+$ T-cell attenuation of cutaneous Herpes Simplex Virus infection reduces the average viral copy number of the ensuing latent infection. Immunology and Cell Biology *86*, 666-675.

Wakim, L. M., Waithman, J., Van Rooijen, N., Heath, W. R., and Carbone, F. R. (2008c). Dendritic cell-induced memory T cell activation in nonlymphoid tissues. Science *319*, 198-202.

Wallach, D., Fellous, M., and Revel, M. (1982). Preferential effect of γ interferon on the synthesis of HLA antigens and their mRNAs in human cells. Nature *299*, 833-836.

Wang, J., and Quake, S. R. (2014). RNA-guided endonuclease provides a therapeutic strategy to cure latent herpesviridae infection. Proceedings of the National Academy of Sciences *111*, 13157-13162.

Wang, K., Lau, T. Y., Morales, M., Mont, E. K., and Straus, S. E. (2005a). Laser-capture microdissection: Refining estimates of the quantity and distribution of latent Herpes Simplex Virus 1 and Varicella-Zoster Virus DNA in human trigeminal ganglia at the single-cell level. Journal of Virology *79*, 14079-14087.

Wang, Q.-Y., Zhou, C., Johnson, K. E., Colgrove, R. C., Coen, D. M., and Knipe, D. M. (2005b). Herpesviral Latency-Associated Transcript gene promotes assembly of heterochromatin on viral lytic-gene promoters in latent infection. Proceedings of the National Academy of Sciences of the United States of America *102*, 16055-16059.

Watson, G., Xu, W., Reed, A., Babra, B., Putman, T., Wick, E., Wechsler, S. L., Rohrmann, G. F., and Jin, L. (2012). Sequence and comparative analysis of the genome of HSV-1 strain McKrae. Virology *433*, 528-537.

Watson, R. J., and Clements, J. B. (1980). A Herpes Simplex Virus type 1 function continuously required for early and late virus RNA synthesis. Nature *285*, 329-330.

Webre, J. M., Hill, J. M., Nolan, N. M., Clement, C., McFerrin, H. E., Bhattacharjee, P. S., Hsia, V., Neumann, D. M., Foster, T. P., Lukiw, W. J., *et al.* (2012). Rabbit and mouse models of HSV-1 latency, reactivation, and recurrent eye diseases. Journal of Biomedicine and Biotechnology *2012*, 18.

Weir, J. P. (2001). Regulation of Herpes Simplex Virus gene expression. Gene *271*, 117-130.

Weller, T. H., and Stoddard, M. B. (1952). Intranuclear inclusion bodies in cultures of human tissue inoculated with Varicella vesicle fluid. The Journal of Immunology *68*, 311-319.

Wheatley, S. C., Dent, C. L., Wood, J. N., and Latchman, D. S. (1992). Elevation of cyclic AMP levels in cell lines derived from latently infectable sensory neurons increases their permissivity for herpes virus infection by activating the viral immediate-early 1 gene promoter. Molecular Brain Research *12*, 149-154.

Whitley, R. J., Kimberlin, D. W., and Roizman, B. (1998). Herpes Simplex Viruses. Clinical Infectious Diseases *26*, 541-555.

Wiertz, E. J. H. J., Jones, T. R., Sun, L., Bogyo, M., Geuze, H. J., and Ploegh, H. L. (1996). The Human Cytomegalovirus US11 gene product dislocates MHC class I heavy chains from the endoplasmic reticulum to the cytosol. Cell *84*, 769-779.

Willey, D. E., Trousdale, M. D., and Nesburn, A. B. (1984). Reactivation of murine latent HSV infection by epinephrine iontophoresis. Investigative Ophthalmology and Visual Science *25*, 945-950.

Wisner, T. W., Sugimoto, K., Howard, P. W., Kawaguchi, Y., and Johnson, D. C. (2011). Anterograde transport of Herpes Simplex Virus capsids in neurons by both separate and married mechanisms. Journal of Virology *85*, 5919-5928.

Wojtasiak, M., Pickett, D. L., Tate, M. D., Bedoui, S., Job, E. R., Whitney, P. G., Brooks, A. G., and Reading, P. C. (2010). Gr-1^{+} cells, but not neutrophils, limit virus replication and lesion development following flank infection of mice with Herpes Simplex Virus type-1. Virology *407*, 143-151.

Wollenberg, A., Zoch, C., Wetzel, S., Plewig, G., and Przybilla, B. (2003). Predisposing factors and clinical features of eczema herpeticum: A retrospective analysis of 100 cases. Journal of the American Academy of Dermatology *49*, 198-205.

Wong, G. H. W., Bartlett, P. F., Clark-Lewis, I., McKimm-Breschkin, J. L., and Schrader, J. W. (1984). Interferon-γ induces the expression of H-2 and Ia antigens on brain cells. Journal of Neuroimmunology *7*, 255-278.

Wong, Y. C., Lin, L. C., Melo-Silva, C. R., Smith, S. A., and Tscharke, D. C. (2011). Engineering recombinant poxviruses using a compact GFP-blasticidin resistance fusion gene for selection. Journal of Virological Methods *171*, 295-298.

Wu, C. A., Nelson, N. J., McGeoch, D. J., and Challberg, M. D. (1988). Identification of Herpes Simplex Virus type 1 genes required for origin-dependent DNA synthesis. Journal of Virology *62*, 435-443.

Xiao, A., Cheng, Z., Kong, L., Zhu, Z., Lin, S., Gao, G., and Zhang, B. (2014). CasOT: A genome-wide Cas9/gRNA off-target searching tool. Bioinformatics *30*, 1180-1182.

Xie, S., Shen, B., Zhang, C., Huang, X., and Zhang, Y. (2014). sgRNAcas9: A software package for designing CRISPR sgRNA and evaluating potential off-target cleavage sites. PLoS ONE *9*, e100448.

Yewdell, J., and Bennink, J. (1989). Brefeldin A specifically inhibits presentation of protein antigens to cytotoxic T lymphocytes. Science *244*, 1072-1075.

Yordy, B., Iijima, N., Huttner, A., Leib, D., and Iwasaki, A. (2012). A neuron-specific role for autophagy in antiviral defense against Herpes Simplex Virus. Cell Host and Microbe *12*, 334-345.

York, I. A., Roop, C., Andrews, D. W., Riddell, S. R., Graham, F. L., and Johnson, D. C. (1994). A cytosolic Herpes Simplex Virus protein inhibits antigen presentation to $CD8^+$ T lymphocytes. Cell *77*, 525-535.

Young, R. C., Hodge, D. O., Liesegang, T. J., and Baratz, K. H. (2010). Incidence, recurrence, and outcomes of Herpes Simplex Virus eye disease in Olmsted County, Minnesota, 1976-2007: The effect of oral antiviral prophylaxis. Archives of Ophthalmology *128*, 1178-1183.

Yuan, M., Zhang, W., Wang, J., Al Yaghchi, C., Ahmed, J., Chard, L., Lemoine, N. R., and Wang, Y. (2015). Efficiently editing the Vaccinia Virus genome by using the CRISPR-Cas9 system. Journal of Virology *89*, 5176-5179.

Yuen, T. J., Flesch, I. E. A., Hollett, N. A., Dobson, B. M., Russell, T. A., Fahrer, A. M., and Tscharke, D. C. (2010). Analysis of A47, an immunoprevalent protein of vaccinia virus, leads to a reevaluation of the total antiviral $CD8^+$ T cell response. Journal of Virology *84*, 10220-10229.

Zabolotny, J. M., Krummenacher, C., and Fraser, N. W. (1997). The Herpes Simplex Virus type 1 2.0-kilobase latency-associated transcript is a stable intron which branches at a guanosine. Journal of Virology *71*, 4199-4208.

Zhen, S., Hua, L., Liu, Y. H., Gao, L. C., Fu, J., Wan, D. Y., Dong, L. H., Song, H. F., and Gao, X. (2015). Harnessing the clustered regularly interspaced short palindromic repeat (CRISPR)/CRISPR-associated Cas9 system to disrupt the Hepatitis B Virus. Gene Therapy.

Zheng, C., Lin, F., Wang, S., and Xing, J. (2011). A novel virus-encoded nucleocytoplasmic shuttling protein: The UL3 protein of Herpes Simplex Virus type 1. Journal of Virological Methods *177*, 206-210.

Zhou, C., and Knipe, D. M. (2002). Association of Herpes Simplex Virus type 1 ICP8 and ICP27 proteins with cellular RNA polymerase II holoenzyme. Journal of Virology *76*, 5893-5904.

Zhou, G., Du, T., and Roizman, B. (2013). HSV carrying WT REST establishes latency but reactivates only if the synthesis of REST is suppressed. Proceedings of the National Academy of Sciences *110*, E498-506.

Zhou, G., Galvan, V., Campadelli-Fiume, G., and Roizman, B. (2000a). Glycoprotein D or J delivered in *trans* blocks apoptosis in SK-N-SH cells induced by a Herpes Simplex Virus 1 mutant lacking intact genes expressing both glycoproteins. Journal of Virology *74*, 11782-11791.

Zhou, Z. H., Dougherty, M., Jakana, J., He, J., Rixon, F. J., and Chiu, W. (2000b). Seeing the Herpesvirus capsid at 8.5 Å. Science *288*, 877-880.

Zhu, J., Koelle, D. M., Cao, J., Vazquez, J., Huang, M. L., Hladik, F., Wald, A., and Corey, L. (2007). Virus-specific $CD8^+$ T cells accumulate near sensory nerve endings in genital skin during subclinical HSV-2 reactivation. The Journal of Experimental Medicine *204*, 595-603.

Zhu, J., Peng, T., Johnston, C., Phasouk, K., Kask, A. S., Klock, A., Jin, L., Diem, K., Koelle, D. M., Wald, A*., et al.* (2013). Immune surveillance by $CD8\alpha\alpha^+$ skin-resident T cells in human herpes virus infection. Nature *497*, 494-497.

Zhu, L. J., Holmes, B. R., Aronin, N., and Brodsky, M. H. (2014). CRISPRseek: A bioconductor package to identify target-specific guide RNAs for CRISPR-Cas9 genome-editing systems. PLoS ONE *9*, e108424.

Ziegler, H., Muranyi, W., Burgert, H. G., Kremmer, E., and Koszinowski, U. H. (2000). The luminal part of the murine Cytomegalovirus glycoprotein gp40 catalyzes the retention of MHC class I molecules. The EMBO Journal *19*, 870-881.

Ziegler, H., Thäle, R., Lucin, P., Muranyi, W., Flohr, T., Hengel, H., Farrell, H., Rawlinson, W., and Koszinowski, U. H. (1997). A mouse Cytomegalovirus glycoprotein retains MHC class I complexes in the ERGIC/*cis*-Golgi compartments. Immunity *6*, 57-66.

Zinkernagel, R. M., and Doherty, P. C. (1974). Restriction of *in vitr*o T cell mediated cytotoxicity in lymphocytic choriomeningitis within a syngeneic or semiallogeneic system. Nature *248*, 701-702.

Zwaagstra, J. C., Ghiasi, H., Slanina, S. M., Nesburn, A. B., Wheatley, S. C., Lillycrop, K., Wood, J., Latchman, D. S., Patel, K., and Wechsler, S. L. (1990). Activity of Herpes Simplex Virus type 1 Latency-Associated Transcript (LAT) promoter in neuron-derived cells: Evidence for neuron specificity and for a large LAT transcript. Journal of Virology *64*, 5019-5028.

Zweerink, H. J., and Stanton, L. W. (1981). Immune response to Herpes Simplex Virus infections: Virus-specific antibodies in sera from patients with recurrent facial infections. Infection and Immunity *31*, 624-630.